THE UNIVERSITY
of EDINBURGH

Early Parasite-Host Interactions in Controlled Human Malaria Infection

Kathryn Milne

A thesis submitted for the degree of

Doctor of Philosophy

University of Edinburgh

July 2018

Declaration

I declare that the content of this thesis is my own work, and that any collaborative input has been stated clearly in the text. No material presented in this thesis has been submitted to any other university for any other degree.

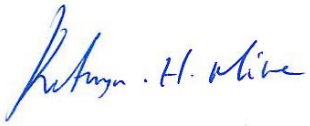

Kathryn Milne

Acknowledgements

First and foremost I would like to thank my supervisors Dr Phil Spence and Prof. J. Alexandra Rowe who together, have mentored me with patience and encouragement from start to finish. I am grateful to them for the opportunity to work on such an interesting project, and for their knowledge and expertise in the field. Their excitement for this project helped motivate me throughout. I would also like to thank Dr Amy Buck for acting on my thesis committee, and for her constructive input along the way.

Financial support for my studentship was provided by the Medical Research Council, to whom I would like to thank. My sincere gratitude goes out to Dr Simon Draper (The Jenner Institute), for allowing me access to volunteer samples, and for his continued collaboration with the lab. Thanks also to Dr Ruth Payne for providing the clinical data and being quick to respond to my incessant emails. I am particularly grateful to Dr Alasdair Ivens (University of Edinburgh), for collaborating with me on the host transcriptional data analysis, and for his patience with the project. I would also like to thank Dr Adam Reid, Dr Mandy Sanders, and Geetha Sankaranarayanan (Wellcome Trust Sanger Institute) for their collaboration on the parasite RNA-sequencing and for sharing their expert knowledge of low-input RNA work.

A huge thank-you to the members of the Rowe/Spence lab, past and present, for all of the invaluable advice and laughter throughout. I would particularly like to thank Ahmed, Yvonne and Martha for their training and assistance with parasite culture, and for helping me find my feet when I first arrived in the lab. A special thanks to Wiebke, Diana, Flo and Ed for all of the interesting discussions, your shared love of gin, and for helping make my time in the lab both productive and fun.

Finally, a very special thanks to my family; to my parents, for their never-ending support and encouragement; to my sister Laura, for understanding the struggles and for being there to lend an ear; to my brother David, for always taking a genuine interest in my studies, and to my boyfriend Kyle for providing the weekly food packages when my funding ran out. Thanks for keeping me smiling.

Lay summary

Malaria is a global health burden, killing more than 400,000 people each year. The disease, which mostly affects children under 5 years, is caused by the *Plasmodium falciparum* parasite. When inside the mammalian host, *P. falciparum* parasites invade red blood cells, where they mature and multiply in numbers. To ensure their continued survival, they express a protein on the surface of the red blood cell, which allows them to stick to cells lining the walls of small blood vessels in host tissues. This affords the parasite a means to escape destruction by the spleen, but has devastating consequences for the host by leading to the obstruction of blood flow and causing damage to vital organs. During infection in non-immune individuals, *P. falciparum* parasites are predicted to express a specific sub-set of these proteins. These so called group-“A” and/ or “B/A” proteins have been associated with severe disease outcome, whereas other subtypes have been linked to mild/uncomplicated infection. This suggests that during first exposure to *P. falciparum*, clinical outcome may be determined by the parasite. Yet, severe disease has also been linked to actions of the host immune system. Upon sensing the invading *P. falciparum* parasite, innate immune cells respond to target and destroy parasite-infected red blood cells. This results in the activation of pro-inflammatory responses thought to be crucial for the early control of parasite growth. However, when inflammatory responses persist or become dysregulated they can also contribute to pathological disease.

It is likely that both parasite and host-mediated factors contribute to severe disease pathology at later stages of infection but their influence at the early stages, as *drivers* of this response, has not been defined. This study aimed to investigate the early interactions between the *P. falciparum* parasite and the non-immune human host, using controlled human malaria infection (deliberate infection of adult volunteers). Data presented in this thesis highlight an inter-individual variability in host immune responses to primary *P. falciparum* infection. Whereas most volunteers demonstrated a classic inflammatory-type response and reported symptoms of malaria, some suppressed inflammation, and others failed to elicit a response in the time frame assessed. Parasites isolated from these volunteers were not found to express the group-A, B/A disease-associated gene/protein subtypes, nor appeared to have any influence on the diversity of host immune responses observed. These findings suggest that it is most likely early decisions of the innate immune response that determine

clinical outcome during primary infection, and that host genetics and/or environmental factors is what drives diversity in responses.

Abstract

Severe malaria infections cause over 400,000 deaths annually, mostly among African children under 5 years of age. In order to reduce the burden of this disease, focus must be placed on understanding what drives pathogenesis in those at greatest risk. It is increasingly appreciated that early immune responses such as inflammation and phagocytosis, although important for host defense, can also contribute to pathogenesis when unrestrained. However, most studies of human malaria have been conducted at the terminal stages of infection, making it difficult to identify the early immune events that may be dictating clinical outcome. The expression of *Plasmodium falciparum* erythrocyte membrane 1 (PfEMP1), along with other variant surface antigens (VSAs), is also thought to influence disease severity, by mediating parasite-host interactions that lead to obstruction of blood flow and organ dysfunction in the non-immune host. Yet, whether these parasite proteins actually drive pathology has been difficult to assess. It is likely that a contribution of both parasite genetics and host immune responses is involved in the progression to severe disease, but how the two might interact to drive this outcome has not yet been explored. Using controlled human malaria infection (CHMI), this study aimed to: (1) characterise the early immune response to *P. falciparum* during primary infection and investigate inter-individual variability within the cohort, (2) assess patterns of parasite VSA expression during infection in the malaria-naïve host and (3) determine the influence of parasite VSA expression on the developing immune response, and vice versa.

Microarray analysis of the host (whole blood) response to *P. falciparum* revealed a dichotomous pattern of gene expression, with volunteers demonstrating either up-regulation or down-regulation of genes associated with the innate inflammatory response, cell signaling and metabolism. This inter-individual variability correlated with chemokine levels in the plasma and clinical adverse events, but not with parasite growth in the circulation. RNA-sequencing of parasites, isolated from the blood of these individuals, demonstrated broad-level expression of PfEMP1-encoding *var* genes. However, expression was dominated by variants out-with those that have been associated with severe disease, and was remarkably similar across samples from all volunteers despite the observed diversity in host responses. Although we cannot speculate as to the severity of outcome in the volunteers, these findings challenge some key concepts in the field, for instance: (1) expression of group-A (disease-

associated) PfEMP1 is not driving, nor is required for early disease outcome in malaria-naïve individuals and (2) the host immune response is not directed by parasite gene expression, and vice versa; the type of host immune response elicited has little influence of parasite VSA expression early in infection. Focus should now be placed on understanding the diversity of host immune responses produced during primary *P. falciparum* infection, the clinical outcome(s) associated with these responses and the host genetic/environmental factors that may serve to protect against severe malaria disease.

Abbreviations

°C	Degree Celsius
AE	Adverse Events
AIM2	Absent In Melanoma 2
ALP	Alaline phosphatase
ALT	Alanine aminotransferase
AMA1	Apical Membrane Antigen 1
ANG-2	Angiopoeitin-2
APC	Allophycocyanin
AS01B	Adjuvant System (01B)
ATS	Acid Terminal Segment
BC.1	"Baseline Control" number 1
BCG	Bacillus Calmette–Guérin
BMI	Body Mass Index
bp	base pairs
C -1	Challenge minus one day (day before challenge)
C +2	Challenge plus two days (2 days post infection)
C. albicans	*Candida albicans*
CCL2 (MCP1)	Chemokine Ligand 2
CCVTM	Centre for Clinical Vaccinology and Tropical Medicine
cDNA	Complimentary Deoxyribonucleic Acid
CHMI	Controlled Human Malaria Infection
CIDR	Cysteine Rich Interdomain Region
cir	*P. chabaudi* interspersed repeat
CLRs	C-type lectin receptors
CM	Cerebral Malaria
CMV	Cytomegalovirus
CXCL10 (IP-10)	Chemokine (c-x-c motif) Ligand 10
CXCL9 (MIG)	Chemokine (c-x-c motif) Ligand 9
DBL	Duffy Binding-Like
DC	Domian cassette
DCs	Dendritic cells
DEGs	Differentially Expressed Genes
DEPC	Diethyl Pyrocarbonate
dH20	Distilled water
DNA	Deoxyribonucleic acid
dNTPs	Deoxyribonucleic triphosphates
DoD	Day of Diagnosis
dsDNA	double standed DNA
DTT	Dithiothreitol
E. coli	*Escherichia coli*
EDTA	Ethylenediaminetetraacetic acid

ELISA	Enzyme-Linked Immunosorbent Assay
EPCR	Endothelial Protein C Receptor
eQTLs	Expression Quantitative Trait Loci
EVs	Extracellular Vesicles
FACS	Fluorescence Activated Cell Sorting
FBCs	Full Blood Counts
FBS	Fetal Bovine Serum
FCS	Fetal Calf Serum
FITC	Fluorescein isothiocyanate
FU	Fluorescence Units
g (rcf)	relative centrifugal force
g/dL	Grams Per Decilitre
GPI	Glycosylphosphatidylinositol
HBEC	Human Brain Endothelial Cells
HRP	Horse Radish Peroxidase
HTA	Human Transcriptome Array
i.p	Intrapleural
i.v	intraveneous
ICAM-1	Intracellular Adhesion Molecule-1
IE	Infected Erythrocytes
IFNα	Interferon alpha
IFNαR1/2	Interferon alpha receptor 1/2
IFNβ	Interferon beta
IFNγ	Interferon gamma
IFNγR2	Interferon gamma receptor 2
Ig	Immunoglobulin
IL-	Interleukin
IPA	Ingenuity Pathway Analysis
IRF-9	Interferon Regulatory Factor-9
ISG	Interferon-Stimulated Genes
ISGF3	Interferon-stimulated gene factor 3
ISPCR	Illumina Sequencing PCR (primers)
ISREs	Interferon-Stimulated Regulatory Elements
JAK1	Janus-activated kinase 1
JAK2	Janus-activated kinase 2
kbp	Kilo base-pairs
LAIR-1	Leucocyte-associated immunoglobulin-like receptor 1
LILRB1	Leucocyte immunoglobulin-like receptor B1
LLQ	Lower Limit of Quantification
LNA	Locked Nucleic Acids
LPS	Lipopolysaccharide
LRR	Leucine Rich Repeat
M	Molar

MAPK	Mitogen-Activated Protein Kinase
MDA5	Melanoma Differentiation-Associated protein 5
MgCl2	Magnesium chloride
mL	Millilitre
MM1	Master Mix 1
MM2	Master Mix 2
mRNA	messenger Ribonucleic Acid
MyD88	Myeloid differentiation factor 88
NF-κB	Nuclear Factor kappa-light-chain-enhancer of activated B cells
ng/µl	Nanograms Per Microlitre
NHS	National Health Service
NIHR	National Institute for Health Research
NK cells	Natural killer cells
NLRs	Nucleotide-binding oligomerisation domain-Like Receptors
nm	Nanomolar
NO	Nitric Oxide
nt	nucleotides
NTS	N-terminal Segment
O.D	Optical Density
Oligo-dT	Primer is single-stranded sequence of deoxythymine (dT)
p.i	Post-infection
p/mL	Parasites Per Millilitre
PAMPs	Parasite Associated Molecular Patterns
PBMCs	Peripheral Blood Mononuclear Cells
PBS	Phosphate Buffered Saline
PCA	Principle Component Analysis
PCR	Polymerase Chain Reaction
pcv	Packed cell volume
PE	Phycoerythrin
Pen/strep	Penicillin/Streptomycin
PEs	Parasitised erythrocytes
Pf	*Plasmodium falciparum*
PfEMP1	Plasmodium falciparum Erythrocyte Membrane Protein-1
PfHRPII	Plasmodium falciparum Histidine Rich Protein II
pg/mL	Picograms Per Millilitre
PI1	Parasite Inoculum (sample replicate 1)
PI2	Parasite Inoculum (sample replicate 2)
PMR	Parasite Multiplication Rate
PMT	Photomultiplier Tubes
PRRs	Pattern Recognition Recepors
QIMR	Queensland Institute of Medical Research
qPCR	Quantitative Polymerase Chain Reaction
RBC	Red Blood Cells

rif	repetitive interspersed family
RIG-I	retinoic acid-inducible gene I
RIN	RNA Integrity Number
rlog	Regularised Logarithm
RLRs	Retinoic acid-inducible gene-I-Like Receptors
rma	Robust Multi-array Average
RNA	Ribonucleic acid
RNA-seq	RNA-sequencing
rpm	Rotations Per Minute
RPMI	Roswell Park Memorial Institute
rRNA	Ribosomal Ribonucleic Acid
RT	Reverse Transcription
RUMC	Radbound University Nijmegen Medical Centre
SA-PE	Streptavidin-Phycoerthrin
SEB	Staphylococcal Enterotoxin type B
SMA	Severe Malaria Anemia
SNP	Single Nucleotide Polymorphism
STAT1	Signal transducer and activator of transcription 1
STAT2	Signal transducer and activator of transcription 2
stevor	sub-telomeric variable open reading frame
STING	Stimulator of Interferon Genes
sTREM-1	Soluble Triggering Receptor Expressed on Myeloid cells-1
TGFβ	Transforming Growth Factor beta
TH1	T helper 1 cells
TLRs	Toll-like receptors
TMB	3,3',5,5'-tetramethylbenzidine
TNF	Tumour Necrosis Factor
TNFα	Tumour Necrosis Factor alpha
TREM-1	Triggering Receptor Expressed on Myeloid cells-1
TRIF	TIR domain-containing adaptor inducing IFN-β
TSO	Template Switching Oligomer
TYK2	Tyrosine-protein Kinase 2
VEGF	Vascular endothelial growth factor
VSA	Variant Surface Antigen
WTCRF	Wellcome Trust Clinical Research Facility
µg/mL	Micrograms Per Millilitre
µl	Microlitre
µM	Micomolar

TABLE OF CONTENTS

FIGURES and TABLES

Chapter 1: Introduction

1 Introduction

This chapter includes a general introduction to malaria and the thesis topic. A specific introduction is provided for each results chapter.

1.1 Malaria- a general background

1.1.1 The burden of malaria

Malaria is a global health burden with over 3 billion people at risk of the disease, and estimated annual cases of over 400 million (Hay *et al.* 2004) (WHO malaria report, 2017). Over the course of the previous century, malaria has been successfully eliminated from developed countries with temperate and sub-tropical climates, including North America and Europe. Today, people at greatest risk are those living in tropical countries of Africa, Asia and South America, with sub-Saharan Africa and India accounting for approximately 90% of cases worldwide (figure 1.1). Efforts made by the Roll Back Malaria partnership and other public health coalitions have contributed to an estimated 60% decline in global malaria mortality rates since 2000. Between 2000 and 2015, approximately 6.2 million lives were saved as a result of scaled-up interventions (http://www.rollbackmalaria.org/index.html.). In 2016, the global tally of malaria-associated deaths reached 445,000, similar to that observed in 2015. Furthermore, the number of reported cases increased by 5 million. Therefore, although the incidence of malaria has fallen globally over the past two decades, the rate of decline appears to have now stalled (WHO malaria report, 2017).

In addition to its impact on human disease and mortality, malaria also has significant socio-economic consequences. Poverty is concentrated in the same geographical areas that frame malaria transmission, and the extent of the correlation suggests the two are closely related (Sachs and Malaney 2002). Furthermore, malaria-endemic countries demonstrate lower rates of economic growth compared to non-malarious countries (Sachs and Malaney 2002, Orem *et al.* 2012). Data collected from 62 independent businesses in Greater Accra, Ashanti and Western Regions of Ghana, from 2012 to 2014, revealed an estimated loss of approximately US$6.58 million to malaria, 90% of which were costs directly related to staff absenteeism and treatment/prevention of malaria in staff and their dependents (Nonvignon *et al.* 2016).

Thus, in order to help eradicate poverty in these areas, there is a need for greater private sector investment in malaria control.

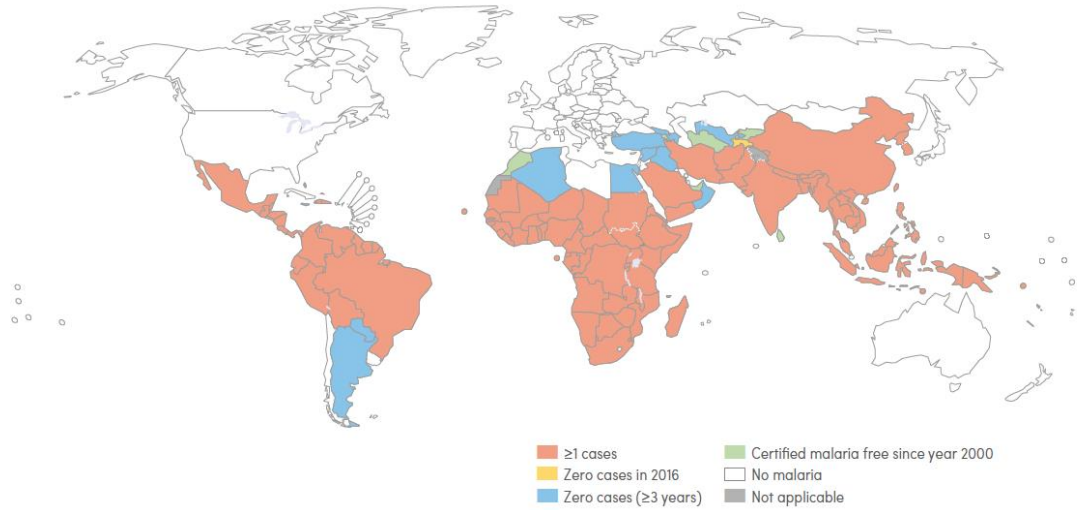

Figure 1.1 | Map of countries and territories with indigenous cases of malaria in 2000 and their status by 2016. Countries with zero indigenous cases over (at least) the past 3 consecutive years are eligible to request certification of malaria-free status from the World Health Organization (WHO). All countries within the WHO European Region reported zero indigenous cases in 2016. In 2016, the greatest number of malaria cases (90%) were reported across sub-Saharan Africa and India. Data source: WHO database. (Figure from the World Malaria Report 2017).

A combination of interventions including timely diagnosis, treatment with effective drugs, and the use of protective measures such as bed nets and insecticides have aided the decline in malaria incidence and vector control (Goodman *et al.* 1999). However, the emergence of drug and insecticide-resistant parasite strains continues to pose a major threat to current preventative/curative therapies. The leading malaria vaccine candidate, RTS,S, provides around 25 - 35% protection in in those at greatest risk of severe disease (Rts 2015). Although this represents a major advance in malaria vaccine development, these levels of protection are far from sufficient. Greater investment therefore needs to be placed in understanding the more basic aspects of the immune response to the parasite, in order to keep reducing (and eventually eliminate) the global malaria burden.

1.1.2 The malaria parasite

Malaria is caused by the apicomplexan parasite *Plasmodium*. The *Plasmodiu*m parasite has co-evolved with the mosquito vector and its host for millions of years, demonstrating an ability to infect many vertebrates including birds, reptiles and

mammals. In humans, malaria can be caused by five *Plasmodium* species; namely *P. falciparum, P. vivax*, *P. ovale*, *P. malariae* and *P. knowlesi*, which have diverse geographical distributions and infection characteristics (Table 1.1). *P. falciparum* is common across the tropics, but is most prevalent in sub-Saharan Africa. It causes the most life-threatening forms of malaria disease and is responsible for the greatest mortality of the five human-infectious species. *P. vivax*, once prevalent in temperate areas of Europe and North America, now occurs most commonly in South America and Asia. Infections with *P. vivax* have been known to cause febrile illness and, in some reported cases, severe disease (Manning *et al.* 2011, Rahimi *et al.* 2014, Barber *et al.* 2015), however this remains controversial. Microscopically confirmed *P. ovale* is rare outside of West Africa, but a major characteristic of this species, along with *P. vivax* is its ability to form hypnozoites (dormant stages of the parasite residing in the liver), which can lead to relapse of infections for up to 1 year after the initial mosquito-bite (White 2011, White and Imwong 2012). *P. malariae* is geographically wide-spread but is associated with infrequent and mild infections, thus having little impact on the public health burden. A major concern with this species however, is its tendency to remain undetected in asymptomatic individuals, therefore serving as reservoirs for ongoing transmission to the mosquito vector. The zoonotic species *P. knowlesi* was first described in 1931, in a long-tail macaque (*Maccaca fascicularis*) and has since been found responsible for over half of all human malaria cases reported in the Malaysian part of Borneo, (Singh *et al.* 2004). Infections with this species are concentrated in Malaysia, where severe disease and death have been reported (Cox-Singh *et al.* 2010, Fatih *et al.* 2012, Willmann *et al.* 2012). Moreover, reports of emerging resistance of *P. knowlesi* to chloroquine and mefloquine are of growing concern (Fatih *et al.* 2013).

Table 1.1 | Characteristics of the five *Plasmodium* species causing malaria in humans

	P. falciparum	*P. vivax*	*P. ovale*	*P. malariae*	*P. knowlesi*
Geographical distribution	Pan-tropical, most common in Africa	Pan-tropical, most common in Asia and South America	Africa, most common in West-Africa	Tropical regions world-wide	South-East Asia, most common in Malaysia
Global Prevalence	High	High	Low	Low	Low (focally high)
Proportion where endemic	80-90%	50-80%	5-8%	0.5-3%	1-60%
Risk of mortality	High	High	Low	Low	High
Risk of drug-resistance	High	High	Low	Low	High
Relapse-formation of hypnozoites	No	Yes	Yes	No	No?
Erythrocyte preference	Normocyte and reticulocytes	Reticulocytes	Normocytes	Reticulocytes	Normocyte and reticulocytes
Duration of one blood-stage cycle	48h	48h	48h	72h	24h
Animal reservoir	No	No	No	No?	yes, monkeys

1.1.3 The life-cycle of *Plasmodium*

Our understanding of malaria transmission can be largely credited to Alphonse Laveran and Ronald Ross, whose contributions to the field of malaria research cannot be overestimated. Ross was awarded the Nobel Prize in 1902, for his discovery of *Plasmodium* parasites in the salivary glands of tropical mosquitoes (Nobel Media AB http://www.nobelprize.org/nobel_prizes/medicine/laureates/1902). Recognition was later given to Laveran (in 1907), for his detection of *Plasmodium* gametocytes in the blood of infected individuals, and linking this to malaria disease (Nobel Media AB http://www.nobelprize.org/nobel_prizes/medicine/laureates/1907).

Malaria is a vector-borne disease that is transmitted to humans by *Plasmodium*-infected female *Anopheles* mosquitoes. As a consequence, the distribution of malaria is restricted to geographical areas where the *Anopheles* mosquito can thrive. High temperatures, rainfall and humidity are ideal breeding conditions for the 25 anthropophilic species that can transmit malaria to humans (Sinka *et al.* 2012). Transmission relies on a complex interplay between the parasite, mosquito and human host (figure 1.2). Following sexual reproduction in the midgut of the female *Anopheles* mosquito, haploid sporozoites accumulate in the salivary glands of the vector and are injected into the skin of the human host during a blood meal. Experimental models have shown that typically few (as little as 1 to 100) motile sporozoites are released during one infectious bite (Beier *et al.* 1991). Sporozoites migrate to the liver and replicate within hepatocytes for the next ~5 - 15 days (depending on the *Plasmodium* species), to form schizonts, containing 10,000 to 30,000 merozoites, which are then released back into the blood stream (Prudencio *et al.* 2006). Some species of malaria (*P. vivax* and *P. ovale*) are able to form hypnozoites, dormant stages of liver-stage parasites which can be re-activated to resume replication at a later time (Shanks and White 2013). Once in the blood stream, each merozoite is able to invade one erythrocyte, initiating the asexual intra-erythrocytic stage of the cycle. Within the erythrocyte, merozoites form rings that mature into pigmented trophozoites, which then undergo schizogony to form schizonts containing up to 32 new daughter merozoites. These merozoites can in turn multiply, leading to exponential growth in non-immune individuals (Simpson *et al.* 2002). Some blood-stage parasites differentiate into the sexual form of the parasite termed gametocytes, which can then be ingested by the

mosquito vector during feeding to re-start the cycle (Silvestrini *et al.* 2000, Buchholz *et al.* 2011, Dantzler *et al.* 2015, Tiburcio *et al.* 2015).

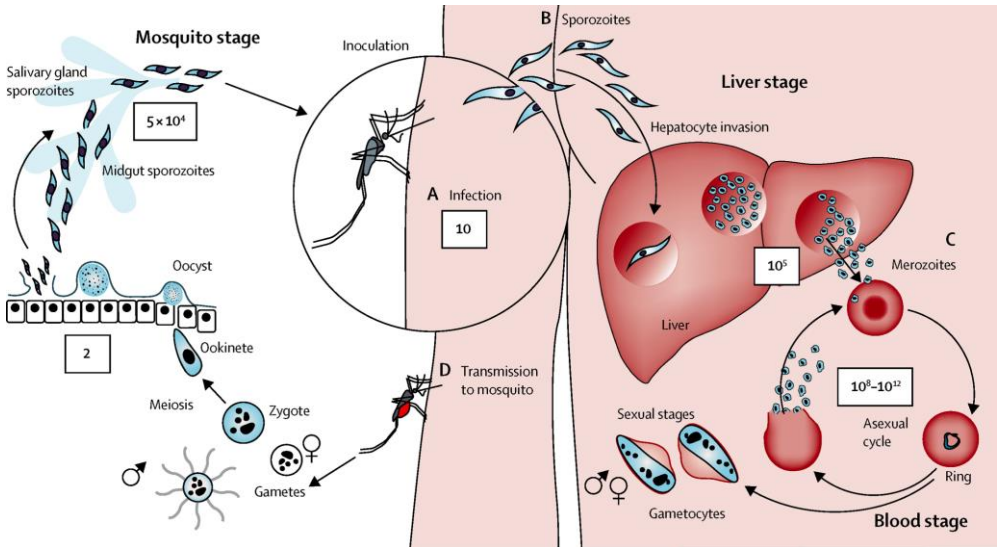

Figure 1.2 | The life-cycle of *Plasmodium*. An illustration of the various developmental stages of *Plasmodium* (from infection to transmission) within the mosquito vector and human host. **A)** A female anopheles mosquito inoculates approximately 10 sporozoites into the dermis, some of which reach the liver and establish an infection of hepatocytes. **B)** Inside hepatocytes the parasite undergoes a period of asexual replication lasting 5 – 15 days (depending on *Plasmodium* species), giving rise to between $1x10^4$ – $3x10^4$ merozoites, per infected liver cell. **C)** After release into the blood-stream, the merozoites invade erythrocytes and mature (from rings, to trophozoites, to schizonts) and replicate asexually. Thus, each blood-stage schizont can give rise to up to ~32 new daughter merozoites. It is this exponential blood-stage replication phase that gives rise to the morbidity and mortality associated with malaria disease. **D)** Some blood-stage parasites develop into male or female gametocytes: the transmissible forms of the parasite. After being ingested by a feeding mosquito, the gametes fuse to form a zygote, which become motile ookinetes with the ability to traverse the midgut wall of the mosquito where they reside as oocysts. Oocysts can give rise to $5x10^4$ haploid sporozoites after replication, which migrate to the salivary glands where they can then be introduced into a new host upon the next feed. Figure was reproduced from White *et al*. 2014.

Infections with malaria parasites remain asymptomatic during the liver-stage replication phase, whereas all morbidity and mortality associated with malaria disease is attributed to the blood-stage of the parasite life cycle.

1.1.4 Manifestations of disease

In human malaria infection, disease can present in differing degrees: mild/uncomplicated, and severe. Most malaria infections are uncomplicated, whereby patients experience non-specific symptoms such as fever, chills and myalgia. These are normally observed about 7 to 14 days post-infection (White *et al.* 2014), and are easily resolved with appropriate treatment. If left untreated however, uncomplicated malaria can rapidly progress to severe disease. The clinical features of severe malaria are characteristically diverse, and are influenced by both age and transmission intensity. In sub-Saharan Africa, where *P. falciparum* predominates, inoculation rates

can be as high as 1,000 (bites) per year. In such settings, morbidity and mortality from malaria are pronounced during early childhood, but by adulthood infections are mostly asymptomatic (Dondorp *et al.* 2008, von Seidlein *et al.* 2012). In areas where transmission is low and erratic (termed unstable), symptomatic disease is observed at all ages, as protective immunity is often not acquired. Severe anemia (haemoglobin concentration <5g/dl) is the main manifestation of malaria disease in young children living in areas of high transmission (Calis *et al.* 2008) (figure 1.3), and is thought to be a combined result of accelerated splenic removal of un-parasitised red blood cells, erythrocyte destruction during parasite schizogeny and ineffective erythropoiesis (Graham 2008). Metabolic acidosis and hypoglycemia are also features commonly linked to fatal outcome in children (English *et al.* 1996, Mackintosh *et al.* 2004, Maitland and Marsh 2004), resulting from the accumulation of organic acids such as lactic acid, in tissues where sequestered parasites obstruct microcirculatory flow (Day 2000, Day *et al.* 2000). In adults, acute respiratory distress (breathing difficulties) is a major complication in those with severe *falciparum* malaria. It often manifests after the start of antimalarial treatment and its pathogenesis is not fully understood, although is likely due to acidosis (Taylor *et al.* 2012, Hanson *et al.* 2013). Renal failure, as a result of acute kidney injury, is also common in adult patients, and is frequently accompanied by the dysfunction of other vital organs- leading to high mortality (Nguansangiam *et al.* 2007). Severe jaundice, resulting from hepatocyte injury, haemolyisis and cholestasis is also more common in adults than in children (figure 1.3). The most striking manifestation of severe disease however is cerebral malaria (CM), characterised by seizures, coma and death (Grau and Craig 2012, Ponsford *et al.* 2012). In fatal cases of CM, capillaries and venules in the brain become clogged with parasitised erythrocytes, leading to extensive microvascular obstruction and impaired perfusion, which is thought to be the crucial pathophysiological process involved (Beare *et al.* 2009, Maude *et al.* 2009). CM has been shown to occur in all age groups, but may have slightly different pathogenic features between children and adults; cerebral oedema is frequently reported in children, but less so in the majority of adult cases (Idro *et al.* 2005, Medana *et al.* 2011, Potchen *et al.* 2012, Seydel *et al.* 2015, Mohanty *et al.* 2017). CM has a 15 - 25% case-fatality rate, even with appropriate medical intervention (Marsh *et al.* 1995, Murphy and Breman 2001). Many of the syndromes cause rapid deterioration, and 50-80% of malaria deaths in hospital occur within 24

hours of admission, (Marsh *et al.* 1995, Schellenberg *et al.* 1999, Ranque *et al.* 2008), highlighting the importance of prompt triage and treatment.

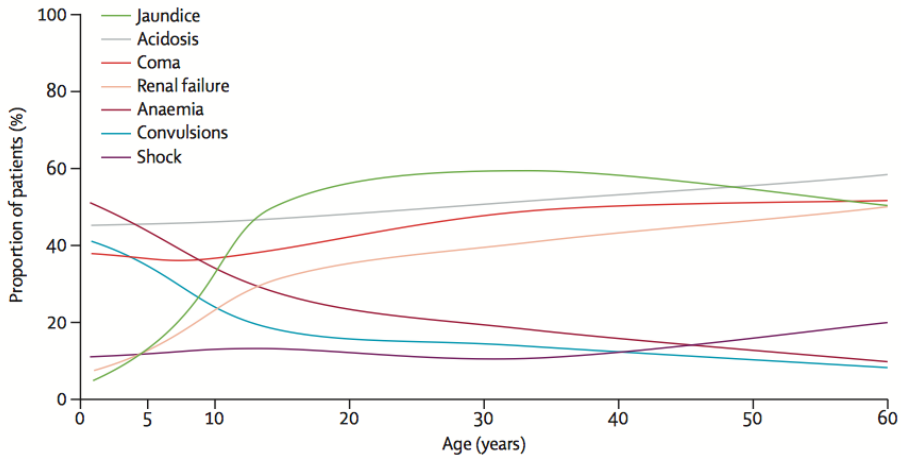

Figure 1.3 | Manifestations of severe *P. falciparum* malaria by age. Graph shows the proportion of patients (%) (y-axis) with observed symptoms of each of the listed clinical manifestations of severe *P. falciparum*, as a relation to patient age (x-axis). Figure reproduced from White *et al,* 2014.

1.2 Naturally Acquired Immunity to Malaria

In areas where malaria is endemic, severe disease is associated almost exclusively with the very young, whereas older children and adults develop naturally acquired immunity with continued exposure to the *Plasmodium* parasite (Gupta *et al.* 1999, Barry and Hansen 2016) (figure 1.4). Naturally acquired immunity is compromised however, in pregnant women, especially in primigravidae, and in adults who return to malaria-endemic regions after a period of absence (Doolan *et al.* 2009). Thus, interventions that reduce exposure below a level capable of maintaining immunity may compromise protection against severe malaria in the majority, and risk increased incidence of severe infections (Snow *et al.* 1997, Romi *et al.* 2002), although this remains controversial.

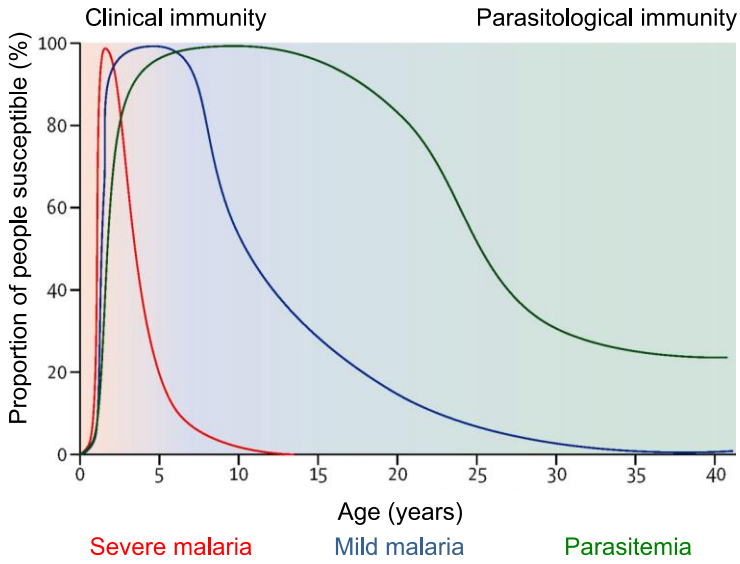

Figure 1.4. | Naturally acquired immunity as a relation between age and malaria severity. All infants are initially susceptible to severe malaria (red line), but clinical immunity is acquired with repeated exposure, which makes symptoms of malaria milder (blue line), while parasites are still present in the blood-stream of almost every child. Parasitological immunity is slow to develop and many people harbour microscopically-detectable blood-stage parasites well into adulthood (green line). The here shown timings for the development of clinical and parasitological immunity are typical for areas of moderate transmission. Figure reproduced from Marsh *et al.* 2006 and Langhorne *et al*. 2008.

Despite decades of research, the underlying mechanisms of naturally acquired immunity to malaria are not fully understood. The protection associated with the very gradual acquisition of anti-parasite immunity (figure 1.4) appears largely dependent on antibodies capable of recognising blood-stage antigens (Garraud *et al.* 2003, Duah *et al.* 2010). Transfer of immunoglobulin (Ig) from clinically immune adults to children with high-density infections is able to reduce parasite numbers, and attenuate clinical symptoms (Cohen *et al.* 1961). Moreover, immune IgG inhibits *P. falciparum* growth *in vitro* (Mitchell *et al.* 1976). It is therefore likely that protection against high density infection requires the induction of antibodies capable of recognising multiple antigens, and in malaria endemic areas, the breadth and magnitude of the malaria-specific antibody response correlates with increasing age and exposure (Dorfman *et al.* 2005, Weiss *et al.* 2010). Conversely, immunity to (severe) clinical disease develops much more quickly (figure 1.4). In areas of high transmission, it is estimated that 10 – 20% of all children will suffer an episode of severe malaria before the onset of partial immunity but once suffered, will likely be protected from subsequent severe infections (Gupta *et al.* 1999, Goncalves *et al.* 2014). In an important study by Goncalves *et al*, the incidence of *P. falciparum* infection and associated disease was documented in a large cohort of (882) Tanzanian children, by monitoring the children from birth, for up to 4 years of age. Of these 882 children, 102 (~11%) experienced an episode(s) of severe

malaria which, in the majority of cases, was restricted to the first, second or third infection. As is consistent with the schematic shown in figure 1.4, the incidence of severe malaria decreased considerable after infancy, whereas the incidence of high-density parasitaemia was similar among all age groups of children (Goncalves *et al.* 2014). These data suggest that the rapid development of immunity to severe (life-threatening) disease is not associated with better control of parasite growth, and occurs early in life at a time where limited exposure to the parasite has not yet afforded an accumulation of protective antibodies. It is therefore speculated that innate immune responses play a crucial role in shaping outcome of infection in the malaria-naive (Langhorne *et al.* 2008, Liehl and Mota 2012, Wu *et al.* 2014), however it is not yet clear why some children are more susceptible to severe malaria than others.

1.3 The innate immune response to malaria

Innate responses are the major forces combating infection in non-immune individuals, and thus are predicted to influence clinical outcome during primary infection with *P. falciparum*. Over recent years, various strategies have been employed to investigate innate host responses to malaria infection. Cross-sectional and longitudinal studies of malaria-endemic populations have afforded the analysis of genetic and/or immunological features associated with disease severity. Studies of controlled human malaria infection in non-immune volunteers have been useful for examining the early stages of infection, although the ethical necessity to treat (most often) before the onset of clinical symptoms precludes the correlation of variables with disease outcome. Autopsy studies of fatal malaria have yielded some important insights, but studies are small and likely confounded by artifacts of death and/or co-morbidities.

In vitro model systems have been widely utilised to study the response of primary host cells, such as peripheral blood mononuclear cells (PBMCs) and endothelial cells, or cell lines upon exposure to *Plasmodium*. These experiments are easily manipulated and permit controlled exposure of host cells to parasite, but are reductionist in nature. Murine models have also been used to investigate the host response to malaria, as a variety of *Plasmodium* strains naturally infect rodents. These models have to be considered carefully however, as the combination of parasite strain and genetic background of the host greatly influences the course and outcome of infection. While

no single model fully recapitulates *P. falciparum* malaria, various aspects of human malaria infection can be probed using the appropriate model.

Research suggests that host innate responses to malaria can mediate both protection and pathology, evidence for which will be discussed in the following sections.

1.3.1 Phagocytic clearance of parasitised erythrocytes

Phagocytosis of parasitised erythrocytes (PEs) and merozoites by myeloid cells is thought to be a primary mechanism for controlling parasite growth in non-immune individuals. This is underlined by evidence from *in vitro* studies confirming the ability of monocytes, macrophages and neutrophils to phagocytose PEs, independently of malaria-specific antibodies (Trubowitz and Masek 1968, Su *et al.* 2002). The non-opsonic uptake of mature-stage PEs by macrophages is largely mediated by scavenger receptor CD36 (McGilvray *et al.* 2000, Serghides *et al.* 2003, Patel *et al.* 2004), likely through the engagement of parasite proteins such as *P. falciparum* erythrocyte membrane protein-1 (PfEMP1), exposed on the surface of the red blood cell (RBC) (Baruch *et al.* 1996). There is also evidence to suggest that ring-stage PEs can be opsonised by complement proteins and natural IgG, and thus targeted for destruction via complement and Fc receptor-dependent pathways (Turrini *et al.* 1992, Ayi *et al.* 2004). In support of this, a loss of function mutation in the Fc gamma receptor IIb, which normally inhibits IgG-mediated phagocytosis, has been shown to enhance the opsonic PE internalisation by macrophages *in vitro* and reduced parasitaemia in the *Plasmodium chabaudi* mouse model (Clatworthy *et al.* 2007). Although, this association has not been upheld in a more recent, and much larger, genetic study on human malaria infection (Rockett *et al.* 2014). During infection in the RBC, parasites break down haemoglobin, producing haemozoin as a by-product. Haemozoin is insoluble in the phagolysosome, and thus persists in the cell following phagocytosis of PEs. In malaria infected humans and mice, haemozoin-laden myeloid cells are found abundant in the blood and particularly the spleen- the primary site of PE clearance (Coban *et al.* 2010). *In vitro* studies of dendritic cell (DC) activation, in response to *Plasmodium,* have demonstrated the efficient phagocytosis and phagosomal maturation of infected erythrocytes (Bettiol *et al.* 2010). Yet, results also suggest for a dose-dependent inhibition of DC maturation (Elliott *et al.* 2007) that occurs at high concentrations of infected erythrocytes. This is characterised by a failure of DCs to up-

regulate the co-stimulatory molecules required for full effector function (Urban *et al.* 1999). In line with this, DCs extracted from malaria-infected humans show an impaired capacity to mature, produce pro-inflammatory cytokines and present antigens to T cells (Woodberry *et al.* 2012, Loughland *et al.* 2016, Gotz *et al.* 2017, Loughland *et al.* 2017). Thus, it appears that malaria does not induce classical activation of DCs. However, it is important to note that human studies are limited to assessment of circulating cells, and it is possible that fully functioning DCs are migrating into tissues where they exert their effects as mediators of innate host defense.

Based on these data, myeloid cells, particularly monocytes (given their location in the blood and capacity to phagocytose) are speculated to play a crucial role in the innate response to malaria. In a study of controlled human malaria infection with *P. vivax,* volunteers were found to have elevated levels of the ($CD16^{+}CD14^{+}$) monocyte subset at diagnosis, compared to baseline. Moreover, these cells displayed enhanced phagocytic activity in response to infection (Antonelli *et al.* 2014). Parasite clearance by monocytes/macrophages has also been explored using the *P. chabaudi* mouse model, where resolution of infection has been shown to be dependent on recruitment of a $CD11b^{hi}Ly6C^{+}$ monocyte population from the bone marrow to the spleen. These cells demonstrated extensive phagocytic activity towards PEs *in vitro* and *in vivo* (Sponaas *et al.* 2009). Macrophages have also been shown to control parasitaemia during non-lethal *P. yoelii* infection (Couper *et al.* 2007).

The phagocytosis of parasitised erythrocytes therefore appears to correlate with better control of malaria infection in humans and mice. However phagocytosis is tightly linked to inflammation, which also plays an important role in the innate response.

1.3.2 The systemic inflammatory response to malaria infection

In studies of semi-immune populations and experimental vaccine trials, robust T-helper cell-1 (TH1) responses, in particular IFNγ production, has been associated with protection. While memory T cells are the major source of IFNγ (Schoenborn and Wilson 2007), it can also be produced by innate immune cells, and has been shown to exert effector functions relevant for non-immune individuals, such as enhanced phagocytosis of PEs (Su *et al.* 2002, Horowitz *et al.* 2010). In line with this, exposure of malaria-naïve PBMCs to *P. falciparum* induces production of IFNγ in NK cells, gamma

delta (γδ) T cells and (cross-reactive) alpha beta (αβ) T cells in an IL-12 dependent manner (Hensmann and Kwiatkowski 2001, Horowitz *et al.* 2010). In controlled human malaria infection, early IFNγ responses correlate with lower parasite densities, suggesting better control of parasite growth. However, there is considerable inter-individual variation in this response (Walther *et al.* 2006). In African children, severe malaria syndromes have been associated with promoter variants that reduce transcription of IFNγ and/or IL-12p40 (Cabantous *et al.* 2005, Marquet *et al.* 2008). Yet, this finding has been contested by a more recent genetic screening in a large cohort of individuals, where almost all protective mutations were found to be associated exclusively with red cell genes (Rockett *et al.* 2014). In *P. chabaudi*-resistant mice, deficiency in the IL-12p40 subunit reduces IFNγ induction and increases mortality (Su and Stevenson 2002), suggesting a key role of this cytokine in host defense. However, evidence is controversial across the different models of infection, and its protective capacity may be context and species dependent. More recently, studies in both mice and humans have identified production of Type I IFNs (IFNα/β) among the earliest of host cytokine responses during *Plasmodium* infection, however the extent to which they mediate protection remains to be defined (Rocha *et al.* 2015, Montes de Oca *et al.* 2016, Yu *et al.* 2016, Zander *et al.* 2016).

Tumour Necrosis Factor (TNF), produced early in infection by monocytes/macrophages, is another cytokine thought to be critical for the control of parasite replication. In a prospective study of children in Papua New Guinea, *ex vivo* stimulation of PBMCs with *P. falciparum* revealed patterns of TNF production that correlated with protection (Robinson *et al.* 2009). The protective functions of TNF are thought to be induced through the generation of nitric oxide (NO) (Rockett *et al.* 1992). Moreover, TNF has been shown to enhance killing of parasitised erythrocytes *in vitro*, and administration of exogenous TNF reduces parasitaemia in both *P. chabaudi* and *P. yoelii*- infected mice (Clark *et al.* 1987, Taverne *et al.* 1987). Importantly, high levels of TNF correlated with a rapid parasitological cure in patients, supporting a protective role of this cytokine in the clearance of *P. falciparum* parasites (Kremsner *et al.* 1995). However, elevated levels of TNF have also been associated with severe malaria disease (Kwiatkowski *et al.* 1990, Awandare *et al.* 2006, Boeuf *et al.* 2012).

It is likely that anti-inflammatory responses, such as interleukin-10 (IL-10) and transforming growth factor-β (TGFβ) production, play an important role in the resolution

of infection by preventing malaria-associated immunopathology (Linke *et al.* 1996, Omer and Riley 1998). However, the timing of these responses appears to be a critical. Data from models of lethal *P. yoelii* and *P. chabaudi* infections suggests an association between early production of transforming growth factor-β (TGFβ), low IFNγ and uncontrolled parasitaemia. In these infection settings, inhibition of TGFβ enhanced pro-inflammatory responses, reduced parasitaemia and improved survival (Tsutsui and Kamiyama 1999, Omer *et al.* 2003). Furthermore, in studies of controlled human malaria infection, early production TGFβ coinciding with parasites entering the circulation, correlated with reduced plasma levels of pro-inflammatory cytokines and increased rates of parasite replication, although this response was not observed in all volunteers (Walther *et al.* 2005). Additionally, blood-stage *P. falciparum* infection was found to promote the development of parasite-specific IL-10 producing TH1 cells in malaria-naïve volunteers. This parasite-induced IL-10 suppressed inflammatory cytokine responses and was associated with higher parasite burdens (Montes de Oca *et al.* 2016).

Thus, data from both human and mouse models suggest an important role of the systemic inflammatory response in host protection from malaria. However, contradictory evidence from the field underscores the complexity involved in mechanisms of host defense against *Plasmodium*. For instance, whereas tumor necrosis factor alpha (TNFα), Interferon gamma (IFNγ), Interleukin (IL)- 1β, IL-2, IL-6, IL-8, IL-10 and IL-12 have been reported in children and adults with symptomatic *P. falciparum* malaria, compared to asymptomatic and healthy controls (Day *et al.* 1999, Lyke *et al.* 2004, Walther *et al.* 2006, Mirghani *et al.* 2011), higher levels of the same pro-inflammatory cytokines have been observed in non-severe *P. vivax* infections (Zeyrek *et al.* 2006, Jain *et al.* 2010, Goncalves *et al.* 2012, Scherer *et al.* 2016).

Strategies used to contain pathogens are harsh by nature, and if responses are excessive or dysregulated, they can often become detrimental to the host. The pathology associated with severe malaria anemia (SMA) is a prime example of this. Low plasma IL-10 or high TNF/IL-10 ratios have been consistently observed in children with SMA compared to mild malaria (Kurtzhals *et al.* 1998, Othoro *et al.* 1999, May *et al.* 2000, Perkins *et al.* 2000, Awandare *et al.* 2006, Thuma *et al.* 2011). The ability of IL-10 to suppress pro-inflammatory cytokine production by PBMCs in response to

P. falciparum (Ho et al. 1998) has given rise to the hypothesis that unrestrained inflammatory responses contribute to the pathology of SMA. Impaired erythropoiesis is one of the hallmark characteristics associated with SMA, as is the destruction of unparasitised RBCs (Graham 2008). TNF has been shown to suppress erythropoiesis *in vitro* (Broxmeyer *et al.* 1986) and in chronically exposed mice (Johnson *et al.* 1989). Furthermore, pro-inflammatory cytokines are predicted to enhance phagocytosis of RBCs via activation of macrophages (Burchard *et al.* 1995, Salmon *et al.* 1997), although evidence is indirect in murine models of infection.

An ability to keep inflammatory responses in check may therefore protect children against severe malaria, at time when they are yet to develop protective antibodies (Portugal *et al.* 2013). However, there is an increasing need to identify the key parasite-host interactions that induce inflammation so that interventions can be better targeted to downstream events.

1.3.3 Innate sensing of malaria parasites

In contrast to viral and bacterial infections, for which many pattern recognition receptors and signaling pathways are well defined, our understanding of the parasite-associated molecular patterns (PAMPs) and reciprocal host receptors involved in the response to *Plasmodium*, is still limited. In the context of human malaria infection, *P. falciparum* presents itself in many different forms. Thus, it is of considerable interest to define the *Plasmodium* parasite molecules being recognised by the host. Evidence from a large body of studies in both mouse models and human infection has highlighted a role of key parasite recognition receptors (PRRs), including toll-like receptors (TLRs), retinoic acid-inducible gene-I-like receptors (RLRs), cytosolic DNA sensors and nucleotide-binding oligomerisation domain-like receptors (NLRs) in host defense against *Plasmodium* parasites (Gazzinelli and Denkers 2006, Liehl and Mota 2012, Gazzinelli *et al.* 2014, Oviedo-Boyso *et al.* 2014, Wu *et al.* 2014). However, the significance of each has been much debated.

1.3.3.1 Toll-like receptors (TLR)

TLRs are widely expressed in a cell-type specific manner, and each recognises a distinct set of ligands. TLR 1, 2, 4, 5 and 6 are detected on the cell surface, and in

intracellular compartments. TLR4 senses lipopolysaccharide (LPS), and other microbial products, as well as “danger signals” released from dead or dying cells. TLR2 forms heterodimers with TLR1 or TLR6 to recognise ligands such as lipoproteins and yeast cell wall, whereas TLR5 detects flagellin. TLR3, 7, 8 and 9 sense nucleic acids; TLR9 recognises CpG DNA, while TLR3, TLR7 and TLR8 detect RNA (Akira *et al.* 2006, Kawai and Akira 2006, Kawai and Akira 2010). Ligand binding interactions induce TLR dimerisation and recruitment of adaptor proteins (such as Myeloid differentiation factor 88 (MyD88) and TIR domain-containing adaptor inducing IFN-β (TRIF)), to initiate signaling cascades. Signalling via MyD88 leads to activation of MAPKs and NF-κB, transcription of pro-inflammatory cytokines and chemokines, and generation of anti-microbial effectors such as Nitric Oxide (NO) (Yamamoto *et al.* 2004, Akira *et al.* 2006, Coban *et al.* 2007, Litvak *et al.* 2009). The TRIF-dependent pathway is unique to TLR3 and TLR4, and results in activation of IRF3 and transcription of Type I Interferons (IFNs)- important for the control of viral infection (Akira *et al.* 2006).

TLRs have been shown to be important for innate and adaptive immune responses in a variety of infectious disease models, as has been previously reviewed (Trinchieri and Sher 2007, Palm and Medzhitov 2009). In the *Plasmodium berghei* ANKA model, mice deficient of MyD88 demonstrate impaired production of pro-inflammatory cytokines, and mutations in TLR9, TLR2 and TLR2/4 were shown to provide protection against cerebral malaria (Coban *et al.* 2007, Griffith *et al.* 2007). In human studies, *Plasmodium*-mediated enhancement of TLR responsiveness in immune cells has been described. In a study comparing PBMC expression profiles isolated from volunteers experimentally infected (pre-symptomatic), with those from individuals naturally infected in the field (symptomatic), common to both was an up-regulation of toll-like receptor signaling through NF-κB pathways (TLR1, TLR2, TLR4 and TLR8), as well as expression of genes such as TNFα, IFNγ and IL-1β (Ockenhouse *et al.* 2006). A similar observation was documented in PBMCs which had been isolated from individuals, in a subsequent study of controlled human malaria infection (CHMI) (McCall *et al.* 2007). Moreover, acute infection in Ghanaian school children and a Brazilian cohort has been shown to present with augmented reactivity to TLR stimulation (Hartgers *et al.* 2008, Franklin *et al.* 2009). Thus, evidence suggests that TLRs play an important role during initiation of the host inflammatory response to *Plasmodium* infection, but the extent of their involvement remains to be defined.

1.3.3.2 Nod-like receptors (NLR)

NLRs are cytosolic PRRs, implicated in inflammatory responses to pathogens and environmental hazards. Their protein structure consists of a C-terminal Leucine Rich Repeat (LRR) domain involved in ligand sensing; a central nucleotide-binding domain, which mediates oligomerization; and a variable N-terminal domain. NLR proteins Nod1 and Nod2 recognise components of bacterial peptidoglycan, and activate NF-κB for downstream transcription of pro-inflammatory cytokines (Girardin *et al.* 2003, Girardin *et al.* 2003). Nod proteins have also been shown to induce activation of Type I IFNs in response to bacteria and viruses (Herskovits *et al.* 2007, Sabbah *et al.* 2009). Other NLRs, such as NLRP3, self-assemble to form inflammasome complexes when activated. This leads to the auto-activation of Caspase-1, driving the maturation and secretion of IL-1β and IL-18 (Lee *et al.* 2009, Latz 2010).

Like TLRs, NLRs have been shown to contribute to both innate and adaptive immune responses, and to a variety of pathogens. Moreover, dysregulated NLR signaling has been implicated in the pathogenesis of diseases such as atherosclerosis, inflammatory bowel disease, asthma and gout (Davis *et al.* 2011, Magalhaes *et al.* 2011). Interestingly, activation of the NLRP3 inflammasome, and resulting IL-1β production, has recently been associated with malaria infection in both mouse and human models of the disease (Ataide *et al.* 2014, Kalantari *et al.* 2014). In the second study, NLRP3 inflammasome activation was found to be dependent on the initial activation of TLR9, highlighting the cooperative and synergistic nature of PRRs during the innate host response (Kalantari *et al.* 2014).

1.3.3.3 Other pattern recognition receptors (PRRs)

Among other PRRs implicated in the induction of inflammation are the C-type lectin receptors (CLRs), which detect pathogen carbohydrate components, and the Rig-like receptors (RLRs), which recognise double-stranded RNA in the cytoplasm (Takeuchi and Akira 2010, Goubau *et al.* 2013, McNab *et al.* 2015). When activated, RLRs induce Type-I IFN responses, and so far have been linked to host defense against RNA viruses; DNA viruses; intracellular bacteria (due to reverse transcription of microbial DNA) (Chiu *et al.* 2009) and extracellular bacteria (by an unknown mechanism)(Kong *et al.* 2009). Given that Type-I IFN induction is observed during malaria infection in both mouse and human models (Rocha *et al.* 2015, Montes de Oca *et al.* 2016,

Spaulding *et al.* 2016, Yu *et al.* 2016, Zander *et al.* 2016), RLRs are also predicted to be involved in the host response to *Plasmodium*, although precise mechanisms of interactions are yet to be defined. Other PRRs are responsible for the detection of cytoplasmic DNA, such as the AIM2 inflammasome, as has been implicated during *Plasmodium* infection (Kalantari *et al.* 2014) and DAI receptor (Takaoka *et al.* 2007, Hornung *et al.* 2009, Hornung and Latz 2010, Sharma *et al.* 2011, Roers *et al.* 2016, Sisquella *et al.* 2017). Thus, every pathogen type is sensed by multiple host receptors during infection.

1.3.3.4 Parasite-associated molecular patterns (PAMPs)

Extensive attempts have been made to define the "malaria toxin" that induces inflammatory responses. Previous efforts were complicated by a lack of understanding of innate immunity, but with recent advances in PRR discovery, interest in this field has been revived.

Of the PAMPs that have been implicated in driving the host inflammatory response, glycosylphosphatidylinositol (GPI) has been studied most comprehensively. Protozoa make extensive use of GPIs to anchor membrane proteins (Gowda *et al.* 1997), and are thus thought to be essential for parasite viability (Naik *et al.* 2000). Both free and membrane-associated *Pf*GPIs are thought to be released upon schizont rupture, triggering the production of pro-inflammatory cytokines, such as TNF (Schofield and Hackett 1993, Tachado *et al.* 1996, Naik *et al.* 2000). This process is thought to be dependent on TLR2 (Zhu *et al.* 2005, Durai *et al.* 2013). However, GPI has also been shown to act as a ligand for TLR4, albeit to a lesser extent (Krishnegowda *et al.* 2005). In support of these findings, SNPs related to TLR2 and TLR4 pathways have been associated with human malaria disease, suggesting that recognition of *Pf*GPI is a crucial step in preventing pathology (Mockenhaupt *et al.* 2006, Mockenhaupt *et al.* 2006, Ferwerda *et al.* 2007, Leoratti *et al.* 2008, Hamann *et al.* 2010). However, the effects of these TLR variants are not fully understood, and it is important to consider the complex role of inflammation in severe malaria disease. Interestingly, human studies have shown a correlation between levels of anti-GPI antibodies with increasing age in malaria-endemic regions (Naik *et al.* 2000, Boutlis *et al.* 2002, de Souza *et al.* 2002), suggesting that GPI neutralisation may contribute to protection from severe

malaria. This is consistent with data from mouse models of *P. berghei* infection, whereby immunisation with the *Pf*GPI glycan core prevented cerebral, pulmonary and systemic manifestations compared to un-immunised controls (Schofield *et al.* 2002). Overall, these data implicate *Pf*GPI, through interactions with TLR2 and TLR4, as an important PAMP during initiation of the inflammatory response to the malaria parasite.

Haemoglobin degradation is an obligate process for the survival of *P. falciparum* parasites. This process takes place during the asexual cycle in the blood, and results in the production of malarial haemozoin. Upon lysis of infected RBCs, the release of haemozoin into the blood, along with other parasite components, coincides with induction of pro-inflammatory cytokines (Liehl and Mota 2012). Thus, it has been implicated in the induction of malaria-associated fever. Haemozoin-loaded macrophages can induce expression of pro-inflammatory cytokine genes (Shio *et al.* 2009), and dendritic cells (DCs) have also been found responsive to stimulation (Parroche *et al.* 2007). Studies have shown that haemozoin purified from *P. falciparum* is a ligand for TLR9 (Coban *et al.* 2005, Coban *et al.* 2010). However, this finding has been contested by others showing that only natural haemozoin contaminated with *Plasmodium* DNA is able to trigger activation of the immune response (Parroche *et al.* 2007). Others provide evidence for the interaction being TLR-independent (Togbe *et al.* 2007). In line with this, nucleotide-binding oligomerization domain-like receptors (NLRs) have also been implicated in haemozoin-induced inflammation. Activation of the NLRP3 inflammasome drives production of pyrogenic IL-1β, and has been associated with disease severity in various mouse models of malaria infection (Dostert *et al.* 2009, Shio *et al.* 2009, Kalantari *et al.* 2014). Thus, irrespective of the mechanism, there is robust evidence implicating haemozoin, either alone, or in complex with other parasite molecules, as a potent activator of the innate immune response during *Plasmodium* infection.

There is also evidence for a role of *Plasmodium* nucleic acids (DNA and RNA) in the initiation of inflammation during infection. When delivered into the cytosol of various cell types, *Plasmodium*-derived AT-rich genomic DNA triggers the induction of Type I IFN responses via a pathway involving Interferon regulator factor 3-7 (IRF3/IRF7), TANK-binding kinase 1 (TBK1), stimulator of interferon genes (STING) and cGAS (Sharma *et al.* 2011, Wu *et al.* 2013). In line with this, *Plasmodium* RNA has also been

linked to induction of Type I IFN responses following recognition by retinoic acid-inducible gene-I-like receptors, RIG-I and/or melanoma-differentiation-associated protein 5 (MDA5), as has been reviewed (Goubau *et al.* 2013, McNab *et al.* 2015). The mechanisms of such interactions are still unclear, but have been discussed in recent literature (Kalantari *et al.* 2014, Sisquella *et al.* 2017).

1.3.3.5 Linking the innate immune response to protection and/or pathology

Despite recent advances in our understanding of the innate immune response to *Plasmodium*, many questions still remain regarding the initiation and propagation of responses that lead to severe malaria disease in human infection. What is the relative importance of the different parasite stimuli and host sensors, and how do they interact? What are the key cell types and signaling pathways involved? Do these pathways contribute to protection and/or development of severe disease?

In order to fully understand the key parasite-host interactions responsible for onset of disease, it is important to consider the parasite and host factors predicted to influence clinical outcome.

1.4 Factors influencing disease outcome

A range of host polymorphisms have been associated with protection from severe malaria (de Mendonca *et al.* 2012). The best characterised of these include: blood group O (Rowe *et al.* 2007), sickle cell (HbS) (Aidoo *et al.* 2002), α+ thalassemia (Wambua *et al.* 2006, Opi *et al.* 2014) and glucose-6-phosphate dehydrogenase deficiency (Ruwende *et al.* 1995, Rockett *et al.* 2014). These polymorphisms are common in Africa, and thus may protect the majority of children, whereas those lacking these polymorphisms could be at greater risk of severe disease. Certain environmental factors have also been shown to influence differences in disease susceptibility. The use of bed nets, the level of fitness, co-infections, past infection history and nutritional status are factors contributing to variability in clinical outcome (Bartoloni and Zammarchi 2012, Goncalves *et al.* 2014).

Parasite specific factors such as parasite multiplication rates (PMR) and choice of invasion pathway have also been linked to disease outcome, although evidence is controversial. Whereas higher PMRs have been associated with severe disease in adults (Chotivanich *et al.* 2000), no such correlation was observed in African children with severe versus uncomplicated malaria (Deans *et al.* 2006). Furthermore, differences in clinical outcome have been documented when comparing infections involving sialic acid-dependent and sialic acid-independent invasion pathways (Bowyer *et al.* 2015, Mensah-Brown *et al.* 2015), although these data are contradictory to earlier studies of clinical isolates (Deans *et al.* 2007, Gomez-Escobar *et al.* 2010).

There is substantial evidence that the parasite-encoded variant surface antigens (VSAs), on the surface of PEs, are the decisive determinants of clinical outcome during *P. falciparum* malaria (Hviid 2010). There are several VSAs expressed by *P. falciparum*, the best characterised of which is *P. falciparum* Erythrocyte Membrane Protein 1 (PfEMP1), encoded by *var* genes. Expression of PfEMP1 gives rise to the ability of infected erythrocytes to agglutinate, rosette and adhere to endothelial cells, enabling them to sequester out of the circulation and avoid clearance by the spleen (Pain *et al.* 2001, Doumbo *et al.* 2009, Rowe *et al.* 2009). Switching between PfEMP1 variants correlates with changes in the antigenic and adhesion phenotype of the parasite, and the expression of specific PfEMP1 types has been associated with severe malaria (Bull *et al.* 2000, Jensen *et al.* 2004, Bull *et al.* 2005, Kyriacou *et al.* 2006, Lavstsen *et al.* 2012). An overview of *var* genes, PfEMP1, and their associated virulence is discussed in the following section.

1.5 *Var* Genes, PfEMP1 and Parasite Virulence

1.5.1 PfEMP1 variant surface antigens

Each parasite genome has approximately 60 *var* genes encoding 60 variants of PfEMP1 (Smith *et al.* 1995). *Var* genes are activated in a mutually exclusive fashion whereby just one is expressed at any given time, while all others are transcriptionally silenced (Dzikowski *et al.* 2006). During infection, *P. falciparum* parasites are able to switch expression between different *var* genes as a means to evade the developing host immune response. This, in turn, gives rise to variable expression of PfEMP1

types. The global *var* gene repertoire present in the parasite population is highly diverse. However, recent evidence suggests that every parasite *var* gene repertoire is organised similarly (Kraemer and Smith 2003, Lavstsen *et al.* 2003, Kraemer *et al.* 2007). The majority of *var* genes (and hence PfEMP1) can be classified into groups (A, B, C or E) on the basis of various structural features: upstream sequence, chromosome location and direction of transcription. Both group-A and B *var* genes are located in the sub-telomeric regions near the chromosome ends, but have an opposing direction of transcription; group-A towards the telomeres and group-B towards the centromere. Group-C *var* genes are located at chromosome internal clusters (Gardner *et al.* 2002). *Var* genes are made up of two exons; the hypervariable exon 1, encoding for the extracellular region involved in adhesion interactions and the transmembrane, conserved exon 2, which encodes the acid terminal segment (ATS). The extracellular region of the PfEMP1 is made up of the N-terminal segment (NTS), Duffy binding-like domains (DBL) and cysteine rich interdomain regions (CIDR) (figure 1.5). The DBL domains can be classified into six types (α, β, γ, δ, ε and ζ) and the CIDR into four groups (α, β, δ and γ). Furthermore, 23 functionally conserved tandem domains of DBL-CIDR, termed 'domain cassettes' (DC) have also been described (Rask *et al.* 2010). Each molecule of PfEMP1 contains a number of functional cytoadhesive domains, and depending on domain composition, demonstrate diverse cytoadhesive functions (Kraemer and Smith 2006, Hviid and Jensen 2015, Bull and Abdi 2016). The DBLβ domains of group-A and B PfEMP1, for instance, have been implicated in the binding of the host receptor ICAM-1 (Bengtsson *et al.* 2013, Gullingsrud *et al.* 2013), whereas the CIDRα2-6 domains of group-B and C PfEMP1 have been shown to interact with CD36 (Miller *et al.* 2002, Robinson *et al.* 2003).

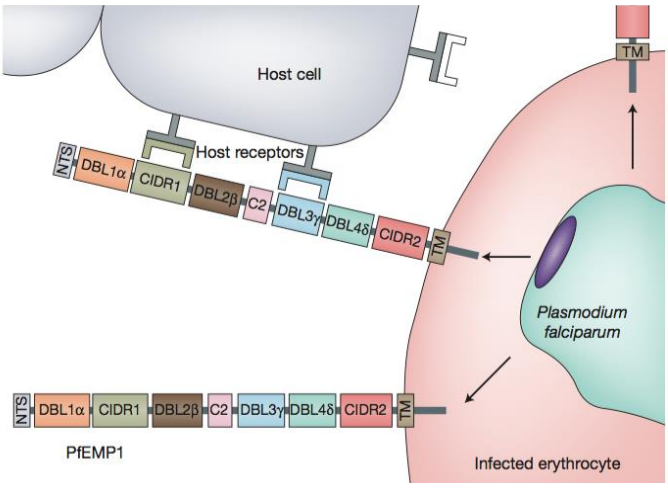

Figure 1.5 | Schematic representation of a parasite-derived PfEMP1 protein variant on the surface of an infected erythrocyte. The extracellular region of the PfEMP1 is involved in adhesion interactions with host cell receptors and is made up of the N-terminal segment (NTS), Duffy binding-like domains (DBL) and cysteine rich interdomain regions (CIDR). The DBL domains can be classified into six types (α, β, γ, δ, ε and ζ) and the CIDR into four groups (α, β, δ and γ). Only one PfEMP1 variant is expressed per cell at any given time. The number, location and type of DBL and CIDR domains vary among PfEMP1 variants, giving rise to variable domain compositions and diversity in adhesion specificities. This schematic shows a hypothetical model of a PfEMP1 variant. TM, transmembrane region. Figure was taken from Rowe *at al*. 2009.

1.5.2 PfEMP1-associated virulence

The interaction of PfEMP1 proteins with endothelial and circulating cells causes obstruction of blood flow and tissue perfusion, contributing to organ failure in the non-immune host (Dondorp *et al.* 2000, Dondorp *et al.* 2004, Dondorp *et al.* 2008). However, the vast majority of *P. falciparum* infections do not lead to severe disease and only certain types of PfEMP1, with specific adhesion specificities, have been implicated in pathology (Hviid and Jensen 2015, Bull and Abdi 2016). Group-A PfEMP1 proteins have a structure consisting of a DBLα1 and a CIDRα1/β/γ/δ (non-CD36 binding) domain and their pattern of expression has been linked to severe disease outcome in numerous studies (Kirchgatter and Portillo Hdel 2002, Bull *et al.* 2005, Kaestli *et al.* 2006, Kyriacou *et al.* 2006, Rottmann *et al.* 2006, Normark *et al.* 2007, Falk *et al.* 2009, Warimwe *et al.* 2009, Kalmbach *et al.* 2010, Lavstsen *et al.* 2012, Warimwe *et al.* 2012, Bertin *et al.* 2013, Almelli *et al.* 2014, Abdi *et al.* 2015, Bertin *et al.* 2016, Jespersen *et al.* 2016, Mkumbaye *et al.* 2017, Shabani *et al.* 2017, Tonkin-Hill *et al.* 2018). However, data on the host cell receptors associated with these parasite-host interactions are largely inconclusive (Rowe *et al.* 2009, Craig *et al.* 2012). Sequestration of mature infected erythrocytes in the microvasculature of the brain is one of the key features of cerebral malaria pathology and parasites that transcribe a subset of group-A and B/A *var* genes encoding 'Domain cassette (DC) 8 and 13' type

PfEMP1 have been associated with this pathology, in children specifically (MacPherson *et al.* 1985, Bertin *et al.* 2013, Almelli *et al.* 2014, Milner *et al.* 2014). Infected erythrocytes that express these variants have been reported to bind EPCR, expressed on human brain endothelial cells (HBEC), implicating this host receptor in the interaction (Turner *et al.* 2013). Owing to the difficulty of performing the relevant experiments however, there is yet limited evidence for a direct association between EPCR binding and cerebral malaria, and the host receptor ICAM-1 has also been implicated with various degrees of controversy (Ockenhouse *et al.* 1991, Turner *et al.* 1994, Newbold *et al.* 1997). Most B- and C-type PfEMP1 have a 4-domain extracellular structure including a CD36-binding head consisting of a DBLα0 and a CIDRα2–6, plus another DBL and CIDR domain (Kraemer and Smith 2003). The expression of group-B PfEMP1 has been associated with both severe and mild malaria (Kaestli *et al.* 2006, Rottmann *et al.* 2006, Merrick *et al.* 2012, Almelli *et al.* 2014), whereas group-C PfEMP1 have only been found expressed in parasites causing asymptomatic infections and in long-term *in vitro* cultivated parasites (Jensen *et al.* 2004, Sharp *et al.* 2006, Frank *et al.* 2007, Enderes *et al.* 2011).

1.5.3 PfEMP1 selection in the human host

Because of their exposure on the surface of infected erythrocytes during blood-stage infection, VSAs such as PfEMP1 are targets of naturally acquired immunity (Bull *et al.* 1998, Bull *et al.* 2000, Chan *et al.* 2012). This is thought to impose a selection pressure on the infecting parasite population, causing them to switch expression between different PfEMP1 variants in order to evade the host immune system and establish chronic infection (Smith *et al.* 1995, Bull *et al.* 1998, Chan *et al.* 2012). Interestingly, healthy individuals (having experienced previous episodes of malaria), asymptomatic individuals and those recovering from disease demonstrate high levels of antibodies to a broad repertoire of PfEMP1 (Bull *et al.* 1998, Ofori *et al.* 2002, Hviid 2005). Thus production of antibodies, capable of neutralising binding of PfEMP1s to host cell receptors, may be important in the development of immunity to severe disease (Marsh *et al.* 1989, Dobbs and Dent 2016).

As previously discussed, in areas of high malaria transmission, immunity to severe disease develops rapidly (Langhorne *et al.* 2008, Goncalves *et al.* 2014). One popular

explanation for this in the scientific community is that restricted subtypes of disease-causing PfEMP1 variants are specialised for infection in malaria-naïve hosts, and upon development of antibodies to these variants, children are subsequently protected from severe infection (Bull *et al.* 1999, Bull *et al.* 2000, Nielsen *et al.* 2002, Staalsoe *et al.* 2003, Jensen *et al.* 2004, Abdi *et al.* 2017). In line with this, it is predicted that PfEMP1 of the group-A, B/A subclass confer a growth advantage in the immunologically naïve host through mechanisms that allow them to adhere to a more diverse range of endothelial cells, and thus more efficiently escape clearance from the spleen (Abdi *et al.* 2017). However, this has been extremely difficult to test in the field, owing to the difficulty in controlling for current and past infection history. In one recent study, controlled human malaria infection (CHMI) of 28 Kenyan adults was used to investigate an association between pre-existing antibodies against infected erythrocytes, and parasite expression of group-A and DC-8-like PfEMP1 (Abdi *et al.* 2017). The study reports that in individuals with high levels of pre-existing antibodies, lower levels of group-A *var* transcripts are detected in parasites that go on to establish blood-stage infection, compared to volunteers with low levels of pre-existing antibodies. Based on these data, the authors propose a model whereby group-A and DC8-and 13-type PfEMP1 confer a fitness advantage in the naïve host, and suggest for dominant expression of these variants in all cases of primary infection with *P. falciparum* (Abdi et al. 2017). However, alternative models of *var* gene/PfEMP1 selection have been proposed (Peters *et al.* 2002, Lavstsen *et al.* 2005, Wang *et al.* 2009, Bachmann *et al.* 2011, Bachmann *et al.* 2016). In another study of CHMI, parasite *var* gene expression was assessed following sporozoite infection of non-immune volunteers. Analysis was limited to just one blood sample containing mRNA material sufficient for qPCR, but reported the detection of 90% of all *var* gene transcripts (Wang *et al.* 2009), suggesting a theory whereby at the onset of blood-stage infection, *P. falciparum* (3D7-strain) gene expression is based on a strategy that allows all or most PfEMP1 variants to be expressed. Similar broad-level detection of *var* gene variants has since been documented by Bachmann *et al,* although there appeared dominant expression of group-B variants in this cohort of 18 volunteers (Bachmann *et al.* 2016). In contrast, studies of *P. falciparum in vitro* cultures established from parasites isolated from non-immune individuals, display a dominant group-A transcript pattern (Lavstsen *et al.* 2005, Bachmann *et al.* 2011). However results from these studies are confounded by a possible bias in transcription profile due to *var* gene switching of cultured parasites; a

well-documented phenomenon (Roberts *et al.* 1992, Horrocks *et al.* 2004, Peters *et al.* 2007, Bachmann *et al.* 2011). Therefore, in order to understand what drives severe disease in the malaria-naïve, it is important to investigate this parasite-host interaction further.

1.5.4 Other variant surface antigens

The *P. falciparum* genome consists of other multi-gene families with a potential influence on parasite virulence. These include the repetitive interspersed family (*rif*), which encode RIFINS, and sub-telomeric variable open reading frame (*stevor*), which encode STEVORS (Kyes *et al.* 1999, Lavazec *et al.* 2007, Joannin *et al.* 2008). These proteins are expressed on the surface of infected erythrocytes (Bachmann *et al.* 2015), however their role in malaria is unclear due to the limited studies available (Abdel-Latif *et al.* 2003, Niang *et al.* 2009, Chan *et al.* 2014, Niang *et al.* 2014). RIFINS have been implicated in severe malaria given their ability to form rosettes upon binding to uninfected red cells (Goel *et al.* 2015). Whereas, in another study they have been shown to interact with the host inhibitory receptors; leucocyte immunoglobulin-like receptor B1 (LILRB1) and leucocyte-associated immunoglobulin-like receptor 1 (LAIR1), in a process thought to inhibit activation of LILRB1-expressing B cells and natural killer cells (Saito *et al.* 2017). Thus, *P. falciparum*-derived RIFINs may utilise immune inhibitory receptors to achieve immune evasion. The role of these VSAs, and their interaction with the human host, also warrants further exploration.

1.5.5 Understanding the innate immune response to *P. falciparum*

Malaria is a complex disease, not least in part due to the heterogeneity between, and within, the clinically-defined syndromes. Interpreting how immunity develops is further complicated by the various host and parasite factors influencing susceptibility and protection. Most observations of the innate immune responses to human malaria are derived either from *in vitro* studies or from cross-sectional epidemiological studies conducted at a time when the infection has already led to disease. Furthermore, in the setting of natural infection: previous exposure, infective dose, age, genetic diversity and co-infections are all confounding factors. Therefore, in order to better delineate the innate immune response to *P. falciparum* infection in the human host, we need to consider a model that limits the introduction of variability.

Controlled Human Malaria Infection (CHMI) offers a unique opportunity to study the earliest immune events during *P. falciparum* infection in the human host, in a setting where many of the above-listed variables can be excluded. CHMI, and its applications will be discussed in the following section.

1.6 Controlled Human Malaria Infection

The deliberate infection of human volunteers with malaria is not a recent practice. During the early twentieth century, artificial induction of malaria-fever, termed "malariatherapy" served as the most effective treatment for neurosyphillis in the pre-penicillin era; a discovery which earned Julius Wagner Von Jauregg the 1927 Nobel Prize in Medicine (figure 1.6). During the 1920s to 1950s, thousands of patients were infected with *Plasmodium*, providing the largest body of data on the human response to controlled malaria infection. These data are still very much relevant today (Austin *et al.* 1992, Collins and Jeffery 1999, Molineaux *et al.* 2002, Collins *et al.* 2004). Although the aim of these studies was not to assess the early immune events during malaria, they provide the first evidence for inter-individual variation in response to controlled malaria infection, as well as detailed information on parasite growth kinetics within the human host (McKenzie *et al.* 2001, McKenzie *et al.* 2002, Molineaux *et al.* 2002). Many fundamental insights can be attributed to these historical studies of malariatherapy and their significance to the field of malaria research must not be overlooked.

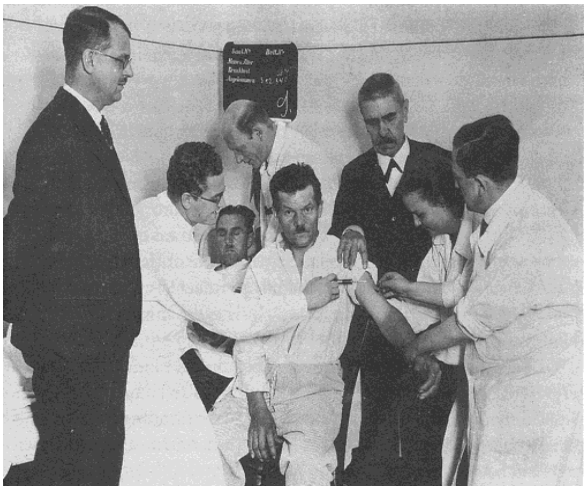

Figure 1.6 | Malariatherapy in the early 20th century. Julius Wagner-Jauregg (black suit, facing camera) oversees the transfusion of blood from a malaria patient to a psychiatric patient suffering from neurosyphilis (center) for induction of malaria-fever at Horton Hospital, Epsom, in 1934. (Photograph sourced from the Institut für Gescjocjte der Medizin Vienna, Austria and reproduced in Raju, T.N. 2006). Figure taken from Raju, T.N. 2006.

Controlled Human Malaria infection (CHMI), is now the most practiced controlled human infection model worldwide, and is a critical tool for the assessment of new malaria vaccine candidates. Field studies are often complex and expensive to organise, requiring large numbers of participants to allow for variables such as genetic heterogeneity and co-infections, whereas CHMI requires relatively small numbers of healthy volunteers per trial. To date, over 3,000 human volunteers have been safely exposed to *P. falciparum* infection across four specialised centres, namely the Walter Reed Army Institute, Silver Spring, Maryland (USA), the University of Oxford (UK), the Radbound University Nijmegen Medical Centre (RUMC, The Netherlands) and the Queensland Institute of Medical Research (QIMR), Brisbane, Australia (Roestenberg *et al.* 2017).

Traditionally, malaria vaccines are designed to target different life cycle stages of the parasite, using antigens expressed at either the pre-erythrocytic or blood-stages. Depending on the type of vaccine being tested, different models of CHMI are routinely used to infect volunteers.

1.6.1 Mosquito-bite challenge model

Exposure to five infectious mosquito bites, via the mosquito-bite challenge model,

mimics the natural route of infection leading to detection of blood-stage parasites by thick blood film approximately 9 - 11 days later, at which point drug treatment is initiated (Roestenberg *et al.* 2012). Most volunteers undergoing the mosquito-bite challenge experience non-specific symptoms of uncomplicated malaria, with fever and headaches being most common. The prepatent period (time from exposure to positive thick smear) is used to estimate efficacy of the vaccine, and is supplemented by exact measurements of parasite numbers in the blood using quantitative RealTime (qRT) PCR (Hermsen *et al.* 2001), allowing for calculation of parasite multiplication rates within the human host. Pooled data from clinical trials at RUMC have shown that an estimated 23 to 5,273 (mean 500) merozoites per mL are released within the first erythrocytic cycle, approximately 6.5 days after mosquito bite (Roestenberg *et al.* 2012), however this number is likely highly variable between volunteers. Once in the circulation, *P. falciparum* parasites follow a pattern of synchronous replication, multiplying approximately 10.8-fold every 48 hours (Roestenberg *et al.* 2012). Due to the nature of CHMI diagnosis criteria, volunteer infections are terminated after just 2 - 3 erythrocytic replication cycles following mosquito-bite challenge. This short time frame has been deemed inappropriate for the assessment of partially effective blood-stage vaccines, which may demonstrate effects only after several replication cycles in the blood (Sanderson *et al.* 2008, Sheehy *et al.* 2013). In this instance, volunteers are instead infected by *intravenous (iv)* injection of PEs (blood-stage challenge model).

1.6.2 Blood-stage challenge model

All blood inoculum used in recent trials of blood-stage vaccines has come from one of two donors experimentally infected with the 3D7 reference strain of *P. falciparum* (Cheng et al. 1997*)*. Injection of 1,800 parasitised erythrocytes *iv* leads to blood-stage parasitaemia that can be detected by qRT PCR after 3.5 days, reaching thick-film positivity (diagnosis) at 8 days post-infection. Thus, a greater number of erythrocytic cycles in which to monitor the effects of vaccines targeting blood-stage parasites are afforded (Sanderson *et al.* 2008). However, inoculum dose has varied greatly between different trials using this model: from 30 to 6,000 parasitised erythrocytes (Cheng *et al.* 1997, Pombo *et al.* 2002). One major advantage of the blood-stage challenge model is that every volunteer within the same trial can be guaranteed an identical immune challenge, whereby the dose and timing of parasites entering circulation is stringently

controlled (Duncan and Draper 2012, Payne *et al.* 2016). Moreover, given that the number of PEs being used to initiate infection is known, it allows for much more accurate modelling of parasite growth with each 48-hour cycle of replication in the blood (Douglas *et al.* 2013). However, individuals undergoing *P. falciparum* infection by blood-stage challenge experience fewer symptoms compared to those following mosquito-bite, for reasons that are not understood (Duncan and Draper 2012). This precludes the (already difficult) correlation of host responses variables with clinical outcome.

1.6.3 Sporozoite infection model

The recent availability of cryopreserved parasites from Sanaria Inc. provides an appealing alternative to current models of CHMI, whereby volunteers are infected by intravenous inoculation of cryopreserved sporozoites (PfSPZ challenge) (Lyke *et al.* 2015, Mordmuller *et al.* 2015). Here, the number of sporozoites injected can be controlled, minimising inter-individual variation and strengthening statistical power compared to the mosquito-bite model. Its use has already been shown to be safe, well tolerated and infectious for a large proportion of tested individuals (Roestenberg *et al.* 2013, Shekalaghe *et al.* 2014).

1.6.4 Standardisation of CHMI

The advance of molecular technology for fast and accurate parasite detection is beginning to diversify the design of CHMI and there has been recent discussion over how best to standardise studies (Roestenberg *et al.* 2017). At some trial sites, qRT PCR is replacing microscopy for diagnosis, as a more sensitive method for detecting blood-stage parasites. In this instance, drug treatment is initiated when parasite densities (p/mL) surpass a predefined threshold (Burel *et al.* 2016). This approach is thought to improve safety, reducing the clinical burden without compromising the evaluation of protective efficacy (Walk *et al.* 2016, Stanisic *et al.* 2018). In other studies, infections have been allowed to continue beyond the thick film threshold if clinical symptoms are absent (Roestenberg *et al.* 2017). Most CHMI trials have been performed using the 3D7 or parental NF54 strain of *P. falciparum,* however, the long-term culture of this strain has sparked concerns over its likely divergence from field

strains. The introduction of a more diverse range of *Plasmodium* genotypes has therefore been proposed, to bridge the gap between strain-specific *P. falciparum* developed for CHMI, and strains found in the natural endemic setting (Roestenberg *et al.* 2017). The general design of CHMI in current trials, however, is similar and results are highly reproducible across sites, highlighting the robustness of this model (Roestenberg *et al.* 2012).

1.6.5 CHMI for studying host and parasite immunobiology

Over recent years, the CHMI model has been exploited beyond its use anti-malaria vaccine screening, and is being increasingly applied to more basic research questions. Many sub-studies undertaken within the frame-work of drug or vaccine evaluation have already provided some valuable insights, as summarised in table 1.2 (Peters *et al.* 2002, Lavstsen *et al.* 2005, Walther *et al.* 2005, Ockenhouse *et al.* 2006, Walther *et al.* 2006, Wang *et al.* 2009, Teirlinck *et al.* 2011, Turner *et al.* 2011, Woodberry *et al.* 2012, Arevalo-Herrera *et al.* 2014, Scholzen *et al.* 2014, Rojas-Pena *et al.* 2015, Teirlinck *et al.* 2015, Arevalo-Herrera *et al.* 2016, Bachmann *et al.* 2016, Burel *et al.* 2016, Loughland *et al.* 2016, Montes de Oca *et al.* 2016, Stanisic *et al.* 2016, Tran *et al.* 2016, Burel *et al.* 2017, Loughland *et al.* 2017, Gardinassi *et al.* 2018, Rothen *et al.* 2018). Importantly, CHMI has provided evidence which supports the inter-individual variability in host responses to controlled *Plasmodium* infection, first documented in early studies of malariatherapy (Molineaux *et al.* 2002). Following mosquito-bite challenge with *P. falciparum* (3D7 strain), Walther *et al* were able to group volunteers according to their cytokine response profiles, which ranged from anti-inflammatory (associated with the upregulation of TGF-β), to pro-inflammatory (characterised by detectable IL-12p70, and high levels of IFNγ). Moreover, pro-inflammatory responses in these individuals were associated with better control of parasite growth, and development of clinical symptoms (Walther *et al.* 2006). In a more recent study, Burel *et al* report a dichotomy in volunteer miRNA expression patterns following direct blood inoculation of *P. falciparum*-infected erythrocytes (Burel *et al.* 2017). Thus, inter-individual variability in the host immune response to controlled *P. falciparum* infection has been reported at both the transcript and protein level, highlighting an important gap in our understanding of human malaria infection.

Table 1.2 | CHMI for studying host/ parasite immunobiology: a summary

Publication reference	Study site	Plasmodium species	Study type	CHMI model	Focus of study	Cohort size	Volunteer immune status	Key finding(s)
Peters *et al.* 2002	QIMR, Brisbane, Australia	*P. falciparum*	Parasite genetics	Blood-stage	Parasite *var* gene profiling	2	malaria-naive	The composition and frequency of *var* transcript expression differs markedly between parasites isolated after infection in the human host and the parasite population used to infect
Lavstsen *et al.* 2005	RUMC, Nijmegen, Netherlands	*P. falciparum*	Parasite genetics	Mosquito-bite	Parasite *var* gene profiling	10	malaria-naive	Parasites isolated form volunteers (2nd and 3rd generation parasites, following hepatic release) have dominant expression of group-A and B *var* gene variants
Walther *et al.* 2005	CCVTM, Oxford/ LSHTM, London	*P. falciparum*	Host immunology	Mosquito-bite	The host regulatory T cell (Treg) response	26	malaria-naive	Cells with the characteristics of Treg cells are rapidly induced following blood-stage infection and are associated with a burst of TGFβ production, decreased proinflammatory cytokine production, and decreased antigen-specific immune responses
Ockenhouse *et al.* 2006	WRAIR, US Cameroon, West Africa	*P. falciparum*	Host immunology	Mosquito-bite Natural infection	Comparison of transcriptional immune events during *P. falciparum* infection in pre-symtomatic (malaria-naive CHMI) vs symptomatic (naturally-infected, Cameroon)	22 15	malaria-naive previously exposed (Cameroonian adults)	TLR signalling is upregulated in both pre-symptomatic and symptomatic individuals, as well as genes that function in phagocytosis and inflammation. Differences between pre-symptomatic and symptomatic volunteers were linked to genes that regulate the induction of apoptosis.
Walther *et al.* 2006	CCVTM, Oxford/ LSHTM. London	*P. falciparum*	Host immunology	Mosquito-bite	Host cytokine response kinetics (PBMCs and whole blood)	18	malaria-naive	Volunteers infected by CHMI have diverse cytokine responses to *P. falciparum*. Proinflammatroy responses are associated with better control of parasite growth and adverse clinical events
Mccall *et al.* 2007	RUMC, Nijmegen, Netherlands	*P. falciparum*	Host immunology	Mosquito-bite	TLR responses during acute-phase *P. falciparum* infection in the malaria-naive	15	malaria-naive	TLR4 responses were characterised by the up-regulation of proinflammatory cytokines during infection, compared to baseline. TLR2/TLR1 responses demonstrated increases in both pro- and anti-inflammatory cytokine production.
Wang *et al.* 2009	RUMC, Nijmegen, Netherlands	*P. falciparum*	Parasite genetics	Mosquito-bite	Parasite *var* gene profiling	1	malaria-naive	At the onset of blood-stage infection in the naive host, all (or most) parasite *var* gene variants are expressed
Teirlinck *et al.* 2011	RUMC, Nijmegen, Netherlands	*P. falciparum*	Host immunology	Blood-stage or PfSPZ challenge	Longevity and composition of host cellular immune responses	15	malaria-naive	Cellular responses to both *Pf*SPZ and *Pf*RBCs are induced and remain undiminished for up to 14 months after a single infection. Both innate and adaptive lymphocyte subsets contribute to the increased IFNγ response (αβT cells, γδT cells and NK cells).
Turner *et al.* 2011	RUMC, Nijmegen, Netherlands	*P. falciparum*	Host immunology	Mosquito-bite	Screening for anti-VSA antibodies in volunteer plasma	44	malaria-naive	Antibodies against PfEMP1, RIFIN, MSP3 and GLURP are aquired after a single, low density *P. falciparum* infection in malaria-naive individuals
Woodberry *et al.* 2012	QIMR, Brisbane, Australia	*P. falciparum*	Host immunology	Blood-stage	The kinetics of Dendritic Cell (DC) apoptosis/loss during *P. falciparum* infection	10	malaria-naive	In primary infection, loss of dendritic cell numbers and function occurs early during the prepatent period. Remaining DCs demonstrated a reduced ability to uptake particulate antigen.
Arevalo-Herrera *et al.* 2014	Malaria Vaccine and Drug Development Centre (CECIV, Cali, Columbia)	*P. vivax*	Host immunology	Mosquito-bite	Parasitaemia levels, clinical manifestations and immune responses during infection with *P. vivax*	7 9	malaria-naive adults (Cali, Columbia) semi-immune (adults) (Buenaventura, Columbia)	Malaria-naive and semi-immune individuas demonstrate comparable prepatent periods during infection with *P. vivax*. Malaria-naive volunteers develop classic malaria-associated symptoms, whereas semi-immune volunteers display minor or no symptoms at the day of diagnosis.

Scholzen *et al.* 2014	RUMC, Nijmegen, Netherlands	*P. falciparum*	Host immunology	cryopreserved sporozoites (PfSPZ challenge)	The dynamics of BAFF induction and B cell subset activation and composition in the blood	18	malaria-naïve	BAFF and BAFF receptor levels correlate with B cell subset activation and redistribution in CHMI
Rojas-Pena *et al.* 2015	Malaria Vaccine and Drug Development Centre (CECIV, Cali, Columbia)	*P. vivax*	Host immunology	Mosquito-bite	Comparison of (whole blood) transcriptional profiles in naïve versus semi-immune volunteers experimentally infected with *P. vivax*	7 9	malaria-naïve adults (Cali, Columbia) semi-immune (adults) (Beunaventura, Columbia)	Whole-blood transcriptome analysis revealed a strong interferon response, and down-regulation of transcripts linked to inflammation and innate immunity in response to *P. vivax* infection, in both naïve and semi-immune volunteers.
Teirlinck *et al.* 2015	RUMC, Nijmegen, Netherlands	*P. falciparum*	Host immunology	Mosquito-bite	Composition and activation status of monocytes and dendritic cells in the blood	18	malaria-naïve	*P. falciparum* activation induces activation of monocytes and CD16+ dendritic cells (DCs) and induces up-regulation of CD16 and CD1c expression
Arevalo-Herrera *et al.* 2016	Malaria Vaccine and Drug Development Centre (CECIV, Cali, Columbia)	*P. vivax*	Host immunology	Mosquito-bite	Antibody profiling in naïve and semi-immune volunteers experimentally infected with *P. vivax*	7 9	malaria-naïve adults (Cali, Columbia) semi-immune (adults) (Beunaventura, Columbia)	Higher serological (antibody) responses were detected in semi-immune volunteers, compared to malaria-naïve volunteers, although malaria-naïve volunteers also had pre-existing antibodies. Semi-immune volunteers without fever displayed a lower response to challenge.
Bachmann *et al.* 2016	The Institute of Tropical Medicine (Tubingen, Germany)	*P. falciparum*	Parasite genetics	Mosquito-bite	Parasite *var* gene profiling	18	malaria-naïve	Broad-level detection of parasite *var* gene variants after ~3 replication cycles in the blood *Var* gene expression dominated by those of the group-B and, to a lesser extent, group-A sub-types
Burel *et al.* 2016	QIMR, Brisbane, Australia	*P. falciparum* & *P. vivax*	Host immunology	Blood-stage	Profiling the host cellular response during infection with *P. falcairum*, compred to *P. vivax*	19 (*Pf*) 8 (*Pv*)	malaria-naïve	*P. vivax* but not *P. falciparum* blood-stage infection in the human host is associated with the expansion of a CD8+ T cell population with cytotoxic potential
Loughland *et al.* 2016	QIMR, Brisbane, Australia	*P. falciparum*	Host immunology	Blood-stage	The maturation status of (CD1c+) myeloid DCs and their associated cytokine production	62	malaria niave	*P. falciparum* infection is associated with reduced CD1c+ myeloid dendritic cell HLA-DR and CD86 expression, but enhanced TNF production
Montes de Oca *et al.* 2016	QIMR, Brisbane, Australia	*P. falciparum*	Host immunology	Blood-stage	Immuno-regulatory networks during the host response to *P. falciparum*	65	malaria-naïve	Type I IFNs suppress innate immune cell function and parasite-specific CD4+ T cell IFNγ production, and promote the development of parasite-specific IL-10 producing Th1 (Tr1) cells.
Stanisic *et al.* 2016	QIMR, Brisbane, Australia	*P. falciparum*	Parasite immunobiology	Blood-stage	Characterisation of *P. falciparum* parasite strains (NF54, 3D7B and 7G8) for assessment of *in vivo* infectivity in the malaria naïve host	3	malaria-naïve	Infectivity of *P. falciparum* in malaria-naïve individuals is associated with knob expression and cytoadherence of the parasite
Tran *et al.* 2016	RUMC, Nijmegen, Netherlands Kalifabougou, Mali	*P. falciparum*	Host immunology	Mosquito-bite Natural infection	Comparison of (whole-blood) RNA-seq profiles in adults who are naturally exposed and i) asymptomatic or ii) febrile, to those who were previoulsy malaria-naïve	5 8	malaria-naïve (Dutch adults) previously exposed (Malian adults)	Malaria-naïve individuals demonstrate much higher activation of pathways downstream of pro-inflammatory cytokines, compared to malaria-experienced Malawian volunteers. Febrile and asymptomatic profiles were indistinguishable, with the exception of genes activated by pro-inflammatory cytokines.
Burel *et al.* 2017	QIMR, Brisbane, Australia	*P. falciparum*	Host immunology	Blood-stage	Assessment of early immune events (miRNA expression profiles) and evidence for inter-individual variation in host responses	21	malaria-naïve	Volunteers displayed a dichotomous pattern of high or low expression of a defined set of micro-RNAs (miRNAs), which correlated variation in parasite growth rate. High miRNA responders had higher numbers of activated cD4+ T cells and enhanced antimalarial antibody responses
Loughland *et al.* 2017	QIMR, Brisbane, Australia	*P. falciparum*	Host immunology	Blood-stage	The activation and cytokine production of plasmacytoid dendritic cells (pDCs) during *P. falciaprum* infection	59	malaria-naïve	Plasmacytoid DCs (pDCs) appear inactive during sub-microscopic *P. falciparum* blood-stage infection, yet retain their ability to respond to TLR stimulation
Gardinassi *et al.* 2018	Malaria Vaccine and Drug Development Centre (CECIV, Cali, Columbia)	*P. vivax*	Host immunology	Mosquito-bite	Integrative metabolomics and transcriptomics signatures of clinical tolerance to *P. vivax*	7 9	malaria-naïve adults (Cali, Columbia) semi-immune (adults) (Beunaventura, Columbia)	At baseline, naïve and semi-immune volunteers differed in the expression of interferon-related genes, neutrophil and B cell signatures that progressed with distinct kinetics after infection. Metabolomics data highlighted differences in amino acid pathways and lipid metabolism between the two groups.
Rothen *et al.* 2018	Ifakara Health Institute, Bagamoyo, Tanzania	*P. falciparum*	Host immunology	cryopreserved sporozoites (PfSPZ challenge)	Transcriptional analysis of early host immune events (whole blood)	10	previously exposed (Tanzanian adults)	Grouping volunteers based on prepatent period identified 265 genes whose expression levels were linked to time of blood-stage parasitaemia detection. Modules associated with these 265 genes were linked to regulation of transcription, cell cycle and erythrocyte development.

1.7 Scope of this thesis

The development of effective preventative/curative therapies for malaria requires a better understanding of what constitutes protection in those at greatest risk of severe disease. In children with limited immunity to *P. falciparum*, most episodes of severe disease appear restricted to the 1st, 2nd or 3rd malaria infection, suggesting an important role of the innate immune response in determining outcome of infection. Therefore, investigation into the earliest immune events during infection in the malaria-naive is essential. When it comes to anti-malaria vaccine design, there are important practical implications in understanding diversity in host immune responses. Yet, the host and/or parasite factors driving inter-individual variation remain undefined. One potential source is differential expression of parasite VSAs, however little work has been done to investigate their influence on the developing host immune response in the malaria-naïve. Furthermore, although the expression of particular PfEMP1 variants has been associated with different clinical outcomes, little is known about their expression at the onset of infection. This is also true for other multi-gene family members such as the RIFINS and STEVORS, whereby research into their role as VSAs is limited to just a handful of studies.

The CHMI model offers a unique opportunity to investigate the earliest immune events taking place during primary infection with *P. falciparum.* Yet most studies to date have been limited to the assessment of host immune responses in isolation, without considering the influence of parasite gene expression on developing host immunities and associated clinical outcome(s). With this in mind, this project explores the hypothesis that inter-individual variability in the immune response to primary *P. falciparum* infection is driven by parasite VSA expression, and has three key objectives, each of which will be addressed in the chapters outlined overleaf:

Chapter 3 objectives: To characterise the earliest immune events during *P. falciparum* infection in the malaria-naïve host, and assess inter-individual variation within the cohort.

Chapter 4 objectives: To investigate parasite multi-gene family expression (*var, rif* and *stevor*), and determine their influence on the developing host immune response, and vice versa.

Chapter 5 objectives: To optimise a method for direct *ex vivo* RNA-sequencing of parasites isolated at the onset of infection, and at multiple time points throughout, with the aim of investigating *in vivo* VSA selection in non-immune individuals.

Chapter 2: Materials and Methods

2 Materials and Methods

Samples used for investigating early parasite-host interactions in Controlled Human Malaria Infection were collected from volunteers enrolled in a phase I/IIa vaccine study that took place from March to December 2014 at the Centre for Clinical Vaccinology and Tropical Medicine (CCVTM), Oxford *(Clinical/ Trials.gov i.d: NCT02044198*). The trial was designed and conduced by a team lead by Dr Simon Draper at the Jenner Institute, University of Oxford. This chapter describes the protocol for CHMI, and gives details of the host/parasite sample collection used for my sub-study. Sections marked (*) indicate the sample processing steps performed by me. Specific materials and methods have been included in subsequent chapters.

2.1 Controlled Human Malaria Infection (CHMI)

2.1.1 Study Design and Ethical Approvals

The study was designed to assess the safety, immunogenicity and efficacy of the AMA1 FMP2.1/AS01B asexual blood-stage candidate as a vaccine for *P. falciparum* malaria. To assess vaccine efficacy, all volunteers underwent blood-stage challenge with *P. falciparum* (3D7 strain) - infected erythrocytes, results from which have been previously published (Payne *et al.* 2016).

Ethical approval for this study was given by the United Kingdom National Health Service (NHS) Research Ethics Service (Oxfordshire Research Ethics Committee A, reference 13/SC/0596) and the Western Institutional Review Board in the United States (reference 20131985). The study was approved by the United Kingdom Medicines and Healthcare Products Regulatory Agency (reference 21584/0326/001-0001) and was conducted in full concordance with the Declaration of Helsinki 2008.

2.1.2 Volunteer Cohort and Inclusion/Exclusion Criteria

Volunteers were recruited at multiple trial sites across the UK: the Centre for Clinical Vaccinology and Tropical Medicine (CCVTM), Oxford; the Hammersmith National Institute for Health Research (NIHR)/Wellcome Trust Clinical Research Facility (WTCRF), London; and the NIHR WTCRF, Southampton. The original vaccine study recruited 30 volunteers in total: 15 to receive the candidate vaccine and 15 to act as unvaccinated, infectivity controls (Payne *et al.* 2016). Given my interest in the host

response to *P. falciparum* infection during primary exposure to the parasite, the volunteer cohort for my sub-study included 14 (unvaccinated) controls only. All volunteers gave written informed consent prior to participation. Recruited volunteers were healthy, malaria-naïve male or non-pregnant females aged 18 – 45 years. Table 3.1 (chapter 3) provides more detailed information on the 14 participants in this study. A full list of volunteer inclusion and exclusion criteria is provided in Appendix 1.

2.1.3 Blood-stage CHMI

The inoculum used for CHMI was prepared and cryopreserved at the QIMR in Brisbane, Australia, in 1994 and consisted of *P. falciparum* (3D7-strain) infected erythrocytes taken from a single donor. Details of inoculum production have been previously published (Cheng *et al.* 1997).

The inoculum was prepared for use in this blood-stage CHMI, as has been described previously (Payne *et al.* 2016)**.** In brief, a single vial of inoculum was thawed, washed and diluted under aseptic conditions in a derogated containment level III laboratory area, using solutions licensed for clinical use and single-use disposable consumables. Inoculum was administered *intravenously* (*iv)* in a 5 mL volume of 0.9% saline, at an estimated dose of 1,000 parasitised erythrocytes (PEs) per volunteer. A limiting dilution assay for assessment of inoculum viability later confirmed this dose to be 690 ring-stage PEs. All volunteers were inoculated at the CCVTM, within 2 hours and 13 minutes of inoculum preparation. Following CHMI, blood was collected from each volunteer the day after inoculum challenge (C +1), and twice daily from C +2. Thick blood films were evaluated by experienced microscopists and qPCR was performed for quantification of parasites/ mL of blood (p/mL). qPCR confirmed that all volunteers in the study were successfully infected. Treatment with the combination drug Riamet® was prescribed to volunteers when two out of three diagnosis criteria were met: a positive thick blood film and/or qPCR ≥500 parasites/mL and/or symptoms consistent with malaria infection All volunteers were monitored for at least two days following their initial course of drug-therapy.

2.1.4 Parasite qPCR

Parasite qPCR was performed on C +1, and twice daily from C +2, by staff at the Jenner Institute. Details of the protocol have been previously published (Sheehy *et al.* 2012). Briefly, blood was depleted of white cells and the DNA extracted from a 0.5 mL volume using the Qiagen Blood Mini Kit. 10% of each extraction was then run in triplicate for qPCR (equating to 150 µL of blood directly assessed). Previously published primers with TaqMan™ probe (5′ FAM-AAC AAT TGG AGG GCA AG-NFQ-MGB 3′) were used to amplify the *P. falciparum* 18s ribosomal region (Applied Biosystems, Foster City, CA). Parasites per mL equivalent mean values were generated by a standard TaqMan™ absolute quantitation, against a defined plasmid standard curve with an ABI StepOne Plus machine and v2.3 software. Results obtained using a dilution series of microscopically-counted cultured parasites suggested that this method has a lower limit of quantification (LLQ, defined as %CV<20%) of around 20 p/mL blood. Thus, mean parasite equivalent values below 20 p/mL or with only one positive replicate of three tested were classed as negative. Raw qPCR data is provided in Appendix 2.

2.1.5 Modelling of Parasite Multiplication Rate (PMR)

Parasite Multiplication Rate (PMR) was modeled by Dr Alexander Douglas, using a linear model fitted to $\log_{10}$-transformed qPCR data as previously published (Douglas *et al.* 2013)**.** PMR was calculated for all volunteers that underwent blood-stage CHMI, given they all had ≥ 5 data points above the lower limit of quantification (the criterion for modeling PMR using this method).

2.1.6 Full blood counts

Full blood counts (FBCs) were carried out by NHS staff in the haematology department at either one of the Churchill or John Radcliffe Hospitals in Oxford, at baseline (C -1), C +6 and day of diagnosis (DoD) for each volunteer. These data provide an accurate measurement of total red and white cell counts per mL of blood, as well as a break-down of the contribution from individual leukocyte subsets; neutrophils, lymphocytes, monocytes, eosinophils and basophils.

2.1.7 Volunteer clinical assessments

Measurements of temperature, heart rate and blood pressure were recorded for every volunteer, at each clinic visit during CHMI and as a follow-up during their course of drug-therapy. Adverse Events (AEs) were also monitored at each visit, with volunteers being asked to grade any symptoms likely related to their malaria infection as mild, moderate or severe according to the below specifications:

- **Grade 0:** None
- **Grade 1:** Transient or mild discomfort (<48 hours); no medical intervention/therapy required
- **Grade 2:** Mild to moderate limitation in activity - some assistance may be needed; no or minimal medical intervention/therapy required
- **Grade 3:** Marked limitation in activity, some assistance usually required; may require medical intervention/therapy

Solicited AEs included symptoms such as nausea, headaches, diarrhoea and rigors. Samples for biochemistry analysis were taken at baseline (C -1), C +6 and day of diagnosis and were processed by NHS staff in the biochemistry department at either the Churchill or John Radcliffe hospital in Oxford. Biochemistry analyses included the quantitative assessment of electrolytes, urea, creatinine, bilirubin, alanine aminotransferase, alkaline phosphatase and albumin**.**

2.2 Sample collection and processing*

All venipuncture was carried out by trained medical staff at the CCVTM in Oxford.

2.2.1.1 List of Materials

Reagent	Supplier	Catalog Number
1.5 mL Eppendorf® tubes	Sigma-Aldrich	T9661-1000EA
2 mL K3 EDTA Vacuette tubes	Becton Dickinson (BD)	367836
2 mL Lithiam Heparin Vacuette tubes	Grenier Bio-One	454089
6 mL Lithiam Heparin Vacuette tubes	Grenier Bio-One	456084
9 mL Lithiam Heparin Vacuette tubes	Grenier Bio-One	455084
Casyton counting buffer	Sedna Scientific	43003
Casyton tubes	Sedna Scientific	43001
FCS (heat-inactivated, filtered and batch tested)	Biosera	S1810
L-Glutamine	Gibco	25030-24
Leucosep tubes	Grenier Bio-One	227209
Lymphoprep	Axis Shield	1114545
Penicillin/Streptomycin	Gibco BRL/Invitrogen	15140-122
RPMI	Sigma-Aldrich	R0883
Tempus™ Blood RNA Tubes	Applied Biosystems	4342792
TRIzol™	Ambion (Life technologies)	115596026

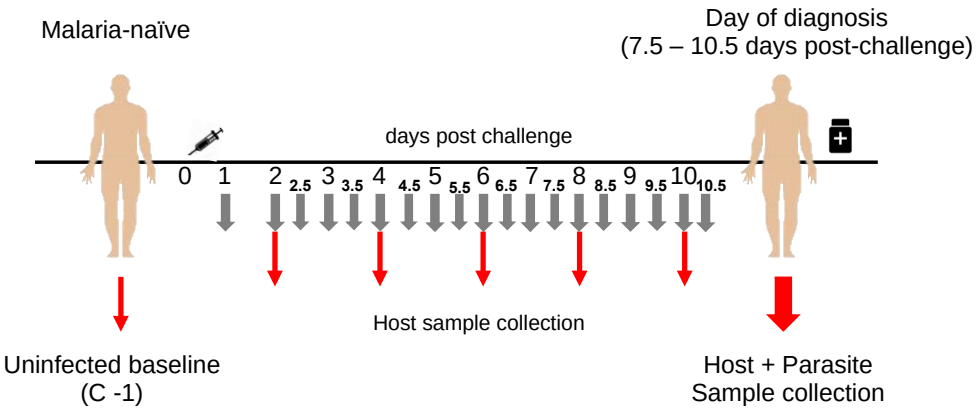

Figure 2.1 | CHMI Sample Collection and Schedule. Grey arrows represent the blood collection schedule for qPCR analysis. Red arrows represent bleeds taken for analysis of the host response to *P. falciparum* infection. Thick red arrow at diagnosis (ranging 7.5 – 10.5 days post-challenge) represents a larger (67 mL) blood volume collected for host and parasite analysis.

A 2 mL volume of blood was collected in EDTA tubes (Beckton Dickinson) for routine qPCR on the morning of C +1, and twice daily from C +2 (represented by grey arrows in figure 2.1).

An additional (17 mL) volume of blood was collected at each volunteer's baseline (C -1), and at 48 hour intervals post infection (C +2, C +4, C +6, C +8…) up to (and including) day of diagnosis for analysis of the host response to *P. falciparum* infection (red arrows in figure 2.1). This blood volume was divided as per sample processing requirements:

2.2.1.2 Samples for whole-blood transcriptome analysis

3 mL was collected directly into 6 mL Tempus™ reagent (Tempus™ Blood RNA Tube, Applied Biosystems) for whole-blood transcriptome analysis. Immediately following blood-draw, tempus tubes were shaken for 10 seconds to ensure thorough mixing, as per manufacturer's guidelines. Tubes were frozen and stored at -70ºC prior to RNA extraction.

2.2.1.3 Isolation of plasma and Peripheral Blood Mononuclear Cells (PBMCs)

14 mL of blood was collected in lithium heparin tubes (Grenier Bio-One) for isolation of plasma and PBMCs. Following collection, blood was transferred to a pre-prepared 50 mL Leucosep tube (Grenier Bio-One) containing 15 mL lymphoprep (Axis Shields) for centrifugation at 1,000g, for 13 minutes at room temperature. Following centrifugation, 2 mL was collected from the plasma fraction and transferred to 4x 1.5 mL Eppendorf tubes (Sigma) for snap-freezing on dry ice and storage at -70ºC. The remaining supernatant from the Leucosep tube (containing the PBMC fraction) was then transferred to a fresh 50 mL falcon tube and centrifuged at 18,000 *rpm* (Thermo Scientific, Heraeus Megafuge 40R) for 5 minutes before 2x washes in 20 mL RPMI wash media (500 mL RPMI, 1% Penicillin/Streptomycin, 1% L-glutamine). PBMCs were resuspended in a 10 mL volume of culture media (500 mL RPMI, 1% Pen/Strep, 1% L-glutamine, 10% FCS) and counted on an automated CASY® Counter (TTC model), using a programme set to measure a cell diameter range of 5.75 μM – 15 μM. PBMCs were resuspended at a final concentration of $1x10^7$/mL and split into 2x 1.5 mL Eppendorf tubes for pelleting by centrifugation at 3,000 *rpm* (Thermo Scientific, Heraeus Megafuge 40R) for 5 minutes. PBMCs were then resuspended in 1 mL TRIzol™ reagent (Ambion), mixed and incubated for 5 minutes at 37ºC before being snap-frozen on dry ice and stored at -70ºC.

2.2.1.4 Samples for *ex vivo* Parasite RNA-sequencing

At day of diagnosis (ranging C +7.5 – C +10.5), a 50 mL volume of blood was collected into lithium heparin tubes (Grenier Bio-One) for isolation/purification of *P. falciparum* parasites (see chapter 4, section 4.4.2).

On the day of challenge, 2 mL of (surplus) blood-inoculum used to infect the volunteers were collected and transferred in to 2x 1.5 mL Eppendorf tubes. Samples were centrifuged at 3,000 *rpm* (Beckman Coulter, Allegra x-12 R) for 5 minutes before aspirating the supernatant and resuspension of the pellets in 1 mL TRIzol™ reagent. Resuspended samples were mixed by pipetting and then incubated at 37°C for 5 minutes, to ensure thorough homogenisation. Samples were snap-frozen on dry ice and stored at -70°C prior to RNA extraction (see chapter 4, section 4.4.3).

2.3 Statistical Analysis*

Unless otherwise stated, statistical analyses were performed using GraphPad Prism (software version 7.0b). For comparisons between different time-points within the same group of volunteers, a Wilcoxon signed-rank test was used. For comparisons between different volunteer groups, a non-parametric, unpaired U-test was used (Mann-Whitney). Pairwise comparisons (correlation analyses) were performed using non-parametric, two-tailed Spearman's rank correlation.

Chapter 3: Diversity in the Host Response to *P. falciparum* Infection

3 Diversity in the Host Response to *P. falciparum* Infection

3.1 Abstract

In areas where malaria is endemic, severe disease is associated almost exclusively with children under the age of five, having had little or no previous exposure to the *Plasmodium* parasite. A better understanding of the earliest immune responses to *P. falciparum* in the malaria-naïve is thus of great importance. Herein, controlled human malaria infection was used to investigate the early immune events following primary infection of 14 healthy volunteers with blood-stage *Plasmodium falciparum*. Furthermore, responses were compared among individuals to assess diversity in the host response. By day 8 of infection, a dichotomous pattern of gene expression was detected in the blood, with volunteers responding by up-regulation of genes classically associated with the innate inflammatory response, or by down-regulation of genes linked to inflammation, cell signaling and metabolism. Four volunteers in the cohort failed to elicit an immune response in the time frame assessed. The observed inter-individual variability in host transcriptional responses correlated with chemokine levels in the plasma, but not with parasite growth kinetics in the blood. These results highlight the need for further investigation into factors driving diversity in the human response to *Plasmodium falciparum.*

3.2 Introduction

Malaria has an associated pattern of disease that ranges from asymptomatic, to death, with children under the age of five, living in sub-Saharan Africa, being at greatest risk of severe disease (WHO malaria report, 2017). Recent evidence has suggested that immunity to severe (life-threatening) disease occurs rapidly in areas where transmission rates are high, and often within the first few years of life (Goncalves *et al.* 2014). This paradigm suggests for an essential role of the innate immune response, at a time where limited exposure to the parasite has not yet afforded a build-up of protective antibodies (Molineaux *et al.* 2002, Langhorne *et al.* 2008). However, it is not yet clear why certain children respond more adversely to infection than others, and the molecular mechanisms that underpin such inter-individual variability are not well understood. The ability to mount an effective immune response to infection is determined by a combination of factors including environmental exposure, and host genetics (Oosting *et al.* 2016, Ter Horst *et al.*

2016). Thus, interpreting how immunity to *Plasmodium* infection develops is complex. Most observations of the human response to *P. falciparum* have been made in the setting of natural infection where previous exposure, infective dose, developing immunity, genetic variability and co-infections are confounding factors. Moreover, the short time-window in which to monitor the earliest of immune responses is extremely limiting in this setting.

Studies of malariatherapy, dating back to the early twentieth century, provided the first evidence for inter-individual variation in host responses to controlled *Plasmodium* infection. In a setting where parasite strain, dose and level of previous exposure was controlled for, individuals displayed marked differences in their ability to control parasite growth, and in the severity of symptoms presented (Collins and Jeffery 1999, Collins *et al.* 2004). Concordant with this, heterogeneity in innate immune responses has been reported in individuals experimentally infected with *P. falciparum* sporozoites (Walther *et al.* 2006) and more recently, in volunteers infected by direct blood inoculation of *P. falciparum*-infected erythrocytes (Burel *et al.* 2017). Therefore, the diversity in the human response to controlled *P. falciparum* infection, and the immune mechanisms underpinning such diversity, warrants further investigation.

Controlled Human Malaria Infection (CHMI) offers a unique opportunity to study the earliest molecular events following primary exposure of the human immune system to *P. falciparum;* the species responsible for the most severe forms of malaria disease. Infecting volunteers by direct blood inoculation (blood-stage model) ensures that every individual receives an identical immune challenge, whereby the dose and timing of parasites entering circulation is stringently controlled (Duncan and Draper 2012, Payne *et al.* 2016). By sampling volunteers over a time-course of infection, we can begin to investigate the order and timing of key immune events, whilst assessing inter-individual variability in host responses.

3.3 Hypotheses and specific aims

This chapter investigates the hypotheses that individuals demonstrate variability in response to controlled *P. falciparum* infection, and that the type of immune response produced will influence parasite growth in the circulation, or vice versa.

Specific aims

1. To characterise the earliest immune events in response to primary infection with *P. falciparum,* and assess inter-individual variation within the cohort.
2. To investigate a relationship between host immune response(s) and parasite growth in the circulation.
3. To predict the associated clinical outcome(s) in volunteers, using biomarkers of severe disease.

3.4 Methods

3.4.1 List of Materials

Reagent	Supplier	Catalog Number
1.5 mL DNA LoBind Eppendorf® tubes	Eppendorf	22431021
50 mL Falcon tubes	Becton Dickinson (BD)	352098
Sterile D10 ST pipette tips	Gilson	F171101
Sterile D200 ST pipette tips	Gilson	F171301
Sterile D1000 ST pipette tips	Gilson	F171501
Tempus™ Blood RNA Tubes	Applied Biosystems	4342792
Tempus™ Spin RNA Isolation Kit	Applied Biosystems	4380204
AbsoluteRNA wash solution	Applied Biosystems	4305545
RNA 6000 Nano Chip Bioanalyzer Kit	Agilent	5067-1511
Ultrapure DEPC H_20	Thermo Fisher Scientific	750024
Anti-*Pf*HRP2 IgM	Abcam	ab9206
Anti-*Pf*HRP2-HRP IgG	Abcam	MPFG-55P
Casein in PBS blocking reagent	Thermo Fisher Scientific	37528
NUNC MaxiSorp 96 well, flat-bottom ELISA plates (uncoated)	BioLegend	423501
1x PBS	Gibco	20012-019
Recombinant *Pf*HRP2 protein	Gifted from Dr david Sullivan, John Hopkins University	-
Sulfuric acid (1-2M)	Sigma-Aldrich	339741-100ML
TMB Substrate	Sigma-Aldrich	T0440-100ML
Angiopoietin-2 Quantikine ELISA Kit	R&D Systems	DANG20
LEGENDplex™ custom-panel kit for 13 analytes (Human)	BioLegend ®	92919
MultiScreen® HTS Vacuum Manifold	(Merk) Millipore	MSVMHTS00
Nunc 96-well v-bottom Microwell plates	Scientific Laboartoy Supplies	249570
Sterile, Low protein Binding 96-well plates with 1.2 µm filter wells	(Merk) Millipore	MSBVS1210
Anti-CMV IgG Human ELISA Kit	Abcam	ab108724

3.4.2 Volunteer Sample Collection

For analysis of the host transcriptional response to infection with *P. falciparum,* volunteers were bled (3 mL into Tempus™ Blood RNA Tubes, Applied biosystems) the day before challenge (C -1), and at 48 hour intervals post infection (C +2, C +4, C +6, C +8…) up to (and including) day of diagnosis (see figure 2.1). Immediately following blood-draw, tempus tubes were shaken for 10 seconds to ensure thorough mixing, as per manufacturer's guidelines. Tubes were frozen and stored at -70°C prior to RNA extraction.

3.4.3 Baseline Controls Bleeds

To control for every-day fluctuations in host gene expression, four volunteers were recruited at the University of Edinburgh to act as uninfected (baseline) controls. Volunteers were bled (3 mL into Tempus™ Blood RNA Tubes, Applied biosystems) over a time course matched with that of the infected volunteers during CHMI (every 48 hours, over a period of 12 days). The uninfected volunteers (2 male, 2 female) were white Caucasian, had a mean age of 24 years (22 – 25 years), with no previous history of malaria infection.

3.4.4 RNA Extraction

RNA extraction was done using the Tempus™ Spin RNA Isolation Kit (Applied Biosystems). Note that this kit is not compatible for the isolation of small RNAs (<200 nt in length), due to the low molecular weight cut-off from the columns provided (approximately 200 bp). In brief, samples were thawed at room temperature, topped up to 12 mL volumes with 1x PBS (Tempus™ Spin RNA Isolation Kit) and mixed before centrifugation at 3,000g at 4°C for 30 minutes. The supernatant was discarded, and the pellet resuspended in 400 µl of "RNA Resuspension Solution" for transferal to a spin filter for a series of 30 second centrifugation spins at 16,000g and 4°C, using the wash solutions provided. A DNAse treatment step using "AbsoluteRNA wash solution" (Applied Biosystems), for 20 minutes at room temperature, was included for the removal of genomic DNA. The purified RNA was incubated in 100 µl "Nucleic Acid Purification Elution Solution" for 2 minutes at 70°C before being eluted off the filter.

3.4.5 RNA Quantification and QC

Samples were quantified by nanodrop (ND-1000, software version 3.5.2) and normalised to a final concentration of 50 ng/µl in DEPC H_20 (Thermo Fisher Scientific), where possible. The ratios of absorbance at A260nm/280nm and A260nm/230nm were used to assess sample purity, with an A260/280 ratio of ~2.0 and an A260/230 ratio of 2.0-2.2 generally accepted as "pure" for RNA. The Agilent 2100 Bioanalyzer, RNA 6000 Nano chip assay for total eukaryotic RNA (RNA concentration range of 25 ng/µl -500 ng/µl) was used to assess the RNA integrity number (RIN), as per the manufacturer's instructions. A RIN value of $\geq$ 7.0 is generally accepted as being indicative of high quality RNA for use in downstream molecular applications.

3.4.6 Microarray for Whole-blood Transcriptome Analysis

Preparation of RNA samples for microarray analysis, and running of the microarray itself was performed by Dr Robert Holt, and others, at Hologic (Tepnel Pharma Services, West Lothian, UK). Data acquisition and sample QC was performed by Dr Alasdair Ivens at the University of Edinburgh.

3.4.6.1 Sample Randomisation and Microarray

RNA samples were randomized and assigned a sample code before shipment to Hologic, blinding them to sample identity. This measure was taken to ensure unbiased sample-chip positioning, and provides confidence that any differential intensity observed is more likely to reflect true differential expression. Samples were assessed using the Affymetrix GeneChip® human Transcriptome Array (HTA, version 2.0: www.affymetrix.com); designed for improved detection of transcript isoforms, compared to previous chip versions. 70% of probes comprising the HTA v2.0 are designed to cover exons for coding transcripts, and the remaining 30%, to cover exon-exon splice junctions and non-coding transcripts.

3.4.6.2 Data Acquisition and Sample QC

Data was acquired using the function rma (robust multi-array average) from the package affy (Gautier *et al.* 2004), for background correction and probeset

summarisation. Samples were QC analysed using the *arrayQualityMetrics* package in Bioconductor (Kauffmann and Huber 2010). The package utilises three visualisation tools to score arrays and identify outliers, namely: the MA plot, the boxplot and heatmap. An array was classed as an outlier if it was detected as such for two or more of these matrices.

3.4.7 Gene expression analysis

All steps involved in the conceptual/biological analyses of the host transcriptional response were derived from myself, with contribution from my two supervisors. All statistical analyses and graphical presentations of the microarray data, were done in collaboration with Dr Alasdair Ivens (University of Edinburgh), using R-Bioconductor. Samples collected the day before challenge (C -1) served as internal baseline controls for the corresponding volunteers, whereas expression values from the four uninfected volunteers provided a background cut-off for the level of variance expected due to everyday fluctuations in gene expression. Analysis was performed on transcripts of known protein-coding function only, and excluded all small RNAs of < 200 nt in length (see section 3.4.4).

3.4.7.1 Top 100 most variably expressed genes through time

In order to determine potential diversity within the cohort, patterns of differential gene expression unique to each individual were first assessed. To ensure that even the earliest of events would be detected, a list of the top 100 most variably expressed genes through time (C -1 through to day of diagnosis) was composed for each volunteer. Top 100 gene lists were created by **1)** calculating the within-gene median expression through the patient time-course (for every gene in the dataset) **2)** calculating the difference from that median at each time-point in the patient time-course **3)** calculating the variance of these differences, to give one value per gene **4)** sorting genes based on this variance value (high – low), and selecting the top 100. Volunteer gene lists were selected independently and thus are unique to each individual. Heatmaps were created using the *Heatmap.2* software package (R-Bioconductor).

3.4.7.2 Global gene set analysis

The global gene set was used for determining overlapping expression profiles within the cohort. The gene set was composed by pooling the 'top 100' genes for each of the 14 volunteers (n = 1,400 genes), and then removing any shared (redundant) genes from the list. This resulted in a set of 517 genes for analysis, which was applied to all 14 infected, and the 4 uninfected controls. Principle component analysis (PCA) was performed on the 517 gene set for **1)** all infected, all time-points (82 samples) and **2)** all infected, diagnosis time-point only (14 samples). PCA plots were created in 3 dimensions, using the *PCA-prcomp* software package (R-Bioconductor).

3.4.7.3 Analysis of within-volunteer "distance travelled"

For assessment of the within-volunteer "distance travelled", Principle Component Analysis was performed on each individual, using expression data restricted to the 517 global gene set. Data was plotted in 2-dimensions: PC1 against PC2, covering the largest proportion of variance observed within the volunteer dataset. Once plotted, the distance travelled between each sequential time-point in the volunteer time-course was calculated using Pythagoras Theorem ($a^2 + b^2 = c^2$). "Total distance" was taken as the sum of each sequential distance travelled, and "final distance", calculated by drawing a direct line between the first time-point and the last.

3.4.8 Ingenuity Pathway Analysis

Ingenuity pathway analysis (IPA) core analysis (IPA®, QIAGEN Redwood City www.qiagen.com/ingenuity) was utilised to investigate the canonical pathways significantly perturbed during primary *P. falciparum* infection. IPA utilises the Ingenuity knowledge base; built upon a wide range of published information including textbooks, reviews, biomedical literature and a variety of public databases to provide insight into molecular and chemical interactions in the context of human disease and infection.

So as to extend analysis beyond the 517 global gene set, and to give more statistical power to the software, all gene features on the array were considered for IPA. Genes without annotation, and those encoding small RNAs (< 200 nt in length)

were excluded. To investigate pathways associated with the variability in host response, analysis was performed on genes differentially expressed between the “classical” and “non-classical” responder groups at diagnosis, using an adjusted p-value cut-off of 0.05. To investigate the pathways associated specifically with members of the “classical” and “non-classical” responder groups, individual analysis was performed on volunteers 16 and 19, respectively. In this instance, genes demonstrating a ≥ 1.5 fold change at diagnosis (relative to median expression) were considered. IPA was also used to predict the upstream regulators responsible for the gene expression patterns observed in the dataset. The analysis examines the known targets of each upstream regulator, and compares the targets’ direction of change to expectations derived from the literature. The software then issues a prediction of downstream activation or inhibition (z-score). IPA does not make an activation or inhibition prediction for the upstream regulator itself, but provides a value of significant overlap (Fisher’s Exact p-value), based on known interactions from published data.

3.4.9 PfHRPII ELISA

An ELISA was set up to quantify levels of *P. falciparum* Histidine Rich Protein II (PfHRPII) in the plasma of volunteers. The protocol was modified from that used with the commercially available ‘Anti-HRP2 ELISA kit’ (Celllabs), and from that previously published (Martin *et al.* 2009)**.** In brief, wells of a 96-well ELISA plate (BioLegend) were coated with 100 µl anti-HRP2 IgM antibody (1 µg /mL), overnight at 4^{o}C and then blocked using 200 µl/ well of Casein buffer (1% w/v casein in PBS, Thermo Fisher Scientific) for 2 hours at room temperature. Supernatant was removed and wells of the plate washed x3 in 200 µl/ well Casein buffer. 50 µl of plasma samples were diluted in an equal volume of Casein buffer before addition to the plate. The standard curve was prepared by diluting recombinant PfHRPII protein (Dr David Sullivan, John Hopkins University) to 125 ng/mL in PBS and making 1:2 serial dilutions to cover the range; 125 ng/mL – 0.061 ng/mL. “Blank” wells of PBS served as negative controls. Plasma samples, controls and standards were added to the plate (in duplicate), and the plate sealed for incubation at room temperature for 1 hour. Supernatants were discarded and the plate washed x3 in Casein buffer before addition of 100 µl anti-HRPII IgG-HRP conjugate antibody (0.05 µg /mL) to each well. The plate was then incubated for 1 hour at room temperature before 3x

washes with PBS (200 µl/well). 100 µl of 3,3',5,5'-tetramethylbenzidine (TMB) substrate was then added to each well of the plate, and plate incubated for 5 - 10 minutes, whilst protected from light. The reaction was stopped with use of 1M Sulfuric acid (50 µl/well) and optical densities determined by use of a microplate reader (Multiskan Ascent, Lab systems) with wavelength set to 405 nm. Standard curves were constructed by plotting mean absorbance of each standard (y-axis) against (log10) concentration (ng/mL) on the x-axis and interpolating using the Sigmoidal, 4 PL function in GraphPad Prism.

3.4.10 LEGENDplex™ for Quantification of Cytokines/Chemokines in Volunteer Plasma

A chosen set of 12 analytes; CCL2 (MCP1), CXCL9 (MIG) CXCL10 (IP-10), Interferon alpha (IFNα), Interferon gamma (IFNγ), Interleukin-1β (IL-1β), Interleukin-6 (IL-6), Interleukin-8 (IL-8), Interleukin-10 (IL-10), Interleukin-17 (IL-17), Interleukin 18 (IL-18) and Tumour necrosis factor alpha (TNFα), were quantified in the plasma of volunteers using a custom-designed multiplex assay from BioLegend® (www.biolegend.com/legendplex). Plasma collected at time-points spanning the full infection time course (including baseline), for 13 of the 14 volunteers was screened. These samples, run in duplicate (and with the inclusion of standard and control samples) reached maximum kit capacity and hence one volunteer (volunteer #20) was excluded. Plasma sample were not collected for the 4 uninfected (baseline) controls.

Plasma samples were diluted 1:2, and standard prepared by making 1:4 serial dilutions of stock (8-point standard curve). The assay was performed as per the manufacturer's guidelines in 2x 96-well, low protein-binding filter-bottom plates (Merck). In brief, wells were wetted with 100 µl of 1x "wash buffer", plates incubated at room temperature for 1 minute, and then placed on a vacuum manifold (MultiScreen® HTS, Merck) (≤ 10 Hg applied for 5-10 seconds) for removal of residual liquid from the wells. 25 µl of "matrix B" and "assay buffer" was added to the standard and test sample wells, respectively, before addition of 25 µl standard and plasma to the appropriate wells. The aliquot of mixed beads was vortexed before addition to each well on the plate, in 25 µl volumes. Plates were then sealed, covered to protect from light and incubated at room temperature for 2 hours, on a

plate shaker set to 500 *rpm* (ThermoMixer C, Eppendorf®). Following incubation, supernatant was filtered from the wells using the vacuum manifold, as before and then plate washed x2 with 200 µl/ well of "wash buffer". 25 µl of detection antibodies were added to each well, plate sealed, covered and then incubated for 1 hour before the addition of 25 µl of Streptavidin-Phycoerythrin (SA-PE) to each well. Plates were incubated for 30 minutes at room temperature, supernatant filtered, and the plate washed x2 using 200 µl/well of "wash buffer". Beads were resuspended in 150 µl "wash buffer" using the plate shaker and then transferred, as appropriate, to 2x Nunc 96 well v-bottom plates (Scientific Laboratory Supplies) for running on the flow cytometer. Fluorescence was measured using an automated plate counter and BD™ LSRFortessa™ flow cytometer running FACSDiva™. The PE (575 – 585 nm) and APC (660 nm) channels were used for bead classification, according to PMT voltages that had been set up in advance, using the "Setup Beads-3" provided with the kit. Samples were read in the order prescribed by a template containing details of sample/plate layout, and data analysed using the LEGENDplex™ data analysis software provided with the kit. Data is presented as the raw concentrations (pg/mL) through time, and as fold-change from baseline, at each subsequent time-point in the infection time course. Fold-change was calculated by dividing the concentration measured at C +2, C +4, C +6 etc, by the concentration as measured the day before challenge (C -1) for each corresponding volunteer. In the event where analytes were undetectable, samples were assigned the largest integer below the limit of detection for that particular analyte (details of which were provided in the kit manual).

3.4.11 Angiopoietin-2 ELISA

Levels of Angiopoietin-2 (ANG-2) in volunteer plasma were quantified using the Human Angiopoietin-2 Quantikine ELISA kit from R&D Systems, as per the manufacturer's instructions. Plasma collected at baseline (C -1) and day of diagnosis for each of the 14 volunteers was assayed in duplicate (n = 56 samples). In brief, plasma samples were diluted five-fold using the "Calibrator Diluent" provided with the kit, and standard prepared by 2-fold serial dilutions of the standard stock (final range; 3,000 pg/mL – 46.9 pg/mL). 100 µl of "Assay Diluent" was added to each well of the plate followed by 50 µl of standard, control or sample (to appropriate wells) for a 2-hour incubation at room temperature, using a microplate shaker (ThermoMixer C, Eppendorf®) set to 500 *rpm*. Wells were aspirated and

washed x4 in 400 µl “Wash Buffer”, ensuring complete removal of liquid after each wash. 200 µl of the “Human Angiopoietin-2 Conjugate” was added to each well and the plate incubated as before. The plate was washed x4 and then 200 µl of “Substrate Solution” was added to each well for 30 minutes incubation at room temperature. 50 µl of “Stop Solution” was then added to each well and within 30 minutes, the optical densities (O.D) were determined with use of a microplate reader (Multiskan Ascent, Lab systems), by subtracting readings measured at 570 nm wavelength from readings measured at 450 nm wavelength. Sample and standard readings were background-corrected by subtracting the mean O.D reading taken from duplicate “blank” wells containing 150 µl of “Assay Diluent”. A standard curve was constructed by plotting the mean absorbance of each standard (y-axis) against concentration (pg/mL) on the x-axis and drawing a line of best fit (R^2value = 0.998). Levels of ANG-2 in the plasma were read off the curve and multiplied five-fold to correct for the original 1:5 dilution made. Data is presented as the mean of duplicate samples.

3.4.12 Anti-Cytomegalovirus (CMV) IgG ELISA

Qualitative assessment of Anti-CMV IgG antibodies in volunteer plasma was done using the Anti-CMV IgG Human ELISA Kit from Abcam, as per the manufacturer’s guidelines. In brief, plasma samples collected at baseline (C -1) from the 14 infected were diluted 1:100 with “IgG Sample Diluent”, and added (in duplicate) in 100 ul volumes to wells of the pre-coated plate. 100 µl of the “CMV IgG positive control”, “negative control” and “CMV IgG cut-off” solutions were then added, in duplicate and two wells of 100 µl PBS served as the substrate “blank”. Wells were covered in foil, and incubated for 1 hour at 37^{o}C before aspiration of supernatant and 3x washes with 300 µl of 1x “Wash Solution”. Wells were then inverted and blotted to ensure removal of residual liquid before addition of 100 µl “CMV anti-IgG HRP conjugate”, for incubation at room temperature for 30 minutes. After another 3x washes with 1x “Wash Solution”, 100 µl “TMB Substrate Solution” was added to each well, and plate incubated for exactly 15 minutes at room temperature, protected from light. “Stop Solution” was then added (100 µl/ well) and optical densities read by measuring absorbance at both 450 nm and 620 nm on a microplate reader (Multiskan Ascent, Lab systems). The mean, background-subtracted absorbance was calculated for each sample, and compared to the mean absorbance value of the “CMV IgG Cut-off

control". The "CMV IgG Cut-off control" is a titration of the purified human anti-CMV IgG, used for the positive control. Samples were considered positive if their absorbance value was >10% over the cut-off value, by converting O.D values to Standard Units using the following equation: (mean) absorbance value [x10] / (mean) absorbance value for the cut-off control. The cut-off control = 10 standard units, samples with < 9 standard units are defined as CMV-negative, and samples with > 11 standard units are defined as CMV-positive.

3.5 Results

3.5.1 Volunteer Characteristics

Infected volunteers had a mean age of 24 years (ranging 19 – 34 years) and were 71% Male (table 3.1). Mean time to qPCR detection and thick smear positivity (prepatent period) was 5 days (5 – 7 days) and 9 days (7.5 – 10.5 days), respectively. Parasitaemia (p/mL) at diagnosis ranged 1,440/mL - 273,247/mL and parasite multiplication rates (mean; 10.0 and range; 6.7 – 12.8) were comparable with that of previous CHMI studies using *P. falciparum* 3D7-strain (Roestenberg *et al.* 2012, Sheehy *et al.* 2013).

Table 3.1 | Volunteer characteristics

Volunteer i.d	Age (years)	Gender	Country of birth	Time to qPCR detection (days)	Parasite Multiplication Rate (PMR/48 hours)	Prepatent period (days)	p/mL at diagnosis
12	20	M	UK	5.0	12.8	7.5	1,645
13	27	M	Belgium	5.0	8.9	10.5	70,368
16	21	M	UK	5.0	11.9	10.0	273,247
17	34	M	Albania	6.5	6.7	10.5	16,911
18	23	F	Switzerland	5.0	11.3	8.5	19,670
19	20	M	UK	5.0	9.7	8.5	6,932
20	27	M	UK	5.0	12.8	8.5	15,025
22	19	F	UK	7.0	6.8	10.0	8,865
24	20	M	UK	5.0	9.4	10.0	43,707
26	24	F	UK	5.0	9.9	9.0	9,133
27	19	M	UK	5.0	11.2	9.0	13,421
106	22	F	UK	5.0	11.3	8.5	16,162
206	29	M	Kenya	5.0	9.9	10.0	185,576
208	34	M	Pakistan	5.5	7.1	9.0	1,440

3.5.2 RNA quality

The Agilent bioanalyzer software tool calculates RIN scores based on the ratio of the ribosomal bands as well as the presence or absence of degradation products. RIN values ranged from 6.5 - 9.9 (figure 3.1), with 98% of samples having RIN

scores of > 7, indicative of high quality RNA. All 114 samples were processed for microarray analysis.

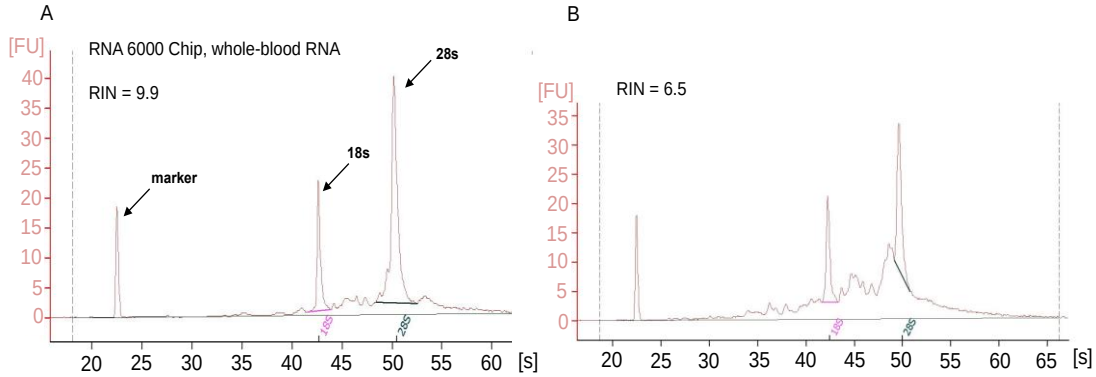

Figure 3.1 | Bioanalyzer electropherograms of total RNA from two representative samples of highest (A) and lowest (B) achieved RNA integrity. Y-axis shows fluorescence units (FU) against time in seconds (s) on the x-axis. Peaks represent; marker, mRNA, 18s subunit and 28s subunit ribosomal RNA. (Plots generated through the bioanalyzer (Agilent Technologies)).

3.5.3 Sample Exclusion

Based on the QC criteria, 7 samples in the microarray dataset were identified as outliers. Failed samples included; C -1 and C +4 for volunteer #26, C +2 for volunteer #27, C +4 for volunteer #208, C -1 and C +6 for baseline control number 3 (BC.3) and C +12 for BC.4, resulting in incomplete time-courses for these volunteers.

3.5.4 The Host (Whole Blood) Transcriptional Response to *P. falciparum* Infection

3.5.4.1 Diversity in the host (whole blood) transcriptional response to blood-stage *P. falciparum*

To assess diversity in the host response to *P. falciparum* infection, a list of the top 100 most variably expressed genes through time (C -1 through to day of diagnosis) was composed for each individual, and thus patterns of gene expression compared. Top 100 gene lists are provided for the 14 infected and 4 uninfected volunteers, in Appendix 3. In figure 3.2, top 100 genes are presented as heatmaps of the log-2 fold change (deviation from median expression), through time (positive fold-changes in red and negative fold-changes in blue).

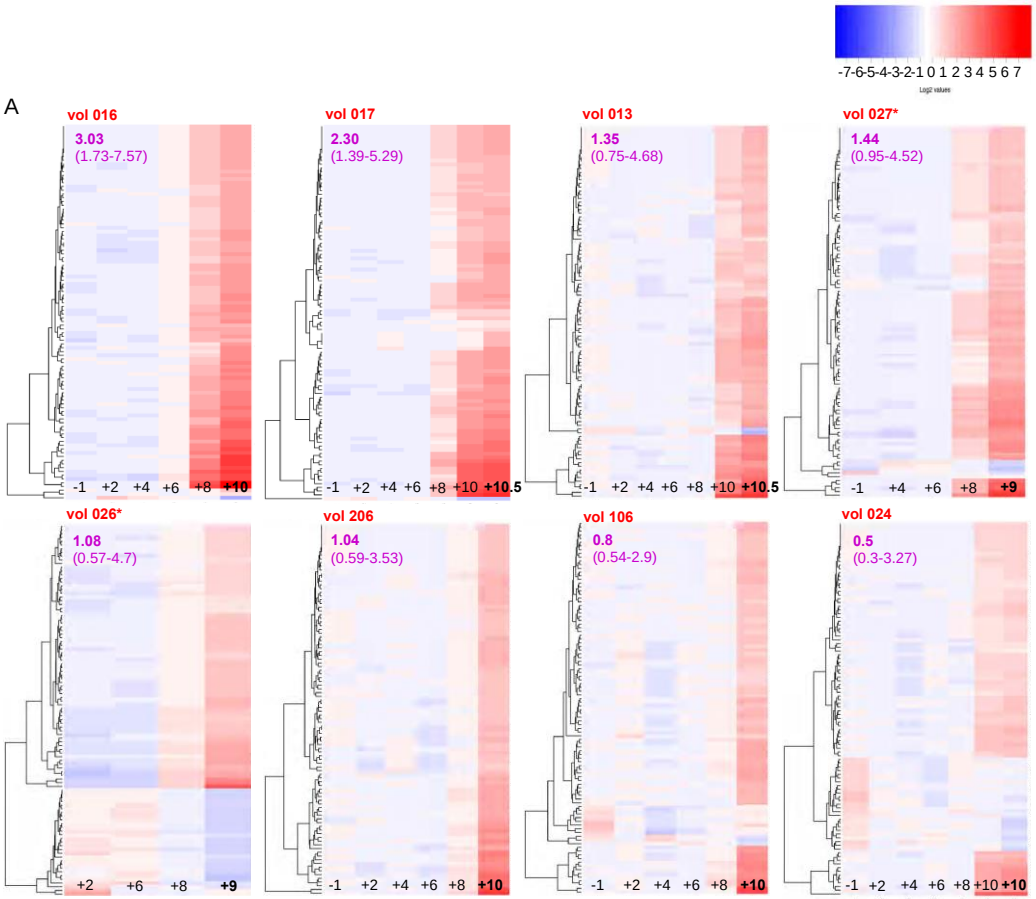

Figure 3.2 (Part A) | Diversity in the host transcriptional response to *P. falciparum* infection (legend continues on next page)

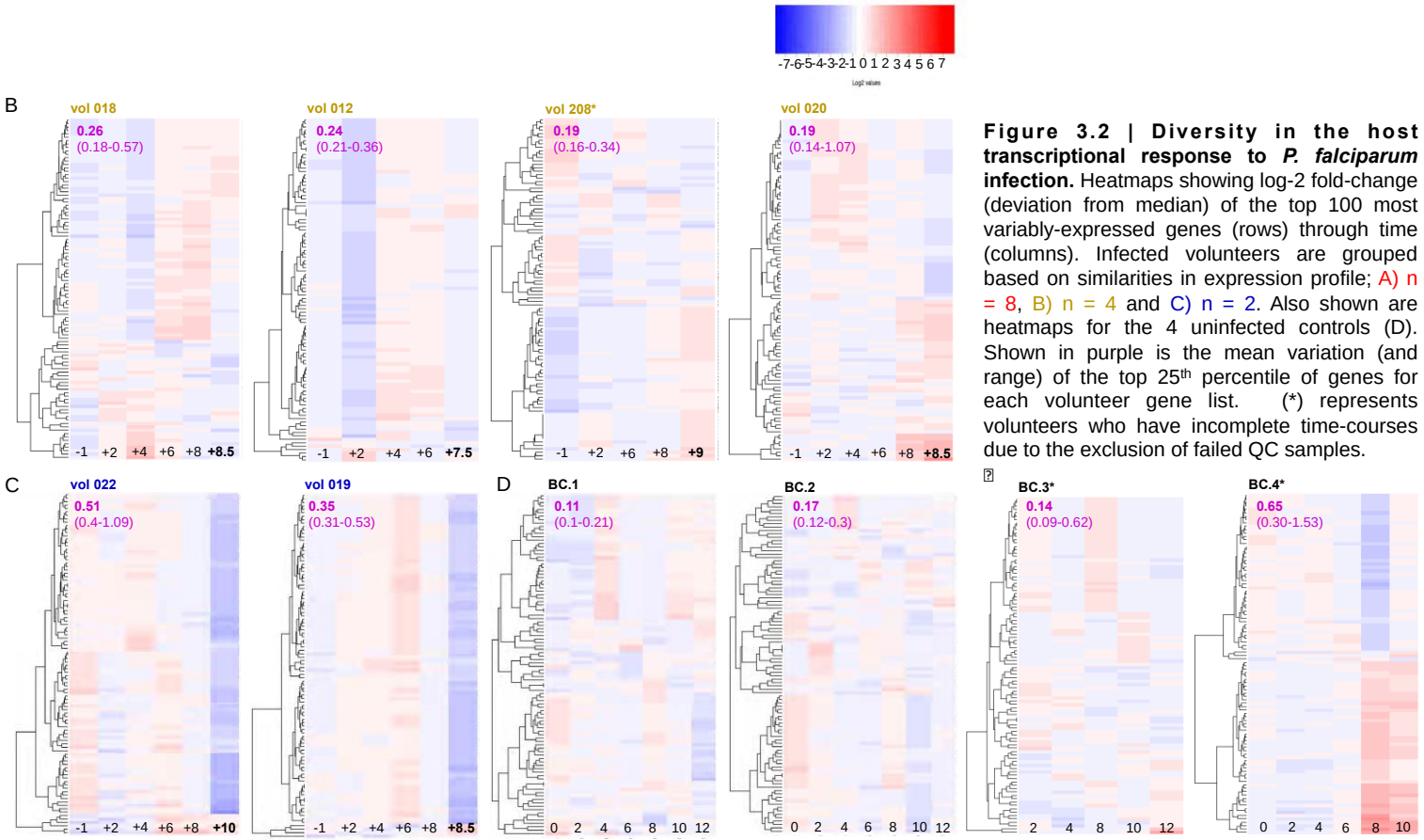

Figure 3.2 | Diversity in the host transcriptional response to *P. falciparum* infection. Heatmaps showing log-2 fold-change (deviation from median) of the top 100 most variably-expressed genes (rows) through time (columns). Infected volunteers are grouped based on similarities in expression profile; A) n = 8, B) n = 4 and C) n = 2. Also shown are heatmaps for the 4 uninfected controls (D). Shown in purple is the mean variation (and range) of the top 25th percentile of genes for each volunteer gene list. (*) represents volunteers who have incomplete time-courses due to the exclusion of failed QC samples.

Figure 3.2 (Parts B, C &D) | Diversity in the host transcriptional response to *P. falciparum* infection

Based on these data, 8 of the 14 volunteers responded to *P. falciparum* malaria infection by up-regulating genes typically associated with the innate inflammatory response, namely: Interferon-stimulated genes (ISGs), members of the inflammasome activation pathway, complement receptors and pattern recognition receptors, as has been previously documented in studies of CHMI (Montes de Oca *et al.* 2016, Loughland *et al.* 2017). Of the most variably expressed genes in this set of volunteers, the most strongly up-regulated included CXCL10, a chemokine produced by many cells of the immune system in response to stimulation with IFNγ, and a biomarker associated with increased risk of cerebral malaria and death in infected humans (Jain *et al.* 2008, Wilson *et al.* 2011, Gotz *et al.* 2017). Also among the most variably expressed genes were FCγR1 (high affinity IgG Fc receptor); SERPING 1, involved in regulation of complement activation; CARD17, a regulator of IL-1β production; RSAD2, which encodes a protein of known anti-viral function and acts to promote production of Type1 interferons (IFNs) in plasmacytoid DCs, and STAT1/STAT2, the signal transducers and transcription activators that mediate cell response to IFNs. Interestingly, among the top 12 most variable genes for all 8 volunteers was CD274 (PDL-1), which encodes an inhibitory ligand which when bound to its PD1 receptor, acts to block T cell activation and cytokine production. On the other hand, 2 of the 14 volunteers in the cohort had a very different type of response, whereby a large proportion of their top 100 genes were suppressed in response to infection (figure 3.2, panel C). Genes down-regulated in these volunteers included the c-type lectins CLEC4E and CLEC7A, glycoproteins with cell signaling properties as well as functions in pattern recognition of mycobacteria and pathogenic fungi; ALAS2 and FECH, enzymes involved in the heme biosynthesis pathway; GYPA, the major intrinsic membrane protein of the erythrocyte, bearing receptors for the MN blood-group antigens, and a range of genes associated with cell signaling and metabolism eg LRRK2, MBOAT2 and RGS18. Four of the fourteen volunteers did not produce a detectable response in the time frame assessed (figure 3.2, panel B). When considering the variance levels for the top 25th percentile of “variable” genes (figure 3.2), these 4 individuals had levels comparable to that of the uninfected controls (mean variance of the top 25th percentile of genes in the 4 uninfected controls = 0.27). Notably, of the volunteers who did respond, their responses were undetectable in the blood until 8 days post-infection (C +8).

This was a surprising finding, and can perhaps be explained by the uncharacteristically low-dose inoculum given to volunteers in this CHMI study (~690 PEs). Inoculum dose has been shown to be inversely correlated with pre-patent period (Glynn and Bradley 1995). It is difficult to speculate how the 4 unresponsive volunteers would have gone on to respond if given more time before initiation of drug treatment. Based on their top 100 gene list, volunteer #20 had 54% of genes shared with those belonging to larger responder group, and looked as if they were trending towards up-regulation of said genes towards the end of their infection time course. However, based on variance levels, volunteer #20 was responding no more than the uninfected controls. The stringent cut-offs used for diagnosis in studies of CHMI (first microscopic detection of parasites), means that volunteer infections are terminated when parasitaemias are still magnitudes lower than would be observed in the field. Nevertheless, analysis of gene expression patterns, at multiple time-points in individuals receiving identical immune challenge, has revealed diversity in the host response to primary infection with *P. falciparum.*

3.5.4.2 Dichotomy in the host transcriptional response to blood-stage *P. falciparum* infection

Having established inter-individual variation in the host response to blood-stage infection with *P. falciparum*, volunteer profiles were compared using a global gene-set to determine potential groupings within the cohort. For this analysis, the top 100 genes for each volunteer were pooled to comprise a list of 1,400 genes. Given that many of the genes were shared between volunteers however, the final set of (non-redundant) genes used for analysis totaled just 517. A list of the 517 genes is provided in Appendix 4. Based on this global gene set, a heatmap displaying the raw expression data for each of the 14 infected, and 4 uninfected volunteers was created, allowing for direct comparison between volunteers (figure 3.3, part A). Visualising the data this way highlighted a dichotomy in the host response, whereby volunteers could be grouped as either “classical responders”: up-regulating clusters of genes linked to the onset of inflammation and Interferon responses (n = 8), or as “non-classical responders”: suppressing a completely different set of genes (n = 2). For the purpose of classification, volunteers that failed to elicit a response in the time frame assessed are hereon referred to as “unknowns” (n = 4). Based on their top 100 most variable gene lists, the 8 “classical” responders showed a significant

overlap in expression profiles, with the two most diverse volunteers in the group sharing 79% of genes. These 8 volunteers continued to demonstrate similar patterns of expression when the comparison was extended to the global gene set of 517, as clusters of genes being up- or down-regulated were consistent across all in the group. Another two of the volunteers could be also grouped based on a high percentage of overlapping genes in the global gene set (volunteer 22 had 59% of genes shared with volunteer 19). Importantly, the genes shared between these individuals were distinct from those of the 8 “classical” responders and were mostly down-regulated in response to infection. For confirmation of groupings by statistical means, Principle Component Analysis was performed on the (82) samples comprising the infection time courses for each of the 14 infected volunteers (figure 3.3, part B), as well as the (14) samples taken at the last, day of diagnosis time-point only (figure 3.3, part C). In PCA plot B a clear divergence is observed, with all 8 volunteers (in red) grouping separately from the rest of the volunteers at day of diagnosis. A similar observation was noted for the two “non-classical” responders (in blue) at day of diagnosis, but in the opposite direction along PC1; the Principle Component encoding the largest percentage of variance in the dataset. This confirmed the two groups to be distinct from one another in their transcriptional response to infection with *P. falciparum,* and thus established the use of the 517 global gene set for determining host responder status.

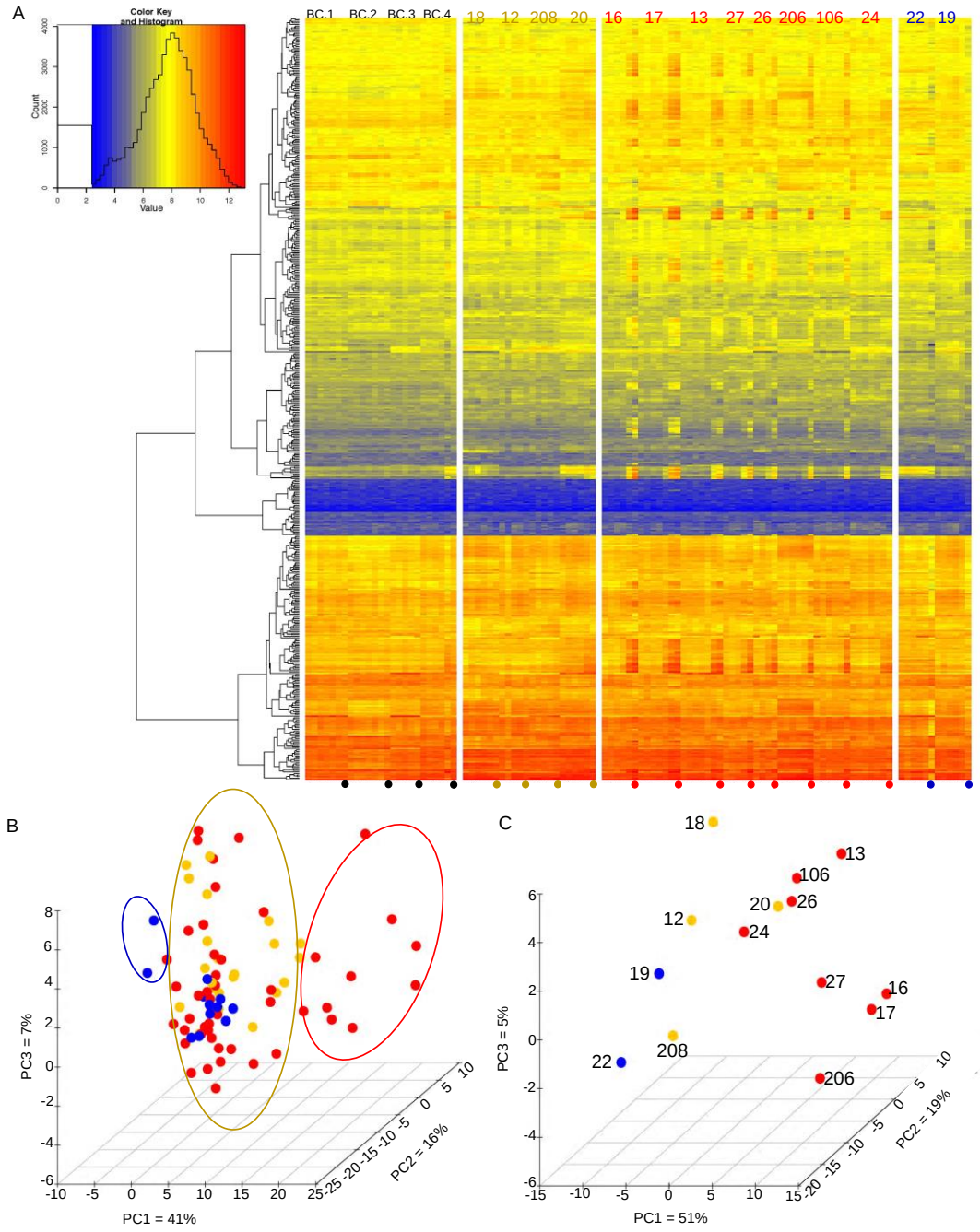

Figure 3.3 | Dichotomy in the host transcriptional response to blood-stage *P. falciparum* infection. **A)** Heatmap of raw expression data for the 517 genes (ordered by variance along the y-axis) through time (x-axis). Volunteers are grouped by similarities in expression profile and colour-coded as such; uninfected controls (black), "unknowns" (yellow), "classical" responders (red) and "non-classical" responders (blue). Volunteer I.Ds are shown along the top, and end-points (diagnosis) for each volunteer are marked by coloured dots along the bottom. **B)** Principle Component Analysis of the same 517 genes for the 82 samples comprising all time-points, for all infected volunteers and **C)** the 14 samples comprising day of diagnosis only (volunteer I.Ds are marked). The variation encoded by each principle component (1, 2 and 3) is presented along each axis, as a percentage of the total variation in the dataset.

3.5.4.3 Within-volunteer distance travelled

Another way to distinguish the responder volunteers from the "unknowns" was to consider the within-volunteer "distance travelled", or movement from baseline (C -1), through to day of diagnosis. Thus, Principle Component Analysis was performed to assess within-volunteer variation, and data plotted in two-dimensions: Principle Component 1 (PC1) against Principle Component 2 (PC2), accounting the majority of all variation encoded within the volunteer's dataset. The scaling of each PCA plot was set to match, and "distance travelled" between each time point calculated using "Pythagoras' Theorem" as previously described (section 3.4.7.3). Four individual PCA plots (one volunteer representative from each transcriptional group) are shown in figure 3.4; uninfected control BC.2, "unknown" responder 018, "classical" responder 016 and "non-classical" responder 022. Data presented highlights a far reduced "distance travelled" in the baseline control (BC.2) and the "unknown" responder (018) when compared to that of responder volunteers 16 and 22. This analysis was consistent with the classification of the "unknowns" based on their levels of gene variance (figure 3.2). A break-down of "distance travelled" and "final distance" is provided for each volunteer in Appendix 5.

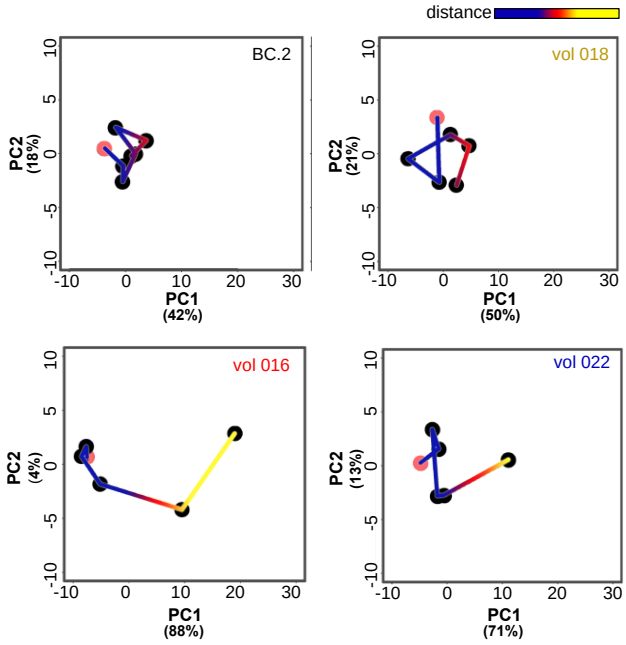

Figure 3.4 | Within-volunteer distance travelled. Analysis was performed using the 517 global gene set. Data is presented in 2- dimensions (PC1 on the x-axis against PC2 on the y-axis). Percentage (%) variance encoded by each PC is shown. Plots for one representative volunteer from each response group, plus one baseline control are shown; baseline control no. 2 (black), "unknown" volunteer 18 (yellow), "classical" responder volunteer 16 (red) and "non-classical" responder volunteer 22 (blue). Distance travelled is scaled as in the key shown above.

3.5.5 Hematological perturbations during acute-phase *P. falciparum* infection

When investigating inter-individual variation in gene expression patterns in peripheral blood, it is important to consider the relative proportions of specific blood cell subsets within each individual. Full blood counts (FBCs) were carried out by NHS staff in the haematology department at either one of the Churchill or John Radcliffe Hospitals in Oxford, at baseline (C -1), C +6 and day of diagnosis (DoD) for each volunteer. Measurements of total red and white cell counts per mL of blood, as well as a break-down of the contribution from individual leukocyte subsets; neutrophils, lymphocytes, monocytes, eosinophils and basophils were provided for each volunteer (Table 3.2).

Figure 3.5 (parts A – C) displays mean absolute cell counts within each responder group, at baseline, C +6 and day of diagnosis. Within the group of 8 “classical” responders; neutrophils, monocytes, eosinophils and basophils were within the healthy reference range, and showed little fluctuation in numbers throughout the course of infection. A significant drop in lymphocyte numbers (from $2.17x10^6$/mL to $1.01x10^6$/mL, $p = 0.0078$) was observed at diagnosis in these volunteers, however (figure 3.5, part A). This effect was due to a decrease in lymphocyte counts across all volunteers in the group, but was most marked in 3 out of the 8 individuals (16, 17 and 26), who became lymphopenic at diagnosis ($<1x10^6$ lymphocytes/mL of whole blood, figure 3.5 part D). Comparison of lymphocyte counts between groups did not reveal any significant differences, at any of the three time-points (table 3.2). Within the group of 2 “non-classical” responders, mean neutrophil counts were slightly below the healthy reference range at baseline and C +6: $1.77x10^6$/mL and $1.57x10^6$/mL, respectively, but increased at diagnosis ($2.76x10^{6/}$mL, not significant). Low neutrophil counts were observed in volunteer 22, specifically. A similar pattern was observed for lymphocyte numbers, whereas monocytes, eosinophils and basophils showed little fluctuation throughout the course of infection. In the case of the 4 “unknown” volunteers, all cell types were within the healthy reference range throughout, and showed little fluctuation in numbers. Thus, the only significant perturbation observed in response to blood-stage *P. falciparum* infection was a drop in lymphocyte counts at diagnosis, in the 8 “classical” responder volunteers. This was also evident when considering the relative blood cell proportions in each individual, at diagnosis compared to baseline (figure 3.5, part E and F). Given that

lymphopenia is a key feature of inflammatory disease, these data support transcript-level inflammation in the 8 “classical” responders. However, data also suggest a potential influence of differing cell proportions on the transcript-level variation observed within the cohort. Thus, in order to validate the diversity in host responses to *P. falciparum* infection, responses were also compared at the protein level.

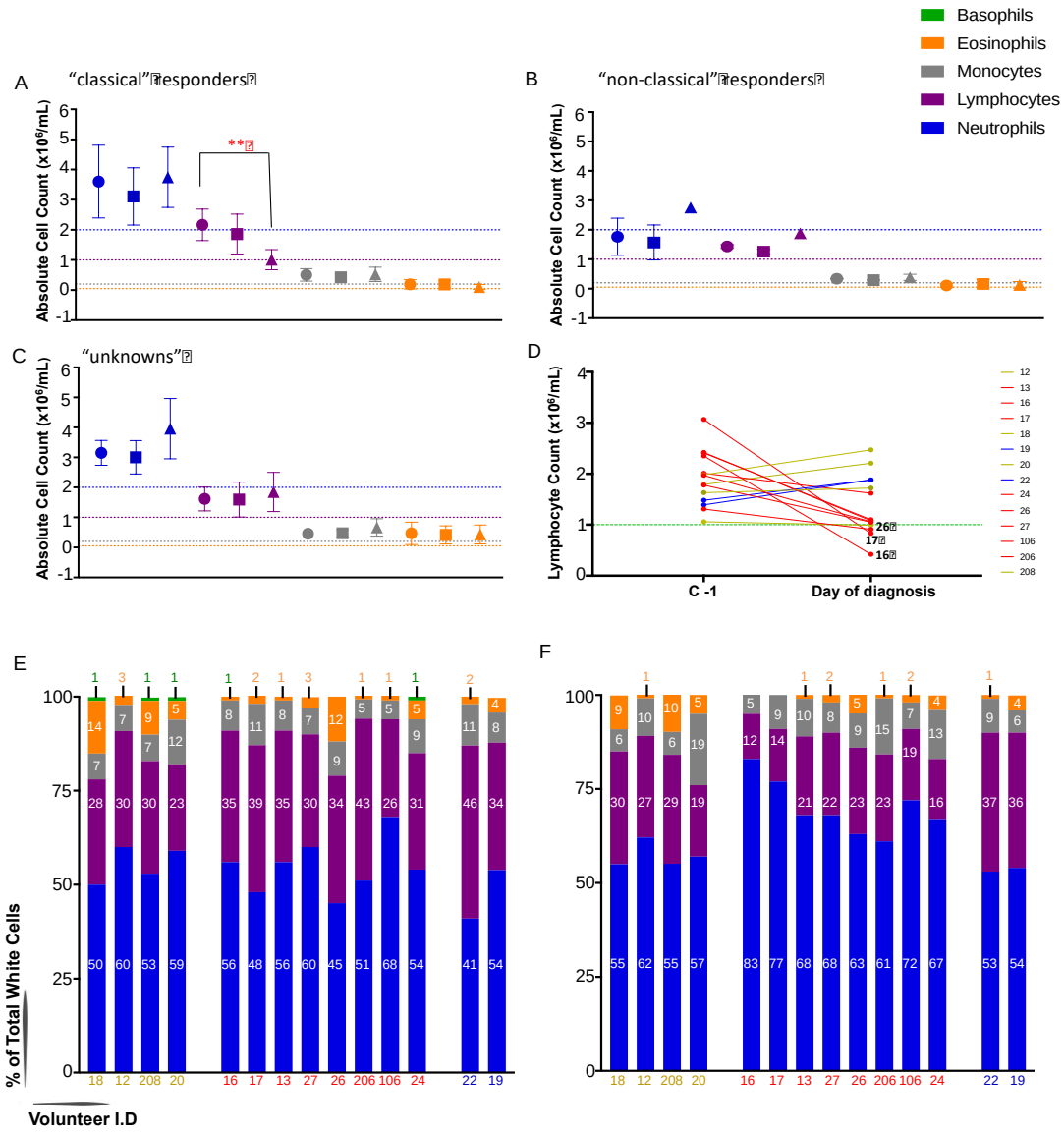

Figure 3.5 | Haematological perturbations during blood-stage *P. falciparum* infection. Top panel graphs show the absolute cell counts for neutrophils, lymphocytes, monocytes, eosinophils and basophils as measured at baseline (circles), C +6 (squares) and day of diagnosis (triangles) in the 8 "classical" responders (A), the 2 "non-classical" responders (B) and the 4 "unknown" volunteers (C). Data is presented as the mean and standard deviation. Coloured (horizontal) lines denote the lower cut-off of the healthy reference range for each corresponding cell subset. Statistical analysis was done using Wilcoxon signed rank test (** = significant drop in lymphocyte count at diagnosis in the "classical" responders, p-value = 0.0078). D) Lymphocyte counts at baseline (C -1) and day of diagnosis, presented for each volunteer in the; "unknowns" (yellow); "classical" responders (red) and "non-classical" responders (blue). Green line denotes lymphopenia at <1x10^6 cells/mL. Volunteer I.Ds for the three "classical" responders who became lymphopenic at diagnosis are shown. Bottom panel graphs show the percentage (%) of each cell subset contributing to total white cell count (y-axis) for each volunteer (x-axis) at baseline (E) and diagnosis (F). Numbers on bars (or attached to bars) denote the % of cells attributed to each cell type. A colour key for cell type is provided.

Table 3.2 | Full blood count analysis

	Neutrophils (x10^6/mL)			Lymphocytes (x10^6/mL)			Monocytes (x10^6/mL)			Eosinophils (x10^6/mL)			Basophils (x10^6/mL)			Total White Cells (x10^6/mL)			Platelets (x10^6/mL)			Erythrocytes (x10^9/mL)		
	2.0 - 7.0 (x10^6/mL)			1.0 - 4.0 (x10^6/mL)			0.2 - 1.0 (x10^6/mL)			0.0 - 0.5 (x10^6/mL)			0.0 - 0.1 (x10^6/mL)			4.0 - 11.0 (x10^6/mL)			150 - 400 (x10^6/mL)			3.8 - 5.5 (x10^6/mL)		
Volunteer I.D (diagnosis)	C -1	C +6	Diagnosis	C -1	C +6	Diagnosis	C -1	C +6	Diagnosis	C -1	C +6	Diagnosis	C -1	C +6	Diagnosis	C -1	C +6	Diagnosis	C -1	C +6	Diagnosis	C -1	C +6	Diagnosis
18 (C +8.5)	3.54	3.48	4.53	1.98	2.14	2.47	0.49	0.47	0.49	0.99	0.6	0.74	0.07	0.07	0.08	7.07	6.70	8.24	196.00	192.00	221.00	4.73	4.58	4.48
12 (C +7.5)	3.47	3.49	5.07	1.79	1.47	2.21	0.4	0.33	0.82	0.17	0.11	0.08	0.00	0.00	0.00	5.78	5.45	8.17	229.00	252.00	242.00	4.78	4.75	4.72
208 (C +9)	2.88	2.57	3.26	1.63	1.94	1.72	0.38	0.46	0.36	0.49	0.74	0.65	0.05	0.06	0.06	5.44	5.72	5.92	266.00	283.00	274.00	4.81	5.07	5.32
20 (C +8.5)	2.72	2.48	2.97	1.06	0.83	0.99	0.55	0.62	0.99	0.23	0.21	0.26	0.05	0.04	0.00	4.61	4.13	5.21	265.00	267.00	256.00	4.89	4.86	4.72
Group Mean	*3.15*	*3.01*	*3.96*	*1.62*	*1.60*	*1.85*	*0.46*	*0.47*	*0.67*	*0.47*	*0.42*	*0.43*	*0.04*	*0.04*	*0.04*	*5.73*	*5.50*	*6.89*	*239.00*	*248.50*	*248.25*	*4.80*	*4.82*	*4.81*
16 (C +10)	3.78	3.7	2.91	2.35	2.04	0.42	0.52	0.51	0.18	0.07	0.13	0	0.00	0.00	0.00	6.72	6.38	3.51	198.00	177.00	82.00	4.95	4.5	4.48
17 (C +10.5)	3.77	4.44	4.55	3.07	3.16	0.83	0.86	0.77	0.53	0.16	0.17	0.06	0.00	0.00	0.00	7.86	8.53	5.91	228.00	250.00	176.00	4.75	4.47	4.50
13 (C +10.5)	3.22	2.63	5.24	2.01	1.49	1.62	0.46	0.32	0.77	0.06	0.09	0.08	0.00	0.00	0.00	5.75	4.53	7.71	256.00	238.00	229.00	4.55	4.78	5.01
27 (C +9)	4.84	3.81	3.35	2.42	2.33	1.08	0.56	0.49	0.39	0.24	0.42	0.1	0.00	0.00	0.00	8.07	7.05	4.93	226.00	226.00	209.00	4.76	4.44	4.61
26 (C +9)	1.74	1.82	2.5	1.31	1.27	0.91	0.35	0.25	0.36	0.46	0.29	0.16	0.00	0.00	0.00	3.86	3.63	3.97	224.00	215.00	193.00	4.16	4.11	4.06
206 (C +10)	2.11	1.83	2.78	1.78	1.91	1.05	0.21	0.37	0.68	0.08	0.04	0.05	0.00	0.00	0.00	4.13	4.15	4.55	169.00	154.00	144.00	5.31	5.23	5.21
106 (C +8.5)	5.15	3.12	4.02	1.97	1.56	1.06	0.38	0.25	0.39	0.08	0.1	0.11	0.00	0.05	0.00	7.57	5.03	5.58	234.00	242.00	252.00	4.48	4.33	4.57
24 (C +10)	4.2	3.51	4.6	2.41	1.12	1.1	0.7	0.43	0.89	0.39	0.27	0.27	0.08	0.05	0.00	7.78	5.32	6.87	278.00	288.00	291.00	5.09	4.99	5.07
Group Mean	*3.60*	*3.11*	*3.74*	*2.17*	*1.86*	*1.01***	*0.51*	*0.42*	*0.52*	*0.19*	*0.19*	*0.10*	*0.01*	*0.01*	*0.00*	*6.47*	*5.58*	*5.38*	*226.63*	*223.75*	*197.00*	*4.76*	*4.61*	*4.69*
22 (C +10)	1.32	1.15	2.69	1.48	1.32	1.88	0.35	0.28	0.46	0.06	0.06	0.05	0.00	0.03	0.00	3.22	2.81	5.08	175.00	200.00	168.00	4.31	4.36	4.39
19 (C +8.5)	2.21	1.99	2.82	1.39	1.2	1.88	0.33	0.3	0.31	0.16	0.26	0.26	0.00	0.00	0.00	4.10	3.75	5.23	182.00	170.00	184.00	4.95	4.75	4.90
Group Mean	*1.77*	*1.57*	*2.76*	*1.44*	*1.26*	*1.88*	*0.34*	*0.29*	*0.39*	*0.11*	*0.16*	*0.16*	*0.00*	*0.02*	*0.00*	*3.66*	*3.28*	*5.16*	*178.50*	*185.00*	*176.00*	*4.63*	*4.56*	*4.65*

** Significant drop in lymphocyte numbers at day of diagnosis in the "classical" responders (Wilcoxon signed rank test, p = 0.0078)

Green type indicates healthy reference range

3.5.6 Quantification of plasma cytokines and chemokines for validation of the host transcriptional response

A chosen set of 12 analytes; CCL2 (MCP-1), CXCL9 (MIG) CXCL10 (IP-10), IFNα, IFNγ, IL-1β, IL- 6, IL-8, IL-10, IL-17, IL-18 and TNFα, were quantified in the plasma of volunteers. Analytes selected for analysis were chosen based on their known association with inflammation and/or predefined role in human malaria infection and thus were used not only to validate the diversity in host transcriptional responses, but to try to predict severity of outcome. High levels of the cytokines; TNFα, IFNγ, IL-1β, IL-6, IL-8 IL-10 and IL-18 have been reported in both children and adults with symptomatic *P. falciparum* (Day *et al.* 1999, Lyke *et al.* 2004, Walther *et al.* 2006, Mirghani *et al.* 2011), whereas CXCL9, CXCL10 and CCL2 are considered robust biomarkers of severe disease (Abrams *et al.* 2003, Armah *et al.* 2007, Jain *et al.* 2008, Ayimba *et al.* 2011, Wilson *et al.* 2011). Plasma samples from 13 of the 14 infected (volunteer ♯20 excluded due to limited kit capacity) were screened using the (custom-designed) LegendPlex™ assay from BioLegend®. Analysis included all infection time-points, with samples collected the day before challenge (C -1) providing a baseline read-out for each corresponding volunteer. The normalised concentrations as measured for all 12 analytes tested, through each individual's time-course of infection can be found in Appendix 6.

Results from this analysis confirmed the diversity in host responses observed at the transcript level, with CXCL10 and CXCL9 found elevated (> 1.5-fold from baseline) in 8 and 6 of the 8 "classical" responders, respectively (figure 3.6). CCL2 looked to be following a similar trend, however this response was less marked (Appendix 6). Importantly, CXCL10 was found as the gene most strongly up-regulated in response to *P. falciparum* infection in 6 of the 8 "classical" responders, and was within the top 4 most strongly up-regulated genes for the group as a whole. The biggest fold-change observed above baseline for CXCL10 and CXCL9 was in volunteer ♯16; the most inflammatory volunteer in the cohort (35-fold and 38-fold, respectively). These chemokines are considered robust biomarkers of severe malaria disease, and thus results suggest that if left untreated, these 8 volunteers would have likely gone on to become seriously ill. IFNγ is thought to be one of the key mediators of the immune effector mechanisms essential for initial control of malaria infections in the non-

immune, but there is also evidence that IFNγ levels need to be carefully balanced to avoid immune pathology (Good and Doolan 1999, Plebanski and Hill 2000). Interestingly, IFNγ (Type II IFN) was only detected in three of the most inflammatory volunteers of the same group (♯16, ♯17 and ♯13), and not until the end of their infection time-course (C +10 onwards). The biggest fold-change observed above baseline was in volunteer ♯16 (63-fold), followed by volunteer ♯17 (25-fold) and volunteer ♯13 (4-fold). INFα (Type I IFN), was detectable in 11 of the 13 volunteers screened in this analysis, but demonstrated no trend. Levels of INFα varied little throughout infection, and concentrations were observed within a similar range for all volunteers (Appendix 6).

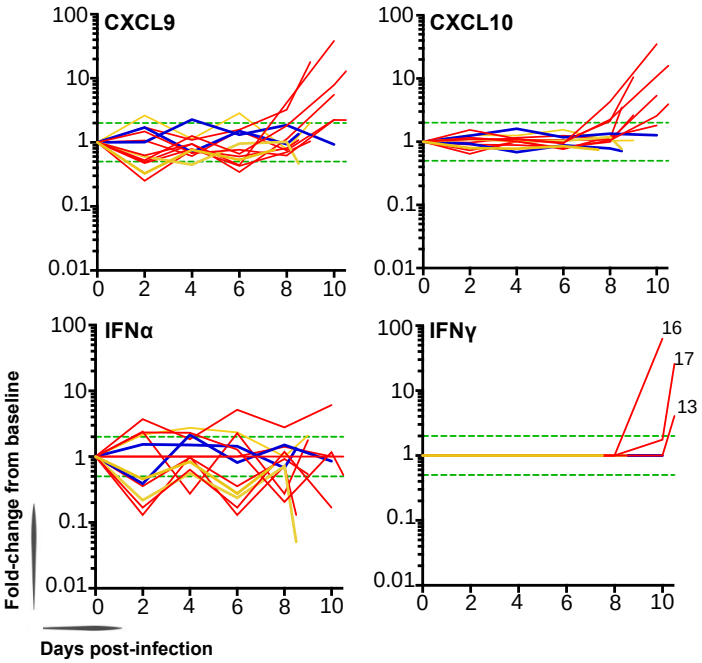

Figure 3.6 | Cytokine and chemokine production during blood-stage *P. falciparum* infection
Levels of CXCL9, CXCL10, IFNα and IFNγ were quantified in volunteer plasma, by multiplex assay (BioLegend®). Data is presented as fold change from baseline (y-axis), at each time-point in infection (x-axis) for 13 of the 14 infected volunteers. Volunteers are colour-coded as per transcriptional response group; 'unknown" volunteers 12, 18 and 208 (yellow); "classical" responders 13, 16, 17, 24, 26, 27, 106 and 206 (red); and "non-classical" responders 19 and 22 (blue). Green line indicates a 1.5-fold increase in concentration relative to baseline. For the IFNγ plot, the volunteer I.Ds for which elevated levels were found, are shown.

Figure 3.7 displays the concentrations of CXCL10, CXCL9, CCL2, IFNγ, IFNα, TNFα, IL-10, and IL-6 as measured throughout the course of each individual's infection time-course. In volunteers of the "unknown" group (♯18, ♯12, and ♯208), the kinetics of cytokine and chemokine production appear to reflect their

transcriptional profile whereby no obvious fluctuation in response to infection is observed. Where IL-10 appears to be dropping from baseline at certain time-points, this is likely explained by concentrations being below or very close to the limit of detection (0.8 pg/mL). Observations within the group of 8 “classical” responders suggest a kinetic whereby levels of CXCL10, CXCL9, and CCL2 can be found elevated from C +8 onwards in the majority of individuals. The response of these chemokines occurs in advance of a spike in INFγ as observed in three volunteers, suggesting that the early transcript-level IFN-stimulated responses detected from C +8 onwards is not being driven by IFNγ in the circulation. When considering that levels of IFNα appear similar to the “unknown” volunteers, and that little fluctuation is observed throughout infection, results suggest that the whole-blood IFN-signature observed in these 8 “classical” responders, is instead being driven by IFNβ (not tested), or by IFNs (INFα and/or IFNβ and/or IFNγ) stimulation in host tissue(s). In three of the “classical” responders, an increase in IL-10 production (> 2-fold above baseline) was also observed for volunteers: ♯16 (19-fold) and ♯27 (3-fold) from C +8, and in volunteer ♯17 (4-fold) from C +10. Interestingly, 2 out of 3 of these IL-10 producers (♯16 and ♯17) were also shown to produce INFγ (figure 3.6). This observation is consistent with data showing the two cytokines to be co-regulated during the host response to *P. falciparum* infection (Brustoski *et al.* 2005, Jagannathan *et al.* 2014, Villegas-Mendez *et al.* 2016), and may be indicative of immune-regulatory mechanisms at play in these inflammatory volunteers. The cytokine/chemokine profile for volunteer ♯16 validates transcriptional data highlighting this individual as the most inflammatory in the cohort. This volunteer demonstrated elevated plasma levels of CCL2, CXCL10, CXCL9, INFγ, IL-10 and IL-6; all of which have been associated with symptomatic malaria infection (Day *et al.* 1999, Lyke *et al.* 2004, Walther *et al.* 2006, Mirghani *et al.* 2011). *In vivo*, IL-6 and TNFα production has been associated with cerebral malaria (Kwiatkowski *et al.* 1990, Wenisch *et al.* 1999, Lyke *et al.* 2004). However, elevated levels of TNFα has also been linked to parasite clearance and resolution of fever (Kremsner *et al.* 1995). TNFα was detected in 11 of the 13 volunteers tested, but at a limited number of time-points for each. Its concentration did not appear to fluctuate in response to *P. falciparu*m infection, with the exception of volunteer ♯22 of the “non-classical” responders whereby a 2.6-fold increase in concentration was observed at their day of diagnosis time-point (C +10). It has been suggested that IL-18, along with IL-12,

plays an important role in initiating the inflammatory cytokine cascade during acute-phase infection with *P. falciparum,* and associations have been reported between circulating levels of these cytokines and risk of severe *Plasmodium falciparum* malaria (Malaguarnera *et al.* 2002). IL-18 was detected at similar concentrations for all 13 volunteers screened in this cohort, and concentrations varied little in response to *P. falciparum* infection during the time frame assessed (Appendix 6).

IL-1β was largely undetectable (limit of detection = 0.9 pg/mL) with the exception of volunteers ♯12, ♯13, ♯19, ♯22 and ♯208, and no obvious fluctuations in concentration were observed throughout infection in these individuals (Appendix 6). This was also true for IL-17 (limit of detection = 1.9 pg/mL). Importantly, IL-1β is highly unstable (degrades very quickly) *ex vivo*, which may have affected the ability to detect it in volunteer plasma. IL-8 was detectable in just three volunteers, and at a maximum of just two time-points for each (limit of detection = 1.0 pg/mL). Thus, due to issues of assay sensitivity and/or cytokine instability, I was unable to compare levels of these inflammatory mediators in volunteer plasma. Nevertheless, results from this analysis validate the diversity in host responses observed at the transcript level and confirm, at the protein level, the inflammatory gene signature observed in the 8 “classical” responders.

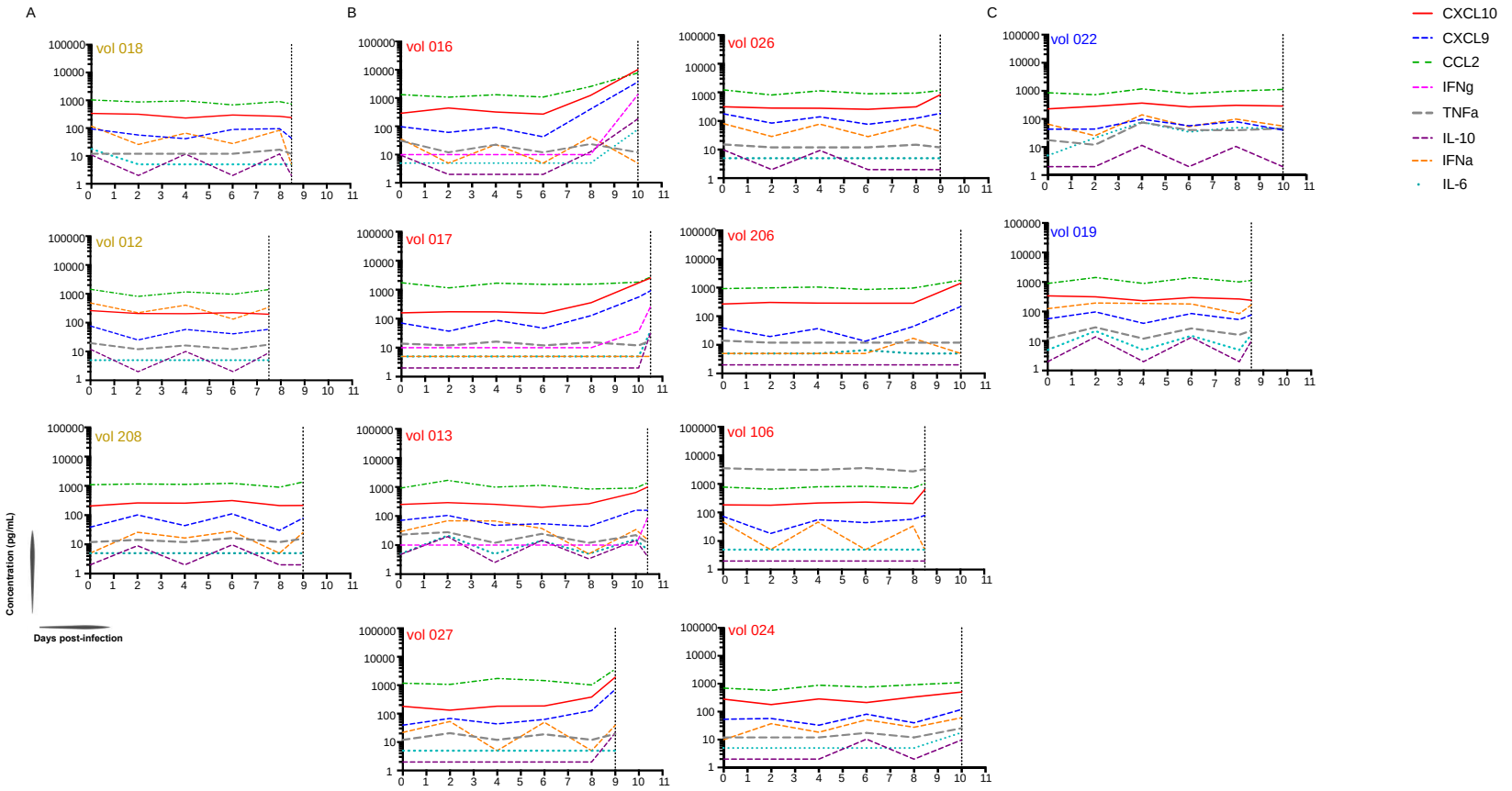

Figure 3.7 | Kinetics of cytokine and chemokine production during blood-stage *P. falciparum* infection. Concentrations of CXCL10, CXCL9, CCL2, INF**γ**, TNF**α**, IL-10, IFN**α** and IL-6 were quantified in volunteer plasma, by muliplex assay (BioLegend®). Graphs show concentration (pg/mL) of each cytokine (y-axis) through time (x-axis). Plots are shown for three of the four individuals in the "unknown" group (panel A), the eight "classical" responder group (panel B) and the two "non-classical" responder group (panel C). Black vertical line denotes day of diagnosis. A colour-key for each analyte is provided.

3.5.7 Biological pathways affected during *P. falciparum* blood-stage infection

Ingenuity pathway analysis (IPA) core analysis was utilised to investigate the canonical pathways significantly perturbed during primary *P. falciparum* infection. For this analysis, all gene features on the array (with the exception of those without annotation, and those encoding small RNAs <200 nt) were considered.

3.5.7.1 In the "classical" relative to "non-classical" responders

In order to investigate the immune signaling pathways associated with the variability in host responses, differentially expressed genes (DEGs) between the "classical" responders (n = 8), and the "non-classical" responders (n = 2) were considered for pathway analysis. Using a p-value < 0.05 (adjusted for multiple comparisons using the Benjamini-Hochberg method) resulted in 882 genes differentially expressed between the two groups at diagnosis (560 up and 322 down in the "classical" responders). Figure 3.8, part A shows the top 20 pathways significantly associated with these genes. IFN signalling and activation of the innate inflammatory response (Fcγ receptor-mediated phagocytosis, dendritic cell maturation, toll-like receptor signaling and activation of the inflammasome) were found enriched within the response of the "classical" responder group. Figure 3.8, part B displays the top 20 upstream regulators associated with the genes differentially expressed between the two groups. IFNα ($3.9x10^{-20}$), STAT1 ($9.7x10^{-19}$) and IFNγ ($9.7x10^{-16}$) were predicted with greatest significance, acting upstream of 47, 32 and 49 genes in the dataset, respectively.

To further dissect the biological pathways associated with the "classical" responder group, or the "non-classical" responders specifically, analysis was performed on a representative volunteer from each group.

A

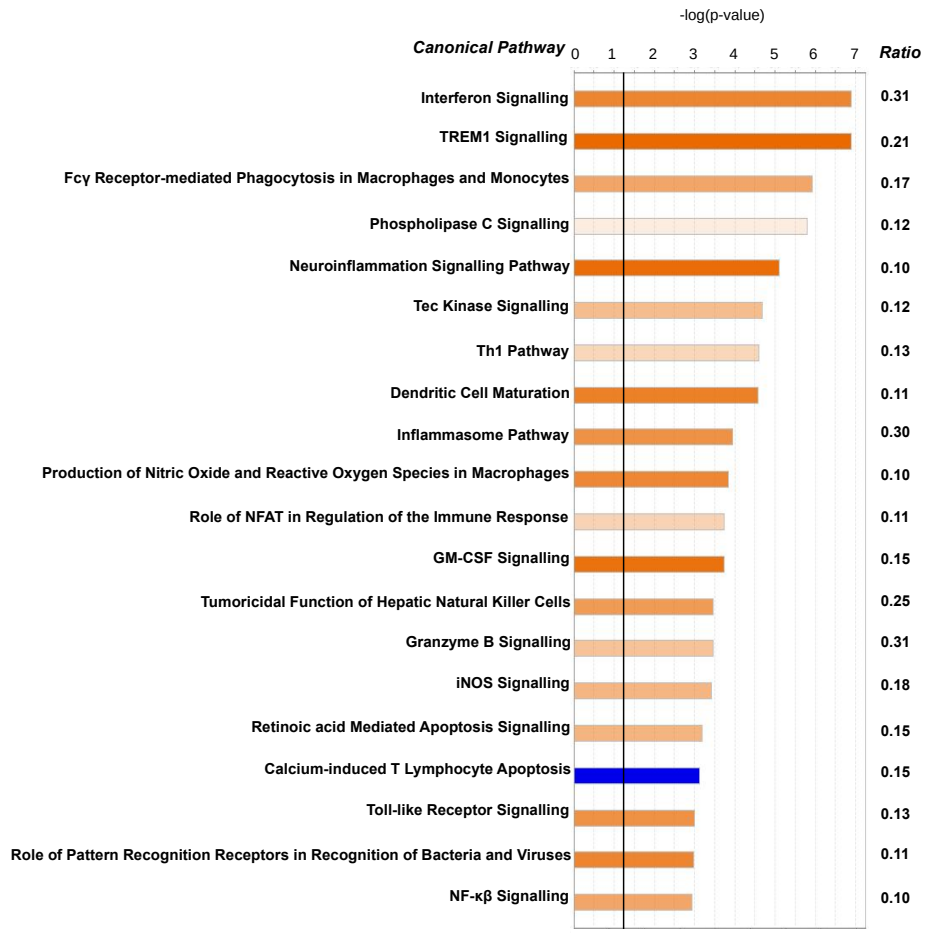

B

Upstream Regulator	Molecule Type	Predicted Activation State	Activation z-score	p-value of overlap	Number of Target Molecules
Interferon alpha	group	Activated	3.869	$3.93x10^{-20}$	47
STAT1	transcription regulator	Activated	4.887	$9.74x10^{-19}$	32
IFNG	cytokine	Activated	5.934	$9.73x10^{-16}$	49
TGM2	enzyme	Activated	4.61	$4.68x10^{-11}$	32
IRF1	transcription regulator	Activated	2.598	$8.53x10^{-10}$	14
CEBPA	transcription regulator	Activated	2.706	$1.07x10^{-9}$	23
TNF	cytokine	Activated	5.076	$3.07x10^{-9}$	48
RELA	transcription regulator	Activated	3.517	$4.47x10^{-9}$	26
MAPK1	kinase	Inhibited	-4.191	$1.75x10^{-8}$	26
CD40LG	cytokine	Activated	2.193	$4.15x10^{-8}$	17
TLR7/8	group	Activated	3.317	$3.91x10^{-7}$	11
IL1B	cytokine	Activated	3.939	$5.76x10^{-7}$	25
IRF4	transcription regulator	Inhibited	-2.491	$1.15x10^{-6}$	12
IFNL1	cytokine	Activated	3.44	$4.64x10^{-6}$	12
PRL	cytokine	Activated	3.672	$4.69x10^{-6}$	14
TLR9	transmembrane receptor	Activated	2.164	$5.33x10^{-6}$	11
SAFB	other	Inhibited	-2.111	$5.33x10^{-6}$	11
NFkB (complex)	complex	Activated	2.155	$5.82x10^{-6}$	26
IRF9	transcription regulator	Activated	2.186	$6.16x10^{-6}$	6
IFNA2	cytokine	Activated	3.638	$7.28x10^{-6}$	14

Figure 3.8 | Canonical pathways and upstream regulators significantly associated with gene differentially expressed between the "classical" and "non-classical" responder groups. A) The top 20 most significantly-enriched pathways are presented. Bars represent the –log p-value for the statistical test of the probability of molecules within the dataset being associated with the canonical pathway by random chance alone (Fisher's exact right-tailed test). Threshold (black vertical line) indicates significance at p = 0.05 (-log p = 1.3). Bar shading represents predicted pathway activation (orange), pathway inhibition (blue) or an equal chance of activation or inhibition (white), based on the calculated z-score. The ratio of genes differentially expressed in the dataset to total number of genes associated with the pathway is shown on the right. **B)** Top 20 most significantly-associated molecules predicted to be regulating differential gene expression observed in the dataset (p- value of overlap, Fisher's exact right-tailed test). Predicted activation status, as based on the calculated z-score is shown for each, as is as the number of target molecules in the dataset predicted to be affected. (Analysis was generated through use of QIAGEN'S Ingenuity Pathway Analysis (IPA ®, Qiagen, Redwood City, www.qiagen.com/ingenuity)).

3.5.7.2 In the "classical" responder volunteer ♯16

Genes demonstrating a ≥ 1.5 fold increase over median expression at diagnosis, in volunteer ♯16 were considered for analysis. Using this fold-change cut-off resulted in 762 genes (531 up and 231 down) differentially expressed in this volunteer. Figure 3.9 shows the top 20 most significantly enriched pathways associated with their response. "Interferon signaling" was the most significantly enriched ($p = 2.44x10^{-14}$) with 44% of genes associated with this pathway (16 out of 36) found differentially expressed in response to *P. falciparum* infection in this volunteer (figure 3.9). The observed effect was due to the genes; BAK1, IFI6, IFI35, IFIT1, IFIT3, IFITM1, IRF1, ISG15, JAK2, MX1, OAS1, PSMB8, SOCS1, STAT1, STAT2, and TAP1, all of which were up-regulated. Interferons (IFN) are cytokines that play a central role in initiating immune responses, most commonly associated with the antiviral response. They are divided into three classes: Type I (predominantly IFN-α, -β and -κ), Type II (IFN-γ) and Type III (IFN-λ1 and -λ2 also known as IL-28 and IL-29) (Ivashkiv and Donlin 2014). The Interferon Signalling pathway is initiated upon binding of Type I and Type II IFNs to IFNAα1/2 and/or IFNγR2, and activation of the tyrosine kinases JAK1, JAK2 or TYK2 (figure 3.10). In the case of Type I IFNs, both STAT1 and STAT2 are required to form a heterodimer which, once phosphorylated, associates with IFN gene regulatory factor-9 (IRF-9) (Yan *et al.* 1996). The resultant trimeric transcription factor, ISGF3, binds to the IFN-stimulated regulatory elements (ISREs) to induce the expression of many IFN-α/β-regulated genes (Schneider *et al.* 2014). Both STAT1 and STAT2 were found strongly up-regulated in the dataset, suggesting a key role of Type I IFNs in the response of the "classical" responders. Furthermore, increased expression of the cytosolic PRRs DDX58 (RIG-I) and IFIH1 (MDA-5) was observed within the group of volunteers (figure 3.11 and top 100 gene lists). These receptors are responsible for the recognition of RNA and are highly associated with the induction of Type I IFNs. (McNab *et al.* 2015). Importantly, Type I IFN responses have been previously reported in a study of CHMI with *P. falciparum* (Montes de Oca *et al.* 2016).

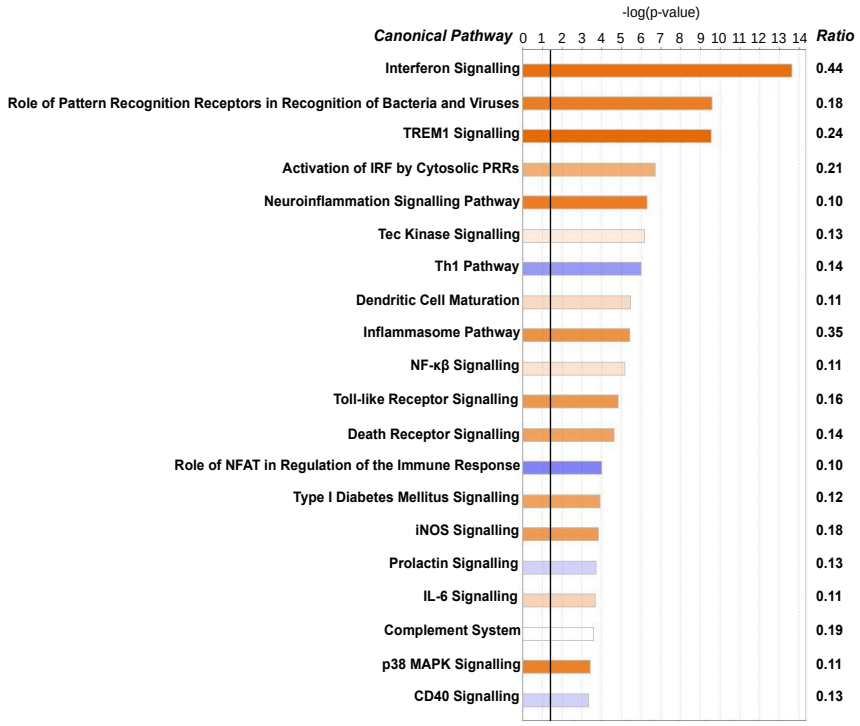

Figure 3.9 | Canonical pathways significantly enriched in volunteer ♯16 of the "classical" responder group. The top 20 most significantly-enriched pathways are presented. Bars represent the –log p-value for the statistical test of the probability of molecules within the dataset being associated with the canonical pathway by random chance alone (Fisher's exact right-tailed test). Threshold (black vertical line) indicates significance at p = 0.05 (-log p = 1.3). Bar shading represents predicted pathway activation (orange), pathway inhibition (blue) or an equal chance of activation or inhibition (white) based on the calculated z-score. The ratio of genes differentially expressed in the dataset to total number of genes associated with each pathway is shown on the right. (Analysis was generated through use of QIAGEN'S Ingenuity Pathway Analysis (IPA®, Qiagen, Redwood City.www.qiagen.com/ingenuity)).

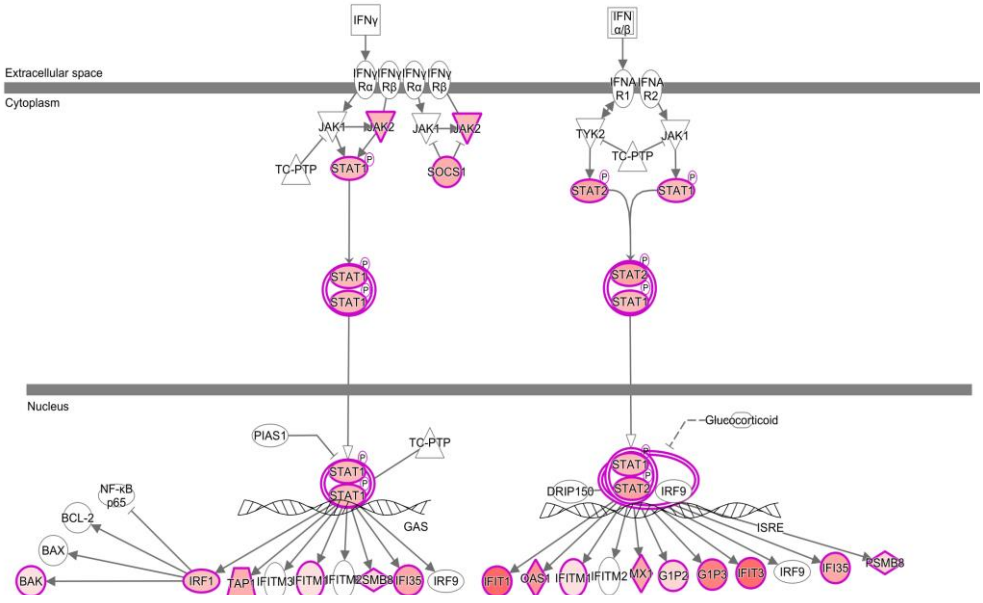

Figure 3.10 | Interferon (IFN) signalling pathway. Interferon signalling pathway initiated through binding of Type I and Type II IFNs to IFN**α**R1/2 and INF**γ**R (receptors) respectively. Red colour-shading indicates molecules that are up-regulated in the dataset, with double-borders in purple indicating protein complexes affected by the differentially expressed genes. Pathway analysis was generated through the use of QIAGEN's Ingenuity Pathway Analysis (IPA®, QIAGEN Redwood City, www.qiagen.com/ingenuity)).

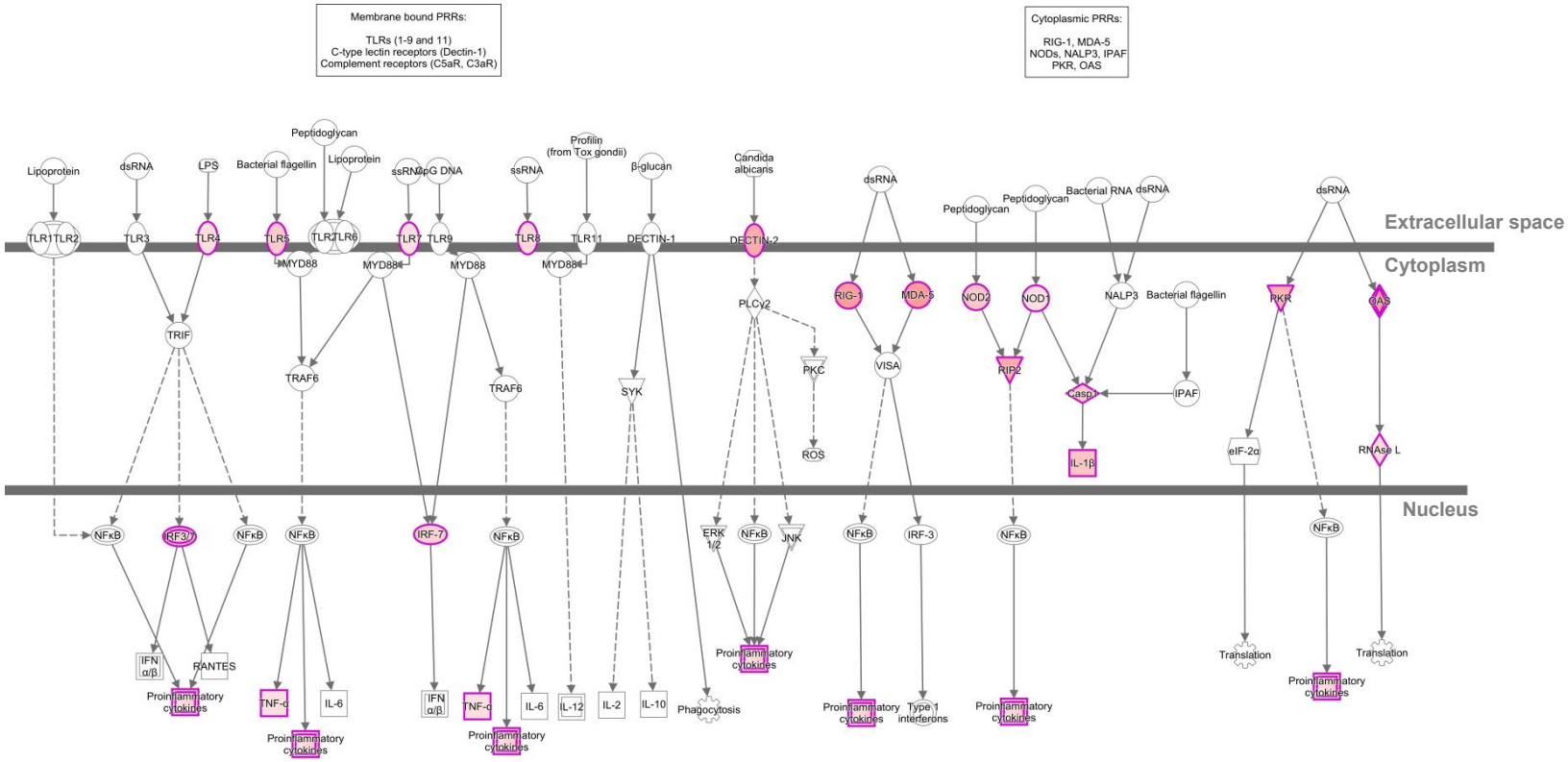

Figure 3.11 | Pattern Recognition Receptors involved in recognition of blood-stage *P. falciparum*. Recognition of conserved microbial structures and PAMPs by membrane-bound and cytosolic PRRs of the innate immune system, resulting in downstream proinflammatory cytokine production. Red color shading indicates genes that are upregulated in the dataset, with double-borders in pink indicating protein complexes affected by the differentially expressed genes. Pathway analysis was generated through the use of QIAGEN's Ingenuity Pathway Analysis (IPA® QIAGEN,Redwood City, www.qiagen.com/ingenuity).

The Inflammasome signaling pathway was also significantly enriched ($p = 3.9x10^{-6}$) with 35% of genes (7 out of 20) in the pathway differentially expressed (figure 3.9). The observed effect was due to the genes: AIM2, CASP1, CASP5, IL-1β, NOD2, P2RX7 and TLR4, all of which were found up-regulated. Inflammasomes are immune system complexes that regulate the activation of caspase-1 upon sensing of infectious microbes. Several families of PRRs can serve as nucleators of inflammasome complexes, including the absent in melanoma 2 (AIM)-like receptors, found up-regulated in the dataset (figure 3.12) (Latz 2010). Activation of the inflammasome pathway via AIM2, suggests recognition of parasite nucleic acids in the cytosol, consistent with the observed up-regulation of the cytosolic PRRs; RIG-I and MDA-5. Also found up-regulated in the dataset were three key molecules of the NLRP1 and NLRP3 inflammasome complexes; NOD2, caspase-1 and caspase-5. Upon sensing pathological stimuli, the relevant NOD-like receptor (NLR) or AIM2 oligomerise with scaffold protein ASC, which then binds and activates pro-caspase-1. Active caspase-1 functions to cleave the pro-inflammatory IL-1 family of cytokines into their bioactive forms; IL-1β and IL-18 and as a consequence, leads to pyroptosis (Latz 2010). Thus activation of inflammasomes has been implicated in a variety of inflammatory processes and disorders, including that of *Plasmodium* malaria infection (Ataide *et al.* 2014, Kalantari *et al.* 2014, Hirako *et al.* 2015). In line with this very inflammatory response, TREM-1 signalling was the third most significantly associated pathway in this volunteer (figure 3.9). When activated, triggering receptor expressed on myeloid cells 1 (TREM-1) acts to amplify neutrophil and monocyte-mediated inflammatory responses through the recruitment of adaptor proteins such as DAP-12 (Bouchon *et al.* 2000), thereby promoting the production of pro-inflammatory cytokines, as well as increased surface expression of cell activation markers (Charles *et al.* 2016). In the context of human malaria infection, high plasma levels of sTREM-1 have been shown to predispose patients to a phenotype of severe disease (Adukpo *et al.* 2016). Taken together, results suggest a model whereby cells of the innate immune system, upon detection of parasite nucleic acids, stimulate production of IFNs and other pro-inflammatory cytokines, leading to inflammation and, most likely, damaging effects to the host. However, this response was only observed in 8 of the 14 infected volunteers.

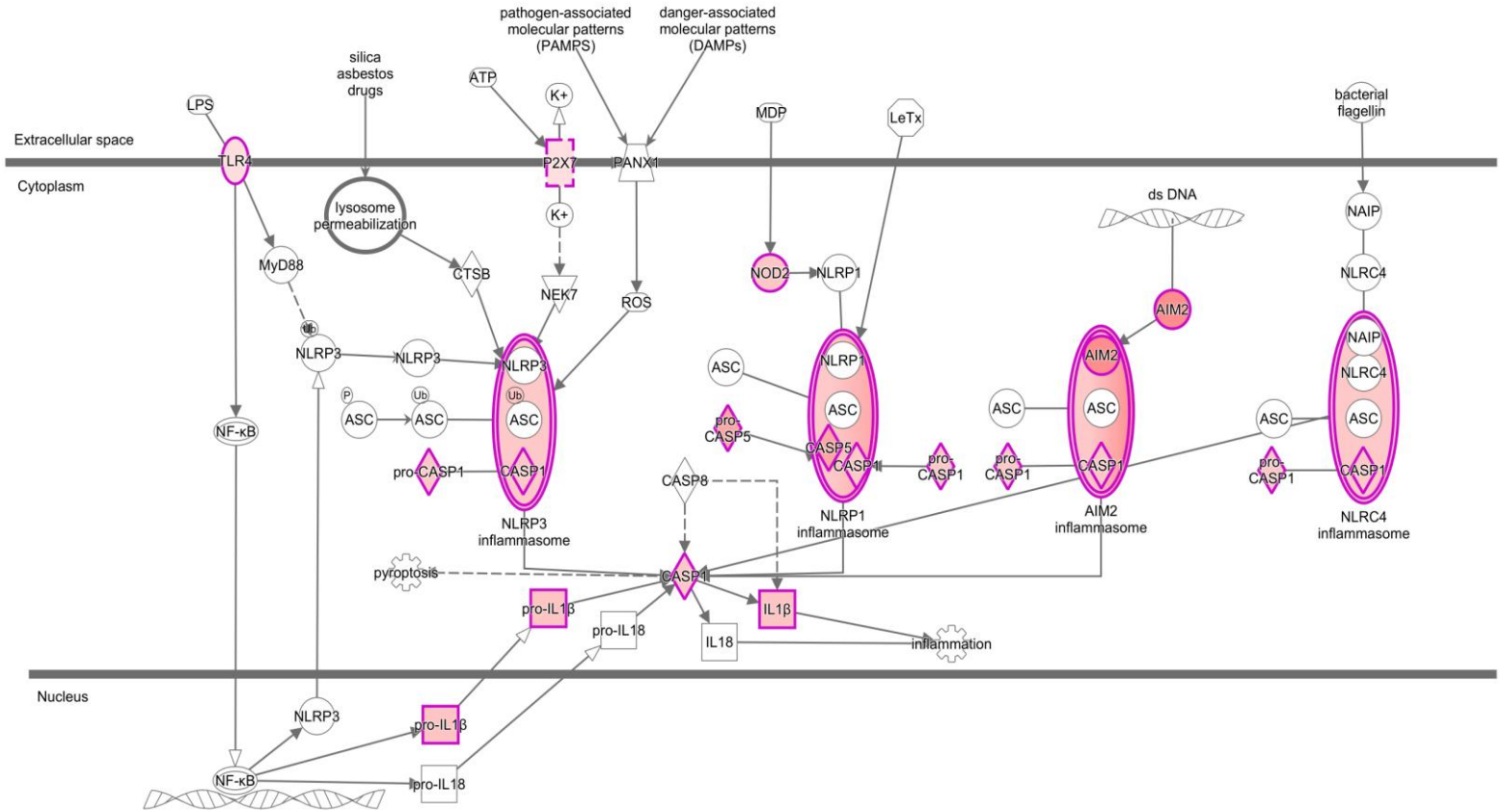

Figure 3.12 | Inflammasome Signalling Pathway. Initiation of inflammasome assembly/activation in the cytosol after sensing of pathogen-associated molecular patterns (PAMPs) or danger-associated molecular patterns (DAMPs). Red color shading indicates genes that are upregulated in the dataset, with double-borders in pink indicating protein complexes affected by the differentially expressed genes. Pathway analysis was generated through the use of QIAGEN's Ingenuity Pathway Analysis (IPA® QIAGEN, Redwood City, www.qiagen.com/ingenuity).

3.5.7.3 In the "non-classical" responder volunteer ♯19

Pathway analysis was also performed on volunteer ♯19 of the "non-classical" responders. Using a fold-change cut-off of 1.5 resulted in 797 genes differentially expressed at diagnosis (104 up and 693 down) in this volunteer. Figure 3.13 displays the top 20 pathways associated with their response. Interestingly, several of the most significantly overrepresented pathways overlapped with that of "classical" responder ♯16, but had opposing activity. Within the top 20 were: the inflammasome pathway, TREM-1 signaling, Nf-κβ and Toll-like receptor signaling, all of which were inhibited in response to *P. falciparum* blood-stage infection. Inhibition of inflammasome signaling was associated with the down-regulation of CASP1, CASP5, CASP8, NAIP and NLRP3, encompassing 25% of molecules in the pathway. Expression of TREM-1 was also repressed. Thus, the response in the "non-classical" volunteers appeared to be a highly suppressive one, in contrast to that of the "classical" responders. The most significantly enriched pathway in this volunteer was that of death receptor signaling (figure 3.13). The observed effect was due to 11 genes; APAF1, BIRC2, CASP8, CFLAR, NAIP, PARP8, PARP14, PARP15, ROCK1, TANK and TNFSF10, all of which were down-regulated. Apoptosis can be induced through the activation of death receptors including Fas, TNFαR, DR3, DR4, and DR5 by their respective ligands (figure 3.14). Death receptor ligands characteristically initiate signaling for the recruitment of specialised adaptor proteins and activation of caspase cascades. Activation of caspase-8, for instance, stimulates apoptosis via two parallel cascades: it can directly cleave and activate caspase-3, or alternatively, it can cleave Bid, a pro-apoptotic Bcl-2 family protein. Truncated Bid (tBid) translocates to mitochondria, leading to activation of caspase-9 and -3. Activation of caspase-3 leads to downstream signaling, and apoptosis of cells (Kaufmann *et al.* 2012). Programmed cell death plays a crucial role in development and tissue homeostasis. It has also been shown to serve a protective role, by eliminating cells that are abnormal and potentially dangerous (Fuchs and Steller 2011). Thus, abnormal regulation of this process may prove detrimental to the host, but it is yet unclear what effect this may have in the context of *P. falciparum* malaria infection.

It is reasonable to hypothesise that by suppressing the activity of the innate immune response early in infection, volunteers ♯19 and ♯22 may demonstrate a reduced

ability to control parasite growth in the circulation. Or vice versa, parasite growth kinetics may influence the type of host response produced. Thus, it was important to consider a potential correlation between host responder status and parasite growth kinetics in the blood.

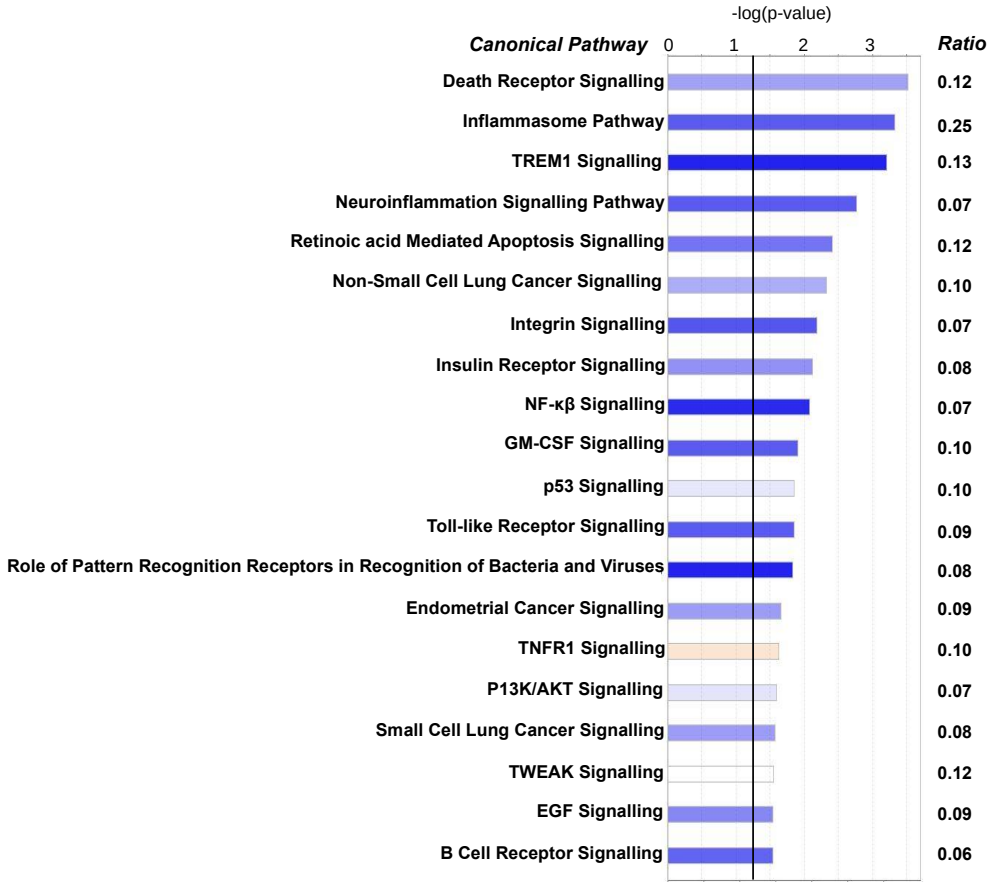

Figure 3.13 | Canonical pathways significantly enriched in volunteer ♯19 of the "non-classical" responder group. The top 20 most significantly-enriched pathways are presented. Bars represent the –log p-value for the statistical test of the probability of molecules within the dataset being associated with the canonical pathway by random chance alone (Fisher's exact right-tailed test). Threshold (black vertical line) indicates significance at p = 0.05 (-log p = 1.3). Bar shading represents predicted pathway activation (orange), pathway inhibition (blue) or an equal chance of activation or inhibition (white), based on the calculated z-score. The ratio of genes differentially expressed in the dataset to total number of genes associated with the pathway is shown on the right. (Analysis was generated through use of QIAGEN'S Ingenuity Pathway Analysis (IPA ®, Qiagen, Redwood City, www.qiagen.com/ingenuity)).

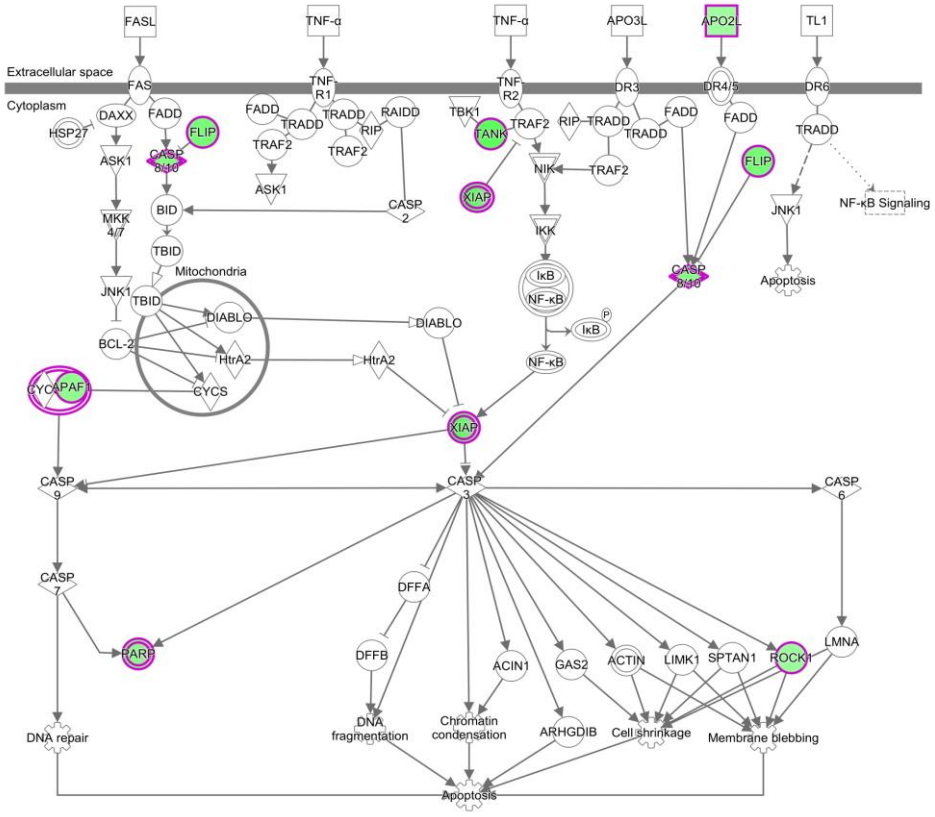

Figure 3.14 | Death receptor signalling pathway. Green color shading indicates genes that are downregulated in the dataset, with double-borders in pink indicating protein complexes affected by the differentially expressed genes. Pathway analysis was generated through the use of QIAGEN's Ingenuity Pathway Analysis (IPA® QIAGEN, Redwood City, www.qiagen.com/ingenuity).

3.5.8 Relationship between host responder status and parasite growth in the blood

Observations from populations of repeated malaria exposure have suggested that innate immunity is triggered when parasite density surpasses a predefined threshold (Kwiatkowski and Nowak 1991). This hypothesis is extremely difficult to investigate in the setting of natural infection. In studies of CHMI however, volunteers are monitored from as early as day 1 post-infection, allowing for detection of immune events at the onset. Moreover, volunteers were sampled twice daily, for quantification of parasites in the circulation. Figure 3.15, part A compares parasite densities between two volunteers; one who failed to elicit a response (volunteer ♯18), and one of the most inflammatory volunteers in the cohort (volunteer ♯17), as measured at the time-point when activation of the innate immune response was first detected (8 days post-infection). Volunteer ♯17 initiated a detectable immune

response to 157 p/mL, whereas volunteer ♯18 failed to elicit a response to *P. falciparum* at a density far greater (8,735 p/mL). Furthermore, day of diagnosis parasitaemias for the other three "unknown" responders; ♯12, ♯20 and ♯208, were higher than those observed for volunteer ♯17 at C +8 (1,645 p/mL, 15, 025 p/mL and 1,440 p/mL respectively). Thus, results suggest that there is a parasite density threshold for the onset of the innate immune response, but that this threshold is highly variable between individuals.

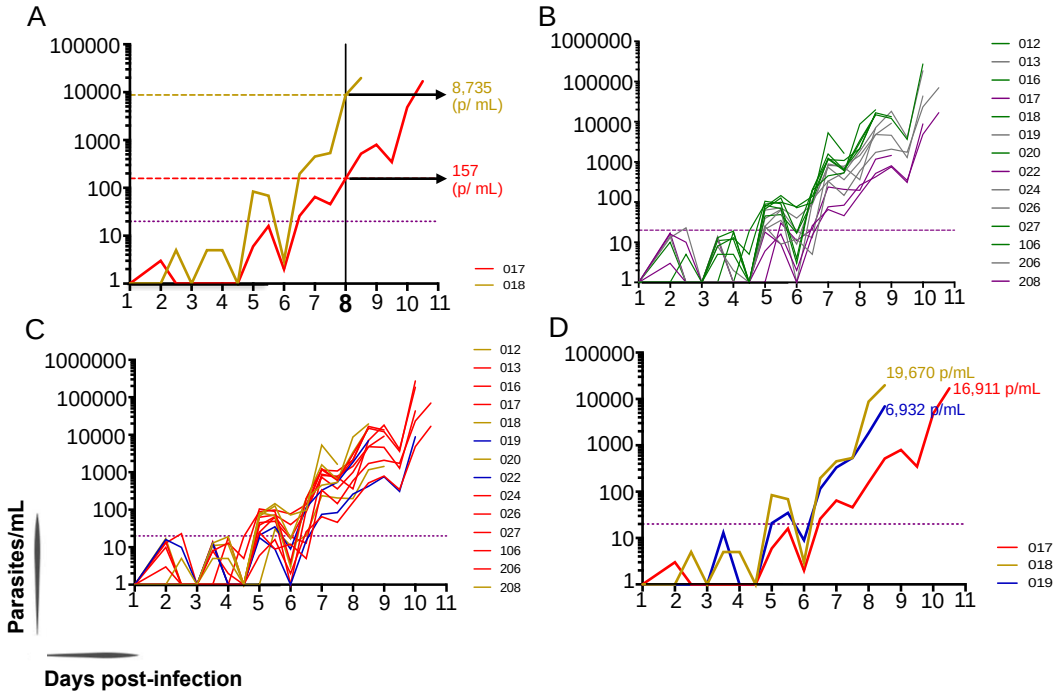

Figure 3.15 | Relationship between host transcriptional status and parasite growth in the blood cycle. Parasites/mL of blood (y-axis) as quantified by qPCR are shown against time on the x-axis. **A)** Parasite growth curves for "unknown" responder; 18 (yellow), and "classical" responder; 17 (red). Parasites/mL as measured at 8 days post infection is shown for each. **B)** Parasite growth curves for all 14 infected volunteers, colour-coded according to parasite multiplication rate: <8 (slow/purple), 8 – 10 (intermediate/grey) and >10 (fast/green) and according to transcriptional response group; "unknowns" (yellow), "classical" responders (red) and "non-classical" responders (blue) in **C**. **D)** Parasite growth curves for volunteers 17, 18 and 19, colour-coded as per transcriptional response group. Day of diagnosis parasitaemias (p/mL) are shown for each. Horizontal purple line represents the qPCR lower limit of quantification at 20 p/mL.

One major advantage of the blood-stage CHMI model is the ability to control for the dose and timing of parasites entering host circulation, allowing for more accurate modelling of parasite growth with each 48-hour cycle of replication in the blood (Douglas *et al.* 2013). Considering the diversity of transcriptional responses observed in this volunteer cohort, parasite multiplication rates (PMR) (Table 3.1) were used to investigate the relationship between host responder status, and

parasite growth in the blood. Volunteers were grouped as having either slow, intermediate or fast-growing parasites using arbitrary cut-offs for PMR: <8, 8 – 10, >10 respectively. Figure 3.15, parts B and C show parasite densities (p/mL) plotted against time, for the 14 volunteers. When colour-coded according to PMR (part B), a clear pattern is observed. This pattern, however, is completely lost when volunteers are re-colour-coded according to transcriptional response profile: “unknowns” in yellow, “classical” responders in red, and “non-classical” responders in blue (part C). These results suggest that there is no direct relationship between host transcriptional responder status, and PMR in the circulation. Given that the majority of all transcriptional events were recorded in the last two time-points of infection, parasite densities measured at day of diagnosis were compared to determine any influence on volunteer responder status. The parasite density measured at diagnosis for the “classical” responders (median = 30,309 p/mL) was found to be higher than that of the two other groups (“non-classical” responders = 7,899 and “unknowns” = 8,335) (Table 3.3), which likely reflects the longer prepatent period (time to thick film smear positivity) observed for these volunteers (median = 10.0 days). However, parasite densities were highly variable between individuals within the same group, and were not sufficient to explain the inflammatory response of the “classical” responders considering that volunteers of the unresponsive “unknown” group had comparable parasites/mL when assessed at the individual level (figure 3.16). Figure 3.15, part D highlights the diverse range of p/mL recorded at day of diagnosis, in three representative volunteers (one “classical” responder (♯17), one “non-classical responder (♯19) and one “unknown” volunteer (♯18)). Of these three, the highest parasite density was observed in the unresponsive, “unknown” volunteer ♯18 (19,670 p/mL). Results therefore suggest that the diversity in host immune responses to blood-stage *P. falciparum* infection is not being driven by differences in parasite growth, or densities at time of sampling.

Table 3.3 | Parasite growth parameters by host transcriptional response group

	"classical" responders	"non-classical" responders	"unknown" volunteers	All volunteers
Number in group	8	2	4	14
Median time to qPCR detection in days (range)	5.0 (5.0 - 6.5)	6.0 (5.0 - 7.0)	5.0 (no range)	5.0 (5.0 - 7.0)
Median Parasite Multiplication Rate (range)	9.9 (6.7 - 11.9)	8.3 (6.8 - 9.7)	12.1 (7.1 - 12.8)	9.9 (6.7 - 12.8)
Median prepatant period in days (range)	10.0 (8.5 - 10.5)	9.0 (8.5 - 10.0)	8.5 (7.5 - 9.0)	9.0 (7.5 - 10.5)
Median parasite density (p/mL) at diagnosis (range)	30,309 (9,133 - 273,247)	7,899 (6,932 - 8,865)	8,335 (1,645 - 19,670)	15,594 (1,440 - 273,247)

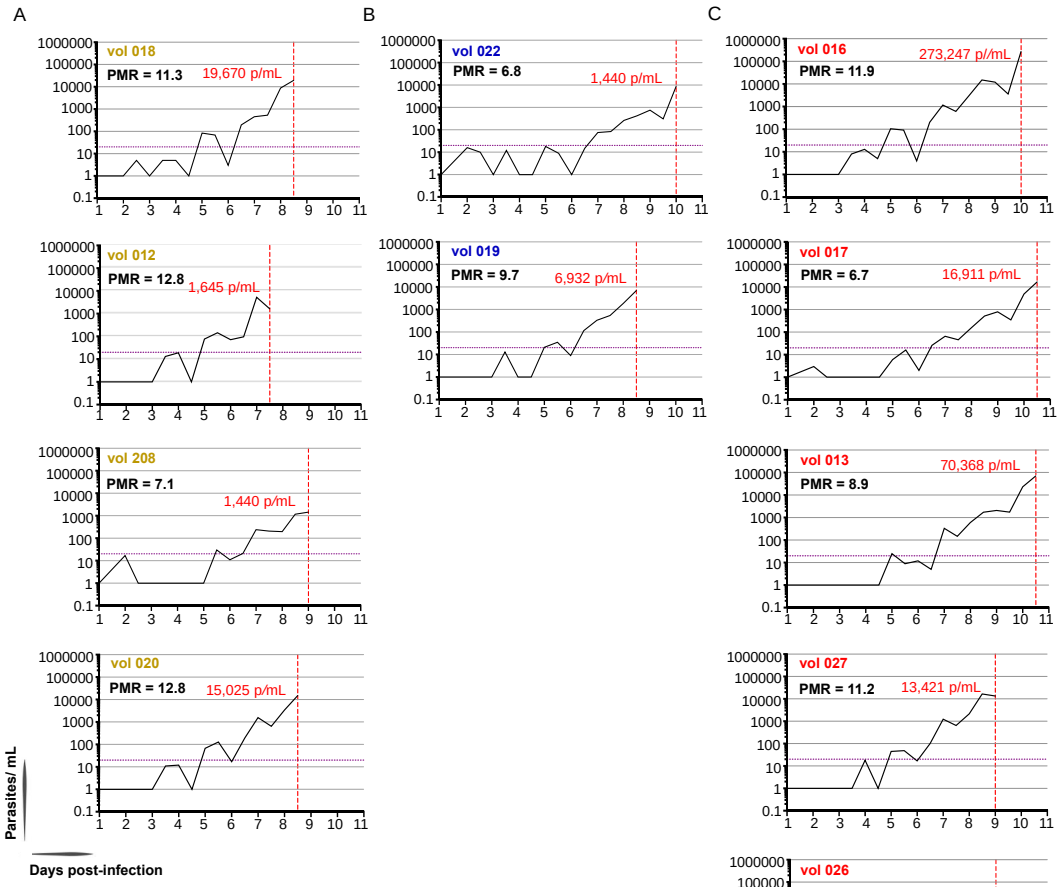

Figure 3.16 | Parasite growth curves. Graphs show number of parasites per mL of blood (y-axis) through time (x-axis), as measured by qPCR. Plots are shown for each individual in the "unknown" group (panel A), the "non-classical" responder group (panel B) and the "classical" responder group (panel C). The parasite multiplications rate (PMR) and parasitaemia at day of diagnosis (vertical red line) is shown for each volunteer. Dashed purple line represents the qPCR lower limit of quantification (20 p/mL).

Figure 3.16 | Parasite growth curves (legend above).

One of the key pathological features of *P. falciparum* infection is that the mature blood stage parasites (pigmented trophozoites and schizonts) are sequestered in the microvasculature (Miller *et al.* 2002). Thus, recognising that the above analysis was limited to monitoring parasite numbers only in the circulation, an ELISA was set up to quantify levels of *P. falciparum* Histidine Rich protein II (PfHRPII) in volunteer plasma, as a more accurate read-out of total parasite burden (Dondorp *et al.* 2005) (see methods section 3.4.9). PfHRPII is a *falciparum*-specific antigen, produced in all blood-stages of the parasites life-cycle (Parra *et al.* 1991). A substantial amount of the water-soluble protein is secreted by the parasite, into the host bloodstream during infection, allowing for its detection and quantification. However, screening of PfHRPII is carried out, most commonly, by rapid diagnostic testing in populations of natural infection where parasite densities typically reach 2 - 3 orders of magnitude higher levels than those observed in studies of CHMI. Figure 3.17 displays the 12-point standard curve of recombinant PfHRPII used for quantification in the ELISA (dilution range = 125 – 0.06 ng/mL, R^2 = 0.993). In order to conserve precious samples, the ELISA was first tested on plasma collected on day of diagnosis (peak parasitaemia) for volunteer ♯16, demonstrating the highest observed parasite density within the cohort (273,247 p/mL). PfHRPII was undetectable in this sample, suggesting that the ELISA method is not sensitive enough to detect this parasite protein at the low level parasitaemias typically observed in volunteers following CHMI. Nevertheless, studies carried out in the field have shown a direct correlation between parasite numbers in the circulation as measured by qPCR, and levels of PfHRPII in the plasma of patients (Silamut and White 1993, Dondorp *et al.* 2005, Dobbs *et al.* 2017). Thus, considering that there is no association between parasite numbers in the circulation and host responder status in this cohort of volunteers, I would not expect total parasite burden to be a determinant of host responder status at this early stage of infection.

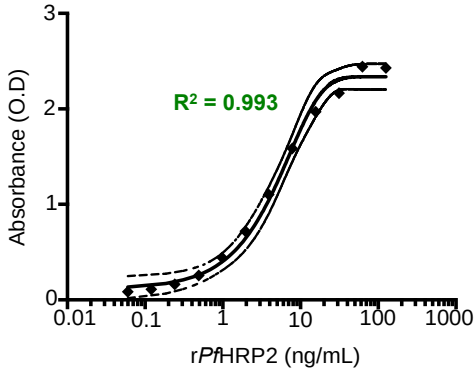

Figure 3.17 | Sigmoidal curve of the (log_{10}) PfHRPII ELISA standard concentrations (125 – 0.06 ng/mL range) on the x-axis against absorbance (O.D) on the y-axis. Interpolation was done using the Sigmoidal, 4PL function in GraphPad Prism. R^2 value is shown in green, with dashed lines representing the upper and lower 95% confidence intervals.

3.5.9 Relationship between host responder status and CMV positivity

There is evidence to suggest that microbial exposure (or past infection history) is a likely driver of immune variation, and a particularly robust example is that of cytomegalovirus (CMV), a viral infection that has marked effects on the immune phenotypes of humans (Sylwester *et al.* 2005, Brodin *et al.* 2015, Shmeleva *et al.* 2015). The prevalence of human CMV infection varies greatly depending on geographic and socioeconomic backgrounds of the population, but has been recognised in every human population studied (Krech *et al.* 1971, Nankervis 1976). Given the observed heterogeneity in immune responses, anti-CMV IgG seropositivity was assessed in volunteers, to investigate a potential relationship with responder status.

Table 3.4 displays the calculated ELISA standard units, relative to the anti-CMV IgG "cut-off control" (see section 3.4.12). Results show that 5 out of 14 (35%) of volunteers were positive for anti-CMV IgG (standard units > 11). Although 4 of the 5 positive volunteers fall within the "classical" responder group, CMV seropositivity cannot be used to explain the transcriptional response groups observed, as the four remaining "classical" responders are negative for anti-CMV IgG. Furthermore, a higher proportion of volunteers in the cohort belong to the "classical" responder group compared to any other, thereby increasing the likelihood of finding CMV-positive individuals within this group. Interestingly, volunteers who were positive for

anti-CMV IgG by ELISA (n = 5) were found to have significantly lower parasite multiplication rates (PMR/48 hours) when compared to volunteers that were negative for anti-CMV IgG (n = 9) (figure 3.18). However, this will need to be tested on a larger number of volunteers to determine true significance. There was no significant difference in the parasite densities observed at diagnosis between the two groups (figure 3.18).

Table 3.4| Volunteer anti-CMV IgG seropositivity status

Volunteer i.d	Standard unit	anti-CMV IgG positive?	P/mL at diagnosis	PMR/48 hours
12	2.4	N	1,645	12.8
13	33.5	Y	70,368	8.9
16	2.2	N	273,247	11.9
17	49.6	Y	16,911	6.7
18	1.6	N	19,670	11.3
19	1.8	N	6,932	9.7
20	2.2	N	15,025	12.8
22	3.0	N	8,865	6.8
24	30.03	Y	43,707	9.4
26	9.7	N	9,133	9.9
27	2.5	N	13,421	11.2
106	2.3	N	16,162	11.3
206	34.4	Y	185,576	9.9
208	33.7	Y	1,440	7.1

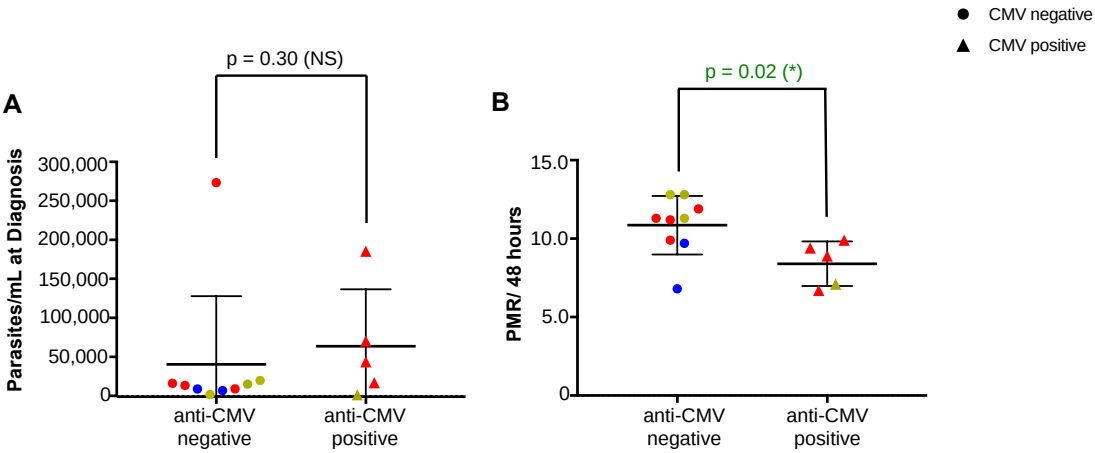

Figure 3.18 | Relationship between CMV seropositivity and parasite growth in the blood. Anti-CMV IgG seropositivity was assessed in each volunteer by ELISA, using baseline (C -1) plasma samples from the 14 infected volunteers. Data shown are the median and standard deviations of pairwise comparisons between parasite densities (parasites/mL at diagnosis) in the anti-CMV IgG negative volunteers (n = 9) and anti-CMV IgG positive volunteers (n = 5) **(A),** and between Parasite Multiplication Rates (PMR/48 hours) in **B**. Volunteers have been colour-coded as per transcriptional response group; "classical" responders in red, "non-classical" responders in blue and "unknown" volunteers in yellow. Comparisons were made using non-parametric Mann-Whitney U test. *P < 0.005. NS = Not significant.

3.5.10 Relationship between host responder status and clinical outcome

As is standard protocol during CHMI, volunteers were safety-assessed at each clinic visit, by monitoring temperature, heart rate and blood pressure. With the exception of fever in one “classical” responder (volunteer ♯17) on day of diagnosis (figure 3.19), no marked changes were observed in any volunteer safety measurements throughout the duration of infection (see Appendix 7 for volunteer clinical data). At baseline, C +6 and diagnosis, volunteers were also screened for perturbations in the biochemical markers; sodium, potassium, urea, creatinine, bilirubin, alanine aminotransferase (ATL), alkaline phosphatase (ALP), albumin and haemoglobin. Analysis of volunteer biochemistry was performed across the groups to determine any associated signs of liver dysfunction. With the exception of a drop in albumin levels at C +6 days post-infection, in the “classical” responders, no significant changes in biochemistry were observed in any of the volunteers, in response to infection with blood-stage *P. falciparum* (Table 3.5).

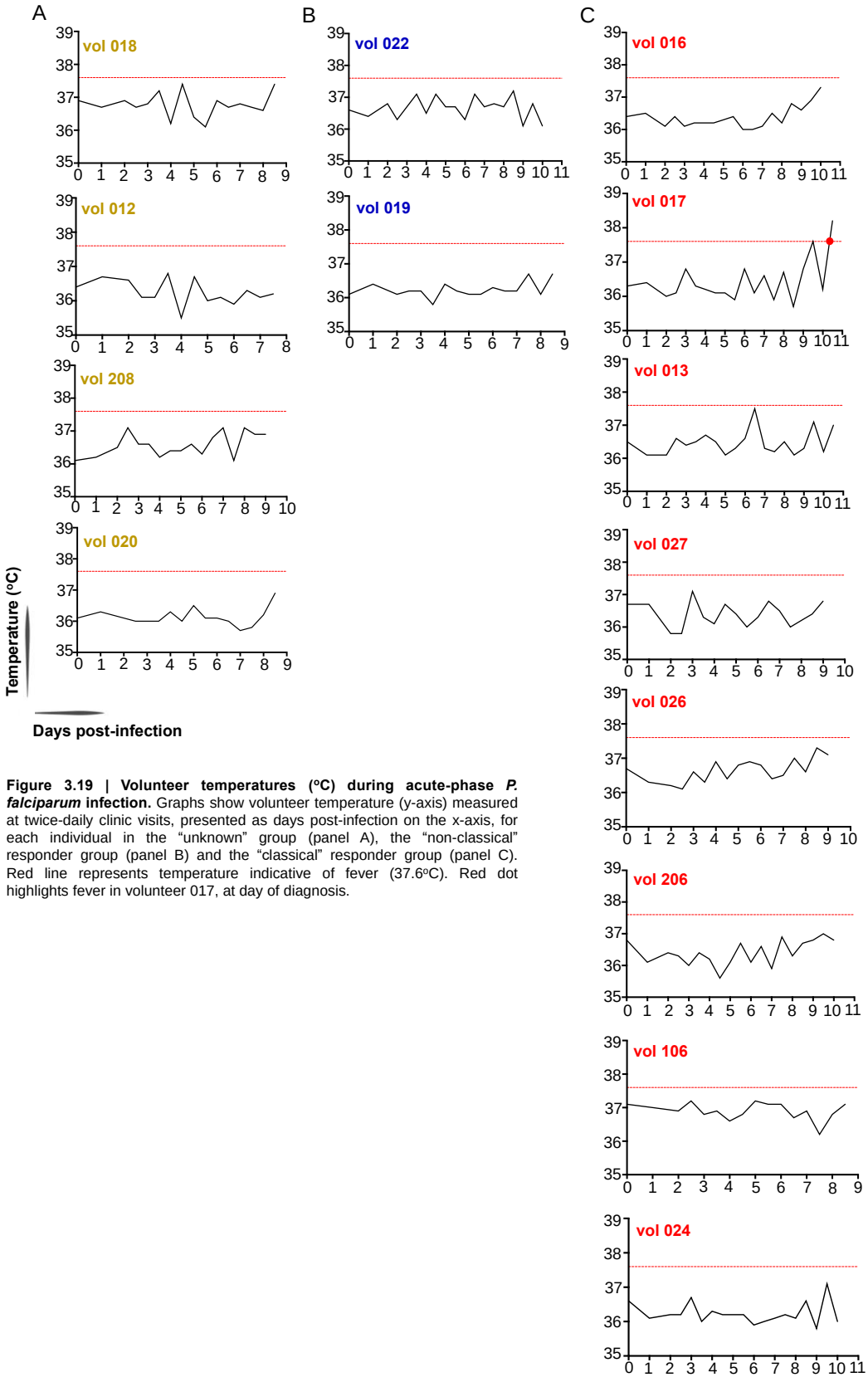

Figure 3.19 | Volunteer temperatures (ºC) during acute-phase *P. falciparum* infection. Graphs show volunteer temperature (y-axis) measured at twice-daily clinic visits, presented as days post-infection on the x-axis, for each individual in the "unknown" group (panel A), the "non-classical" responder group (panel B) and the "classical" responder group (panel C). Red line represents temperature indicative of fever (37.6ºC). Red dot highlights fever in volunteer 017, at day of diagnosis.

Figure 3.19 | Volunteer temperatures (ºC) during acute-phase *P. falciparum* infection (see legend above)

Table 3.5 | Table of volunteer Biochemistry

	Sodium (mmol/L)			Potassium (mmol/L)			Urea (mmol/L)			Creatinine (µmol/L)			Bilirubin (µmol/L)			ALT (IU/L)			ALP (IU/L)			Albumin (g/L)			Haemoglobin (g/dL)		
	135.0 - 145.0 mmol/L			3.5 - 5.1 mmol/L			4.0 - 8.2 mmol/L			50.0 - 110.0 µmol/L			3.0 - 22.0 µmol/L			7.0 - 56.0 IU/L			45.0 - 180.0 IU/L			35.0 - 50.0 g/L			12.0 - 18.0 g/dL		
Volunteer I.D (gender)	C -1	C +6	Diagnosis	C -1	C +6	Diagnosis	C -1	C +6	Diagnosis	C -1	C +6	Diagnosis	C -1	C +6	Diagnosis	C -1	C +6	Diagnosis	C -1	C +6	Diagnosis	C -1	C +6	Diagnosis	C -1	C +6	Diagnosis
18 (F)	138.0	140.0	141.0	4.0	3.8	3.3	5.0	4.1	5.1	47.0	46.0	52.0	10.0	9.0	5.0	14.0	10.0	8.0	178.0	165.0	176.0	44.0	42.0	43.0	14.4	13.7	13.2
12 (M)	142.0	140.0	142.0	3.7	3.9	3.7	5.1	4.4	4.3	56.0	53.0	64.0	12.0	11.0	14.0	12.0	13.0	18.0	164.0	154.0	161.0	45.0	43.0	46.0	14.2	14.3	13.7
208 (M)	140.0	139.0	140.0	3.2	3.9	3.6	3.8	5.1	3.9	71.0	74.0	67.0	27.0	25.0	23.0	14.0	12.0	16.0	147.0	142.0	131.0	45.0	47.0	46.0	14	15	15.1
20 (M)	141.0	142.0	141.0	3.4	3.8	3.6	5.8	6.1	5.5	67.0	73.0	70.0	14.0	16.0	8.0	37.0	27.0	28.0	117.0	116.0	113.0	45.0	46.0	44.0	14.3	14	13.2
Group Mean	*140.3*	*140.3*	*141.0*	*3.6*	*3.85*	*3.55*	*4.9*	*4.925*	*4.7*	*60.3*	*61.5*	*63.3*	*15.8*	*15.3*	*12.5*	*19.3*	*15.5*	*17.5*	*151.5*	*144.3*	*145.3*	*44.8*	*44.5*	*44.8*	*14.2*	*14.3*	*13.8*
16 (M)	140.0	141.0	139.0	4.3	3.8	3.6	4.6	4.0	3.6	81.0	80.0	73.0	12.0	12.0	9.0	19.0	14.0	30.0	137.0	133.0	133.0	49.0	43.0	44.0	15.7	14.2	14.4
17 (M)	141.0	140.0	139.0	3.9	4.0	3.9	5.8	6.7	5.2	64.0	60.0	67.0	11.0	8.0	10.0	36.0	25.0	35.0	133.0	144.0	137.0	45.0	46.0	46.0	15.3	14.5	14.0
13 (M)	142.0	142.0	140.0	3.8	4.0	3.8	5.2	5.0	5.6	63.0	81.0	69.0	8.0	9.0	6.0	20.0	18.0	26.0	153.0	140.0	159.0	45.0	43.0	47.0	13.6	14.2	14.7
27 (M)	139.0	142.0	142.0	3.4	4.0	3.4	6.0	4.0	5.3	62.0	62.0	68.0	19.0	10.0	13.0	21.0	12.0	15.0	158.0	156.0	177.0	51.0	48.0	51.0	14.2	13.7	13.8
26 (F)	142.0	143.0	140.0	3.8	4.7	3.4	4.5	3.6	5.3	64.0	70.0	62.0	16.0	15.0	17.0	19.0	22.0	18.0	110.0	105.0	108.0	45.0	44.0	45.0	12.3	12.0	11.4
206 (M)	143.0	143.0	140.0	3.6	3.4	4.2	3.4	5.2	4.6	80.0	84.0	91.0	14.0	14.0	11.0	13.0	13.0	13.0	158.0	143.0	165.0	47.0	45.0	45.0	15.9	15.6	15.6
106 (F)	139.0	140.0	140.0	3.9	3.7	3.5	4.2	3.7	4.0	57.0	56.0	59.0	24.0	24.0	27.0	8.0	10.0	8.0	183.0	150.0	162.0	45.0	42.0	45.0	13.0	12.5	12.9
24 (M)	142.0	142.0	145.0	3.4	4.0	3.4	6.2	5.1	4.5	70.0	75.0	72.0	10.0	11.0	9.0	13.0	12.0	16.0	158.0	152.0	166.0	49.0	46.0	52.0	13.5	13.2	13.2
Group Mean	*141.0*	*141.6*	*140.6*	*3.8*	*4.0*	*3.7*	*5.0*	*4.7*	*4.8*	*67.6*	*71.0*	*70.1*	*14.3*	*12.9*	*12.8*	*18.6*	*15.8*	*20.1*	*148.8*	*140.4*	*150.9*	*47.0*	*44.6**	*46.9*	*14.2*	*13.7*	*13.8*
22 (F)	142.0	140.0	140.0	3.9	3.7	3.5	3.4	3.7	3.2	56.0	57.0	46.0	9.0	8.0	7.0	8.0	8.0	11.0	145.0	157.0	146.0	46.0	48.0	48.0	12.8	13.0	12.9
19 (M)	141.0	141.0	139.0	3.3	3.8	3.3	4.0	4.3	3.8	65.0	78.0	75.0	8.0	19.0	10.0	20.0	16.0	15.0	144.0	137.0	147.0	48.0	47.0	48.0	14.9	14.5	14.6
Group Mean	*141.5*	*140.5*	*139.5*	*3.6*	*3.8*	*3.4*	*3.7*	*4.0*	*3.5*	*60.5*	*67.5*	*60.5*	*8.5*	*13.5*	*8.5*	*14.0*	*12.0*	*13.0*	*144.5*	*147.0*	*146.5*	*47.0*	*47.5*	*48.0*	*13.9*	*13.8*	*13.8*

* Significant drop in albumin levels at C +6 in the "classical" responders (Wilcoxon signed rank test, p = 0.0234)

Green type indicates healthy reference range for human adults

Angiopoietin-2 (ANG-2) is a secreted glycoprotein that plays a complex role in angiogenesis and inflammation. As a marker of endothelial cell activation, serum levels of ANG-2 in healthy individuals are normally low, whereas increased levels are associated with disease states that cause inflammation and vascular permeability (Fagiani and Christofori 2013). In the context of malaria infection, increased levels of ANG-2 have been widely associated with severe clinical outcome (Viebig *et al.* 2005, Yeo *et al.* 2008) and more recently, as a predictor of mortality in patients presenting with cerebral malaria (Lovegrove *et al.* 2009, Conroy *et al.* 2012). Therefore, to assess the relationship between host responder status and clinical outcome, an ELISA was used to quantify levels of ANG-2 in the plasma of volunteers. A mean concentration of 2,352.62 pg/mL ANG-2 was detected in volunteer plasma at baseline (C -1), and demonstrated little increase in response to *P. falciparum* infection (2,407.23 pg/mL at diagnosis) (figure 3.20, part A). Moreover, ANG-2 concentrations were comparable between the "classical" responder, "non-classical" responder and "unknown" groups at diagnosis (figure 3.20, part B), and showed no significant correlation with parasitaemia (figure 3.20, part C). Interestingly, a 1.6-fold increase in ANG-2 levels was detected in volunteer ♯16 at diagnosis; the most inflammatory responder in the cohort (Table 3.6). Although only observed in one volunteer, it may be indicative of increased ANG-2 production in response to systemic inflammation, or increasing parasite sequestration, and endothelial cell activation. Therefore, it will be important to validate these findings in a larger cohort of individuals.

Table 3.6 | Angiopoietin-2 levels at C -1 and diagnosis

Volunteer I.D	C -1	Diagnosis	Fold change at Diagnosis
18	1913.33	2032.08	1.06
12	3357.08	3457.08	1.03
208	1461.25	1686.25	1.15
20	1938.33	2457.08	1.27
Group Mean	**2167.50**	**2408.13**	**1.11**
16	3069.58	4884.17	1.61
17	1513.33	2236.25	1.48
13	3523.75	2046.67	1.35
27	2105.00	2067.50	0.98
26	2180.00	1840.42	0.84
206	2742.50	1952.92	0.71
106	2438.33	2498.75	1.02
24	3017.50	3096.67	1.03
Group Mean	**2573.75**	**2577.92**	**1.00**
19	1946.67	1948.75	1.00
22	1730.00	1496.67	0.87
Group Mean	**1838.33**	**1722.71**	**0.94**

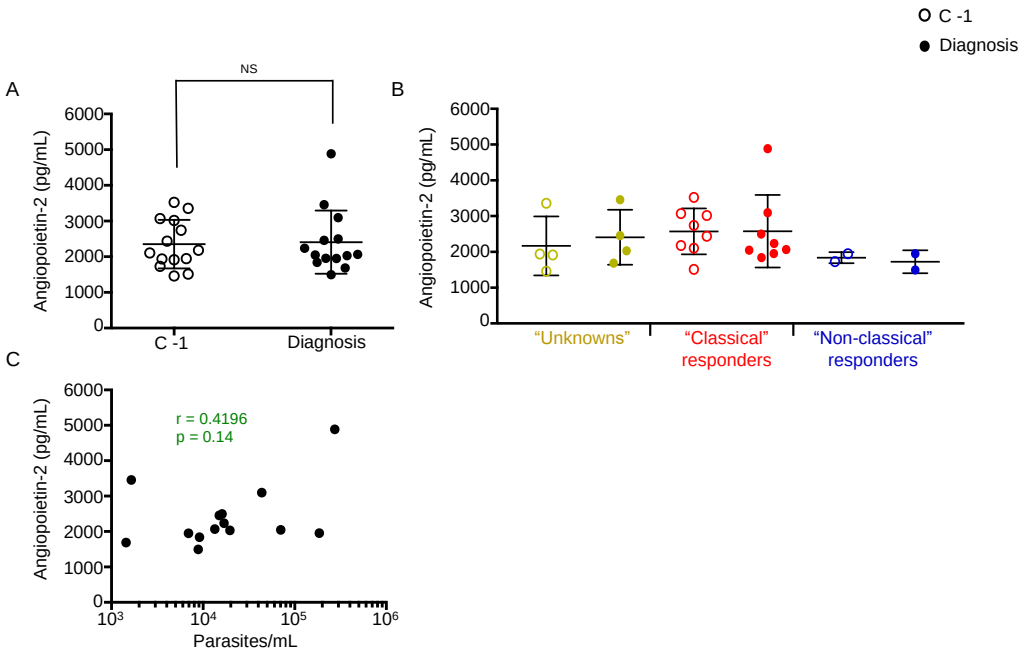

Figure 3.20 | Angiopoietin-2 levels during blood-stage *P. falciparum* infection. A) Angiopoietin-2 levels (pg/mL) as measured in volunteer plasma, at baseline/C -1 (open circles) and diagnosis (closed circles) for all 14 infected. The mean and standard deviation is shown. **B)** comparison of Angiopoietin-2 levels at C -1 and diagnosis within and between groups; "unknown" volunteers ♯12, ♯18, ♯20 and ♯208 (yellow), "classical" responders ♯13, ♯16, ♯17, ♯24, ♯26, ♯27, ♯106 and ♯206 (red) and "non-classical" responders ♯19 and ♯22 (blue). The mean and standard deviation is shown. **C)** Relationship between parasitaemia at diagnosis, as measured by qPCR (parasites/mL), and levels of Angiopoietin-2 (pg/mL) at diagnosis. Spearman's rank correlation coefficient (r) and p-value is shown on the graph. ELISA was performed by Diana Munoz Sandoval. NS = Not Significant.

As a routine measure, volunteers were asked to grade any symptoms experienced during the CHMI follow-up period, using a severity score (see chapter 2, section 2.1.7). Symptoms included; pyrexia, feverishness, rigor, chills, sweats, headaches, myalgia, arthralgia, back pain, fatigue, nausea, vomiting and diarrhoea. Volunteers that reported most frequent and more severe symptomology were those belonging to the "classical" responder group (figure 3.21), with the three most inflammatory volunteers (♯16, ♯17 and ♯13) reporting grade 3 severity for fatigue, headaches and fever. Thus, although subjective, symptomology that could be assessed during the CHMI follow-up period appeared to correlate with host responder status.

Figure 3.21 | Reported clinical events. Heatmaps of volunteer clinical events, as reported on diary cards during CHMI follow-up period. Volunteers were asked to grade symptoms (y-axis) at each twice-daily clinic visit post-CHMI throughout the duration of their infections (x-axis), according to the scale above: 0 = symptom absent, 1 = symptom causing mild or transient discomfort, with no medical intervention required, 2 = symptom causing mild to moderate limitation in activity, with minimal medical intervention required and 3 = symptom causing marked limitation in activity, assistance or medical intervention required. Volunteers are grouped based on transcriptional response profile; “unknown” volunteers (yellow), “classical” responders (red) and “non-classical” responders (blue).

3.6 Discussion

The clinical outcomes associated with malaria infection are characteristically diverse, and appear strongly influenced by the type of immune response elicited early in infection. An effective response can control parasite growth without causing damage to the host, whereas unregulated activation of innate immune cells can result in the over-production of pro-inflammatory cytokines, leading to pathology (Gazzinelli *et al.* 2014). The multifactorial nature of clinical disease has greatly confounded efforts to define mechanisms of pathogenesis, as well as correlates of protection. Thus, greater investment needs to be placed in understanding the most basic aspects of the human response to *Plasmodium falciparum*.

CHMI offers the opportunity to dissect host-pathogen interactions at an unprecedented level of detail. Over recent years, an increasing number of researchers have utilised this model to investigate the early host response to *P. falciparum* (see chapter 1, section 1.6.5). Where this study offers an important advantage over others however, is the sampling of volunteers over a time-course throughout infection, thus allowing each individual to be treated as their own experiment. Importantly, this was conducive to the assessment of inter-individual variability in host responses. When responses were compared across volunteers, distinct patterns of gene expression were evident in whole blood. 8 out of 14 volunteers responded by up-regulation of genes associated with the innate inflammatory response, many of which were interferon-stimulated genes. In contrast, 2 volunteers had a very distinct response, suppressing genes associated with the inflammatory response, cell signaling and metabolism. In 4 out of 14 volunteer (29%), no response was detected in the time frame assessed.

Further validating the inter-individual variation in host immune response to *P. falciparum*, were levels of chemokines detected in the plasma of volunteers. CXCL10 (IP-10) and CXCL9 (MIG) were found elevated in the 8 “classical” responders but in none of the others, reflecting volunteer responder status as defined by microarray. Elevated levels of these chemokines has been associated with more severe disease in malaria patients (Schofield and Grau 2005, Ayimba *et al.* 2011) and thus, may be predictive of a more adverse outcome in this group of 8

volunteers; something otherwise impossible to assess in studies of CHMI. Consistent with the transcriptomics data, cytokine and chemokine analysis in the group of "unknown" volunteers suggest little in the way of a response to *P. falciparum* infection within the time frame assessed. Moreover, volunteer ♯16, demonstrating the most marked up-regulation of innate/inflammatory response genes at the transcript level, displayed the biggest fold-change (from baseline) in levels of CCL2, CXCL10, CXCL9, INFγ, IL-10 and IL-6, all of which have been associated with symptomatic malaria infection (Day *et al.* 1999, Abrams *et al.* 2003, Lyke *et al.* 2004, Walther *et al.* 2006, Armah *et al.* 2007, Jain *et al.* 2008, Ayimba *et al.* 2011, Mirghani *et al.* 2011, Wilson *et al.* 2011). Full blood count analysis revealed a significant decrease in the blood proportion of lymphocytes at diagnosis compared to baseline, in these 8 volunteers. 3 out of the 8 in this group (volunteers ♯16, ♯17 and ♯26) were lymphopenic (had $<1x10^6$ lymphocytes/mL of whole blood) by day of diagnosis. This is consistent with studies of malaria patients exhibiting high levels of inflammation in the natural infection setting (Hviid *et al.* 1997). Thus, based on these data it appears that increased production of CXCL9 and CXCL10 at the transcript and protein level, along with decreased numbers of lymphocytes in the blood, may serve as biomarkers of a more inflammatory, adverse clinical outcome during primary infection with blood-stage *P. falciparum* (3D7).

In the "classical" responder group, pathway analysis revealed a signature consistent with activation of both Type II (IFNγ), and Type I (IFNα/β) signalling, as has been previously published in studies of CHMI (Montes de Oca *et al.* 2016, Gardinassi *et al.* 2018). Although well described in the context of anti-viral defense, the role of Type I IFNs in immunity to other pathogens is less clear. They have been highlighted in a regulatory capacity in models of Listeria monocytogens and Tuberculosis, demonstrating inhibitory effects on various innate immune cells including macrophages, monocytes and neutrophils, leading to higher infection burdens and severe pathology. (Auerbuch *et al.* 2004, Carrero *et al.* 2004, Berry *et al.* 2010, Desvignes *et al.* 2012, McNab *et al.* 2015). To date, the functional roles of Type I IFNs during *Plasmodium* infection have mainly focused on mouse models of lethal, experimental cerebral malaria (ECM), and evidence has been controversial. Disruption to Type I IFN signalling in mice lacking the IFNα/β receptor enhanced the survival of *P. berghei*-infected *and P. yoelii*-infected mice, and in all cases was

accompanied by a decrease in immune cell activation, and unregulated parasite growth (Haque *et al.* 2011, Ball *et al.* 2013, Haque *et al.* 2014, Spaulding *et al.* 2016, Zander *et al.* 2016). Yet, counterevidence form *P. berghei*- infected mice receiving daily i.p injections of recombinant IFNα suggest a protective role of Type I IFNs, whereby mice had better control of parasite densities, and reduced incidence of cerebral malaria compared to wild-type mice (Vigario *et al.* 2007). Limited data from studies of human malaria infection are also controversial. Up-regulation of the Type I IFN pathway has been associated with mild malaria compared to severe disease, in a cohort of Malawian children (Krupka *et al.* 2012) whereas, in the setting of experimentally-induced infection, Type I IFN-driven neutrophil activation correlated with increased levels of circulating transaminases, indicative of liver pathology (Rocha *et al.* 2015). Furthermore, a study carried out in the Gambia revealed that two SNPs (17470-G/G and L168V-G/G) in the gene encoding IFNαR1 are associated with protection against severe and cerebral malaria (Aucan *et al.* 2003). Thus, the capacity to which Type I IFN responses mediate susceptibility/protection during primary infection with *P. falciparum* remains to be defined.

The erythrocytic stage of infection is characterised by a strong proinflammatory response, hallmarked by the production of large amounts of IFNγ (Type II IFN). During this phase, IFNγ is thought to play a key role in the activation of phagocytic cells, promoting clearance of infected red blood cells and thus controlling parasitaemia (Riley and Stewart 2013). The kinetics of IFNγ production during the earliest stages of the acute-phase of human *P. falciparum* infection however have not been well defined. In this cohort of volunteers, IFNγ was undetectable in the plasma at baseline and, with the exception of 3 volunteers, remained undetectable during the CHMI follow-up period. Interestingly, a spike in IFNγ levels was observed in three of the most inflammatory responders, but not until the end of their infection time-course (diagnosis time-point). Importantly, recent evidence suggests a dominant role of Type I IFNs, over that of IFNγ during the initiation of the inflammatory response to malaria. Data from both mouse and human models of *Plasmodium* infection have shown an ability of Type I IFNs to suppress IFNγ-driven cellular responses at this early stage in infection (Haque *et al.* 2014, Montes de Oca *et al.* 2016). Furthermore, studies suggest that this dominant Type I IFN response is

associated with the expression of negative regulators such PDL-1, which work to inhibit adaptive responses (Haque *et al.* 2011, Yu *et al.* 2016, Zander *et al.* 2016). This paradigm has also been demonstrated in the context of viral infection (Shaabani *et al.* 2016), and may be consistent with our transcriptional dataset, whereby volunteers displaying the strongest Type I IFN response, also had up-regulated expression of CD274 (PDL-1), SOCS1, SOCS3, and down-regulation expression of CD40L. However, given that there is substantial overlap in the genes they regulate, it is difficult to speculate a dominant role of either Type I or Type II responses in this cohort of volunteers. Furthermore, there is evidence to suggest that the two can work cooperatively, through the regulated expression of STAT1 (Gough *et al.* 2010), although the precise mechanisms of this cross-talk have not been examined in the context of *Plasmodium* infection. Surprisingly, levels of (Type I) IFNα detected in the plasma did not appear to fluctuate in response to infection, suggesting that transcript-level interferon-stimulated responses are observed before an increase in circulating interferon can be detected. One possible explanation for this is that the initial production of IFNs, in response to *P. falciparum,* does not occur systemically, but instead is an upstream event that takes place in tissue(s). This hypothesis is supported by recent evidence implicating plasmacytoid dendritic cells (pDCs), in the bone marrow, as the main source of systemic Type I IFNs, following TLR7/MyD88-mediated sensing of parasites in *P. yoelii*-infected mice (Spaulding *et al.* 2016). Thus, the strong interferon-stimulated gene signature detected in the blood of these volunteers may be an effect of cells being activated by Type I IFNs (and/or Type II IFNs) in the bone marrow and being subsequently released into the circulation. It is important to note that human malaria is a multi-organ disease, involving a vast range of cell-types and tissues that cannot be accessed for investigation. Thus, only in conjunction with appropriate mouse models will we be able to gain a full appreciation of the mechanisms mediating protection/susceptibility to this parasite.

In line with studies implicating the role of Type I IFNs in the initiation of deleterious inflammatory responses, also found activated in these volunteers were pathways for inflammasome and TREM1 signalling. Inflammasome signalling was associated with up-regulation of AIM2, CASP1 and CASP5, suggesting activation of both AIM2 and NLRP3 inflammasomes, in response to cytosolic sensing of parasite DNA and

haemozoin, respectively (Kalantari *et al.* 2014). Also found up-regulated were the cytosolic PRRs; DDX58 (RIG-I) and IFIH1 (MDA-5), responsible for the recognition of RNA (McNab *et al.* 2015). The processes by which phagocytic cells of the immune system are able to detect and process parasite-derived molecules via cytosolic PRRs, inducing Type I IFN responses, have been discussed in recent literature (Kalantari *et al.* 2014, Sisquella *et al.* 2017).

It is difficult to predict what effect the suppressive response may mean for clinical outcome in the two volunteers of the "non-classical" responder group. Death receptors play a central role in instructive/ programmed cell death. Their activation is typically observed during viral infection, and in the context of malignantly-transformed or excessively activated cells. In these settings, programmed cell death serves as a host defense mechanism, by eliminating cells that are potentially dangerous (Fuchs and Steller 2011), whilst preventing initiation of inflammatory pathways (Bruchhaus *et al.* 2007). Abnormal regulation of this process may therefore prove detrimental to the host, but there is it yet unclear what effect this may have in the context of *P. falciparum* infection. Pathway analysis also revealed inhibition of those linked to the innate immune response, such as TREM-1 signalling, in these "non-classical" responders. It is possible that early suppression of innate inflammatory responses may inhibit the overproduction of pro-inflammatory mediators, thus helping to reduced pathology. On the other hand, it may reflect a reduced ability to control parasite growth, leading to more severe disease outcome later in infection. Thus, it was important to consider a potential correlation between host responder status and parasite growth in the blood.

Parasite multiplication rates, as measured over each 48-hour parasite growth cycle in the blood, were not influenced by host transcriptional response status, and vice versa. This is in line with the recent reanalysis of historical malariatherapy data, suggesting a host-specific influence on acquired immunity, independent of parasite growth kinetics during primary infection (Molineaux *et al.* 2002). Importantly, individuals who elicited a robust inflammatory response (the 8 "classical" volunteers) had no better control of parasite growth than those who failed to respond within the time assessed (the 4 "unknowns"). This contests previously published data associating innate inflammatory responses with enhanced parasite clearance in the

malaria-naïve host (Walther *et al.* 2005, Walther *et al.* 2006, Horowitz *et al.* 2010, Haque *et al.* 2011, Montes de Oca *et al.* 2016). Also interesting was the lack of response detected in the group of “unknowns”, as all four reached comparable- and in some cases higher- parasitaemias to the “classical” responders. This suggests that there is likely a parasite density threshold for activation of host immune responses, and that it is highly variable between individuals.

There is evidence to suggest that microbial exposure (or past infection history) is a driver of immune variation, and CMV seropositivity has been shown to influence variability in host immune responses (Sylwester *et al.* 2005, Schoenfisch *et al.* 2011, Brodin *et al.* 2015, Shmeleva *et al.* 2015). The prevalence of human CMV infection varies greatly depending on geographic and socioeconomic backgrounds of the population, reaching ~30 - 80% in adults (Dollard *et al.* 2011). Thus, CMV IgG seropositivity was assessed in the volunteers, to investigate an association with host responder status. 35% of volunteers (5/14) tested positive for anti-CMV IgG; 4 in the “classical” responder group and 1 in the “unknowns”. Therefore, CMV IgG seropositivity does not explain the variation in host response observed in this cohort of volunteers, as only 50% of “classical” responders are seropositive for CMV. Interestingly, volunteers who were seropositive for anti-CMV IgG were found to have significantly lower parasite multiplication rates when compared to volunteers that were seronegative. However, this ELISA is designed to be semi-quantitative and with just 14 volunteers, this association will need to be investigated using a greater number of individuals before drawing any conclusions.

One of the major limitations of CHMI is the early termination of volunteer infections, often at a time preceding any clinical symptomology. Thus, in an attempt to predict the clinical severity that may have eventuated had infection been allowed to continue without drug treatment, levels of Angiopoietin-2 (ANG-2) were quantified in the plasma of these individuals. The only volunteer demonstrating elevated ANG-2 levels (>1.5 fold increase) at diagnosis was the “classical” responder ♯16. It is difficult to speculate a trend based on n = 1, but it may be indicative of endothelial cell activation in response to systemic inflammation, or upon reaching a threshold of parasite density (volunteer ♯16 had the highest parasite density at 273,247 p/mL). Overall, results may reflect too early a time-point, or parasitaemias too low for ANG-

2 production in response to CHMI with blood-stage *P. falciparum,* and suggest that activation of the endothelium is a secondary event to inflammation in this setting. Symptoms reported by volunteers during the CHMI follow-up period did suggest a relationship between host responder status and clinical outcome, however. Volunteers within the "classical" responder group reported more frequent and more severe clinical events, compared to those of the "non-classical" responders and "unknown" volunteers. The type of response produced following blood-stage CHMI thus appears to predict clinical outcome. However, it is unfortunate to have to rely on such subjective means for a clinical read-out in studies of CHMI.

It is important to consider the other potential limitations of this study. Due to restrictions in blood volume/sampling of volunteers throughout the CHMI follow-up period, my analysis of the host transcriptional response was confined to a 48-hourly time course. This sampling schedule may have been too infrequent to detect certain immune events, and/or transient patterns of gene expression out-with the designated collection times. Furthermore, although the whole-blood transcriptome has provided a great overview of the early immune events during primary *P. falciparum* infection, this study would have benefited from a combined analysis of cellular subsets, to determine the key immune cells associated with the response(s). This will be an important consideration for future trial design. Analysis based on transcriptome data is also restricted in that evidence for gene expression/regulation does not necessary translate to protein production. Importantly, this study has revealed evidence for inter-individual variability in the host response to primary *P. falciparum* infection, however was limited in its statistical power due the small number of volunteers enrolled in control group (n = 14). I fully acknowledge that the results presented within this chapter are preliminary, and may be at risk of bias due to the small cohort of volunteers used in the study. Interpretations of these results are in no way conclusive, but are intended to better inform future hypothesis-driven studies of the host response to *P. falciparum* infection. It will therefore be crucial to validate the observations from this study using larger cohorts of volunteers across more studies.

In conclusion CHMI in 14 previously malaria-naïve volunteers has revealed a possible dichotomy in the host immune response to *P. falciparum* blood stage

infection. Responder status did not appear to be associated with parasite growth kinetics, but correlated with chemokine levels in the plasma. Results suggest important practical implications in understanding the diversity of clinical responses to vaccination and induction of effective anti-pathogen immunity. Thus, investment should be placed on understanding the contribution of host and parasite genetics, to inter-individual variability in immune responses to *P. falciparum*.

Chapter 4: *P. falciparum* Gene Expression in the Malaria-Naïve Host

4 *P. falciparum* Gene Expression in the Malaria-Naïve Host

4.1 Abstract

P. falciparum gene expression- specifically *var* gene expression- is predicted to dictate clinical outcome in the non-immune host. In particular, *var* genes encoding a restricted subset of group-A, B/A *Plasmodium falciparum* erythrocyte membrane protein 1 (PfEMP1) variant surface antigens have been associated with severe malaria disease, giving rise to the hypothesis that these *var* gene variants are dominantly expressed in individuals that have yet to develop an immune response to the parasite. However, the extent to which parasite gene expression influences the developing host immune response remains unclear. Herein, parasites isolated from the blood of 12 volunteers undergoing controlled infection with *P. falciparum* (3D7-strain) were analysed by RNA-sequencing to investigate expression of the *var*, *rif* and *stevor* multi-gene families. Moreover, parasites isolated at the end of volunteer infections were compared to those recovered from the inoculum used to infect, to investigate evidence for VSA selection *in vivo*. On the day of microscopic patency (day of diagnosis), a broad repertoire of *var* transcripts were detected in volunteer samples, and those that demonstrated highest expression were of the group-B subtype. Interestingly, *var* and *rif* gene profiles were almost identical across the 12 volunteer and 2 inoculum samples, suggesting there was little diversity within the cohort and that *in vivo* selection forces had not been activated in this setting. These data provide first evidence that the inter-individual variation in host immune responses, during primary infection with *P. falciparum*, is not driven by parasite gene expression but is instead more likely associated with factors intrinsic to the host.

4.2 Introduction

The virulence of *Plasmodium falciparum* is directly linked to the expression of parasite variant surface antigens (VSAs), the best characterised of which is *P. falciparum* Erythrocyte Membrane Protein 1. The expression of PfEMP1 on the surface of infected erythrocytes enables the parasite to adhere to a large variety of host receptors on microvasculature linings, in order to avoid passage through the spleen and subsequent clearance (Looareesuwan *et al.* 1987, Kyes *et al.* 2001).

This parasite survival strategy leads to the obstruction of blood flow, contributing to impaired perfusion in vital host organs- the main cause of pathology associated with infections with this species of malaria parasite (Dondorp *et al.* 2000, Dondorp *et al.* 2004, Dondorp *et al.* 2008, Hanson *et al.* 2012). There is good evidence that PfEMP1, exposed on the surface of infected cells, are natural targets of the developing antibody response of the host (Bull *et al.* 1998, Chan *et al.* 2012). This is thought to impose a selection pressure on the infecting parasite population, causing them to switch expression between different PfEMP1 variants in order to evade the host immune system and establish chronic infection (Smith *et al.* 1995, Bull *et al.* 1998, Chan *et al.* 2012). Allowing for this switch in PfEMP1 is the repertoire of ~60 *var* genes encoding these proteins. On the basis of the full genomic sequence of the *P. falciparum* 3D7 clone, *var* genes have been classified into three major groups (A, B and C) and two intermediate groups (B/A and B/C), defined by the presence of one of three conserved 5′ upstream sequences (UpsA, UpsB or UpsC) and by the gene's position and orientation within the chromosome (summarised in table 4.1). (Kraemer and Smith 2003, Lavstsen *et al.* 2003, Kraemer *et al.* 2007). All group-A genes have a DBLα1 type N-terminal domain and a lower number of conserved cysteine resides compared to the group-B, B/C and C genes that have DBLα0 N-terminal domains. Furthermore, the group-A and B/A members are larger and have more complex domain structures (Lavstsen *et al.* 2003, Robinson *et al.* 2003). The 3D7 reference clone possesses 10 group-A *var* genes, including the inter-strain conserved subfamilies *var1* and *var3,* 37 group-B members, 13 group-C genes and var2CSA, belonging to the conserved var2 sub-family. This group-E member is the dominant *var* gene transcribed in pregnancy-associated malaria, found expressed at high levels in parasites isolated from placentas (Kyes *et al.* 2003, Salanti *et al.* 2003). Four and nine of the 3D7 clone *var* gene members form chimeras of group B/A and B/C respectively. (Lavstsen *et al.* 2003). The expression of *var* genes occurs in a mutually exclusive fashion, such that just one is activated by each parasite at any given time (Dzikowski *et al.* 2006, Voss *et al.* 2006). In a population of infecting parasites however, this can give rise to broad expression of up to all ~60 members, and associated PfEMP1.

Table 4.1 | Characteristics of *P. falciparum* (3D7) *var* gene groups

var subgroup	Upstream Sequence	Position	Orientation (direction of transcription)	Median transcript size (kb)	No. of genes in 3D7
A	UpsA	Subtelomeric	Telomeric	9.2	10
B/A	UpsB	Subtelomeric	Centromeric	8.8	4
B	UpsB	Subtelomeric	Centromeric	6.6	24
B/C	UpsB	Central	Telomeric	6.7	9
C	UpsC	Central	Telomeric	6.6	13
E	UpsE	-	-	9.2	1

In areas of high malaria transmission, immunity to severe (life-threatening) disease develops more rapidly than immunity to mild malaria, as children grow older (Langhorne *et al.* 2008, Goncalves *et al.* 2014). One popular explanation for this in the scientific community is that restricted subtypes of disease-causing PfEMP1 variants are specialised for infection in malaria-naïve hosts, and upon development of antibodies to these PfEMP1, children are subsequently protected from severe infection (Bull *et al.* 1999, Bull *et al.* 2000, Nielsen *et al.* 2002, Staalsoe *et al.* 2003, Jensen *et al.* 2004, Abdi *et al.* 2017). Various studies have attempted to profile the *var* gene expression patterns associated with severe disease, using clinical *P. falciparum* isolates from children diagnosed with severe and mild malaria (Kirchgatter and Portillo Hdel 2002, Bull *et al.* 2005, Kaestli *et al.* 2006, Kyriacou *et al.* 2006, Rottmann *et al.* 2006, Normark *et al.* 2007, Falk *et al.* 2009, Warimwe *et al.* 2009, Kalmbach *et al.* 2010, Lavstsen *et al.* 2012, Warimwe *et al.* 2012, Bertin *et al.* 2013, Almelli *et al.* 2014, Abdi *et al.* 2015, Bertin *et al.* 2016, Jespersen *et al.* 2016, Mkumbaye *et al.* 2017, Shabani *et al.* 2017, Tonkin-Hill *et al.* 2018). However, results from these studies have proven inconclusive, potentially as a result of differences in methodologies used to measure *var* gene expression. The most common strategy uses degenerate primer pairs to target and amplify unique DBLα sequence tags for sequencing, and has implicated the group-A *var* genes exclusively, demonstrating that *P. falciparum* parasites expressing a higher proportion of these variants are positively associated with severe/symptomatic malaria disease (Kirchgatter and Portillo Hdel 2002, Bull *et al.* 2005, Kyriacou *et al.* 2006, Falk *et al.* 2009, Warimwe *et al.* 2009, Warimwe *et al.* 2012). However, this method requires the sequencing of a large number of clones for statistical significance and is inherently susceptible to primer bias. Other researchers have utilised qPCR primers designed to quantify more directly the transcript abundance of group-A, B and C *var* genes and conserved sequence blocks of DBL-domain cassettes. In the majority of these studies a higher frequency of group-A, B and

subsets of group-A and B PfEMP1 variants containing domain cassette 13 and 8 were detected in patients suffering with severe malaria disease, compared to those with mild or asymptomatic infections (Kaestli *et al.* 2006, Rottmann *et al.* 2006, Lavstsen *et al.* 2012, Abdi *et al.* 2015), whereas one found an association between increased transcripts of group-C *var* type and cerebral malaria (Kalmbach *et al.* 2010). More recently, RNA sequencing has been used to analyse gene expression patterns in clinical isolates of severe and uncomplicated malaria in Papuan patients, confirming the up-regulation of a subset of PfEMP1 proteins (containing DBLα1 domains) previously associated with severe malaria infections (Tonkin-Hill *et al.* 2018). Despite discrepancies in these results, it has been hypothesised that a restricted subset of group-A and/or B/A *var* genes/PfEMP1 is responsible for the pathogenesis of severe disease. Given that severe infections are most commonly observed in children with limited prior exposure to the *Plasmodium* parasite, there is a need to investigate *var* gene expression in a representative population of malaria-naïve individuals.

Four previous studies have utilised the controlled human malaria infection (CHMI) model to assess *var* gene expression during primary infection in the human host, reporting variable findings (Peters *et al.* 2002, Lavstsen *et al.* 2005, Wang *et al.* 2009, Bachmann *et al.* 2016). In the original study by Peters *et al*, *var* transcription profiles were assessed in parasites isolated from two volunteers on day 12 and 13 following infection with *P. falciparum* 3D7, and they report dominant expression of one group-B *var*, comprising ~40% of the sequences cloned from each individual. On the other hand, Wang *et al* report broad-level activation of ~90% of all *var* genes at the early onset of blood-stage infection (Wang *et al.* 2009). However, this study was limited to a single volunteer from which sufficient parasite material could be recovered for analysis. In a more recent study, parasite populations from 18 volunteers were found to express virtually identical transcript patterns that were dominated by the subtelomeric group-B *var* genes and, to a lesser extent, group-A (Bachmann *et al.* 2016). Unlike patients suffering with malaria following natural infection in the field, volunteers enrolled in studies of CHMI are only allowed to progress through a few cycles of parasite replication in the blood before they have to be treated. As a consequence, patients have very low levels of parasitaemia and often do not develop clinical symptoms (Sauerwein *et al.* 2011). Due to the reduced parasite material available in these volunteers, Lavstsen *et al* included a step for *in*

vitro culture of parasites for approximately one month prior to analysis, to ensure sufficient RNA material for qPCR, following isolation from the human host (Lavstsen *et al.* 2005). However, *P. falciparum* has been reported to switch *var* gene expression at variable rates *in vitro,* giving rise to potential bias in gene selection (Roberts *et al.* 1992, Horrocks *et al.* 2004, Peters *et al.* 2007, Bachmann *et al.* 2011). In this instance, *var* gene expression profiles in the cultures at the time of transcriptional analysis may not reflect the expression profile at the time of blood collection, making it difficult to interpret results. Therefore, it is important to clarify these contradicting data in order to better understand parasite *var* gene expression in the naïve human host.

In recent years, RNA sequencing (RNA-seq) has allowed many advances in the characterisation and quantification of transcriptomes and can now be successfully performed at the single cell level (Liu and Trapnell 2016, Reid *et al.* 2018). Providing that parasite samples can be prepared to sufficient purity, this method offers an appealing alternative to qPCR for the analysis of *ex vivo* parasite gene expression. It also holds a major advantage over *var*-specific qPCR, in that analysis is not limited to one multi-gene family. The *P. falciparum* genome consists of other multi-gene families encoding VSAs with potential influence on host immunity and clinical outcome. These include the repetitive interspersed family (*rif*), encoding RIFINS and sub-telomeric variable open reading frame (*stevor)* encoding STEVORS, for which 143 and 32 members have been found in the 3D7 genome, respectively (Kyes *et al.* 1999, Lavazec *et al.* 2007, Joannin *et al.* 2008, Bachmann *et al.* 2012, Wahlgren *et al.* 2017). These proteins are expressed on the surface of infected erythrocytes and thus are thought to be important for the sequestration of parastised erythrocytes and the pathogenesis of severe malaria (Niang *et al.* 2009, Niang *et al.* 2014, Goel *et al.* 2015, Wahlgren *et al.* 2017). In an important study by Bachmann *et al*, the expression dynamics of *rif* and *stevor*-encoded proteins were assessed in clinical *P. falciparum* isolates, using quantitative real-time PCR (Bachmann *et al.* 2012). Interestingly, both *rif* and *stevor* multi-gene families were found overexpressed in clinical isolates, relative to 3D7-strain parasites, and demonstrated a complex pattern of expression during clinical progression (Bachmann *et al.* 2012). Results are suggestive of diverse functional roles of the RIFIN and STEVOR proteins *in vivo*, yet little information is currently available on how they may influence disease progression and the developing host immune response. Having previously

demonstrated diversity in the host responses to controlled *P. falciparum* infection, I wanted to profile *var, rif and stevor* gene expression in the malaria-naïve host, and investigate the influence of parasite VSA expression as a driver of this inter-individual variability.

4.3 Hypothesis and specific aims

This chapter investigates the hypotheses that a subset of group-A and/or B/A disease-associated *var* genes are dominantly expressed in the naïve human host, and that inter-individual variation in parasite gene expression will reflect the inter-individual variation observed in host immune responses.

Specific aims

1. To isolate parasites from the blood of volunteers during controlled human malaria infection, in sufficient numbers and purity for direct *ex vivo* RNA-sequencing.
2. To investigate multi-gene family (*var, rif* and *stevor*) selection in the naïve host, by comparing parasites isolated at time of patent infection with samples of parasite inoculum used to infect.
3. To determine inter-individual variation in parasite gene expression, consistent with the inter-individual variation in host immune responses observed within the cohort.

4.4 Methods

Analysis of *P. falciparum* gene expression in the naive host was done in collaboration with Dr Adam Reid, Dr Mandy Sanders and Geetha Sankaranarayanan, at the Wellcome Trust Sanger in Cambridge, UK. Their contribution has been stated in the relevant sections that follow.

4.4.1 List of materials

Reagent	Supplier	Catalog Number
1.5 mL Eppendorf® tubes	Sigma-Aldrich	T9661-1000EA
50 mL Falcon tubes	Becton Dickinson (BD)	352098
50 mL luer syringe	Becton Dickinson (BD)	12339159
250 mL centrifuge bottles	Corning Life Sciences	CLS 431842
Sterile D200 ST pipette tips	Gilson	F171301
Sterile D1000 ST pipette tips	Gilson	F171501
PBS (1x)	Gibco	20012-019
Leucoflex LXT filters	Scottish National Blood Transfusion Service	-
Saponin	Sigma-Aldrich	8047-15-2
TRIzol™	Ambion (Life technologies)	115596026
0.5 mL DNA LoBind Eppendorf® tubes	Eppendorf	22431005
1.5 mL DNA LoBind Eppendorf® tubes	Eppendorf	22431021
UltraPure Ethanol	Sigma-Aldrich	51976
Bromochloropropane	Sigma-Aldrich	B9673-200mL
DEPC H_2O	Thermo Fisher Scientific	750024
Globin-Zero® Gold kit	Epicentre (Illumina)	GZG1224
Linear acrylamide	Ambion (Life technologies)	AM9520
Magnetic Core Kit (beads)	Epicentre (Illumina)	MR211124C
DynaMag™-2 Magnet	Thermo Fisher Scientific	12321D
RNA 6000 Pico Chip Bioanalyzer Kit	Agilent	
Sterile D10 ST pipette tips	Gilson	F171101
Sterile D200 ST pipette tips	Gilson	F171301
Sterile D1000 ST pipette tips	Gilson	F171501
Zymo-Spin RNA Clean and Concentrator™ -5 kit	Zymo Research	R1016
Agencourt Ampure XP beads	Beckman Coulter	A63881
Betaine (BioUltra >99.0 %)	Sigma-Aldrich	61962
dNTP mix (10 mM)	Fermentas	R0192
DynaMag™-2 Magnet	Thermo Fisher Scientific	12321D
High Sensitivity DNA Bioanalyzer kit	Agilent	5067-4626
ISPCR primer (10 uM) (5′-AAGCAGTGGTATCAACGCAGAGT-3′)	Biomers.net	-
KAPA HiFi HotStart ReadyMix (2× KAPA)	Biosystems	KK2601
LNA-modified TSO (5′-AAGCAGTGGTATCAACGCAGAGTACATrGrG+G-3′)	www.exiqon.com	-
MgCl2	Ambion (Life technologies)	AM9530G
Oligo-dT30VN (5′–AAGCAGTGGTATCAACGCAGAGTACT30VN-3′)	biomers.net	-
Qbit™ ds DNA high sensitivity assay kit	Thermo Fisher Scientific	Q32851
Recombinant RNase inhibitor	Clontech	2313A
Superscript II reverse transcriptase kit*	Thermo Fisher Scientific	18064-014

4.4.2 Isolation of *P. falciparum* (3D7-strain) parasites from whole human blood

Isolation of *P. falciparum* parasites was performed during the volunteer diagnosis period (ranging C +7.5 days– C +10.5 days post-CHMI). Parasites were isolated from 13 of the 14 infected volunteers (no sample for volunteer #22). Unless otherwise stated, all materials were single-use and disposable to prevent cross-contamination between volunteers.

4.4.2.1 Leucodepletion

In advance of blood collection, filtering apparatus was set up comprising a 50 mL capacity syringe with plunger removed (Becton Dickinson), connected to a leucoflex LXT filter (Scottish National Blood Transfusion Service) with 250 mL capacity centrifuge bottle (Corning Life Sciences) for collection of flow-through. For each volunteer, 50 mL blood was pooled into one 50 mL falcon tube (Becton Dickinson) and transferred to the syringe for passage through leucodepletion filter. To ensure maximal recovery of parasite-infected erythrocytes, filters were washed through with 200 mL 1x PBS (Gibco) and left to run dry before collection of flow-through for centrifugation at 1,000g for 10 minutes, at room temperature. Supernatant was then discarded, being careful not to disturb the pellet. From this point in the protocol, all samples and reagents were kept at 4^{o}C.

4.4.2.2 Erythrocyte Lysis and cryopreservation of parasite pellets

Erythrocyte pellets (containing ring-stage parasites) from the previous step were resuspended in 0.015% saponin (Sigma-Aldrich) in PBS, in a final volume 9x that of the pellet volume (varied between volunteers). Samples were incubated for 10 minutes on ice to ensure the efficient lysis of red cells and then centrifuged at 15,000g for 10 minutes, with the brake off. The supernatant was discarded and the pellets resusupend in 1 mL cold PBS, added directly to the predicted pellet location (marked on the centrifuge bottle prior to spin). Resuspended samples were then transferred to 1.5 mL Eppendorf tubes and centrifuged at 16,000g for 5 minutes, before removal of supernatant. Parasite pellets were resuspended in 1 mL TRIzol^{TM} reagent, mixed and then incubated for 5 minutes at 37^{o}C before being snap-frozen on dry ice and stored at -70^{o}C.

4.4.3 Parasite RNA Extraction and Clean-up

Unless otherwise stated, all steps in the RNA extraction/ clean-up protocol were performed at 4^{o}C, using RNAse-free/sterile materials and molecular biology- grade reagents.

4.4.3.1 RNA Extraction and purification

Parasites in TRIzol™ (including the two inoculum samples) were thawed at room temperature, before addition of 200 µl (0.2x original TRIzol™ volume) bromochloropropane (Sigma-Aldrich). Tubes were vortexed, incubated for 3 minutes at room temperature and then centrifuged at 12,000g and 4^{o}C, for 15 minutes. ~500 µl of aqueous phase was then transferred to a fresh 1.5 mL Eppendorf tube, and diluted 1:1 in 100% ethanol (Sigma-Aldrich) for purification with RNA Clean and Concentrator™-5 kit (Zymo Research). In brief, the aqueous phase/ethanol mix was added to a zymo-spin column, with collection tube, and centrifuged at 12,000g for 30 seconds. Column flow-through was discarded and purification proceeded as follows: 30 second spin with 400 µl "RNA Prep Buffer", 30 second spin with 700 µl "RNA Wash Buffer", and a 2 minute spin with 400 µl "RNA Wash Buffer". The column was then transferred to a fresh 1.5 mL Eppendorf tube, and 14µl DNAse/RNAse-free water added for incubation at RT for 5 minutes. RNA was eluted off the column by centrifugation at 4^{o}C for 30 seconds. At this stage in the protocol, a 4 µl aliquot of the eluted sample was taken for quantification by nanodrop and/or the Agilent 2100 Bioanalyzer RNA 6000 Pico Chip assay for Total RNA (RNA concentration range of 50 pg/µl - 5,000 pg/µl).

4.4.3.2 Depletion of Globin mRNA and Ribosomal RNA

RNA was depleted of ribosomal RNA (rRNA) and globin mRNA using the Globin-Zero® Gold kit from Illumina, as per manufacturer's instructions. Kit specifications suggest a minimum starting input of ≥ 1 µg RNA. In cases where this was not possible, reagent volumes were adjusted (indicated by blue type) to suit lower-input RNA yields ranging either 100 – 250 ng RNA ('low input 1") or 250 – 1 µg RNA ("low input 2"), as per manufacturer's guidelines below:

Preparation of magnetic beads

Magnetic beads were resuspended and aliquoted in 225 ul (90 µl) volumes per sample reaction, for 2x washes in 225 ul (90 µl) RNAse-free water, using the DynaMag™-2 Magnet (Thermo Fisher Scientific). Final resuspension of beads was in 65 ul (35 µl) of "resuspension solution", with addition of 1 ul (0.5 µl) "RiboGuard RNAse Inhibitor". Magnetic beads were set aside at room temperature until use.

Preparation of samples for magnetic bead reaction

Kit reagents were thawed on ice before use, and combined in the order below to make up a 40 µl (20 µl) volume. Once combined, reagents were mixed and incubated at 68ºC for 10 minutes and then again, for 5 minutes at room temperature.

For RNA yields ≥1 µg;

- 16 µl RNAse-free water
- 4 µl Globin-Zero® Gold Reaction Buffer
- 1 – 5 µg RNA (10 µl volume)
- 10 µl Globin-Zero® Gold Removal Solution

For RNA yields 250 ng – 1 µg;

- 3 µl RNAse-free water
- 2 µl Globin-Zero® Gold Reaction Buffer
- 250 ng – 1 µg RNA (10 µl volume)
- 5 µl Globin-Zero® Gold Removal Solution

For RNA yields 100 ng – 250 ng;

- 5.5 µl RNAse-free water
- 2 µl Globin-Zero® Gold Reaction Buffer
- 100 ng – 250 ng RNA (10 µl volume)
- 2.5 µl Globin-Zero® Gold Removal Solution

Magnetic bead reaction for removal of Globin mRNA and rRNA

Treated RNA was added to the 1.5 mL Eppendorf tube containing washed magnetic beads, tubes vortexed and then incubated for 5 minutes at room temperature. Samples were mixed once again, incubated at 50ºC for 5 minutes and then transferred to the magnetic stand. After 1 minute, supernatant (containing the RNA) was pipetted off and transferred to a fresh for 1.5 mL Eppendorf tube for a second incubation in the magnetic stand. RNA was then topped up to 180 µl volumes using RNAse-free water for overnight precipitation with ethanol.

Ethanol precipitation

Globin and rRNA-depleted RNA was precipitated in 600 µl ethanol (100%) and 18 µl 3M sodium acetate, overnight at 4ºC. 2 µl linear acrylamide (Ambion) served as co-precipitant. RNA was pelleted by centrifugation at 12,000g for 20 minutes, and washed x2 in 75% ethanol. Samples were air-dried for 5 minutes before resuspension in 12 µl DEPC H_20 (Thermo Fisher Scientific) and incubation at 65ºC for 5 minutes. RNA for use in first-strand cDNA synthesis/amplification was stored at -70ºC until use.

4.4.4 RNA quantification and QC

To ensure the efficient depletion of ribosomal RNA, 1 µl from every sample was run on the Agilent 2100 bioanalyzer using the RNA 6000 Pico Chip assay (RNA quantification range: 50 pg/µl – 5,000 pg/µl). Following depletion of globin and ribosomal RNA, sample yields were too low to be quantified by nanodrop or Qbit fluorometer, and thus the RNA 6000 Pico Chip assay was also used for quantification purposes.

4.4.5 Smart-seq2 for first strand synthesis and amplification of cDNA

First strand synthesis and PCR was performed by Geetha Sankaranarayanan, at the Wellcome Trust Sanger institute in Cambridge. The protocol used was adapted from that previously published (Picelli *et al.* 2014), and optimised for use with low-input (single-cell level) *P. falciparum* RNA (Reid *et al.* 2018). All steps were performed in clean lab areas designated exclusively for either low-input RNA, or low-input DNA work. DNA and RNA reagents were stored separately, in single-use aliquots to avoid free-thaw cycles. All plastic-wear was PCR clean, and pipettes RNAse/DNAse-treated before use.

Master mixes for the reverse transcription reaction were prepared in 0.2 mL PCR strip-tubes (Eppendorf®) on ice in enough volume for all, plus one additional reaction. Volumes below are calculated for 10 reactions. In all cases, 2 µl of globin/rRNA-depleted RNA (variable concentrations) was reverse transcribed as described.

4.4.5.1 Reverse Transcription Reaction

Master Mix 1 – (10 reactions)
- 1 µl (100 µM) oligo-dT30VN
- 10 µl (10 µM) dNTPs
- 9 µl DEPC H_20

Master Mix 2 - (10 reactions)
- 1 µl (100 µM) TSO primer
- 0.6 µl $MgCl_2$
- 20 µl Betaine
- 20 µl Superscript buffer
- 5 µl DTT
- 2. 5 µl RNAse Inhibitor
- 5 µl Super Script II
- 2.9 µl DEPC H_2O

2 µl of RNA was incubated with an equal volume Master Mix 1 (MM1), for 3 minutes at 72°C to allow the oligo-dT primer to hybridized to the poly-A tail of the mRNA molecules. The 3′ end of this oligonucleotide contains 'VN', where 'N' is any base and 'V' is either A, C or G. The two terminal nucleotides are necessary for anchoring the oligonucleotide to the beginning of the poly-A tail and to avoid unnecessary amplification of a long stretch of adenosines. The free dNTPs are added in this initial mix to improve the yield of the RT-PCR, likely through mechanisms that stabilize RNA-primer hybridizations. Samples were placed back on ice immediately following incubation and then 5.5 µl of Master Mix 2 (MM2) was added to obtain a final reaction volume of 9.5 µl. The reaction was mixed and then spun down in a minifuge before incubation in a thermal cycler with heated lid as below:

Cycle	Temp.	Time	Purpose
1	42°C	90 minutes	Reverse Transcription (RT) and template-switching
2 - 11	50°C	2 minutes	Unfolding of RNA secondary structures
	42°C	2 minutes	Completion/continuation of RT and template switching
12	70°C	15 minutes	Enzyme inactivation
13	4°C	Hold	Safe storage

Reactions were then diluted 1:5 by addition of 40 µl DEPC H_2O (Thermo Fisher Scientific).

The PCR master mix was prepared on ice, by combining the below components;

PCR Mastermix - (volumes for 1 reaction)

- 2.5 µl KAPA HiFi HotStart ReadyMix (2x)
- 0.25 µl (10 µM) Illumina Sequencing PCR (ISPCR) primer
- 2.75 µl DEPC H_20

4.4.5.2 PCR

15 µl of PCR Master Mix was added to 10 µl of (diluted) RNA sample from the RT reaction, tubes vortexed and then spun down in a minifuge. PCR was performed in a different thermal cycler, as below:

Cycle	Denature	Anneal	Extend	Hold
1	98°C, 3 minutes	-		-
2 - 26*	98°C, 20 seconds	67°C, 15 seconds	72°C, 6 minutes	-
27	-	-	72°C, 5 minutes	-
28	-	-		4°C

* In all cases, 25 cycles of amplification were performed

The absence of DNA contamination was confirmed by the absence of amplification product in a reverse transcriptase (RT) negative control that was included for every PCR run.

4.4.5.3 cDNA purification

cDNA samples were purified with use of AMPure XP beads (Beckman Coulter), as per manufacturer's guidelines. In brief, beads were equilibrated at room temperature and resuspended (1:1) in 25 µl volumes for incubation with 25 µl cDNA. The beads/cDNA mix were incubated in the DynaMag™-2 Magnet (Termo Fisher Scientific) for ~5 minutes and supernatant removed. Whilst still in the magnetic stand, beads were washed x2 in 180 µl of freshly prepared 80% ethanol by incubating for 30 seconds, and then ethanol discarded. Tubes were removed from the magnet, centrifuged for ~7 seconds at 8,500g and returned to the magnet for removal of any residual ethanol. Beads were air-dried for up to 5 minutes, and then DNA was eluted off the beads in 20 µl of DEPC H_2O. Tubes were vortexed, contents spun down and then incubated for 5 minutes at room temperature, off the magnetic

stand. As a final step, tubes were placed back on the magnetic stand and incubated for 2 minutes before transferal of supernatant (containing the cDNA) to fresh 1.5 mL Eppendorf tubes.

4.4.5.4 cDNA quantification and QC

cDNA samples were quantified using the Qbit® Fluorometer 2.0 and dsDNA High Sensitivity assay, with quantitation range; 10 pg/µl - 100 ng/µl (Thermo Fisher Scientific). The Agilent 2100 Bioanalyzer, High sensitivity DNA assay (DNA size range; 50 – 7,000 bp) was used to assess DNA quality and sizing.

4.4.6 NEB NEXTflex® for preparation of RNA-seq libraries

cDNA libraries were prepared by Geetha Sankaranarayanan, at the Wellcome Trust Sanger Institute, using the NEB NEXTflex® PCR-free kit (Bioo Scientific, catalog number: NOVA-5144-01), as per manufacturer's instructions. In brief, 500 ng of cDNA (in 40 ul volumes DEPC H_2O) was fragmented to 400 - 600 bp using a Covaris AFA™Ultrasonicator before incubation with NEXTflex® PCR-free End Repair Buffer mix and End Repair Enzyme Mix for 30 minutes at 22^{o}C. The cDNA was purified using AMPure XP beads (Beckman Coulter) for size selection at 300 – 400 bp, as per manufacturer's instructions, prior to 3' end adenylation using NEXTfelx® PCR-free Adenylation Mix and incubation at 37^{o}C for 30 minutes. The index adapters were ligated to the cDNA strands by incubating at 22^{o}C for 15 minutes, in the presence of NEXTfelx® PCR-free Ligation Mix and DNA adaptor indexes. Excess adaptors were removed using AMPure XP beads (Beckman Coulter), according to manufacturer's instructions. Libraries were then quality assessed using the Agilent Bioanalyser, High Sensitivity DNA chip and quantified by Qbit® 2.0 Fluorometer, under standard operating procedures.

4.4.7 RNA-sequencing and data analysis

RNA-sequencing and data analysis was performed by Dr Adam Reid at the Wellcome Trust Sanger institute. Samples were sequenced using the Illumina HiSeqv4 platform to produce 75 bp paired-end reads, which were then mapped to the *P. falciparum* v3 gene sequences as described in the GeneDB genome database for prokaryotic and eukaryotic pathogens (http://www.genedb.org), using

the Kallisto v0.42.3 quantification platform (Logan-Klumpler *et al.* 2012, Bray *et al.* 2016). Variable sequencing depth was detected across samples and thus read counts were normalised by regularized logarithm transformation (rlog), using DESeq2 v1.16.1. This process was performed by 1) calculating the log_2 value for each gene, in each sample 2) calculating the geometric average (average of the log_2-transformed values) for each gene, across samples 3) subtracting the geometric average from the log(counts) for each gene, in each sample. This allows for the identification of genes that are expressed at levels significantly below or above the average. 4) The final "scaling factor" was then calculated for each sample by taking the median of all (log) gene values (within that sample) and converting this median value back into a "normal number". 5) The original (raw) read counts were then divided by the "scaling factor" associated with each corresponding sample, to produce "rlog" values. (Love *et al.* 2014). The rlog values were used for further analysis. Note that only genes with ≥ 5 reads in at least one sample were included in this analysis. Unless otherwise stated, a corrected p-value of 0.01 was used for differential expression analysis. EdgeR v3.8.6 was used to determine differential expression across all patient samples (Robinson *et al.* 2010).

4.5 Results

4.5.1 Volunteer parasitaemias at day of diagnosis

Isolation of parasites for *ex vivo* RNA-seq was performed on the day of volunteer diagnosis (positive thick film smear by microscopy), prior to initiation of treatment. This time point was selected to ensure peak parasitaemia, and thus the increased likelihood of achieving sufficient material for sequencing. Parasite isolation was performed on 13 of the 14 infected volunteers that underwent CHMI (volunteer ♯22 was excluded from analysis due to a reduced blood volume available for collection on day of diagnosis). On average, this subset of volunteers became positive by thick film smear ~9 days post infection (range = 7.5 – 10.5), and thus parasites were predicted to be either in the 4^{th}, 5^{th} or 6^{th} generation (Table 4.2). Parasitaemias ranged 1,440 – 273,247 parasites/mL of blood, as measured by qPCR. Excluding any potential loss in parasite numbers during the isolation process, this equated to a range of 72,000 – 13,662,350 parasites, in the 50 mL blood volumes collected. Percentage parasitaemia was calculated using the reference number of

erythrocytes/mL of whole blood for healthy adult males ($5.4x10^9$/mL) and females ($4.8x10^9$/mL) (https://www.nhs.uk/conditions/red-blood-count/).

Table 4.2 | Volunteer infection kinetics

Volunteer i.d	Day of diagnosis	Predicted parasite generation	P/mL of blood	Total parasites (in 50 mL of blood)	% parasitemia
208	C +9.0	5th	1,440	**72,000**	0.00003
12	C +7.5	4th	1,645	**82,250**	0.00003
19	C +8.5	5th	6,932	**346,600**	0.0001
26	C +9.0	5th	9,133	**456,650**	0.0002
27	C +9.0	5th	13,421	**671,050**	0.0003
20	C +8.5	5th	15,025	**751,250**	0.0003
106	C +8.5	5th	16,162	**808,100**	0.0003
17	C +10.5	6th	16,911	**845,550**	0.0003
18	C +8.5	5th	19,670	**983,500**	0.0004
24	C +10.0	6th	43,707	**2,185,350**	0.0008
13	C +10.5	6th	70,368	**3,518,400**	0.001
206	C +10.0	6th	185,576	**9,278,800**	0.003
16	C +10.0	6th	273,247	**13,662,350**	0.005

In addition to the 13 parasite samples isolated at day of diagnosis, two samples of the inoculum used to infect volunteers were also processed for analysis, as described in Materials and Methods section 2.2.1.4. RNA from inoculum samples was preserved, and processed alongside RNA from the 13 volunteer samples as described in section 4.4.3.1.

4.5.2 Quantity and quality assessment of RNA and cDNA libraries

One of the major issues in isolating parasites from whole human blood for RNA-seq analysis is the potential contamination with host material. Although samples were depleted of leucocytes and red cells during sample processing, it was predicted that the RNA extracted from the isolated parasite samples would also contain RNA from the host. As much as 70% of the mRNA in a (blood) total RNA sample can be globin mRNA, with the remaining total RNA composed of greater than 90% ribosomal RNA (rRNA). Neither globin mRNA nor rRNA provide valuable sequencing information and thus were removed from the RNA samples prior to RNA-seq. The combined Globin-Zero® Gold kit from Illumina was used for this purpose, as described in section 4.4.3.2. Bioanalyzer electropherograms were generated pre- and post-depletion to confirm effective removal of 18S and 28S rRNA peaks (Figure 4.1).

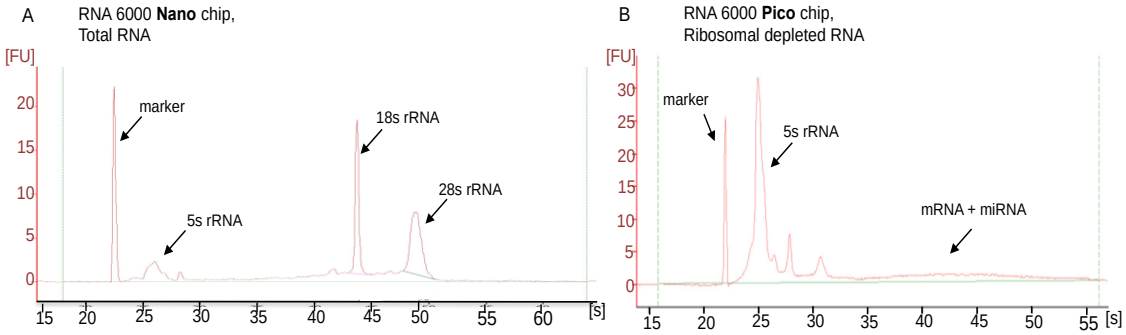

Figure 4.1 | Quality control ribosomal RNA removal. Electropherograms showing fluorescence units (FU) on the y-axis, versus time (s) on the x-axis. **A)** total RNA from isolated paraistes from volunteer 16; marker (25 nt), mRNA and 5s rRNA (<200 nt), 18s subunit rRNA (~2,000 nt) and 28s subunit rRNA (~5,000 nt). **B)** Ribosomal depleted RNA from volunteer 16 parasite sample; marker (25 nt) and mRNA + miRNA (100 – 2,000 nt). (Plots generated using the bioanalyser (Agilent Technologies)).

The two main subunits of human ribosomal RNA are 18S and 28S with sizes 1,869 nt and 5,070 nt, respectively. Post-ribosomal depletion bioanalyzer traces suggested complete elimination of the previously observed ribosomal peaks, which was a requirement for taking the samples forward for library preparation. Following depletion of ribosomal RNA and globin mRNA, the majority of samples were too low in concentration for quantification by nanodrop (quantification range 0.4 – 15,000 ng/µl), thus samples were instead quantified using the Agilent bioanalyzer and RNA 6000 Pico Chip assay (quantification range 50 – 5,000 pg/µl), either neat or following a 1:10 dilution. Table 4.3 displays the concentration and yield for each RNA sample recovered. Samples were quantified within the range 0.05 – 71.7 ng/µl, with volunteers ♯208 and ♯206 representing either end of the scale, respectively. RNA concentration did not correlate with parasitaemia at time of sampling, indicating either sensitivity issues during the quantification of such low levels, or host RNA contributing to the measurement. This highlights the two biggest technical hurdles in using CHMI for analysis of parasite gene expression; limited parasite material available (due to early termination of volunteer infections), and host contamination during parasite isolation.

Table 4.3 | Bioanalyzer quantification of purified RNA samples

Sample/volunteer i.d	Total parasites (in 50mL whole blood)	Concentration (ng/µl)	Recovered yield (ng)
208	72,000	0.053	0.53
12	82,250	4.840	48.4
19	346,600	0.736	36.8
26	456,650	0.158	7.88
27	671,050	0.150	7.51
20	751,250	0.394	19.7
106	808,100	0.926	46.3
17	845,550	1.964	98.2
18	983,500	5.181	259.0
24	2,185,350	0.097	4.85
13	3,518,400	0.166	8.28
206	9,278,800	71.660	716.6
16	13,662,350	0.344	3.44
Parasite Inoculum (PI1)	N/A	0.281	14.05
Parasite Inoculum (PI2)	N/A	0.113	5.63

All 15 samples (including the two from the inoculum) met the quantification requirements for first strand cDNA synthesis and amplification using the Smart-seq2 protocol (10 pg – 10 ng), however, following Smart-seq2 amplification, the sample from volunteer ♯208 did not produce sufficient cDNA for downstream library prep and thus was excluded from further analysis. For all remaining samples (n = 14), the NEB NEXTflex® kit (requiring 500 ng cDNA) was used to produce libraries for RNA-seq (see section 4.4.6). Libraries were quality assessed using the Agilent Bioanalyzer High Sensitivity DNA chip (Agilent Technologies). Figure 4.2 displays the electropherograms of the libraries prepared from representative samples ♯24 (with lower-end RNA yield) and ♯18 (higher-end RNA yield). The median of cDNA libraries was observed, as expected, at approximately 300 bp (~500 - 600 bp with the inclusion of NEB NEXTflex® sequencing adapters). The NEB NEXTflex® libraries showed high symmetry within their distribution and high similarity across cDNA library samples.

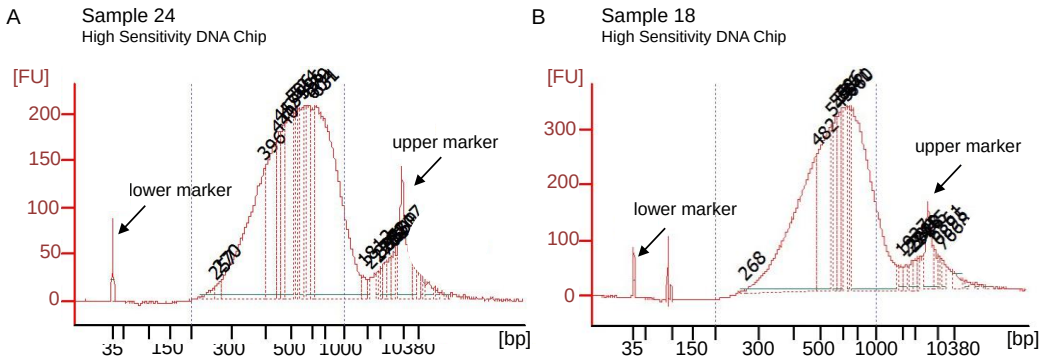

Figure 4.2 | Quality assessment of cDNA libraries
Electropherograms showing fluorescence units (FU) on the y-axis, against base-pairs (bp) on the x-axis. Plots show the cDNA libraries prepared from paraistes recovered from volunteer 24 **(A)** and volunteer 18 **(B)**, using the NEB NEXTflex® kit (Bioo Scientific). Lower (36 bp) and upper (10,380 bp) markers are shown. ((Plots generated using the bioanalyser (Agilent Technologies)).

4.5.3 Read counts and coverage

Table 4.4 displays the total read counts measured for each sample, as well as the total (and percentage) that mapped to either the human or *P. falciparum* reference genome. The percentage of reads mapped to the human genome ranged from 23.05% (sample ♯13) to 94.4% (sample ♯206), with median = 89.0%, suggesting that RNA preparations made from the isolated parasite samples contained a high proportion of host material, as expected. The number of reads mapped to the *P. falciparum* genome ranged from 107,149 (sample ♯206) – 2,732,963 (sample ♯27*),* with median = 884,333 and were sufficient for analysis of all samples. Importantly, despite the limited parasite material available, and thus low RNA inputs, good gene coverage was detected for all patient samples (median number of *P. falciparum* genes identified with ≥5 reads = 2,518 and range = 1,159 – 3,671). Furthermore, reads could be detected across the full length of genes, despite the high number of amplification cycles performed in the PCR, which can sometimes lead to a signal bias towards either the 5' or 3' end of transcripts (Reid *et al.* 2018). Figure 4.3 displays the read counts per nucleotide, covering the entire length of the most abundantly transcribed *var* gene in the dataset (PF3D7_1041300/ PF10_0406), for three representative samples (♯12, ♯17 and ♯206) with some of the lowest total coverage.

Table 4.4 | Human and *P. falciparum* read count data

Sample i.d	Total number of reads	Number of reads mapping to human genome	% Human reads	Number of reads mapping *to P. falciparum* genome	% *P. falciparum reads*	Number of *P. falciparum* genes identified (≥ 5 reads)
12	31,107,828	28,411,691	91.33	308597	0.99	1,777
13	31,881,266	7,347,443	23.05	19109979	59.94	3,659
16	29,587,516	4,795,353	16.21	20153999	68.12	3,671
17	30,403,052	27,229,953	89.56	607603	2.00	2,224
18	29,309,712	26,730,785	91.20	572011	1.95	2,088
19	31,709,640	28,305,560	89.26	719902	2.27	2,183
20	34,842,860	28,644,454	82.21	3659914	10.50	2,850
24	31,551,748	12,990,026	41.17	15241324	48.31	3,526
26	29,971,040	26,633,150	88.86	730380	2.44	1,585
27	29,816,582	24,766,881	83.06	2732963	9.17	2,968
106	31,630,498	28,254,712	89.33	1381624	4.37	2,524
206	35,448,282	33,468,007	94.41	107149	0.30	1,159
Parasite inoculum (PI1)	27,546,798	24,571,235	89.20	818425	2.97	1,513
Parasite inoculum (PI2)	28,193,120	25,029,688	88.78	950240	3.37	1,731

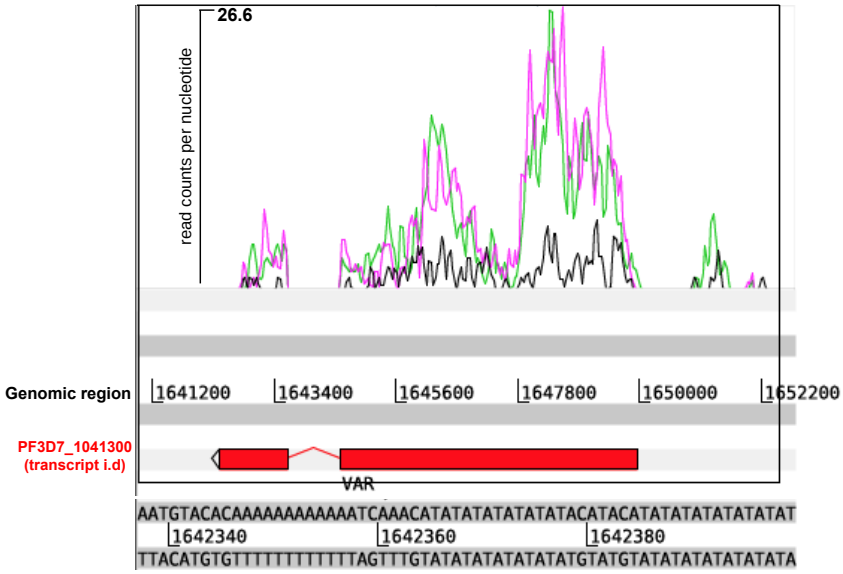

Figure 4.3 | Read count coverage over the *var* gene PF3D7_1041300, for three representative samples of low *P. falciparum* read counts; 12 (pink line), 17 (green line) and 206 (black line). Gene is composed of 2 exons and is located at a genome region spanning 1,642,401 – 1,649,948 base pairs (bp) (total transcript length = 6.6 kbp). Read counts per nucleotide is shown on the y-axis (maximum read height is shown). Note that plot represents read counts before rlog normalisation and thus samples cannot be compared for differences in gene expression. Figure produced by Dr Adam Reid, Wellcome Trust Sanger Institute.

4.5.4 Differential expression analysis between parasites isolated from inoculum samples, and parasites recovered from infected volunteers at the day of patent infection

In order to investigate evidence for VSA selection in the naive host, differential expression analysis was performed on parasites isolated from the two samples of blood-stage inoculum used to infect, and parasites recovered from the volunteers at the day of patent infection, following 5-6 replication cycles in the blood. Analysis revealed 203 differentially expressed genes (DEGs) between the two different sample types (Appendix 8). Of the 203 differentially expressed genes, 132 were found more highly expressed in the volunteer samples and mainly included genes encoding transcription factors, RNA binding proteins, heat-shock proteins and proteins involved in DNA repair and RNA processing. 37 of these 132 genes (28%) were conserved or hypothetical proteins of unknown function. Interestingly, the most differentially expressed (7.6 fold-increase in the volunteer samples) was the *rif* gene PF3D7_0401600.1/ PFD0070c. This gene encodes a group-A RIFIN protein and is described as strain-transcendent, having been detected in 3D7, HB3, IT and Dd2 *P.*

falciparum strains (Claessens *et al.* 2011). In one study, it has been found transcribed at high levels in parasite populations enriched for parasites that bind to the human endothelial receptors P-selectin, E-selectin, CD9 and CD151 (Metwally *et al.* 2017), however limited information is currently available with regards to its function. Of the differentially expressed genes found at lower levels in the volunteer samples (n = 71), five were *var* genes- PF3D7_0632800/ MAL6P1.1; PF3D7_0223500/ PFB1055c; PF3D7_1300100/ PF13_0001; PF3D7_0100100/ PFA0005w and PF3D7_0712000/ PF07_0049). Four of these genes encode group-B PfEMP1, whereas PF3D7_0712000/ PF07_0049 belongs to the group-C subset. Reduced expression of these variants may be suggestive *in vivo var* gene switching mechanisms at play, or may simply reflect differences between the preparation of the inoculum and patient samples prior to analysis. For instance, whereas parasites in the patient samples were processed for analysis (at 4^{o}C) within 4 hours of isolation from fresh blood, parasites in the inoculum samples had been previously cryopreserved, and then thawed and incubated at room temperature for up to 3 hours before the addition of stabilising TRIzol reagent. Thus, it is possible that the viability of parasites may have been compromised during processing, and it is unclear if- and how- the presence of differential levels of degraded parasite RNA affects measurements of gene expression. Importantly, the two inoculum samples (PI1 and PI2), representing the only replicate samples in the dataset, were found to be significantly positively correlated for *var* and *rif* gene expression, as expected (spearman rank coefficient, r = 0.951, p= < 0.0001) (Figure 4.4).

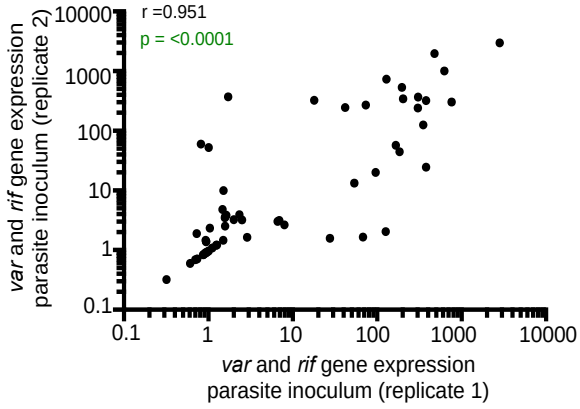

Figure 4.4 | Correlation analysis of *var* and *rif* (rlog) expression in the two replicate inoculum samples
The pairwise Spearman's rank correlation demonstrating a positive, significant correlation between the (rlog) expression values for the detectable *var* and *rif* transcripts in parasite inoculum replicate 1 (x-axis) and parasite inoculum replicate 2 (y-axis). The Spearman's rank correlation coefficient (r) is shown, along with p. value (p < 0.0001). Significance was defined as p = <0.05.

4.5.5 *Var* Gene Expression in Controlled Human *Plasmodium falciparum* Infection

There is evidence to implicate the group-A and B/A *var* genes/PfEMP1 proteins, in the pathogenesis of severe malaria infection. Given that severe disease is most commonly observed in children with limited prior exposure to the *Plasmodium* parasite, there is a need to investigate *var* gene expression in a representative population of malaria-naive individuals.

Analysis of *var* gene profiles in 12 volunteers during CHMI revealed the detection of 58/61 (95%) *var* gene variants at day of patent infection (table 4.5). Just three group-A *var* genes- (PF3D7_0533100/PFE1640w, PF3D7_1150400/PF11_0521 and PF3D7_0600400/MAL6P1.314) were undetectable by definition of the set cut-off (≥ 5 reads in at least one sample). Importantly, this broad-level detection of variants is consistent with data from three previously published studies of parasite *var* gene expression in controlled human malaria infection (Lavstsen *et al.* 2005, Wang *et al.* 2009, Bachmann *et al.* 2016).

Table 4.5 | Number of each *var* gene subgroup detected in the dataset

var subgroup	Upstream Sequence	Position	Orientation (direction of transcription)	No. of genes in 3D7	No. of genes detected in volunteer cohort
A	UpsA	Subtelomeric	Telomeric	10	7
B/A	UpsB	Subtelomeric	Centromeric	4	4
B	UpsB	Subtelomeric	Centromeric	24	24
B/C	UpsB	Central	Telomeric	9	9
C	UpsC	Central	Telomeric	13	13
E	UpsE	-	-	1	1

Interestingly, *var* gene expression profiles were remarkably uniform across volunteers (Figure 4.5). Genes demonstrating the highest levels of expression were largely of the group-B subclass, however also included 3 genes from the B/C subgroup (PF3D7_0712800/ MAL7P1.55, PF3D7_0421100/ PFD1005c and PF3D7_0809100/ PF08_0103), 2 from the B/A subgroup (PF3D7_0632500**/** PFF1580c and PF3D7_1200400/ PFL0020w), 1 group-C gene (PF3D7_0421300/ PFD1015c) and the conserved group-E gene (PF3D7_1200600**/** VAR2SCA) (table 4.6). Across all volunteers, the highest transcript levels were detected for PF3D7_1041300/ PF10_0406 (rlog median = 11.07; range: 8.94 – 11.68), followed by PF3D7_1200100/ PFL0005w (rlog median = 9.12; range: 8.04 – 10.24), PF3D7_0712800/ MAL7P1.55 (rlog median = 8.02; range: 4.61 – 9.59),

PF3D7_0421100/ PFD1005c (rlog median = 7.88; range: 6.06 – 8.54), PF3D7_0421300/ PFD1015c (rlog median = 7.49; range: 6.08 – 8.21) and PF3D7_1100100/ PF11_0007 (rlog median = 7.22; range: 4.93 – 9.11) (figure 4.6). Five out of the six genes are categorised as either group-B or group-B/C *var* genes, suggesting dominant expression of the UpsB genes *in vivo*. This is in agreement with previously published data from Bachmann *et al*, who upon infection of 18 volunteers with *P. falciparum* (N5F4), detected broad expression of *var* genes, and group-B variants as the most highly expressed (figure 4.8) (Bachmann *et al.* 2016). Conversely, members of the group A *var* genes, were detected at the lowest levels in this dataset (figure 4.5, table 4.6).

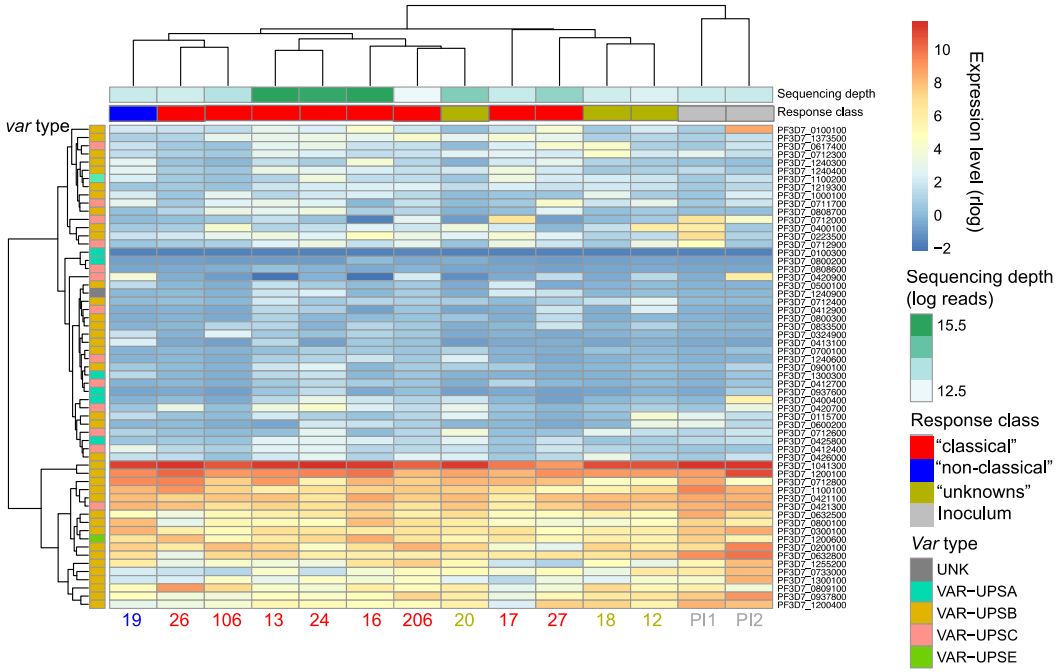

Figure 4.5 | Comparison of *var* gene expression across the volunteer cohort and inoculum samples
Heatmap showing normalised (rlog) values for all detectable *var* transcripts. Each row represents a *var* gene (annotated on the left hand side), and each column represents a volunteer or inoculum sample (annotated along the bottom, and colour coded as per transcriptional response class; "classical" responders (red), "non-classical" responders (blue), "unknowns" (yellow), or as parasite inoculum samples (PI1 and PI2) in grey). *Var* type is shown and sample sequencing depth is indicated, as per the colour keys provided. (Heatmap generated by Dr Adam Reid, Wellcome Trust Sanger Institute).

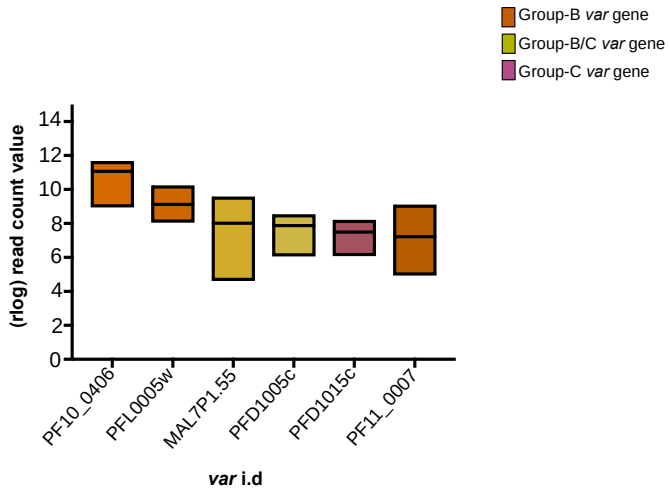

Figure 4.6 | Top six *var* gene variants in patients samples. Graph displays the normalised (rlog) read counts for the six *var* gene variants with highest transcript levels across the 12 patient samples. Each box represents the median and range for one of the six genes (annotated on the x-axis). Boxes have been colour-coded as per *var* gene sub-group (B, B/C or C). A colour-key is provided.

Figure 4.7 provides a schematic representation of the PfEMP1 domain architecture for those encoded by the top six most highly expressed *var* genes in the dataset (PF10_0406, PFL0005w, MAL7P1.55, PFD1005c, PFD1015c and PF11_0007). All six represent small PfEMP1 and are similar in structure, comprising four extracellular domains; the semi-conserved DBLα0-CIDRα head structure (commonly associated with CD36 binding) (Smith *et al.* 2001, Robinson *et al.* 2003), followed by a DBLδ-CIDRβ/γ/δ tandem domain. DBL and CIDR domains have been further sub-classified (denoted by numbers) according to (Rask *et al.* 2010). Binding of the CD36 receptor on host endothelial cells appears to be mediated by several CIDRα class domains (Baruch *et al.* 1995, Baruch *et al.* 1997, Gamain *et al.* 2001, Smith *et al.* 2001), but is limited to those of the B and C subgroups (Robinson *et al.* 2003, Turner *et al.* 2013). In contrast, group-A PfEMP1 have two distinct protein head structures; DBLα1-CIDRα1 and DBLα1-CIDRβ/γ/δ (Rask *et al.* 2010) which have been linked to binding activity for endothelial protein C receptor (EPCR) (Turner *et al.* 2013), and higher rates of rosetting (Russell *et al.* 2005, Ghumra *et al.* 2012), common in more severe infections (Carlson *et al.* 1990, Rowe *et al.* 1995). As previously noted, the group-A *var* genes were detected at very low levels in this dataset.

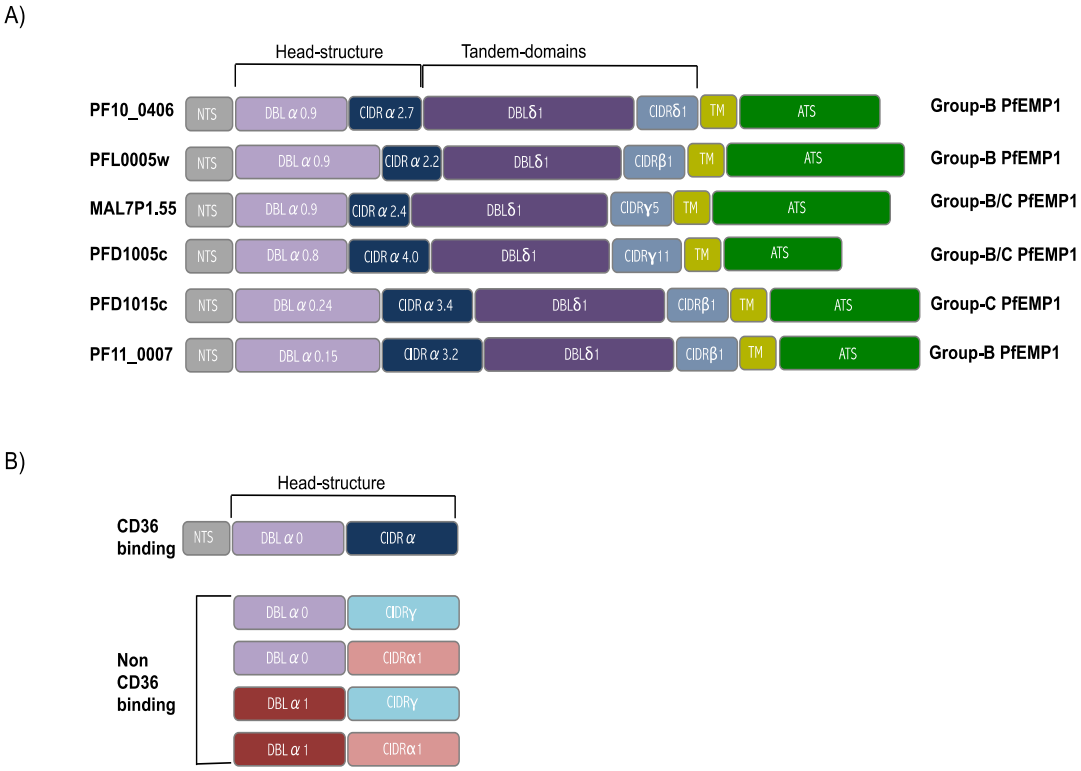

Figure 4.7 | PfEMP1 domain architectures for the variants encoded by the six most highly expressed *var* genes in the dataset (PF10_0406, PFL0005w, MAL7P1.55, PFD1015c, PFD1015c and PF11_0007). PfEMP1 proteins have multiple domains including (from N- to C-terminal): the N-terminal segment (NTS), Duffy binding-like (DBL) domains, Cysteine-rich inter-domain regions (CIDR), one transmembrane region (TM) and the acidic terminal segment (ATS). Six major classes of DBL domains have been proposed based on amino acid sequence similarity: DBLα, β, γ, δ, ζ, and ε, whereas CIDR domains have been divided into five major classes: CIDRα, β, γ, δ and pam. DBL and CIDR domains have been further sub-classified (denoted by numbers) according to Rask *et al.*, 2010. **A)** The domain structure for each associated PfEMP1 protein has been annotated using the VarDom server (http://www.cbs.dtu.dk/services/VarDom/). **B)** summarises the PfEMP1 head-structure domains that have been associated with CD36 binding and non-CD36 binding PfEMP1. For each PfEMP1, the *var* gene i.d and associated group is shown.

Table 4.6 | Normalised (rlog) read counts for all detectable *var* genes in the 12 patient and 2 inoculum samples (same order as heatmap)

transcript i.d	*var* i.d	*var* group	v019	v026	v106	v013	v024	v016	v206	v020	v017	v027	v018	v012	median of patient samples	PI1	PI2	median of inoculum samples
PF3D7_0100100	PFA0005w	B	2.02	1.79	1.48	2.84	2.28	4.30	1.93	0.24	1.61	4.00	0.70	2.24	**1.97**	0.79	8.54	**4.66**
PF3D7_1373500	PF130364	B	0.89	1.04	3.04	3.07	3.31	2.85	4.24	2.90	4.02	3.08	0.94	1.27	**2.97**	1.00	1.70	**1.35**
PF3D7_0617400	MAL6P1.252	C	1.84	0.74	0.37	2.81	3.13	1.76	1.66	0.06	2.29	4.09	4.22	0.98	**1.80**	0.70	1.94	**1.32**
PF3D7_0712300	MAL7P1.50	B/C	1.51	0.94	0.61	2.89	2.38	1.44	1.80	2.60	2.63	2.15	4.34	2.10	**2.12**	2.73	1.60	**2.16**
PF3D7_1240300	PFL1950w	B/C	2.81	0.36	0.05	1.57	0.75	3.98	1.28	-0.21	2.00	2.83	1.14	0.65	**1.21**	0.33	0.29	**0.31**
PF3D7_1240400	PFL1955w	B/C	2.71	0.78	0.51	3.13	2.76	2.34	1.61	2.08	3.44	2.00	0.71	0.98	**2.04**	1.52	0.71	**1.12**
PF3D7_1100200	PF11_0008	A	2.30	0.69	0.39	1.04	3.57	1.55	1.55	0.53	3.42	2.20	2.16	1.87	**1.71**	0.66	1.84	**1.25**
PF3D7_1219300	PFL0935c	B	0.59	0.69	0.44	1.87	2.23	2.36	2.51	1.49	2.33	1.79	2.07	1.79	**1.83**	0.66	1.34	**1.00**
PF3D7_1000100	PF10_0001	B	2.16	0.58	2.79	1.20	2.06	2.40	1.40	0.17	0.52	0.58	2.91	0.80	**1.30**	0.55	2.27	**1.41**
PF3D7_0711700	PF07_0048	C	2.92	0.72	2.51	3.06	2.48	-0.02	1.62	0.10	0.64	4.17	1.90	2.90	**2.19**	0.69	1.91	**1.30**
PF3D7_0808700	PF08_0106	B/C	0.22	1.25	3.19	2.71	3.47	0.89	1.24	-0.20	0.27	2.43	0.26	0.62	**1.07**	0.30	0.26	**0.28**
PF3D7_0712000	PF07_0049	C	0.08	0.28	0.61	1.58	0.38	-1.68	2.72	-0.81	6.62	-0.65	0.16	0.64	**0.33**	6.59	4.33	**5.46**
PF3D7_0400100	PFD0005w	B	0.65	0.85	4.15	1.13	1.62	2.59	1.88	3.62	2.13	-0.03	1.59	6.03	**1.75**	6.09	0.73	**3.41**
PF3D7_0223500	PFB1055c	B	1.72	2.01	3.05	3.43	2.47	4.78	3.36	2.68	4.04	2.49	1.03	1.47	**2.59**	6.98	1.04	**4.01**
PF3D7_0712900	MAL7P1.56	C	0.59	0.75	1.00	2.42	3.27	1.66	2.87	0.45	3.31	1.87	0.65	3.31	**1.76**	4.79	0.65	**2.72**
PF3D7_0100300	PFA0015c	A	-1.65	-1.64	-1.66	-1.63	-1.67	-1.67	-1.61	-1.67	-1.64	-1.67	-1.64	-1.63	**-1.65**	-1.64	-1.64	**-1.64**
PF3D7_0800200	PF08_0141	A	-0.76	-0.70	-0.84	-0.84	-0.83	0.15	-0.39	-0.24	-0.73	-0.86	-0.74	-0.60	**-0.74**	-0.71	-0.74	**-0.72**
PF3D7_0808600	PF08_0107	C	-0.57	-0.50	-0.34	0.27	-0.12	-0.41	-0.16	-0.52	-0.54	-0.65	-0.55	-0.39	**-0.46**	-0.52	-0.55	**-0.53**
PF3D7_0420900	PFD1000c	C	3.84	-0.23	-0.78	-2.16	-0.09	-2.10	2.15	-1.29	-0.37	1.55	-0.38	1.35	**-0.30**	-0.29	5.90	**2.80**
PF3D7_0500100	PFE0005w	B	1.51	-0.06	-0.31	1.66	0.85	0.09	0.66	-0.42	2.15	-0.39	-0.16	0.17	**0.13**	-0.10	-0.15	**-0.12**
PF3D7_1240900	PFL1970w	B/C	-0.08	0.05	-0.20	1.88	2.27	0.04	0.83	-0.34	2.19	1.75	-0.05	0.30	**0.18**	0.01	-0.05	**-0.02**
PF3D7_0712400	PF07_0050	B/C	0.08	0.19	-0.04	2.08	0.71	1.19	0.99	0.88	0.12	0.91	1.67	2.82	**0.89**	0.15	0.11	**0.13**
PF3D7_0412900	PFD0630c	C	-0.32	-0.16	-0.45	1.35	0.92	-0.70	0.59	-0.59	-0.25	1.95	-0.26	2.27	**-0.20**	-0.20	-0.26	**-0.23**
PF3D7_0800300	PF08_0140	B/A	-0.29	-0.17	-0.37	1.03	-0.05	0.13	0.40	0.48	-0.24	1.54	-0.25	0.01	**-0.02**	-0.20	-0.25	**-0.23**
PF3D7_0833500	MAL7P1.212	B	-0.12	0.01	1.24	1.18	-0.20	1.24	0.69	-0.30	-0.08	1.91	-0.09	1.04	**0.35**	-0.03	-0.08	**-0.06**
PF3D7_0324900	PFC1120c	B	1.72	-0.09	2.45	0.67	0.41	1.05	0.67	-0.48	-0.18	-0.45	-0.19	0.15	**0.28**	-0.13	-0.19	**-0.16**
PF3D7_0413100	PFD0635c	B/C	2.28	-0.40	-0.71	1.31	-0.74	0.72	0.41	-0.88	-0.50	-0.34	-0.51	-0.14	**-0.37**	-0.44	-0.50	**-0.47**
PF3D7_0700100	MAL8P1.220	B	-0.17	-0.06	-0.22	0.25	1.01	0.66	0.50	1.13	-0.13	-0.26	0.46	0.12	**0.18**	-0.09	0.46	**0.18**
PF3D7_1240600	PFL1960w	C	-0.20	-0.05	-0.30	0.93	1.14	1.95	0.67	2.30	-0.14	-0.39	-0.15	0.18	**0.06**	-0.09	-0.15	**-0.12**
PF3D7_0900100	PFI0005w	B	0.70	0.10	-0.13	1.97	2.54	-0.02	0.85	0.98	0.78	-0.22	0.01	0.34	**0.52**	0.06	1.22	**0.64**
PF3D7_1300300	PF13_0003	A	1.41	-0.07	-0.29	1.38	1.84	-0.06	0.59	-0.10	-0.16	-0.36	-0.16	0.14	**-0.07**	-0.11	0.54	**0.22**
PF3D7_0412700	PFD0625c	C	-0.17	-0.06	-0.23	0.64	1.38	0.76	0.54	-0.29	1.19	0.00	-0.14	0.13	**0.07**	-0.09	0.50	**0.21**
PF3D7_0937600	PFI1820w	A	-0.56	-0.41	-0.65	0.60	1.47	-0.38	0.26	-0.74	-0.50	-0.72	-0.50	-0.20	**-0.45**	-0.45	0.93	**0.24**
PF3D7_0400400	PFD0020c	A (var3)	-0.13	0.07	-0.42	1.37	3.22	1.87	1.15	1.98	-0.05	-0.75	-0.06	0.41	**0.24**	0.01	5.70	**2.86**
PF3D7_0420700	PFD0995c	C	0.49	3.11	0.26	3.41	4.31	2.35	1.56	3.05	0.55	0.03	0.54	0.89	**1.23**	0.60	3.32	**1.96**
PF3D7_0115700	PFA0765c	B	1.55	0.37	0.05	2.02	0.89	0.44	1.30	2.65	0.30	-0.14	0.29	3.99	**0.66**	2.79	1.65	**2.22**
PF3D7_0600200	MAL6P1.316	B/A	-0.08	0.08	-0.26	-0.60	2.11	1.77	0.98	-0.04	-0.03	-0.44	-0.04	3.36	**-0.03**	3.00	1.40	**2.20**
PF3D7_0712600	PF07_0051	C	1.06	0.39	0.09	0.20	2.75	0.10	1.28	3.68	0.32	0.38	2.78	1.64	**0.72**	1.23	1.97	**1.60**
PF3D7_0425800	PFD1235w	A	0.52	0.61	0.41	2.57	2.76	2.38	1.38	2.67	0.56	1.80	0.55	0.79	**1.09**	1.32	1.69	**1.51**
PF3D7_0412400	PFD0615c	C	2.98	1.39	0.90	2.42	2.62	1.21	1.40	1.76	0.55	1.98	1.26	0.82	**1.40**	0.58	0.55	**0.57**
PF3D7_0426000	PFD1245c	B	1.70	1.49	0.42	2.02	2.73	1.13	2.57	2.36	0.62	1.32	3.12	0.89	**1.59**	0.65	1.80	**1.23**
PF3D7_1041300	PF10_0406	B	11.23	11.44	10.65	11.40	11.68	11.40	10.33	11.30	9.84	8.94	10.91	10.79	**11.07**	11.47	11.53	**11.50**
PF3D7_1200100	PFL0005w	B	9.46	10.24	8.96	9.27	9.50	9.95	8.04	8.65	8.17	9.20	9.04	8.90	**9.12**	8.90	10.94	**9.92**
PF3D7_0712800	MAL7P1.55	B/C	9.43	9.59	7.52	9.02	5.57	8.12	7.43	8.19	8.13	7.91	4.61	4.90	**8.02**	8.57	4.61	**6.59**
PF3D7_1100100	PF11_0007	B	8.16	9.11	7.33	5.82	6.79	7.34	7.56	7.40	6.76	4.93	5.64	7.12	**7.22**	9.57	8.25	**8.91**
PF3D7_0421100	PFD1005c	B/C	8.07	7.36	7.75	7.91	6.43	8.54	7.43	8.02	6.06	7.84	8.04	8.07	**7.88**	8.57	8.33	**8.45**
PF3D7_0421300	PFD1015c	C	8.13	7.90	6.91	7.32	6.73	7.57	6.65	7.72	6.08	7.42	8.21	7.65	**7.49**	8.25	8.51	**8.38**
PF3D7_0632500	MAL6P1.4	B/A	4.86	3.62	5.31	5.94	6.35	7.39	5.78	7.07	5.09	4.91	5.64	5.16	**5.47**	8.46	6.97	**7.72**
PF3D7_0800100	PF08_0142	B	8.05	3.07	5.21	5.05	4.72	8.00	6.70	6.12	4.53	3.92	3.97	4.72	**4.89**	7.38	5.84	**6.61**
PF3D7_0300100	PFC0005w	B	8.27	5.73	5.05	6.93	6.45	6.10	6.68	6.41	6.77	4.79	5.91	5.87	**6.26**	7.67	8.42	**8.04**
PF3D7_1200600	PFL0030c	E/var2CSA	6.64	8.02	5.07	6.25	7.11	8.39	6.65	5.39	6.54	5.21	5.81	5.55	**6.39**	7.52	5.47	**6.50**
PF3D7_0200100	PFB0010w	B	7.42	6.14	7.96	7.33	4.41	6.83	8.34	7.34	4.16	2.71	7.37	6.06	**7.08**	7.01	9.51	**8.26**
PF3D7_0632800	MAL6P1.1	B	6.97	3.12	7.12	7.49	5.79	5.88	5.76	6.19	6.24	6.59	6.67	7.46	**6.41**	9.29	9.98	**9.63**
PF3D7_1255200	PFL2665c	B	6.14	3.11	4.10	3.68	3.60	6.58	7.40	5.19	1.86	1.03	4.87	3.11	**3.89**	5.38	7.94	**6.66**
PF3D7_0733000	PF07_0139	B	2.20	1.78	1.20	4.21	1.64	3.93	4.96	5.09	4.03	5.01	3.33	6.25	**3.98**	6.20	8.07	**7.13**
PF3D7_1300100	PF13_0001	B	2.00	2.30	4.46	3.01	4.59	3.79	4.38	2.68	1.39	3.51	2.58	4.19	**3.26**	4.16	8.34	**6.25**
PF3D7_0809100	PF08_0103	B/C	4.92	8.92	7.14	4.31	3.95	6.05	4.95	6.13	2.84	3.87	7.21	5.27	**5.11**	5.75	3.72	**4.74**
PF3D7_0937800	PFI1830c	B	4.84	3.77	3.82	4.62	4.44	5.00	7.34	6.05	3.30	5.30	6.32	6.60	**4.92**	7.62	9.07	**8.34**
PF3D7_1200400	PFL0020w	B/A	3.09	3.40	3.95	5.33	5.08	4.83	4.95	5.79	2.28	7.47	7.34	5.59	**5.02**	8.24	7.91	**8.08**

4.5.5.1 Comparison of *ex vivo* parasite *var* gene profiles with previous studies of CHMI

Considering the differences in methodologies used for *var* gene profiling, I was interested to compare patterns of *var* gene expression observed in this dataset, with those previously reported in studies of CHMI (Peters *et al.* 2002, Lavstsen *et al.* 2005, Wang *et al.* 2009, Bachmann *et al.* 2016). In the original study, Peters *et al* show expression of *var* gene variants belonging mainly to groups A and B, with dominant expression coming from a single B-type PfEMP1 transcript (PF3D7_1100100/ PF11_0007) (Peters *et al.* 2002). Interestingly, this variant was detected among the top 6 most highly expressed *var* genes in my dataset (rlog median = 7.22; range: 4.93 – 9.11) (figure 4.6). Observations made by Peters *et al*, however, contradict the broad-level detection of almost all *var* gene variants (95%) within this study.

More consistent with my results is the recent data from Bachmann *et al,* demonstrating the expression of a broad range of *var* gene variants, with highest level expression coming from the group-B subclass (Bachmann *et al.* 2016). Figure 4.8 compares the expression patterns of all detectable *var* genes, across the different subgroups. The most highly expressed variant in the study by Bachmann *et al* (PF3D7_0632800/ MAL6P1.1) was found as the 8th most highly expressed within this cohort of volunteers. Analysis of the top 20 expressed variants across both studies revealed 11 shared genes (PF3D7_0632800/ MAL6P1.1; PF3D7_0937800/ PFI1830c; PF3D7_0800100/ PF08_0142; PF3D7_1255200/ PFL2665c; PF3D7_0223500/ PFB1055c; PF3D7_1373500/ PF13_0364; PF3D7_1300100/ PF13_0001; PF3D7_0632500/ MAL6P1.4; PF3D7_1041300/ PF10_0406; PF3D7_1100100/ PF11_0007 and PF3D7_1200100/ PFL0005w), 10 of which belong to the group-B *var* subclass. However, there are also some inconsistencies between the two datasets, which may be a result of the different methodologies used to measure *var* gene expression (qPCR vs RNA-seq) or due to the different models of CHMI used to infect volunteers (mosquito-bite vs blood-stage). For instance, in the study by Bachmann *et al*, the group-A variant PF3D7_0400400/ PFD0020c was among the top 5 most highly expressed, whereas this *var* gene was detected with some of the lowest levels across the dataset. Nevertheless, when considering all *var* gene variants, a significant positive correlation in expression was

observed between the two studies (figure 4.9). Interestingly, apart from slight differences in frequencies, the expression patterns reported by Bachmann *et al*, were almost identical to those reported in a previous study of CHMI, albeit based on parasites from a single volunteer (Wang *et al.* 2009). In this study by Wang *et al*, PF3D7_0632800/ MAL6P1.1 was also found expressed at the highest level, and all other *var* gene variants had a similar hierarchy of expression, dominated by those of the group-B subclass. Thus, my analysis of parasite *var* gene expression in volunteers following blood-stage CHMI demonstrates similarities with those previously published across different studies of mosquito-bite CHMI. However, it will be important to investigate parasite *var* gene expression by RNA-seq (as was used in this study), using the mosquito-bite challenge model.

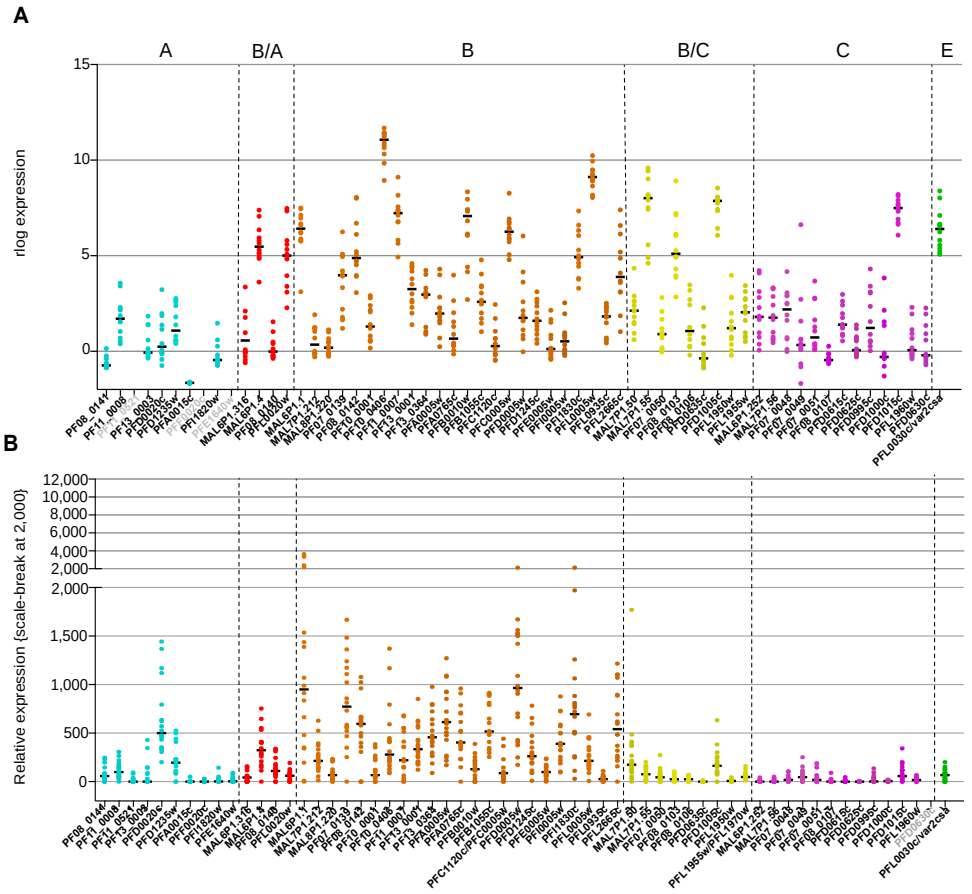

Figure 4.8 | Comparison of *ex vivo* parasite *var* gene expression profiles in human volunteers. A) RNA-seq analysis of parasite populations isolated at day of patent infection (thick film smear positivity), from 12 malaria-naïve volunteers following blood-stage CHMI with *P. falciparum* (3D7-strain). The distribution of the rlog expression (read counts) per *var* gene is presented as a dot plot for all volunteer samples. Each point represents a *var* gene rlog value and the median expression is marked. **B)** Data from Bachmann *et al.* 2016. qRT-PCR analysis of parasite populations isolated at day of patent infection (defined as thick film smear positivity) from 18 malaria-naïve volunteers following mosquito-bite CHMI with *P. falciparum* (NF54). The distribution of the relative gene expression per *var* gene is shown in a dot plot for all volunteer samples. Each point represents a *var* gene expression value relative to the normalising gene *sbp1* observed per volunteer sample and the median expression per *var* gene is

marked. For both plots, *var* gene names and groups are indicated (v*ar* genes in grey = not detected). Note that scales do not match in these plots.

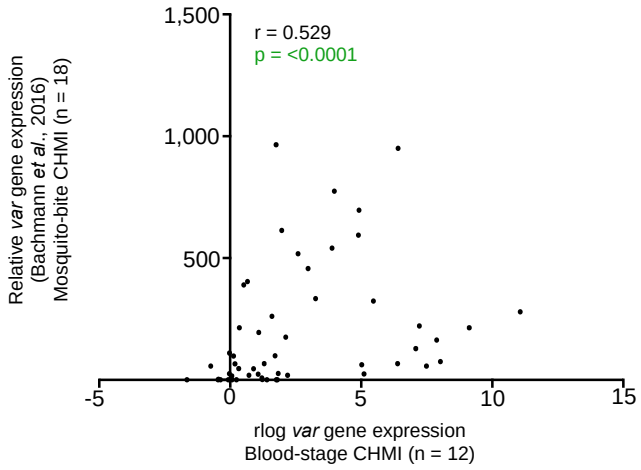

Figure 4.9 | Comparison of *ex vivo* parasite *var* gene expression profiles in human volunteers following blood-stage and mosquito-bite CHMI. Spearman's rank correlation demonstrating a positive, significant correlation between parasite populations recovered at day of patent infection (defined by thick film smear positivity) from n = 12 volunteers following blood-stage CHMI (median rlog values on the x-axis) and from n = 18 volunteers following mosquito-bite CHMI (median expression values on the y-axis). The Spearman's rank correlation coefficient (r) is shown, along with p. value (p = < 0.0001). Significance was defined as p = <0.05.

4.5.5.2 Relationship between group A, B/A *var* expression and parasite growth in the blood

Based on their association with severe disease, it has been predicted that PfEMP1 of the group-A, B/A subclass confer a growth advantage in the immunologically naïve host through mechanisms that allow them to adhere to a more diverse range of endothelial cells, and thus more efficiently escape clearance from the spleen (Abdi *et al.* 2017). However, direct evidence is still needed to support an intrinsic growth advantage over other PfEMP1 types in the absence of antibody pressure (Warimwe *et al.* 2009, Warimwe *et al.* 2012). Using arbitrary cut-offs based on the calculated parasite multiplication rates (PMRs), volunteers in this cohort had been previously grouped into those having "fast" (PMR > 10), "intermediate" (PMR = 8 - 10) and "slow" (PMR <8) growing parasites (see chapter 3, section 3.5.8 and table 3.1). In order to investigate evidence for a growth advantage of the group-A and/or B/A *var* genes, their expression levels were compared across the parasite samples

of variable PMR class (figure 4.10). It is important to note that just 1 of 3 belonging to the “slow” group were included in this analysis, as parasite RNA-seq was not performed on samples ♯22 and ♯208. For all 7 detectable group-A variants in the dataset, there was no trend suggestive of higher expression in parasites with “fast” PMR, compared to those with “intermediate” or “slow” PMR (figure 4.10, part A). This was also true for PF3D7_0800300/ PF08_0140, PF3D7_0600200/ MAL6P1.316 and PF3D7_0632500/ MAL6P1.4 of the B/A subgroup (figure 4.10, part B). There did look to be a trend towards higher expression of the group B/A variant PF3D7_1200400/ PFL0020w in those parasites with “fast” PMR compared to “intermediate” and slow “PMR”. However, when considering this *var* gene, as well as the two other most highly expressed variants of the group-A and B/A subclasses (PF3D7_0632500/ MAL6P1.4 and PF3D7_1100200/ PF11_0008), there was no correlation detected between expression levels and PMR (figure 4.10, parts D and E). It is important to note that these data are limited, however, by the small number of samples available in this study of CHMI. Thus, analysis of group-A and B/A *var* gene expression in parasites with variable growth rates in the naïve host will need to be extended to future trials.

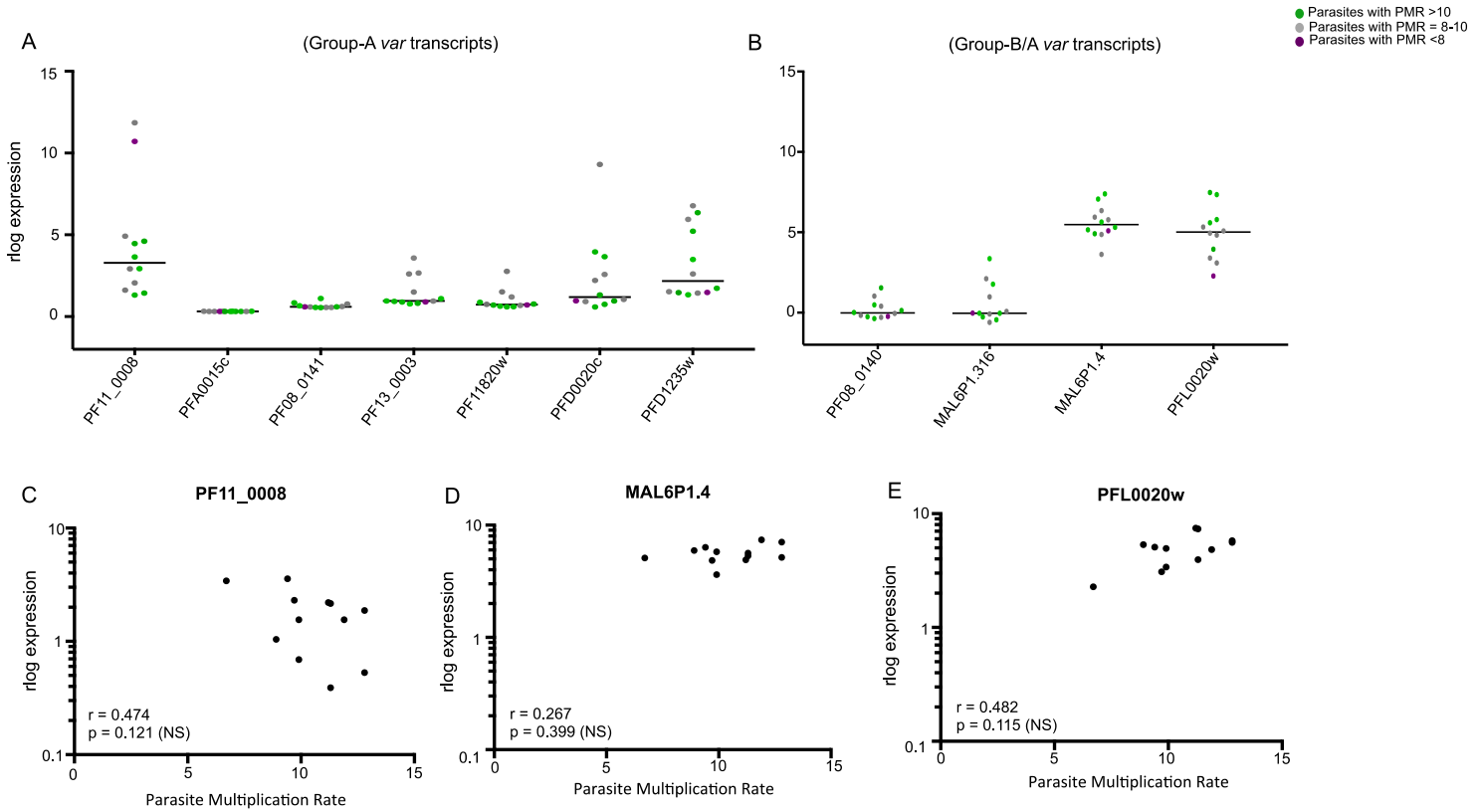

Figure 4.10 | Relationship between group-A / group-B/A *var* gene expression and parasite growth in the blood. Panels **A** and **B** show the rlog expression levels for the 7 and 4 detectable group-A and B/A *var* transcripts in the dataset, respectively. Each dot represents a *var* gene expression value, per volunteer sample (n=12). The median expression value is marked. Volunteer samples have been colour-coded by Parasite Multiplication Rate (PMR); fast (PMR >10) in green; intermediate (PMR = 8-10) in grey and slow (PMR <8) in purple. *Var* gene names are indicated. Panels C, D and E show the Spearman's rank correlation between rlog expression and PMR, for the three group-A, B/A *var* genes with highest expression levels; PF11_0008 (group-A); MAL6P1.4 (group-B/A) and PFL0020w (group-B/A). Spearman's rank correlation coefficient (r) is shown, along with p. value. Significance was defined as p = <0.05 (NS = Not significant).

4.5.5.3 Investigating evidence for *var* gene selection in the naïve human host

The comparison of *var* gene expression between parasites isolated from the blood-stage inoculum, and parasites recovered from volunteers at day of patent infection revealed the two to be consistently different, as is shown by the heatmap-based clustering (figure 4.5). Differential expression analysis revealed five *var* genes (PFF1595c/ PF3D7_0632800, PFB1055c/ PF3D7_0223500, PF13_0001/ PF3D7_1300100, PFA005w/ PF3D7_0100100 and PF07_0049/ PF3D7_071200) to be expressed at significantly lower levels in the volunteer samples compared to the inoculum (Appendix 8), which may represent the initial stages of *var gene* selection. Within the time frame assessed however, there was little evidence for this given that the majority of all variants (95%) were still detectable on the day of patent (microscopically-positive) infection, and the most highly expressed *var* gene variant in the volunteer samples, was also the most highly expressed in the inoculum samples (figure 4.5 and table 4.6). Furthermore, pairwise comparisons of *var* gene expression in parasites of the 5th generation (isolated at C +8 - C +10, n = 6 samples) with those of the 6th generation in the blood cycle (isolated from C +10, n = 5 samples), revealed the two to be significantly positively correlated (figure 4.10, part A). This was also true for the pairwise comparison between patient samples (median expression) and the inoculum used to infect (figure 4.10). Results suggest that following 5 - 6 replication cycles in the blood, *var* gene selection forces had not yet been activated in this *in vivo* setting.

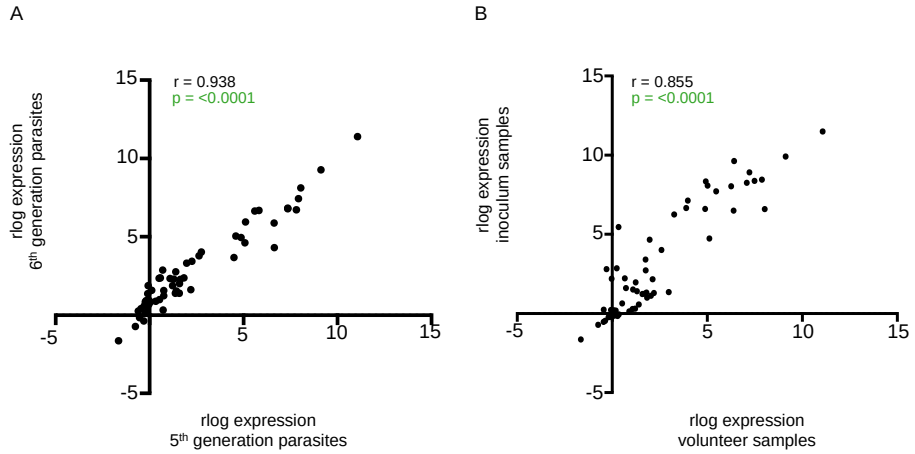

Figure 4.11 | Comparison of (rlog) *var* gene expression between parasites isolated at different stages in the blood cycle, and to those recovered from the inoculum. A) demonstrates the pairwise Spearman's rank correlation between the median (rlog) expression values for all detectable *var* transcripts in samples from 5th

generation parasites (samples 18, 19, 20, 26, 27 and 106) and 6th generation parasites in the blood cycle (samples 13, 16, 17, 24 and 206). **B)** demonstrates the pairwise Spearman's rank correlation between the median (rlog) expression values for all detectable *var* transcripts in the volunteer samples (n = 12) vs the inoculum samples (n = 2). For both plots, the Spearman's rank correlation coefficient (r) is shown, along with p. value (p = < 0.0001). Significance was defined as p = <0.05.

4.5.5.4 Relationship between parasite *var* gene expression and the developing immune response in the malaria-naïve host

Having observed inter-individual variation in the host immune response to *P. falciparum* (chapter 3), I wanted to investigate a similar variability in parasite gene expression, which may be indicative of a causal relationship. Furthermore, it was hypothesised that parasites isolated from the 8 "classical" responders (♯13, ♯16, ♯17, ♯24, ♯26, ♯27, ♯106, and ♯206), showing a pronounced inflammatory response at both the transcriptional and protein level, would have a distinct *var* expression profile when compared to the rest. As is shown in figure 4.5 however, v*ar* gene profiles were remarkably similar across volunteers, and Principle Component Analysis did not reveal any divergence between the two groups, highlighting a clear overlap in expression profiles (figure 4.12).

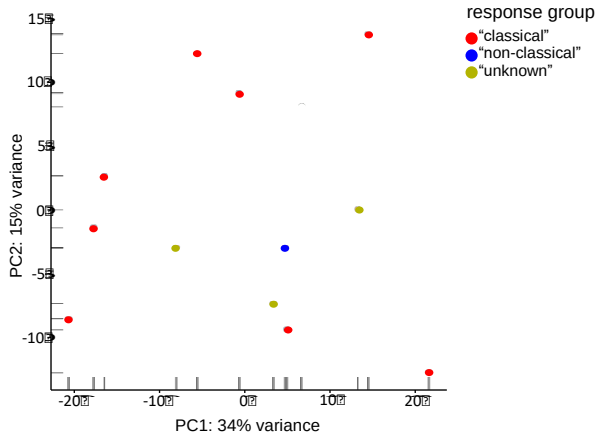

Figure 4.12 | Principle Component Analysis of parasite *var* gene expression across the volunteer cohort. Principle Component Analysis was performed on the detectable *var* transcripts in the 12 successfully sequenced parasite samples from the 8 "classical" responders (♯13, ♯16, ♯17, ♯24, ♯26, ♯27, ♯106 and ♯206) in red, the "non-classical" responders (♯19) in blue, and 3 of the "unknown" volunteers (♯12, ♯18 and ♯20) in yellow. Data is presented in two dimensions: PC1 on the x-axis against PC2 on the y-axis. The variation encoded by each is presented as a percentage of the total variation in the dataset. A colour key for host transcriptional response group is provided.

When comparing the proportional distribution of *var* transcripts by *var* group affiliation (A, B/A, B, B/C, C and E), individuals showed remarkable similarities, irrespective of the host transcriptional response groupings presented in chapter 3 (figure 4.13). As previously discussed, the group-B variants were attributed to the largest proportion of total *var* expression in all patient samples (range: 58.1% - 87.2% and mean: 75.6%), followed by the group-B/C variants (range: 9.4% - 21.5% and mean: 14.0%), group-C *var* genes (range: 3.4% - 9.4% and mean: 5.0%), the group-B/A variants (range: 0.4% - 8.9% and mean: 2.6%), group-E (var2CSA) (range: 0.9% - 5.5% and mean: 2.5%) and then the group-A *var* genes (range: 0.1% - 0.7% and mean: 0.3%). Volunteer sample ♯27, of the "classical" host responder group had the most unique *var* group distribution, with a lower contribution of the group-B variants, and a higher contribution from the group-B/A, B/C and C variants compared to the other samples (figure 4.13). The proportional distribution of *var* gene groups in the patient samples demonstrated a slightly higher contribution of the B/C variants to the (mean) total expression (14.0%) compared to that of the inoculum samples (6.5%), but otherwise had a very similar distribution profile.

Pairwise comparison of *var* gene expression in volunteer ♯16 (the most inflammatory "classical" responder in the cohort) and volunteer ♯19 ("non-classical" responder) revealed a significant positive correlation between the two (figure 4.14, part A). Positive correlations in *var* gene expression were also observed for group-level comparisons between the "classical" responders (n = 8) and the "unknown" volunteers (n = 3) (figure 4.14, part B); the "classical" responders and the "non-classical" responder volunteer ♯19 (figure 4.14, part C); as well as the "unknown" volunteers and "non-classical" responder volunteer ♯19 (figure 4.14, part D). Results suggest that inter-individual variation in host immune responses to *P. falciparum* during primary infection, is not driven by differences in parasite *var* gene expression, and thus it is important to investigate the role of multi-gene families coding for other VSAs.

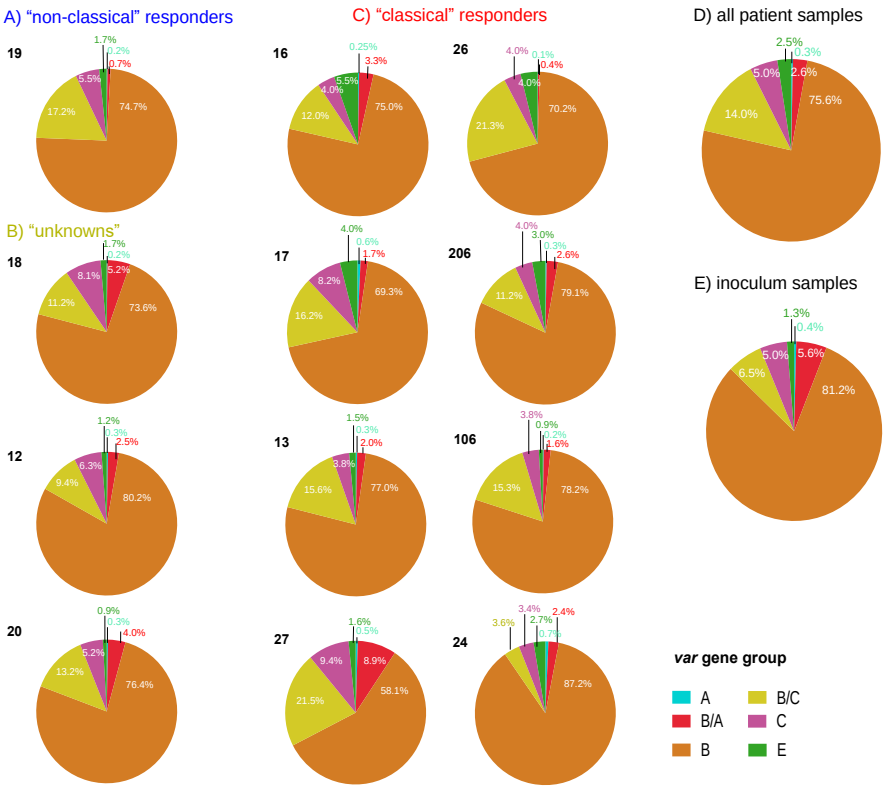

Figure 4.13 | Proportion of *var* gene expression by group. The distribution of *var* transcripts according to *var* group affiliation in shown as the proportion of total *var* gene expression for individual volunteer samples **(A-C)**. Samples have been grouped according to host transcriptional response class; "non-classical" responder ǂ19 **(A)**; "unknowns"-ǂ18, ǂ12 and ǂ20 **(B)** and "classical" responders- ǂ16, ǂ17, ǂ13, ǂ27, ǂ26, ǂ206, ǂ106 and ǂ24 **(C)**. The proportion of *var* gene expression by group, across all patient samples (n=12) is shown in D. E) shows the proportion of *var* gene expression (mean) by group, for the two replicate inoculum samples. A *var* gene group colour-code is provided.

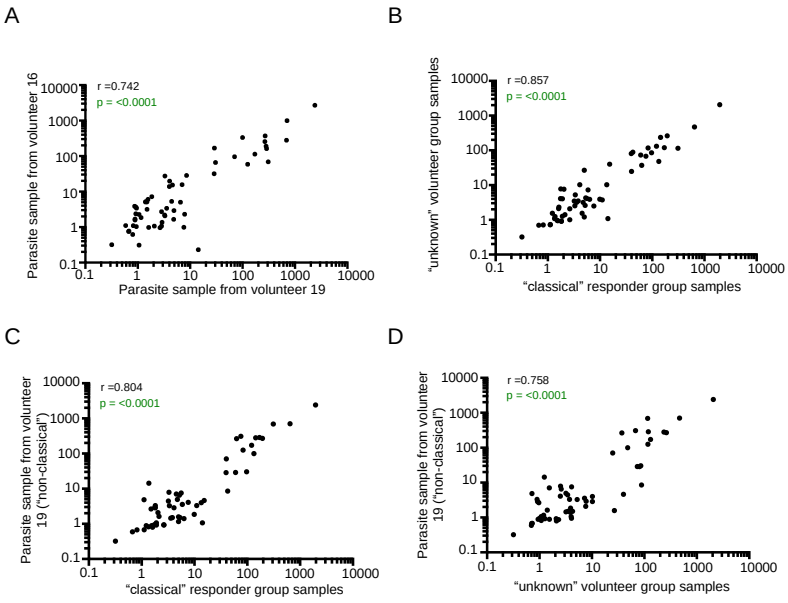

Figure 4.14 | Comparison of (rlog) *var* gene expression between parasites isolated from volunteers with variable host immune responses to *P. falciparum* infection. The pairwise Spearman's rank correlation demonstrating a positive, significant correlation between the (rlog) expression values for the detectable *var*

transcripts in parasite samples from volunteer ♯16 ("classical" responder) and ♯19 ("non-classical" responder) in **A**. Plots **B - D** show group-level correlations of the mean (rlog) expression values for the detectable *var* transcripts in the "unknown" volunteer group (12, 18 and 20) vs the "classical" responder group (♯13, ♯16, ♯17, ♯24, ♯26, ♯27, ♯106 and ♯206) in **B**, the "non-classical" responder volunteer (19) vs the "classical" responder group in **C**, and the "non-classical" responder volunteer (#19) vs the "unknown" volunteer group samples in **D**. For each plot, the Spearman's rank correlation coefficient (r) is shown, along with p. value (p<0.0001). Significance was defined as p = <0.05.

4.5.5.5 *Rif* and *stevor* gene expression in Controlled Human *Plasmodium falciparum* Infection

Whereas the *var* multi-gene family of *P. falciparum* has been well characterised, far less is understood about the role of *rif* and *stevor* genes in the context of severe malaria disease. The *rif* and *stevor* gene families encode the variant antigens *P. falciparum* repetitive interspersed families of polypeptides (RIFINs) and STEVOR, respectively, which can be found on the surface of parasite-infected red blood cells where they are thought to mediate adhesion, thus contributing to pathology (Wahlgren *et al.* 2017). RIFINs and STEVORs appear to be predominantly expressed by freshly isolated *P. falciparum* strains, and by parasites enriched for adhesion *in vitro* (Fernandez *et al.* 1999, Kyes *et al.* 1999, Blythe *et al.* 2008). 70% of all RIFINs belong to a subgroup A (A-RIFINs), and have an insertion of 25 amino acids at the N-terminus, that is absent in B-RIFINs. The A- and B-subgroups of RIFIN proteins also differ in the number of cysteine residues they contain (10 and 8, respectively). These proteins also localise to different compartments of infected erythrocytes and are predicted to have different functions. A-type RIFIN proteins are associated with the Maurer's cleft, a membranous network that is involved in the export of proteins from the parasite cytosol to the erythrocyte surface. B-type RIFINs, however, appear to be mostly retained inside the parasite (Joannin *et al.* 2008). STEVORs resemble B-RIFINs, in that they lack the N-terminus insertion sequence of the A-RIFINs (Wahlgren *et al.* 2017). 143 and 32 members of the *rif* and *stevor* gene families have been found in the 3D7 reference genome, respectively and their expression has been reported at various stages of the *P. falciparum* life cycle (Petter *et al.* 2007, Khattab *et al.* 2008, Claessens *et al.* 2011, Khattab and Meri 2011). Interestingly, their expression patterns seem to occur in a highly organised, sequential manner starting with the transcription of *var* genes at the ring stage (3–18 hours post infection) (Kyes *et al.* 2000, Llinas *et al.* 2006), followed by the expression of *rif* genes (12–27 hours post infection) (Kyes *et al.*

1999, Kyes *et al.* 2000, Llinas *et al.* 2006, Wang *et al.* 2009), and then transcription of the *stevor* gene family (22–32 hours post infection) (Kaviratne *et al.* 2002, Lavazec *et al.* 2007). In most parasites, PfEMP1 proteins are not expressed alone, but together with RIFINs and STEVORs (Fernandez *et al.* 1999, Kaviratne *et al.* 2002), suggesting that these proteins may be involved in key parasite-host interactions during primary *P. falciparum* infection. Therefore, in order to investigate the influence of parasite gene expression on the host immune response, RNA-seq was also used to quantify the expression of these multi-gene families during controlled human infection in the naïve host.

Of the 32 *stevor* gene members in the *P. falciparum* (3D7) genome, just 3 were detected (PF3D7_0832000, PF3D7_0300900 and PF3D7_0617600), and at low levels across all. PF3D7_0832000 demonstrated the highest level of expression, but was variable between volunteers; (highest in parasites isolated from volunteer ♯24 (rlog = 4.53), followed by volunteer ♯13 (rlog = 2.97), volunteer ♯20 (rlog = 2.09) and volunteer ♯16 (rlog = 0.36). Thus, although this gene had variable expression, it did not follow the same trend in variability in host transcriptional responses. It is important to note that the stage specific expression of parasite multi-gene families (*var* genes: 3-18 hours post infection (p.i), *rif* genes: 12–27 hours p.i and *stevor* genes: 22–32 hours p.i) may explain the failure to detect the majority of *stevor* variants in these patient samples. Only immature ring stages of *P. falciparum* merozoites are found in the circulation of the human host, whereas the more mature stages (trophozoites and schizonts) are sequestered in the microvasculature (Miller *et al.* 2002), making them inaccessible during parasite isolation from whole blood.

Of the 143 *rif* gene members present in the *P. falciparum* (3D7) genome, 43 were detected within the volunteer cohort (figure 4.15). The majority of variants were transcribed at very low levels however, and often in just one or two samples (table 4.7). Across all volunteer samples, one A-type *rif* variant (PFD0070c/ PF3D7_0401600) was dominantly expressed, (rlog median = 5.96; range: 4.98 – 7.08), followed by the B-type variant PFD1010w/ PF3D7_0421200 (rlog median = 1.89; range: 0.71 – 3.91). Interestingly, the most highly expressed *rif* gene (PFD0070c/ PF3D7_0401600) was found to be expressed at significantly lower levels in the two inoculum samples (rlog median = 2.37) compared the parasites

recovered at day of patent infection in the volunteers (table 4.7). Given that this variant was the most highly expressed across all, it is unlikely to represent *in vivo* selection but instead may reflect differences in how the samples were prepared for sequencing, as has been previously discussed (see section 4.5.4). As with the *var* genes, the uniformity in *rif* variant expression across volunteers reinforces the concept that immune variation is not driven by parasite gene expression, highlighting an important gap in our understanding of the diversity in the human response to *P. falciparum* infection.

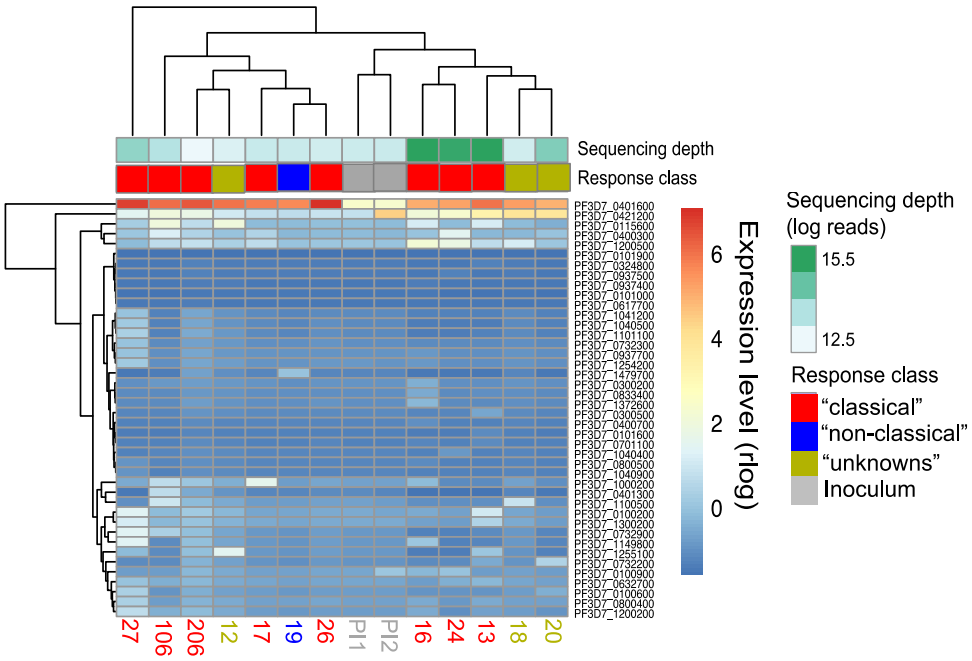

Figure 4.15 | Comparison of *rif* gene expression across the volunteer cohort and inoculum samples. Heatmap showing normalised (rlog) expression values for all detectable *rif* transcripts. Each row represents a *rif* gene (transcript i.d annotated on the left hand side), and each column represents a volunteer or inoculum sample (annotated along the bottom, and colour-coded as per transcriptional response class; "classical" responder (red), "non-classical" responder (blue), "unknown" (yellow), or as parasite inoculum samples (PI1 and PI2) in grey). Sample sequencing depth is indicated, as per the colour key provided. A colour key for rlog expression values is also shown. (Heatmp generated by Dr Adam Reid, Wellcome Trust Sanger Institute).

Table 4.7 | Normalised (rlog) read counts for all detectable *rif* genes in the 12 patient and 2 inoculum samples (same order as heatmap)

transcript i.d	v027	v106	v206	v012	v017	v019	v026	v016	v024	v013	v018	v020	median of volunteer samples	PI1	PI2	median of inoculum samples
PF3D7_0401600.1	6.77	6.06	6.39	5.97	5.81	5.68	7.08	5.01	5.18	6.02	5.31	4.98	5.89	2.41	2.33	2.37
PF3D7_0421200	1.48	2.01	1.77	1.09	0.77	0.71	0.86	2.13	2.35	3.28	3.91	3.81	1.89	0.82	4.42	2.62
PF3D7_0115600	0.28	2.04	0.69	2.01	-0.13	-0.19	-0.04	1.13	-0.15	1.14	-0.14	-0.41	0.12	-0.08	-0.14	-0.11
PF3D7_0400300	0.13	1.26	0.46	0.05	0.43	-0.26	-0.14	0.01	1.53	-0.28	-0.22	0.03	0.04	-0.17	-0.21	-0.19
PF3D7_1200500	-0.17	0.74	0.82	0.33	0.75	-0.01	0.10	2.20	1.84	0.72	1.17	0.08	0.73	0.06	0.02	0.04
PF3D7_0101900	-1.58	-1.58	-1.51	-1.54	-1.56	-1.56	-1.55	-1.52	-1.59	-1.59	-1.56	-1.58	-1.56	-1.55	-1.56	-1.55
PF3D7_0324800	-1.44	-1.43	-1.31	-1.36	-1.39	-1.40	-1.39	-1.44	-1.44	-1.28	-1.40	-1.44	-1.40	-1.39	-1.39	-1.39
PF3D7_0937500	-1.44	-1.43	-1.32	-1.37	-1.40	-1.41	-1.39	-1.44	-1.32	-1.42	-1.40	-1.44	-1.40	-1.39	-1.40	-1.40
PF3D7_0937400	-1.48	-1.47	-1.36	-1.41	-1.44	-1.44	-1.43	-1.36	-1.48	-1.48	-1.44	-1.48	-1.44	-1.43	-1.44	-1.44
PF3D7_0101000	-1.52	-1.51	-1.42	-1.46	-1.49	-1.49	-1.48	-1.45	-1.52	-1.50	-1.49	-1.52	-1.49	-1.48	-1.49	-1.48
PF3D7_0617700	-1.44	-1.48	-1.39	-1.43	-1.46	-1.46	-1.45	-1.49	-1.44	-1.49	-1.46	-1.49	-1.46	-1.45	-1.46	-1.45
PF3D7_1041200	0.05	-1.26	-0.59	-0.92	-1.12	-1.17	-1.07	-1.32	-1.31	-1.32	-1.13	-1.29	-1.15	-1.09	-1.13	-1.11
PF3D7_1040500	0.23	-1.27	-0.55	-0.90	-1.12	-1.17	-1.06	-1.34	-1.34	-1.34	-1.13	-1.31	-1.15	-1.09	-1.13	-1.11
PF3D7_1101100	0.33	-1.26	-0.51	-0.87	-1.11	-1.15	-1.04	-1.34	-1.34	-1.28	-1.11	-1.31	-1.13	-1.07	-1.11	-1.09
PF3D7_0732300	0.02	-1.12	-0.70	-0.88	-1.00	-1.02	-0.97	-1.14	-1.14	-1.14	-1.00	-1.14	-1.01	-0.98	-1.00	-0.99
PF3D7_0937700	0.00	-1.04	-0.62	-0.81	-0.93	-0.95	-0.89	-0.89	-1.06	-1.06	-0.93	-1.05	-0.93	-0.91	-0.93	-0.92
PF3D7_1254200	0.22	-1.02	-0.56	-0.76	-0.90	-0.92	-0.86	-0.88	-1.01	-1.05	-0.90	-1.04	-0.90	-0.88	-0.90	-0.89
PF3D7_1479700	-1.42	-1.38	-0.68	-1.01	-1.22	-0.01	-1.16	-1.45	-1.45	-1.45	-1.22	-1.43	-1.30	-1.19	-1.22	-1.20
PF3D7_0300200	-1.06	-0.83	-0.73	-0.87	-0.96	-0.98	-0.94	-0.44	-1.06	-1.06	-0.97	-1.06	-0.97	-0.95	-0.97	-0.96
PF3D7_0833400	-1.13	-1.12	-0.82	-0.95	-1.04	-1.05	-1.01	-0.48	-1.13	-1.06	-1.04	-1.13	-1.04	-1.02	-1.04	-1.03
PF3D7_1372600	-1.12	-1.11	-0.74	-0.90	-1.01	-1.03	-0.98	-0.21	-1.09	-1.12	-1.01	-1.12	-1.02	-0.99	-1.01	-1.00
PF3D7_0300500	-1.20	-1.18	-0.92	-1.04	-1.11	-1.13	-1.09	-1.20	-1.20	-0.62	-1.11	-1.20	-1.12	-1.10	-1.11	-1.11
PF3D7_0400700	-1.28	-1.27	-1.09	-1.17	-1.22	-1.23	-1.21	-0.98	-1.25	-1.28	-1.22	-1.28	-1.23	-1.21	-1.22	-1.22
PF3D7_0101600	-1.34	-1.33	-1.17	-1.24	-1.28	-1.29	-1.27	-1.34	-1.34	-1.08	-1.29	-1.34	-1.29	-1.28	-1.29	-1.28
PF3D7_0701100	-1.30	-1.29	-1.13	-1.20	-1.25	-1.26	-1.24	-1.22	-1.31	-1.11	-1.25	-1.31	-1.25	-1.24	-1.25	-1.25
PF3D7_1040400	-1.25	-1.23	-1.02	-1.11	-1.17	-1.19	-1.16	-1.25	-0.81	-1.25	-1.18	-1.25	-1.18	-1.16	-1.17	-1.17
PF3D7_0800500	-0.93	-1.23	-1.03	-1.11	-1.17	-1.18	-1.16	-1.15	-1.24	-1.24	-1.17	-1.24	-1.17	-1.16	-1.17	-1.17
PF3D7_1040900	-0.89	-1.26	-1.06	-1.15	-1.21	-1.22	-1.19	-1.28	-1.28	-1.28	-1.21	-1.28	-1.21	-1.20	-1.21	-1.20
PF3D7_1000200	-0.54	0.73	0.12	-0.37	1.59	-0.76	-0.60	-0.13	-1.12	-1.12	-0.70	-1.02	-0.57	-0.64	-0.70	-0.67
PF3D7_0401300	-1.45	0.75	-0.48	-0.90	-1.17	-1.23	-1.10	-1.53	-1.53	-1.53	-1.18	-1.47	-1.20	-1.13	-1.18	-1.15
PF3D7_1100500	-0.98	0.99	-0.13	-0.50	-0.73	-0.78	-0.66	-1.03	-1.03	-1.03	0.87	-0.99	-0.75	-0.69	-0.73	-0.71
PF3D7_0100200	1.37	-0.15	0.21	-0.25	-0.55	-0.61	-0.47	-0.48	-0.67	1.09	-0.56	-0.79	-0.47	-0.50	-0.55	-0.53
PF3D7_1300200	1.14	-0.25	0.01	-0.32	-0.54	-0.58	-0.48	-0.70	-0.75	0.45	-0.54	-0.73	-0.51	-0.50	-0.54	-0.52
PF3D7_0732900	1.38	0.37	-0.08	-0.55	-0.86	-0.92	-0.77	-1.26	-1.26	-1.07	-0.87	-1.17	-0.86	-0.81	-0.86	-0.84
PF3D7_1149800	1.40	-1.09	-0.10	-0.57	-0.88	-0.94	-0.79	0.09	-1.28	-1.18	-0.89	-1.19	-0.88	-0.83	-0.88	-0.86
PF3D7_1255100	-0.18	-1.14	-0.06	1.50	-0.89	-0.95	-0.80	-1.39	-1.39	0.14	-0.89	-1.27	-0.89	-0.84	-0.89	-0.86
PF3D7_0732200	-1.10	-1.07	-0.34	-0.70	-0.93	-0.98	-0.87	-1.14	-1.14	-0.48	-0.94	0.45	-0.94	-0.90	-0.94	-0.92
PF3D7_0100900	-0.77	-0.75	-0.25	-0.49	-0.64	-0.67	-0.60	-0.24	0.01	-0.78	-0.64	-0.77	-0.64	-0.62	0.13	-0.24
PF3D7_0632700	0.06	-0.42	-0.26	-0.47	-0.61	-0.63	-0.57	-0.72	-0.38	-0.26	-0.61	-0.71	-0.52	-0.59	-0.61	-0.60
PF3D7_0100600	0.35	-0.92	-0.41	-0.64	-0.79	-0.82	-0.75	-0.95	-0.95	-0.95	-0.79	-0.43	-0.79	-0.77	-0.79	-0.78
PF3D7_0800400	0.39	-0.78	-0.29	-0.52	-0.67	-0.70	-0.63	-0.46	-0.81	-0.50	-0.67	-0.65	-0.64	-0.64	-0.67	-0.66
PF3D7_1200200	0.71	-0.45	-0.16	-0.54	-0.79	-0.84	-0.72	-0.48	-1.00	-0.71	-0.79	-0.97	-0.71	-0.75	-0.79	-0.77

4.6 Discussion

The inter- and intra-clonal variability of *P. falciparum var* genes have hampered attempts to investigate the roles of the encoded PfEMP1 proteins in the pathogenesis of malaria in the field. To date, the most popular strategy has involved the use of degenerate primers, and qPCR approaches to quantify *var* gene transcripts found in patient isolates of variable clinical outcome. Using this method, numerous studies have implicated a subset of group-A, B/A *var* gene variants in severe disease outcome following infection with *P. falciparum* (Kirchgatter and Portillo Hdel 2002, Bull *et al.* 2005, Kaestli *et al.* 2006, Kyriacou *et al.* 2006, Rottmann *et al.* 2006, Normark *et al.* 2007, Falk *et al.* 2009, Warimwe *et al.* 2009, Kalmbach *et al.* 2010, Lavstsen *et al.* 2012, Warimwe *et al.* 2012, Bertin *et al.* 2013, Almelli *et al.* 2014, Abdi *et al.* 2015, Bernabeu *et al.* 2016, Bertin *et al.* 2016, Jespersen *et al.* 2016, Mkumbaye *et al.* 2017, Shabani *et al.* 2017, Tonkin-Hill *et al.* 2018). Given that severe disease is most commonly observed in young children having had limited exposure to the *Plasmodium* parasite, it has been hypothesised that group-A and/or B/A variants are dominantly expressed in the malaria-naïve.

In this study, parasites isolated from the blood of 12 volunteers undergoing CHMI with *P. falciparum* (3D7-strain) were analysed by RNA-seq, to characterise expression of *var* gene variants in the naïve host. All volunteers received direct blood-stage challenge of ~690 parasitised erythrocytes. At day of patent infection (7.5 - 10.5 days later), 95% of the 3D7 *var* gene variants were detected across the cohort. Moreover, those with highest levels of expression belonged to the group-B subclass. This was in agreement with three previous studies of CHMI showing similar broad expression of group-B *var* gene variants following mosquito-bite challenge (Lavstsen *et al.* 2005, Wang *et al.* 2009, Bachmann *et al.* 2016), although contradicts data from another (Peters *et al.* 2002). In the original study by Peters *et al*, *var* expression was analysed using semi-quantitative RT-PCR followed by sequencing of a large number of clones, revealing the dominant expression of a single B-group variant (PF3D7_1100100/ PF11_0007). One possible explanation for this divergent observation is that the semi-quantitative RT-PCR method used is susceptible to primer and cloning bias, which can result in the overestimation of transcript frequencies. Furthermore, this study was limited to just two volunteers. Using a different method Wang *et al*, detected much broader expression of variants

but report a different group-B *var* gene as being dominantly transcribed (PF3D7_0632800/ MAL6P1.1). This study however, was limited by low parasitaemias, meaning that just one blood sample, from one volunteer, gave sufficient mRNA for quantitative analysis of NF54-expressed *var* genes.

Despite the limitations of these studies, two models of *in vivo var* gene selection have been proposed. The first suggests that switching of *var* genes comes about via an ordered hierarchical program, meaning that most parasites express a single *var* type in the first generation after egress from the liver. In subsequent replication cycles the parasite switches to other variants, determined by the intrinsic rate for each gene to be turned on or off. This model would allow for efficient evasion of the host immune system, without exposing the remaining PfEMP1 variants to the immune system (Peters *et al.* 2002, Bachmann *et al.* 2011). The second model proposes that the parasite population released from the liver express all *var* genes and later on, immune pressures force selection of parasites expressing certain PfEMP1 variants with optimal adhesion properties, for which the human host has no pre-existing variant-specific immunity (Wang *et al.* 2009).

Results from this study correlate well with Bachmann *et al* in support of the second model whereby, at the earliest stages of infection in the naïve host, parasites express a broad repertoire of *var* gene variants with no single one being dominantly transcribed (Bachmann *et al.* 2016). This concept supports the early exploration of the suitability of available host sequestration receptors, at a time when specific antibody-mediated immune responses are unlikely to be controlling the first waves of parasite growth. With use of the blood-stage challenge model, my study was able to expand on this analysis, offering a direct comparison between transcript patterns of parasites in the inoculum and parasites recovered from patient samples, to investigate evidence for *var* gene selection *in vivo*. The most highly expressed variant at day of patent infection in the volunteers (following ~5 parasite replication cycles in the blood) was also the most highly expressed in the inoculum used to infect, suggesting that *var* gene selection forces had not been activated in this infection setting. Interestingly, parasites had a mean parasite multiplication rate of 10.0 (range 6.7 – 12.8) consistent with other studies of CHMI, and thus were able to successfully establish infection, and multiply in the human host without selection of

specific *var* gene variants predicted to have a growth advantage and enhanced abilities to sequester and escape splenic clearance (Warimwe *et al.* 2009, Warimwe *et al.* 2012, Abdi *et al.* 2017). Moreover, based on data from historical malaria-therapy studies, it can be speculated that an estimated 50% (likely more) of volunteers in this cohort, if left un-treated, would have gone on to develop symptoms of malaria disease following just a few more cycles of parasite replication in the blood (Glynn *et al.* 1995). Yet, the disease-associated *var* gene variants were not amongst those dominantly expressed in these individuals. This finding therefore challenges some key concepts in the field and raises some questions with regards to the importance of PfEMP1 proteins for the growth and survival of parasites *in vivo*, and their association with disease severity during primary infection.

Having observed diversity in the host immune response to *P. falciparum*, I wanted to investigate the relationship between host and parasite gene expression using parasites isolated from the same cohort of volunteers. Interestingly, *var and rif* gene expression was found to be remarkably uniform across all volunteer samples. Pairwise comparisons between the different host transcriptional groups revealed parasite *var* gene expression to be significantly positively correlated across all. Furthermore, the percentage distribution of *var* genes by *var* gene group was highly consistent irrespective of immune response class. Results suggest that the host immune response is not directed by parasite gene expression, and vice versa; the type of host immune response elicited has little influence of parasite VSA expression early in infection. Instead, it is likely that host genetics and/or environmental factors are the cause of variability in immune responses. In recent years, this has been researched in great depth, offering up some interesting insights into the drivers of immune variation during the host response to pathogen insult (Brodin *et al.* 2015, Chen *et al.* 2016, Nedelec *et al.* 2016, Oosting *et al.* 2016, Schirmer *et al.* 2016, Ter Horst *et al.* 2016).

One of the key pathological features of *P. falciparum* malaria infection is that the mature blood stage parasites (pigmented trophozoites and schizonts) are sequestered in the microvasculature (Miller *et al.* 2002). Therefore, a potential limitation of studies such as these is the restricted access to parasites found in circulation, which may not accurately represent the sequestered population. It is

also important to note that volunteers in this study were infected using the direct blood-stage challenge model of CHMI, which does not rely on vector transmission and thus bypasses the skin and liver infectious stages in the human host. Interestingly, there is evidence to suggest that mosquito transmission modifies parasite virulence by re-setting expression of virulence genes (Spence *et al.* 2013, Bachmann *et al.* 2016). For the rodent malaria parasite *Plasmodium chabaudi,* this has been shown to correlate with altered expression of the *cir* (chabaudi interspersed repeats) multi-gene family. In the study by Spence *et al*, mosquito-transmission resulted in a broader expression of these *cir* genes, and attenuated symptoms of disease when compared to parasites that had been serially blood-passaged (Spence *et al.* 2013), albeit following a much higher number of blood passages than was applied to the inoculum used in this study of CHMI (figure 4.16) (Cheng *et al.* 1997, Payne *et al.* 2016). Although my results appear to correlate well with previous studies of parasite *var* gene expression following mosquito-bite CHMI (Wang *et al.* 2009, Bachmann *et al.* 2016), it will therefore be important to compare results of the two infection models using my method for direct *ex vivo* parasite RNA-seq.

It is also important to consider the potential limitations with use of the RNA-seq protocol for the measurement of parasite *var* gene expression. In the Smart-Seq2 protocol, designed for low input RNA yields (see section 4.4.5), only full-length transcripts are targeted for amplification in the PCR reaction, which may introduce a potential amplification bias towards the genes of shorter length. This may be particularly relevant for the analysis of *var* gene expression levels, as many (specifically, the group-A *var* genes) are larger in size compared to genes of the other subclasses (table 4.1). Importantly, in a recent study of single-cell RNA-seq using *P. falciparum* (trophozoite, schizont and gametocyte stages), Reid *et al* demonstrate the ability to detect the expression of longer length *P. falciparum* genes with use of the same Smart-seq2 protocol (Reid *et al.* 2018). This is thought to be due to internal poly-A priming by the Oligo-dT primer, resulting in the reverse transcription of fragments of long genes; a phenomenon commonly reported with its use (Nam *et al.* 2002). Giving confidence to my dataset was the detection of the group-B/A *var* gene; PF3D7_0632500/ PFF1580c, as one of the longest of the *var*

genes variants (11.9 kb), and one of the most abundantly expressed (top 11) across all in the cohort. Nevertheless, optimisation of the protocol to reduce the number of amplification cycles performed prior to transcript fragmentation may help to limit the potential bias towards smaller length genes, and thus will be considered for future experiment design.

It is important to acknowledge that results presented within this chapter may be at risk of bias due to the small number of parasite samples available for assessment in this study. This is especially relevant when considering the comparison of parasite gene expression between previously stratified volunteer groups, as is discussed in chapter 3. My interpretations of the results presented in this chapter are not intended to be conclusive, but observational.

In summary, parasites isolated at the early stages of infection in the naive host appear to transcribe a broad repertoire of *var* gene variants, with those of the group-B subclass having highest levels of expression. Moreover, *var* gene selection forces do not appear active during the first 5 - 6 replication cycles in the blood. These data contest the popular hypothesis that group-A and or B/A *var* genes actively dominate infection in the naïve host. Furthermore, parasite virulence gene expression does not influence the developing host immune response during primary infection, considering that *var* and *rif* profiles were uniform across volunteers. This highlights a need to better understand the host genetic and environmental factors giving rise to variability in immune responses during *P. falciparum* malaria infection. Importantly, I have shown for the first time that RNA-sequencing can be successfully applied for *ex vivo* analysis of *P. falciparum* gene expression during CHMI. In this study however, analysis was restricted to parasites recovered at day of patent infection (peak parasitaemia), following direct blood-stage inoculation. These data would be complimented by a study conducive to the assessment of parasite gene expression at earlier time-points in infection, as well as a comparison of parasite VSA expression following vector transmission. As a next step, my protocol for *ex vivo* parasite RNA-seq will therefore need to be optimised for use with the much lower parasite densities predicted at the onset of blood-stage infection following mosquito bite CHMI, which may prove more challenging.

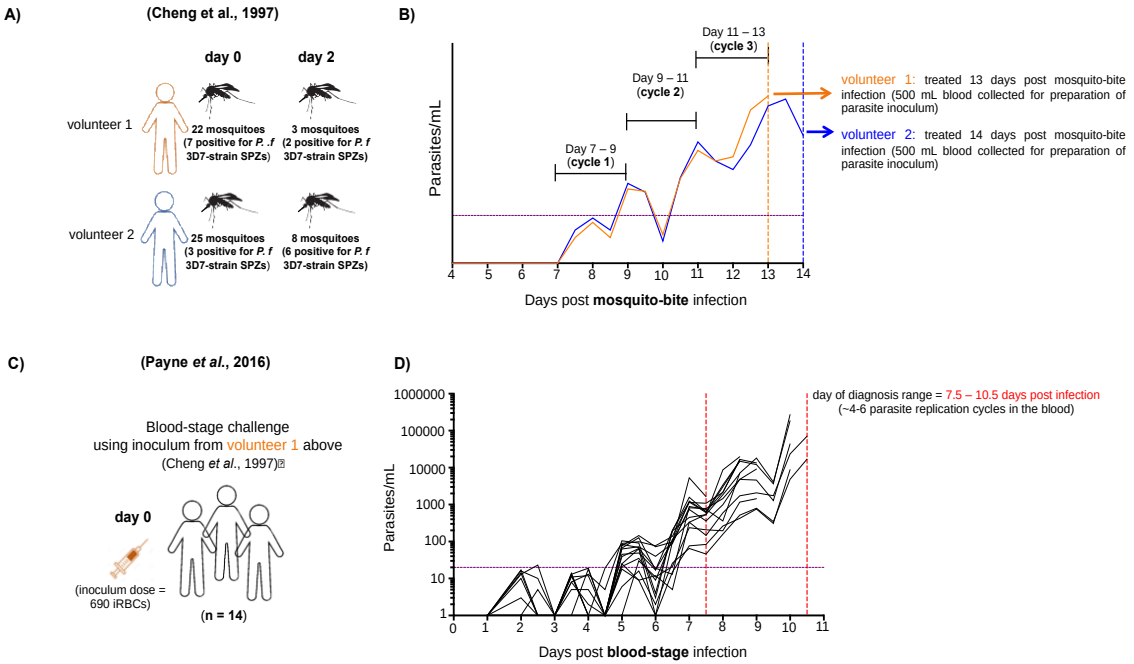

Figure 4.16 | History of the parasite inoculum used for blood-stage CHMI. A) Laboratory-reared *Anopheles stephensi* mosquitoes infected with *P. falciparum* clone 3D7A were used to infect 2 volunteers at the Queensland institute of Medical research (QIMR) (Cheng *et al*., 1997). On day 0, volunteer 1 (orange) was exposed to the bites of 22 mosquitoes (7 of which were found positive for *P. f* 3D7 sporozoites (SPZs)), and two days later was exposed to the bites of another 3 mosquitoes (2 of which were found positive for *P. f* 3D7 SPZs). On day 0, volunteer 2 (blue) was exposed to the bites of 25 mosquitoes (3 of which were found positive for *P. f* 3D7 sporozoites (SPZs)), and two days later was exposed to the bites of another 8 mosquitoes (6 of which were found positive for *P. f* 3D7 SPZs). From day 4 following mosquito-bite infection, parasite densities were monitored by both PCR and microscopy in the two volunteers. **B)** Schematic showing the course of parasite growth in the two volunteers. Parasites could be detected in the blood from ~ 7 days post mosquito-bite (after egress from the liver), and continued to grow for ~ 3-4 cycles of replication in the circulation, until treatment was administered at 13 days post infection (volunteer 1), and at 14 days post infection (volunteer 2). Before the administration of drug treatment, a unit of blood (500 mL) was collected from each volunteer for preparation of the blood-stage inoculum to be used in subsequent blood-stage CHMI trials. **C)** Schematic diagram to indicate use of blood-stage inoculum (prepared from blood of volunteer 1 in Cheng *at al*., 1997), in my study (Payne et al., 2016). 14 malaria-naïve volunteers were infected upon injection with ~690 parasitised erythrocytes (iRBCs) and parasite density was monitored by qPCR at twice-daily time-points, until diagnosis and administration of drug treatment. **D)** Graph displays the number of parasites/mL of blood as measured by qPCR (y-axis), through time (x-axis) for each of the 14 volunteers. Day of diagnosis ranged 7.5 – 10.5 days post infection (after ~4-6 parasite replication cycles in the blood). Dashed vertical lines denote day of diagnosis (or range of diagnosis). Dashed horizontal line indicates the lower limit of detection by qPCR (20 p/mL).

Chapter 5: Optimising a Protocol for *ex vivo* Parasite RNA-seq during mosquito-bite CHMI

5 Optimising a Protocol for *ex vivo* Parasite RNA-seq during mosquito-bite CHMI

5.1 Abstract

The expression of parasite *var* genes is thought to be influenced by the developing host immune response, yet current knowledge of *var* gene switching parameters is limited to studies based on *in vitro* cultured parasites in the absence of immune pressure. Moreover, despite clear associations between group-A, B/A PfEMP1s and severe disease, *var* gene expression has not yet been assessed at the very onset of infection, which limits our understanding of their influence on host clinical outcome. Having previously demonstrated the successful application of *ex vivo* parasite RNA-seq in a blood-stage model of controlled human malaria infection, I wanted to extend my analysis of *var* gene expression to the blood stages following immediate egress from the liver. Herein, optimisation was performed on various steps of the RNA-seq protocol with the aim to recover sufficient *P. falciparum* ring-stages at the onset, and at subsequent time points following mosquito-transmission in the naïve host. At days 9 and 10 post-infection (~cycle 2 in the blood), a good number of *P. falciparum* genes could be detected in parasites isolated from 5 volunteers. However, the detection of VSA genes was markedly reduced when compared to parasites isolated on day 11 post-challenge. Hence, low parasite densities and host contamination restrict the application of this protocol, precluding the assessment of *var* gene expression at these early time-points. Profiling of *var* genes on day 11 post mosquito-bite challenge (~cycle 3 in the blood) revealed broad level detection of variants, this time inclusive of the group-A subclass. Interestingly, *var* gene expression patterns were more variable across volunteers, compared to observations from the previous blood-stage challenge. Results suggest that diversity in *var* gene expression may be dictated by events occurring in either the mosquito vector or liver stages, before entering the blood-phase. However, it will be important to assess *var* gene expression in the first blood cycle, using a more appropriate method for parasite isolation and/or gene expression analysis to validate this hypothesis.

5.2 Introduction

The mutually exclusive switching between *var* gene variants affords the *P. falciparum* parasite an immune evasion strategy, and a means to exploit different host tissues (Roberts *et al.* 1992, Smith *et al.* 1995). In non-immune individuals, this parasite survival strategy can have fatal consequences by leading to the obstruction of blood flow, and contributing to impaired perfusion in vital host organs (Dondorp *et al.* 2000, Dondorp *et al.* 2008, Warimwe *et al.* 2009, Hanson *et al.* 2012, Warimwe *et al.* 2013). Although a restricted subset of group-A, B/A PfEMP1 variants has been associated with severe clinical outcomes (Jensen *et al.* 2004, Bull *et al.* 2005, Kaestli *et al.* 2006, Rottmann *et al.* 2006, Warimwe *et al.* 2009), little is known about *var* gene expression at the onset of infection and our current understanding of *var* gene switching parameters is largely restricted to studies based on *in vitro* cultured parasites (Kyes *et al.* 2003, Horrocks *et al.* 2004, Horrocks *et al.* 2004, Peters *et al.* 2007, Recker *et al.* 2011, Zhang *et al.* 2011, Noble *et al.* 2013). In this setting, it has been speculated that rates at which *var* genes become activated and deactivated is non-random, and is dependent on chromosomal position. For instance, genes occupying subtelomeric loci (group-A and B types) tended to switch off faster than those positioned more centrally in the chromosome (Frank *et al.* 2007). This concept is supported by the more recent findings of Noble *et al*, who, with use of a diverse set of clonal parasite cultures, revealed a global hierarchy in *var* gene activation, favouring those in central chromosomal locations (Noble *et al.* 2013). However, most studies of this nature have been limited due to restrictions in the number of variants considered, as well as time points at which gene transcription levels were measured. Moreover, the diversity and order of PfEMP1 variants in the human host is thought to be influenced by the developing immune response (Kyriacou *et al.* 2006), which is something that cannot be assessed in these experiments.

In the previous chapter, I demonstrated the application of *ex vivo* parasite RNA-seq during a study of blood-stage CHMI, for the assessment of *var, rif* and *stevor* expression in the naïve host. RNA-sequencing at day of patent infection (positive thick film microscopy) revealed broad level detection of *var* gene variants, with the group-B subclass demonstrating highest levels of expression. Moreover, parasites recovered after ~5 - 6 replication cycles in the blood had similar expression profiles to that of parasites isolated from the inoculum used to infect. This suggested that *var* gene selection forces were not yet activate in this infection setting. These two observations

contradict the hypothesis that group-A and/or B/A PfEMP1s are actively selected during the blood-phase of infection in the malaria-naïve host. However, the blood-stage challenge model is not conducive to the assessment of *var* gene expression immediately following liver egress. Thus, it was important to extend my analysis to earlier stages of infection, and to compare patterns of parasite gene expression following direct blood challenge, to those observed following vector transmission.

In continued collaboration with Professor Adrian Hill and Dr Simon Draper at the Jenner institute in Oxford, I was granted access to blood samples from 5 (unvaccinated control) volunteers undergoing mosquito-bite CHMI at the CCVTM, in January 2017 (*Clinical/ Trails.gov i.d: NCT02905019*). Sampling for my sub-study was designed to allow for the assessment of parasite *var* gene expression from C +7 (predicted onset of blood-phase infection), and at subsequent daily time points until the termination of volunteer infections (at first microscopic detection). Based on data from previous mosquito-bite trials carried at the CCVTM (Roestenberg *et al.* 2012), parasite densities were predicted to be extremely low, particularly during the first and second replication cycles in blood; ~40 – 50 p/mL and 400 – 500 p/mL, respectively (table 5.1). This highlights the major limitation of the CHMI model for the analysis of parasite gene expression, as has been previously discussed (Peters *et al.* 2002, Lavstsen *et al.* 2005, Wang *et al.* 2009, Bachmann *et al.* 2016). For RNA-sequencing of parasites that have been isolated from whole human blood, it is also important to consider the potential host contaminants, which may act to dwarf the valuable sequencing information coming from the parasite. Thus, in order to ensure maximal recovery and purity of *P. falciparum* rings stages in this study, it was important to optimise the protocol used for parasite isolation and *ex vivo* RNA-seq.

Table 5.1 | Comparison of parasitological data from CHMI trials (table modified from Roestenberg *et al.*, 2012)

Trial centre	RUNMC I	RUNMC II	CCVTM, Oxford	USMMVP
Number of volunteers	20	43	65	47
Methodology				
Mosquito *P.f* strain	NF54	NF54	3D7	NF54
Number of infected mosquitoes	4-7	5	5	5
Exposure time to mosquitoes (min)	10	10	5	5
Parasitological data				
Mean peak parasitemia (p/mL)	7,076	15,901	9,055	-
Mean parasite denisty first cycle (p/mL)	567	456	48	-
Mean Parasite Multiplication Rate (PMR)	11.8	11.1	11.6	-

RUNMC I = Radbound University Nijmegen Medical Centre, cohort I
RUNMC II = Radbound University Nijmegen Medical Centre, cohort 2
CCVTM = Centre for Clinical Vaccinology and Clinical Medicine (University of Oxford)
USMMVP = U.S Military Malaria Vaccine Program

5.3 Chapter aims

This chapter provides details of the work carried out to optimise the protocol used for *ex vivo* parasite RNA-seq, and demonstrates its application to the mosquito-bite challenge model for assessment of parasite VSA expression early in the naïve host.

Specific aims

1. To improve the recovery and purity of *P. falciparum* ring-stages from whole human blood, using numbers representative of those predicted immediately following liver egress after mosquito-bite challenge.
2. To determine how early in infection (and thus the lower limit of parasites/mL) this protocol can be successfully applied.
3. To investigate parasite *var* and *rif* gene expression early following mosquito-transmission in the naïve human host.

5.4 Methods

The optimisation of *ex vivo* parasite RNA-seq required readily available samples of *in vitro* cultured *P. falciparum* (3D7-strain). Provided below are details of the *in vitro P. falciparum* culture. A description of the methods used for each optimisation step is provided in the relevant sections that follow.

5.4.1 *P. falciparum* culture

All work with *P. falciparum* was carried out in a biosafety level 3 laboratory and where possible, in a Class II biological safety cabinet under sterile conditions. All materials and reagents used for culturing were sterile and the solutions warmed to 37°C for use.

5.4.1.1 List of Materials

Reagent	Supplier	Catalog Number
Absolute Methanol	Fisher Scientific	10516279
AlbuMAX® II Lipid-Rich BSA	Termo Fisher Scientific	11021
D-sorbitol	Sigma-Aldrich	S-3889
Gentamicin Sulfate	Lonza	17-518Z
Giemsa	TCS Biosciences	HS295
Glucose	Scientific Laboratory Supplies	CHE1806
Glycerol	Thermo Fisher Scientific	4392215
HEPES	Lonza	17-737F
Human Serum	Scottish National Blood Transfusion Service	-
L-glutamine	Thermo Fisher Scientific	25030
NaOH	Fisher Scientific	10675692
O^+ erythrocytes	Scottish National Blood Transfusion Service	-
PBS tablets	Merk	109468
Roswell Park Memorial (RPMI) 1640 medium	Lonza	BE12-167F
Leucoflex LXT filters	Macopharma	-

Incomplete RPMI medium

RPMI 1640 medium
25 mM Hepes
20 mM glucose
2 mM L-glutamine
25 µg/mL gentamicin

Complete RPMI medium

RPMI 1640 medium
25 mM Hepes
20 mM glucose
2 mM L-glutamine
25 µg/mL gentamicin
0.25% AlbuMAX® II
5% pooled human serum

Freezing medium (glycerolyte)

57% glycerol
0.14 M sodium lactate
4 mM potassium chloride
24 mM sodium phosphate

Synchronising medium

5% D-sorbitol
dH_2O

5.4.1.2 General

P. falciparum (3D7A) parasites were cultured in O^+ erythrocytes (Scottish National Blood Transfusion Service) in RPMI 1640 media (Lonza), adjusted to pH 7.2 – 7.3 using 1M NaOH (Fisher Scientific), and supplemented with 25 mM Hepes (Lonza), 20 mM glucose (Scientific Laboratory Supplies), 2 mM L-glutamine (Thermo Fisher Scientific), 25 µg/mL gentamicin sulfate (Lonza), 0.25% AlbuMAX® II Lipid-Rich BSA (Thermo Fisher Scientific) and 5% pooled human serum (Scottish National Blood Transfusion Service), comprising “Complete RPMI medium”. Cultures were incubated

at 37ºC in 1% O_2, 3% CO_2 and 96% N gas (BOC gases). On a daily basis (or every two days in some cases), smears were made from ~250 ul of culture and stained with Giemsa (TCS Biosciences) for assessment of parasitaemia. Parasites were diluted in O^+ erythrocytes when necessary, to allow for reinvasion and for maintenance of desired parasitaemia.

5.4.1.3 Giemsa staining for determination of parasitaemia

250 µl volumes of parasite culture were centrifuged at 8,500g for ~7 seconds, and pellets reconstituted in approximately 30 µl of the supernatant to achieve a 30 - 50% haematocrit for smearing. 10 µl volumes of resuspension were smeared at an angle of about 45º on clean glass slides. Smears were air dried, fixed with absolute methanol (Fisher Scientific) and air-dried again, before flooding with filtered 10% v/v Giemsa in Giemsa buffer made up of PBS pH 7.2 (Merck). Stain was left for 15 - 25 minutes before being washed off with water, and air-dried. The smears were viewed under oil with the 100X objective on a light microscope (Leica Microsystems, Leica DM1000). Parasitaemia was determined by counting the number of infected erythrocytes (IEs) and uninfected erythrocytes per field, until a minimum of 500 cells had been counted in at least 3 different fields.

5.4.1.4 Washing of erythrocytes for culture

Blood used for parasite cultures was obtained weekly, from donors at the Scottish National blood Transfusion Service. In preparation for use, whole blood was first filtered of leucocytes by passing through a Leucoflex LXT filter (Macopharma). Recovered erythrocytes were then centrifuged 2,400g for 15 minutes, and pelleted cells washed x2 at 20 - 30% haematocrit in “incomplete RMPI medium” at 2,400g for 15 minutes. Erythrocytes were resuspended at a final haematocrit of 50% in “incomplete RPMI medium”, and stored at 4ºC for a maximum of 1 week.

5.4.1.5 Synchronising parasites with Sorbitol

For experiments requiring synchronous ring-stage merozoites only (representative of the stages found in human circulation), the more mature parasite forms (> 20 hours post-invasions) were lysed using 5% sorbitol in dH_2O. Cultures to be treated were centrifuged at 800g for 4 minutes, the supernatant removed and pelleted cells

resuspended in 7 mL 5% sorbitol. Cells were then incubated at 37ºC for 15 minutes. Suspensions were centrifuged at 800g for removal of supernatant, and then washed twice in 13 mL “incomplete RPMI”. Final suspensions were at 2% haematocrit in “complete RPMI medium”, for returning to culture prior to use in experiments. After every sorbitol treatment, an aliquot of culture was used to make a smear for confirmation of lysis of the mature-stage IEs.

5.4.1.6 Cryopreservation of IEs

Cultures were centrifuged at 800g for 4 minutes, and supernatant removed prior to the gradual addition of glyercerolyte (57% glycerol, 0.14 M sodium lactate, 4 mM potassium chloride, 24 mM sodium phosphate at pH 6.8) as follows: Glycerolyte, 0.33 times the packed cell volume (pcv) of the pellet, was added to the cells slowly and drop-wise, with constant agitation to ensure uniform mixing. The suspension was then left to stand for 5 minutes before addition of the next volume of glycerolyte; 1.33 times the pcv this time, added as before. The suspension was aliquoted into cryovials and stored at -70ºC for 24 hours before transferring to liquid nitrogen for longer-term storage.

5.4.1.7 Thawing of IEs

Cryopreserved IEs (1 mL aliquots) were thawed at 37ºC and transferred to 50 mL falcon tubes before addition of 200 µl 12% NaCl, slowly and drop-wise. With each drop, tubes were agitated to ensure uniform mixing of suspension. After 5 minutes rest, a 10 mL volume of 1.8% NaCl was added, slowly and drop-wise as above, followed by a 10 mL volume of 0.9% NaCl/0.2% glucose. Suspensions were centrifuged at 800g for 4 minutes, and the pelleted cells washed in 20 mL “incomplete RPMI medium”. Cells were resuspended at 2% haematocrit in “complete RPMI medium” for culture, and an aliquot taken to make a smear for determination of parasitaemia. Cultures were then gassed with a mixture of 1% O_2, 3% CO_2 and 96% N, and incubated at 37ºC.

5.5 Protocol Optimisation

5.5.1 List of materials

Reagent	Supplier	Catalog Number
Leucoflex LXT filters	Macopharma	-
0.5 mL DNA LoBind Eppendorf® tubes	Eppendorf	22431005
1.5 mL DNA LoBind Eppendorf® tubes	Eppendorf	22431021
1x PBS	Gibco	20012-019
250 mL centrifuge bottles	Corning Life Sciences	CLS 431842
anti-human CD45-FITC (HI30)	eBioscience	11-0459-42
EDTA	Invitrogen	AM9260G
FCS	Gibco	16080-044
Multispot slides	Hendley-Essex	PH001
Saponin	Sigma-Aldrich	8047-15-2
Zymo-Spin RNA Clean and Concentrator™ -5 kit	Zymo Research	R1016
Globin-Zero® Gold kit	Epicentre (Illumina)	GZG1224
RNA 6000 Pico Chip Bioanalyzer Kit	Agilent	5067-1513
Ultrapure DEPC H_20	Thermo Fisher Scientific	750024
0.2 mL Eppendorf® PCR strip tubes	Eppendorf	951010022
Agencourt Ampure XP beads	Beckman Coulter	A63881
Betaine (BioUltra >99.0 %)	Sigma-Aldrich	61962
DEPC H_2O	Thermo Fisher Scientific	750024
dNTP mix (10 mM)	Fermentas	R0192
DynaMag™-2 Magnet	Thermo Fisher Scientific	12321D
High Sensitivity DNA Bioanalyzer kit	Agilent	5067-4626
ISPCR primer (10 uM) (5′-AAGCAGTGGTATCAACGCAGAGT-3′)	Biomers.net	-
KAPA HiFi HotStart ReadyMix (2× KAPA)	Biosystems	KK2601
LNA-modified TSO (5′-AAGCAGTGGTATCAACGCAGAGTACATrGrG+G-3′)	www.exiqon.com	-
MgCl2	Ambion (Life technologies)	AM9530G
Oligo-dT30VN (5′–AAGCAGTGGTATCAACGCAGAGTACT30VN-3′)	biomers.net	-
Qbit™ ds DNA high sensitivity assay kit	Thermo Fisher Scientific	Q32851
Recombinant RNase inhibitor	Clontech	2313A
Superscript II reverse transcriptase kit*	Thermo Fisher Scientific	18064-014
UltraPure Ethanol	Sigma-Aldrich	51976

5.5.2 Isolation of parasites from whole human blood

One of the major concerns with direct *ex vivo* parasite RNA-seq is contamination with host material. The constituents of human peripheral blood include 93 - 96% erythrocytes (3,800 – 6,200 x10^6/mL), 4 - 7% platelets (140 – 450 x10^6/mL) and 0.1-0.2% leucocytes (4.1 – 10.9 x10^6/mL). In the first and second blood cycles following mosquito-bite challenge, parasitaemias are predicted to be as low as 40 p/mL and 400 p/mL, respectively (Roestenberg *et al.* 2012). Therefore, to maximise the likelihood that a sufficient number of sequenced reads would map to the *P. falciparum* genome without being dwarfed by those mapping to the human genome, parasite samples needed to be purified. Mature erythrocytes, although anucleated, contain large quantities of polyadenylated globin, which is a contaminating factor for down-stream RNA-seq. Furthermore, these cells make up 93 - 96% of whole blood. Thus, a crucial step during the purification process was to remove red cells, along with leucocytes, from final parasite preparations.

5.5.2.1 Leucodepletion

Leucocyte depletion was to be performed as per the previous blood-stage CHMI trial (chapter 4, section 4.4.2.1), using Leucoflex LXT filters (Macopharma). These filters are designed for use in blood-transfusion services and thus were predicted to be highly efficient for the removal of leucocytes from whole blood. In order to test their efficiency before application in the mosquito-bite CHMI, an experiment was set up to quantify the percentage of leucocytes in blood samples post-filtration, using CD45 as a marker for white blood cells. For each experiment run, a 10 µl sample of fresh whole blood (predicted to contain ~$4.0x10^7$ RBCs and ~$4.0x10^4$ leucocytes) served as the "pre-filtration" positive control, and a duplicate sample of unstained blood served as the negative control. Filter efficiency was tested using 20 mL volumes of whole blood (representative of the volume to be collected from volunteers in the trial) and then staining 3x 10 µl (replicate samples) of filter flow-though. Staining was performed using 5 µl (0.25 µg/test) of anti-human CD45-FITC (eBioscience), in a 100 µl volume of FACs buffer (PBS with 2% FCS and 5mM EDTA), for 20 minutes whilst protected from light. After staining, cells were washed x3 with 1 mL FACs buffer and then acquired using the BD™ LSR-II and FACSDiva™ software. For each experiment run, $3x10^6$ events were acquired.

Figure 5.1 displays the gating strategy used for calculating the percentage of CD45+ leucocytes in the pre- and post-filtered samples of blood in representative experiment 1 of 5. In the positive control stain (unfiltered blood), percentage CD45+ cells were within the expected range for the population of leucocytes in whole human blood (0.1 – 0.2%). Gating on the CD45+ population in the post-filtered samples consistently revealed percentage levels below that of the negative unstained control, confirming the highly efficient depletion of leucocytes with use of these filters. Table 5.2 displays the percentage of CD45+ cells calculated pre- and post-filtration for each replicate, in each of the 5 independent experiment runs.

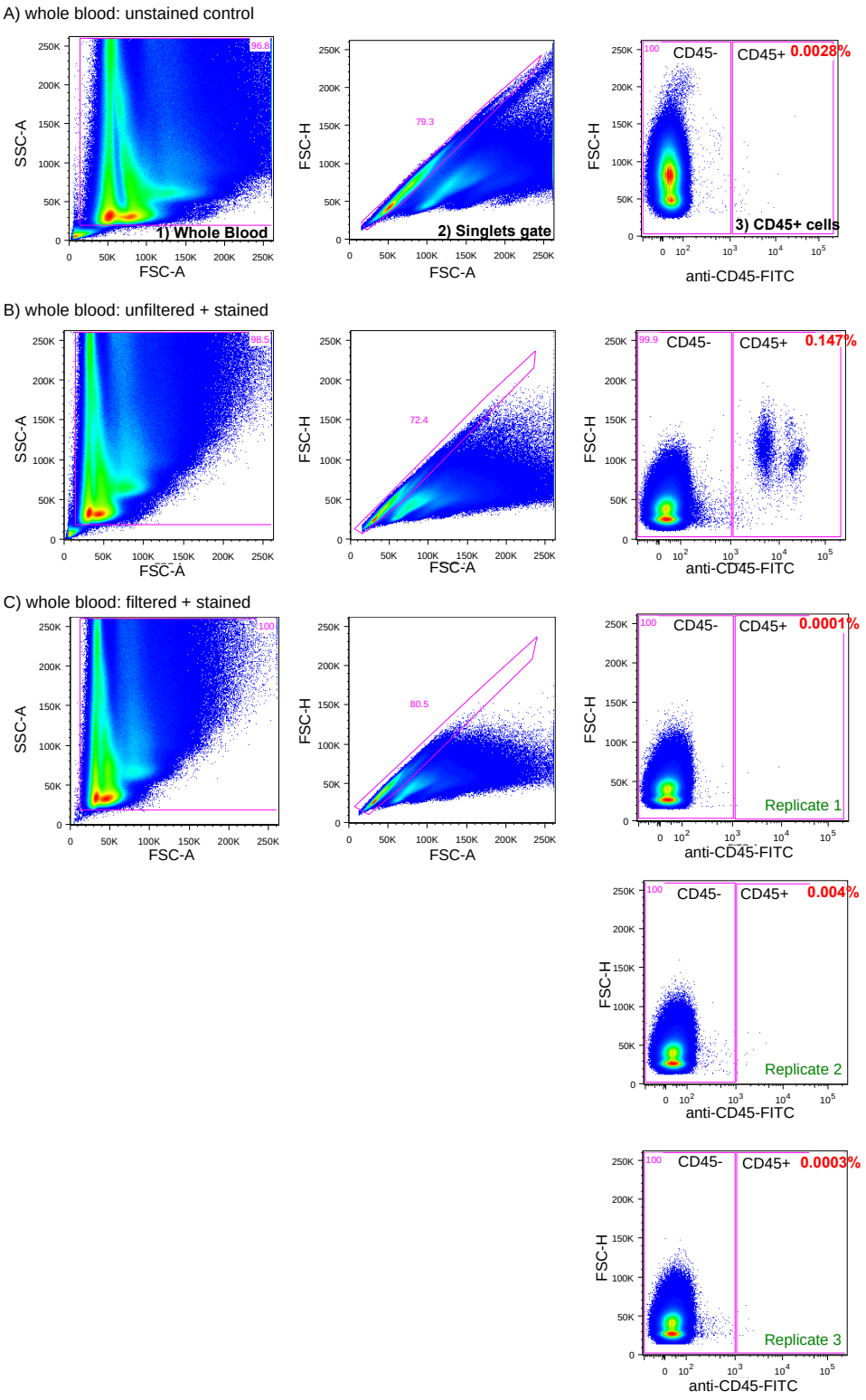

Figure 5.1 | Gating strategy used for the assessment of CD45+ cells in samples of whole-blood. The percentage (%) of CD45+ leucocytes was assessed in samples of whole blood pre- **(B)** and post- **(C)** filtration following staining with anti-CD45-FITC. Unstained blood served as the negative control **(A).** 1) Psuedo-colour plots showing FSC-A on the x-axis vs SSC-A on the y-axis, for gating on whole-blood cell populations (erythrocytes, platelets and leucocytes). 2) Plots showing FSC-A on the x-axis vs FSC-H on the y-axis for gating on single cells (singlets) and exclusion of doublets. 3) anti-CD4-FITC vs FSC-H for distinction of CD45- and CD45+ cell populations following each condition tested (% CD45+ cells are shown in red).

Table 5.2 | Percentage of CD45+ cells pre- and post-filtration of whole blood

	Percentage CD45+ cells					
			post-filtration			
	unstained control	pre-filtration	replicate 1	replicate 2	replicate 3	mean of replicates
Experiment 1	0.0028	0.147	0.0001	0.0040	0.0003	0.0015
Experiment 2	0.0045	0.210	0.0001	0.0004	0.0050	0.0018
Experiment 3	0.0017	0.156	0.0020	0.0020	0.0008	0.0016
Experiment 4	0.0024	0.188	0.0030	0.0006	0.0003	0.0013
Experiment 5	0.0038	0.102	0.0009	0.003	0.0001	0.0013

5.5.2.2 Red cell lysis and recovery of ring-stage parasites

Saponin works to lyse red blood cells by making the lipid bilayer permeable to macromolecules. During this process, the *Plasmodium* parasite is left intact with its parasite membrane and parasitophorous vacuole (Cordery *et al.* 2007, Kyes *et al.* 2007, Lemieux *et al.* 2013). 0.015% saponin in PBS was shown to successfully lyse red cells following isolation from the human host in the previous trial, however this protocol step had not been optimised and there was a concern that using too high a concentration may result in the unnecessary loss of ring-stage parasites. Given the extremely low parasitaemias predicted at the early stages following mosquito-bite challenge, it was thus important to establish the concentration at which optimal recovery of ring-stage parasites would be achieved, without compromising the efficiency of red cell lysis.

So as to represent the *P. falciparum* stages present in the circulation of the human host, all experiments were performed using *in vitro* (3D7-strain) cultured parasites that had been synchronised at the ring stage (see section 5.1.3.4). Percentage parasitaemia was determined on the morning of each experiment (see section 5.1.3.2) and the number of RBCs/mL counted by haemocytometer. Samples were prepared by centrifugation of culture at 800g for 4 minutes, to pellet the red cells. The volume of packed red cells (typically ~300 – 500 µl) was then split equally between the number of tubes/concentrations to be tested to ensure each sample contained the same starting number of ring-stage parasites. Red cell lysis was performed by incubation with saponin (Sigma-Aldrich) at 0.0015%, 0.0025%, 0.00375% 0.005%, 0.0075%, 0.01%, 0.015% or 0.03%, using a ratio of 1:9 (packed red cells: saponin), for 10 minutes on ice. After incubation, samples were centrifuged at 12,000g for 5 minutes at 4^{o}C and then washed x2 in 1 mL PBS. 2 µl of each pellet was then diluted 1:2 in human serum

(Scottish National Blood Transfusion Service) for addition to a well of a multispot slide (Hendley-Essex) for fixing with methanol and staining with 10% Giemsa for 1 hour. Slide preparations were viewed under oil with the 100x objective on a light microscope (Leica Microsystems, Leica DM1000) and the ratio of ring-stage parasites: RBCs were counted in 40 random fields.

In an initial experiment, saponin concentrations of 0.0015%, 0.0025% and 0.00375% were found to insufficiently lyse red cells. When incubation times were extended to 1 hour, no visual indication of red cell lysis was observed and thus these concentrations were excluded from further analysis. Table 5.3 displays the counts for the samples of ring-stage parasites and RBCs following saponin lysis at 0.03%, 0.015%, 0.01%, 0.0075% and 0.005% saponin in PBS. Results suggested an inverse correlation between increasing concentrations of saponin and the number of RBCs in the parasite prep, as expected. However, with increasing concentrations of saponin, a decreased number of ring-stage parasites was also observed (0.0075% mean = 4,079; 0.01% mean = 3,804; 0.015% mean = 2,599; and 0.03% = 2,487). Although these differences are minimal, the trend was consistent across all independent experiments suggesting that ring-stage parasites may be sensitive to subtle differences in the saponin concentration used for red cell lysis. At the lowest concentration of 0.005%, the ratio of rings:RBCs was estimated at 6:1. Compared to the (93:1) ratio that was observed with the 0.015% concentration used in the first trial, this was considered too high a drop in red cell lysis efficiency. The difference in ring counts between 0.015% and 0.0075% concentrations (1.6-fold) suggested that this 2-fold dilution would give optimal recovery of rings, while maintaining an acceptable efficiency of red cell lysis for use in the mosquito-bite CHMI. When tested on 20 mL volumes of leucodepleted blood (representative of the volume to be collected during the mosquito-bite CHMI), 0.0075% saponin worked to successfully lyse the ~8 mL volume of packed red cells (40% haematocrit in whole human blood). Figure 5.2 shows representative images of smears made following red cell lysis with 0.015%, 0.01% and 0.0075% saponin.

Table 5.3 | Ring-stage parasites and RBC counts following Saponin lysis

	ring-stage parasite/ RBC counts (in 40 fields)									
	0.03% saponin		0.015% saponin		0.01% saponin		0.0075% saponin		0.005% saponin	
	rings / RBC count	rings/RBC ratio	rings / RBC count	rings/RBC ratio	rings / RBC count	rings/RBC ratio	rings / RBC count	rings/RBC ratio	rings / RBC count	rings/RBC ratio
Experiment 1	2988 / 10	299:1	3209 / 56	50:1	N/A	N/A	4862 / 210	23:1	4917 / 434	11:1
Experiment 2	1986 / 7	284:1	2354 / 38	62:1	N/A	N/A	3361 / 143	24:1	3478 / 580	6:1
Experiment 3	N/A	N/A	2594 / 18	144:1	5243 / 224	23:1	4260 / 260	16:1	N/A	N/A
Experiment 4	N/A	N/A	2651 / 9	295:1	3215 / 76	42:1	4288 / 81	53:1	N/A	N/A
Experiment 5	N/A	N/A	2187 / 20	109:1	2954 / 34	75:1	3628 / 52	70:1	3120 /1040	3:1
mean	**2487 / 9**	**276:1**	**2599 / 28**	**93:1**	**3804 / 111**	**34:1**	**4079 / 149**	**27:1**	**3838 / 685**	**6:1**

N/A = Not assessed
RBC = Red Blood Cell

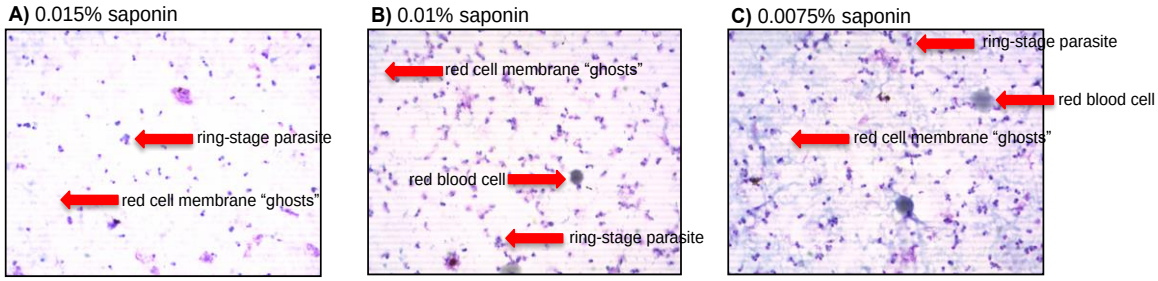

Figure 5.2 | Quantifying *P. falciparum* (3D7) ring-stage recovery following saponin-lysis of RBCs. Giemsa-stained smears of *in vitro* parasite preparations following red blood cell lysis with saponin at 0.015% **(A)**, 0.01% **(B)** and 0.0075% **(C).** Images represent one field of view, taken under 100x objective (LEICA DM LB2 microscope and Yencam HD camera (Yenway microscopes)). *P. falciparum* (3D7) ring-stage parasites, red blood cells and red cell membrane "ghosts" are indicated.

Following red cell lysis, samples were to be centrifuged to pellet the parasite ring stages and dispose of the supernatant. In the previous trial, centrifugation was performed at 15,000g, for 10 minutes (see chapter 4, section 4.4.2.2). However, in an experiment set up to optimise centrifugation speed and duration, some parasite ring-stages were found present in the supernatant using these settings. This centrifugation step was therefore adjusted to 18,000g, for 20 minutes to ensure optimal recovery of parasites during the mosquito-bite CHMI. Furthermore, an additional step was included to wash parasite pellets of any free globin that may have resulted following the lysis of red cells, as described below.

Washing of parasite pellets

Samples were centrifuged at 16,000g for 5 minutes and then, to ensure maximal recovery of isolated parasites, the supernatants from each tube were collected into fresh 1.5 mL Eppendorfs labelled "S1", and pellets stored on ice. "S1" tubes were centrifuged at 16,000g for 5 minutes to pellet any residual parasite material, and as before, supernatants from "S1" tubes were then transferred into fresh 1.5 mL Eppendorfs, labelled "S2". "S2" supernatants were centrifuged, and the supernatant

transferred into tubes labelled “S3” for a final spin at 16,000g for 5 minutes. The recovered parasite pellets from each supernatant spin were then pooled back into the tube containing the original parasite pellet by resuspending in 1 mL cold PBS. Pellets were then washed x3 by centrifugation at 16,000g for 5 minutes, again collecting the supernatants from each pellet wash (to be centrifuged at the end, before pooling together with the original). Washed pellets were resuspended in 1 mL TRIzol™ reagent, then mixed by pipetting before incubation at 37^{o}C for 5 minutes. Pellets were snap-frozen on dry-ice and transferred to -70^{o}C for storage until RNA extraction.

5.5.3 RNA extraction and quantification

RNA extraction was to be performed, with inclusion of globin and rRNA-removal, as had been optimised for the previous trial (see chapter 4, section 4.4.3). However, at such low levels of RNA out-put (picogram quantities), it becomes difficult to accurately quantify samples. This can be an issue for the downstream application of the Smart-seq2 protocol, specifically, for directing the number of PCR amplification cycles to be performed following first strand cDNA synthesis. For the previous trial, quantification of RNA (after globin and rRNA removal) relied on the use the Agilent Bioanalyzer and RNA 6000 Pico Chip assay (quantification range 50 - 5,000 pg/µl). As is shown in chapter 4, figure 4.1 (part B), a proportion of the estimated concentration was being attributed to the presence of small RNAs (< 200 nt), which was likely to have caused an over-estimation in the measurement coming from the larger (> 200 nt) message (mRNA) of interest. For this reason, it was decided that exclusion of small RNAs would be necessary for more accurate quantification and more efficient amplification in downstream steps.

The exclusion of small RNAs (< 200 nt) was to be performed using the ZymoSpin RNA Clean and Concentrator Kit™- 5 (Zymo Research), as per manufacturer’s guidelines. Before application to the trial samples, the protocol was first optimised using RNA that had been extracted from mock samples containing (~1x10^{7}) *in vitro* (3D7-strain) ring-stage parasites, lysed of RBCs. After the removal of globin mRNA and rRNA (see chapter 4, section 4.4.3), samples were resuspended in a volume of 50 µl DEPC H_2O (Thermo Fisher scientific), for immediate mixing with 100 µl of “RNA binding buffer” (50 µl ethanol + 50 µl buffer). Samples were transferred to a zymo spin column with

collection tube and centrifuged at 12,000g for 30 seconds, at 4ºC. At this stage, flow through (containing small RNAs < 200 nt) was kept aside for assessment of kit efficiency. 400 µl of "RNA prep buffer" was then added to the column (containing RNAs > 200 nt), centrifuged at 12,000g, at 4 ºC for 30 seconds, and flow-through discarded. RNA was then washed x2 in 700 µl, then 400 µl "RNA wash buffer" before transferal to a fresh 1.5 mL eppendorf tube. 10 µl of DEPC H_2O was then added to the column matrix, which was centrifuged for 30 seconds at 4ºC for elution of RNA. Samples were run on the Agilent bioanalyzer RNA 6000 Pico Chip assay to ensure efficient depletion of RNAs < 200 nt.

Samples treated with the ZymoSpin RNA Clean and Concentrator kit™-5 demonstrated a partial reduction in the presence small RNAs (representative Figure 5.3). By comparing the same samples before and after exclusion, results across 3 independent experiments suggested that the small RNA fraction (miRNA and 5s rRNA <200 nt) contributes to ~80% of the ribosomal-depleted RNA concentration (table 5.4). Thus, although the kit did not remove 100% of the small RNA fraction, this step was considered important to include in order to accurately quantify samples for downstream Smart-seq2.

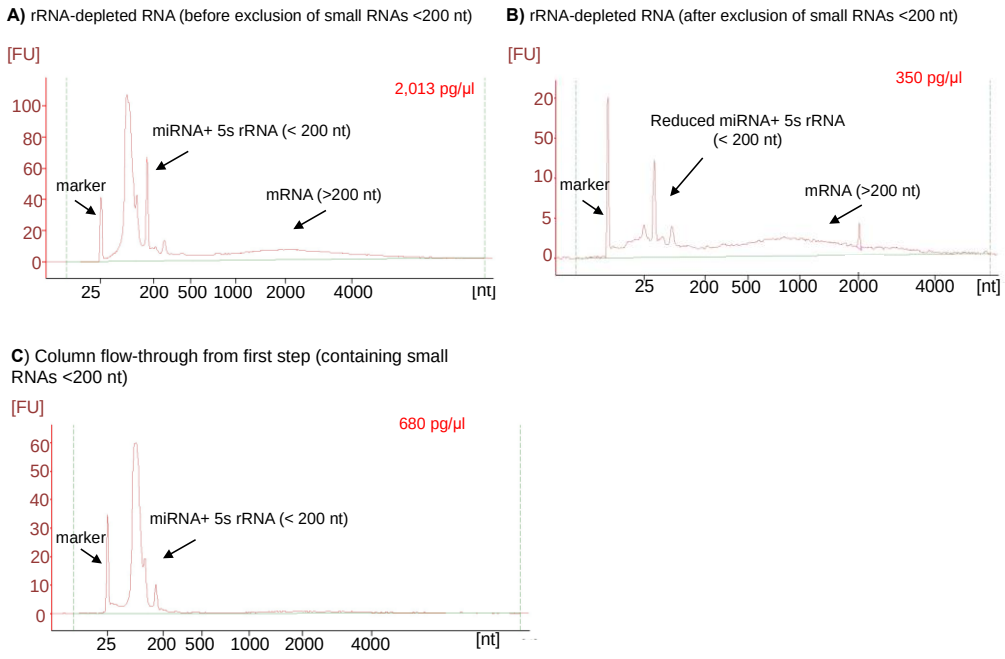

Figure 5.3 | Depletion of small RNAs (<200 nt) using Zymo Spin RNA Clean and Concentrator Kit™- 5. . Fuorescence units (FU) are shown on the y axis, versus nucleotide length (nt) on the x-axis. Plot shows ribosomal-depleted RNA before small RNA exclusion in A, ribosomal-depleted RNA after small RNA exclusion in B, and the flow-

through from step one of protocol (containing the excluded small RNAs) in C. Peaks have been annotated, and measured concentrations (pg/µl) are shown in red. Note that scales are different between plots (Plots generated by the bioanalyzer (Agilent Technologies)).

Table 5.4 | RNA concentrations before and after exclusion of small (<200 nt) RNA, across three independent experiments

	rRNA-depleted RNA (before exlusion of small RNA <200 nt)	rRNA-depleted RNA (after exlusion of small RNA <200 nt)	Column flow-through (containing small RNA <200 nt)
Experiment 1	2,013 pg/µl	350 pg/µl	680 pg/µl
Experiment 2	5,957 pg/µl	654 pg/µl	1,345 pg/µl
Experiment 3	2,571 pg/µl	419 pg/µl	952 pg/µl

5.5.4 Smart-seq2 for first strand cDNA synthesis and amplification

The Smart-seq2 protocol for first-strand cDNA synthesis and amplification has been specifically designed for use with low-input quantities of RNA (10 pg – 10 ng range), and has been shown to give the greatest coverage of genes in mammalian cells at the single-cell level (Picelli *et al.* 2013, Picelli *et al.* 2014, Reid *et al.* 2018). This makes it ideal for use in *ex vivo* parasite RNA-seq during studies of CHMI, where RNA material is extremely limited (Reid *et al.* 2018). Smart-seq2, as performed by Geetha Sankaranarayanan during the previous trial, has been described in full in chapter 4, section 4.4.5. Figure 5.4 below outlines the key steps.

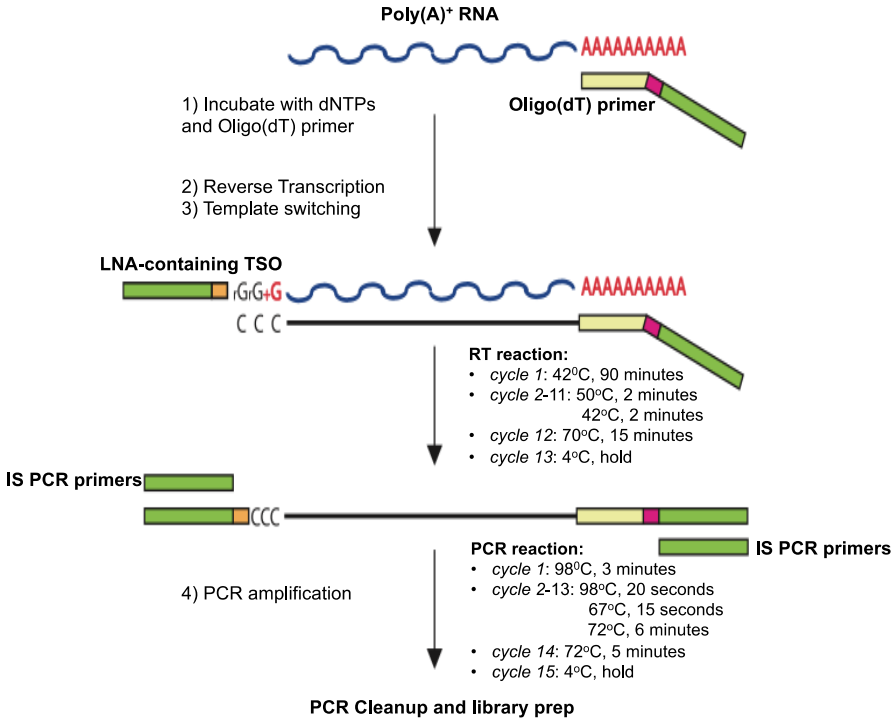

Figure 5.4 | Smart-Seq2 for first strand synthesis and amplification. Flowchart highlighting the key protocol steps. **1**) Incubation of purified Poly(A)+ RNA with dNTPs and Oligo (dT) for priming of samples for reverse transcription.

2) Reverse transcription using a Template Switching Oligomer (TSO) carrying two riboguanosines in the third- and second-last positions, and a modified guanosine to produce a locked nucleic acid (LNA) as the last base at the 3' end, for template switching **(3). 4)** Amplification of cDNA by PCR (~10-12 cycles recommended). Poly(A)+ = polyadenylated, dNTPs = deoxyribonucleic triphosphates, RT = Reverse Transcription, IS PCR = Illumina Sequencing PCR primers. Figure modified from Picelli *et al.* 201

1) **Priming for the RT reaction**- Samples are primed for the RT-reaction upon incubation with free dNTPs and tailed oligo-dT oligonucleotides (30-nt poly-dT stretch and a 25-nt universal 5' anchor sequence). The free dNTPs are added in this initial step to improve the yield of RT-PCRs, likely through mechanisms that stabilise RNA-primer hybridisations.

2) **Reverse Transcription-** as described using the original Smart-seq protocol is normally performed at 42^{o}C for 90 minutes (the optimal conditions for Superscript II^{TM}, according to the manufacturer). However, with the inclusion of betaine (1M) to increase protein thermal-stability during the RT reaction in the Smart-seq2 protocol, the temperature is allowed to reach to 50^{o}C for 2 minute intervals, to promote the unfolding of any secondary RNA structures, thus helping to maximize enzyme efficiency and cDNA yield.

3) Template Switching- relies on 2 - 5 un-templated nucleotides being added to the cDNA 3' end when the reverse transcriptase reaches the 5' end of the RNA. To achieve this, Smart-seq2 uses a template switching oligomer (TSO) carrying two riboguanosines in the third- and second-last positions, and a modified guanosine to produce a locked nucleic acid (LNA) as the last base. Upon reaching the 5' end of the RNA transcript, the Superscript II™ enzyme is able switch template and synthesise a complementary sequence to the TSO, meaning that every full-length cDNA carries the entire 5' end of the transcript, and an additional artificial sequence, which in this case is the same as the one located at the 5' end of the Oligo-dT primer. This makes it possible to perform the subsequent PCR using a single primer.

4) PCR amplification- is performed using a limited number of cycles (recommended 10 - 12), or just as many as needed to produce enough material for going into library prep (usually ~1 - 2 nanograms is sufficient). Following

amplification, samples were to be purified with use of Agencourt Ampure XP beads, as per manufacturer's guidelines (see chapter 4, section 4.4.5.3).

During the processing of samples from the previous trial, the recommended number of PCR cycles (10 - 12) did not give sufficient cDNA material for library prep using the NEB NEXTflex® kit (Bioo Scientific). For this reason, all samples were put through an arbitrary 25 cycles of PCR. This step in the protocol had not be optimsied for variable quantities of starting RNA input however, and over-amplification risks inefficiency in the RT reaction, and the introduction of technical variability due to amplification bias (Oshlack and Wakefield 2009, Stegle *et al.* 2015). Importantly, the Smart-seq2 protocol uses template switching technology, resulting in a bias towards genes that are reverse transcribed in full during the RT reaction (full length genes). This may be particularly relevant for *var* gene profiling as many of the genes (particularly those of the A and B/A groups) are large in size, at ~ 10 - 12 kb in length (see table 4.1). Thus, reducing the number of amplification cycles performed at this stage may help to limit the bias towards genes of shorter length. It was therefore decided that for use in the mosquito-bite CHMI, it would be important to first optimise the number of PCR cycles to be applied to samples, based on a predicted range of RNA concentrations following parasite isolation from the human host.

Based on the RNA yields recovered from parasites at day of patent infection in the blood-stage CHMI (see chapter 4, table 4.3), it was predicted that parasites isolated (at more frequent, and earlier time-points) during the mosquito-bite CHMI would produce yields between 10 pg - 1 ng of mRNA. The number of PCR cycles was thus optimised using RNA samples that had been depleted of globin mRNA, ribosomal RNA and small RNAs (< 200 nt) following extraction from *in vitro* cultured (ring-stage) 3D7 parasites, and then diluted as appropriate to give 10 pg, 50 pg, 100 pg, 500 pg or 1 ng in 2 µl volumes (required for the initial RT reaction). The RT reaction was performed exactly as described previously (see section 4.4.5.1). Based on the commercial Smart-seq (version 4) guidelines, the optimal PCR cycle number was determined as that resulting in a target cDNA yield of ~3 - 17 ng, when measured by Qbit™ fluorometer and dsDNA High Sensitivity kit (Thermo-Fisher Scientifc). Furthermore, quality assessment by Agilent 2100 bioanalyzer and High Sensitivity DNA Kit (Agilent Technologies) was used confirm the presence of a clean cDNA product spanning 300 – 10,000 base-pairs (bp),

as is shown in Figure 5.5. Each experiment run included three replicates, and a Minus Reverse Transcriptase (-RT) control to ensure the absence of DNA contamination.

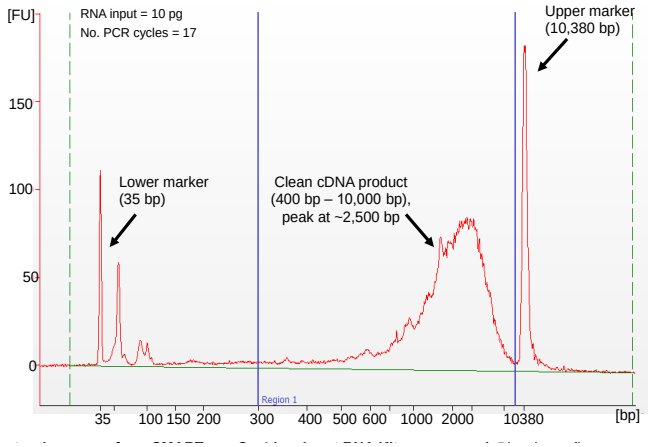

Figure 5.5 | Example electropherogram from SMART-seq® v4 low-input RNA kit user manual. Plot shows fluorescence units (FU) on the y-axis versus base-pairs (bp) along the x-axis, for a cDNA sample following synthesis and 17 cycles of PCR amplification using Smart-seq v4. Lower and upper marker peaks are displayed at 35 bp and 10,380 bp, respectively. Amplified cDNA product spans 300 bp – 10,000 bp (region 1), with a clean peak at ~2,500 bp as is indicative of a successful reaction.

cDNA yields, as measured for each replicate sample across all experiments, are provided in Appendix 9**.** Table 5.5 displays the mean yield (ng) of the replicate samples for each condition tested.

Table 5.5 | Optimising Smart-seq2 PCR cycle number based on cDNA yield

	cDNA yield (ng)										
	13 cycles	**14 cycles**	**15 cycles**	**16 cycles**	**17 cycles**	**18 cycles**	**19 cycles**	**20 cycles**	**21 cycles**	**22 cycles**	**25 cycles**
10 pg RNA						5.65[a]	9.05[b]	11.7[b]	36.1[b]	53.2[b]	1499.3[b]
50 pg RNA					7.4[a]	13.2[a]	20.6[b]				
100 pg RNA			3.2[a]	9.9[a]	19.6[a]	52.5[b]	134.5[b]				
500 pg RNA			12.5[a]	21.3[a]	34.2[a]						
1 ng RNA	7.5[a]	13.7[a]	48.7[b]		72.9[b]						

PCR cycle number not assessed

a mean of 6 replicates, across 2 independent experiemt runs

b mean of 3 replicates, from 1 experiment

Results suggested that the number of PCR cycles required to give ~3 – 17 ng cDNA, was variable depending on the starting RNA amount (10 pg, 50 pg, 100 pg, 500 pg or 1 ng), as expected. When 25 cycles of PCR was applied to 10 pg starting mRNA, the recovered yield (1,499.3 ng) far exceeded the amount required for going into downstream library prep (few nanograms). When starting with 10 pg of RNA, 20 cycles

of PCR resulted in a mean yield of 11.7 ng cDNA, within the predicted size range (300 – 10,000 bp) when quality assessed by bioanalyzer (Figure 5.6, part A). 18 and 19 cycles of PCR also produced cDNA yields within the target range. With increasing concentrations of RNA, decreasing numbers of PCR amplification cycles were required (table 5.5). Figure 5.6 (B - E) shows representative electropherograms of cDNA amplification product following 18, 17, 16 and 13 cycles of PCR for 50 pg, 100 pg, 500 pg and 1 ng starting amounts of mRNA, respectively. Based on these experiments, an optimal number of PCR cycles was proposed for each amount of input mRNA predicted to be recovered from parasites during the mosquito-bite CHMI (table 5.6).

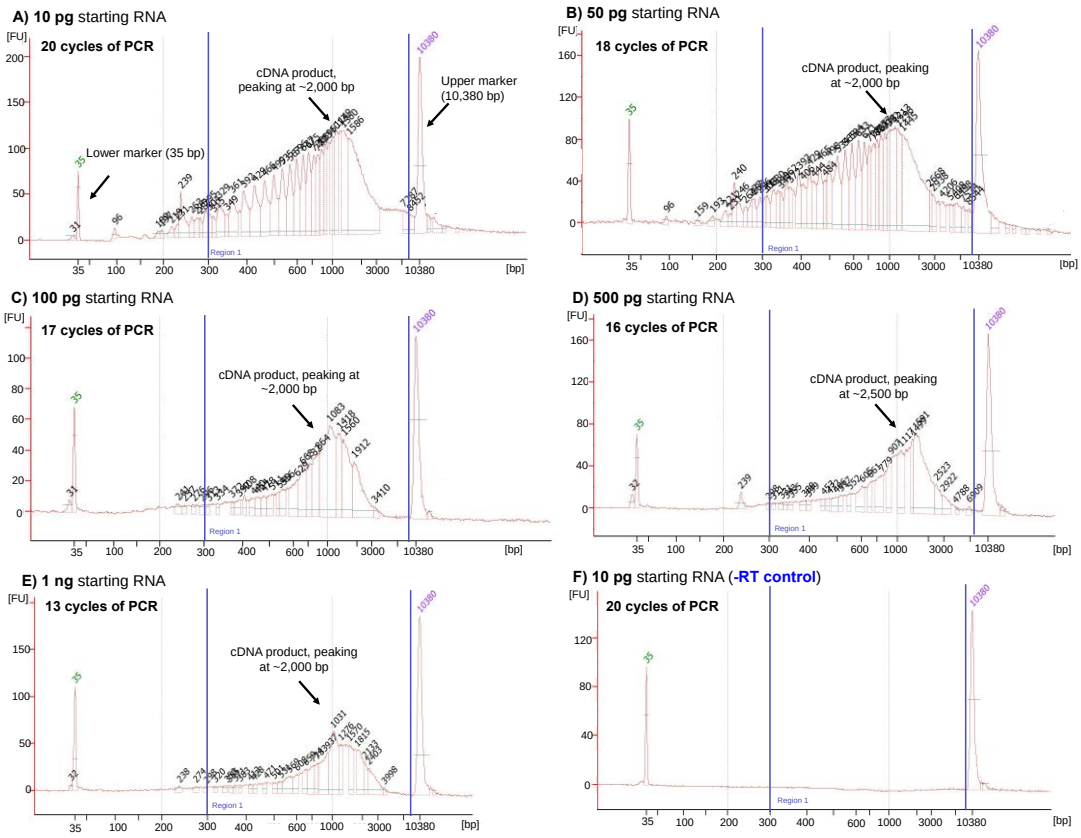

Figure 5.6 | Electropherograms of cDNA product following amplification using an optimised number of PCR cycles. RNA samples were prepared from *in vitro* cultured *P. falciparum* (3D7) ring-stage parasites, and reverse transcribed using Smart-seq2. Plots show fluorescence units (FU) on the y-axis against base-pairs (bp) along the x-axis for the cDNA produced from 10 pg **(A),** 50 pg **(B),** 100 pg **(C),** 500 pg **(D)** and 1 ng **(E)** starting RNA input. The number of PCR cycles applied to each sample is shown. **(F)** shows a plot of negative amplification for a representative sample processed without the reverse transcriptase enzyme (-RT control). Peaks at 35 bp and 10,380 bp represent the lower and upper markers of the Agilent 2100 HS DNA Chip, respectively. Region 1 highlights the predicted region for the cDNA amplification product (300 bp – 10,000 bp). (Plots generated by the Agilent 2100 bioanalyzer (Agilent Technologies)).

Table 5.6 | Proposed PCR cycle number for the predicted amounts of input RNA

Input Amount of RNA	Number of PCR cycles to apply
1 ng	13 - 14
500 pg	15 - 16
100 pg	16 - 17
50 pg	17 - 18
10 pg	18 - 20

5.5.5 Library prep and RNA-seq

Library prep was to be performed by Geetha Sankaranarayanan at the Wellcome Trust Sanger Institute, as with the previous trial. In this instance however, it was decided that the Nextera XT library prep kit (Illumina) would be best suited, having been optimised for low-input (1 ng) DNA, therefore allowing for a reduced number of amplification cycles during the Smart-seq2 protocol. The success of this kit is dependent on the accurate quantification of cDNA, thus before shipment, samples were to be quantified using the Qbit fluorometer 2.0 and dsDNA High Sensitivity kit (Thermo Fisher Scientific).

Library prep was to be performed as per manufacturer's instructions. In brief, 1 ng of cDNA (0.2 ng/µl, in 5 µl volumes) is incubated with 10 µl of Nextera XT "Tagment Buffer" and 5 µl of "Amplicon Tagment Mix" in a well of 96-well, PCR plate. DNA is then tagmented (fragmented and tagged with adaptor sequences) by incubating at 55^{o}C for 5 minutes, using a thermal cycler with heated lid. Following incubation, 5 µl of "Neutralize Tagment Buffer" is added to the well, and plate is centrifuged at 280g and 20^{o}C for 1 minute, prior to incubation at room temperature for 5 minutes. 5 µl of each index adapter (Index I (i7) and Index 2 (i5)), along with 15 µl of "Nextera XT PCR Master Mix" is then added to the 25 µl of tagmented DNA for amplification using a limited-cycle PCR program (table 5.7). After amplification, library DNA is treated with AMPure XP (Beckman Coulter) beads to purify, and then 1 µl of undiluted library is run on the Agilent bioanalyzer High sensitivity DNA chip (Agilent Technologies) for quality assessment.

Table 5.7 | Nextera XT PCR program

Cycle	Temperature	Duration
cycle 1	72°C	3 minutes
cycle 2	95°C	30 seconds
cycle 3 - 15	95°C	10 seconds
	55°C	30 seconds
	72°C	30 seconds
cycle 16	72°C	5 minutes
cycle 17	4°C	Hold

RNA-sequencing of samples was to be performed by Dr Adam Reid (Wellcome Trust Sanger Institute), as described previously (see chapter 4 section 4.4.7).

5.5.6 Summary of protocol amendments

The protocol used for *ex vivo* parasite RNA-seq during the original (blood-stage) CHMI trial is described in full, in chapter 4 methods. Table 5.8 summarises the amendments made to the protocol for use in the mosquito-bite CHMI, based on the optimisation experiments discussed in this chapter.

Table 5.8 | Summary of protocol amendments for use in mosquito-bite CHMI

Protocol step	Procedure used in Original (blood-stage) CHMI trial	*Amendment(s)* made for follow-up mosquito-bite CHMI trial	Reason for protocol amendment
Leucodepletion	Leucodepletion by filtration (LEUCOFLEX LXT filters, Macopharma)	-	-
Red cell lysis and recovery of rings	0.015% saponin in PBS 10 minute incubation at 4°C Centrifugation at 15,000g for 10 minutes	0.0075% saponin in PBS 10 minute incubation at 4°C Centrifugation at 18,000g for 20 minutes	0.0075% saponin gives better recovery of rings. Faster and longer centrifugation to recover rings otherwise lost in the supernatant
RNA extraction and quantification	Depletion of globin mRNA and rRNA, Quantification by Bioanalyzer (Pico Chip)	Depletion of globin mRNA, rRNA and small RNAs Quantification by Bioanalyzer (Pico Chip)	More accurate quantification for downstream Smart-seq2
Smart-seq2 for first strand cDNA synthesis and amplification	Reverse transcription, 25 cycles of PCR	Reverse transcription, optimised number of PCR cycles (input-dependent)	Reduced risk of over-amplification / bias towards genes of shorter length
Library prep	NEB NEXTflex® kit (Bioo Scientific)	Nextera™ XT kit (Illumina)	Optimised for use with lower input DNA (1 ng)
RNA-seq	Illumina sequecning (paired-end, HiSeqv4)	-	-

5.5.7 Test run using *in vitro* "mock" samples

In order to test run the fully optimised protocol before application during the mosquito-bite CHMI, two samples of *in vitro* cultured (3D7) parasites were prepared and run through the protocol, for subsequent RNA-seq analysis. I was interested to know whether it would be possible to detect expression of parasite genes in the earliest stages of infection, after just one or two cycles following parasite egress from the liver. To explore this, samples were prepared using representative numbers of ring-stage

parasites (~40 p/mL and ~400 p/mL respectively), based on previous data from mosquito-bite challenges performed at the CCVTM, Oxford (Roestenberg *et al.* 2012). Samples were controlled for the total blood volumes that had originally been allocated during the challenge follow-up period, such that the "cycle 1 mock" contained 2,000 parasites in 50 mL of whole blood, and "cycle 2 mock" contained 8,000 parasites in 20 mL of whole blood. Parasites were purified, RNA extracted and cDNA amplified as per the protocol amendments summarised above. Library prep and RNA-sequencing was performed by collaborators at the Wellcome Trust Sanger Institute), as previously described in chapter 4, sections 4.4.6 and 4.4.7.

RNA-sequencing results showed the ability to detect the expression of *P. falciparum* genes in these samples (table 5.9). For "cycle 1 mock" and "cycle 2 mock", 658 and 786 genes were found with at ≥ 5 reads mapping to the reference genome, respectively. Although this was an encouraging result, it is important to note that the number of genes observed for each represents a small proportion of the > 5,000 genes present in the *P. falciparum* (3D7) reference genome (Gardner *et al.* 2002). Moreover, just four (PF3D7_1200100/ PFL0005w, PF3D7_1200600/ PFL0030c, PF3D7_0412900/ PFD0630c and PF3D7_1041300/ PF10_0406) and six (PF3D7_0712800/ MAL7P1.55, PF3D7_0800100/ PF08_0142, PF3D7_0421300/ PFD1015c, PF3D7_1200600/ PFL0030c, PF3D7_1200100/ PFL0005w and PF3D7_1041300/ PF10_0406) *var* gene variants were detected (with ≥ 5 reads) in the "cycle 1 mock" and "cycle 2 mock" samples, respectively. It has been shown previously that parasites adapted to long-term culture (as with the parasites used for mock sample preparation here), tend to transcribe a reduced number of *var* gene variants (Peters *et al.* 2007, Zhang *et al.* 2011), which may partly explain this observation. However, considering the overall reduction in the number of detectable genes in these samples (mean = 722), compared to that in samples isolated at day of patent infection in the previous trial (see chapter 4, table 4.4), results suggest that the low parasite densities expected at the onset of infection may limit the number of genes that can be successfully detected using this protocol.

Table 5.9| Number of detectable genes in "cycle 1 mock" and "cycle 2 mock" samples

Sample I.D	Number of parasites in sample	RNA concentration (ng/µl	RNA yield (ng)	Number of *P. falciprum* genes identified (≥ 5 reads)	Number of *P. falciprum* genes identified (≥ 10 reads)
"cycle 1 mock"	2,000	0.20	1.99	658	426
"cycle 2 mock"	8,000	8.33	8.33	786	428

5.5.8 Application of optimised protocol to mosquito-bite CHMI

The protocol described within was applied to a mosquito-bite CHMI study that took place at the CCVTM in Oxford, in January 2017 (*Clinical/ Trails.gov i.d: NCT02905019*). Sampling for my sub-study was designed to test how early in infection parasites could be isolated for successful RNA-sequencing, following liver egress at ~6 - 7 days post-infection. Parasites (in 20 mL volumes of blood) were isolated from 5 (unvaccinated) control volunteers on day 7 post-infection (C +7) and at subsequent 24 hour time-points, until the termination of volunteer infections at first microscopic detection (ranging C +11 - C +12).

5.5.8.1 Parasite densities following mosquito-bite CHMI

As is routine practice for studies of CHMI, qPCR was used to monitor parasite density at twice-daily time points throughout the duration of the challenge follow-up period. Figure 5.7 displays the parasite growth curves for the 5 volunteers; ♯1037, ♯1068, ♯1073, ♯1074 and ♯1076, and the parasite densities (p/mL) as measured at day of diagnosis for each. Compared to the previous blood-stage challenge trial, parasite densities following mosquito-bite CHMI were consistently lower (mean; 4,658 p/mL and range; 1,453 – 10,466 p/mL versus mean; 48,722 p/mL and range; 1,440 – 273,247 p/mL). In this study, just one of five volunteers (20%) was diagnosed at a parasite density ≥ 10,000 parasites/mL, compared to the 9/14 (64%) as was observed following blood-stage CHMI. Based on these data, it was decided that parasites isolated at the C +7 and C +8 time points, where densities were below or just above the lower limit of qPCR detection (20 p/mL), would be too low in numbers to give sufficient RNA material for successful RNA-seq considering the likely host contamination in these samples. Thus, focus was placed on the parasites recovered at the three time-points; C +9, C +10 and C +11, by which time parasitaemias (in 20 mL volumes of blood) were in the range ~1,000 – 200,000.

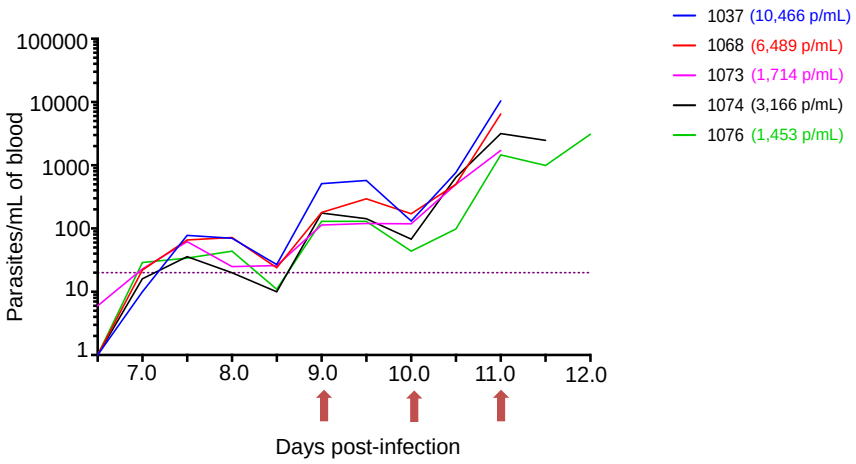

Figure 5.7 | Parasite growth following mosquito-bite CHMI. Graph shows the number of parasites per mL of blood (y-axis) through time (x-axis), as measured by qPCR. A colour key is provided for each of the 5 volunteers, along with the parasite density (p/mL) as measured at day of diagnosis for each. Dashed purple line represents the qPCR lower limit of quantification (20 p/mL). Red arrows denote the sampling time-points at which isolated parasites were assessed by RNA-sequencing.

5.5.8.2 Number of *P. falciparum* genes detected at 9, 10 and 11 days post mosquito-bite CHMI

In order to compare the number of genes detected in these samples to that of the "cycle 1 mock, "cycle 2 mock" and the 12 patient samples from the blood-stage challenge trial, only genes that had ≥ 5 reads (in at least one sample) were considered for analysis. As expected, parasite samples isolated at C +11 (from volunteers ♯1037, ♯1068 and ♯1074) gave the best coverage of genes (1,285, 1,915 and 2,323, respectively), most likely reflecting the higher parasitaemias in these volunteers, at this time-point (table 5.10). On the other hand, parasite samples from volunteers ♯1073 and ♯1076 demonstrated best coverage at C +10, when parasite densities had not yet reached their peak. Parasites from volunteer ♯1074 gave the best coverage of genes (2,323), representing 44% of the 5,268 genes belonging to the *P. falciparum* genome (Gardner *et al.* 2002). When compared to the 12 patient samples from the blood-stage challenge (day of diagnosis mean: 2,518 and range: 1,159 – 3,671), coverage in these samples was slightly lower overall (C +11 mean: 1,235 and range: 221 – 2,323). However, for volunteers ♯1037, ♯1068 and ♯1074, where parasite densities reached >3,000 p/mL (~60,000 total), the number of genes that could be detected was highly comparable to that observed for the majority of volunteers in the previous trial (see section 4.5.3, table 4.4).

The total parasite numbers predicted (in 20 mL) at C +9 (mean: 4,444 and range: 2,600 – 10,220) were within a similar range to those used to create the “cycle 1 mock” and “cycle 2” mock samples, and demonstrated a similar number of detectable genes (median: 414 genes and range: 219 - 570). This observation was also true of the C +10 samples (mean coverage: 596 genes and range: 348 - 904). Importantly, the detection of *var*, and *rif* genes was markedly reduced in these earlier samples, for volunteers ♯1037, ♯1068 and ♯1074 (table 5.10). No *stevor* genes were detected in any volunteer, at any time-point. As previously noted, maximal gene coverage (including the VSAs of interest) was taken as C +10 for volunteers ♯1073 and ♯1076. However, detection was lowest overall in these individuals. A full list of the *var* and *rif* genes detected for each volunteer, is provided in Appendix 10.

Thus, despite optimisation, the protocol for *ex vivo* RNA-seq described within appears restricted by the low parasite densities in the first two blood cycles and/or host contamination, precluding the ability to assess *var* gene expression at the onset of infection. The gene coverage detected at C +11, for volunteers ♯1037, ♯1068 and ♯1074, and C +10, for volunteers ♯1073 and ♯1076 was considered sufficient to make some preliminary observations of *var* gene expression following mosquito-bite CHMI.

Table 5.10 | Number of *P. falciparum* genes detected in parasites isolated at 9, 10 and 11 days post mosquito-bite CHMI

Volunteer i.d/ time-point	Parasites/mL	Total parasites (in 20 mL)	No. of genes detetced (≥ 5 reads)	No. of *var* genes detected	No. of *rif* genes detected	No. of *stevor* genes detected
1037 C +9	511	10,220	570	2	0	0
C +10	131	2,620	619	8	0	0
C +11	10,466	209,320	1,285	29	1	0
1068 C +9	180	3,600	432	1	0	0
C +10	171	3,420	422	2	1	0
C +11	6,489	129,780	1,915	31	3	0
1074 C +9	176	3,520	558	3	0	0
C +10	68	1,360	348	0	1	0
C +11	3,166	63,320	2,323	33	2	0
1073 C +9	114	2,280	290	1	0	0
C +10	119	2,380	686	17	0	0
C +11	1,714	34,280	429	2	0	0
1076 C +9	130	2,600	219	1	0	0
C +10	44	880	904	10	1	0
C +11	1,453	29,060	221	0	0	0

5.5.8.3 Parasite *var* gene expression following mosquito transmission in the naïve host

Figure 5.8 displays the read counts for all detectable *var* genes at either C +11 (for volunteers ♯1037, ♯1068 and ♯1074) or at C +10 (for volunteers ♯1073 and ♯1076). Consistent with observations from the blood-stage challenge trial, a high proportion of *var* gene variants (38/61, 62%) were detected with reads ≥ 5 reads (in at least one sample). In parasite samples from volunteers ♯1074, ♯1068 and ♯1037, showing the greatest coverage of genes, 55%, 51% and 48% of all variants were detected, respectively (figure 5.8). These 3 individuals had shared expression of 23 *var* genes, including variants from the group-A, B/A, B, B/C subclasses, and var2csa (group-E). However, read count hierarchies for these common genes were variable between volunteer samples. When considering the entire cohort (n = 5), just two variants were shared across all (PF3D7_0632800/ MAL6P1.1 and PF3D7_0400100/ PFD0005w). MAL6P1.1 was found with the highest number of associated read counts in volunteer ♯1074, and was within the top ten genes with highest read counts for volunteers ♯1037 (3rd), ♯1068 (9th), ♯1076 (9th) (figure 5.8). A similar observation was made for PFD0005w, which was detected among the top ten for volunteers ♯1073 (1st), ♯1074 (6th), ♯1037 (7th) and ♯1076 (8th). Interestingly, these group-B *var* genes have been reported as the most highly expressed in two previous studied of mosquito-bite CHMI (Wang *et al.* 2009, Bachmann *et al.* 2016), showing consistency between the three datasets. MAL6P1.1 was also found expressed at high levels in the 12 volunteers that received the blood-stage challenge. Yet, PFD0005w was among the variants detected at some of the lowest levels (see chapter 4, table 4.6 and figure 4.5).

In contrast to what was observed in the blood-stage trial, group-A genes were reported with some of the highest associated read counts in these 5 volunteers, although at variable levels across the 5 volunteers (figure 5.8). For instance, PF3D7_0400400/ PFD0020c was found among the top four in volunteers ♯1074 (read count = 795), ♯1068 (read count = 176) and ♯1073 (read count = 299) (similar to previous reports) (Wang *et al.* 2009, Bachmann *et al.* 2016), but was detected with a low read count in volunteer ♯1037 (read count = 5), and not at all in volunteer ♯1076 (figure 5.8). Other group-A *var* genes found shared between volunteers included PF3D7_0425800/ PFD1235w (in volunteers ♯1037, ♯1068, ♯1074 and ♯1076), PF3D7_1100200/ PF11_0008 (in volunteers ♯1068, ♯1074 and ♯1076) and PF3D7_1300300/ PF13_0003

(in volunteers ♯1068 and ♯1075). Of the top six most highly expressed variants detected following blood-stage CHMI (chapter 4, figure 4.6), four (PF3D7_1041300/ PF10_0406, PF3D7_1200100/ PFL0005W, PF3D7_0421100/ PFD1005c, and PF3D7_1100100/ PF11_0007) were detected in the 3 volunteers with best gene coverage in this trial (figure 5.8).

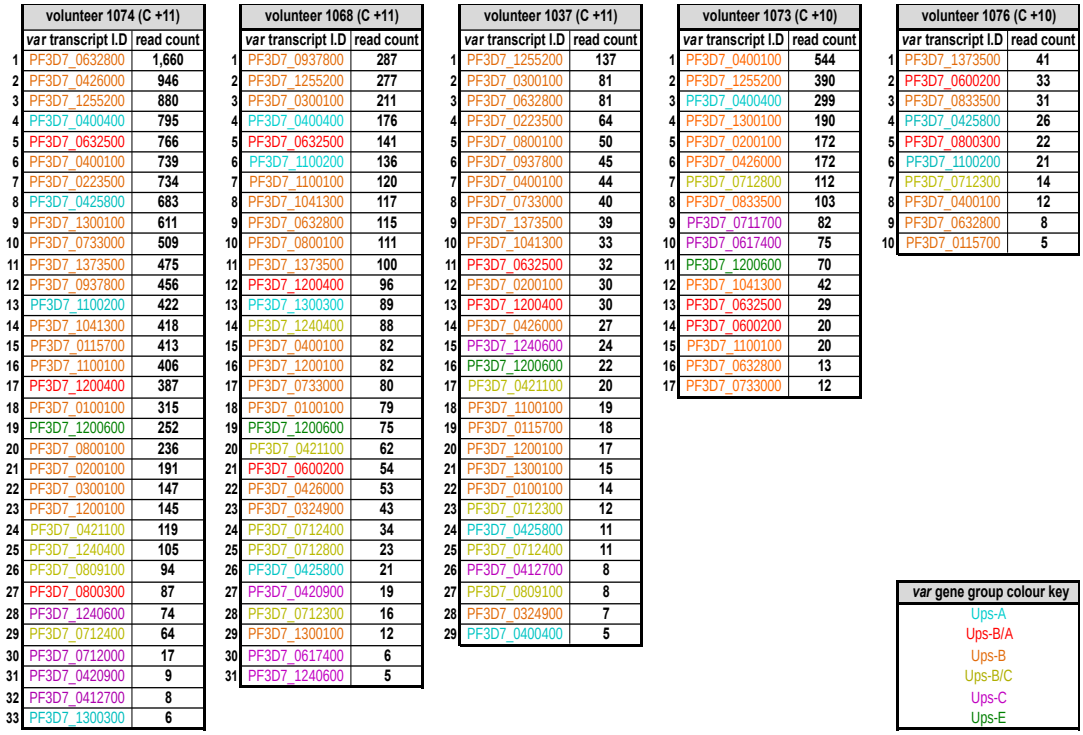

volunteer 1074 (C +11)

	var transcript I.D	read count
1	PF3D7_0632800	1,660
2	PF3D7_0426000	946
3	PF3D7_1255200	880
4	PF3D7_0400400	795
5	PF3D7_0632500	766
6	PF3D7_0400100	739
7	PF3D7_0223500	734
8	PF3D7_0425800	683
9	PF3D7_1300100	611
10	PF3D7_0733000	509
11	PF3D7_1373500	475
12	PF3D7_0937800	456
13	PF3D7_1100200	422
14	PF3D7_1041300	418
15	PF3D7_0115700	413
16	PF3D7_1100100	406
17	PF3D7_1200400	387
18	PF3D7_0100100	315
19	PF3D7_1200600	252
20	PF3D7_0800100	236
21	PF3D7_0200100	191
22	PF3D7_0300100	147
23	PF3D7_1200100	145
24	PF3D7_0421100	119
25	PF3D7_1240400	105
26	PF3D7_0809100	94
27	PF3D7_0800300	87
28	PF3D7_1240600	74
29	PF3D7_0712400	64
30	PF3D7_0712000	17
31	PF3D7_0420900	9
32	PF3D7_0412700	8
33	PF3D7_1300300	6

volunteer 1068 (C +11)

	var transcript I.D	read count
1	PF3D7_0937800	287
2	PF3D7_1255200	277
3	PF3D7_0300100	211
4	PF3D7_0400400	176
5	PF3D7_0632500	141
6	PF3D7_1100200	136
7	PF3D7_1100100	120
8	PF3D7_1041300	117
9	PF3D7_0632800	115
10	PF3D7_0800100	111
11	PF3D7_1373500	100
12	PF3D7_1200400	96
13	PF3D7_1300300	89
14	PF3D7_1240400	88
15	PF3D7_0400100	82
16	PF3D7_1200100	82
17	PF3D7_0733000	80
18	PF3D7_0100100	79
19	PF3D7_1200600	75
20	PF3D7_0421100	62
21	PF3D7_0600200	54
22	PF3D7_0426000	53
23	PF3D7_0324900	43
24	PF3D7_0712400	34
25	PF3D7_0712800	23
26	PF3D7_0425800	21
27	PF3D7_0420900	19
28	PF3D7_0712300	16
29	PF3D7_1300100	12
30	PF3D7_0617400	6
31	PF3D7_1240600	5

volunteer 1037 (C +11)

	var transcript I.D	read count
1	PF3D7_1255200	137
2	PF3D7_0300100	81
3	PF3D7_0632800	81
4	PF3D7_0223500	64
5	PF3D7_0800100	50
6	PF3D7_0937800	45
7	PF3D7_0400100	44
8	PF3D7_0733000	40
9	PF3D7_1373500	39
10	PF3D7_1041300	33
11	PF3D7_0632500	32
12	PF3D7_0200100	30
13	PF3D7_1200400	30
14	PF3D7_0426000	27
15	PF3D7_1240600	24
16	PF3D7_1200600	22
17	PF3D7_0421100	20
18	PF3D7_1100100	19
19	PF3D7_0115700	18
20	PF3D7_1200100	17
21	PF3D7_1300100	15
22	PF3D7_0100100	14
23	PF3D7_0712300	12
24	PF3D7_0425800	11
25	PF3D7_0712400	11
26	PF3D7_0412700	8
27	PF3D7_0809100	8
28	PF3D7_0324900	7
29	PF3D7_0400400	5

volunteer 1073 (C +10)

	var transcript I.D	read count
1	PF3D7_0400100	544
2	PF3D7_1255200	390
3	PF3D7_0400400	299
4	PF3D7_1300100	190
5	PF3D7_0200100	172
6	PF3D7_0426000	172
7	PF3D7_0712800	112
8	PF3D7_0833500	103
9	PF3D7_0711700	82
10	PF3D7_0617400	75
11	PF3D7_1200600	70
12	PF3D7_1041300	42
13	PF3D7_0632500	29
14	PF3D7_0600200	20
15	PF3D7_1100100	20
16	PF3D7_0632800	13
17	PF3D7_0733000	12

volunteer 1076 (C +10)

	var transcript I.D	read count
1	PF3D7_1373500	41
2	PF3D7_0600200	33
3	PF3D7_0833500	31
4	PF3D7_0425800	26
5	PF3D7_0800300	22
6	PF3D7_1100200	21
7	PF3D7_0712300	14
8	PF3D7_0400100	12
9	PF3D7_0632800	8
10	PF3D7_0115700	5

var gene group colour key

Ups-A
Ups-B/A
Ups-B
Ups-B/C
Ups-C
Ups-E

Figure 5.8 | List of detectable *var* genes (and associated read counts) following mosquito-bite CHMI in 5 volunteers. Figure displays the full list of *var* genes and associated read counts, as detected by *ex vivo* RNA-seq at 10 days post mosquito-bite challenge (C +10) for volunteers 1073 and 1076, and at 11 days post mosquito-bite challenge (C +11) for volunteers 1037, 1068 and 1074. Note that data is not normalised (rlog converted) thus read count values are not directly comparable between volunteers. A colour key for *var* group affiliation is provided.

I was interested to assess the proportional distribution of parasite *var* transcripts by *var* group affiliation (A, B/A, B, B/C, C and E) in these 5 volunteers (figure 5.9). Consistent with observations from the previous blood-stage challenge, the group-B variants were attributed to the largest proportion of total *var* expression in all patient samples (range: 45.5% - 81.0% and mean: 66.1%). However, in this study, the group-A variants were attributed to a second highest proportion of total read counts (range: 2.0% – 22.1% and mean: 13.27%), followed by those of the B/A group (range: 2.1% - 25.8% and mean: 10.9%), the B/C variants (range: 2.9% - 7.9% and mean: 5.3%), the group-C var genes

(range: 0% - 6.7% and mean: 2.4%) and then var2csa (range: 0% - 3% and mean: 2.0%). Interestingly, the proportional distribution of each *var* gene group appeared to be more variable following mosquito-bite CHMI, compared to the patterns observed following blood-stage challenge (see chapter 4, figure 4.13). Parasites from volunteers ♯1074 and ♯1068, demonstrating the best coverage of genes at C +11, had remarkably similar *var* group distribution profiles (figure 5.9). However, this pattern was not observed in parasites from volunteer ♯1037 (demonstrating a similar number of detectable genes). This volunteer had reduced contribution from the group-A variants, and a larger proportion of group-B and C variants attributed to their total *var* read counts. Volunteer ♯1076 displayed the most unique *var* group distribution pattern within the cohort (figure 5.9), however this parasite sample had the poorest coverage of *var* genes (n = 10), which is likely skewing the distribution profile towards those select few with high read counts, and hence may be misrepresentative of its expression pattern had a broader range of variants been detected.

Nevertheless, *var* gene expression profiles appear to be more variable across volunteers following mosquito-transmission, albeit based on this small cohort of n = 5. It is possible that this variability may be an effect of ectopic *var* gene recombination events that take place during meiosis in the mosquito-vector (Freitas-Junior *et al.* 2000, Taylor *et al.* 2000, Claessens *et al.* 2014), and hence why it was not observed following direct blood-stage inoculation in the previous trial. Based on these preliminary observations of the read count data, it will be therefore be important to next compare the normalised (rlog) *var* gene expression levels between volunteers, and between different trials. These data were not available at time of thesis submission.

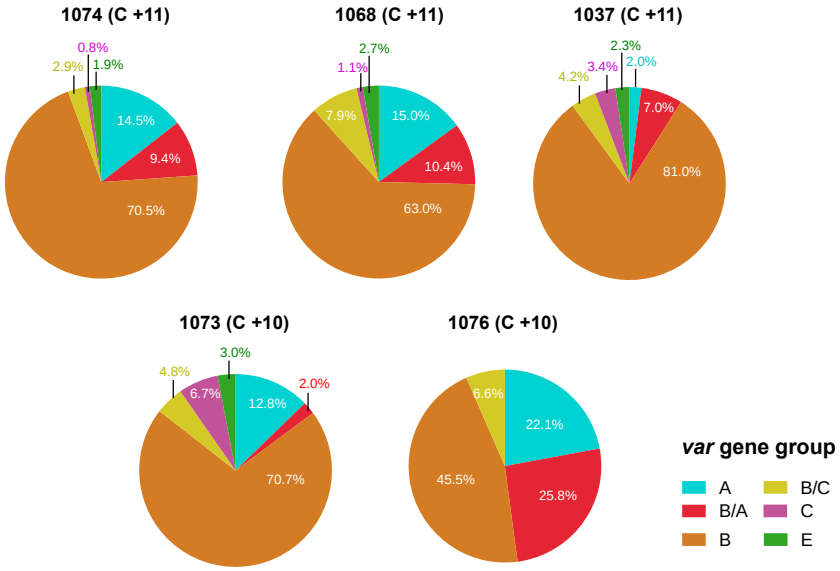

Figure 5.9 | Percentage distribution of *var* transcripts by *var* gene group. The distribution of *var* transcripts according to *var* group affiliation in shown as the proportion of total *var* gene read counts, for individual volunteer samples as measured at either C +11 (1074, 1068 and 1037) or C +10 (1073 and 1076). A *var* gene group colour-code is provided.

5.5.8.4 Parasite *rif* gene expression following mosquito transmission in the naïve host

Of the 143 *rif* gene members in the *P. falciparum* (3D7) genome, just 3 (PF3D7_0401600, PF3D7_0400500 and PF3D7_1200500) were detected following mosquito-bite CHMI in this study, and only in certain volunteers (Appendix 10). Of the 3, the most widely detected (and displaying highest read counts) was PF3D7_0401600, encoding a group-A RIFIN. This variant was found expressed in parasites isolated from the three volunteers demonstrating the best gene coverage (♯1074, ♯1068 and ♯1037), and at both C +10 and C +11 time points in two of these three individuals (♯1074 and ♯1068). Interestingly, this *rif* gene variant was also found dominantly expressed in volunteer samples from the previous blood-stage CHMI study (chapter 4, figure 4.15). There is currently limited information with regards to the function of this protein, although it has been found transcribed at high levels in parasite populations enriched for parasites that bind to the human endothelial receptors P-selectin, E-selectin, CD9 and CD151 (Metwally *et al.* 2017), It will therefore be important to investigate the adhesive properties of this RIFIN further, to determine its role early during infection in the non-immune host.

5.6 Discussion

The switching between hyper-variable *var* genes affords *P. falciparum* parasites a means to evade the developing host immune response and establish chronic infection (Roberts *et al.* 1992, Smith *et al.* 1995). This is thought to explain, in part, the delay to naturally acquired immunity, which coincides with a transition from acute and severe infection in young infants, to asymptomatic carriage in older individuals (Marsh and Snow 1997). The severe disease associated with young children (< 5 years) has been linked specifically to a subset of group-A, B/A *var* genes/PfEMP1, suggesting that these variants confer a fitness advantage in the immunologically naïve host (Jensen *et al.* 2004, Bull *et al.* 2005, Kaestli *et al.* 2006, Rottmann *et al.* 2006). This, in turn, has given rise to the hypothesis that *var* gene expression (and the acquisition of anti-PfEMP1 immunity) follows an ordered pattern, with group-A variants being the first to be recognised by the developing host immune response (Warimwe *et al.* 2009, Cham *et al.* 2010, Abdi *et al.* 2016). Contradictory to this hypothesis however, is data from studies of CHMI (including those discussed in the previous chapter of this thesis), which demonstrates activation of all, or the majority of *var* gene variants upon infection in the naïve host (Lavstsen *et al.* 2005, Wang *et al.* 2009, Bachmann *et al.* 2016). These studies propose a model whereby, at the onset of infection (and in the absence of antibody-specific immune selection forces), parasites express a broad repertoire of *var* gene variants for the early exploration of host sequestration receptors. This is in line with results reported in the previous chapter of this thesis, showing consistent patterns of *var* gene expression between parasites isolated from the 3rd blood cycle (inoculum sample) and parasites recovered after a further 5 - 6 cycles in the blood (volunteer samples). In this setting, *var* gene switching was not observed. Furthermore, the disease-associated group-A, B/A *var* gene variants were detected at some of the lowest levels in these non-immune individuals. However, this analysis was restricted to a short time-window, and was not conducive to the assessment of *var* gene expression immediately following liver egress (cycles 1 and 2 in the blood).

In order to better understand the parameters of *var* gene selection *in vivo*, and hence their influence on host clinical outcome, we need to investigate *var* gene expression patterns from the very onset of infection in the human host. Having previously demonstrated the successful application of *ex vivo* parasite RNA-seq during a study of blood-stage CHMI, I aimed to optimise my protocol for application to parasitaemias as

low as those expected in the first 1 - 2 blood cycles following liver egress (~40 p/mL). Moreover, I wanted to ensure the efficient depletion of all (irrelevant) host contaminants (blood cells and RNA), as is necessary for successful RNA-sequencing. With use of *in vitro* cultured parasites (*P. falciparum* 3D7-strain), I was able to show improved recovery of parasite ring stages from whole human blood, by reducing the concentration of saponin used for red blood cell lysis from 0.015% to 0.0075%. Furthermore, by adjusting centrifugation speeds and duration, I was able to prevent the loss of parasites that had previously been discarded along with the supernatant. A step to wash parasite pellets of residual free globin was also included to improve the purity of final parasite preparations before freezing in TRIzol™ reagent. During the RNA-extraction protocol, I added a step to exclude the presence of small RNAs (< 200 nt in length), for the more accurate quantification and estimation of the PCR cycle number required in the Smart-seq2 protocol. Importantly, I optimised the number of amplification cycles required for the predicted range of parasite RNA yields expected during the mosquito-bite CHMI trial, thereby helping to reduce the risk of technical variation due to amplification bias. This was also afforded by the switching of protocols used for library prep, to a kit designed for use with low-input cDNA yields (1 ng).

RNA-sequencing results from “cycle 1” and “cycle 2” mock samples (consisting of 2,000 and 8,000 ring-stage parasites, respectively) confirmed the ability to detect parasite gene expression from parasite densities representative of those expected after immediate liver egress (~40 – 50 p/mL), and in the subsequent blood cycle (~400 – 500 p/mL). However, it is important to note that a limited number of genes were detectable in these samples (“cycle 1 mock” = 658 and “cycle 2 mock” = 786), considering the > 5,000 genes that make up the 3D7 reference genome. Furthermore, a reduced number of *var* gene variants were detected (4 - 6) compared to parasites isolated on the day of patent infection (positive thick film by microscopy) in the previous blood-stage CHMI trial (58). This may be explained, in part, by the tendency for long-term cultured parasites to have reduced transcription of *var* gene variants; a well described phenomenon (Peters *et al.* 2007, Zhang *et al.* 2011). Therefore, it was important to determine the coverage of *P. falciparum* VSA genes that could be achieved using this protocol, when applied early following mosquito-transmission in the naïve host.

In this study of mosquito-bite CHMI, parasite densities were lower compared to those observed during the blood-stage challenge, albeit based on a small cohort of 5 volunteers. As a consequence, the parasite material recovered at C +7 and C +8 days was presumed to be insufficient for sequencing. At 9 days post infection (mean parasite density: 222 p/mL/ 4,444 parasites total), a good number of *P. falciparum* genes (mean: 414) could be detected using my protocol for *ex vivo* RNA-seq, however coverage was far reduced when compared to the number of genes detectable at C +11 (mean: 1,285). In two volunteers, optimal gene coverage was observed at C +10, when parasite densities had not yet reached their peak. This observation suggests that, as well as low parasitaemias, contaminating host material is likely to have affected the success of this protocol. Thus, despite optimisation, this method for *ex vivo* RNA-seq appears restricted to the 3rd blood cycle onwards. Furthermore, observations from this trial and the previous blood-stage challenge trial imply a parasite density threshold (of ~2,000 p/mL / ~50,000 total) for the sufficient coverage of parasite genes. Interestingly, a recent study using the same Smart-seq2 technology for parasite RNA-sequencing has demonstrated the ability to detect a large proportion of *P. falciparum* genes in the single-cell transcriptomes of parasites at either the asexual trophozoite stage (mean coverage = 1,712 genes) or sexual gametocyte stage (mean coverage = 2,090 genes) (Reid *et al.* 2018). Hence, a similar level of coverage that required ~3,000 p/mL in the CHMI model, but in transcriptomes from a single parasite. However, it is important to note that later stage trophozoites and gametocytes contain larger quantities of RNA material than the ring-stages found in the blood, which may have aided sequencing efficiency. Moreover, single cell preparations made from *in vitro* cultures, are unlikely to contain contaminating host material, which may have otherwise reduced the number of reads mapped to the *P. falciparum* genome. It may be that Fluorescence Activated Cell Sorting (FACS) could offer an alternative approach for the assessment of parasite gene expression at the onset of infection in the human host. Single cell sorting of ring stage-infected erythrocytes would likely reduce the risk of contamination. Furthermore, based on the number of genes detected in single parasite transcriptomes, by Reid *et al*, it is presumed that sorting of just a few ring stage-infected erythrocytes (~10 – 20) would provide sufficient material for sequencing. However, this method may not be appropriate in a setting where the desired cell population is at such low frequencies in the blood (predicted < 0.0003% at the earlier time-points). Moreover, it is difficult to distinguish between ring-stage infected and uninfected erythrocytes without the use of

intracellular DNA dyes and it is not clear what affect these dyes may have on parasite viability and/or gene expression.

Analysis of parasite *var* gene expression in samples isolated at C +10 (for two volunteers, and C +11 (for the remaining three volunteers) revealed the broad expression of variants, consistent with observations from the blood-stage CHMI. Furthermore, variants associated with all subgroups (A, B/A, B, B/C, C and E) were detected across the cohort. *Var* genes detected with highest associated read counts were largely of the group-B and group-A subclasses following mosquito-bite challenge, but demonstrated a variable hierarchy across volunteers. Interestingly, the only two variants detected in all 5 individuals (MAL6P1.1 and PFD0005w) have been reported as the most abundantly expressed variants in two previous studies of mosquito-bite CHMI (Wang *et al.* 2009, Bachmann *et al.* 2016). Moreover, the group-A *var* gene; PFD0020c, detected with some of the highest read counts in 3/5 volunteers in this study, was reported as the 4th and 5t^{h} most highly expressed by Wang *et al* and Bachmann *et al*, respectively (Wang *et al.* 2009, Bachmann *et al.* 2016), demonstrating consistency between the three datasets. Interestingly, this group-A *var* gene variant encodes a PEMP1 protein with an N-terminal region containing DBLα1.7 and CIRDα1.4 (domain cassette13) (Rask *et al.* 2010), and has been linked to severe malaria disease (CM) through its capacity to bind human brain endothelial cells (Claessens *et al.* 2012, Lavstsen *et al.* 2012, Bertin *et al.* 2013, Turner *et al.* 2013, Almelli *et al.* 2014). Based on results from the previous blood-stage CHMI study, parasite *var* gene/PfEMP1 expression is not predicted to influence host immune responses at this early stage of infection. However, it will be interesting to assess host immune responses in these volunteers, given the differing *var* gene expression profiles between these individuals and those following mosquito-bite challenge. Samples of whole blood were collected for transcriptional analysis of the host response in this trial, but results are yet to be analysed.

Despite overlapping expression of *var* gene variants across this cohort, expression hierarchies varied between volunteers. This was reflected in the proportional distribution of *var* gene read counts, by *var* gene group. When compared to the (almost) identical patterns of *var* gene expression observed in volunteers following direct blood inoculation (blood-stage challenge), this observation suggests that *var*

gene recombination events that occur in the mosquito-vector may be driving variability in *var* gene expression profiles before entry to the blood-phase. However, this study was limited to the analysis of *var* gene expression in parasites recovered from the third blood cycle in these volunteers, and it may be that switching events occur during the first two cycles in the blood. This will be important to investigate in future studies, assuming an appropriate method becomes available. This study was also limited by the small cohort, and by the reduced gene coverage in 2 of the 5 volunteers. Therefore, it will be important to validate these findings with use of a much larger cohort, and ideally at more time points during infection. It is also important to consider that all CHMI studies of *P. falciparum* gene expression to date have been done using the 3D7 or the parental NF54 laboratory strain of the parasite (Peters *et al.* 2002, Lavstsen *et al.* 2005, Wang *et al.* 2009, Bachmann *et al.* 2016). It is therefore essential that other strains of the *P. falciparum* species be tested in studies of CHMI, for validation of findings.

Chapter 6: General discussion and Future Directions

6 General discussion and Future Directions

In order to reduce the burden associated with malaria disease, focus needs to be placed on understanding what drives pathogenesis in those at greatest risk. Most observations of human malaria are based on studies conducted at a time when the infection has already led to disease, making it difficult to identify the initiating immune events that may be driving severe disease outcome. Furthermore, the expression of *Plasmodium falciparum* erythrocyte membrane 1 (PfEMP1), along with other variant surface antigens (VSAs), is thought to influence clinical outcome, by mediating the parasite-host interactions that contribute to the obstruction of blood flow and organ dysfunction. However, despite clear associations between group-A, B/A PfEMP1 and severe disease in patients presenting to the clinic, little is known about their expression at the onset of infection. Importantly, not all individuals exposed to *P. falciparum* for the first time develop severe disease and evidence from studies of experimental human malaria infection support marked inter-individual variability in host responses (Walther *et al.* 2006, Burel *et al.* 2017). Yet, out-with the well-described red cell polymorphisms associated with protection, factors influencing diversity in the host response to *P. falciparum* have not been well defined. Therefore, to better understand what drives severe malaria disease, we need to investigate the early parasite-host interactions that are predicted to dictate outcome of infection in the non-immune host.

The aim of this thesis was to investigate patterns of host and parasite gene expression early during infection in the malaria-naïve and to determine the influence of parasite VSA expression on the developing host immune response, and vice versa. This chapter seeks to provide a general overview of findings, limitations of this project and recommendations for future studies. Discussed first will be the host response to *P. falciparum* infection, followed by our analysis of parasite gene expression in the malaria naive host.

6.1 The early host response to primary *P. falciparum* infection

It is increasingly evident that individuals produce diverse responses to *P. falciparum,* yet few studies have been designed in a way that is conducive to the assessment of inter-individual variation. By sampling volunteers over a time-course throughout infection, this study allowed each volunteer to be treated as their own experiment. Furthermore, with use of the blood-stage CHMI model, variables such as liver to blood

inoculum load, and the timing of parasites entering the host circulation (as is expected with use of the mosquito-bite challenge model), could be excluded. This study was therefore uniquely designed to assess inter-individual variation in host immune responses during primary *P. falciparum* infection, and to allow us to investigate the earliest of immune events.

In chapter 3, our analysis of the host (whole blood) transcriptome response to *P. falciparum* infection is presented. These data were complemented by the quantification of cytokines and chemokines in host plasma and parasite growth in the blood, the assessment of haematological perturbations (full blood counts) and the monitoring of clinical adverse events.

6.1.1 Overview of key findings

6.1.1.1 Activation of the immune response and inter-individual variation

An important observation from this study was that 4 volunteers (29% of the cohort) did not produce a detectable transcriptional response, despite having parasite densities comparable to (or exceeding) those who demonstrated marked differential expression of genes in response to *P. falciparum*. This suggests that the parasite density threshold required for activation of the immune response is variable between individuals, something which has only before been suggested in historical studies of malaria-therapy (Glynn and Bradley 1995, Molineaux *et al.* 2002, Dietz *et al.* 2006). In those that did react, a dichotomous pattern of gene expression was detected, confirming inter-individual variability in the early host response. Surprisingly, 2 volunteers demonstrated down-regulation of genes associated with inflammation, cell signaling and metabolism. Moreover, IPA predicted the inhibition of pathways such as interferon signalling and TREM-1 signalling in this group of volunteers. To our knowledge, this study is the first to document this “non-classical” type of response, whereby inflammation is actively suppressed during primary *P. falciparum* infection. On the other hand, 8 volunteers demonstrated up-regulation of genes that were classically associated with innate inflammation.

6.1.1.2 The early host inflammatory response

6.1.1.2.1 Cytosolic sensing of *P. falciparum*

Studies *in vitro*, murine models and human infection have implicated a range of parasite associated molecular patters (PAMPs) and host pattern recognition receptors (PRRs) in initiating the inflammatory response to *Plasmodium,* as has been previously reviewed (Gazzinelli and Denkers 2006, Liehl and Mota 2012, Gazzinelli et al. 2014, Liehl et al. 2014, Oviedo-Boyso et al. 2014). However, evidence has been largely context and species dependent. In the 8 individuals that demonstrated an inflammatory transcriptional signature in this study, among the most up-regulated genes were DDX58 (RIG-I), IFIH1 (MDA5) and TLR7. All three of these cytosolic PRRs are responsible for the detection of RNA (Akira *et al.* 2006, Goubau *et al.* 2013, McNab *et al.* 2015). Interestingly, there is evidence to suggest that RIG-1 and MDA5 may also recognise certain AT-rich DNA motifs, although this is controversial (Goubau *et al.* 2013). Another cytosolic PRR found to be up-regulated in the dataset was AIM2, which recognises double-stranded DNA. This protein has been shown to serve as a potent activator of the inflammasome complex, by initiating the recruitment of caspase-1 precursor and processing of interleukin-1 beta and interleukin-18 (Latz 2010). Genes associated with the NLRP3 inflammasome, including PR2X7 and CASP1, were also expressed. Evidence for dual activation of the AIM2 and NLRP3 inflammasomes has been previously reported in a study of *P. berghei* ANKA infection whereby parasite-produced haemozoin and DNA were thought to be the key inducers of the systemic inflammation (Kalantari *et al.* 2014). As *P. falciparum* infects red blood cells and not leukocytes, it is unclear how parasite nucleic acids come into contact with host cytosolic sensors. However, recent evidence suggests this process may occur though the internalisation of parasite secreted extracellular vesicles (EVs), containing parasitic small RNA and/or genomic DNA (Sisquella *et al.* 2017). In this study by Sisquella *et al,* human monocytes were shown capable of this interaction, via expression of the Stimulator of Interferon genes (STING) cytosolic DNA sensor, resulting in downstream activation immune genes including Type I IFNs.

6.1.1.2.2 Interferon-signalling

Pathway analysis revealed “interferon signaling” to be the most significantly enriched pathway in the response of the 8 inflammatory volunteers. Consistently, both RIG-I and

MDA5 (discussed above) have been widely associated with the induction of Type I IFNs (Yoneyama and Fujita 2004, Kawai *et al.* 2005, Gitlin *et al.* 2006, Kawai and Akira 2006, Besch *et al.* 2009, Broquet *et al.* 2011, McNab *et al.* 2015, Ho *et al.* 2016, Maria *et al.* 2017), suggesting a key role for these cytokines in the early response to *P. falciparum.* This observation is in line with previously reported results from studies in both mouse models of *Plasmodium* infection (Rocha *et al.* 2015, Spaulding *et al.* 2016, Yu *et al.* 2016, Zander *et al.* 2016) and CHMI (Montes de Oca *et al.* 2016, Gardinassi *et al.* 2018), suggesting a "classical" type response from these 8 volunteers. Interestingly, data from both mouse and human models of *Plasmodium* infection have shown an ability of Type I IFNs to suppress IFNγ-driven cellular responses at the early stages of *Plasmodium* infection (Haque *et al.* 2014, Montes de Oca *et al.* 2016). Yet, data from this study suggest that both Type I (IFNα/β) and Type II IFNs (IFNγ) are important mediators in the early response to *P. falciparum*, as CXCL9 and CXCL10 (both induced by IFNγ) were found elevated at the transcript and protein level in these 8 individuals. Importantly, there is substantial overlap in the genes that Type I and Type II IFNs regulate, making it is difficult to interpret whether one type may dominate over the other in this infection setting. Furthermore, there is evidence to suggest that the two can work cooperatively, through the regulated expression of STAT1 (Gough *et al.* 2010), although the mechanisms of this crosstalk have not been defined in the context of *Plasmodium* infection. Surprisingly, IFNγ was not found elevated in host plasma until C +10 (48 hours after the first transcriptional responses could be detected), and only in the 3 most inflammatory volunteers. Furthermore, no detectable increase in circulating IFNα (Type I IFN) was observed throughout. This was another important observation, as it suggests that the initial IFN-signalling event may be occurring in host tissue(s), out-with the blood. In line with this hypothesis, there is evidence to suggest that during severe *P. yoelli* infection in mice, Type I IFNs are largely produced by plasmacytoid DCs in the bone marrow (Spaulding *et al.* 2016).

6.1.1.2.3 Evidence for a role of myeloid cells

Activation of the inflammasome signaling pathway was predicted among the top ten pathways significantly enriched within the group of the 8 inflammatory volunteers, suggesting a key role for myeloid cells in their response. In line with this, TREM-1 (Triggering Receptor Expressed on Myeloid Cells 1)-signalling was also predicted with high significance. This protein is expressed on monocytes, macrophages and

neutrophils (Bouchon *et al.* 2000, Zanzinger *et al.* 2009). Interestingly, full blood count analysis did not reveal any fluctuations in circulating monocytes and neutrophils throughout the course of infection, contradictory to what has been reported in previous studies of CHMI (Antonelli *et al.* 2014, Teirlinck *et al.* 2015), and in studies of infection in the field (Chimma *et al.* 2009, Ogonda *et al.* 2010, Ataide *et al.* 2014, Dobbs *et al.* 2017, Patel *et al.* 2017). However, CXCL10 (produced in large quantities by monocytes), was among the top 10 most up-regulated genes in this group, and was found significantly elevated in the plasma of these volunteers. This protein serves as a chemoattractant for monocytes/macrophages, as well as other cell types including T cells, NK cells and dendritic cells. Interestingly, the response of these 8 volunteers was associated with a significant drop in circulating lymphocytes. Furthermore, CXCL10 was detected in plasma before IL-8 (the chemoattractant for neutrophils) could be observed. Thus, given their capacity to phagocytose and their location in the blood, it is reasonable to speculate that monocytes are among the earliest of cell types responding to *P. falciparum* infection. Evidence from *in vitro* studies has demonstrated an ability of these cells to phagocytose PEs and parasite-secreted EVs, independently of malaria-specific antibodies (Su *et al.* 2002, Sisquella *et al.* 2017). There is also evidence to suggest that ring-stage PEs can be opsonised by complement proteins and natural IgG, and thus targeted for destruction via complement and Fc receptor-dependent pathways (Turrini *et al.* 1992, Ayi *et al.* 2004). Interestingly, the gene encoding FCγR1 (high affinity IgG Fc receptor) was among the top 10 most up-regulated for all 8 volunteers in this group. A recent study has highlighted an ability of monocytes, via expression of a cytosolic DNA sensor, to interact with parasite nucleic acids through phagocytosis of *P. falciparum*-secreted EVs, resulting in downstream activation of Type I IFN responses (Sisquella *et al.* 2017). If the cytosolic receptors found up-regulated in our dataset (RIG-I, MDA5, TLR7 and AIM2) are also capable of this interaction, data presented by Sisquella *et al* may provide the link between the host transcriptional responses reported in our volunteer cohort.

Overall, observations from our study of the early host response to blood-stage *P. falciparum* (3D7) suggest that onset of inflammation likely involves cytosolic host PRRs such as RIG-I, MDA5, AIM2 and TLR7 for the detection of parasite nucleic acids. Activation of these PRRs may lead to the production of Type I IFNs (via RIG-I and MDA5), engagement of the AIM2 and NLRP3 inflammasome complexes in myeloid

cells, the recruitment of immune cells via IFNγ-induced CXCL9 and CXL10, Fc receptor-dependent phagocytosis of PEs by monocytes/macrophages, and the production of pro-inflammatory cytokines, which may be amplified by TREM-1 expression. However, the resulting outcome of the response is difficult to predict.

6.1.1.3 Predicting clinical outcome in the non-immune host

The ethical necessity to treat volunteers before the onset of clinical symptoms in CHMI, precludes our ability to determine disease severity in these 8 inflammatory volunteers. Within the most up-regulated genes expressed by this group, however, were those encoding the chemokines CXCL9 and CXCL10, both of which are considered robust biomarkers of severe malaria disease (Schofield and Grau 2005, Jain *et al.* 2008, Ayimba *et al.* 2011, Wilson *et al.* 2011). Moreover, their transcriptional response coincided with a significant drop in lymphocytes (lymphopenia in three volunteers), which has been reported in malaria patients exhibiting high levels of inflammation in the natural infection setting (Hviid *et al.* 1997). Individuals in this group also reported more frequent and more adverse symptoms, compared to volunteers that did not share this inflammatory transcriptional response. These data thus highlight CXCL9, CXCL10 and lymphopenia as potential biomarkers of disease for use with the CHMI model, something currently lacking. Interestingly, levels of angiopoietin-2 (ANG-2) were found elevated in the most inflammatory volunteer in this group. In the context of malaria infection, increased levels of ANG-2 have been widely associated with severe clinical outcome (Viebig *et al.* 2005, Yeo *et al.* 2008) and more recently, as a predictor of mortality in patients presenting with cerebral malaria (Lovegrove *et al.* 2009, Conroy *et al.* 2012).

In mouse and human models documenting the early production of Type I IFNs during *Plasmodium* infection, this response has been predominantly associated with impaired immune cell responses, unregulated parasite growth and poor host outcome (Haque *et al.* 2014, Rocha *et al.* 2015, Montes de Oca *et al.* 2016, Spaulding *et al.* 2016, Zander *et al.* 2016). In other disease models such as *Listeria monocytogenes* (in mice) and Tuberculosis (mouse and human infection), Type I IFNs have been shown to exert inhibitory effects on immune cells, leading to higher infection burdens and disease (Auerbuch *et al.* 2004, Carrero *et al.* 2004, Berry *et al.* 2010, Desvignes *et al.* 2012, McNab *et al.* 2015). However, their protective role during the host response to viral

infections has been well described (Isaacs and Lindenmann 1957, Muller *et al.* 1994, Schneider *et al.* 2014). Hence, the extent to which Type I IFNs mediate either pathology or protection during primary infection remains to be defined. Also predicted to be activated in these volunteers was the inflammasome pathway and TREM-1 signalling. In mice infected with *P. chabuadi* AS, caspase-1 activation via the NLRP3 inflammasome results in high-level production of IL-1β, and lethal outcome (Ataide *et al.* 2014). Furthermore, a significant increase in the frequency of circulating $CD14^{+}CD16^{-}Caspase\text{-}1^{+}$ and $CD14^{dim}CD16^{+}Caspase\text{-}1^{+}$ monocytes has been reported in the peripheral blood mononuclear cells from febrile patients (Ataide *et al.* 2014). In the broader context of human disease, inflammasome signaling has been implicated in a variety of inflammatory processes and disorders, as has been reviewed (Strowig *et al.* 2012). TREM-1 signalling has been causally implicated in rodent models of inflammatory pathologies, including sepsis (Charles *et al.* 2016), and this is consistently linked to elevated monocyte TREM-1 and plasma sTREM-1 in the corresponding human condition. In malaria infection, TREM-1 has been found at elevated levels on monocytes, and in plasma (sTREM-1) of patients with severe disease (Adukpo *et al.* 2016). Thus, it is plausible to speculate that the 8 volunteers would have gone on to develop severe malaria disease if left untreated. However, the inflammatory response has also been implicated in a protective capacity, in the early control of parasite growth. For instance, the phagocytosis of parasitised erythrocytes (PEs) and merozoites, by myeloid cells, is thought to be important for controlling parasite growth in non-immune individuals based on evidence that this can occur in the absence of malaria-specific antibodies (Trubowitz and Masek 1968, Su *et al.* 2002). Furthermore, in malaria infected humans and mice, haemozoin-laden myeloid cells are found abundant in the blood and particularly the spleen- the primary site of PE clearance (Coban *et al.* 2010). Therefore, it was important to consider the relationship between host immune responses and parasite growth in the blood.

6.1.1.4 Relationship between early host immune responses and parasite growth in the blood

Parasite multiplication rates (PMRs) in this cohort of individuals were similar to those reported in other studies of CHMI with *P. falciparum* (mean: 10 and range: 6.7 – 12.8) (Roestenberg *et al.* 2012, Sheehy *et al.* 2012, Sheehy *et al.* 2013). Importantly,

parasite densities at time of diagnosis were not sufficient to explain the inflammatory response of the 8 “classical” responders. Furthermore, there was no evidence to suggest that the rate of parasite growth in the blood influenced the host transcriptional response, or vice versa. Thus, the 8 volunteers who elicited an early inflammatory response had no better control of parasite growth in the circulation than those who failed to respond. Results from this study thus contest evidence that suggest a key role for the innate immune response in controlling parasite growth early during infection in the non-immune host (Trubowitz and Masek 1968, Clark *et al.* 1987, Taverne *et al.* 1987, Turrini *et al.* 1992, Tsutsui and Kamiyama 1999, McGilvray *et al.* 2000, Su *et al.* 2002, Omer *et al.* 2003, Ayi *et al.* 2004, Walther *et al.* 2005, Walther *et al.* 2006, Robinson *et al.* 2009, Coban *et al.* 2010, Horowitz *et al.* 2010, Willcocks *et al.* 2010). It is important to consider that this evidence has largely been derived from studies carried out *in vitro*, or in mouse models whereby parasite growth kinetics are highly variable between species, and are not necessarily representative of those observed in human *Plasmodium* infections. Importantly, recent reanalysis of data from studies of malaria-therapy suggest that the acquisition of clinical immunity, following repeated re-exposure to *Plasmodium*, is not associated with a reduction in parasite density during the first few infections (Molineaux *et al.* 2002). The same observation has more recently been reported in a large cohort of Tanzanian children (Goncalves *et al.* 2014), highlighting disconnect between the animal models and human infection studies used to investigate the innate immune response during *Plasmodium* infection in the naïve host.

6.1.2 Study limitations

Results from our study of the early host immune response, in conjunction with parasite growth kinetics raise some important questions. For example, is there really a protective function of the innate immune response early during primary infection? Although we saw no evidence for reduced parasite growth during the first ~5 - 6 replication cycles in the blood, we need to consider what effect it may have on sequestered parasites- something that was not assessed in his study. Hence, are we missing evidence for this protective function because it’s happening in the tissues? There is convincing data to show that myeloid cells are able to phagocytose PEs in the spleen, for instance, as haemozoin-laden macrophages have been found abundant in this tissue during human malaria-infection (Coban *et al.* 2010). Yet, whether this is a

feature associated with the early response during primary infection remains unclear. Furthermore, results from this study suggest that initial immune signalling events during the host response to primary *P. falciparum* infection may involve cells located in tissue(s), outwith the blood. This highlights an important limitation of CHMI, and human studies of *Plasmodium* infection more generally, in that current ethical constraints limit our analysis to immune events occurring in host circulation. Malaria is a multi-organ disease involving tissues such as the liver, bone marrow and spleen (Del Portillo *et al.* 2012, Joice *et al.* 2014, Punsawadl *et al.* 2014, Viriyavejakul *et al.* 2014, Obaldia *et al.* 2018) and there are likely important parasite-host interactions occurring at these sites. A central, protective role of the spleen, for instance, has been well described (Chotivanich *et al.* 2002, Engwerda *et al.* 2005, Del Portillo *et al.* 2012). Although many crucial insights into the immune response during *Plasmodium* infection have been gained with use of murine models (Wykes and Good 2009), none fully recapitulate malaria infection in the human host. Therefore, it is likely that future studies of the early host immune response would benefit from continued use of non-human primate models (Cox-Singh *et al.* 2010, Langhorne *et al.* 2011) and/or access to human tissue biopsies, assuming the necessary ethical approvals can be granted.

By selecting to analyse the whole blood response to *P. falciparum*, we have been able to provide an overview of the early transcriptional events. Yet, this study was limited in its ability to dissect the function of specific immune cell subsets in the early host response. Furthermore, it is important to consider that our analysis of the host transcriptional response may not necessarily translate at the protein level. Although we were able to validate the up-regulated expression of certain genes by screening for their corresponding proteins in the plasma, it was not feasible to screen for everything we found differentially expressed.

A key finding reported in this work was the inter-individual variation in host immune responses. However, we were unable to correlate these immune response variables with disease outcome, due to the stringent diagnosis cut-offs used in CHMI. This represents the major limitation of this study. Switching to a higher parasite density cut-off for diagnosis would likely benefit future studies, although may not be feasible due to ethical concerns. An important consideration with use of the CHMI model for studying the host immune response is that volunteers are of adult age (>18 years), and there

are some well-characterised differences between the immune systems of adults and children (Elahi *et al.* 2013, Krow-Lucal *et al.* 2014, Levy and Wynn 2014, Kollmann *et al.* 2017). Furthermore, age-dependent characteristics of clinical outcome in malaria (Baird 1998, Baird *et al.* 1998, Dondorp *et al.* 2008) suggest that progression to severe disease may occur through distinct mechanisms in children. Therefore, findings presented here may not be fully representative of the early immune events occurring during natural *P. falciparum* infection in children <5 years of age- i.e. those at greatest risk of severe disease.

Nevertheless, this study provides important insight into the diversity in early host immune responses to primary *P. falciparum* infection, and highlights an important gap in our understanding of how differing immune responses, at the onset of infection, may contribute to the diversity in clinical outcomes observed at the later stages of disease.

6.1.3 Future considerations

A key finding reported in this work was the inter-individual variation in host immune responses. However, this study is limited in statistical power due to the small number of volunteers (n = 14), of which only 2 produced the “non-classical” type response. It is therefore crucial to test the reproducibility of this observation, using a much larger cohort of individuals, over repeated studies of CHMI. It will also be important to do this using both mosquito-bite and blood-stage challenge models, to explore any differences between the two infection routes. Importantly, our analysis of the host response excluded non-coding transcripts, such as micro RNAs (miRNAs). Yet, microRNAs are important regulators of the immune response, and there is recent evidence to suggest that inter-individual variability during *P. falciparum* infection is also reflected in this non-coding fraction of the host transcriptome (Burel *et al.* 2017). Future analysis should therefore be extended to non-coding, as well as coding transcripts.

Our data give evidence for a transcriptional signature of myeloid cells in the whole blood transcriptional response to *P. falciparum*. These cells are likely important mediators of the response to *P. falciparum*, given their ability to phagocytose and to produce large quantities of inflammatory cytokines. However, their role in protection and/or pathogenesis during primary infection remains to be defined (Serghides *et al.* 2003, Silver *et al.* 2010, Chua *et al.* 2013, Weinberg *et al.* 2016, Dobbs *et al.* 2017).

Thus, future work should consider a focused analysis of monocytes and neutrophils, to determine their activation status during primary *P. falciparum* infection, as well as their contribution to the diversity in host responses. A time-course analysis of these cells would likely give insight into the order and timing of key transcriptional events. Furthermore, experiments designed to test the functional capacity of these cells would also be of interest. For instance, incubating monocytes with parasite-infected RBCs to monitor phagocytic uptake or by re-stimulating these cells *ex vivo*, using *P. falciparum* lysate, to assess cytokine responses, and potential variability between volunteer samples.

6.2 Parasite gene expression in the naïve host

There is substantial evidence for an association between the expression of *P. falciparum* variant surface antigens, in particular group-A and/or group-B/A PfEMP1, and severe clinical outcome (Kirchgatter and Portillo Hdel 2002, Bull *et al.* 2005, Kaestli *et al.* 2006, Kyriacou *et al.* 2006, Rottmann *et al.* 2006, Normark *et al.* 2007, Falk *et al.* 2009, Warimwe *et al.* 2009, Kalmbach *et al.* 2010, Lavstsen *et al.* 2012, Warimwe *et al.* 2012, Bertin *et al.* 2013, Almelli *et al.* 2014, Abdi *et al.* 2015, Bertin *et al.* 2016, Jespersen *et al.* 2016, Mkumbaye *et al.* 2017, Shabani *et al.* 2017, Tonkin-Hill *et al.* 2018). However, the extent to which these variants actually drive pathology has been difficult to assess as little is known about their expression at the onset of infection. Hence, their influence on the developing host immune response, and disease severity, remains elusive. This is also true for the other parasite VSAs with predicted disease-causing characteristics, such as the RIFINSs and STEVORs. Given that severe disease is almost exclusively associated with the very young, having had little or no previous exposure to the *Plasmodium* parasite, our cohort of malaria-naïve volunteers represented an opportunity to assess parasite (*var*, *rif* and *stevor*) expression during the volunteers' first infection.

6.2.1 Overview of key findings

6.2.1.1 *Rif* and *stevor* gene expression in the malaria-naïve host

In most parasites, RIFIN and STEVOR proteins (encoded by the *rif* and *stevor* multi-gene families) are found expressed along with PfEMP1 (Fernandez *et al.* 1999, Kyes *et*

al. 1999, Kaviratne *et al.* 2002), suggesting that they may be involved in key parasite-host interactions during primary *P. falciparum* infection. Furthermore, RIFINS have been implicated in severe malaria given their ability to form rosettes upon binding to uninfected red cells (Goel *et al.* 2015). In this study the majority of detectable *rif* variants were transcribed at very low levels, whereas one A-type *rif* variant (PFD0070c/ PF3D7_0401600) was dominantly expressed in all. Although there is limited information available with regards to its function, this RIFIN protein appears to be strain-transcendent, having been detected in 3D7, HB3, IT and Dd2 *P. falciparum* strains (Claessens *et al.* 2011). Interestingly, this *rif* gene variant was also found dominantly expressed in volunteers following mosquito-bite CHMI. It is thus of considerable interest to better characterise the function of this protein, and its interactions with host cell receptors.

Just 3 (of 32) *stevor* variants were detected in this dataset (PF3D7_0832000, PF3D7_0300900 and PF3D7_0617600), and all at very low levels. This is likely due to the late stage expression of the *stevor* multi-gene family (22–32 hours post infection) (Kaviratne *et al.* 2002, Lavazec *et al.* 2007), on more mature stages (trophozoites and schizonts) that are sequestered in the microvasculature (Miller *et al.* 2002). Parasites isolated from the blood are thus not suitable for investigating expression patterns of this multi-gene family during infection in the human host.

6.2.1.2 *Var* gene expression in the malaria-naive host

Group-A, B/A disease-associated *var* gene/PfEMP1 variants are predicted to dominate expression in the non-immune host. Furthermore, these variants are thought to confer a growth advantage over others in this infection setting, through mechanisms that afford them promiscuity in host cell receptor binding (Abdi *et al.* 2017). Results from this study contradict these hypotheses, showing broad-level detection of variants (95% of the total *var* gene repertoire), with highest expression coming from the group-B subclass. Importantly, these results were consistent with two other studies of parasite *var* gene expression during CHMI (Wang *et al.* 2009, Bachmann *et al.* 2016). The 6 most highly expressed *var* genes in our study (PF10_0406, PFL0005w, MAL7P1.55, PFD1005c, PFD1015c and PF11_0007) were small group-B and C PfEMP1, with structures comprising the semi-conserved DBLα0-CIDRα head structure commonly associated with CD36 binding) (Smith *et al.* 2001, Robinson *et al.* 2003). The

relationship between CD36 binding and pathogenesis has not been well defined, with alternative lines of evidence supporting contradictory models (Newbold *et al.* 1997, Rogerson *et al.* 1999, Aitman *et al.* 2000, Pain *et al.* 2001, Mackintosh *et al.* 2004). Clumping of PEs has been associated with severe disease, and appears to be predominantly mediated by CD36 expressed on platelets (Pain *et al.* 2001). Yet, parasites from children with cerebral malaria tend to have relatively lower CD36 binding (Newbold *et al.* 1997, Rogerson *et al.* 1999) and in more recent studies have been linked to the EPCR-binding (group-A, B/A PfEMP1) variants containing domain cassettes 8 and 13 (Jensen *et al.* 2004, Kyriacou *et al.* 2006, Bertin *et al.* 2013, Almelli *et al.* 2014, Almelli *et al.* 2014). These group-A, B/A variants were detected at some of the lowest levels in this blood-stage challenge trial, and we found no evidence for the group-A, B/A PfEMP1s having a growth advantage upon comparison of rlog expression values across parasite populations with high, intermediate or slow PMRs.

It is reasonable to speculate that in the absence of anti-PfEMP1 specific antibodies (as would be expected during primary infection in the naïve host), *var* gene switching mechanisms are not required. Instead, parasite survival strategies might favour the broad expression of all (or most variants), for sampling the availability of host cell receptors upon entry into a new host. In the limited number of studies that have investigated *var* gene expression in this *in vivo* setting, the majority support this hypothesis, by showing broad-level detection of *var* genes in non-immune volunteers (Lavstsen *et al.* 2005, Wang *et al.* 2009, Bachmann *et al.* 2016). Offering further support to this hypothesis are results presented in chapter 4 of this thesis. With use of the blood-stage challenge model we have been able to directly compare *var* gene expression profiles of parasites isolated from the inoculum used to infect (day 0) and parasites recovered following a further 5 - 6 cycles, in the same infection (volunteer diagnosis samples). Importantly, *var* gene expression patterns between these different stages of infection were found to be significantly positively correlated, as the dominantly expressed variant in the inoculum on day 0 was still the most dominantly expressed in cycles 5 and 6. This suggested that *var* gene switching had not occurred within this time-window. Moreover, parasites isolated from each of the 12 volunteers (for which RNA-seq was successful), demonstrated remarkably similar expression profiles. This was another important observation from our study, as it gives first evidence that factors driving inter-individual variability in host responses to

P. falciparum, during primary infection, appear independent of parasite *var* gene expression, and vice versa; the type of early host immune response elicited has little influence of parasite *var* gene expression.

Although based on a small cohort of n = 5, *var* gene expression profiles measured at C +11 post mosquito-bite CHMI appeared to be more variable between volunteers (chapter 5, figures 5.8 and 5.9), compared to those following blood-stage challenge (chapter 4, figure 4.13). These results, combined with observations from the blood-stage CHMI, suggest that *var* gene/PfEMP1 expression may be randomly selected in the mosquito vector, or liver stages, and upon entry into the circulation remains random (and unchanged) until activation of host antibody responses, when immune pressures may then force selection of specific variants. However, it is presumed that the first signs of malaria disease are apparent before this time. As was shown in the blood-stage challenge, some volunteers had started to develop symptoms of malaria within the time-frame we were able to assess, yet none of the group-A disease-associated variants were found to be expressed in their infecting parasite populations. Furthermore, parasite gene expression had no apparent influence on the inter-individual variability in immune responses observed in this cohort. Although we cannot be sure of the severity of outcome in the volunteers, these findings challenge some key concepts in the field. For instance, expression of group-A, B/A PfEMP1 is not driving, nor is required for disease outcome in the malaria-naive. Moreover, *var* gene expression does not influence the host immune response during primary exposure, and vice versa.

6.2.2 Study limitations

A key finding of this study was that *var* gene switching does not appear to take place during the first 5 - 6 blood cycles in the malaria-naïve host. However, this study was not able to examine *var* gene expression upon immediate egress from the liver, and it may be that switching events occur during these early time points. Therefore, it was important to try and extend our analysis to earlier stages of infection, to determine any influence of parasite *var* gene expression at the onset of host immune responses. In chapter 5 of this thesis, a protocol for the *ex vivo* RNA sequencing of parasites was optimised for application to parasite densities of ~40 – 400 p/mL, as expected immediately following liver egress (cycles 1 and 2). However, in parasites isolated at

C +9 and C +10 post mosquito-bite CHMI (~ cycle 2 in the blood of these volunteers), a markedly reduced number of *P. falciparum* genes (including VSAs) could be detected compared to the later time-point of C +11, and to the diagnosis time-point range (C +7.5 – C +10.5) in the previous blood-stage challenge trial. Results suggested that this was due to a combination of low parasite densities at these time-points but also host contamination, highlighting the two biggest technical challenges in using the CHMI model for this type of analysis. Hence, despite efforts, our method for parasite isolation and RNA-seq appears restricted to cycle 3 onwards, thereby precluding our ability to assess parasite VSA expression any earlier during infection in the naïve host. Only with improved sensitivity of currently available sequencing technologies and more efficient methods for parasite isolation, will this analysis be possible. It is also important to consider that all CHMI studies of *P. falciparum* gene expression to date, have been done using the 3D7 or the parental NF54 laboratory strain of the parasite (Peters *et al.* 2002, Lavstsen *et al.* 2005, Wang *et al.* 2009, Bachmann *et al.* 2016). It is therefore essential that other strains of the *P. falciparum* species be tested in studies of CHMI, for validation of findings.

6.2.3 Future considerations

A key novel finding from our analysis of *P. falciparum* gene expression in the naive host, was that parasite VSA expression (*var* and *rif*) had no apparent influence on the diversity of immune responses observed in the volunteer cohort. This raises an important question: what drives inter-individual variation in the host response to *P. falciparum*? The immune system is thought to be shaped by many different factors such as host genetics, environmental stimuli, the gut microbiome and the various different microbes that an individual encounters in their life time. In recent years, great effort has been made to better understand the factors that determine variability of host immune responses. Key studies, including those performed as part of the Human Functional Genomics Project, have provided some crucial insight (Brodin *et al.* 2015, Li *et al.* 2016, Oosting *et al.* 2016, Schirmer *et al.* 2016, Ter Horst *et al.* 2016, Piasecka *et al.* 2018). In one study, 700 healthy individuals were genotyped in order to assess the impact of genetic heritability on the cytokine production capacity of isolated cells, following stimulation with pathogenic stimuli. Results, when analysed alongside the ~8.0 million detected SNPs, revealed a strong influence of host genetics on inter-individual variation. Furthermore, researchers identified 17 novel eQTLs (genetic

variants that impact transcript abundance for immune genes), most of which were found enriched within monocyte-specific enhancer regions (Li *et al.* 2016). Non-genetic factors, such as age and gender, have also been shown to influence cytokine production. For instance, older age is associated with defects in the production of T-helper cell cytokine responses including IL-22 and IFN**γ**, whereas the production of monocyte-derived cytokines does not appear to be affected (Ter Horst *et al.* 2016). In another study, the affect of age was found to be stimulus-specific, with 40% of genes presenting age-dependent expression in only one or two conditions tested (*E.coli*, BCG, SEB, *C.albicans*, Influenza-A virus). Moreover, the mapping of expression quantitative trait loci (eQTLs) revealed that genetic factors had a stronger effect on variable immune gene regulation than age (Piasecka *et al.* 2018). In addition to host factors, the immune responses of an individual are also likely to be influenced by the environment. Interestingly, environmental factors such as body mass index (BMI) and use of the contraceptive pill were shown to affect circulatory levels of inflammatory mediators including IL-6, IL-18 and IL-1Rα, C-reactive protein and VEGF (Ter Horst *et al.* 2016). The gut microbiome is also thought to be crucial for shaping and modulating immune system responses, as gut microbial dysbioses are commonly linked to aberrant cytokine responses in auto-immune and immune mediated disease (Kosiewicz *et al.* 2011, Gevers *et al.* 2014, Paun *et al.* 2016). As part of the Human Functional Genomics Project, differences in the composition and function of gut microbial communities were assessed to determine how they might contribute to inter-individual variation in the cytokine responses of 500 healthy humans (Schirmer *et al.* 2016). Importantly, between-subject variation in microbial composition was found to be substantial, and was predicted to account for ~5 - 10% of variation in host cell cytokine responses. Interestingly, the most pronounced effect of microbial variation was observed for the production of TNFα, in response to stimulation with C. *albicans* (Schirmer *et al.* 2016). Although the majority of studies discussed here have focused on responses to viral and/or bacterial stimulus, it is likely that host-intrinsic and/or environmental factors are also influencing the human immune response to *Plasmodium*.

Overall, this study provides important insight into the early host response to *P. falciparum* infection in the non-immune host. Our combined analysis of parasite and host gene expression suggest that early decisions of the innate immune response are what determine disease outcome in the malaria-naïve, and that host-intrinsic and/or environmental factors are most likely driving inter-individual variability in responses.

References

Abdel-Latif, M. S., K. Dietz, S. Issifou, P. G. Kremsner and M. Q. Klinkert (2003). "Antibodies to Plasmodium falciparum rifin proteins are associated with rapid parasite clearance and asymptomatic infections." Infect Immun **71**(11): 6229-6233.

Abdi, A. I., S. H. Hodgson, M. K. Muthui, C. A. Kivisi, G. Kamuyu, D. Kimani, S. L. Hoffman, E. Juma, B. Ogutu, S. J. Draper, F. Osier, P. Bejon, K. Marsh and P. C. Bull (2017). "Plasmodium falciparum malaria parasite var gene expression is modified by host antibodies: longitudinal evidence from controlled infections of Kenyan adults with varying natural exposure." BMC Infect Dis **17**(1): 585.

Abdi, A. I., S. M. Kariuki, M. K. Muthui, C. A. Kivisi, G. Fegan, E. Gitau, C. R. Newton and P. C. Bull (2015). "Differential Plasmodium falciparum surface antigen expression among children with Malarial Retinopathy." Sci Rep **5**: 18034.

Abdi, A. I., G. M. Warimwe, M. K. Muthui, C. A. Kivisi, E. W. Kiragu, G. W. Fegan and P. C. Bull (2016). "Global selection of Plasmodium falciparum virulence antigen expression by host antibodies." Sci Rep **6**: 19882.

Abrams, E. T., H. Brown, S. W. Chensue, G. D. Turner, E. Tadesse, V. M. Lema, M. E. Molyneux, R. Rochford, S. R. Meshnick and S. J. Rogerson (2003). "Host response to malaria during pregnancy: placental monocyte recruitment is associated with elevated beta chemokine expression." J Immunol **170**(5): 2759-2764.

Adukpo, S., B. A. Gyan, M. F. Ofori, D. Dodoo, T. P. Velavan and C. G. Meyer (2016). "Triggering receptor expressed on myeloid cells 1 (TREM-1) and cytokine gene variants in complicated and uncomplicated malaria." Trop Med Int Health **21**(12): 1592-1601.

Aidoo, M., D. J. Terlouw, M. S. Kolczak, P. D. McElroy, F. O. ter Kuile, S. Kariuki, B. L. Nahlen, A. A. Lal and V. Udhayakumar (2002). "Protective effects of the sickle cell gene against malaria morbidity and mortality." Lancet **359**(9314): 1311-1312.

Aitman, T. J., L. D. Cooper, P. J. Norsworthy, F. N. Wahid, J. K. Gray, B. R. Curtis, P. M. McKeigue, D. Kwiatkowski, B. M. Greenwood, R. W. Snow, A. V. Hill and J. Scott (2000). "Malaria susceptibility and CD36 mutation." Nature **405**(6790): 1015-1016.

Akira, S., S. Uematsu and O. Takeuchi (2006). "Pathogen recognition and innate immunity." Cell **124**(4): 783-801.

Almelli, T., N. T. Ndam, S. Ezimegnon, M. J. Alao, C. Ahouansou, G. Sagbo, A. Amoussou, P. Deloron and R. Tahar (2014). "Cytoadherence phenotype of

Plasmodium falciparum-infected erythrocytes is associated with specific pfemp-1 expression in parasites from children with cerebral malaria." Malar J **13**: 333.

Almelli, T., G. Nuel, E. Bischoff, A. Aubouy, M. Elati, C. W. Wang, M. A. Dillies, J. Y. Coppee, G. N. Ayissi, L. K. Basco, C. Rogier, N. T. Ndam, P. Deloron and R. Tahar (2014). "Differences in gene transcriptomic pattern of Plasmodium falciparum in children with cerebral malaria and asymptomatic carriers." PLoS One **9**(12): e114401.

Antonelli, L. R., F. M. Leoratti, P. A. Costa, B. C. Rocha, S. Q. Diniz, M. S. Tada, D. B. Pereira, A. Teixeira-Carvalho, D. T. Golenbock, R. Goncalves and R. T. Gazzinelli (2014). "The CD14+CD16+ inflammatory monocyte subset displays increased mitochondrial activity and effector function during acute Plasmodium vivax malaria." PLoS Pathog **10**(9): e1004393.

Arevalo-Herrera, M., D. A. Forero-Pena, K. Rubiano, J. Gomez-Hincapie, N. L. Martinez, M. Lopez-Perez, A. Castellanos, N. Cespedes, R. Palacios, J. M. Onate and S. Herrera (2014). "Plasmodium vivax sporozoite challenge in malaria-naive and semi-immune Colombian volunteers." PLoS One **9**(6): e99754.

Arevalo-Herrera, M., M. Lopez-Perez, E. Dotsey, A. Jain, K. Rubiano, P. L. Felgner, D. H. Davies and S. Herrera (2016). "Antibody Profiling in Naive and Semi-immune Individuals Experimentally Challenged with Plasmodium vivax Sporozoites." PLoS Negl Trop Dis **10**(3): e0004563.

Armah, H. B., N. O. Wilson, B. Y. Sarfo, M. D. Powell, V. C. Bond, W. Anderson, A. A. Adjei, R. K. Gyasi, Y. Tettey, E. K. Wiredu, J. E. Tongren, V. Udhayakumar and J. K. Stiles (2007). "Cerebrospinal fluid and serum biomarkers of cerebral malaria mortality in Ghanaian children." Malar J **6**: 147.

Ataide, M. A., W. A. Andrade, D. S. Zamboni, D. Wang, C. Souza Mdo, B. S. Franklin, S. Elian, F. S. Martins, D. Pereira, G. Reed, K. A. Fitzgerald, D. T. Golenbock and R. T. Gazzinelli (2014). "Malaria-induced NLRP12/NLRP3-dependent caspase-1 activation mediates inflammation and hypersensitivity to bacterial superinfection." PLoS Pathog **10**(1): e1003885.

Aucan, C., A. J. Walley, B. J. Hennig, J. Fitness, A. Frodsham, L. Zhang, D. Kwiatkowski and A. V. Hill (2003). "Interferon-alpha receptor-1 (IFNAR1) variants are associated with protection against cerebral malaria in the Gambia." Genes Immun **4**(4): 275-282.

Auerbuch, V., D. G. Brockstedt, N. Meyer-Morse, M. O'Riordan and D. A. Portnoy (2004). "Mice lacking the type I interferon receptor are resistant to Listeria monocytogenes." J Exp Med **200**(4): 527-533.

Austin, S. C., P. D. Stolley and T. Lasky (1992). "The history of malariotherapy for neurosyphilis. Modern parallels." JAMA **268**(4): 516-519.

Awandare, G. A., B. Goka, P. Boeuf, J. K. Tetteh, J. A. Kurtzhals, C. Behr and B. D. Akanmori (2006). "Increased levels of inflammatory mediators in children with severe Plasmodium falciparum malaria with respiratory distress." J Infect Dis **194**(10): 1438-1446.

Ayi, K., F. Turrini, A. Piga and P. Arese (2004). "Enhanced phagocytosis of ring-parasitized mutant erythrocytes: a common mechanism that may explain protection against falciparum malaria in sickle trait and beta-thalassemia trait." Blood **104**(10): 3364-3371.

Ayimba, E., J. Hegewald, A. Y. Segbena, R. G. Gantin, C. J. Lechner, A. Agosssou, M. Banla and P. T. Soboslay (2011). "Proinflammatory and regulatory cytokines and chemokines in infants with uncomplicated and severe Plasmodium falciparum malaria." Clin Exp Immunol **166**(2): 218-226.

Bachmann, A., M. Petter, R. Krumkamp, M. Esen, J. Held, J. A. Scholz, T. Li, B. K. Sim, S. L. Hoffman, P. G. Kremsner, B. Mordmuller, M. F. Duffy and E. Tannich (2016). "Mosquito Passage Dramatically Changes var Gene Expression in Controlled Human Plasmodium falciparum Infections." PLoS Pathog **12**(4): e1005538.

Bachmann, A., M. Petter, A. K. Tilly, L. Biller, K. A. Uliczka, M. F. Duffy, E. Tannich and I. Bruchhaus (2012). "Temporal expression and localization patterns of variant surface antigens in clinical Plasmodium falciparum isolates during erythrocyte schizogony." PLoS One **7**(11): e49540.

Bachmann, A., S. Predehl, J. May, S. Harder, G. D. Burchard, T. W. Gilberger, E. Tannich and I. Bruchhaus (2011). "Highly co-ordinated var gene expression and switching in clinical Plasmodium falciparum isolates from non-immune malaria patients." Cell Microbiol **13**(9): 1397-1409.

Bachmann, A., J. A. Scholz, M. Janssen, M. Q. Klinkert, E. Tannich, I. Bruchhaus and M. Petter (2015). "A comparative study of the localization and membrane topology of members of the RIFIN, STEVOR and PfMC-2TM protein families in Plasmodium falciparum-infected erythrocytes." Malar J **14**: 274.

Baird, J. K. (1998). "Age-dependent characteristics of protection v. susceptibility to Plasmodium falciparum." Ann Trop Med Parasitol **92**(4): 367-390.

Baird, J. K., S. Masbar, H. Basri, S. Tirtokusumo, B. Subianto and S. L. Hoffman (1998). "Age-dependent susceptibility to severe disease with primary exposure to Plasmodium falciparum." J Infect Dis **178**(2): 592-595.

Ball, E. A., M. R. Sambo, M. Martins, M. J. Trovoada, C. Benchimol, J. Costa, L. Antunes Goncalves, A. Coutinho and C. Penha-Goncalves (2013). "IFNAR1 controls progression to cerebral malaria in children and CD8+ T cell brain pathology in Plasmodium berghei-infected mice." J Immunol **190**(10): 5118-5127.

Barber, B. E., T. William, M. J. Grigg, U. Parameswaran, K. A. Piera, R. N. Price, T. W. Yeo and N. M. Anstey (2015). "Parasite biomass-related inflammation, endothelial activation, microvascular dysfunction and disease severity in vivax malaria." PLoS Pathog **11**(1): e1004558.

Barry, A. and D. Hansen (2016). "Naturally acquired immunity to malaria." Parasitology **143**(2): 125-128.

Bartoloni, A. and L. Zammarchi (2012). "Clinical aspects of uncomplicated and severe malaria." Mediterr J Hematol Infect Dis **4**(1): e2012026.

Baruch, D. I., J. A. Gormely, C. Ma, R. J. Howard and B. L. Pasloske (1996). "Plasmodium falciparum erythrocyte membrane protein 1 is a parasitized erythrocyte receptor for adherence to CD36, thrombospondin, and intercellular adhesion molecule 1." Proc Natl Acad Sci U S A **93**(8): 3497-3502.

Baruch, D. I., X. C. Ma, H. B. Singh, X. Bi, B. L. Pasloske and R. J. Howard (1997). "Identification of a region of PfEMP1 that mediates adherence of Plasmodium falciparum infected erythrocytes to CD36: conserved function with variant sequence." Blood **90**(9): 3766-3775.

Baruch, D. I., B. L. Pasloske, H. B. Singh, X. Bi, X. C. Ma, M. Feldman, T. F. Taraschi and R. J. Howard (1995). "Cloning the P. falciparum gene encoding PfEMP1, a malarial variant antigen and adherence receptor on the surface of parasitized human erythrocytes." Cell **82**(1): 77-87.

Beare, N. A., S. P. Harding, T. E. Taylor, S. Lewallen and M. E. Molyneux (2009). "Perfusion abnormalities in children with cerebral malaria and malarial retinopathy." J Infect Dis **199**(2): 263-271.

Beier, J. C., J. R. Davis, J. A. Vaughan, B. H. Noden and M. S. Beier (1991). "Quantitation of Plasmodium falciparum sporozoites transmitted in vitro by experimentally infected Anopheles gambiae and Anopheles stephensi." Am J Trop Med Hyg **44**(5): 564-570.

Bengtsson, A., L. Joergensen, T. S. Rask, R. W. Olsen, M. A. Andersen, L. Turner, T. G. Theander, L. Hviid, M. K. Higgins, A. Craig, A. Brown and A. T. Jensen (2013). "A novel domain cassette identifies Plasmodium falciparum PfEMP1 proteins binding

ICAM-1 and is a target of cross-reactive, adhesion-inhibitory antibodies." J Immunol **190**(1): 240-249.

Bernabeu, M., S. A. Danziger, M. Avril, M. Vaz, P. H. Babar, A. J. Brazier, T. Herricks, J. N. Maki, L. Pereira, A. Mascarenhas, E. Gomes, L. Chery, J. D. Aitchison, P. K. Rathod and J. D. Smith (2016). "Severe adult malaria is associated with specific PfEMP1 adhesion types and high parasite biomass." Proc Natl Acad Sci U S A **113**(23): E3270-3279.

Berry, M. P., C. M. Graham, F. W. McNab, Z. Xu, S. A. Bloch, T. Oni, K. A. Wilkinson, R. Banchereau, J. Skinner, R. J. Wilkinson, C. Quinn, D. Blankenship, R. Dhawan, J. J. Cush, A. Mejias, O. Ramilo, O. M. Kon, V. Pascual, J. Banchereau, D. Chaussabel and A. O'Garra (2010). "An interferon-inducible neutrophil-driven blood transcriptional signature in human tuberculosis." Nature **466**(7309): 973-977.

Bertin, G. I., T. Lavstsen, F. Guillonneau, J. Doritchamou, C. W. Wang, J. S. Jespersen, S. Ezimegnon, N. Fievet, M. J. Alao, F. Lalya, A. Massougbodji, N. T. Ndam, T. G. Theander and P. Deloron (2013). "Expression of the domain cassette 8 Plasmodium falciparum erythrocyte membrane protein 1 is associated with cerebral malaria in Benin." PLoS One **8**(7): e68368.

Bertin, G. I., A. Sabbagh, N. Argy, V. Salnot, S. Ezinmegnon, G. Agbota, Y. Ladipo, J. M. Alao, G. Sagbo, F. Guillonneau and P. Deloron (2016). "Proteomic analysis of Plasmodium falciparum parasites from patients with cerebral and uncomplicated malaria." Sci Rep **6**: 26773.

Besch, R., H. Poeck, T. Hohenauer, D. Senft, G. Hacker, C. Berking, V. Hornung, S. Endres, T. Ruzicka, S. Rothenfusser and G. Hartmann (2009). "Proapoptotic signaling induced by RIG-I and MDA-5 results in type I interferon-independent apoptosis in human melanoma cells." J Clin Invest **119**(8): 2399-2411.

Bettiol, E., D. L. Van de Hoef, D. Carapau and A. Rodriguez (2010). "Efficient phagosomal maturation and degradation of Plasmodium-infected erythrocytes by dendritic cells and macrophages." Parasite Immunol **32**(6): 389-398.

Blythe, J. E., X. Y. Yam, C. Kuss, Z. Bozdech, A. A. Holder, K. Marsh, J. Langhorne and P. R. Preiser (2008). "Plasmodium falciparum STEVOR proteins are highly expressed in patient isolates and located in the surface membranes of infected red blood cells and the apical tips of merozoites." Infect Immun **76**(7): 3329-3336.

Boeuf, P. S., S. Loizon, G. A. Awandare, J. K. Tetteh, M. M. Addae, G. O. Adjei, B. Goka, J. A. Kurtzhals, O. Puijalon, L. Hviid, B. D. Akanmori and C. Behr (2012). "Insights into deregulated TNF and IL-10 production in malaria: implications for understanding severe malarial anaemia." Malar J **11**: 253.

Bouchon, A., J. Dietrich and M. Colonna (2000). "Cutting edge: inflammatory responses can be triggered by TREM-1, a novel receptor expressed on neutrophils and monocytes." J Immunol **164**(10): 4991-4995.

Boutlis, C. S., D. C. Gowda, R. S. Naik, G. P. Maguire, C. S. Mgone, M. J. Bockarie, M. Lagog, E. Ibam, K. Lorry and N. M. Anstey (2002). "Antibodies to Plasmodium falciparum glycosylphosphatidylinositols: inverse association with tolerance of parasitemia in Papua New Guinean children and adults." Infect Immun **70**(9): 5052-5057.

Bowyer, P. W., L. B. Stewart, H. Aspeling-Jones, H. E. Mensah-Brown, A. D. Ahouidi, A. Amambua-Ngwa, G. A. Awandare and D. J. Conway (2015). "Variation in Plasmodium falciparum erythrocyte invasion phenotypes and merozoite ligand gene expression across different populations in areas of malaria endemicity." Infect Immun **83**(6): 2575-2582.

Bray, N. L., H. Pimentel, P. Melsted and L. Pachter (2016). "Near-optimal probabilistic RNA-seq quantification." Nat Biotechnol **34**(5): 525-527.

Brodin, P., V. Jojic, T. Gao, S. Bhattacharya, C. J. Angel, D. Furman, S. Shen-Orr, C. L. Dekker, G. E. Swan, A. J. Butte, H. T. Maecker and M. M. Davis (2015). "Variation in the human immune system is largely driven by non-heritable influences." Cell **160**(1-2): 37-47.

Broquet, A. H., Y. Hirata, C. S. McAllister and M. F. Kagnoff (2011). "RIG-I/MDA5/MAVS are required to signal a protective IFN response in rotavirus-infected intestinal epithelium." J Immunol **186**(3): 1618-1626.

Broxmeyer, H. E., D. E. Williams, L. Lu, S. Cooper, S. L. Anderson, G. S. Beyer, R. Hoffman and B. Y. Rubin (1986). "The suppressive influences of human tumor necrosis factors on bone marrow hematopoietic progenitor cells from normal donors and patients with leukemia: synergism of tumor necrosis factor and interferon-gamma." J Immunol **136**(12): 4487-4495.

Bruchhaus, I., T. Roeder, A. Rennenberg and V. T. Heussler (2007). "Protozoan parasites: programmed cell death as a mechanism of parasitism." Trends Parasitol **23**(8): 376-383.

Brustoski, K., U. Moller, M. Kramer, A. Petelski, S. Brenner, D. R. Palmer, M. Bongartz, P. G. Kremsner, A. J. Luty and U. Krzych (2005). "IFN-gamma and IL-10 mediate parasite-specific immune responses of cord blood cells induced by pregnancy-associated Plasmodium falciparum malaria." J Immunol **174**(3): 1738-1745.

Buchholz, K., T. A. Burke, K. C. Williamson, R. C. Wiegand, D. F. Wirth and M. Marti (2011). "A high-throughput screen targeting malaria transmission stages opens new avenues for drug development." J Infect Dis **203**(10): 1445-1453.

Bull, P. C. and A. I. Abdi (2016). "The role of PfEMP1 as targets of naturally acquired immunity to childhood malaria: prospects for a vaccine." Parasitology **143**(2): 171-186.

Bull, P. C., M. Berriman, S. Kyes, M. A. Quail, N. Hall, M. M. Kortok, K. Marsh and C. I. Newbold (2005). "Plasmodium falciparum variant surface antigen expression patterns during malaria." PLoS Pathog **1**(3): e26.

Bull, P. C., M. Kortok, O. Kai, F. Ndungu, A. Ross, B. S. Lowe, C. I. Newbold and K. Marsh (2000). "Plasmodium falciparum-infected erythrocytes: agglutination by diverse Kenyan plasma is associated with severe disease and young host age." J Infect Dis **182**(1): 252-259.

Bull, P. C., B. S. Lowe, M. Kortok and K. Marsh (1999). "Antibody recognition of Plasmodium falciparum erythrocyte surface antigens in Kenya: evidence for rare and prevalent variants." Infect Immun **67**(2): 733-739.

Bull, P. C., B. S. Lowe, M. Kortok, C. S. Molyneux, C. I. Newbold and K. Marsh (1998). "Parasite antigens on the infected red cell surface are targets for naturally acquired immunity to malaria." Nat Med **4**(3): 358-360.

Burchard, G. D., P. Radloff, J. Philipps, M. Nkeyi, J. Knobloch and P. G. Kremsner (1995). "Increased erythropoietin production in children with severe malarial anemia." Am J Trop Med Hyg **53**(5): 547-551.

Burel, J. G., S. H. Apte, P. L. Groves, M. J. Boyle, C. Langer, J. G. Beeson, J. S. McCarthy and D. L. Doolan (2017). "Dichotomous miR expression and immune responses following primary blood-stage malaria." JCI Insight **2**(15).

Burel, J. G., S. H. Apte, J. S. McCarthy and D. L. Doolan (2016). "Plasmodium vivax but Not Plasmodium falciparum Blood-Stage Infection in Humans Is Associated with the Expansion of a CD8+ T Cell Population with Cytotoxic Potential." PLoS Negl Trop Dis **10**(12): e0005031.

Cabantous, S., B. Poudiougou, A. Traore, M. Keita, M. B. Cisse, O. Doumbo, A. J. Dessein and S. Marquet (2005). "Evidence that interferon-gamma plays a protective role during cerebral malaria." J Infect Dis **192**(5): 854-860.

Calis, J. C., K. S. Phiri, E. B. Faragher, B. J. Brabin, I. Bates, L. E. Cuevas, R. J. de Haan, A. I. Phiri, P. Malange, M. Khoka, P. J. Hulshof, L. van Lieshout, M. G. Beld, Y. Y. Teo, K. A. Rockett, A. Richardson, D. P. Kwiatkowski, M. E. Molyneux and M. B. van Hensbroek (2008). "Severe anemia in Malawian children." N Engl J Med **358**(9): 888-899.

Carlson, J., H. Helmby, A. V. Hill, D. Brewster, B. M. Greenwood and M. Wahlgren (1990). "Human cerebral malaria: association with erythrocyte rosetting and lack of anti-rosetting antibodies." Lancet **336**(8729): 1457-1460.

Carrero, J. A., B. Calderon and E. R. Unanue (2004). "Type I interferon sensitizes lymphocytes to apoptosis and reduces resistance to Listeria infection." J Exp Med **200**(4): 535-540.

Cham, G. K., L. Turner, J. D. Kurtis, T. Mutabingwa, M. Fried, A. T. Jensen, T. Lavstsen, L. Hviid, P. E. Duffy and T. G. Theander (2010). "Hierarchical, domain type-specific acquisition of antibodies to Plasmodium falciparum erythrocyte membrane protein 1 in Tanzanian children." Infect Immun **78**(11): 4653-4659.

Chan, J. A., F. J. Fowkes and J. G. Beeson (2014). "Surface antigens of Plasmodium falciparum-infected erythrocytes as immune targets and malaria vaccine candidates." Cell Mol Life Sci **71**(19): 3633-3657.

Chan, J. A., K. B. Howell, L. Reiling, R. Ataide, C. L. Mackintosh, F. J. Fowkes, M. Petter, J. M. Chesson, C. Langer, G. M. Warimwe, M. F. Duffy, S. J. Rogerson, P. C. Bull, A. F. Cowman, K. Marsh and J. G. Beeson (2012). "Targets of antibodies against Plasmodium falciparum-infected erythrocytes in malaria immunity." J Clin Invest **122**(9): 3227-3238.

Charles, P. E., R. Noel, F. Massin, J. Guy, P. E. Bollaert, J. P. Quenot and S. Gibot (2016). "Significance of soluble triggering receptor expressed on myeloid cells-1 elevation in patients admitted to the intensive care unit with sepsis." BMC Infect Dis **16**(1): 559.

Chen, L., B. Ge, F. P. Casale, L. Vasquez, T. Kwan, D. Garrido-Martin, S. Watt, Y. Yan, K. Kundu, S. Ecker, A. Datta, D. Richardson, F. Burden, D. Mead, A. L. Mann, J. M. Fernandez, S. Rowlston, S. P. Wilder, S. Farrow, X. Shao, J. J. Lambourne, A. Redensek, C. A. Albers, V. Amstislavskiy, S. Ashford, K. Berentsen, L. Bomba, G. Bourque, D. Bujold, S. Busche, M. Caron, S. H. Chen, W. Cheung, O. Delaneau, E. T. Dermitzakis, H. Elding, I. Colgiu, F. O. Bagger, P. Flicek, E. Habibi, V. Iotchkova, E. Janssen-Megens, B. Kim, H. Lehrach, E. Lowy, A. Mandoli, F. Matarese, M. T. Maurano, J. A. Morris, V. Pancaldi, F. Pourfarzad, K. Rehnstrom, A. Rendon, T. Risch, N. Sharifi, M. M. Simon, M. Sultan, A. Valencia, K. Walter, S. Y. Wang, M. Frontini, S. E. Antonarakis, L. Clarke, M. L. Yaspo, S. Beck, R. Guigo, D. Rico, J. H. A. Martens, W.

H. Ouwehand, T. W. Kuijpers, D. S. Paul, H. G. Stunnenberg, O. Stegle, K. Downes, T. Pastinen and N. Soranzo (2016). "Genetic Drivers of Epigenetic and Transcriptional Variation in Human Immune Cells." Cell **167**(5): 1398-1414 e1324.

Cheng, Q., G. Lawrence, C. Reed, A. Stowers, L. Ranford-Cartwright, A. Creasey, R. Carter and A. Saul (1997). "Measurement of Plasmodium falciparum growth rates in vivo: a test of malaria vaccines." Am J Trop Med Hyg **57**(4): 495-500.

Chimma, P., C. Roussilhon, P. Sratongno, R. Ruangveerayuth, K. Pattanapanyasat, J. L. Perignon, D. J. Roberts and P. Druilhe (2009). "A distinct peripheral blood monocyte phenotype is associated with parasite inhibitory activity in acute uncomplicated Plasmodium falciparum malaria." PLoS Pathog **5**(10): e1000631.

Chiu, Y. H., J. B. Macmillan and Z. J. Chen (2009). "RNA polymerase III detects cytosolic DNA and induces type I interferons through the RIG-I pathway." Cell **138**(3): 576-591.

Chotivanich, K., R. Udomsangpetch, R. McGready, S. Proux, P. Newton, S. Pukrittayakamee, S. Looareesuwan and N. J. White (2002). "Central role of the spleen in malaria parasite clearance." J Infect Dis **185**(10): 1538-1541.

Chotivanich, K., R. Udomsangpetch, J. A. Simpson, P. Newton, S. Pukrittayakamee, S. Looareesuwan and N. J. White (2000). "Parasite multiplication potential and the severity of Falciparum malaria." J Infect Dis **181**(3): 1206-1209.

Chua, C. L., G. Brown, J. A. Hamilton, S. Rogerson and P. Boeuf (2013). "Monocytes and macrophages in malaria: protection or pathology?" Trends Parasitol **29**(1): 26-34.

Claessens, A., Y. Adams, A. Ghumra, G. Lindergard, C. C. Buchan, C. Andisi, P. C. Bull, S. Mok, A. P. Gupta, C. W. Wang, L. Turner, M. Arman, A. Raza, Z. Bozdech and J. A. Rowe (2012). "A subset of group A-like var genes encodes the malaria parasite ligands for binding to human brain endothelial cells." Proc Natl Acad Sci U S A **109**(26): E1772-1781.

Claessens, A., A. Ghumra, A. P. Gupta, S. Mok, Z. Bozdech and J. A. Rowe (2011). "Design of a variant surface antigen-supplemented microarray chip for whole transcriptome analysis of multiple Plasmodium falciparum cytoadherent strains, and identification of strain-transcendent rif and stevor genes." Malar J **10**: 180.

Claessens, A., W. L. Hamilton, M. Kekre, T. D. Otto, A. Faizullabhoy, J. C. Rayner and D. Kwiatkowski (2014). "Generation of antigenic diversity in Plasmodium falciparum by structured rearrangement of Var genes during mitosis." PLoS Genet **10**(12): e1004812.

Clark, I. A., N. H. Hunt, G. A. Butcher and W. B. Cowden (1987). "Inhibition of murine malaria (Plasmodium chabaudi) in vivo by recombinant interferon-gamma or tumor necrosis factor, and its enhancement by butylated hydroxyanisole." J Immunol **139**(10): 3493-3496.

Clatworthy, M. R., L. Willcocks, B. Urban, J. Langhorne, T. N. Williams, N. Peshu, N. A. Watkins, R. A. Floto and K. G. Smith (2007). "Systemic lupus erythematosus-associated defects in the inhibitory receptor FcgammaRIIb reduce susceptibility to malaria." Proc Natl Acad Sci U S A **104**(17): 7169-7174.

Coban, C., T. Horii, S. Akira and K. J. Ishii (2010). "TLR9 and endogenous adjuvants of the whole blood-stage malaria vaccine." Expert Rev Vaccines **9**(7): 775-784.

Coban, C., K. J. Ishii, T. Kawai, H. Hemmi, S. Sato, S. Uematsu, M. Yamamoto, O. Takeuchi, S. Itagaki, N. Kumar, T. Horii and S. Akira (2005). "Toll-like receptor 9 mediates innate immune activation by the malaria pigment hemozoin." J Exp Med **201**(1): 19-25.

Coban, C., K. J. Ishii, S. Uematsu, N. Arisue, S. Sato, M. Yamamoto, T. Kawai, O. Takeuchi, H. Hisaeda, T. Horii and S. Akira (2007). "Pathological role of Toll-like receptor signaling in cerebral malaria." Int Immunol **19**(1): 67-79.

Coban, C., M. Yagi, K. Ohata, Y. Igari, T. Tsukui, T. Horii, K. J. Ishii and S. Akira (2010). "The malarial metabolite hemozoin and its potential use as a vaccine adjuvant." Allergol Int **59**(2): 115-124.

Cohen, S., G. I. Mc and S. Carrington (1961). "Gamma-globulin and acquired immunity to human malaria." Nature **192**: 733-737.

Collins, W. E. and G. M. Jeffery (1999). "A retrospective examination of secondary sporozoite- and trophozoite-induced infections with Plasmodium falciparum: development of parasitologic and clinical immunity following secondary infection." Am J Trop Med Hyg **61**(1 Suppl): 20-35.

Collins, W. E., G. M. Jeffery and J. M. Roberts (2004). "A retrospective examination of reinfection of humans with Plasmodium vivax." Am J Trop Med Hyg **70**(6): 642-644.

Conroy, A. L., S. J. Glover, M. Hawkes, L. K. Erdman, K. B. Seydel, T. E. Taylor, M. E. Molyneux and K. C. Kain (2012). "Angiopoietin-2 levels are associated with retinopathy and predict mortality in Malawian children with cerebral malaria: a retrospective case-control study*." Crit Care Med **40**(3): 952-959.

Cordery, D. V., U. Kishore, S. Kyes, M. J. Shafi, K. R. Watkins, T. N. Williams, K. Marsh and B. C. Urban (2007). "Characterization of a Plasmodium falciparum macrophage-migration inhibitory factor homologue." J Infect Dis **195**(6): 905-912.

Couper, K. N., D. G. Blount, J. C. Hafalla, N. van Rooijen, J. B. de Souza and E. M. Riley (2007). "Macrophage-mediated but gamma interferon-independent innate immune responses control the primary wave of Plasmodium yoelii parasitemia." Infect Immun **75**(12): 5806-5818.

Cox-Singh, J., J. Hiu, S. B. Lucas, P. C. Divis, M. Zulkarnaen, P. Chandran, K. T. Wong, P. Adem, S. R. Zaki, B. Singh and S. Krishna (2010). "Severe malaria - a case of fatal Plasmodium knowlesi infection with post-mortem findings: a case report." Malar J **9**: 10.

Craig, A. G., M. F. Khairul and P. R. Patil (2012). "Cytoadherence and severe malaria." Malays J Med Sci **19**(2): 5-18.

Dantzler, K. W., D. B. Ravel, N. M. Brancucci and M. Marti (2015). "Ensuring transmission through dynamic host environments: host-pathogen interactions in Plasmodium sexual development." Curr Opin Microbiol **26**: 17-23.

Davis, B. K., H. Wen and J. P. Ting (2011). "The inflammasome NLRs in immunity, inflammation, and associated diseases." Annu Rev Immunol **29**: 707-735.

Day, M. B. (2000). "Managing the patient with severe respiratory problems." J Calif Dent Assoc **28**(8): 585-589, 591-583, 595-588.

Day, N. P., T. T. Hien, T. Schollaardt, P. P. Loc, L. V. Chuong, T. T. Chau, N. T. Mai, N. H. Phu, D. X. Sinh, N. J. White and M. Ho (1999). "The prognostic and pathophysiologic role of pro- and antiinflammatory cytokines in severe malaria." J Infect Dis **180**(4): 1288-1297.

Day, N. P., N. H. Phu, N. T. Mai, T. T. Chau, P. P. Loc, L. V. Chuong, D. X. Sinh, P. Holloway, T. T. Hien and N. J. White (2000). "The pathophysiologic and prognostic significance of acidosis in severe adult malaria." Crit Care Med **28**(6): 1833-1840.

de Mendonca, V. R., M. S. Goncalves and M. Barral-Netto (2012). "The host genetic diversity in malaria infection." J Trop Med **2012**: 940616.

de Souza, J. B., J. Todd, G. Krishegowda, D. C. Gowda, D. Kwiatkowski and E. M. Riley (2002). "Prevalence and boosting of antibodies to Plasmodium falciparum glycosylphosphatidylinositols and evaluation of their association with protection from mild and severe clinical malaria." Infect Immun **70**(9): 5045-5051.

Deans, A. M., K. E. Lyke, M. A. Thera, C. V. Plowe, A. Kone, O. K. Doumbo, O. Kai, K. Marsh, M. J. Mackinnon, A. Raza and J. A. Rowe (2006). "Low multiplication rates of African Plasmodium falciparum isolates and lack of association of multiplication rate and red blood cell selectivity with malaria virulence." Am J Trop Med Hyg **74**(4): 554-563.

Deans, A. M., S. Nery, D. J. Conway, O. Kai, K. Marsh and J. A. Rowe (2007). "Invasion pathways and malaria severity in Kenyan Plasmodium falciparum clinical isolates." Infect Immun **75**(6): 3014-3020.

Del Portillo, H. A., M. Ferrer, T. Brugat, L. Martin-Jaular, J. Langhorne and M. V. Lacerda (2012). "The role of the spleen in malaria." Cell Microbiol **14**(3): 343-355.

Desvignes, L., A. J. Wolf and J. D. Ernst (2012). "Dynamic roles of type I and type II IFNs in early infection with Mycobacterium tuberculosis." J Immunol **188**(12): 6205-6215.

Dietz, K., G. Raddatz and L. Molineaux (2006). "Mathematical model of the first wave of Plasmodium falciparum asexual parasitemia in non-immune and vaccinated individuals." Am J Trop Med Hyg **75**(2 Suppl): 46-55.

Dobbs, K. R. and A. E. Dent (2016). "Plasmodium malaria and antimalarial antibodies in the first year of life." Parasitology **143**(2): 129-138.

Dobbs, K. R., P. Embury, J. Vulule, P. S. Odada, B. A. Rosa, M. Mitreva, J. W. Kazura and A. E. Dent (2017). "Monocyte dysregulation and systemic inflammation during pediatric falciparum malaria." JCI Insight **2**(18).

Dollard, S. C., S. A. Staras, M. M. Amin, D. S. Schmid and M. J. Cannon (2011). "National prevalence estimates for cytomegalovirus IgM and IgG avidity and association between high IgM antibody titer and low IgG avidity." Clin Vaccine Immunol **18**(11): 1895-1899.

Dondorp, A. M., V. Desakorn, W. Pongtavornpinyo, D. Sahassananda, K. Silamut, K. Chotivanich, P. N. Newton, P. Pitisuttithum, A. M. Smithyman, N. J. White and N. P. Day (2005). "Estimation of the total parasite biomass in acute falciparum malaria from plasma PfHRP2." PLoS Med **2**(8): e204.

Dondorp, A. M., C. Ince, P. Charunwatthana, J. Hanson, A. van Kuijen, M. A. Faiz, M. R. Rahman, M. Hasan, E. Bin Yunus, A. Ghose, R. Ruangveerayut, D. Limmathurotsakul, K. Mathura, N. J. White and N. P. Day (2008). "Direct in vivo assessment of microcirculatory dysfunction in severe falciparum malaria." J Infect Dis **197**(1): 79-84.

Dondorp, A. M., P. A. Kager, J. Vreeken and N. J. White (2000). "Abnormal blood flow and red blood cell deformability in severe malaria." Parasitol Today **16**(6): 228-232.

Dondorp, A. M., S. J. Lee, M. A. Faiz, S. Mishra, R. Price, E. Tjitra, M. Than, Y. Htut, S. Mohanty, E. B. Yunus, R. Rahman, F. Nosten, N. M. Anstey, N. P. Day and N. J. White (2008). "The relationship between age and the manifestations of and mortality associated with severe malaria." Clin Infect Dis **47**(2): 151-157.

Dondorp, A. M., E. Pongponratn and N. J. White (2004). "Reduced microcirculatory flow in severe falciparum malaria: pathophysiology and electron-microscopic pathology." Acta Trop **89**(3): 309-317.

Doolan, D. L., C. Dobano and J. K. Baird (2009). "Acquired immunity to malaria." Clin Microbiol Rev **22**(1): 13-36, Table of Contents.

Dorfman, J. R., P. Bejon, F. M. Ndungu, J. Langhorne, M. M. Kortok, B. S. Lowe, T. W. Mwangi, T. N. Williams and K. Marsh (2005). "B cell memory to 3 Plasmodium falciparum blood-stage antigens in a malaria-endemic area." J Infect Dis **191**(10): 1623-1630.

Dostert, C., G. Guarda, J. F. Romero, P. Menu, O. Gross, A. Tardivel, M. L. Suva, J. C. Stehle, M. Kopf, I. Stamenkovic, G. Corradin and J. Tschopp (2009). "Malarial hemozoin is a Nalp3 inflammasome activating danger signal." PLoS One **4**(8): e6510.

Douglas, A. D., N. J. Edwards, C. J. Duncan, F. M. Thompson, S. H. Sheehy, G. A. O'Hara, N. Anagnostou, M. Walther, D. P. Webster, S. J. Dunachie, D. W. Porter, L. Andrews, S. C. Gilbert, S. J. Draper, A. V. Hill and P. Bejon (2013). "Comparison of modeling methods to determine liver-to-blood inocula and parasite multiplication rates during controlled human malaria infection." J Infect Dis **208**(2): 340-345.

Doumbo, O. K., M. A. Thera, A. K. Kone, A. Raza, L. J. Tempest, K. E. Lyke, C. V. Plowe and J. A. Rowe (2009). "High levels of Plasmodium falciparum rosetting in all clinical forms of severe malaria in African children." Am J Trop Med Hyg **81**(6): 987-993.

Duah, N. O., D. J. Miles, H. C. Whittle and D. J. Conway (2010). "Acquisition of antibody isotypes against Plasmodium falciparum blood stage antigens in a birth cohort." Parasite Immunol **32**(2): 125-134.

Duncan, C. J. and S. J. Draper (2012). "Controlled human blood stage malaria infection: current status and potential applications." Am J Trop Med Hyg **86**(4): 561-565.

Durai, P., R. G. Govindaraj and S. Choi (2013). "Structure and dynamic behavior of Toll-like receptor 2 subfamily triggered by malarial glycosylphosphatidylinositols of Plasmodium falciparum." FEBS J **280**(23): 6196-6212.

Dzikowski, R., M. Frank and K. Deitsch (2006). "Mutually exclusive expression of virulence genes by malaria parasites is regulated independently of antigen production." PLoS Pathog **2**(3): e22.

Elahi, S., J. M. Ertelt, J. M. Kinder, T. T. Jiang, X. Zhang, L. Xin, V. Chaturvedi, B. S. Strong, J. E. Qualls, K. A. Steinbrecher, T. A. Kalfa, A. F. Shaaban and S. S. Way (2013). "Immunosuppressive CD71+ erythroid cells compromise neonatal host defence against infection." Nature **504**(7478): 158-162.

Elliott, S. R., T. P. Spurck, J. M. Dodin, A. G. Maier, T. S. Voss, F. Yosaatmadja, P. D. Payne, G. I. McFadden, A. F. Cowman, S. J. Rogerson, L. Schofield and G. V. Brown (2007). "Inhibition of dendritic cell maturation by malaria is dose dependent and does not require Plasmodium falciparum erythrocyte membrane protein 1." Infect Immun **75**(7): 3621-3632.

Enderes, C., D. Kombila, M. Dal-Bianco, R. Dzikowski, P. Kremsner and M. Frank (2011). "Var Gene promoter activation in clonal Plasmodium falciparum isolates follows a hierarchy and suggests a conserved switching program that is independent of genetic background." J Infect Dis **204**(10): 1620-1631.

English, M., C. Waruiru, E. Amukoye, S. Murphy, J. Crawley, I. Mwangi, N. Peshu and K. Marsh (1996). "Deep breathing in children with severe malaria: indicator of metabolic acidosis and poor outcome." Am J Trop Med Hyg **55**(5): 521-524.

Engwerda, C. R., L. Beattie and F. H. Amante (2005). "The importance of the spleen in malaria." Trends Parasitol **21**(2): 75-80.

Fagiani, E. and G. Christofori (2013). "Angiopoietins in angiogenesis." Cancer Lett **328**(1): 18-26.

Falk, N., M. Kaestli, W. Qi, M. Ott, K. Baea, A. Cortes and H. P. Beck (2009). "Analysis of Plasmodium falciparum var genes expressed in children from Papua New Guinea." J Infect Dis **200**(3): 347-356.

Fatih, F. A., A. Siner, A. Ahmed, L. C. Woon, A. G. Craig, B. Singh, S. Krishna and J. Cox-Singh (2012). "Cytoadherence and virulence - the case of Plasmodium knowlesi malaria." Malar J **11**: 33.

Fatih, F. A., H. M. Staines, A. Siner, M. A. Ahmed, L. C. Woon, E. M. Pasini, C. H. Kocken, B. Singh, J. Cox-Singh and S. Krishna (2013). "Susceptibility of human Plasmodium knowlesi infections to anti-malarials." Malar J **12**: 425.

Fernandez, V., M. Hommel, Q. Chen, P. Hagblom and M. Wahlgren (1999). "Small, clonally variant antigens expressed on the surface of the Plasmodium falciparum-infected erythrocyte are encoded by the rif gene family and are the target of human immune responses." J Exp Med **190**(10): 1393-1404.

Ferwerda, B., M. B. McCall, S. Alonso, E. J. Giamarellos-Bourboulis, M. Mouktaroudi, N. Izagirre, D. Syafruddin, G. Kibiki, T. Cristea, A. Hijmans, L. Hamann, S. Israel, G. ElGhazali, M. Troye-Blomberg, O. Kumpf, B. Maiga, A. Dolo, O. Doumbo, C. C. Hermsen, A. F. Stalenhoef, R. van Crevel, H. G. Brunner, D. Y. Oh, R. R. Schumann, C. de la Rua, R. Sauerwein, B. J. Kullberg, A. J. van der Ven, J. W. van der Meer and M. G. Netea (2007). "TLR4 polymorphisms, infectious diseases, and evolutionary pressure during migration of modern humans." Proc Natl Acad Sci U S A **104**(42): 16645-16650.

Frank, M., R. Dzikowski, B. Amulic and K. Deitsch (2007). "Variable switching rates of malaria virulence genes are associated with chromosomal position." Mol Microbiol **64**(6): 1486-1498.

Franklin, B. S., P. Parroche, M. A. Ataide, F. Lauw, C. Ropert, R. B. de Oliveira, D. Pereira, M. S. Tada, P. Nogueira, L. H. da Silva, H. Bjorkbacka, D. T. Golenbock and R. T. Gazzinelli (2009). "Malaria primes the innate immune response due to interferon-gamma induced enhancement of toll-like receptor expression and function." Proc Natl Acad Sci U S A **106**(14): 5789-5794.

Freitas-Junior, L. H., E. Bottius, L. A. Pirrit, K. W. Deitsch, C. Scheidig, F. Guinet, U. Nehrbass, T. E. Wellems and A. Scherf (2000). "Frequent ectopic recombination of virulence factor genes in telomeric chromosome clusters of P. falciparum." Nature **407**(6807): 1018-1022.

Fuchs, Y. and H. Steller (2011). "Programmed cell death in animal development and disease." Cell **147**(4): 742-758.

Gamain, B., J. D. Smith, L. H. Miller and D. I. Baruch (2001). "Modifications in the CD36 binding domain of the Plasmodium falciparum variant antigen are responsible for the inability of chondroitin sulfate A adherent parasites to bind CD36." Blood **97**(10): 3268-3274.

Gardinassi, L. G., M. Arevalo-Herrera, S. Herrera, R. J. Cordy, V. Tran, M. R. Smith, M. S. Johnson, B. Chacko, K. H. Liu, V. M. Darley-Usmar, Y. M. Go, H. C. Ma, D. P. Jones, M. R. Galinski and S. Li (2018). "Integrative metabolomics and transcriptomics

signatures of clinical tolerance to Plasmodium vivax reveal activation of innate cell immunity and T cell signaling." Redox Biol **17**: 158-170.

Gardner, M. J., N. Hall, E. Fung, O. White, M. Berriman, R. W. Hyman, J. M. Carlton, A. Pain, K. E. Nelson, S. Bowman, I. T. Paulsen, K. James, J. A. Eisen, K. Rutherford, S. L. Salzberg, A. Craig, S. Kyes, M. S. Chan, V. Nene, S. J. Shallom, B. Suh, J. Peterson, S. Angiuoli, M. Pertea, J. Allen, J. Selengut, D. Haft, M. W. Mather, A. B. Vaidya, D. M. Martin, A. H. Fairlamb, M. J. Fraunholz, D. S. Roos, S. A. Ralph, G. I. McFadden, L. M. Cummings, G. M. Subramanian, C. Mungall, J. C. Venter, D. J. Carucci, S. L. Hoffman, C. Newbold, R. W. Davis, C. M. Fraser and B. Barrell (2002). "Genome sequence of the human malaria parasite Plasmodium falciparum." Nature **419**(6906): 498-511.

Garraud, O., S. Mahanty and R. Perraut (2003). "Malaria-specific antibody subclasses in immune individuals: a key source of information for vaccine design." Trends Immunol **24**(1): 30-35.

Gautier, L., L. Cope, B. M. Bolstad and R. A. Irizarry (2004). "affy--analysis of Affymetrix GeneChip data at the probe level." Bioinformatics **20**(3): 307-315.

Gazzinelli, R. T. and E. Y. Denkers (2006). "Protozoan encounters with Toll-like receptor signalling pathways: implications for host parasitism." Nat Rev Immunol **6**(12): 895-906.

Gazzinelli, R. T., P. Kalantari, K. A. Fitzgerald and D. T. Golenbock (2014). "Innate sensing of malaria parasites." Nat Rev Immunol **14**(11): 744-757.

Gevers, D., S. Kugathasan, L. A. Denson, Y. Vazquez-Baeza, W. Van Treuren, B. Ren, E. Schwager, D. Knights, S. J. Song, M. Yassour, X. C. Morgan, A. D. Kostic, C. Luo, A. Gonzalez, D. McDonald, Y. Haberman, T. Walters, S. Baker, J. Rosh, M. Stephens, M. Heyman, J. Markowitz, R. Baldassano, A. Griffiths, F. Sylvester, D. Mack, S. Kim, W. Crandall, J. Hyams, C. Huttenhower, R. Knight and R. J. Xavier (2014). "The treatment-naive microbiome in new-onset Crohn's disease." Cell Host Microbe **15**(3): 382-392.

Ghumra, A., J. P. Semblat, R. Ataide, C. Kifude, Y. Adams, A. Claessens, D. N. Anong, P. C. Bull, C. Fennell, M. Arman, A. Amambua-Ngwa, M. Walther, D. J. Conway, L. Kassambara, O. K. Doumbo, A. Raza and J. A. Rowe (2012). "Induction of strain-transcending antibodies against Group A PfEMP1 surface antigens from virulent malaria parasites." PLoS Pathog **8**(4): e1002665.

Girardin, S. E., I. G. Boneca, L. A. Carneiro, A. Antignac, M. Jehanno, J. Viala, K. Tedin, M. K. Taha, A. Labigne, U. Zahringer, A. J. Coyle, P. S. DiStefano, J. Bertin, P. J. Sansonetti and D. J. Philpott (2003). "Nod1 detects a unique muropeptide from gram-negative bacterial peptidoglycan." Science **300**(5625): 1584-1587.

Girardin, S. E., I. G. Boneca, J. Viala, M. Chamaillard, A. Labigne, G. Thomas, D. J. Philpott and P. J. Sansonetti (2003). "Nod2 is a general sensor of peptidoglycan through muramyl dipeptide (MDP) detection." J Biol Chem **278**(11): 8869-8872.

Gitlin, L., W. Barchet, S. Gilfillan, M. Cella, B. Beutler, R. A. Flavell, M. S. Diamond and M. Colonna (2006). "Essential role of mda-5 in type I IFN responses to polyriboinosinic:polyribocytidylic acid and encephalomyocarditis picornavirus." Proc Natl Acad Sci U S A **103**(22): 8459-8464.

Glynn, J. R. and D. J. Bradley (1995). "Inoculum size, incubation period and severity of malaria. Analysis of data from malaria therapy records." Parasitology **110 (Pt 1)**: 7-19.

Glynn, J. R., W. E. Collins, G. M. Jeffery and D. J. Bradley (1995). "Infecting dose and severity of falciparum malaria." Trans R Soc Trop Med Hyg **89**(3): 281-283.

Goel, S., M. Palmkvist, K. Moll, N. Joannin, P. Lara, R. R. Akhouri, N. Moradi, K. Ojemalm, M. Westman, D. Angeletti, H. Kjellin, J. Lehtio, O. Blixt, L. Idestrom, C. G. Gahmberg, J. R. Storry, A. K. Hult, M. L. Olsson, G. von Heijne, I. Nilsson and M. Wahlgren (2015). "RIFINs are adhesins implicated in severe Plasmodium falciparum malaria." Nat Med **21**(4): 314-317.

Gomez-Escobar, N., A. Amambua-Ngwa, M. Walther, J. Okebe, A. Ebonyi and D. J. Conway (2010). "Erythrocyte invasion and merozoite ligand gene expression in severe and mild Plasmodium falciparum malaria." J Infect Dis **201**(3): 444-452.

Goncalves, B. P., C. Y. Huang, R. Morrison, S. Holte, E. Kabyemela, D. R. Prevots, M. Fried and P. E. Duffy (2014). "Parasite burden and severity of malaria in Tanzanian children." N Engl J Med **370**(19): 1799-1808.

Goncalves, R. M., K. K. Scopel, M. S. Bastos and M. U. Ferreira (2012). "Cytokine balance in human malaria: does Plasmodium vivax elicit more inflammatory responses than Plasmodium falciparum?" PLoS One **7**(9): e44394.

Good, M. F. and D. L. Doolan (1999). "Immune effector mechanisms in malaria." Curr Opin Immunol **11**(4): 412-419.

Goodman, C. A., P. G. Coleman and A. J. Mills (1999). "Cost-effectiveness of malaria control in sub-Saharan Africa." Lancet **354**(9176): 378-385.

Gotz, A., M. S. Tang, M. C. Ty, C. Arama, A. Ongoiba, D. Doumtabe, B. Traore, P. D. Crompton, P. Loke and A. Rodriguez (2017). "Atypical activation of dendritic cells by Plasmodium falciparum." Proc Natl Acad Sci U S A **114**(49): E10568-E10577.

Goubau, D., S. Deddouche and C. Reis e Sousa (2013). "Cytosolic sensing of viruses." Immunity **38**(5): 855-869.

Gough, D. J., N. L. Messina, L. Hii, J. A. Gould, K. Sabapathy, A. P. Robertson, J. A. Trapani, D. E. Levy, P. J. Hertzog, C. J. Clarke and R. W. Johnstone (2010). "Functional crosstalk between type I and II interferon through the regulated expression of STAT1." PLoS Biol **8**(4): e1000361.

Gowda, D. C., P. Gupta and E. A. Davidson (1997). "Glycosylphosphatidylinositol anchors represent the major carbohydrate modification in proteins of intraerythrocytic stage Plasmodium falciparum." J Biol Chem **272**(10): 6428-6439.

Graham, S. M. (2008). "Severe anemia in Malawian children." N Engl J Med **358**(21): 2290; author reply 2291.

Grau, G. E. and A. G. Craig (2012). "Cerebral malaria pathogenesis: revisiting parasite and host contributions." Future Microbiol **7**(2): 291-302.

Griffith, J. W., C. O'Connor, K. Bernard, T. Town, D. R. Goldstein and R. Bucala (2007). "Toll-like receptor modulation of murine cerebral malaria is dependent on the genetic background of the host." J Infect Dis **196**(10): 1553-1564.

Gullingsrud, J., T. Saveria, E. Amos, P. E. Duffy and A. V. Oleinikov (2013). "Structure-function-immunogenicity studies of PfEMP1 domain DBL2betaPF11_0521, a malaria parasite ligand for ICAM-1." PLoS One **8**(4): e61323.

Gupta, S., R. W. Snow, C. A. Donnelly, K. Marsh and C. Newbold (1999). "Immunity to non-cerebral severe malaria is acquired after one or two infections." Nat Med **5**(3): 340-343.

Hamann, L., G. Bedu-Addo, T. A. Eggelte, R. R. Schumann and F. P. Mockenhaupt (2010). "The toll-like receptor 1 variant S248N influences placental malaria." Infect Genet Evol **10**(6): 785-789.

Hanson, J., S. W. Lam, K. C. Mahanta, R. Pattnaik, S. Alam, S. Mohanty, M. U. Hasan, A. Hossain, P. Charunwatthana, K. Chotivanich, R. J. Maude, H. Kingston, N. P. Day, S. Mishra, N. J. White and A. M. Dondorp (2012). "Relative contributions of macrovascular and microvascular dysfunction to disease severity in falciparum malaria." J Infect Dis **206**(4): 571-579.

Hanson, J. P., S. W. Lam, S. Mohanty, S. Alam, R. Pattnaik, K. C. Mahanta, M. U. Hasan, P. Charunwatthana, S. K. Mishra, N. P. Day, N. J. White and A. M. Dondorp (2013).

"Fluid resuscitation of adults with severe falciparum malaria: effects on Acid-base status, renal function, and extravascular lung water." Crit Care Med **41**(4): 972-981.

Haque, A., S. E. Best, A. Ammerdorffer, L. Desbarrieres, M. M. de Oca, F. H. Amante, F. de Labastida Rivera, P. Hertzog, G. M. Boyle, G. R. Hill and C. R. Engwerda (2011). "Type I interferons suppress CD4(+) T-cell-dependent parasite control during blood-stage Plasmodium infection." Eur J Immunol **41**(9): 2688-2698.

Haque, A., S. E. Best, M. Montes de Oca, K. R. James, A. Ammerdorffer, C. L. Edwards, F. de Labastida Rivera, F. H. Amante, P. T. Bunn, M. Sheel, I. Sebina, M. Koyama, A. Varelias, P. J. Hertzog, U. Kalinke, S. Y. Gun, L. Renia, C. Ruedl, K. P. MacDonald, G. R. Hill and C. R. Engwerda (2014). "Type I IFN signaling in CD8- DCs impairs Th1-dependent malaria immunity." J Clin Invest **124**(6): 2483-2496.

Hartgers, F. C., B. B. Obeng, A. Voskamp, I. A. Larbi, A. S. Amoah, A. J. Luty, D. Boakye and M. Yazdanbakhsh (2008). "Enhanced Toll-like receptor responsiveness associated with mitogen-activated protein kinase activation in Plasmodium falciparum-infected children." Infect Immun **76**(11): 5149-5157.

Hay, S. I., C. A. Guerra, A. J. Tatem, A. M. Noor and R. W. Snow (2004). "The global distribution and population at risk of malaria: past, present, and future." Lancet Infect Dis **4**(6): 327-336.

Hensmann, M. and D. Kwiatkowski (2001). "Cellular basis of early cytokine response to Plasmodium falciparum." Infect Immun **69**(4): 2364-2371.

Hermsen, C. C., D. S. Telgt, E. H. Linders, L. A. van de Locht, W. M. Eling, E. J. Mensink and R. W. Sauerwein (2001). "Detection of Plasmodium falciparum malaria parasites in vivo by real-time quantitative PCR." Mol Biochem Parasitol **118**(2): 247-251.

Herskovits, A. A., V. Auerbuch and D. A. Portnoy (2007). "Bacterial ligands generated in a phagosome are targets of the cytosolic innate immune system." PLoS Pathog **3**(3): e51.

Hirako, I. C., C. Gallego-Marin, M. A. Ataide, W. A. Andrade, H. Gravina, B. C. Rocha, R. B. de Oliveira, D. B. Pereira, J. Vinetz, B. Diamond, S. Ram, D. T. Golenbock and R. T. Gazzinelli (2015). "DNA-Containing Immunocomplexes Promote Inflammasome Assembly and Release of Pyrogenic Cytokines by CD14+ CD16+ CD64high CD32low Inflammatory Monocytes from Malaria Patients." MBio **6**(6): e01605-01615.

Ho, M., T. Schollaardt, S. Snape, S. Looareesuwan, P. Suntharasamai and N. J. White (1998). "Endogenous interleukin-10 modulates proinflammatory response in Plasmodium falciparum malaria." J Infect Dis **178**(2): 520-525.

Ho, T. H., C. Kew, P. Y. Lui, C. P. Chan, T. Satoh, S. Akira, D. Y. Jin and K. H. Kok (2016). "PACT- and RIG-I-Dependent Activation of Type I Interferon Production by a Defective Interfering RNA Derived from Measles Virus Vaccine." J Virol **90**(3): 1557-1568.

Hornung, V., A. Ablasser, M. Charrel-Dennis, F. Bauernfeind, G. Horvath, D. R. Caffrey, E. Latz and K. A. Fitzgerald (2009). "AIM2 recognizes cytosolic dsDNA and forms a caspase-1-activating inflammasome with ASC." Nature **458**(7237): 514-518.

Hornung, V. and E. Latz (2010). "Intracellular DNA recognition." Nat Rev Immunol **10**(2): 123-130.

Horowitz, A., K. C. Newman, J. H. Evans, D. S. Korbel, D. M. Davis and E. M. Riley (2010). "Cross-talk between T cells and NK cells generates rapid effector responses to Plasmodium falciparum-infected erythrocytes." J Immunol **184**(11): 6043-6052.

Horrocks, P., S. Kyes, R. Pinches, Z. Christodoulou and C. Newbold (2004). "Transcription of subtelomerically located var gene variant in Plasmodium falciparum appears to require the truncation of an adjacent var gene." Mol Biochem Parasitol **134**(2): 193-199.

Horrocks, P., R. Pinches, Z. Christodoulou, S. A. Kyes and C. I. Newbold (2004). "Variable var transition rates underlie antigenic variation in malaria." Proc Natl Acad Sci U S A **101**(30): 11129-11134.

Hviid, L. (2005). "Naturally acquired immunity to Plasmodium falciparum malaria in Africa." Acta Trop **95**(3): 270-275.

Hviid, L. (2010). "The role of Plasmodium falciparum variant surface antigens in protective immunity and vaccine development." Hum Vaccin **6**(1): 84-89.

Hviid, L. and A. T. Jensen (2015). "PfEMP1 - A Parasite Protein Family of Key Importance in Plasmodium falciparum Malaria Immunity and Pathogenesis." Adv Parasitol **88**: 51-84.

Hviid, L., J. A. Kurtzhals, B. Q. Goka, J. O. Oliver-Commey, F. K. Nkrumah and T. G. Theander (1997). "Rapid reemergence of T cells into peripheral circulation

following treatment of severe and uncomplicated Plasmodium falciparum malaria." Infect Immun **65**(10): 4090-4093.

Idro, R., N. E. Jenkins and C. R. Newton (2005). "Pathogenesis, clinical features, and neurological outcome of cerebral malaria." Lancet Neurol **4**(12): 827-840.

Isaacs, A. and J. Lindenmann (1957). "Virus interference. I. The interferon." Proc R Soc Lond B Biol Sci **147**(927): 258-267.

Ivashkiv, L. B. and L. T. Donlin (2014). "Regulation of type I interferon responses." Nat Rev Immunol **14**(1): 36-49.

Jagannathan, P., I. Eccles-James, K. Bowen, F. Nankya, A. Auma, S. Wamala, C. Ebusu, M. K. Muhindo, E. Arinaitwe, J. Briggs, B. Greenhouse, J. W. Tappero, M. R. Kamya, G. Dorsey and M. E. Feeney (2014). "IFNgamma/IL-10 co-producing cells dominate the CD4 response to malaria in highly exposed children." PLoS Pathog **10**(1): e1003864.

Jain, V., H. B. Armah, J. E. Tongren, R. M. Ned, N. O. Wilson, S. Crawford, P. K. Joel, M. P. Singh, A. C. Nagpal, A. P. Dash, V. Udhayakumar, N. Singh and J. K. Stiles (2008). "Plasma IP-10, apoptotic and angiogenic factors associated with fatal cerebral malaria in India." Malar J **7**: 83.

Jain, V., P. P. Singh, N. Silawat, R. Patel, A. Saxena, P. K. Bharti, M. Shukla, S. Biswas and N. Singh (2010). "A preliminary study on pro- and anti-inflammatory cytokine profiles in Plasmodium vivax malaria patients from central zone of India." Acta Trop **113**(3): 263-268.

Jensen, A. T., P. Magistrado, S. Sharp, L. Joergensen, T. Lavstsen, A. Chiucchiuini, A. Salanti, L. S. Vestergaard, J. P. Lusingu, R. Hermsen, R. Sauerwein, J. Christensen, M. A. Nielsen, L. Hviid, C. Sutherland, T. Staalsoe and T. G. Theander (2004). "Plasmodium falciparum associated with severe childhood malaria preferentially expresses PfEMP1 encoded by group A var genes." J Exp Med **199**(9): 1179-1190.

Jespersen, J. S., C. W. Wang, S. I. Mkumbaye, D. T. Minja, B. Petersen, L. Turner, J. E. Petersen, J. P. Lusingu, T. G. Theander and T. Lavstsen (2016). "Plasmodium falciparum var genes expressed in children with severe malaria encode CIDRalpha1 domains." EMBO Mol Med **8**(8): 839-850.

Joannin, N., S. Abhiman, E. L. Sonnhammer and M. Wahlgren (2008). "Sub-grouping and sub-functionalization of the RIFIN multi-copy protein family." BMC Genomics **9**: 19.

Johnson, R. A., T. A. Waddelow, J. Caro, A. Oliff and G. D. Roodman (1989). "Chronic exposure to tumor necrosis factor in vivo preferentially inhibits erythropoiesis in nude mice." Blood **74**(1): 130-138.

Joice, R., S. K. Nilsson, J. Montgomery, S. Dankwa, E. Egan, B. Morahan, K. B. Seydel, L. Bertuccini, P. Alano, K. C. Williamson, M. T. Duraisingh, T. E. Taylor, D. A. Milner and M. Marti (2014). "Plasmodium falciparum transmission stages accumulate in the human bone marrow." Sci Transl Med **6**(244): 244re245.

Kaestli, M., I. A. Cockburn, A. Cortes, K. Baea, J. A. Rowe and H. P. Beck (2006). "Virulence of malaria is associated with differential expression of Plasmodium falciparum var gene subgroups in a case-control study." J Infect Dis **193**(11): 1567-1574.

Kalantari, P., R. B. DeOliveira, J. Chan, Y. Corbett, V. Rathinam, A. Stutz, E. Latz, R. T. Gazzinelli, D. T. Golenbock and K. A. Fitzgerald (2014). "Dual engagement of the NLRP3 and AIM2 inflammasomes by plasmodium-derived hemozoin and DNA during malaria." Cell Rep **6**(1): 196-210.

Kalmbach, Y., M. Rottmann, M. Kombila, P. G. Kremsner, H. P. Beck and J. F. Kun (2010). "Differential var gene expression in children with malaria and antidromic effects on host gene expression." J Infect Dis **202**(2): 313-317.

Kauffmann, A. and W. Huber (2010). "Microarray data quality control improves the detection of differentially expressed genes." Genomics **95**(3): 138-142.

Kaufmann, T., A. Strasser and P. J. Jost (2012). "Fas death receptor signalling: roles of Bid and XIAP." Cell Death Differ **19**(1): 42-50.

Kaviratne, M., S. M. Khan, W. Jarra and P. R. Preiser (2002). "Small variant STEVOR antigen is uniquely located within Maurer's clefts in Plasmodium falciparum-infected red blood cells." Eukaryot Cell **1**(6): 926-935.

Kawai, T. and S. Akira (2006). "Innate immune recognition of viral infection." Nat Immunol **7**(2): 131-137.

Kawai, T. and S. Akira (2010). "The role of pattern-recognition receptors in innate immunity: update on Toll-like receptors." Nat Immunol **11**(5): 373-384.

Kawai, T., K. Takahashi, S. Sato, C. Coban, H. Kumar, H. Kato, K. J. Ishii, O. Takeuchi and S. Akira (2005). "IPS-1, an adaptor triggering RIG-I- and Mda5-mediated type I interferon induction." Nat Immunol **6**(10): 981-988.

Khattab, A., I. Bonow, N. Schreiber, M. Petter, C. Schmetz and M. Q. Klinkert (2008). "Plasmodium falciparum variant STEVOR antigens are expressed in merozoites and possibly associated with erythrocyte invasion." Malar J **7**: 137.

Khattab, A. and S. Meri (2011). "Exposure of the Plasmodium falciparum clonally variant STEVOR proteins on the merozoite surface." Malar J **10**: 58.

Kirchgatter, K. and A. Portillo Hdel (2002). "Association of severe noncerebral Plasmodium falciparum malaria in Brazil with expressed PfEMP1 DBL1 alpha sequences lacking cysteine residues." Mol Med **8**(1): 16-23.

Kollmann, T. R., B. Kampmann, S. K. Mazmanian, A. Marchant and O. Levy (2017). "Protecting the Newborn and Young Infant from Infectious Diseases: Lessons from Immune Ontogeny." Immunity **46**(3): 350-363.

Kong, L., L. Sun, H. Zhang, Q. Liu, Y. Liu, L. Qin, G. Shi, J. H. Hu, A. Xu, Y. P. Sun, D. Li, Y. F. Shi, J. W. Zang, J. Zhu, Z. Chen, Z. G. Wang and B. X. Ge (2009). "An essential role for RIG-I in toll-like receptor-stimulated phagocytosis." Cell Host Microbe **6**(2): 150-161.

Kosiewicz, M. M., A. L. Zirnheld and P. Alard (2011). "Gut microbiota, immunity, and disease: a complex relationship." Front Microbiol **2**: 180.

Kraemer, S. M., S. A. Kyes, G. Aggarwal, A. L. Springer, S. O. Nelson, Z. Christodoulou, L. M. Smith, W. Wang, E. Levin, C. I. Newbold, P. J. Myler and J. D. Smith (2007). "Patterns of gene recombination shape var gene repertoires in Plasmodium falciparum: comparisons of geographically diverse isolates." BMC Genomics **8**: 45.

Kraemer, S. M. and J. D. Smith (2003). "Evidence for the importance of genetic structuring to the structural and functional specialization of the Plasmodium falciparum var gene family." Mol Microbiol **50**(5): 1527-1538.

Kraemer, S. M. and J. D. Smith (2006). "A family affair: var genes, PfEMP1 binding, and malaria disease." Curr Opin Microbiol **9**(4): 374-380.

Krech, U., Z. Konjajev and M. Jung (1971). "Congenital cytomegalovirus infection in siblings from consecutive pregnancies." Helv Paediatr Acta **26**(4): 355-362.

Kremsner, P. G., S. Winkler, C. Brandts, E. Wildling, L. Jenne, W. Graninger, J. Prada, U. Bienzle, P. Juillard and G. E. Grau (1995). "Prediction of accelerated cure in Plasmodium falciparum malaria by the elevated capacity of tumor necrosis factor production." Am J Trop Med Hyg **53**(5): 532-538.

Krishnegowda, G., A. M. Hajjar, J. Zhu, E. J. Douglass, S. Uematsu, S. Akira, A. S. Woods and D. C. Gowda (2005). "Induction of proinflammatory responses in macrophages by the glycosylphosphatidylinositols of Plasmodium falciparum: cell signaling receptors, glycosylphosphatidylinositol (GPI) structural requirement, and regulation of GPI activity." J Biol Chem **280**(9): 8606-8616.

Krow-Lucal, E. R., C. C. Kim, T. D. Burt and J. M. McCune (2014). "Distinct functional programming of human fetal and adult monocytes." Blood **123**(12): 1897-1904.

Krupka, M., K. Seydel, C. M. Feintuch, K. Yee, R. Kim, C. Y. Lin, R. B. Calder, C. Petersen, T. Taylor and J. Daily (2012). "Mild Plasmodium falciparum malaria following an episode of severe malaria is associated with induction of the interferon pathway in Malawian children." Infect Immun **80**(3): 1150-1155.

Kurtzhals, J. A., V. Adabayeri, B. Q. Goka, B. D. Akanmori, J. O. Oliver-Commey, F. K. Nkrumah, C. Behr and L. Hviid (1998). "Low plasma concentrations of interleukin 10 in severe malarial anaemia compared with cerebral and uncomplicated malaria." Lancet **351**(9118): 1768-1772.

Kwiatkowski, D., A. V. Hill, I. Sambou, P. Twumasi, J. Castracane, K. R. Manogue, A. Cerami, D. R. Brewster and B. M. Greenwood (1990). "TNF concentration in fatal cerebral, non-fatal cerebral, and uncomplicated Plasmodium falciparum malaria." Lancet **336**(8725): 1201-1204.

Kwiatkowski, D. and M. Nowak (1991). "Periodic and chaotic host-parasite interactions in human malaria." Proc Natl Acad Sci U S A **88**(12): 5111-5113.

Kyes, S., P. Horrocks and C. Newbold (2001). "Antigenic variation at the infected red cell surface in malaria." Annu Rev Microbiol **55**: 673-707.

Kyes, S., R. Pinches and C. Newbold (2000). "A simple RNA analysis method shows var and rif multigene family expression patterns in Plasmodium falciparum." Mol Biochem Parasitol **105**(2): 311-315.

Kyes, S. A., Z. Christodoulou, A. Raza, P. Horrocks, R. Pinches, J. A. Rowe and C. I. Newbold (2003). "A well-conserved Plasmodium falciparum var gene shows an unusual stage-specific transcript pattern." Mol Microbiol **48**(5): 1339-1348.

Kyes, S. A., S. M. Kraemer and J. D. Smith (2007). "Antigenic variation in Plasmodium falciparum: gene organization and regulation of the var multigene family." Eukaryot Cell **6**(9): 1511-1520.

Kyes, S. A., J. A. Rowe, N. Kriek and C. I. Newbold (1999). "Rifins: a second family of clonally variant proteins expressed on the surface of red cells infected with Plasmodium falciparum." Proc Natl Acad Sci U S A **96**(16): 9333-9338.

Kyriacou, H. M., G. N. Stone, R. J. Challis, A. Raza, K. E. Lyke, M. A. Thera, A. K. Kone, O. K. Doumbo, C. V. Plowe and J. A. Rowe (2006). "Differential var gene transcription in Plasmodium falciparum isolates from patients with cerebral malaria compared to hyperparasitaemia." Mol Biochem Parasitol **150**(2): 211-218.

Langhorne, J., P. Buffet, M. Galinski, M. Good, J. Harty, D. Leroy, M. M. Mota, E. Pasini, L. Renia, E. Riley, M. Stins and P. Duffy (2011). "The relevance of non-human primate and rodent malaria models for humans." Malar J **10**: 23.

Langhorne, J., F. M. Ndungu, A. M. Sponaas and K. Marsh (2008). "Immunity to malaria: more questions than answers." Nat Immunol **9**(7): 725-732.

Latz, E. (2010). "The inflammasomes: mechanisms of activation and function." Curr Opin Immunol **22**(1): 28-33.

Lavazec, C., S. Sanyal and T. J. Templeton (2007). "Expression switching in the stevor and Pfmc-2TM superfamilies in Plasmodium falciparum." Mol Microbiol **64**(6): 1621-1634.

Lavstsen, T., P. Magistrado, C. C. Hermsen, A. Salanti, A. T. Jensen, R. Sauerwein, L. Hviid, T. G. Theander and T. Staalsoe (2005). "Expression of Plasmodium falciparum erythrocyte membrane protein 1 in experimentally infected humans." Malar J **4**: 21.

Lavstsen, T., A. Salanti, A. T. Jensen, D. E. Arnot and T. G. Theander (2003). "Sub-grouping of Plasmodium falciparum 3D7 var genes based on sequence analysis of coding and non-coding regions." Malar J **2**: 27.

Lavstsen, T., L. Turner, F. Saguti, P. Magistrado, T. S. Rask, J. S. Jespersen, C. W. Wang, S. S. Berger, V. Baraka, A. M. Marquard, A. Seguin-Orlando, E. Willerslev, M. T. Gilbert, J. Lusingu and T. G. Theander (2012). "Plasmodium falciparum erythrocyte membrane protein 1 domain cassettes 8 and 13 are associated with severe malaria in children." Proc Natl Acad Sci U S A **109**(26): E1791-1800.

Lee, J., I. Tattoli, K. A. Wojtal, S. R. Vavricka, D. J. Philpott and S. E. Girardin (2009). "pH-dependent internalization of muramyl peptides from early endosomes enables Nod1 and Nod2 signaling." J Biol Chem **284**(35): 23818-23829.

Lemieux, J. E., S. A. Kyes, T. D. Otto, A. I. Feller, R. T. Eastman, R. A. Pinches, M. Berriman, X. Z. Su and C. I. Newbold (2013). "Genome-wide profiling of chromosome interactions in Plasmodium falciparum characterizes nuclear architecture and reconfigurations associated with antigenic variation." Mol Microbiol **90**(3): 519-537.

Leoratti, F. M., L. Farias, F. P. Alves, M. C. Suarez-Mutis, J. R. Coura, J. Kalil, E. P. Camargo, S. L. Moraes and R. Ramasawmy (2008). "Variants in the toll-like receptor signaling pathway and clinical outcomes of malaria." J Infect Dis **198**(5): 772-780.

Levy, O. and J. L. Wynn (2014). "A prime time for trained immunity: innate immune memory in newborns and infants." Neonatology **105**(2): 136-141.

Li, Y., M. Oosting, S. P. Smeekens, M. Jaeger, R. Aguirre-Gamboa, K. T. Le, P. Deelen, I. Ricano-Ponce, T. Schoffelen, A. F. Jansen, M. A. Swertz, S. Withoff, E. van de Vosse, M. van Deuren, F. van de Veerdonk, A. Zhernakova, J. W. van der Meer, R. J. Xavier, L. Franke, L. A. Joosten, C. Wijmenga, V. Kumar and M. G. Netea (2016). "A Functional Genomics Approach to Understand Variation in Cytokine Production in Humans." Cell **167**(4): 1099-1110 e1014.

Liehl, P. and M. M. Mota (2012). "Innate recognition of malarial parasites by mammalian hosts." Int J Parasitol **42**(6): 557-566.

Liehl, P., V. Zuzarte-Luis, J. Chan, T. Zillinger, F. Baptista, D. Carapau, M. Konert, K. K. Hanson, C. Carret, C. Lassnig, M. Muller, U. Kalinke, M. Saeed, A. F. Chora, D. T. Golenbock, B. Strobl, M. Prudencio, L. P. Coelho, S. H. Kappe, G. Superti-Furga, A. Pichlmair, A. M. Vigario, C. M. Rice, K. A. Fitzgerald, W. Barchet and M. M. Mota (2014). "Host-cell sensors for Plasmodium activate innate immunity against liver-stage infection." Nat Med **20**(1): 47-53.

Linke, A., R. Kuhn, W. Muller, N. Honarvar, C. Li and J. Langhorne (1996). "Plasmodium chabaudi chabaudi: differential susceptibility of gene-targeted mice deficient in IL-10 to an erythrocytic-stage infection." Exp Parasitol **84**(2): 253-263.

Litvak, V., S. A. Ramsey, A. G. Rust, D. E. Zak, K. A. Kennedy, A. E. Lampano, M. Nykter, I. Shmulevich and A. Aderem (2009). "Function of C/EBPdelta in a regulatory circuit that discriminates between transient and persistent TLR4-induced signals." Nat Immunol **10**(4): 437-443.

Liu, S. and C. Trapnell (2016). "Single-cell transcriptome sequencing: recent advances and remaining challenges." F1000Res **5**.

Llinas, M., Z. Bozdech, E. D. Wong, A. T. Adai and J. L. DeRisi (2006). "Comparative whole genome transcriptome analysis of three Plasmodium falciparum strains." Nucleic Acids Res **34**(4): 1166-1173.

Logan-Klumpler, F. J., N. De Silva, U. Boehme, M. B. Rogers, G. Velarde, J. A. McQuillan, T. Carver, M. Aslett, C. Olsen, S. Subramanian, I. Phan, C. Farris, S. Mitra, G. Ramasamy, H. Wang, A. Tivey, A. Jackson, R. Houston, J. Parkhill, M. Holden, O. S. Harb, B. P. Brunk, P. J. Myler, D. Roos, M. Carrington, D. F. Smith, C. Hertz-Fowler and M. Berriman (2012). "GeneDB--an annotation database for pathogens." Nucleic Acids Res **40**(Database issue): D98-108.

Looareesuwan, S., M. Ho, Y. Wattanagoon, N. J. White, D. A. Warrell, D. Bunnag, T. Harinasuta and D. J. Wyler (1987). "Dynamic alteration in splenic function during acute falciparum malaria." N Engl J Med **317**(11): 675-679.

Loughland, J. R., G. Minigo, J. Burel, P. E. Tipping, K. A. Piera, F. H. Amante, C. R. Engwerda, M. F. Good, D. L. Doolan, N. M. Anstey, J. S. McCarthy and T. Woodberry (2016). "Profoundly Reduced CD1c+ Myeloid Dendritic Cell HLA-DR and CD86 Expression and Increased Tumor Necrosis Factor Production in Experimental Human Blood-Stage Malaria Infection." Infect Immun **84**(5): 1403-1412.

Loughland, J. R., G. Minigo, D. S. Sarovich, M. Field, P. E. Tipping, M. Montes de Oca, K. A. Piera, F. H. Amante, B. E. Barber, M. J. Grigg, T. William, M. F. Good, D. L. Doolan, C. R. Engwerda, N. M. Anstey, J. S. McCarthy and T. Woodberry (2017). "Plasmacytoid dendritic cells appear inactive during sub-microscopic Plasmodium falciparum blood-stage infection, yet retain their ability to respond to TLR stimulation." Sci Rep **7**(1): 2596.

Love, M. I., W. Huber and S. Anders (2014). "Moderated estimation of fold change and dispersion for RNA-seq data with DESeq2." Genome Biol **15**(12): 550.

Lovegrove, F. E., N. Tangpukdee, R. O. Opoka, E. I. Lafferty, N. Rajwans, M. Hawkes, S. Krudsood, S. Looareesuwan, C. C. John, W. C. Liles and K. C. Kain (2009). "Serum angiopoietin-1 and -2 levels discriminate cerebral malaria from uncomplicated malaria and predict clinical outcome in African children." PLoS One **4**(3): e4912.

Lyke, K. E., R. Burges, Y. Cissoko, L. Sangare, M. Dao, I. Diarra, A. Kone, R. Harley, C. V. Plowe, O. K. Doumbo and M. B. Sztein (2004). "Serum levels of the proinflammatory cytokines interleukin-1 beta (IL-1beta), IL-6, IL-8, IL-10, tumor necrosis factor alpha, and IL-12(p70) in Malian children with severe Plasmodium falciparum malaria and matched uncomplicated malaria or healthy controls." Infect Immun **72**(10): 5630-5637.

Lyke, K. E., M. B. Laurens, K. Strauss, M. Adams, P. F. Billingsley, E. James, A. Manoj, S. Chakravarty, C. V. Plowe, M. L. Li, A. Ruben, R. Edelman, M. Green, T. J. Dube, B. K. Sim and S. L. Hoffman (2015). "Optimizing Intradermal Administration of Cryopreserved Plasmodium falciparum Sporozoites in Controlled Human Malaria Infection." Am J Trop Med Hyg **93**(6): 1274-1284.

Mackintosh, C. L., J. G. Beeson and K. Marsh (2004). "Clinical features and pathogenesis of severe malaria." Trends Parasitol **20**(12): 597-603.

MacPherson, G. G., M. J. Warrell, N. J. White, S. Looareesuwan and D. A. Warrell (1985). "Human cerebral malaria. A quantitative ultrastructural analysis of parasitized erythrocyte sequestration." Am J Pathol **119**(3): 385-401.

Magalhaes, J. G., M. T. Sorbara, S. E. Girardin and D. J. Philpott (2011). "What is new with Nods?" Curr Opin Immunol **23**(1): 29-34.

Maitland, K. and K. Marsh (2004). "Pathophysiology of severe malaria in children." Acta Trop **90**(2): 131-140.

Malaguarnera, L., R. M. Imbesi, S. Pignatelli, J. Simpore, M. Malaguarnera and S. Musumeci (2002). "Increased levels of interleukin-12 in Plasmodium falciparum malaria: correlation with the severity of disease." Parasite Immunol **24**(7): 387-389.

Malaguarnera, L., S. Pignatelli, M. Musumeci, J. Simpore and S. Musumeci (2002). "Plasma levels of interleukin-18 and interleukin-12 in Plasmodium falciparum malaria." Parasite Immunol **24**(9-10): 489-492.

Malaguarnera, L., S. Pignatelli, J. Simpore, M. Malaguarnera and S. Musumeci (2002). "Plasma levels of interleukin-12 (IL-12), interleukin-18 (IL-18) and transforming growth factor beta (TGF-beta) in Plasmodium falciparum malaria." Eur Cytokine Netw **13**(4): 425-430.

Manning, L., M. Laman, I. Law, C. Bona, S. Aipit, D. Teine, J. Warrell, A. Rosanas-Urgell, E. Lin, B. Kiniboro, J. Vince, I. Hwaiwhanje, H. Karunajeewa, P. Michon, P. Siba, I. Mueller and T. M. Davis (2011). "Features and prognosis of severe malaria caused by Plasmodium falciparum, Plasmodium vivax and mixed Plasmodium species in Papua New Guinean children." PLoS One **6**(12): e29203.

Maria, N. I., E. C. Steenwijk, I. J. AS, C. G. van Helden-Meeuwsen, P. Vogelsang, W. Beumer, Z. Brkic, P. L. van Daele, P. M. van Hagen, P. J. van der Spek, H. A. Drexhage and M. A. Versnel (2017). "Contrasting expression pattern of RNA-sensing receptors TLR7, RIG-I and MDA5 in interferon-positive and interferon-negative patients with primary Sjogren's syndrome." Ann Rheum Dis **76**(4): 721-730.

Marquet, S., O. Doumbo, S. Cabantous, B. Poudiougou, L. Argiro, I. Safeukui, S. Konate, S. Sissoko, E. Chevereau, A. Traore, M. M. Keita, C. Chevillard, L. Abel and A. J. Dessein (2008). "A functional promoter variant in IL12B predisposes to cerebral malaria." Hum Mol Genet **17**(14): 2190-2195.

Marsh, K., D. Forster, C. Waruiru, I. Mwangi, M. Winstanley, V. Marsh, C. Newton, P. Winstanley, P. Warn, N. Peshu and et al. (1995). "Indicators of life-threatening malaria in African children." N Engl J Med **332**(21): 1399-1404.

Marsh, K., L. Otoo, R. J. Hayes, D. C. Carson and B. M. Greenwood (1989). "Antibodies to blood stage antigens of Plasmodium falciparum in rural Gambians and their relation to protection against infection." Trans R Soc Trop Med Hyg **83**(3): 293-303.

Marsh, K. and R. W. Snow (1997). "Host-parasite interaction and morbidity in malaria endemic areas." Philos Trans R Soc Lond B Biol Sci **352**(1359): 1385-1394.

Martin, S. K., G. H. Rajasekariah, G. Awinda, J. Waitumbi and C. Kifude (2009). "Unified parasite lactate dehydrogenase and histidine-rich protein ELISA for quantification of Plasmodium falciparum." Am J Trop Med Hyg **80**(4): 516-522.

Maude, R. J., N. A. Beare, A. Abu Sayeed, C. C. Chang, P. Charunwatthana, M. A. Faiz, A. Hossain, E. B. Yunus, M. G. Hoque, M. U. Hasan, N. J. White, N. P. Day and A. M. Dondorp (2009). "The spectrum of retinopathy in adults with Plasmodium falciparum malaria." Trans R Soc Trop Med Hyg **103**(7): 665-671.

May, J., B. Lell, A. J. Luty, C. G. Meyer and P. G. Kremsner (2000). "Plasma interleukin-10:Tumor necrosis factor (TNF)-alpha ratio is associated with TNF promoter variants and predicts malarial complications." J Infect Dis **182**(5): 1570-1573.

McCall, M. B., M. G. Netea, C. C. Hermsen, T. Jansen, L. Jacobs, D. Golenbock, A. J. van der Ven and R. W. Sauerwein (2007). "Plasmodium falciparum infection causes proinflammatory priming of human TLR responses." J Immunol **179**(1): 162-171.

McGilvray, I. D., L. Serghides, A. Kapus, O. D. Rotstein and K. C. Kain (2000). "Nonopsonic monocyte/macrophage phagocytosis of Plasmodium falciparum-parasitized erythrocytes: a role for CD36 in malarial clearance." Blood **96**(9): 3231-3240.

McKenzie, F. E., G. M. Jeffery and W. E. Collins (2001). "Plasmodium malariae blood-stage dynamics." J Parasitol **87**(3): 626-637.

McKenzie, F. E., G. M. Jeffery and W. E. Collins (2002). "Plasmodium malariae infection boosts Plasmodium falciparum gametocyte production." Am J Trop Med Hyg **67**(4): 411-414.

McNab, F., K. Mayer-Barber, A. Sher, A. Wack and A. O'Garra (2015). "Type I interferons in infectious disease." Nat Rev Immunol **15**(2): 87-103.

Medana, I. M., N. P. Day, N. Sachanonta, N. T. Mai, A. M. Dondorp, E. Pongponratn, T. T. Hien, N. J. White and G. D. Turner (2011). "Coma in fatal adult human malaria is not caused by cerebral oedema." Malar J **10**: 267.

Mensah-Brown, H. E., N. Amoako, J. Abugri, L. B. Stewart, G. Agongo, E. K. Dickson, M. F. Ofori, J. A. Stoute, D. J. Conway and G. A. Awandare (2015). "Analysis of Erythrocyte Invasion Mechanisms of Plasmodium falciparum Clinical Isolates Across 3 Malaria-Endemic Areas in Ghana." J Infect Dis **212**(8): 1288-1297.

Merrick, C. J., C. Huttenhower, C. Buckee, A. Amambua-Ngwa, N. Gomez-Escobar, M. Walther, D. J. Conway and M. T. Duraisingh (2012). "Epigenetic dysregulation of virulence gene expression in severe Plasmodium falciparum malaria." J Infect Dis **205**(10): 1593-1600.

Metwally, N. G., A. K. Tilly, P. Lubiana, L. K. Roth, M. Dorpinghaus, S. Lorenzen, K. Schuldt, S. Witt, A. Bachmann, H. Tidow, T. Gutsmann, T. Burmester, T. Roeder, E. Tannich and I. Bruchhaus (2017). "Characterisation of Plasmodium falciparum populations selected on the human endothelial receptors P-selectin, E-selectin, CD9 and CD151." Sci Rep **7**(1): 4069.

Miller, L. H., D. I. Baruch, K. Marsh and O. K. Doumbo (2002). "The pathogenic basis of malaria." Nature **415**(6872): 673-679.

Milner, D. A., Jr., R. O. Whitten, S. Kamiza, R. Carr, G. Liomba, C. Dzamalala, K. B. Seydel, M. E. Molyneux and T. E. Taylor (2014). "The systemic pathology of cerebral malaria in African children." Front Cell Infect Microbiol **4**: 104.

Mirghani, H. A., H. G. Eltahir, A. E. TM, Y. A. Mirghani, M. I. Elbashir and I. Adam (2011). "Cytokine profiles in children with severe Plasmodium falciparum malaria in an area of unstable malaria transmission in central Sudan." J Trop Pediatr **57**(5): 392-395.

Mitchell, G. H., G. A. Butcher, A. Voller and S. Cohen (1976). "The effect of human immune IgG on the in vitro development of Plasmodium falciparum." Parasitology **72**(2): 149-162.

Mkumbaye, S. I., C. W. Wang, E. Lyimo, J. S. Jespersen, A. Manjurano, J. Mosha, R. A. Kavishe, S. B. Mwakalinga, D. T. Minja, J. P. Lusingu, T. G. Theander and T. Lavstsen (2017). "The Severity of Plasmodium falciparum Infection Is Associated with Transcript Levels of var Genes Encoding Endothelial Protein C Receptor-Binding P. falciparum Erythrocyte Membrane Protein 1." Infect Immun **85**(4).

Mockenhaupt, F. P., J. P. Cramer, L. Hamann, M. S. Stegemann, J. Eckert, N. R. Oh, R. N. Otchwemah, E. Dietz, S. Ehrhardt, N. W. Schroder, U. Bienzle and R. R. Schumann (2006). "Toll-like receptor (TLR) polymorphisms in African children: Common TLR-4 variants predispose to severe malaria." Proc Natl Acad Sci U S A **103**(1): 177-182.

Mockenhaupt, F. P., L. Hamann, C. von Gaertner, G. Bedu-Addo, C. von Kleinsorgen, R. R. Schumann and U. Bienzle (2006). "Common polymorphisms of toll-like receptors 4 and 9 are associated with the clinical manifestation of malaria during pregnancy." J Infect Dis **194**(2): 184-188.

Mohanty, S., L. A. Benjamin, M. Majhi, P. Panda, S. Kampondeni, P. K. Sahu, A. Mohanty, K. C. Mahanta, R. Pattnaik, R. R. Mohanty, S. Joshi, A. Mohanty, I. W. Turnbull, A. M. Dondorp, T. E. Taylor and S. C. Wassmer (2017). "Magnetic Resonance Imaging of Cerebral Malaria Patients Reveals Distinct Pathogenetic Processes in Different Parts of the Brain." mSphere **2**(3).

Molineaux, L., M. Trauble, W. E. Collins, G. M. Jeffery and K. Dietz (2002). "Malaria therapy reinoculation data suggest individual variation of an innate immune response and independent acquisition of antiparasitic and antitoxic immunities." Trans R Soc Trop Med Hyg **96**(2): 205-209.

Montes de Oca, M., R. Kumar, F. L. Rivera, F. H. Amante, M. Sheel, R. J. Faleiro, P. T. Bunn, S. E. Best, L. Beattie, S. S. Ng, C. L. Edwards, G. M. Boyle, R. N. Price, N. M. Anstey, J. R. Loughland, J. Burel, D. L. Doolan, A. Haque, J. S. McCarthy and C. R. Engwerda (2016). "Type I Interferons Regulate Immune Responses in Humans with Blood-Stage Plasmodium falciparum Infection." Cell Rep **17**(2): 399-412.

Mordmuller, B., C. Supan, K. L. Sim, G. P. Gomez-Perez, C. L. Ospina Salazar, J. Held, S. Bolte, M. Esen, S. Tschan, F. Joanny, C. Lamsfus Calle, S. J. Lohr, A. Lalremruata, A. Gunasekera, E. R. James, P. F. Billingsley, A. Richman, S. Chakravarty, A. Legarda, J. Munoz, R. M. Antonijoan, M. R. Ballester, S. L. Hoffman, P. L. Alonso and P. G. Kremsner (2015). "Direct venous inoculation of Plasmodium falciparum sporozoites for controlled human malaria infection: a dose-finding trial in two centres." Malar J **14**: 117.

Muller, U., U. Steinhoff, L. F. Reis, S. Hemmi, J. Pavlovic, R. M. Zinkernagel and M. Aguet (1994). "Functional role of type I and type II interferons in antiviral defense." Science **264**(5167): 1918-1921.

Murphy, S. C. and J. G. Breman (2001). "Gaps in the childhood malaria burden in Africa: cerebral malaria, neurological sequelae, anemia, respiratory distress, hypoglycemia, and complications of pregnancy." Am J Trop Med Hyg **64**(1-2 Suppl): 57-67.

Naik, R. S., O. H. Branch, A. S. Woods, M. Vijaykumar, D. J. Perkins, B. L. Nahlen, A. A. Lal, R. J. Cotter, C. E. Costello, C. F. Ockenhouse, E. A. Davidson and D. C. Gowda (2000). "Glycosylphosphatidylinositol anchors of Plasmodium falciparum: molecular characterization and naturally elicited antibody response that may provide immunity to malaria pathogenesis." J Exp Med **192**(11): 1563-1576.

Nam, D. K., S. Lee, G. Zhou, X. Cao, C. Wang, T. Clark, J. Chen, J. D. Rowley and S. M. Wang (2002). "Oligo(dT) primer generates a high frequency of truncated cDNAs through internal poly(A) priming during reverse transcription." Proc Natl Acad Sci U S A **99**(9): 6152-6156.

Nankervis, G. A. (1976). "Cytomegalovirus infections in the blood recipient." Yale J Biol Med **49**(1): 13-15.

Nedelec, Y., J. Sanz, G. Baharian, Z. A. Szpiech, A. Pacis, A. Dumaine, J. C. Grenier, A. Freiman, A. J. Sams, S. Hebert, A. Page Sabourin, F. Luca, R. Blekhman, R. D. Hernandez, R. Pique-Regi, J. Tung, V. Yotova and L. B. Barreiro (2016). "Genetic Ancestry and Natural Selection Drive Population Differences in Immune Responses to Pathogens." Cell **167**(3): 657-669 e621.

Newbold, C., P. Warn, G. Black, A. Berendt, A. Craig, B. Snow, M. Msobo, N. Peshu and K. Marsh (1997). "Receptor-specific adhesion and clinical disease in Plasmodium falciparum." Am J Trop Med Hyg **57**(4): 389-398.

Nguansangiam, S., N. P. Day, T. T. Hien, N. T. Mai, U. Chaisri, M. Riganti, A. M. Dondorp, S. J. Lee, N. H. Phu, G. D. Turner, N. J. White, D. J. Ferguson and E. Pongponratn (2007). "A quantitative ultrastructural study of renal pathology in fatal Plasmodium falciparum malaria." Trop Med Int Health **12**(9): 1037-1050.

Niang, M., A. K. Bei, K. G. Madnani, S. Pelly, S. Dankwa, U. Kanjee, K. Gunalan, A. Amaladoss, K. P. Yeo, N. S. Bob, B. Malleret, M. T. Duraisingh and P. R. Preiser (2014). "STEVOR is a Plasmodium falciparum erythrocyte binding protein that mediates merozoite invasion and rosetting." Cell Host Microbe **16**(1): 81-93.

Niang, M., X. Yan Yam and P. R. Preiser (2009). "The Plasmodium falciparum STEVOR multigene family mediates antigenic variation of the infected erythrocyte." PLoS Pathog **5**(2): e1000307.

Nielsen, M. A., T. Staalsoe, J. A. Kurtzhals, B. Q. Goka, D. Dodoo, M. Alifrangis, T. G. Theander, B. D. Akanmori and L. Hviid (2002). "Plasmodium falciparum variant surface antigen expression varies between isolates causing severe and nonsevere malaria and is modified by acquired immunity." J Immunol **168**(7): 3444-3450.

Noble, R., Z. Christodoulou, S. Kyes, R. Pinches, C. I. Newbold and M. Recker (2013). "The antigenic switching network of Plasmodium falciparum and its implications for the immuno-epidemiology of malaria." Elife **2**: e01074.

Nonvignon, J., G. C. Aryeetey, K. L. Malm, S. A. Agyemang, V. N. Aubyn, N. Y. Peprah, C. N. Bart-Plange and M. Aikins (2016). "Economic burden of malaria on businesses in Ghana: a case for private sector investment in malaria control." Malar J **15**: 454.

Normark, J., D. Nilsson, U. Ribacke, G. Winter, K. Moll, C. E. Wheelock, J. Bayarugaba, F. Kironde, T. G. Egwang, Q. Chen, B. Andersson and M. Wahlgren (2007). "PfEMP1-DBL1alpha amino acid motifs in severe disease states of Plasmodium falciparum malaria." Proc Natl Acad Sci U S A **104**(40): 15835-15840.

Obaldia, N., 3rd, E. Meibalan, J. M. Sa, S. Ma, M. A. Clark, P. Mejia, R. R. Moraes Barros, W. Otero, M. U. Ferreira, J. R. Mitchell, D. A. Milner, C. Huttenhower, D. F. Wirth, M. T. Duraisingh, T. E. Wellems and M. Marti (2018). "Bone Marrow Is a Major Parasite Reservoir in Plasmodium vivax Infection." MBio **9**(3).

Ockenhouse, C. F., M. Ho, N. N. Tandon, G. A. Van Seventer, S. Shaw, N. J. White, G. A. Jamieson, J. D. Chulay and H. K. Webster (1991). "Molecular basis of sequestration in severe and uncomplicated Plasmodium falciparum malaria: differential adhesion of infected erythrocytes to CD36 and ICAM-1." J Infect Dis **164**(1): 163-169.

Ockenhouse, C. F., W. C. Hu, K. E. Kester, J. F. Cummings, A. Stewart, D. G. Heppner, A. E. Jedlicka, A. L. Scott, N. D. Wolfe, M. Vahey and D. S. Burke (2006). "Common and divergent immune response signaling pathways discovered in peripheral blood mononuclear cell gene expression patterns in presymptomatic and clinically apparent malaria." Infect Immun **74**(10): 5561-5573.

Ofori, M. F., D. Dodoo, T. Staalsoe, J. A. Kurtzhals, K. Koram, T. G. Theander, B. D. Akanmori and L. Hviid (2002). "Malaria-induced acquisition of antibodies to Plasmodium falciparum variant surface antigens." Infect Immun **70**(6): 2982-2988.

Ogonda, L. A., A. S. Orago, M. F. Otieno, C. Adhiambo, W. Otieno and J. A. Stoute (2010). "The levels of CD16/Fc gamma receptor IIIA on CD14+ CD16+ monocytes are higher in children with severe Plasmodium falciparum anemia than in children with cerebral or uncomplicated malaria." Infect Immun **78**(5): 2173-2181.

Omer, F. M., J. B. de Souza and E. M. Riley (2003). "Differential induction of TGF-beta regulates proinflammatory cytokine production and determines the outcome of lethal and nonlethal Plasmodium yoelii infections." J Immunol **171**(10): 5430-5436.

Omer, F. M. and E. M. Riley (1998). "Transforming growth factor beta production is inversely correlated with severity of murine malaria infection." J Exp Med **188**(1): 39-48.

Oosting, M., M. Kerstholt, R. Ter Horst, Y. Li, P. Deelen, S. Smeekens, M. Jaeger, E. Lachmandas, H. Vrijmoeth, M. Lupse, M. Flonta, R. A. Cramer, B. J. Kullberg, V. Kumar, R. Xavier, C. Wijmenga, M. G. Netea and L. A. Joosten (2016). "Functional and Genomic Architecture of Borrelia burgdorferi-Induced Cytokine Responses in Humans." Cell Host Microbe **20**(6): 822-833.

Opi, D. H., L. B. Ochola, M. Tendwa, B. R. Siddondo, H. Ocholla, H. Fanjo, A. Ghumra, D. J. Ferguson, J. A. Rowe and T. N. Williams (2014). "Mechanistic Studies of the Negative Epistatic Malaria-protective Interaction Between Sickle Cell Trait and alpha(+)thalassemia." EBioMedicine **1**(1): 29-36.

Orem, J. N., J. M. Kirigia, R. Azairwe, I. Kasirye and O. Walker (2012). "Impact of malaria morbidity on gross domestic product in Uganda." Int Arch Med **5**(1): 12.

Oshlack, A. and M. J. Wakefield (2009). "Transcript length bias in RNA-seq data confounds systems biology." Biol Direct **4**: 14.

Othoro, C., A. A. Lal, B. Nahlen, D. Koech, A. S. Orago and V. Udhayakumar (1999). "A low interleukin-10 tumor necrosis factor-alpha ratio is associated with malaria anemia in children residing in a holoendemic malaria region in western Kenya." J Infect Dis **179**(1): 279-282.

Oviedo-Boyso, J., A. Bravo-Patino and V. M. Baizabal-Aguirre (2014). "Collaborative action of Toll-like and NOD-like receptors as modulators of the inflammatory response to pathogenic bacteria." Mediators Inflamm **2014**: 432785.

Pain, A., D. J. Ferguson, O. Kai, B. C. Urban, B. Lowe, K. Marsh and D. J. Roberts (2001). "Platelet-mediated clumping of Plasmodium falciparum-infected erythrocytes is a common adhesive phenotype and is associated with severe malaria." Proc Natl Acad Sci U S A **98**(4): 1805-1810.

Pain, A., B. C. Urban, O. Kai, C. Casals-Pascual, J. Shafi, K. Marsh and D. J. Roberts (2001). "A non-sense mutation in Cd36 gene is associated with protection from severe malaria." Lancet **357**(9267): 1502-1503.

Palm, N. W. and R. Medzhitov (2009). "Pattern recognition receptors and control of adaptive immunity." Immunol Rev **227**(1): 221-233.

Parra, M. E., C. B. Evans and D. W. Taylor (1991). "Identification of Plasmodium falciparum histidine-rich protein 2 in the plasma of humans with malaria." J Clin Microbiol **29**(8): 1629-1634.

Parroche, P., F. N. Lauw, N. Goutagny, E. Latz, B. G. Monks, A. Visintin, K. A. Halmen, M. Lamphier, M. Olivier, D. C. Bartholomeu, R. T. Gazzinelli and D. T. Golenbock (2007). "Malaria hemozoin is immunologically inert but radically enhances innate responses by presenting malaria DNA to Toll-like receptor 9." Proc Natl Acad Sci U S A **104**(6): 1919-1924.

Patel, A. A., Y. Zhang, J. N. Fullerton, L. Boelen, A. Rongvaux, A. A. Maini, V. Bigley, R. A. Flavell, D. W. Gilroy, B. Asquith, D. Macallan and S. Yona (2017). "The fate and lifespan of human monocyte subsets in steady state and systemic inflammation." J Exp Med **214**(7): 1913-1923.

Patel, S. N., L. Serghides, T. G. Smith, M. Febbraio, R. L. Silverstein, T. W. Kurtz, M. Pravenec and K. C. Kain (2004). "CD36 mediates the phagocytosis of Plasmodium falciparum-infected erythrocytes by rodent macrophages." J Infect Dis **189**(2): 204-213.

Paun, A., C. Yau and J. S. Danska (2016). "Immune recognition and response to the intestinal microbiome in type 1 diabetes." J Autoimmun **71**: 10-18.

Payne, R. O., K. H. Milne, S. C. Elias, N. J. Edwards, A. D. Douglas, R. E. Brown, S. E. Silk, S. Biswas, K. Miura, R. Roberts, T. W. Rampling, N. Venkatraman, S. H. Hodgson, G. M. Labbe, F. D. Halstead, I. D. Poulton, F. L. Nugent, H. de Graaf, P. Sukhtankar, N. C. Williams, C. F. Ockenhouse, A. K. Kathcart, A. N. Qabar, N. C. Waters, L. A. Soisson, A. J. Birkett, G. S. Cooke, S. N. Faust, C. Woods, K. Ivinson, J. S. McCarthy, C. L. Diggs, J. Vekemans, C. A. Long, A. V. Hill, A. M. Lawrie, S. Dutta and S. J. Draper (2016). "Demonstration of the Blood-Stage Plasmodium falciparum Controlled Human Malaria Infection Model to Assess Efficacy of the P. falciparum Apical Membrane Antigen 1 Vaccine, FMP2.1/AS01." J Infect Dis **213**(11): 1743-1751.

Perkins, D. J., J. B. Weinberg and P. G. Kremsner (2000). "Reduced interleukin-12 and transforming growth factor-beta1 in severe childhood malaria: relationship of cytokine balance with disease severity." J Infect Dis **182**(3): 988-992.

Peters, J., E. Fowler, M. Gatton, N. Chen, A. Saul and Q. Cheng (2002). "High diversity and rapid changeover of expressed var genes during the acute phase of Plasmodium falciparum infections in human volunteers." Proc Natl Acad Sci U S A **99**(16): 10689-10694.

Peters, J. M., E. V. Fowler, D. R. Krause, Q. Cheng and M. L. Gatton (2007). "Differential changes in Plasmodium falciparum var transcription during adaptation to culture." J Infect Dis **195**(5): 748-755.

Petter, M., M. Haeggstrom, A. Khattab, V. Fernandez, M. Q. Klinkert and M. Wahlgren (2007). "Variant proteins of the Plasmodium falciparum RIFIN family show distinct subcellular localization and developmental expression patterns." Mol Biochem Parasitol **156**(1): 51-61.

Piasecka, B., D. Duffy, A. Urrutia, H. Quach, E. Patin, C. Posseme, J. Bergstedt, B. Charbit, V. Rouilly, C. R. MacPherson, M. Hasan, B. Albaud, D. Gentien, J. Fellay, M. L. Albert, L. Quintana-Murci and C. Milieu Interieur (2018). "Distinctive roles of age, sex, and genetics in shaping transcriptional variation of human immune responses to microbial challenges." Proc Natl Acad Sci U S A **115**(3): E488-E497.

Picelli, S., A. K. Bjorklund, O. R. Faridani, S. Sagasser, G. Winberg and R. Sandberg (2013). "Smart-seq2 for sensitive full-length transcriptome profiling in single cells." Nat Methods **10**(11): 1096-1098.

Picelli, S., O. R. Faridani, A. K. Bjorklund, G. Winberg, S. Sagasser and R. Sandberg (2014). "Full-length RNA-seq from single cells using Smart-seq2." Nat Protoc **9**(1): 171-181.

Plebanski, M. and A. V. Hill (2000). "The immunology of malaria infection." Curr Opin Immunol **12**(4): 437-441.

Pombo, D. J., G. Lawrence, C. Hirunpetcharat, C. Rzepczyk, M. Bryden, N. Cloonan, K. Anderson, Y. Mahakunkijcharoen, L. B. Martin, D. Wilson, S. Elliott, S. Elliott, D. P. Eisen, J. B. Weinberg, A. Saul and M. F. Good (2002). "Immunity to malaria after administration of ultra-low doses of red cells infected with Plasmodium falciparum." Lancet **360**(9333): 610-617.

Ponsford, M. J., I. M. Medana, P. Prapansilp, T. T. Hien, S. J. Lee, A. M. Dondorp, M. M. Esiri, N. P. Day, N. J. White and G. D. Turner (2012). "Sequestration and microvascular congestion are associated with coma in human cerebral malaria." J Infect Dis **205**(4): 663-671.

Portugal, S., S. K. Pierce and P. D. Crompton (2013). "Young lives lost as B cells falter: what we are learning about antibody responses in malaria." J Immunol **190**(7): 3039-3046.

Potchen, M. J., S. D. Kampondeni, K. B. Seydel, G. L. Birbeck, C. A. Hammond, W. G. Bradley, J. K. DeMarco, S. J. Glover, J. O. Ugorji, M. T. Latourette, J. E. Siebert, M. E. Molyneux and T. E. Taylor (2012). "Acute brain MRI findings in 120 Malawian children with cerebral malaria: new insights into an ancient disease." AJNR Am J Neuroradiol **33**(9): 1740-1746.

Prudencio, M., A. Rodriguez and M. M. Mota (2006). "The silent path to thousands of merozoites: the Plasmodium liver stage." Nat Rev Microbiol **4**(11): 849-856.

Punsawadl, C., C. Setthapramote and P. Viriyavejakul (2014). "Cellular-mediated immune responses in the liver tissue of patients with severe Plasmodium falciparum malaria." Southeast Asian J Trop Med Public Health **45**(5): 973-983.

Rahimi, B. A., A. Thakkinstian, N. J. White, C. Sirivichayakul, A. M. Dondorp and W. Chokejindachai (2014). "Severe vivax malaria: a systematic review and meta-analysis of clinical studies since 1900." Malar J **13**: 481.

Ranque, S., B. Poudiougou, A. Traore, M. Keita, A. A. Oumar, I. Safeukui, S. Marquet, S. Cabantous, M. Diakite, D. Mintha, M. B. Cisse, M. M. Keita, A. J. Dessein and O. K. Doumbo (2008). "Life-threatening malaria in African children: a prospective study in a mesoendemic urban setting." Pediatr Infect Dis J **27**(2): 130-135.

Rask, T. S., D. A. Hansen, T. G. Theander, A. Gorm Pedersen and T. Lavstsen (2010). "Plasmodium falciparum erythrocyte membrane protein 1 diversity in seven genomes--divide and conquer." PLoS Comput Biol **6**(9).

Recker, M., C. O. Buckee, A. Serazin, S. Kyes, R. Pinches, Z. Christodoulou, A. L. Springer, S. Gupta and C. I. Newbold (2011). "Antigenic variation in Plasmodium falciparum malaria involves a highly structured switching pattern." PLoS Pathog **7**(3): e1001306.

Reid, A. J., A. M. Talman, H. M. Bennett, A. R. Gomes, M. J. Sanders, C. J. R. Illingworth, O. Billker, M. Berriman and M. K. Lawniczak (2018). "Single-cell RNA-seq reveals hidden transcriptional variation in malaria parasites." Elife **7**.

Riley, E. M. and V. A. Stewart (2013). "Immune mechanisms in malaria: new insights in vaccine development." Nat Med **19**(2): 168-178.

Roberts, D. J., A. G. Craig, A. R. Berendt, R. Pinches, G. Nash, K. Marsh and C. I. Newbold (1992). "Rapid switching to multiple antigenic and adhesive phenotypes in malaria." Nature **357**(6380): 689-692.

Robinson, B. A., T. L. Welch and J. D. Smith (2003). "Widespread functional specialization of Plasmodium falciparum erythrocyte membrane protein 1 family members to bind CD36 analysed across a parasite genome." Mol Microbiol **47**(5): 1265-1278.

Robinson, L. J., M. C. D'Ombrain, D. I. Stanisic, J. Taraika, N. Bernard, J. S. Richards, J. G. Beeson, L. Tavul, P. Michon, I. Mueller and L. Schofield (2009). "Cellular tumor necrosis factor, gamma interferon, and interleukin-6 responses as correlates of immunity and risk of clinical Plasmodium falciparum malaria in children from Papua New Guinea." Infect Immun **77**(7): 3033-3043.

Robinson, M. D., D. J. McCarthy and G. K. Smyth (2010). "edgeR: a Bioconductor package for differential expression analysis of digital gene expression data." Bioinformatics **26**(1): 139-140.

Rocha, B. C., P. E. Marques, F. M. Leoratti, C. Junqueira, D. B. Pereira, L. R. Antonelli, G. B. Menezes, D. T. Golenbock and R. T. Gazzinelli (2015). "Type I Interferon Transcriptional Signature in Neutrophils and Low-Density Granulocytes Are Associated with Tissue Damage in Malaria." Cell Rep **13**(12): 2829-2841.

Rockett, K. A., M. M. Awburn, B. B. Aggarwal, W. B. Cowden and I. A. Clark (1992). "In vivo induction of nitrite and nitrate by tumor necrosis factor, lymphotoxin, and interleukin-1: possible roles in malaria." Infect Immun **60**(9): 3725-3730.

Rockett, K. A., G. M. Clarke, K. Fitzpatrick, C. Hubbart, A. E. Jeffreys, K. Rowlands, R. Craik, M. Jallow, D. J. Conway, K. A. Bojang, M. Pinder, S. Usen, F. Sisay-Joof, G. Sirugo, O. Toure, M. A. Thera, S. Konate, S. Sissoko, A. Niangaly, B. Poudiougou, V. D. Mangano, E. C. Bougouma, S. B. Sirima, D. Modiano, L. N. Amenga-Etego, A. Ghansah, K. A. Koram, M. D. Wilson, A. Enimil, J. Evans, O. Amodu, S. Olaniyan, T. Apinjoh, R. Mugri, A. Ndi, C. M. Ndila, S. Uyoga, A. Macharia, N. Peshu, T. N. Williams, A. Manjurano, E. Riley, C. Drakeley, H. Reyburn, V. Nyirongo, D. Kachala, M. Molyneux, S. J. Dunstan, N. H. Phu, N. T. N. Quyen, C. Q. Thai, T. T. Hien, L. Manning, M. Laman, P. Siba, H. Karunajeewa, S. Allen, A. Allen, T. M. E. Davis, P. Michon, I. Mueller, A. Green, S. Molloy, K. J. Johnson, A. Kerasidou, V. Cornelius, L. Hart, A. Vanderwal, M. SanJoaquin, G. Band, S. Q. Le, M. Pirinen, N. Sepulveda, C. C. A. Spencer, T. G. Clark, T. Agbenyega, E. Achidi, O. Doumbo, J. Farrar, K. Marsh, T. Taylor, D. P. Kwiatkowski and M. G. E. Netwo (2014). "Reappraisal of known malaria resistance loci in a large multicenter study." Nat Genet **46**(11): 1197-1204.

Roers, A., B. Hiller and V. Hornung (2016). "Recognition of Endogenous Nucleic Acids by the Innate Immune System." Immunity **44**(4): 739-754.

Roestenberg, M., E. M. Bijker, B. K. Sim, P. F. Billingsley, E. R. James, G. J. Bastiaens, A. C. Teirlinck, A. Scholzen, K. Teelen, T. Arens, A. J. van der Ven, A. Gunasekera, S. Chakravarty, S. Velmurugan, C. C. Hermsen, R. W. Sauerwein and S. L. Hoffman (2013). "Controlled human malaria infections by intradermal injection of cryopreserved Plasmodium falciparum sporozoites." Am J Trop Med Hyg **88**(1): 5-13.

Roestenberg, M., S. J. de Vlas, A. E. Nieman, R. W. Sauerwein and C. C. Hermsen (2012). "Efficacy of preerythrocytic and blood-stage malaria vaccines can be assessed in small sporozoite challenge trials in human volunteers." J Infect Dis **206**(3): 319-323.

Roestenberg, M., B. Mordmuller, C. Ockenhouse, A. Mo, M. Yazdanbakhsh and P. G. Kremsner (2017). "The frontline of controlled human malaria infections: A report from the controlled human infection models Workshop in Leiden University Medical Centre 5 May 2016." Vaccine **35**(51): 7065-7069.

Roestenberg, M., G. A. O'Hara, C. J. Duncan, J. E. Epstein, N. J. Edwards, A. Scholzen, A. J. van der Ven, C. C. Hermsen, A. V. Hill and R. W. Sauerwein (2012). "Comparison of clinical and parasitological data from controlled human malaria infection trials." PLoS One **7**(6): e38434.

Rogerson, S. J., R. Tembenu, C. Dobano, S. Plitt, T. E. Taylor and M. E. Molyneux (1999). "Cytoadherence characteristics of Plasmodium falciparum-infected erythrocytes from Malawian children with severe and uncomplicated malaria." Am J Trop Med Hyg **61**(3): 467-472.

Rojas-Pena, M. L., A. Vallejo, S. Herrera, G. Gibson and M. Arevalo-Herrera (2015). "Transcription Profiling of Malaria-Naive and Semi-immune Colombian Volunteers in a Plasmodium vivax Sporozoite Challenge." PLoS Negl Trop Dis **9**(8): e0003978.

Romi, R., M. C. Razaiarimanga, R. Raharimanga, E. M. Rakotondraibe, L. H. Ranaivo, V. Pietra, A. Raveloson and G. Majori (2002). "Impact of the malaria control campaign (1993-1998) in the highlands of Madagascar: parasitological and entomological data." Am J Trop Med Hyg **66**(1): 2-6.

Rothen, J., C. Murie, J. Carnes, A. Anupama, S. Abdulla, M. Chemba, M. Mpina, M. Tanner, B. K. Lee Sim, S. L. Hoffman, R. Gottardo, C. Daubenberger and K. Stuart (2018). "Whole blood transcriptome changes following controlled human malaria infection in malaria pre-exposed volunteers correlate with parasite prepatent period." PLoS One **13**(6): e0199392.

Rottmann, M., T. Lavstsen, J. P. Mugasa, M. Kaestli, A. T. Jensen, D. Muller, T. Theander and H. P. Beck (2006). "Differential expression of var gene groups is associated with morbidity caused by Plasmodium falciparum infection in Tanzanian children." Infect Immun **74**(7): 3904-3911.

Rowe, A., J. Obeiro, C. I. Newbold and K. Marsh (1995). "Plasmodium falciparum rosetting is associated with malaria severity in Kenya." Infect Immun **63**(6): 2323-2326.

Rowe, J. A., A. Claessens, R. A. Corrigan and M. Arman (2009). "Adhesion of Plasmodium falciparum-infected erythrocytes to human cells: molecular mechanisms and therapeutic implications." Expert Rev Mol Med **11**: e16.

Rowe, J. A., I. G. Handel, M. A. Thera, A. M. Deans, K. E. Lyke, A. Kone, D. A. Diallo, A. Raza, O. Kai, K. Marsh, C. V. Plowe, O. K. Doumbo and J. M. Moulds (2007). "Blood group O protects against severe Plasmodium falciparum malaria through the mechanism of reduced rosetting." Proc Natl Acad Sci U S A **104**(44): 17471-17476.

Rts, S. C. T. P. (2015). "Efficacy and safety of RTS,S/AS01 malaria vaccine with or without a booster dose in infants and children in Africa: final results of a phase 3, individually randomised, controlled trial." Lancet **386**(9988): 31-45.

Russell, C., O. Mercereau-Puijalon, C. Le Scanf, M. Steward and D. E. Arnot (2005). "Further definition of PfEMP-1 DBL-1alpha domains mediating rosetting adhesion of Plasmodium falciparum." Mol Biochem Parasitol **144**(1): 109-113.

Ruwende, C., S. C. Khoo, R. W. Snow, S. N. Yates, D. Kwiatkowski, S. Gupta, P. Warn, C. E. Allsopp, S. C. Gilbert, N. Peschu and et al. (1995). "Natural selection of hemi- and heterozygotes for G6PD deficiency in Africa by resistance to severe malaria." Nature **376**(6537): 246-249.

Sabbah, A., T. H. Chang, R. Harnack, V. Frohlich, K. Tominaga, P. H. Dube, Y. Xiang and S. Bose (2009). "Activation of innate immune antiviral responses by Nod2." Nat Immunol **10**(10): 1073-1080.

Sachs, J. and P. Malaney (2002). "The economic and social burden of malaria." Nature **415**(6872): 680-685.

Saito, F., K. Hirayasu, T. Satoh, C. W. Wang, J. Lusingu, T. Arimori, K. Shida, N. M. Q. Palacpac, S. Itagaki, S. Iwanaga, E. Takashima, T. Tsuboi, M. Kohyama, T. Suenaga, M. Colonna, J. Takagi, T. Lavstsen, T. Horii and H. Arase (2017). "Immune evasion of Plasmodium falciparum by RIFIN via inhibitory receptors." Nature **552**(7683): 101-105.

Salanti, A., T. Staalsoe, T. Lavstsen, A. T. Jensen, M. P. Sowa, D. E. Arnot, L. Hviid and T. G. Theander (2003). "Selective upregulation of a single distinctly structured var gene in chondroitin sulphate A-adhering Plasmodium falciparum involved in pregnancy-associated malaria." Mol Microbiol **49**(1): 179-191.

Salmon, M. G., J. B. De Souza, G. A. Butcher and J. H. Playfair (1997). "Premature removal of uninfected erythrocytes during malarial infection of normal and immunodeficient mice." Clin Exp Immunol **108**(3): 471-476.

Sanderson, F., L. Andrews, A. D. Douglas, A. Hunt-Cooke, P. Bejon and A. V. Hill (2008). "Blood-stage challenge for malaria vaccine efficacy trials: a pilot study with discussion of safety and potential value." Am J Trop Med Hyg **78**(6): 878-883.

Sauerwein, R. W., M. Roestenberg and V. S. Moorthy (2011). "Experimental human challenge infections can accelerate clinical malaria vaccine development." Nat Rev Immunol **11**(1): 57-64.

Schellenberg, D., C. Menendez, E. Kahigwa, F. Font, C. Galindo, C. Acosta, J. A. Schellenberg, J. J. Aponte, J. Kimario, H. Urassa, H. Mshinda, M. Tanner and P. Alonso (1999). "African children with malaria in an area of intense Plasmodium falciparum transmission: features on admission to the hospital and risk factors for death." Am J Trop Med Hyg **61**(3): 431-438.

Scherer, E. F., D. G. Cantarini, R. Siqueira, E. B. Ribeiro, E. M. Braga, A. C. Honorio-Franca and E. L. Franca (2016). "Cytokine modulation of human blood viscosity from vivax malaria patients." Acta Trop **158**: 139-147.

Schirmer, M., S. P. Smeekens, H. Vlamakis, M. Jaeger, M. Oosting, E. A. Franzosa, T. Jansen, L. Jacobs, M. J. Bonder, A. Kurilshikov, J. Fu, L. A. Joosten, A. Zhernakova, C. Huttenhower, C. Wijmenga, M. G. Netea and R. J. Xavier (2016). "Linking the Human Gut Microbiome to Inflammatory Cytokine Production Capacity." Cell **167**(4): 1125-1136 e1128.

Schirmer, M., S. P. Smeekens, H. Vlamakis, M. Jaeger, M. Oosting, E. A. Franzosa, R. Ter Horst, T. Jansen, L. Jacobs, M. J. Bonder, A. Kurilshikov, J. Fu, L. A. B. Joosten, A. Zhernakova, C. Huttenhower, C. Wijmenga, M. G. Netea and R. J. Xavier (2016). "Linking the Human Gut Microbiome to Inflammatory Cytokine Production Capacity." Cell **167**(4): 1125-1136 e1128.

Schneider, W. M., M. D. Chevillotte and C. M. Rice (2014). "Interferon-stimulated genes: a complex web of host defenses." Annu Rev Immunol **32**: 513-545.

Schoenborn, J. R. and C. B. Wilson (2007). "Regulation of interferon-gamma during innate and adaptive immune responses." Adv Immunol **96**: 41-101.

Schoenfisch, A. L., S. C. Dollard, M. Amin, L. I. Gardner, R. S. Klein, K. Mayer, A. Rompalo, J. D. Sobel and M. J. Cannon (2011). "Cytomegalovirus (CMV) shedding is highly correlated with markers of immunosuppression in CMV-seropositive women." J Med Microbiol **60**(Pt 6): 768-774.

Schofield, L. and G. E. Grau (2005). "Immunological processes in malaria pathogenesis." Nat Rev Immunol **5**(9): 722-735.

Schofield, L. and F. Hackett (1993). "Signal transduction in host cells by a glycosylphosphatidylinositol toxin of malaria parasites." J Exp Med **177**(1): 145-153.

Schofield, L., M. C. Hewitt, K. Evans, M. A. Siomos and P. H. Seeberger (2002). "Synthetic GPI as a candidate anti-toxic vaccine in a model of malaria." Nature **418**(6899): 785-789.

Scholzen, A., A. C. Teirlinck, E. M. Bijker, M. Roestenberg, C. C. Hermsen, S. L. Hoffman and R. W. Sauerwein (2014). "BAFF and BAFF receptor levels correlate with B cell subset activation and redistribution in controlled human malaria infection." J Immunol **192**(8): 3719-3729.

Serghides, L., T. G. Smith, S. N. Patel and K. C. Kain (2003). "CD36 and malaria: friends or foes?" Trends Parasitol **19**(10): 461-469.

Seydel, K. B., S. D. Kampondeni, C. Valim, M. J. Potchen, D. A. Milner, F. W. Muwalo, G. L. Birbeck, W. G. Bradley, L. L. Fox, S. J. Glover, C. A. Hammond, R. S. Heyderman, C. A. Chilingulo, M. E. Molyneux and T. E. Taylor (2015). "Brain swelling and death in children with cerebral malaria." N Engl J Med **372**(12): 1126-1137.

Shaabani, N., V. Duhan, V. Khairnar, A. Gassa, R. Ferrer-Tur, D. Haussinger, M. Recher, G. Zelinskyy, J. Liu, U. Dittmer, M. Trilling, S. Scheu, C. Hardt, P. A. Lang, N. Honke and K. S. Lang (2016). "CD169(+) macrophages regulate PD-L1 expression via type I interferon and thereby prevent severe immunopathology after LCMV infection." Cell Death Dis **7**(11): e2446.

Shabani, E., B. Hanisch, R. O. Opoka, T. Lavstsen and C. C. John (2017). "Plasmodium falciparum EPCR-binding PfEMP1 expression increases with malaria disease severity and is elevated in retinopathy negative cerebral malaria." BMC Med **15**(1): 183.

Shanks, G. D. and N. J. White (2013). "The activation of vivax malaria hypnozoites by infectious diseases." Lancet Infect Dis **13**(10): 900-906.

Sharma, S., R. B. DeOliveira, P. Kalantari, P. Parroche, N. Goutagny, Z. Jiang, J. Chan, D. C. Bartholomeu, F. Lauw, J. P. Hall, G. N. Barber, R. T. Gazzinelli, K. A. Fitzgerald and D. T. Golenbock (2011). "Innate immune recognition of an AT-rich stem-loop DNA motif in the Plasmodium falciparum genome." Immunity **35**(2): 194-207.

Sharp, S., T. Lavstsen, Q. L. Fivelman, M. Saeed, L. McRobert, T. J. Templeton, A. T. Jensen, D. A. Baker, T. G. Theander and C. J. Sutherland (2006). "Programmed transcription of the var gene family, but not of stevor, in Plasmodium falciparum gametocytes." Eukaryot Cell **5**(8): 1206-1214.

Sheehy, S. H., A. D. Douglas and S. J. Draper (2013). "Challenges of assessing the clinical efficacy of asexual blood-stage Plasmodium falciparum malaria vaccines." Hum Vaccin Immunother **9**(9): 1831-1840.

Sheehy, S. H., C. J. Duncan, S. C. Elias, P. Choudhary, S. Biswas, F. D. Halstead, K. A. Collins, N. J. Edwards, A. D. Douglas, N. A. Anagnostou, K. J. Ewer, T. Havelock, T. Mahungu, C. M. Bliss, K. Miura, I. D. Poulton, P. J. Lillie, R. D. Antrobus, E. Berrie, S. Moyle, K. Gantlett, S. Colloca, R. Cortese, C. A. Long, R. E. Sinden, S. C. Gilbert, A. M. Lawrie, T. Doherty, S. N. Faust, A. Nicosia, A. V. Hill and S. J. Draper (2012). "ChAd63-MVA-vectored blood-stage malaria vaccines targeting MSP1 and AMA1: assessment of efficacy against mosquito bite challenge in humans." Mol Ther **20**(12): 2355-2368.

Sheehy, S. H., A. J. Spencer, A. D. Douglas, B. K. Sim, R. J. Longley, N. J. Edwards, I. D. Poulton, D. Kimani, A. R. Williams, N. A. Anagnostou, R. Roberts, S. Kerridge, M. Voysey, E. R. James, P. F. Billingsley, A. Gunasekera, A. M. Lawrie, S. L. Hoffman and A. V. Hill (2013). "Optimising Controlled Human Malaria Infection Studies Using Cryopreserved P. falciparum Parasites Administered by Needle and Syringe." PLoS One **8**(6): e65960.

Shekalaghe, S., M. Rutaihwa, P. F. Billingsley, M. Chemba, C. A. Daubenberger, E. R. James, M. Mpina, O. Ali Juma, T. Schindler, E. Huber, A. Gunasekera, A. Manoj, B. Simon, E. Saverino, L. W. Church, C. C. Hermsen, R. W. Sauerwein, C. Plowe, M. Venkatesan, P. Sasi, O. Lweno, P. Mutani, A. Hamad, A. Mohammed, A. Urassa, T. Mzee, D. Padilla, A. Ruben, B. K. Sim, M. Tanner, S. Abdulla and S. L. Hoffman (2014). "Controlled human malaria infection of Tanzanians by intradermal injection of aseptic, purified, cryopreserved Plasmodium falciparum sporozoites." Am J Trop Med Hyg **91**(3): 471-480.

Shio, M. T., S. C. Eisenbarth, M. Savaria, A. F. Vinet, M. J. Bellemare, K. W. Harder, F. S. Sutterwala, D. S. Bohle, A. Descoteaux, R. A. Flavell and M. Olivier (2009). "Malarial hemozoin activates the NLRP3 inflammasome through Lyn and Syk kinases." PLoS Pathog **5**(8): e1000559.

Shmeleva, E. V., S. E. Boag, S. Murali, K. Bennaceur, R. Das, M. Egred, I. Purcell, R. Edwards, S. Todryk and I. Spyridopoulos (2015). "Differences in immune responses between CMV-seronegative and -seropositive patients with myocardial ischemia and reperfusion." Immun Inflamm Dis **3**(2): 56-70.

Silamut, K. and N. J. White (1993). "Relation of the stage of parasite development in the peripheral blood to prognosis in severe falciparum malaria." Trans R Soc Trop Med Hyg **87**(4): 436-443.

Silver, K. L., S. J. Higgins, C. R. McDonald and K. C. Kain (2010). "Complement driven innate immune response to malaria: fuelling severe malarial diseases." Cell Microbiol **12**(8): 1036-1045.

Silvestrini, F., P. Alano and J. L. Williams (2000). "Commitment to the production of male and female gametocytes in the human malaria parasite Plasmodium falciparum." Parasitology **121 Pt 5**: 465-471.

Simpson, J. A., L. Aarons, W. E. Collins, G. M. Jeffery and N. J. White (2002). "Population dynamics of untreated Plasmodium falciparum malaria within the adult human host during the expansion phase of the infection." Parasitology **124**(Pt 3): 247-263.

Singh, B., L. Kim Sung, A. Matusop, A. Radhakrishnan, S. S. Shamsul, J. Cox-Singh, A. Thomas and D. J. Conway (2004). "A large focus of naturally acquired Plasmodium knowlesi infections in human beings." Lancet **363**(9414): 1017-1024.

Sinka, M. E., M. J. Bangs, S. Manguin, Y. Rubio-Palis, T. Chareonviriyaphap, M. Coetzee, C. M. Mbogo, J. Hemingway, A. P. Patil, W. H. Temperley, P. W. Gething, C. W. Kabaria, T. R. Burkot, R. E. Harbach and S. I. Hay (2012). "A global map of dominant malaria vectors." Parasit Vectors **5**: 69.

Sisquella, X., Y. Ofir-Birin, M. A. Pimentel, L. Cheng, P. Abou Karam, N. G. Sampaio, J. S. Penington, D. Connolly, T. Giladi, B. J. Scicluna, R. A. Sharples, A. Waltmann, D. Avni, E. Schwartz, L. Schofield, Z. Porat, D. S. Hansen, A. T. Papenfuss, E. M. Eriksson, M. Gerlic, A. F. Hill, A. G. Bowie and N. Regev-Rudzki (2017). "Malaria parasite DNA-harbouring vesicles activate cytosolic immune sensors." Nat Commun **8**(1): 1985.

Smith, J. D., C. E. Chitnis, A. G. Craig, D. J. Roberts, D. E. Hudson-Taylor, D. S. Peterson, R. Pinches, C. I. Newbold and L. H. Miller (1995). "Switches in expression of Plasmodium falciparum var genes correlate with changes in antigenic and cytoadherent phenotypes of infected erythrocytes." Cell **82**(1): 101-110.

Smith, J. D., B. Gamain, D. I. Baruch and S. Kyes (2001). "Decoding the language of var genes and Plasmodium falciparum sequestration." Trends Parasitol **17**(11): 538-545.

Snow, R. W., J. A. Omumbo, B. Lowe, C. S. Molyneux, J. O. Obiero, A. Palmer, M. W. Weber, M. Pinder, B. Nahlen, C. Obonyo, C. Newbold, S. Gupta and K. Marsh (1997). "Relation between severe malaria morbidity in children and level of Plasmodium falciparum transmission in Africa." Lancet **349**(9066): 1650-1654.

Spaulding, E., D. Fooksman, J. M. Moore, A. Saidi, C. M. Feintuch, B. Reizis, L. Chorro, J. Daily and G. Lauvau (2016). "STING-Licensed Macrophages Prime Type I IFN Production by Plasmacytoid Dendritic Cells in the Bone Marrow during Severe Plasmodium yoelii Malaria." PLoS Pathog **12**(10): e1005975.

Spence, P. J., W. Jarra, P. Levy, A. J. Reid, L. Chappell, T. Brugat, M. Sanders, M. Berriman and J. Langhorne (2013). "Vector transmission regulates immune control of Plasmodium virulence." Nature **498**(7453): 228-231.

Sponaas, A. M., A. P. Freitas do Rosario, C. Voisine, B. Mastelic, J. Thompson, S. Koernig, W. Jarra, L. Renia, M. Mauduit, A. J. Potocnik and J. Langhorne (2009). "Migrating monocytes recruited to the spleen play an important role in control of blood stage malaria." Blood **114**(27): 5522-5531.

Staalsoe, T., M. A. Nielsen, L. S. Vestergaard, A. T. Jensen, T. G. Theander and L. Hviid (2003). "In vitro selection of Plasmodium falciparum 3D7 for expression of variant surface antigens associated with severe malaria in African children." Parasite Immunol **25**(8-9): 421-427.

Stanisic, D. I., J. Gerrard, J. Fink, P. M. Griffin, X. Q. Liu, L. Sundac, S. Sekuloski, I. B. Rodriguez, J. Pingnet, Y. Yang, Y. Zhou, K. R. Trenholme, C. Y. Wang, H. Hackett, J. A. Chan, C. Langer, E. Hanssen, S. L. Hoffman, J. G. Beeson, J. S. McCarthy and M. F. Good (2016). "Infectivity of Plasmodium falciparum in Malaria-Naive Individuals Is Related to Knob Expression and Cytoadherence of the Parasite." Infect Immun **84**(9): 2689-2696.

Stanisic, D. I., J. S. McCarthy and M. F. Good (2018). "Controlled Human Malaria Infection: Applications, Advances, and Challenges." Infect Immun **86**(1).

Stegle, O., S. A. Teichmann and J. C. Marioni (2015). "Computational and analytical challenges in single-cell transcriptomics." Nat Rev Genet **16**(3): 133-145.

Strowig, T., J. Henao-Mejia, E. Elinav and R. Flavell (2012). "Inflammasomes in health and disease." Nature **481**(7381): 278-286.

Su, Z., A. Fortin, P. Gros and M. M. Stevenson (2002). "Opsonin-independent phagocytosis: an effector mechanism against acute blood-stage Plasmodium chabaudi AS infection." J Infect Dis **186**(9): 1321-1329.

Su, Z. and M. M. Stevenson (2002). "IL-12 is required for antibody-mediated protective immunity against blood-stage Plasmodium chabaudi AS malaria infection in mice." J Immunol **168**(3): 1348-1355.

Sylwester, A. W., B. L. Mitchell, J. B. Edgar, C. Taormina, C. Pelte, F. Ruchti, P. R. Sleath, K. H. Grabstein, N. A. Hosken, F. Kern, J. A. Nelson and L. J. Picker (2005). "Broadly targeted human cytomegalovirus-specific CD4+ and CD8+ T cells dominate the memory compartments of exposed subjects." J Exp Med **202**(5): 673-685.

Tachado, S. D., P. Gerold, M. J. McConville, T. Baldwin, D. Quilici, R. T. Schwarz and L. Schofield (1996). "Glycosylphosphatidylinositol toxin of Plasmodium induces nitric oxide synthase expression in macrophages and vascular endothelial cells by a protein tyrosine kinase-dependent and protein kinase C-dependent signaling pathway." J Immunol **156**(5): 1897-1907.

Takaoka, A., Z. Wang, M. K. Choi, H. Yanai, H. Negishi, T. Ban, Y. Lu, M. Miyagishi, T. Kodama, K. Honda, Y. Ohba and T. Taniguchi (2007). "DAI (DLM-1/ZBP1) is a cytosolic DNA sensor and an activator of innate immune response." Nature **448**(7152): 501-505.

Takeuchi, O. and S. Akira (2010). "Pattern recognition receptors and inflammation." Cell **140**(6): 805-820.

Taverne, J., J. Tavernier, W. Fiers and J. H. Playfair (1987). "Recombinant tumour necrosis factor inhibits malaria parasites in vivo but not in vitro." Clin Exp Immunol **67**(1): 1-4.

Taylor, H. M., S. A. Kyes and C. I. Newbold (2000). "Var gene diversity in Plasmodium falciparum is generated by frequent recombination events." Mol Biochem Parasitol **110**(2): 391-397.

Taylor, W. R. J., J. Hanson, G. D. H. Turner, N. J. White and A. M. Dondorp (2012). "Respiratory manifestations of malaria." Chest **142**(2): 492-505.

Teirlinck, A. C., M. B. McCall, M. Roestenberg, A. Scholzen, R. Woestenenk, Q. de Mast, A. J. van der Ven, C. C. Hermsen, A. J. Luty and R. W. Sauerwein (2011). "Longevity and composition of cellular immune responses following experimental Plasmodium falciparum malaria infection in humans." PLoS Pathog **7**(12): e1002389.

Teirlinck, A. C., M. Roestenberg, E. M. Bijker, S. L. Hoffman, R. W. Sauerwein and A. Scholzen (2015). "Plasmodium falciparum Infection of Human Volunteers Activates Monocytes and CD16+ Dendritic Cells and Induces Upregulation of CD16 and CD1c Expression." Infect Immun **83**(9): 3732-3739.

Ter Horst, R., M. Jaeger, S. P. Smeekens, M. Oosting, M. A. Swertz, Y. Li, V. Kumar, D. A. Diavatopoulos, A. F. Jansen, H. Lemmers, H. Toenhake-Dijkstra, A. E. van Herwaarden, M. Janssen, R. G. van der Molen, I. Joosten, F. C. Sweep, J. W. Smit, R. T. Netea-Maier, M. M. Koenders, R. J. Xavier, J. W. van der Meer, C. A. Dinarello, N. Pavelka, C. Wijmenga, R. A. Notebaart, L. A. Joosten and M. G. Netea (2016). "Host and Environmental Factors Influencing Individual Human Cytokine Responses." Cell **167**(4): 1111-1124 e1113.

Ter Horst, R., M. Jaeger, S. P. Smeekens, M. Oosting, M. A. Swertz, Y. Li, V. Kumar, D. A. Diavatopoulos, A. F. M. Jansen, H. Lemmers, H. Toenhake-Dijkstra, A. E. van Herwaarden, M. Janssen, R. G. van der Molen, I. Joosten, F. Sweep, J. W. Smit, R. T. Netea-Maier, M. Koenders, R. J. Xavier, J. W. M. van der Meer, C. A. Dinarello, N. Pavelka, C. Wijmenga, R. A. Notebaart, L. A. B. Joosten and M. G. Netea (2016). "Host and Environmental Factors Influencing Individual Human Cytokine Responses." Cell **167**(4): 1111-1124 e1113.

Thuma, P. E., J. van Dijk, R. Bucala, Z. Debebe, S. Nekhai, T. Kuddo, M. Nouraie, G. Weiss and V. R. Gordeuk (2011). "Distinct clinical and immunologic profiles in severe malarial anemia and cerebral malaria in Zambia." J Infect Dis **203**(2): 211-219.

Tiburcio, M., M. W. Dixon, O. Looker, S. Y. Younis, L. Tilley and P. Alano (2015). "Specific expression and export of the Plasmodium falciparum Gametocyte EXported Protein-5 marks the gametocyte ring stage." Malar J **14**: 334.

Togbe, D., L. Schofield, G. E. Grau, B. Schnyder, V. Boissay, S. Charron, S. Rose, B. Beutler, V. F. Quesniaux and B. Ryffel (2007). "Murine cerebral malaria development is independent of toll-like receptor signaling." Am J Pathol **170**(5): 1640-1648.

Tonkin-Hill, G. Q., L. Trianty, R. Noviyanti, H. H. T. Nguyen, B. F. Sebayang, D. A. Lampah, J. Marfurt, S. A. Cobbold, J. S. Rambhatla, M. J. McConville, S. J. Rogerson, G. V. Brown, K. P. Day, R. N. Price, N. M. Anstey, A. T. Papenfuss and M. F. Duffy (2018). "The Plasmodium falciparum transcriptome in severe malaria reveals altered expression of genes involved in important processes including surface antigen-encoding var genes." PLoS Biol **16**(3): e2004328.

Tran, T. M., M. B. Jones, A. Ongoiba, E. M. Bijker, R. Schats, P. Venepally, J. Skinner, S. Doumbo, E. Quinten, L. G. Visser, E. Whalen, S. Presnell, E. M. O'Connell, K.

Kayentao, O. K. Doumbo, D. Chaussabel, H. Lorenzi, T. B. Nutman, T. H. Ottenhoff, M. C. Haks, B. Traore, E. F. Kirkness, R. W. Sauerwein and P. D. Crompton (2016). "Transcriptomic evidence for modulation of host inflammatory responses during febrile Plasmodium falciparum malaria." Sci Rep **6**: 31291.

Trinchieri, G. and A. Sher (2007). "Cooperation of Toll-like receptor signals in innate immune defence." Nat Rev Immunol **7**(3): 179-190.

Trubowitz, S. and B. Masek (1968). "Plasmodium falciparum: phagocytosis by polymorphonuclear leukocytes." Science **162**(3850): 273-274.

Tsutsui, N. and T. Kamiyama (1999). "Transforming growth factor beta-induced failure of resistance to infection with blood-stage Plasmodium chabaudi in mice." Infect Immun **67**(5): 2306-2311.

Turner, G. D., H. Morrison, M. Jones, T. M. Davis, S. Looareesuwan, I. D. Buley, K. C. Gatter, C. I. Newbold, S. Pukritayakamee, B. Nagachinta and et al. (1994). "An immunohistochemical study of the pathology of fatal malaria. Evidence for widespread endothelial activation and a potential role for intercellular adhesion molecule-1 in cerebral sequestration." Am J Pathol **145**(5): 1057-1069.

Turner, L., T. Lavstsen, S. S. Berger, C. W. Wang, J. E. Petersen, M. Avril, A. J. Brazier, J. Freeth, J. S. Jespersen, M. A. Nielsen, P. Magistrado, J. Lusingu, J. D. Smith, M. K. Higgins and T. G. Theander (2013). "Severe malaria is associated with parasite binding to endothelial protein C receptor." Nature **498**(7455): 502-505.

Turner, L., C. W. Wang, T. Lavstsen, S. B. Mwakalinga, R. W. Sauerwein, C. C. Hermsen and T. G. Theander (2011). "Antibodies against PfEMP1, RIFIN, MSP3 and GLURP are acquired during controlled Plasmodium falciparum malaria infections in naive volunteers." PLoS One **6**(12): e29025.

Turrini, F., H. Ginsburg, F. Bussolino, G. P. Pescarmona, M. V. Serra and P. Arese (1992). "Phagocytosis of Plasmodium falciparum-infected human red blood cells by human monocytes: involvement of immune and nonimmune determinants and dependence on parasite developmental stage." Blood **80**(3): 801-808.

Urban, B. C., D. J. Ferguson, A. Pain, N. Willcox, M. Plebanski, J. M. Austyn and D. J. Roberts (1999). "Plasmodium falciparum-infected erythrocytes modulate the maturation of dendritic cells." Nature **400**(6739): 73-77.

Viebig, N. K., U. Wulbrand, R. Forster, K. T. Andrews, M. Lanzer and P. A. Knolle (2005). "Direct activation of human endothelial cells by Plasmodium falciparum-infected erythrocytes." Infect Immun **73**(6): 3271-3277.

Vigario, A. M., E. Belnoue, A. C. Gruner, M. Mauduit, M. Kayibanda, J. C. Deschemin, M. Marussig, G. Snounou, D. Mazier, I. Gresser and L. Renia (2007). "Recombinant human IFN-alpha inhibits cerebral malaria and reduces parasite burden in mice." J Immunol **178**(10): 6416-6425.

Villegas-Mendez, A., T. N. Shaw, C. A. Inkson, P. Strangward, J. B. de Souza and K. N. Couper (2016). "Parasite-Specific CD4+ IFN-gamma+ IL-10+ T Cells Distribute within Both Lymphoid and Nonlymphoid Compartments and Are Controlled Systemically by Interleukin-27 and ICOS during Blood-Stage Malaria Infection." Infect Immun **84**(1): 34-46.

Viriyavejakul, P., V. Khachonsaksumet and C. Punsawad (2014). "Liver changes in severe Plasmodium falciparum malaria: histopathology, apoptosis and nuclear factor kappa B expression." Malar J **13**: 106.

von Seidlein, L., R. Olaosebikan, I. C. Hendriksen, S. J. Lee, O. T. Adedoyin, T. Agbenyega, S. B. Nguah, K. Bojang, J. L. Deen, J. Evans, C. I. Fanello, E. Gomes, A. J. Pedro, C. Kahabuka, C. Karema, E. Kivaya, K. Maitland, O. A. Mokuolu, G. Mtove, J. Mwanga-Amumpaire, B. Nadjm, M. Nansumba, W. P. Ngum, M. A. Onyamboko, H. Reyburn, T. Sakulthaew, K. Silamut, A. K. Tshefu, N. Umulisa, S. Gesase, N. P. Day, N. J. White and A. M. Dondorp (2012). "Predicting the clinical outcome of severe falciparum malaria in african children: findings from a large randomized trial." Clin Infect Dis **54**(8): 1080-1090.

Voss, T. S., J. Healer, A. J. Marty, M. F. Duffy, J. K. Thompson, J. G. Beeson, J. C. Reeder, B. S. Crabb and A. F. Cowman (2006). "A var gene promoter controls allelic exclusion of virulence genes in Plasmodium falciparum malaria." Nature **439**(7079): 1004-1008.

Wahlgren, M., S. Goel and R. R. Akhouri (2017). "Variant surface antigens of Plasmodium falciparum and their roles in severe malaria." Nat Rev Microbiol **15**(8): 479-491.

Walk, J., R. Schats, M. C. Langenberg, I. J. Reuling, K. Teelen, M. Roestenberg, C. C. Hermsen, L. G. Visser and R. W. Sauerwein (2016). "Diagnosis and treatment based on quantitative PCR after controlled human malaria infection." Malar J **15**(1): 398.

Walther, M., J. E. Tongren, L. Andrews, D. Korbel, E. King, H. Fletcher, R. F. Andersen, P. Bejon, F. Thompson, S. J. Dunachie, F. Edele, J. B. de Souza, R. E. Sinden, S. C. Gilbert, E. M. Riley and A. V. Hill (2005). "Upregulation of TGF-beta, FOXP3, and CD4+CD25+ regulatory T cells correlates with more rapid parasite growth in human malaria infection." Immunity **23**(3): 287-296.

Walther, M., J. Woodruff, F. Edele, D. Jeffries, J. E. Tongren, E. King, L. Andrews, P. Bejon, S. C. Gilbert, J. B. De Souza, R. Sinden, A. V. Hill and E. M. Riley (2006). "Innate immune responses to human malaria: heterogeneous cytokine responses to blood-stage Plasmodium falciparum correlate with parasitological and clinical outcomes." J Immunol **177**(8): 5736-5745.

Wambua, S., T. W. Mwangi, M. Kortok, S. M. Uyoga, A. W. Macharia, J. K. Mwacharo, D. J. Weatherall, R. W. Snow, K. Marsh and T. N. Williams (2006). "The effect of alpha+-thalassaemia on the incidence of malaria and other diseases in children living on the coast of Kenya." PLoS Med **3**(5): e158.

Wang, C. W., C. C. Hermsen, R. W. Sauerwein, D. E. Arnot, T. G. Theander and T. Lavstsen (2009). "The Plasmodium falciparum var gene transcription strategy at the onset of blood stage infection in a human volunteer." Parasitol Int **58**(4): 478-480.

Wang, C. W., P. A. Magistrado, M. A. Nielsen, T. G. Theander and T. Lavstsen (2009). "Preferential transcription of conserved rif genes in two phenotypically distinct Plasmodium falciparum parasite lines." Int J Parasitol **39**(6): 655-664.

Warimwe, G. M., G. Fegan, J. N. Musyoki, C. R. Newton, M. Opiyo, G. Githinji, C. Andisi, F. Menza, B. Kitsao, K. Marsh and P. C. Bull (2012). "Prognostic indicators of life-threatening malaria are associated with distinct parasite variant antigen profiles." Sci Transl Med **4**(129): 129ra145.

Warimwe, G. M., T. M. Keane, G. Fegan, J. N. Musyoki, C. R. Newton, A. Pain, M. Berriman, K. Marsh and P. C. Bull (2009). "Plasmodium falciparum var gene expression is modified by host immunity." Proc Natl Acad Sci U S A **106**(51): 21801-21806.

Warimwe, G. M., M. Recker, E. W. Kiragu, C. O. Buckee, J. Wambua, J. N. Musyoki, K. Marsh and P. C. Bull (2013). "Plasmodium falciparum var gene expression homogeneity as a marker of the host-parasite relationship under different levels of naturally acquired immunity to malaria." PLoS One **8**(7): e70467.

Weinberg, J. B., A. D. Volkheimer, M. P. Rubach, S. M. Florence, J. P. Mukemba, A. R. Kalingonji, C. Langelier, Y. Chen, M. Bush, T. W. Yeo, D. L. Granger, N. M. Anstey and E. D. Mwaikambo (2016). "Monocyte polarization in children with falciparum malaria: relationship to nitric oxide insufficiency and disease severity." Sci Rep **6**: 29151.

Weiss, G. E., B. Traore, K. Kayentao, A. Ongoiba, S. Doumbo, D. Doumtabe, Y. Kone, S. Dia, A. Guindo, A. Traore, C. Y. Huang, K. Miura, M. Mircetic, S. Li, A. Baughman, D. L. Narum, L. H. Miller, O. K. Doumbo, S. K. Pierce and P. D. Crompton (2010). "The

Plasmodium falciparum-specific human memory B cell compartment expands gradually with repeated malaria infections." PLoS Pathog **6**(5): e1000912.

Wenisch, C., K. F. Linnau, S. Looaresuwan and H. Rumpold (1999). "Plasma levels of the interleukin-6 cytokine family in persons with severe Plasmodium falciparum malaria." J Infect Dis **179**(3): 747-750.

White, N. J. (2011). "Determinants of relapse periodicity in Plasmodium vivax malaria." Malar J **10**: 297.

White, N. J. and M. Imwong (2012). "Relapse." Adv Parasitol **80**: 113-150.

White, N. J., S. Pukrittayakamee, T. T. Hien, M. A. Faiz, O. A. Mokuolu and A. M. Dondorp (2014). "Malaria." Lancet **383**(9918): 723-735.

Willcocks, L. C., E. J. Carr, H. A. Niederer, T. F. Rayner, T. N. Williams, W. Yang, J. A. Scott, B. C. Urban, N. Peshu, T. J. Vyse, Y. L. Lau, P. A. Lyons and K. G. Smith (2010). "A defunctioning polymorphism in FCGR2B is associated with protection against malaria but susceptibility to systemic lupus erythematosus." Proc Natl Acad Sci U S A **107**(17): 7881-7885.

Willmann, M., A. Ahmed, A. Siner, I. T. Wong, L. C. Woon, B. Singh, S. Krishna and J. Cox-Singh (2012). "Laboratory markers of disease severity in Plasmodium knowlesi infection: a case control study." Malar J **11**: 363.

Wilson, N. O., V. Jain, C. E. Roberts, N. Lucchi, P. K. Joel, M. P. Singh, A. C. Nagpal, A. P. Dash, V. Udhayakumar, N. Singh and J. K. Stiles (2011). "CXCL4 and CXCL10 predict risk of fatal cerebral malaria." Dis Markers **30**(1): 39-49.

Woodberry, T., G. Minigo, K. A. Piera, F. H. Amante, A. Pinzon-Charry, M. F. Good, J. A. Lopez, C. R. Engwerda, J. S. McCarthy and N. M. Anstey (2012). "Low-level Plasmodium falciparum blood-stage infection causes dendritic cell apoptosis and dysfunction in healthy volunteers." J Infect Dis **206**(3): 333-340.

Wu, J., L. Sun, X. Chen, F. Du, H. Shi, C. Chen and Z. J. Chen (2013). "Cyclic GMP-AMP is an endogenous second messenger in innate immune signaling by cytosolic DNA." Science **339**(6121): 826-830.

Wu, J., L. Tian, X. Yu, S. Pattaradilokrat, J. Li, M. Wang, W. Yu, Y. Qi, A. E. Zeituni, S. C. Nair, S. P. Crampton, M. S. Orandle, S. M. Bolland, C. F. Qi, C. A. Long, T. G. Myers, J. E. Coligan, R. Wang and X. Z. Su (2014). "Strain-specific innate immune signaling pathways determine malaria parasitemia dynamics and host mortality." Proc Natl Acad Sci U S A **111**(4): E511-520.

Wykes, M. N. and M. F. Good (2009). "What have we learnt from mouse models for the study of malaria?" Eur J Immunol **39**(8): 2004-2007.

Yamamoto, M., S. Yamazaki, S. Uematsu, S. Sato, H. Hemmi, K. Hoshino, T. Kaisho, H. Kuwata, O. Takeuchi, K. Takeshige, T. Saitoh, S. Yamaoka, N. Yamamoto, S. Yamamoto, T. Muta, K. Takeda and S. Akira (2004). "Regulation of Toll/IL-1-receptor-mediated gene expression by the inducible nuclear protein IkappaBzeta." Nature **430**(6996): 218-222.

Yan, H., K. Krishnan, A. C. Greenlund, S. Gupta, J. T. Lim, R. D. Schreiber, C. W. Schindler and J. J. Krolewski (1996). "Phosphorylated interferon-alpha receptor 1 subunit (IFNaR1) acts as a docking site for the latent form of the 113 kDa STAT2 protein." EMBO J **15**(5): 1064-1074.

Yeo, T. W., D. A. Lampah, R. Gitawati, E. Tjitra, E. Kenangalem, K. Piera, R. N. Price, S. B. Duffull, D. S. Celermajer and N. M. Anstey (2008). "Angiopoietin-2 is associated with decreased endothelial nitric oxide and poor clinical outcome in severe falciparum malaria." Proc Natl Acad Sci U S A **105**(44): 17097-17102.

Yoneyama, M. and T. Fujita (2004). "[RIG-I: critical regulator for virus-induced innate immunity]." Tanpakushitsu Kakusan Koso **49**(16): 2571-2578.

Yu, X., B. Cai, M. Wang, P. Tan, X. Ding, J. Wu, J. Li, Q. Li, P. Liu, C. Xing, H. Y. Wang, X. Z. Su and R. F. Wang (2016). "Cross-Regulation of Two Type I Interferon Signaling Pathways in Plasmacytoid Dendritic Cells Controls Anti-malaria Immunity and Host Mortality." Immunity **45**(5): 1093-1107.

Zander, R. A., J. J. Guthmiller, A. C. Graham, R. L. Pope, B. E. Burke, D. J. Carr and N. S. Butler (2016). "Type I Interferons Induce T Regulatory 1 Responses and Restrict Humoral Immunity during Experimental Malaria." PLoS Pathog **12**(10): e1005945.

Zanzinger, K., C. Schellack, N. Nausch and A. Cerwenka (2009). "Regulation of triggering receptor expressed on myeloid cells 1 expression on mouse inflammatory monocytes." Immunology **128**(2): 185-195.

Zeyrek, F. Y., M. A. Kurcer, D. Zeyrek and Z. Simsek (2006). "Parasite density and serum cytokine levels in Plasmodium vivax malaria in Turkey." Parasite Immunol **28**(5): 201-207.

Zhang, Q., Y. Zhang, Y. Huang, X. Xue, H. Yan, X. Sun, J. Wang, T. F. McCutchan and W. Pan (2011). "From in vivo to in vitro: dynamic analysis of Plasmodium falciparum var gene expression patterns of patient isolates during adaptation to culture." PLoS One **6**(6): e20591.

Zhu, J., G. Krishnegowda and D. C. Gowda (2005). "Induction of proinflammatory responses in macrophages by the glycosylphosphatidylinositols of Plasmodium falciparum: the requirement of extracellular signal-regulated kinase, p38, c-Jun N-terminal kinase and NF-kappaB pathways for the expression of proinflammatory cytokines and nitric oxide." J Biol Chem **280**(9): 8617-8627.

Appendix 1: Volunteer Inclusion and Exclusion Criteria

Inclusion Criteria

- Healthy, male or non-pregnant female adult aged 18 - 45 years.
- Subject willing and able to give written informed consent for participation in the study.
- Resident in or near Oxford for the duration of the CHMI part of the study. Or for volunteers not living in Oxford: agreement to stay in arranged accommodation close to the trial centre during a part of the study (from the day before CHMI until anti-malarial treatment is completed).
- Female subjects of child bearing potential willing to practice continuous effective contraception for the duration of the study.
- Able (in the Investigator's opinion) and willing to comply with all study requirements.
- Willing to allow his or her General Practitioner and consultant, if appropriate, to be notified of participation in the study.
- Agreement to permanently refrain from blood donation, as per current UK Blood Transfusion and Tissue Transplantation Services guidelines
- Reachable (24 hours a day) by mobile phone during the period between CHMI and completion of antimalarial treatment.
- Willingness to take a curative anti-malaria regimen following CHMI.
- Answer all questions on the informed consent questionnaire correctly.

Exclusion Criteria

- History of clinical malaria (any species).
- Travel to a malaria endemic region during the study period or within the preceding six months with significant risk of malaria exposure.

- Use of systemic antibiotics with known antimalarial activity within 30 days of CHMI (e.g. trimethoprim-sulfamethoxazole, doxycycline, tetracycline, clindamycin, erythromycin, fluoroquinolones and azithromycin).
- Prior receipt of an investigational malaria vaccine or any other investigational vaccine likely to impact on interpretation of the trial data.
- Receipt of an investigational product in the 30 days preceding enrolment, or planned receipt during the study period.
- History of sickle cell anaemia, sickle cell trait, thalassaemia or thalassaemia trait or any haematological condition that could affect susceptibility to malaria infection.
- Any confirmed or suspected immunosuppressive or immunodeficient state, including HIV infection; asplenia; recurrent, severe infections and chronic (more than 14 days) immunosuppressant medication within the past 6 months (inhaled and topical steroids are allowed).
- Use of immunoglobulins or blood products within 3 months prior to enrolment or previous severe adverse reaction to a blood transfusion.
- History of allergic disease or reactions likely to be exacerbated by any component of the vaccine (or malaria infection).
- Any history of anaphylaxis post vaccination.
- Pregnancy, lactation or intention to become pregnant during the study.
- Use of medications known to cause prolongation of the QT interval ***and*** existing contraindication to the use of Malarone.
- Use of medications known to have a potentially clinically significant interaction with Riamet *and* Malarone.
- Contraindications to the use of all three proposed anti-malarial medications; Riamet, Malarone and Chloroquine.
- Any clinical condition known to prolong the QT interval.
- Family history of congenital QT prolongation or sudden death.

- Positive family history in 1st and 2nd degree relatives < 50 years old for cardiac disease.
- History of cardiac arrhythmia, including clinically relevant bradycardia.
- An estimated, ten year risk of fatal cardiovascular disease of ≥5%, as estimated by the Systematic Coronary Risk Evaluation (SCORE) system
- Any clinically significant abnormal finding on biochemistry or haematology blood tests, urinalysis or clinical examination. In the event of abnormal test results, confirmatory repeat tests may be requested at the discretion of the Investigator. Absolute values for exclusion for confirmed abnormal results are shown in Appendix A.
- History of cancer (except basal cell carcinoma of the skin and cervical carcinoma in situ).
- History of serious psychiatric condition that may affect participation in the study.
- Any other serious chronic illness requiring hospital specialist supervision.
- Suspected or known current alcohol abuse as defined by an alcohol intake of greater than 42 standard UK units every week.
- Suspected or known injecting drug abuse in the 5 years preceding enrolment.
- Seropositive for hepatitis B surface antigen (HBsAg).
- Seropositive for hepatitis C virus (antibodies to HCV) at screening.
- Any other significant disease, disorder, or finding which may significantly increase the risk to the volunteer because of participation in the study, affect the ability of the volunteer to participate in the study or impair interpretation of the study data.
- Volunteers unable to be closely followed for social, geographic or psychological reasons.

Appendix 2: Post-challenge qPCR data (p/mL)

		Post-challenge time-point																		
Volunteer ID	**Day of Diagnosis**	**C +1**	**C +2**	**C +2.5**	**C +3**	**C +3.5**	**C +4**	**C +4.5**	**C +5**	**C +5.5**	**C +6**	**C +6.5**	**C +7**	**C +7.5**	**C +8**	**C +8.5**	**C +9**	**C +9.5**	**C +10**	**C +10.5**
012	**C +7.5**	N	N	N	N	13	19	N	76	146	72	97	5268	1645						
013	**C +10.5**	N	N	N	N	N	N	N	25	9	12	5	334	147.018356	595	1722	2091	1740	23346	70368
016	**C +10**	N	N	N	N	8	13	5	105	91	4	202	1179	610	3026	14951	12105	3636	**273247**	
017	**C +10.5**	N	3	N	N	1	N	N	6	16	2	26	65	46	157	518	798	347	4858	**16911**
018	**C +8.5**	N	1	5	N	5	5	N	84	69	3	195	452	536	8735	**19670**				
019	**C +8.5**	N	N	N	N	13	N	N	21	35	9	115	332	540	1846	**6932**				
020	**C +8.5**	N	N	N	N	11	12	N	67	127	17	195	1578	641	3405	**15025**				
022	**C +10**	N	16	10	N	12	N	N	18	9	N	15	76	84	263	425	756	310	**8865**	
024	**C +10**	N	14	N	N	N	N	N	25	64	N	98	737	361	994	4814	4604	1288	**43707**	
026	**C +9**	N	13	23	N	14	N	N	63	72	40	88	822	785	1455	4817	**9133**			
027	**C +9**	N	N	N	N	N	18	N	45	49	17	102	1246	642	2160	16625	**13421**			
104	**C +9**	N	8	10	N	7	17	31	170	291	14	357	2971	3589	4788	16899	**54085**			
106	**C +8.5**	N	10	N	N	N	N	19	89	99	77	138	1145	1084	2137	**16162**				
206	**C +10**	N	N	N	N	8	2	N	39	65	19	13	889	736	360	7115	18143	4062	**185576**	
208	**C +9**	N	17	N	N	N	N	N	15	30	11	21	238	208	197	1169	**1440**			

= diagnosed (no further samples)

= low level positive PCR <20 p/mL in at least one replicate and below minimum positive reporting criteria (early indication of likely positivity - all here have ultimately gone reliably positive)

red = 2/3 replicates with significant differences but mean >20

= point of diagnosis

= values altered following QC process (no substantial changes)

N = no amplification

Appendix 2: raw qPCR data. Parasite qPCR was performed on C +1 (1 day after inoculum challenge) and twice daily from C +2. 150 µl volumes of leucocyte-depleted blood were run in triplicate, using TaqMan™ probe (5′ FAM-AAC AAT TGG AGG GCA AG-NFQ-MGB 3′) to amplify the *P. falciparum* 18s ribosomal region. Values below 20 p/mL (lower limit of quantification), or with only one positive replicate of three tested, were classed as negative.

Appendix 3: Top 100 (most variable) gene lists ("classical" responders)

Interferon-stimulated genes (ISGs) are indicated by green type

Top 25 genes, for which top 25th percentile variation was calculated, are boxed in pink

Top	16	Variance factor	17	Variance factor	13	Variance factor	27	Variance factor
1	CXCL10	7.57	ANKRD22	5.29	CXCL10	4.68	CXCL10	4.52
2	ANKRD22	7.05	IFI44L	4.20	ANKRD22	3.29	ANKRD22	3.50
3	FCGR1A	5.11	SERPING1	3.85	FCGR1A	2.49	SERPING1	2.96
4	IFI44L	5.00	CXCL10	3.84	FCGR1B	2.33	IFI44L	2.83
5	FCGR1B	4.69	RSAD2	3.36	PDL1	1.97	RSAD2	2.21
6	PDL1	4.24	FCGR1A	3.36	SERPING1	1.95	FCGR1A	1.88
7	RSAD2	4.12	PDL1	3.21	GBP1	1.74	TNFAIP6	1.80
8	SERPING1	4.11	P2RY14	3.19	GBP5	1.71	GBP5	1.65
9	IDO1	3.67	CARD17	3.18	IFI44L	1.65	PDL1	1.62
10	TNFAIP6	3.34	FCGR1B	2.88	P2RY14	1.60	FCGR1B	1.61
11	IFI44	3.33	IFI44	2.64	RSAD2	1.43	P2RY14	1.50
12	P2RY14	3.27	TNFAIP6	2.32	MYOF	1.40	CXCL9	1.46
13	CARD17	3.03	GBP5	2.30	GBP4	1.35	IFI44	1.44
14	GBP1	2.66	GBP1	2.06	TNFAIP6	1.33	CARD17	1.40
15	GBP5	2.65	IFIT1	2.01	CXCL9	1.22	GBP1	1.40
16	IFIT3	2.51	IDO1	1.95	LAP3	1.20	IFIT3	1.27
17	IFIT1	2.46	IFIT3	1.89	IFIT3	1.14	GBP4	1.26
18	PDCD1LG2	2.29	PDCD1LG2	1.68	IFI44	0.99	IFIT1	1.19
19	GBP4	2.13	LAP3	1.64	IFIT1	0.90	OAS3	1.18
20	HERC5	1.97	IFI6	1.48	IDO1	0.89	PDCD1LG2	1.16
21	EPSTI1	1.86	GBP4	1.48	EPSTI1	0.87	MYOF	1.15
22	CEACAM1	1.84	OAS3	1.47	STAT1	0.80	EPSTI1	1.13
23	MYOF	1.75	GBP6	1.42	CARD17	0.78	IFI6	1.10
24	IFI6	1.74	HERC5	1.42	IFI6	0.77	HERC5	1.03
25	PLSCR1	1.73	PRRG4	1.39	SAMD9L	0.75	PRRG4	0.95
26	OAS3	1.66	AIM2	1.28	WARS	0.74	IDO1	0.89
27	PSTPIP2	1.60	EPSTI1	1.28	GBP2	0.73	GCH1	0.85
28	LAMP3	1.53	CEACAM1	1.17	IFIT2	0.71	IFIH1	0.76
29	LAP3	1.51	ETV7	1.14	PARP14	0.70	LAP3	0.71
30	CXCL9	1.49	PSTPIP2	1.12	HERC5	0.69	DHRS9	0.70
31	WARS	1.49	SLAMF8	1.12	PLSCR1	0.69	TIFA	0.70
32	SLAMF8	1.45	MYOF	1.08	GBP3	0.69	STAT1	0.69
33	GK	1.45	DHRS9	1.05	GK	0.63	PARP14	0.68
34	SAMD9L	1.41	PLSCR1	1.00	GCH1	0.63	GBP6	0.66
35	ANXA3	1.38	RTP4	0.99	PARP9	0.63	WARS	0.66
36	GBP6	1.38	WARS	0.99	CEACAM1	0.62	PSME2	0.65
37	PARP14	1.31	PARP14	0.97	PSTPIP2	0.61	LAMP3	0.64
38	XAF1	1.30	FRMD3	0.96	SLAMF8	0.61	AIM2	0.63
39	AIM2	1.28	XAF1	0.94	KLRF1	0.60	SAMD9L	0.62
40	PARP9	1.27	CXCL9	0.93	STAT2	0.57	OAS2	0.61
41	IFIT2	1.24	IFIT2	0.88	TIFA	0.56	FRMD3	0.61
42	GPR84	1.22	IFIH1	0.87	OAS3	0.55	ETV7	0.60
43	EFCAB2	1.20	PARP9	0.86	GBP6	0.54	DDX60	0.60
44	GCH1	1.18	OAS1	0.86	IFIH1	0.53	OAS1	0.59
45	KCNJ2	1.17	STAT2	0.84	XAF1	0.52	OASL	0.58
46	IFIH1	1.17	SAMD9L	0.83	ETV7	0.50	GBP3	0.54
47	BMX	1.13	GCH1	0.82	ANXA3	0.49	CEACAM1	0.53
48	TIFA	1.11	CLEC5A	0.82	CASP5	0.49	GRAMD1B	0.52
49	STAT1	1.10	GBP3	0.82	PDCD1LG2	0.48	PSTPIP2	0.52
50	OAS1	1.09	DOCK4	0.80	PRRG4	0.47	XAF1	0.52
51	RTP4	1.08	SEPT4	0.79	LPCAT2	0.45	ALDH1A1	0.51
52	GBP3	1.06	STAT1	0.79	DDX60	0.45	GBP2	0.51
53	GBP2	1.05	TIFA	0.71	TNFSF10	0.45	PARP9	0.49
54	RIG-I	1.05	RIG-I	0.71	AIM2	0.44	TLR7	0.48
55	PRRG4	1.03	GK	0.68	CASP5	0.44	DOCK4	0.46
56	DDX60	1.03	GBP2	0.68	RIG-I	0.43	PLSCR1	0.46
57	ETV7	1.02	DDX60	0.65	DHRS9	0.41	STAT2	0.45
58	DHRS9	1.02	BMX	0.64	TRAFD1	0.41	APOL3	0.45
59	KCNJ15	1.01	KCNJ2	0.64	HCAR2	0.39	SLAMF8	0.45
60	FRMD3	1.01	HSPH1	0.63	TLR7	0.39	IFIT2	0.43
61	CASP5	1.01	HSPA1B	0.62	HCAR3	0.39	IFIT5	0.41
62	SEPT4	1.01	OAS2	0.61	P2RX7	0.38	TNFSF10	0.41
63	STAT2	0.99	HSPA1B	0.61	IFI35	0.38	CD38	0.40
64	CASP5	0.99	IFIT5	0.61	TAP1	0.38	GPR84	0.39
65	HCAR2	0.98	HSPA1B	0.61	TNFSF10	0.38	RIG-I	0.39
66	KLRF1	0.95	OASL	0.60	TAP1	0.38	CLC	0.38
67	DOCK4	0.95	HSPA1B	0.60	TAP1	0.38	P2RX7	0.38
68	LPCAT2	0.95	CMPK2	0.60	TAP1	0.38	SLAMF7	0.37
69	ERLIN1	0.88	TAP1	0.60	TAP1	0.38	EIF2AK2	0.37
70	HCAR3	0.81	TAP1	0.60	TAP1	0.38	UBE2L6	0.37
71	TNFSF10	0.79	TAP1	0.60	TAP1	0.38	MTHFD2	0.36
72	OAS2	0.76	TAP1	0.60	TAP1	0.38	SORT1	0.36
73	IFI35	0.76	TAP1	0.60	KLRD1	0.37	MX1	0.35
74	FAS	0.76	TAP1	0.60	JAK2	0.37	RTP4	0.35
75	TNFSF10	0.75	TAP1	0.60	APOL2	0.36	RIPK2	0.35
76	TAP1	0.75	TAP1	0.60	KCNJ2	0.36	DTX3L	0.35
77	CMPK2	0.75	MX1	0.59	APOL6	0.36	KCNJ2	0.34
78	APOL2	0.75	CASP5	0.58	RTP4	0.36	JAK2	0.34
79	MX1	0.74	EIF2AK2	0.58	PSME2	0.35	EFCAB2	0.34
80	TAP1	0.74	PSME2	0.58	OAS1	0.35	MT2A	0.34
81	TAP1	0.74	IFI35	0.55	LACTB	0.35	TAP1	0.34
82	TAP1	0.74	WDFY1	0.54	SECTM1	0.35	TAP1	0.34
83	FFAR2	0.74	EFCAB2	0.54	OR56B1	0.34	ALOX15	0.34
84	EIF2AK2	0.74	CASP5	0.54	STX11	0.34	SUCNR1	0.33
85	TAP1	0.74	ALPL	0.53	IRF1	0.33	TAP1	0.33
86	TAP1	0.74	UBE2L6	0.52	DTX3L	0.33	TAP1	0.33
87	STEAP4	0.73	APOL2	0.52	UBE2L6	0.33	TAP1	0.33
88	TAP1	0.73	APOL1	0.52	KCNJ15	0.32	TAP1	0.33
89	TAP1	0.73	HIST2H2BF	0.51	APOL1	0.32	TAP1	0.33
90	STX11	0.72	TFEC	0.51	APOL3	0.31	TAP1	0.33
91	OASL	0.70	TNFSF10	0.50	SORT1	0.31	IFI35	0.33
92	TFEC	0.69	KREMEN1	0.50	IL1B	0.31	NBN	0.32
93	CLEC6A	0.67	GPR84	0.48	KREMEN1	0.31	IL5RA	0.32
94	APOL1	0.67	OR56B1	0.48	EIF2AK2	0.30	BST2	0.32
95	DDX60L	0.66	TMEM140	0.47	P2RX7	0.30	WDFY1	0.31
96	CD38	0.66	MT2A	0.47	LAMP3	0.30	KLRB1	0.31
97	IFIT5	0.65	SECTM1	0.46	SLAMF7	0.30	FGL2	0.31
98	RIPK2	0.64	LAMP3	0.46	IL15	0.30	TFEC	0.31
99	TRAFD1	0.63	RIPK2	0.46	FAS	0.29	HCAR3	0.31
100	SLC26A8	0.63	HCAR3	0.46	TNFSF13B	0.29	TNFSF10	0.31

Appendix 3: Top 100 (most variable) gene lists ("classical" responders)

Interferon-stimulated genes (ISGs) are indicated by green type

Top 25 genes, for which top 25th percentile variation was calculated, are boxed in pink

Top	26	Variance factor	206	Variance factor	106	Variance factor	24	Variance factor
1	CXCL10	4.70	CXCL10	3.53	ANKRD22	2.90	CXCL10	3.27
2	ANKRD22	3.14	ANKRD22	2.86	CXCL10	2.77	FCGR1A	1.30
3	SERPING1	2.38	SERPING1	1.89	FCGR1A	1.50	FCGR1B	1.29
4	FCGR1A	2.05	IFI44L	1.86	FCGR1B	1.35	ANKRD22	1.25
5	FCGR1B	2.03	TNFAIP6	1.80	SERPING1	1.31	GBP1	1.16
6	GBP1	1.39	P2RY14	1.77	GBP1	1.15	GBP5	1.11
7	TNFAIP6	1.23	FCGR1A	1.61	PDL1	1.14	SERPING1	1.08
8	GBP5	1.23	FCGR1B	1.45	P2RY14	1.10	GBP4	0.95
9	IGJ	1.15	PDL1	1.42	GBP4	1.10	CXCL9	0.74
10	IFI44L	1.15	CXCL9	1.32	GBP5	1.10	PDL1	0.70
11	GBP4	1.13	GBP1	1.22	MYOF	1.00	STAT1	0.63
12	PDL1	1.13	IFIT3	1.15	SLAMF8	0.81	LAP3	0.59
13	CXCL9	1.08	GBP5	1.04	IFI44L	0.80	IFI44L	0.50
14	SLAMF8	0.88	RSAD2	0.97	RSAD2	0.69	WARS	0.46
15	RSAD2	0.86	LAP3	0.97	EPSTI1	0.66	IFIT3	0.44
16	IFIT3	0.73	CARD17	0.96	LAP3	0.64	EPSTI1	0.43
17	MYOF	0.72	GBP4	0.84	IDO1	0.63	GBP2	0.43
18	PDCD1LG2	0.69	IFI44	0.83	IFIT3	0.62	MYOF	0.38
19	SECTM1	0.63	IFI6	0.74	IGJ	0.60	GBP3	0.37
20	LAP3	0.61	EPSTI1	0.68	PSTPIP2	0.58	PARP14	0.37
21	P2RY14	0.61	MYOF	0.67	TNFAIP6	0.56	SAMD9L	0.36
22	WARS	0.60	STAT1	0.65	STAT1	0.56	PARP9	0.35
23	CARD17	0.57	IFIT1	0.62	WARS	0.55	IFI6	0.34
24	IFI6	0.57	WARS	0.62	TLR7	0.54	GCH1	0.32
25	STAT1	0.57	IDO1	0.59	PARP14	0.54	TNFAIP6	0.30
26	ETV7	0.56	CASP5	0.58	IFI44	0.53	KLRC3	0.30
27	TXNDC5	0.56	PARP14	0.57	GCH1	0.53	KLRC2	0.30
28	GBP2	0.55	SAMD9L	0.56	TXNDC5	0.52	STAT2	0.27
29	OAS3	0.51	PSTPIP2	0.52	GBP3	0.50	ETV7	0.27
30	IL1RL1	0.50	PDCD1LG2	0.51	ALDH1A1	0.50	RSAD2	0.27
31	GBP6	0.50	PARP9	0.50	CXCL9	0.48	KLRF1	0.27
32	GPR84	0.50	PLSCR1	0.49	TIFA	0.47	ALDH1A1	0.26
33	KLRF1	0.49	OAS3	0.49	IFIH1	0.45	IFIT1	0.26
34	UBE2L6	0.49	CEACAM1	0.47	PDCD1LG2	0.40	IFI44	0.25
35	PSME2	0.49	XAF1	0.45	STAT2	0.39	IFIH1	0.25
36	EPSTI1	0.49	GCH1	0.45	SAMD9L	0.38	IFIT2	0.24
37	IL5RA	0.49	GK	0.44	CARD17	0.37	PSTPIP2	0.24
38	SAMD9L	0.47	IL1B	0.44	IFI6	0.37	SLAMF8	0.24
39	GCH1	0.47	IFIT2	0.43	GBP2	0.36	PLSCR1	0.23
40	TNFSF10	0.45	SLAMF8	0.43	HERC5	0.36	SECTM1	0.23
41	UGT2B11	0.45	HERC5	0.42	CD38	0.36	STX11	0.23
42	PRRG4	0.44	PRRG4	0.41	DDX60	0.36	PSME2	0.22
43	PARP9	0.43	KCNJ2	0.40	LACTB	0.35	TLR7	0.22
44	TLR7	0.42	GBP2	0.40	APOL6	0.35	IFIT5	0.22
45	ANKRD36	0.42	TIFA	0.40	ETV7	0.35	UBE2L6	0.22
46	IFI44	0.42	IFIH1	0.39	PSME2	0.35	KIR3DS1	0.20
47	GBP3	0.41	AIM2	0.38	PRRG4	0.35	XAF1	0.20
48	IFIT1	0.40	CLEC4D	0.38	IFIT1	0.34	TAS2R19	0.20
49	ALDH1A1	0.40	GBP3	0.38	SORT1	0.34	DTX3L	0.19
50	MT2A	0.40	OAS1	0.38	PLSCR1	0.33	GZMB	0.19
51	IFIT2	0.39	CASP5	0.38	PARP9	0.33	MYBL1	0.19
52	IDO1	0.38	PLA2G7	0.37	OAS3	0.33	KIR3DL2	0.18
53	AIM2	0.37	TNFSF10	0.37	RIPK2	0.32	TAP1	0.18
54	STX11	0.37	ANXA3	0.36	CCR2	0.31	TAP1	0.18
55	ARL17A	0.37	STAT2	0.36	ICAM1	0.31	TAP1	0.18
56	IFI35	0.36	LPCAT2	0.36	STX11	0.30	TAS2R20	0.18
57	ANKRD36B	0.36	FFAR2	0.35	UBE2L6	0.30	GZMH	0.18
58	PARP14	0.36	GPR84	0.35	CYBB	0.29	TAP1	0.18
59	CCL2	0.36	HCAR2	0.34	APOL3	0.29	TAS2R50	0.18
60	KLRD1	0.34	ETV7	0.34	SECTM1	0.28	RTP4	0.18
61	TAS2R20	0.34	TLR7	0.34	DTX3L	0.28	TAP1	0.18
62	RTP4	0.34	CD38	0.33	TRAFD1	0.28	TAP1	0.18
63	ICAM1	0.33	PSME2	0.33	OAS2	0.28	TAP1	0.18
64	TAS2R31	0.33	TNFSF10	0.32	IFI35	0.27	TAP1	0.18
65	KLRC3	0.33	P2RX7	0.32	CNTNAP3	0.27	APOL6	0.18
66	APOL3	0.33	TFEC	0.32	HLA-DRB4	0.27	APOL3	0.18
67	STAT2	0.33	SORT1	0.32	AIM2	0.27	DTHD1	0.17
68	HERC5	0.32	HCAR3	0.31	CD86	0.26	KIR2DL2	0.17
69	ABCA5	0.32	FPR2	0.31	FRMD3	0.26	OR5A2	0.17
70	SLAMF7	0.31	FGL2	0.30	CCR1	0.26	PRRG4	0.17
71	FRMD3	0.31	ALDH1A1	0.30	ARG1	0.25	NFE2L2	0.17
72	CLC	0.30	APOL3	0.29	P2RX7	0.25	GPR52	0.17
73	HCAR3	0.30	STX11	0.29	PLA2G7	0.25	ANKRD36	0.17
74	CEACAM1	0.30	IFI35	0.29	C3AR1	0.25	OAS2	0.17
75	P2RX7	0.30	LRRK2	0.29	KMO	0.24	GK5	0.16
76	CD209	0.30	FLVCR2	0.29	CEACAM1	0.24	TNFSF10	0.16
77	TIFA	0.28	CLEC6A	0.29	GBP6	0.24	KLRD1	0.16
78	LGALS3BP	0.28	DHRS9	0.29	HIST1H2BM	0.24	ICAM1	0.16
79	PDK4	0.28	SLAMF7	0.29	GK	0.24	IFI35	0.16
80	KREMEN1	0.28	C3AR1	0.28	TNFSF10	0.24	P2RY14	0.16
81	TAS2R46	0.27	KIAA1598	0.28	KCTD12	0.23	DHRS9	0.16
82	KLRC1	0.27	FRMD3	0.28	GLDC	0.23	IRS2	0.15
83	SYNE1	0.27	UBE2L6	0.27	FAM198B	0.23	MAK	0.15
84	XAF1	0.27	CASP1	0.27	DRAM1	0.23	TAS2R31	0.15
85	ALOX15	0.27	GBP6	0.27	GM2A	0.23	APOL1	0.15
86	GOLGA8B	0.27	TNFSF13B	0.26	GBP7	0.22	ANKRD36B	0.15
87	APOL1	0.27	APOBEC3A	0.26	LY86	0.22	OAS3	0.15
88	APOL6	0.27	DRAM1	0.26	IFIT5	0.22	OR56B1	0.15
89	PSTPIP2	0.26	EIF2AK2	0.26	BST2	0.22	FGL2	0.15
90	GOLGA8A	0.26	JAK2	0.26	IRF4	0.21	CASP5	0.14
91	HCAR2	0.26	TAP1	0.26	DEFA1B	0.21	HERC5	0.14
92	OAS2	0.26	CARD16	0.26	LPCAT2	0.21	SH2D1B	0.14
93	TAS2R43	0.26	TAP1	0.26	HSP90B1	0.21	IRF1	0.14
94	KLRC2	0.26	TAP1	0.26	HLA-DMA	0.21	PTGDR	0.14
95	GPR52	0.26	TAP1	0.26	NETO2	0.21	DEFA1B	0.14
96	GOLGA8A	0.26	TAP1	0.25	GPR15	0.21	CARD17	0.13
97	CCR3	0.26	TAP1	0.25	MTHFD2	0.21	DDX60	0.13
98	TAS2R50	0.26	TAP1	0.25	PSMA4	0.21	TRIM21	0.13
99	P2RY13	0.26	TAP1	0.25	OR5V1	0.20	HLA-DMA	0.13
100	CLK1	0.26	ACSL1	0.25	HLA-DRB1	0.20	LGALS9	0.13

Appendix 3: Top 100 (most variable) gene lists ("unknowns")

Interferon-stimulated genes (ISGs) are indicated by green type

Top 25 genes, for which top 25th percentile variation was calculated, are boxed in pink

Top	18	Variance factor	12	Variance factor	208	Variance factor	20	Variance factor
1	**IFIT1**	0.57	TAS2R19	0.36	KIR2DL5B	0.34	**CXCL10**	1.07
2	PTPLAD1	0.36	**IFIT1B**	0.33	KIR3DS1	0.32	ANKRD22	0.51
3	**IFI44L**	0.35	AHSP	0.32	KIR3DL1	0.27	FCGR1A	0.48
4	KLRF1	0.33	PI3	0.31	KIR2DS2	0.25	FCGR1B	0.45
5	**IFI44**	0.32	ARHGEF12	0.30	ZMAT1	0.24	**GBP5**	0.39
6	SH2D1B	0.31	GMPR	0.29	KIR2DS1	0.23	SERPING1	0.38
7	FGFBP2	0.30	CLEC4E	0.29	KIR2DS4	0.23	**GBP1**	0.34
8	**HERC5**	0.28	TESC	0.29	KIR3DL2	0.22	**GBP4**	0.33
9	**RSAD2**	0.27	TAS2R13	0.26	KIR2DL3	0.22	TAS2R13	0.21
10	KLRD1	0.27	CLC	0.26	KIR2DS3	0.21	**CXCL9**	0.20
11	KIR3DS1	0.26	KLRF1	0.26	KIR2DL2	0.20	PDL1	0.20
12	GZMA	0.26	USP12	0.25	AHSP	0.19	TAS2R20	0.20
13	KIR2DL5B	0.26	EPB42	0.24	FGFBP2	0.19	KLRF1	0.19
14	**IFIT3**	0.25	DEFA1B	0.24	NKG7	0.18	TLR7	0.18
15	NKG7	0.23	IL1R2	0.24	TAS2R19	0.18	PDK4	0.18
16	KIR2DL2	0.22	PPBP	0.24	KIR2DL1	0.18	IL1R2	0.17
17	IL1RL1	0.22	RPIA	0.23	ADAM20	0.18	GRAMD1C	0.16
18	PDK4	0.22	SLC4A1	0.23	GZMH	0.17	OR1G1	0.16
19	HIST1H1E	0.21	GYPA	0.23	HCST	0.17	WARS	0.16
20	CD180	0.21	TAS2R50	0.22	CNTNAP3	0.17	CD180	0.16
21	CX3CR1	0.20	SLC14A1	0.22	CCDC88A	0.16	OR5V1	0.16
22	KIR2DL3	0.19	IL5RA	0.22	ALG3	0.16	TAS2R16	0.15
23	CTSW	0.19	EIF1AY	0.22	PDK4	0.16	CLEC12B	0.15
24	**IFIT2**	0.18	DEFA1B	0.21	PTPLAD1	0.16	ZMAT1	0.14
25	**IFI6**	0.18	ALAS2	0.21	PRF1	0.16	OCLM	0.14
26	FCGR1B	0.18	ENKUR	0.20	CTSW	0.16	MYOF	0.14
27	KIR2DL1	0.18	MS4A14	0.20	CCDC18	0.15	KLRC2	0.14
28	TGFBR3	0.17	OR2W3	0.20	COX8A	0.15	TAS2R40	0.14
29	**GBP5**	0.17	MMD	0.19	NFE2L2	0.15	**STAT1**	0.13
30	**MX1**	0.17	CD180	0.19	GCNT4	0.15	**GBP2**	0.13
31	PRF1	0.16	TBCEL	0.19	BAZ2B	0.14	PI3	0.13
32	KIR2DS4	0.16	MBOAT2	0.19	HLA-DRB5	0.14	KLRD1	0.13
33	TAS2R19	0.16	IGF2BP2	0.19	LY96	0.14	CARD17	0.13
34	GNLY	0.16	GRAMD1C	0.19	OR2T3	0.14	KLRC1	0.13
35	CD160	0.16	DEFA1B	0.19	COPE	0.14	SRRM5	0.13
36	OR6X1	0.16	SLC6A8	0.18	DMXL2	0.14	CLK1	0.13
37	ADAM20	0.16	ODC1	0.18	PBOV1	0.14	MMP8	0.13
38	SLAMF7	0.16	RNF10	0.18	OR10T2	0.14	LY6G5B	0.12
39	FCGR1A	0.16	SDPR	0.18	MYOF	0.14	LY6G5B	0.12
40	TOX	0.15	FCER2	0.18	LRRK2	0.13	LY6G5B	0.12
41	SLAMF6	0.15	OR52K2	0.18	SPN	0.13	LY6G5B	0.12
42	KLRB1	0.15	PPM1A	0.17	PMCH	0.13	LY6G5B	0.12
43	CD79A	0.15	KIF27	0.17	TGFBR3	0.13	LY6G5B	0.12
44	OR2AT4	0.15	TMOD1	0.17	SLCO4C1	0.13	SPANXN3	0.12
45	CD40LG	0.15	SFRP2	0.17	TTC14	0.13	KLRC3	0.12
46	**GBP1**	0.15	TSPAN5	0.17	CNTNAP3B	0.13	CLK4	0.12
47	TMEM14E	0.15	RGS18	0.17	**IFNG**	0.13	RSRP1	0.12
48	SERPING1	0.15	CCDC176	0.17	OR51A4	0.13	CLK1	0.12
49	UGT2B11	0.15	MYL4	0.17	CNTLN	0.13	LAP3	0.12
50	PHGR1	0.14	CCR3	0.17	GZMB	0.12	IL18RAP	0.12
51	HCST	0.14	SCLT1	0.16	**GBP4**	0.12	**GBP3**	0.12
52	KIR2DS3	0.14	FAM210B	0.16	TIMM22	0.12	PLGLB1	0.11
53	KIR3DL1	0.14	FECH	0.16	KIR3DL3	0.12	EPSTI1	0.11
54	KIR2DS2	0.14	ANKRD36	0.16	UGT2B11	0.12	TAS2R50	0.11
55	DEFB128	0.14	IRS2	0.16	HIST1H1B	0.12	GNLY	0.11
56	GIMAP7	0.13	SH3BGRL2	0.16	HIST1H2BM	0.12	GCH1	0.11
57	ZMAT1	0.13	PDK4	0.16	KIAA0825	0.12	ARL17A	0.11
58	IL5RA	0.13	ANK1	0.16	C6orf163	0.12	VNN3	0.11
59	HLA-DQA2	0.13	RAB2B	0.16	GPR56	0.12	TIFA	0.10
60	ICOS	0.13	CCDC18	0.16	KLRD1	0.12	APOL3	0.10
61	IL2RB	0.13	TESC	0.16	TNF	0.12	PLGLB1	0.10
62	GPR18	0.13	OR8A1	0.15	TNF	0.12	SCP2D1	0.10
63	TARP	0.13	GYPB	0.15	TNF	0.12	TNFSF10	0.10
64	KLRG1	0.13	UBXN6	0.15	TNF	0.12	ERV3-1	0.10
65	CD3G	0.13	CPEB4	0.15	TNF	0.12	TMEM14E	0.10
66	CD28	0.13	RAB2B	0.15	TNF	0.12	LOC100130705	0.10
67	SLCO4C1	0.13	GPR52	0.15	TNF	0.12	FGFBP2	0.10
68	HIST1H4C	0.13	TMEM63B	0.15	TNF	0.12	ABCA5	0.10
69	IGJ	0.13	OCLM	0.15	CX3CR1	0.12	DUSP1	0.10
70	GPR174	0.13	CA1	0.15	SEPTIN1	0.12	OR52K2	0.10
71	MANEA	0.12	VNN3	0.15	MS4A14	0.12	GZMB	0.10
72	GZMH	0.12	IL1RAP	0.15	GPR52	0.12	**IFI44L**	0.10
73	KLRC4	0.12	THBS1	0.15	CDK2AP2	0.12	NFE2L2	0.10
74	KIR2DS1	0.12	KIF14	0.15	GZMA	0.12	ADAM20P1	0.10
75	SYT11	0.12	TAS2R46	0.15	LOC643802	0.12	CXorf65	0.10
76	USP28	0.12	TFDP1	0.15	OR10A7	0.12	OR4K5	0.10
77	**IFNG**	0.12	DEFB133	0.15	LDHAL6B	0.11	OR4C11	0.10
78	GPR183	0.12	DCUN1D1	0.15	TLR6	0.11	RNF182	0.10
79	RBMXL3	0.12	ALS2CR12	0.15	CBWD2	0.11	LIPN	0.10
80	FCRL6	0.12	CAPRIN2	0.15	MME	0.11	VNN3	0.10
81	RPS5	0.12	ITGB3	0.15	LUC7L3	0.11	SLAMF8	0.10
82	**PARP14**	0.12	C6orf163	0.14	EIF5AL1	0.11	RPIA	0.10
83	KLRC2	0.12	HIST1H3H	0.14	TAS2R31	0.11	HLA-DQA2	0.10
84	FOXR2	0.12	YOD1	0.14	MGAM	0.11	TRPM6	0.10
85	CHRM4	0.12	ADAM20	0.14	GPR148	0.11	CCR3	0.10
86	GPR56	0.11	IL1RL1	0.14	RPS18	0.11	TTC14	0.10
87	KLRC3	0.11	MICALCL	0.14	VCPKMT	0.11	P2RY14	0.10
88	HSPH1	0.11	MXI1	0.14	CD86	0.11	SPANXN2	0.10
89	FAIM3	0.11	CLU	0.14	CD180	0.11	LOC643802	0.10
90	NDRG3	0.11	CD22	0.14	NLRC4	0.11	OR10A2	0.10
91	LMAN1	0.11	SLPI	0.14	PRKACG	0.11	**STAT2**	0.10
92	TAS2R20	0.11	MICAL2	0.14	CBWD5	0.11	ETV7	0.10
93	DOCK4	0.11	PITHD1	0.14	WDFY3	0.11	TAS2R19	0.10
94	**EIF2AK2**	0.11	BIRC2	0.14	SPRR2F	0.11	FLJ45513	0.10
95	OR5D18	0.11	PRKAR2B	0.13	KATNBL1	0.11	SLITRK1	0.10
96	CD96	0.11	TCF7	0.13	FAM105A	0.11	FAM157B	0.10
97	RSL1D1	0.11	GZMB	0.13	PGBD4	0.11	GPR52	0.10
98	TAS2R46	0.11	FOXO3	0.13	ATP2B1	0.11	CCR7	0.10
99	SDAD1	0.11	YBX3	0.13	TAS2R41	0.11	TAS2R46	0.10
100	KRTAP24-1	0.11	FAM104A	0.13	C7orf62	0.11	TNF	0.10

Appendix 3: Top 100 (most variable) gene lists ("non-classical" responders)

Interferon-stimulated genes (ISGs) are indicated by green type

Top 25 genes, for which top 25th percentile variation was calculated, are boxed in pink

Top	19	Variance factor	22	Variance factor
1	RGS18	0.53	ALAS2	1.09
2	CLEC4E	0.51	CLC	0.99
3	USP12	0.46	IFIT1B	0.80
4	IFIT1B	0.44	PPBP	0.71
5	ANKRD36	0.43	IGJ	0.71
6	CLK1	0.42	SLC4A1	0.69
7	GYPA	0.41	TXNDC5	0.55
8	USP15	0.41	CXCR2	0.53
9	CLK1	0.38	OR2W3	0.53
10	ANKRD36B	0.37	SLC25A39	0.52
11	NABP1	0.36	AQP9	0.52
12	LRRK2	0.36	CXCR1	0.52
13	ERV3-1	0.35	STRADB	0.51
14	BIRC2	0.35	SLC25A37	0.51
15	CMAS	0.34	GYPA	0.49
16	VNN3	0.33	GMPR	0.48
17	CCDC18	0.33	PHOSPHO1	0.48
18	CLEC7A	0.33	PF4	0.46
19	MBOAT2	0.33	SNCA	0.45
20	VNN3	0.33	DCAF12	0.45
21	GPCPD1	0.32	FAM46C	0.44
22	RSRP1	0.32	CA1	0.43
23	KIF14	0.32	PI3	0.41
24	IL5RA	0.31	FFAR2	0.40
25	VCPKMT	0.31	IFIT1	0.40
26	ARHGEF12	0.31	VNN3	0.39
27	NAMPT	0.29	YBX3	0.38
28	TTC14	0.29	SH3BGRL2	0.38
29	CCR3	0.29	EPB42	0.38
30	CD58	0.28	FECH	0.37
31	EIF1AY	0.28	HEMGN	0.35
32	PKN2	0.28	STEAP4	0.34
33	SPOPL	0.28	AHSP	0.33
34	CD46	0.28	MME	0.33
35	SWT1	0.28	PROK2	0.33
36	BAZ2B	0.28	CHI3L1	0.32
37	SCLT1	0.28	RGS18	0.32
38	CCNL1	0.28	MXD1	0.32
39	SAT1	0.27	HIST1H4H	0.31
40	PPBP	0.27	RGS2	0.30
41	CLK4	0.27	TMEM56	0.30
42	CYB5R4	0.26	HIST1H3B	0.30
43	OR6X1	0.26	TNFAIP6	0.29
44	KATNBL1	0.26	R3HDM4	0.29
45	DOCK5	0.26	NAMPT	0.29
46	CCNH	0.26	BPGM	0.29
47	SMCHD1	0.26	PF4V1	0.28
48	RGS2	0.26	SLC14A1	0.28
49	VPS8	0.26	MYL4	0.28
50	RIOK3	0.26	KCNJ15	0.28
51	PELI1	0.25	MPP1	0.27
52	SH3BGRL2	0.25	ALPL	0.26
53	ABCA5	0.25	SLC6A8	0.26
54	NKTR	0.25	MARCH8	0.26
55	TLR2	0.25	VNN3	0.25
56	KIAA1551	0.25	CLEC4E	0.25
57	FAM185A	0.25	MGAM	0.25
58	KIF27	0.25	MBNL3	0.25
59	TIA1	0.25	HIST1H2BM	0.25
60	OR10H2	0.25	IFIT2	0.25
61	CLC	0.25	RIOK3	0.25
62	PTGS2	0.24	TMOD1	0.25
63	CAPRIN2	0.24	TSPAN5	0.24
64	PIGB	0.24	VNN2	0.24
65	MS4A14	0.24	RAB2B	0.24
66	UBE2B	0.24	RSAD2	0.23
67	RPIA	0.24	MBOAT2	0.23
68	FCHO2	0.24	GPR97	0.23
69	LUC7L3	0.24	FPR1	0.23
70	GK	0.24	SOD2	0.23
71	TAS2R13	0.24	TBCEL	0.23
72	RPS6KA5	0.24	ALS2CR12	0.22
73	TANK	0.24	VNN2	0.22
74	PDK4	0.23	HIST1H3H	0.22
75	RBM39	0.23	TREM1	0.22
76	TBCEL	0.23	GYPC	0.22
77	PITHD1	0.23	FKBP8	0.21
78	NFXL1	0.22	RAB2B	0.21
79	TLR1	0.22	IGF2BP2	0.21
80	CLEC4D	0.22	CCR3	0.21
81	CBWD5	0.22	EMR3	0.21
82	TXNDC16	0.22	USP12	0.20
83	FGFR1OP2	0.22	SDPR	0.20
84	VPS13A	0.22	GYPB	0.20
85	IL1R2	0.22	MANSC1	0.20
86	DCUN1D1	0.22	HIST1H1E	0.20
87	USP32	0.22	TESC	0.20
88	TSPAN5	0.22	HBZ	0.19
89	CBWD3	0.22	IL1R2	0.19
90	CDC27	0.22	CYP4F3	0.19
91	STXBP3	0.22	MXI1	0.19
92	ATAD5	0.22	FAM157B	0.19
93	CHPT1	0.22	LY6G5B	0.19
94	NT5C3A	0.22	IFIT3	0.19
95	RNASE8	0.22	KLHL14	0.19
96	ZFYVE16	0.22	FBXO7	0.19
97	TAS2R19	0.22	CSF3R	0.19
98	VRK1	0.22	PADI2	0.19
99	ZMAT1	0.21	FAM210B	0.19
100	N4BP2L2	0.21	HCAR2	0.19

Appendix 3: Top 100 (most variable) gene lists ("Baseline controls")

Interferon-stimulated genes (ISGs) are indicated by green type

Top 25 genes, for which top 25th percentile variation was calculated, are boxed in pink

Top	BC.1	Variance factor	BC.2	Variance factor	BC.3	Variance factor	BC.4	Variance factor
1	CASP5	0.30	PI3	0.21	IGJ	0.62	IFI44L	1.53
2	SLPI	0.29	KCNJ15	0.18	TXNDC5	0.25	SERPING1	1.28
3	PDK4	0.28	HCAR3	0.15	PDK4	0.17	IFIT1	1.22
4	PI3	0.26	PROK2	0.14	TMEM81	0.15	RSAD2	1.14
5	ALPL	0.22	ALPL	0.13	HCAR2	0.13	CXCL10	0.90
6	PROK2	0.22	MME	0.13	FCGR1B	0.13	IFI44	0.88
7	SH2D1B	0.21	HCAR2	0.13	OR1G1	0.13	FCGR1A	0.85
8	ANXA3	0.20	IL1R2	0.13	LIPT2	0.13	FCGR1B	0.80
9	CASP5	0.20	CHI3L1	0.13	FCGR1A	0.13	IFIT3	0.71
10	KLRF1	0.19	C4BPA	0.12	KLRF1	0.12	IFI6	0.67
11	ACSL1	0.18	PDK4	0.12	IFNK	0.12	ANKRD22	0.63
12	KIR2DL5B	0.18	DEFA1B	0.11	FFAR2	0.12	HERC5	0.60
13	OR4K5	0.17	PHOSPHO1	0.11	OR1L6	0.11	EPSTI1	0.57
14	KIR2DL3	0.16	OR7G2	0.11	VNN2	0.11	GBP1	0.54
15	OR14J1	0.14	IFNA7	0.11	ACSL1	0.10	OAS3	0.54
16	KIR2DL1	0.14	TNFAIP6	0.11	HCAR3	0.10	IFIT2	0.39
17	FGFBP2	0.13	DEFA1B	0.11	SRRM5	0.10	GBP5	0.39
18	GZMB	0.13	KIR2DL5B	0.10	OR1N2	0.10	PPBP	0.37
19	FFAR2	0.13	CXCR1	0.10	LY96	0.10	ALAS2	0.35
20	OR51A4	0.13	DEFA1B	0.10	AQP9	0.10	CLC	0.35
21	KIR2DL2	0.13	ACSL1	0.10	FPR2	0.10	GBP4	0.34
22	TAS2R40	0.13	CPLX4	0.10	GK	0.10	LAP3	0.32
23	HCAR3	0.13	TAS2R13	0.10	OR7G2	0.10	MYOF	0.32
24	HIST1H1E	0.13	ANXA3	0.10	OR10J1	0.10	MX1	0.31
25	GK	0.12	BCL6	0.10	MME	0.09	PARP14	0.30
26	IL18RAP	0.12	AQP9	0.09	OR10AG1	0.09	TNFAIP6	0.29
27	KIR3DS1	0.12	TREM1	0.09	ZMAT1	0.09	CAPRIN2	0.29
28	MGAM	0.12	ALAS2	0.09	CXorf51A	0.09	PARP9	0.28
29	FPR2	0.12	TAS2R19	0.09	KIR2DL5B	0.09	EPB42	0.28
30	AQP9	0.12	MXD1	0.09	RGS2	0.09	XAF1	0.28
31	KIR2DS3	0.12	FAM157B	0.09	OR51B2	0.09	OAS1	0.28
32	CDR1	0.11	CEACAM8	0.09	STEAP4	0.09	STAT1	0.27
33	HCAR2	0.11	TIGD2	0.09	PROK2	0.09	ALS2CR12	0.26
34	CCL4	0.11	P2RY13	0.09	NAMPT	0.08	MMD	0.26
35	KIR2DS4	0.11	VNN3	0.09	LRRK2	0.08	GMPR	0.26
36	KCNJ15	0.11	OR51A4	0.09	TREM1	0.08	OAS2	0.25
37	FAM129A	0.11	OR5A1	0.09	PCDHB1	0.08	FCHO2	0.25
38	OR5V1	0.11	CPT1A	0.09	VNN2	0.08	AHSP	0.24
39	CLC	0.11	MGAM	0.09	OR51T1	0.08	WARS	0.24
40	KCNJ2	0.10	OR2Y1	0.08	OR5H15	0.08	TESC	0.24
41	PRF1	0.10	CD1C	0.08	TAS2R40	0.08	STAT2	0.24
42	TMEM133	0.10	C5AR2	0.08	TAS2R20	0.08	PSME2	0.23
43	SPRR2F	0.10	VNN3	0.08	HIST1H1B	0.08	FAXDC2	0.23
44	OR2A25	0.10	OR11H1	0.08	PRRG4	0.08	SLC4A1	0.23
45	TAS2R41	0.10	TREML2	0.08	OR8A1	0.08	DDX60	0.22
46	GZMH	0.10	IFI44L	0.08	NFE2L2	0.08	CAPRIN2	0.22
47	DEFA1B	0.10	GK	0.08	OR2B3	0.08	ZMAT1	0.22
48	KIR2DS1	0.10	OR13G1	0.08	OR9A2	0.08	ANKRD36	0.22
49	ERVV-2	0.10	MMP25	0.08	OR14C36	0.08	PHOSPHO1	0.21
50	IFIT1B	0.10	KIR2DL4	0.08	CPLX4	0.08	MYL4	0.21
51	KIR2DS2	0.10	CXCR2	0.08	DNAJB7	0.08	SECTM1	0.21
52	TGFBR3	0.10	RBMXL2	0.08	OR56A5	0.08	PLSCR1	0.21
53	IL1R2	0.09	STEAP4	0.08	SPATA45	0.08	SAMD9L	0.21
54	FPR3	0.09	C18orf54	0.08	TNFAIP6	0.08	KIF14	0.20
55	SPDYE6	0.09	GZMK	0.08	OR6K2	0.08	IFIT1B	0.20
56	NAMPT	0.09	IFIT1B	0.08	DCAF8L2	0.08	OASL	0.20
57	BCL6	0.09	TMEM133	0.08	PAPOLB	0.07	SIGLEC1	0.20
58	KLRD1	0.09	NAMPT	0.08	MGAM	0.07	SH3BGRL2	0.20
59	FCGR1A	0.09	PTGS2	0.07	OR1L8	0.07	CCL2	0.20
60	OR5D14	0.09	OR2L8	0.07	SSMEM1	0.07	EIF2AK2	0.20
61	ACTBL2	0.09	TRHR	0.07	IFIT1	0.07	SLAMF8	0.20
62	FCGR1B	0.09	CYP4F3	0.07	OR2T10	0.07	PDL1	0.20
63	STEAP4	0.09	KCNJ2	0.07	OR8B12	0.07	GYPC	0.19
64	ST20	0.09	NCF4	0.07	ANXA3	0.07	SWT1	0.19
65	KIR3DL1	0.08	SLPI	0.07	KCNJ15	0.07	ANKRD36B	0.19
66	LRRC10	0.08	GNPDA2	0.07	PI3	0.07	CCDC18	0.18
67	AKR1C3	0.08	KIR2DS3	0.07	OR4C16	0.07	IGF2BP2	0.18
68	KREMEN1	0.08	OR10A7	0.07	OR1M1	0.07	IFI35	0.18
69	TRAPPC13	0.08	ESF1	0.07	WDFY3	0.07	PF4	0.18
70	SPATA45	0.08	FAM157A	0.07	TIFAB	0.07	SLC6A8	0.18
71	CXCR1	0.08	BIRC3	0.07	VNN3	0.07	VRK1	0.17
72	OR5V1	0.08	MRGPRX2	0.07	OR2AT4	0.07	TLR7	0.17
73	MAK	0.08	CYP51A1	0.07	MAS1	0.07	STIL	0.17
74	DEFA1B	0.08	CSF2RB	0.07	OR2T34	0.07	UBXN6	0.17
75	CCL4L2	0.08	RGS2	0.07	THRSP	0.07	IFIH1	0.17
76	VNN3	0.08	CSTF2T	0.07	VNN3	0.07	LY6E	0.17
77	CCR3	0.08	TAS2R39	0.07	IFNA7	0.07	GBP2	0.17
78	TAS2R10	0.08	HIST1H1E	0.07	OR5V1	0.07	FKBP8	0.17
79	OR4P4	0.08	OR14A16	0.07	DEFB121	0.07	RGS2	0.17
80	CHI3L1	0.08	RPS18	0.07	CXCR1	0.07	CHI3L1	0.17
81	CNTNAP3	0.08	ST6GALNAC2	0.07	POU3F4	0.07	STEAP4	0.16
82	HRH2	0.08	MMP8	0.07	OR5AC2	0.07	GRAMD1C	0.16
83	IFNG	0.08	MRPL50	0.07	CXorf51A	0.07	LOC643802	0.16
84	MBOAT2	0.08	DNAAF2	0.07	OR5I1	0.07	CCR1	0.16
85	LIMK2	0.08	OR4C16	0.07	TAS2R3	0.07	DMTN	0.16
86	ALPK1	0.08	OCLM	0.07	TNFRSF17	0.07	RGS18	0.16
87	IFI44L	0.08	ANPEP	0.07	GCA	0.07	MT2A	0.16
88	CNTNAP3B	0.07	HIST1H1C	0.07	H1FX	0.07	PF4V1	0.15
89	GCA	0.07	ZIC4	0.07	SDPR	0.07	APOBEC3A	0.15
90	OR52E4	0.07	GPR97	0.07	OR8K3	0.07	ASCC2	0.15
91	WDFY3	0.07	ERV3-1	0.07	C4orf19	0.07	SLC25A39	0.15
92	HIST1H1C	0.07	VNN2	0.07	PRR32	0.07	CMPK2	0.15
93	OR6C4	0.07	SAMD5	0.06	KRTAP25-1	0.07	OR4K5	0.15
94	TAS2R16	0.07	OR52M1	0.06	CLEC4D	0.07	CCNA2	0.15
95	TAAR1	0.07	OR8B8	0.06	TLR2	0.07	EMR3	0.15
96	XCL2	0.07	KRTAP4-6	0.06	TLR6	0.06	HCAR2	0.15
97	SPDYE2	0.07	SPRR2F	0.06	CLEC2B	0.06	CASP5	0.15
98	OR51A2	0.07	CEACAM3	0.06	C3orf79	0.06	KLRF1	0.15
99	GNLY	0.07	HRH2	0.06	FCGR3B	0.06	GYPA	0.15
100	OR51B6	0.07	OR7G3	0.06	IQCF2	0.06	CCR3	0.15

Appendix 5: Dichotomy in the host transcriptional response to blood-stage *P. falciparum* (list of the 517 genes used in the global gene set analysis).

Table shows the 517 genes (gene I.Ds), ordered as per displayed in the heatmap in figure 3.3 (top to bottom). Up-regulated gene clusters observed in the group of “classical” responders are shown in red. Down-regulated gene clusters observed in the “non-classical” responders are shown in blue.

	Gene Symbol	Description	Up-regulated gene clusters in the "classical" volunteers	Down-regulated gene clusters in the "non-classical" volunteers
1	TOX	thymocyte selection-associated high mobility group box		
2	TGFBR3	transforming growth factor, beta receptor III		
3	TNF	tumor necrosis factor		
4	PTPLAD1	protein tyrosine phosphatase-like A domain containing 1		
5	CD40LG	CD40 ligand		
6	SCLT1	sodium channel and clathrin linker 1		
7	CCNL1	cyclin L1		
8	NKTR	natural killer cell triggering receptor		
9	IL18RAP	interleukin 18 receptor accessory protein		
10	HIST1H4H	histone cluster 1, H4h		
11	RIPK2	receptor-interacting serine-threonine kinase 2		
12	GM2A	GM2 ganglioside activator		
13	CCR2	chemokine (C-C motif) receptor 2		
14	WDFY3	WD repeat and FYVE domain containing 3		
15	SPOPL	speckle-type POZ protein-like		
16	TLR1	toll-like receptor 1		
17	CYB5R4	cytochrome b5 reductase 4		
18	MANSC1	MANSC domain containing 1		
19	STXBP3	syntaxin binding protein 3		
20	LUC7L3	LUC7-like 3 (S. cerevisiae)		
21	ERV3-1	endogenous retrovirus group 3, member 1		
22	SYNE1	spectrin repeat containing, nuclear envelope 1		
23	LY6G5B	lymphocyte antigen 6 complex, locus G5B		
24	ANKRD36B	ankyrin repeat domain 36B		
25	TNFSF13B	tumor necrosis factor (ligand) superfamily, member 13b		
26	NBN	nibrin		
27	PSMA4	proteasome (prosome, macropain) subunit, alpha type, 4		
28	APOL3	apolipoprotein L, 3		
29	IFI35	interferon-induced protein 35		
30	BST2	bone marrow stromal cell antigen 2		
31	TRAFD1	TRAF-type zinc finger domain containing 1		
32	CARD16	caspase recruitment domain family, member 16		
33	SORT1	sortilin 1		
34	SLAMF7	SLAM family member 7		
35	HSPH1	heat shock 105kDa/110kDa protein 1		
36	OAS3	2'-5'-oligoadenylate synthetase 3, 100kDa		
37	MX1	MX dynamin-like GTPase 1		
38	PSTPIP2	proline-serine-threonine phosphatase interacting protein 2		
39	CEACAM1	carcinoembryonic antigen-related cell adhesion molecule 1		
40	GBP3	guanylate binding protein 3		
41	UBE2B	ubiquitin-conjugating enzyme E2B		
42	FCHO2	FCH domain only 2		
43	FGFR1OP2	FGFR1 oncogene partner 2		
44	CMAS	cytidine monophosphate N-acetylneuraminic acid synthetase		
45	VRK1	vaccinia related kinase 1		
46	YOD1	YOD1 deubiquitinase		
47	CA1	carbonic anhydrase I		
48	TMEM56	transmembrane protein 56		
49	CHPT1	choline phosphotransferase 1		
50	CAPRIN2	caprin family member 2		
51	SLC14A1	solute carrier family 14 (urea transporter), member 1		
52	MYL4	myosin, light chain 4, alkali; atrial, embryonic		
53	IGF2BP2	insulin-like growth factor 2 mRNA binding protein 2		
54	ANK1	ankyrin 1, erythrocytic		
55	TSPAN5	tetraspanin 5		
56	WDFY1	WD repeat and FYVE domain containing 1		
57	APOL6	apolipoprotein L, 6		
58	OR56B1	olfactory receptor, family 56, subfamily B, member 1		
59	JAK2	Janus kinase 2		
60	ICAM1	intercellular adhesion molecule 1		
61	APOL2	apolipoprotein L, 2		
62	XAF1	XIAP associated factor 1		
63	DDX58	DEAD (Asp-Glu-Ala-Asp) box polypeptide 58		
64	TRIM21	tripartite motif containing 21		
65	IRF1	interferon regulatory factor 1		
66	PSME2	proteasome (prosome, macropain) activator subunit 2 (PA28 beta)		
67	SAT1	spermidine/spermine N1-acetyltransferase 1		
68	DMXL2	Dmx-like 2		
69	CASP1	caspase 1, apoptosis-related cysteine peptidase		
70	LY86	lymphocyte antigen 86		

71	LMAN1	lectin, mannose-binding, 1		
72	LGALS3BP	lectin, galactoside-binding, soluble, 3 binding protein		
73	HLA-DMA	major histocompatibility complex, class II, DM alpha		
74	CDK2AP2	cyclin-dependent kinase 2 associated protein 2		
75	CCR1	chemokine (C-C motif) receptor 1		
76	SDPR	serum deprivation response		
77	MMD	monocyte to macrophage differentiation-associated		
78	THBS1	thrombospondin 1		
79	SH3BGRL2	SH3 domain binding glutamate-rich protein like 2		
80	TLR6	toll-like receptor 6		
81	BAZ2B	bromodomain adjacent to zinc finger domain, 2B		
82	MME	membrane metallo-endopeptidase		
83	KCNJ2	potassium inwardly-rectifying channel, subfamily J, member 2		
84	GK	glycerol kinase		
85	IL1B	interleukin 1, beta		
86	FPR2	formyl peptide receptor 2		
87	KCNJ15	potassium inwardly-rectifying channel, subfamily J, member 15		
88	TCF7	transcription factor 7 (T-cell specific, HMG-box)		
89	SDAD1	SDA1 domain containing 1		
90	CD180	CD180 molecule		
91	TIMM22	translocase of inner mitochondrial membrane 22 homolog (yeast)		
92	IRF4	interferon regulatory factor 4		
93	TXNDC5	thioredoxin domain containing 5 (endoplasmic reticulum)		
94	KIR2DS3	killer cell immunoglobulin-like receptor		
95	KIR2DS1	killer cell immunoglobulin-like receptor		
96	KIR2DS2	killer cell immunoglobulin-like receptor		
97	PPM1A	protein phosphatase, Mg2+/Mn2+ dependent, 1A		
98	CPEB4	cytoplasmic polyadenylation element binding protein 4		
99	HIST1H3H	histone cluster 1, H3h		
100	CLU	clusterin		
101	BPGM	2,3-bisphosphoglycerate mutase		
102	GOLGA8B	golgin A8 family, member B		
103	GOLGA8A	golgin A8 family, member A		
104	CLK1	CDC-like kinase 1		
105	ANKRD36	ankyrin repeat domain 36		
106	KIR3DS1	killer cell immunoglobulin-like receptor		
107	KIR3DL2	killer cell immunoglobulin-like receptor		
108	KIR2DL5B	killer cell immunoglobulin-like receptor		
109	KIR3DL1	killer cell immunoglobulin-like receptor		
110	PTGDR	prostaglandin D2 receptor (DP)		
111	MYBL1	v-myb avian myeloblastosis viral oncogene homolog-like 1		
112	KLRF1	killer cell lectin-like receptor subfamily F, member 1		
113	TARP	TCR gamma alternate reading frame protein		
114	KLRG1	killer cell lectin-like receptor subfamily G, member 1		
115	KLRD1	killer cell lectin-like receptor subfamily D, member 1		
116	GZMH	granzyme H (cathepsin G-like 2, protein h-CCPX)		
117	FCRL6	Fc receptor-like 6		
118	USP28	ubiquitin specific peptidase 28		
119	KIR3DL3	killer cell immunoglobulin-like receptor		
120	HIST2H2BF	histone cluster 2, H2bf		
121	ALG3	ALG3, alpha-1,3- mannosyltransferase		
122	CD86	CD86 molecule		
123	CCDC88A	coiled-coil domain containing 88A		
124	IRS2	insulin receptor substrate 2		
125	KIR2DL2	killer cell immunoglobulin-like receptor		
126	KIR2DL1	killer cell immunoglobulin-like receptor		
127	KIR2DL3	killer cell immunoglobulin-like receptor		
128	KIR2DS4	killer cell immunoglobulin-like receptor		
129	RNF182	ring finger protein 182		
130	TNFAIP6	tumor necrosis factor, alpha-induced protein 6		
131	P2RY14	purinergic receptor P2Y, G-protein coupled, 14		
132	SERPING1	serpin peptidase inhibitor, clade G (C1 inhibitor), member 1		
133	FCGR1A	Fc fragment of IgG, high affinity Ia, receptor (CD64)		
134	PARP9	poly (ADP-ribose) polymerase family, member 9		
135	EPSTI1	epithelial stromal interaction 1 (breast)		
136	IFIT3	interferon-induced protein with tetratricopeptide repeats 3		
137	FCGR1B	Fc fragment of IgG, high affinity Ib, receptor (CD64)		
138	TANK	TRAF family member-associated NFKB activator		
139	NT5C3A	5'-nucleotidase, cytosolic IIIA		
140	TTC14	tetratricopeptide repeat domain 14		
141	CBWD3	COBW domain containing 3		
142	VNN3	vanin 3		
143	PTGS2	prostaglandin-endoperoxide synthase 2		
144	OR52K2	olfactory receptor, family 52, subfamily K, member 2		
145	VPS8	vacuolar protein sorting 8 homolog (S. cerevisiae)		
146	CCNH	cyclin H		
147	N4BP2L2	NEDD4 binding protein 2-like 2		
148	CD58	CD58 molecule		
149	RPS6KA5	ribosomal protein S6 kinase, 90kDa, polypeptide 5		
150	PIGB	phosphatidylinositol glycan anchor biosynthesis, class B		

151	PF4V1	platelet factor 4 variant 1		
152	SLPI	secretory leukocyte peptidase inhibitor		
153	SWT1	SWT1 RNA endoribonuclease homolog (S. cerevisiae)		
154	MBOAT2	membrane bound O-acyltransferase domain containing 2		
155	ALS2CR12	amyotrophic lateral sclerosis 2 (juvenile) chromosome region, candidate 12		
156	GYPB	glycophorin B (MNS blood group)		
157	GYPA	glycophorin A (MNS blood group)		
158	MICALCL	MICAL C-terminal like		
159	PLA2G7	phospholipase A2, group VII (platelet-activating factor acetylhydrolase, plasma)		
160	KIAA1598	KIAA1598		
161	NLRC4	NLR family, CARD domain containing 4		
162	FAM105A	family with sequence similarity 105, member A		
163	C3AR1	complement component 3a receptor 1		
164	PRRG4	proline rich Gla (G-carboxyglutamic acid) 4 (transmembrane)		
165	KREMEN1	kringle containing transmembrane protein 1		
166	ANXA3	annexin A3		
167	LAP3	leucine aminopeptidase 3		
168	GCH1	GTP cyclohydrolase 1		
169	OAS1	2'-5'-oligoadenylate synthetase 1, 40/46kDa		
170	DDX60	DEAD (Asp-Glu-Ala-Asp) box polypeptide 60		
171	MYOF	myoferlin		
172	P2RX7	purinergic receptor P2X, ligand-gated ion channel, 7		
173	LACTB	lactamase, beta		
174	CD38	CD38 molecule		
175	IFIT5	interferon-induced protein with tetratricopeptide repeats 5		
176	IFIH1	interferon induced with helicase C domain 1		
177	OASL	2'-5'-oligoadenylate synthetase-like		
178	APOL1	apolipoprotein L, 1		
179	IFIT2	interferon-induced protein with tetratricopeptide repeats 2		
180	TIA1	TIA1 cytotoxic granule-associated RNA binding protein		
181	CLK4	CDC-like kinase 4		
182	VPS13A	vacuolar protein sorting 13 homolog A (S. cerevisiae)		
183	ZFYVE16	zinc finger, FYVE domain containing 16		
184	CBWD5	COBW domain containing 5		
185	CBWD2	COBW domain containing 2		
186	IL1RAP	interleukin 1 receptor accessory protein		
187	MS4A14	membrane-spanning 4-domains, subfamily A, member 14		
188	KLRC3	killer cell lectin-like receptor subfamily C, member 3		
189	SH2D1B	SH2 domain containing 1B		
190	PDK4	pyruvate dehydrogenase kinase, isozyme 4		
191	ICOS	inducible T-cell co-stimulator		
192	GPR18	G protein-coupled receptor 18		
193	GCNT4	glucosaminyl (N-acetyl) transferase 4, core 2		
194	SYT11	synaptotagmin XI		
195	CD160	CD160 molecule		
196	MANEA	mannosidase, endo-alpha		
197	HIST1H2BM	histone cluster 1, H2bm		
198	HLA-DQA2	major histocompatibility complex, class II, DQ alpha 2		
199	NFXL1	nuclear transcription factor, X-box binding-like 1		
200	KATNBL1	katanin p80 subunit B-like 1		
201	IL1R2	interleukin 1 receptor, type II		
202	CNTNAP3	contactin associated protein-like 3		
203	HBZ	hemoglobin, zeta		
204	TIFA	TRAF-interacting protein with forkhead-associated domain		
205	SLAMF8	SLAM family member 8		
206	PLSCR1	phospholipid scramblase 1		
207	CMPK2	cytidine monophosphate (UMP-CMP) kinase 2, mitochondrial		
208	TLR7	toll-like receptor 7		
209	ALDH1A1	aldehyde dehydrogenase 1 family, member A1		
210	MTHFD2	methylenetetrahydrofolate dehydrogenase		
211	FLVCR2	feline leukemia virus subgroup C cellular receptor family, member 2		
212	ERLIN1	ER lipid raft associated 1		
213	CLEC4D	C-type lectin domain family 4, member D		
214	RTP4	receptor (chemosensory) transporter protein 4		
215	AIM2	absent in melanoma 2		
216	GRAMD1B	GRAM domain containing 1B		
217	CD209	CD209 molecule		
218	DRAM1	DNA-damage regulated autophagy modulator 1		
219	SFRP2	secreted frizzled-related protein 2		
220	CCDC18	coiled-coil domain containing 18		
221	CCDC176	coiled-coil domain containing 176		
222	IFIT1B	interferon-induced protein with tetratricopeptide repeats 1B		
223	AHSP	alpha hemoglobin stabilizing protein		
224	IL5RA	interleukin 5 receptor, alpha		
225	ALOX15	arachidonate 15-lipoxygenase		
226	CCR3	chemokine (C-C motif) receptor 3		
227	EIF1AY	eukaryotic translation initiation factor 1A, Y-linked		
228	VCPKMT	valosin containing protein lysine (K) methyltransferase		
229	LOC643802	u3 small nucleolar ribonucleoprotein protein MPP10-like		
230	TRPM6	transient receptor potential cation channel, subfamily M, member 6		

231	KIF27	kinesin family member 27		
232	TMEM14E	transmembrane protein 14E		
233	TXNDC16	thioredoxin domain containing 16		
234	ATAD5	ATPase family, AAA domain containing 5		
235	ZMAT1	zinc finger, matrin-type 1		
236	FAM185A	family with sequence similarity 185, member A		
237	FLJ45513	uncharacterized LOC729220		
238	CXorf65	chromosome X open reading frame 65		
239	PLGLB1	plasminogen-like B1		
240	GPR15	G protein-coupled receptor 15		
241	Sep-04	septin 4		
242	EFCAB2	EF-hand calcium binding domain 2		
243	CHRM4	cholinergic receptor, muscarinic 4		
244	OR2T3	olfactory receptor, family 2, subfamily T, member 3		
245	NETO2	neuropilin (NRP) and tolloid (TLL)-like 2		
246	FAM198B	family with sequence similarity 198, member B		
247	LIPN	lipase, family member N		
248	LAMP3	lysosomal-associated membrane protein 3		
249	ETV7	ets variant 7		
250	DOCK4	dedicator of cytokinesis 4		
251	DHRS9	dehydrogenase/reductase (SDR family) member 9		
252	CASP5	caspase 5, apoptosis-related cysteine peptidase		
253	TAS2R31	taste receptor, type 2, member 31		
254	GPR52	G protein-coupled receptor 52		
255	NFE2L2	nuclear factor, erythroid 2-like 2		
256	KIAA0825	KIAA0825		
257	MAK	male germ cell-associated kinase		
258	ENKUR	enkurin, TRPC channel interacting protein		
259	KLRC2	killer cell lectin-like receptor subfamily C, member 2		
260	DTHD1	death domain containing 1		
261	KLRC1	killer cell lectin-like receptor subfamily C, member 1		
262	GRAMD1C	GRAM domain containing 1C		
263	RBMXL3	RNA binding motif protein, X-linked-like 3		
264	PHGR1	proline/histidine/glycine-rich 1		
265	SRRM5	serine/arginine repetitive matrix 5		
266	KLHL14	kelch-like family member 14		
267	HIST1H3B	histone cluster 1, H3b		
268	TAS2R43	taste receptor, type 2, member 43		
269	GK5	glycerol kinase 5 (putative)		
270	ABCA5	ATP-binding cassette, sub-family A (ABC1), member 5		
271	C6orf163	chromosome 6 open reading frame 163		
272	SLC26A8	solute carrier family 26 (anion exchanger), member 8		
273	LY96	lymphocyte antigen 96		
274	KMO	kynurenine 3-monooxygenase (kynurenine 3-hydroxylase)		
275	FRMD3	FERM domain containing 3		
276	TFEC	transcription factor EC		
277	GBP7	guanylate binding protein 7		
278	CLEC5A	C-type lectin domain family 5, member A		
279	IDO1	indoleamine 2,3-dioxygenase 1		
280	PDCD1LG2	programmed cell death 1 ligand 2		
281	GBP6	guanylate binding protein family, member 6		
282	BMX	BMX non-receptor tyrosine kinase		
283	OR5A2	olfactory receptor, family 5, subfamily A, member 2		
284	CLEC6A	C-type lectin domain family 6, member A		
285	CCL2	chemokine (C-C motif) ligand 2		
286	PGBD4	piggyBac transposable element derived 4		
287	LOC100130705	uncharacterized LOC100130705		
288	GLDC	glycine dehydrogenase (decarboxylating)		
289	PRKACG	protein kinase, cAMP-dependent, catalytic, gamma		
290	TAS2R41	taste receptor, type 2, member 41		
291	KIF14	kinesin family member 14		
292	CNTLN	centlein, centrosomal protein		
293	ARG1	arginase 1		
294	IL1RL1	interleukin 1 receptor-like 1		
295	CLEC12B	C-type lectin domain family 12, member B		
296	SLITRK1	SLIT and NTRK-like family, member 1		
297	RNASE8	ribonuclease, RNase A family, 8		
298	DEFB128	defensin, beta 128		
299	OR10H2	olfactory receptor, family 10, subfamily H, member 2		
300	EIF5AL1	eukaryotic translation initiation factor 5A-like 1		
301	IL15	interleukin 15		
302	IFNG	interferon, gamma		
303	GPR84	G protein-coupled receptor 84		
304	MMP8	matrix metallopeptidase 8 (neutrophil collagenase)		
305	IFI44	interferon-induced protein 44		
306	HERC5	HECT and RLD domain containing E3 ubiquitin protein ligase 5		
307	RSAD2	radical S-adenosyl methionine domain containing 2		
308	IFIT1	interferon-induced protein with tetratricopeptide repeats 1		
309	IFI44L	interferon-induced protein 44-like		
310	CD274	CD274 molecule		

311	CARD17	caspase recruitment domain family, member 17		
312	CXCL10	chemokine (C-X-C motif) ligand 10		
313	ANKRD22	ankyrin repeat domain 22		
314	SPANXN2	SPANX family, member N2		
315	KRTAP24-1	keratin associated protein 24-1		
316	TAS2R40	taste receptor, type 2, member 40		
317	SPANXN3	SPANX family, member N3		
318	OR10T2	olfactory receptor, family 10, subfamily T, member 2		
319	OR4K5	olfactory receptor, family 4, subfamily K, member 5		
320	OR51A4	olfactory receptor, family 51, subfamily A, member 4		
321	SUCNR1	succinate receptor 1		
322	TAS2R16	taste receptor, type 2, member 16		
323	OR5D18	olfactory receptor, family 5, subfamily D, member 18		
324	OR8A1	olfactory receptor, family 8, subfamily A, member 1		
325	C7orf62	chromosome 7 open reading frame 62		
326	OR2AT4	olfactory receptor, family 2, subfamily AT, member 4		
327	SCP2D1	SCP2 sterol-binding domain containing 1		
328	PBOV1	prostate and breast cancer overexpressed 1		
329	OR4C11	olfactory receptor, family 4, subfamily C, member 11		
330	OR6X1	olfactory receptor, family 6, subfamily X, member 1		
331	PMCH	pro-melanin-concentrating hormone		
332	OR10A2	olfactory receptor, family 10, subfamily A, member 2		
333	OR1G1	olfactory receptor, family 1, subfamily G, member 1		
334	LDHAL6B	lactate dehydrogenase A-like 6B		
335	DEFB133	defensin, beta 133		
336	OR10A7	olfactory receptor, family 10, subfamily A, member 7		
337	GPR148	G protein-coupled receptor 148		
338	SPRR2F	small proline-rich protein 2F		
339	OR5V1	olfactory receptor, family 5, subfamily V, member 1		
340	FOXR2	forkhead box R2		
341	HIST1H1B	histone cluster 1, H1b		
342	UGT2B11	UDP glucuronosyltransferase 2 family, polypeptide B11		
343	TAS2R46	taste receptor, type 2, member 46		
344	TAS2R20	taste receptor, type 2, member 20		
345	TAS2R19	taste receptor, type 2, member 19		
346	TAS2R50	taste receptor, type 2, member 50		
347	ADAM20P1	ADAM metallopeptidase domain 20 pseudogene 1		
348	TAS2R13	taste receptor, type 2, member 13		
349	OCLM	oculomedin		
350	ADAM20	ADAM metallopeptidase domain 20		
351	CXCL9	chemokine (C-X-C motif) ligand 9		
352	TMEM63B	transmembrane protein 63B		
353	TESC	tescalcin		
354	TMOD1	tropomodulin 1		
355	TFDP1	transcription factor Dp-1		
356	BIRC2	baculoviral IAP repeat containing 2		
357	FAM104A	family with sequence similarity 104, member A		
358	PITHD1	PITH (C-terminal proteasome-interacting domain of thioredoxin-like) domain containing 1		
359	GMPR	guanosine monophosphate reductase		
360	EPB42	erythrocyte membrane protein band 4.2		
361	ARHGEF12	Rho guanine nucleotide exchange factor (GEF) 12		
362	RAB2B	RAB2B, member RAS oncogene family		
363	MPP1	membrane protein, palmitoylated 1, 55kDa		
364	TBCEL	tubulin folding cofactor E-like		
365	RPIA	ribose 5-phosphate isomerase A		
366	ODC1	ornithine decarboxylase 1		
367	CDC27	cell division cycle 27		
368	PRKAR2B	protein kinase, cAMP-dependent, regulatory, type II, beta		
369	ITGB3	integrin, beta 3 (platelet glycoprotein IIIa, antigen CD61)		
370	PELI1	pellino E3 ubiquitin protein ligase 1		
371	CD46	CD46 molecule, complement regulatory protein		
372	NABP1	nucleic acid binding protein 1		
373	RSRP1	arginine/serine-rich protein 1		
374	TLR2	toll-like receptor 2		
375	PROK2	prokineticin 2		
376	CYP4F3	cytochrome P450, family 4, subfamily F, polypeptide 3		
377	ARL17A	ADP-ribosylation factor-like 17A		
378	RBM39	RNA binding motif protein 39		
379	PKN2	protein kinase N2		
380	GPCPD1	glycerophosphocholine phosphodiesterase GDE1 homolog (S. cerevisiae)		
381	ATP2B1	ATPase, Ca++ transporting, plasma membrane 1		
382	SLCO4C1	solute carrier organic anion transporter family, member 4C1		
383	HCAR3	hydroxycarboxylic acid receptor 3		
384	HCAR2	hydroxycarboxylic acid receptor 2		
385	FFAR2	free fatty acid receptor 2		
386	STEAP4	STEAP family member 4		
387	PADI2	peptidyl arginine deiminase, type II		
388	CLC	Charcot-Leyden crystal galectin		
389	USP32	ubiquitin specific peptidase 32		
390	RGS18	regulator of G-protein signaling 18		

391	PF4	platelet factor 4		
392	TREM1	triggering receptor expressed on myeloid cells 1		
393	CLEC7A	C-type lectin domain family 7, member A		
394	EMR3	egf-like module containing, mucin-like, hormone receptor-like 3		
395	NAMPT	nicotinamide phosphoribosyltransferase		
396	ACSL1	acyl-CoA synthetase long-chain family member 1		
397	LRRK2	leucine-rich repeat kinase 2		
398	APOBEC3A	apolipoprotein B mRNA editing enzyme, catalytic polypeptide-like 3A		
399	CLEC4E	C-type lectin domain family 4, member E		
400	MGAM	maltase-glucoamylase (alpha-glucosidase)		
401	DOCK5	dedicator of cytokinesis 5		
402	GPR97	G protein-coupled receptor 97		
403	FPR1	formyl peptide receptor 1		
404	DUSP1	dual specificity phosphatase 1		
405	ALPL	alkaline phosphatase, liver/bone/kidney		
406	PI3	peptidase inhibitor 3, skin-derived		
407	RPS18	ribosomal protein S18		
408	GPR174	G protein-coupled receptor 174		
409	HIST1H4C	histone cluster 1, H4c		
410	NDRG3	NDRG family member 3		
411	CD28	CD28 molecule		
412	GPR56	G protein-coupled receptor 56		
413	FGFBP2	fibroblast growth factor binding protein 2		
414	GZMA	granzyme A		
415	KLRC4	killer cell lectin-like receptor subfamily C, member 4		
416	KLRB1	killer cell lectin-like receptor subfamily B, member 1		
417	GZMB	granzyme B		
418	FCER2	Fc fragment of IgE, low affinity II, receptor for (CD23)		
419	CD22	CD22 molecule		
420	IGJ	immunoglobulin J polypeptide		
421	CHI3L1	chitinase 3-like 1 (cartilage glycoprotein-39)		
422	TNFSF10	tumor necrosis factor (ligand) superfamily, member 10		
423	TAP1	transporter 1, ATP-binding cassette, sub-family B (MDR/TAP)		
424	FAS	Fas cell surface death receptor		
425	TMEM140	transmembrane protein 140		
426	UBE2L6	ubiquitin-conjugating enzyme E2L 6		
427	SECTM1	secreted and transmembrane 1		
428	LPCAT2	lysophosphatidylcholine acyltransferase 2		
429	LGALS9	lectin, galactoside-binding, soluble, 9		
430	KCTD12	potassium channel tetramerization domain containing 12		
431	HSPA1B	heat shock 70kDa protein 1B		
432	STAT2	signal transducer and activator of transcription 2, 113kDa		
433	DTX3L	deltex 3 like, E3 ubiquitin ligase		
434	PARP14	poly (ADP-ribose) polymerase family, member 14		
435	WARS	tryptophanyl-tRNA synthetase		
436	OAS2	2'-5'-oligoadenylate synthetase 2, 69/71kDa		
437	EIF2AK2	eukaryotic translation initiation factor 2-alpha kinase 2		
438	GBP4	guanylate binding protein 4		
439	GBP1	guanylate binding protein 1, interferon-inducible		
440	STAT1	signal transducer and activator of transcription 1, 91kDa		
441	GBP2	guanylate binding protein 2, interferon-inducible		
442	STX11	syntaxin 11		
443	SAMD9L	sterile alpha motif domain containing 9-like		
444	GBP5	guanylate binding protein 5		
445	DEFA1B	defensin, alpha 1B		
446	SEPTIN1	septin 1		
447	CD3G	CD3g molecule, gamma (CD3-TCR complex)		
448	CX3CR1	chemokine (C-X3-C motif) receptor 1		
449	HIST1H1E	histone cluster 1, H1e		
450	RPS5	ribosomal protein S5		
451	CCR7	chemokine (C-C motif) receptor 7		
452	FAIM3	Fas apoptotic inhibitory molecule 3		
453	CD79A	CD79a molecule, immunoglobulin-associated alpha		
454	USP15	ubiquitin specific peptidase 15		
455	KIAA1551	KIAA1551		
456	SPN	sialophorin		
457	IL2RB	interleukin 2 receptor, beta		
458	CD96	CD96 molecule		
459	SLAMF6	SLAM family member 6		
460	RSL1D1	ribosomal L1 domain containing 1		
461	HCST	hematopoietic cell signal transducer		
462	COPE	coatomer protein complex, subunit epsilon		
463	GNLY	granulysin		
464	MXI1	MAX interactor 1, dimerization protein		
465	MICAL2	microtubule associated monooxygenase, calponin and LIM domain containing 2		
466	FAM210B	family with sequence similarity 210, member B		
467	SLC6A8	solute carrier family 6 (neurotransmitter transporter), member 8		
468	USP12	ubiquitin specific peptidase 12		
469	UBXN6	UBX domain protein 6		
470	GYPC	glycophorin C (Gerbich blood group)		

471	OR2W3	olfactory receptor, family 2, subfamily W, member 3		
472	HEMGN	hemogen		
473	DCUN1D1	DCN1, defective in cullin neddylation 1, domain containing 1		
474	HLA-DRB5	major histocompatibility complex, class II, DR beta 5		
475	SOD2	superoxide dismutase 2, mitochondrial		
476	SMCHD1	structural maintenance of chromosomes flexible hinge domain containing 1		
477	MXD1	MAX dimerization protein 1		
478	FAM157B	family with sequence similarity 157, member B		
479	CXCR2	chemokine (C-X-C motif) receptor 2		
480	VNN2	vanin 2		
481	CXCR1	chemokine (C-X-C motif) receptor 1		
482	AQP9	aquaporin 9		
483	RGS2	regulator of G-protein signaling 2		
484	PHOSPHO1	phosphatase, orphan 1		
485	FOXO3	forkhead box O3		
486	FECH	ferrochelatase		
487	SLC4A1	solute carrier family 4 (anion exchanger), member 1 (Diego blood group)		
488	PRF1	perforin 1 (pore forming protein)		
489	NKG7	natural killer cell granule protein 7		
490	CTSW	cathepsin W		
491	MT2A	metallothionein 2A		
492	HSP90B1	heat shock protein 90kDa beta (Grp94), member 1		
493	COX8A	cytochrome c oxidase subunit VIIIA (ubiquitous)		
494	HLA-DRB1	major histocompatibility complex, class II, DR beta 1		
495	GIMAP7	GTPase, IMAP family member 7		
496	HLA-DRB4	major histocompatibility complex, class II, DR beta 4		
497	SLC25A37	solute carrier family 25 (mitochondrial iron transporter), member 37		
498	RIOK3	RIO kinase 3		
499	R3HDM4	R3H domain containing 4		
500	FBXO7	F-box protein 7		
501	YBX3	Y box binding protein 3		
502	STRADB	STE20-related kinase adaptor beta		
503	P2RY13	purinergic receptor P2Y, G-protein coupled, 13		
504	CSF3R	colony stimulating factor 3 receptor (granulocyte)		
505	PPBP	pro-platelet basic protein (chemokine (C-X-C motif) ligand 7)		
506	MARCH8	membrane-associated ring finger (C3HC4) 8, E3 ubiquitin protein ligase		
507	FKBP8	FK506 binding protein 8, 38kDa		
508	SNCA	synuclein, alpha (non A4 component of amyloid precursor)		
509	RNF10	ring finger protein 10		
510	FGL2	fibrinogen-like 2		
511	CYBB	cytochrome b-245, beta polypeptide		
512	IFI6	interferon, alpha-inducible protein 6		
513	MBNL3	muscleblind-like splicing regulator 3		
514	FAM46C	family with sequence similarity 46, member C		
515	DCAF12	DDB1 and CUL4 associated factor 12		
516	ALAS2	aminolevulinate, delta-, synthase 2		
517	SLC25A39	solute carrier family 25, member 39		

Appendix 5: Within-volunteer “distance travelled”

volunteer i.d	"Distance travelled" through time						Total Distance	Final Distance
18	C-1 → C +2 6.01	C +2 → C +4 6.04	C +4 → C +6 7.99	C +6 → C +8 3.55	C +8 → **C +8.5** 4.35		27.94	**7.17**
12	C-1 → C +2 9.12	C +2 → C +4 11.39	C +4 → C +6 0.59	C +6 → **C +7.5** 5.66			26.76	**5.79**
208	C-1 → C +2 8.92	C +2 → C +4 missing C +4 sample	C +2 → C +6 5.00	C +6 → C +8 3.61	C +8 → **C +9.0** 2.03		19.56	**10.15**
20	C-1 → C +2 6.24	C +2 → C +4 1.52	C +4 → C +6 3.95	C +6 → C +8 4.16	C +8 → **C +8.5** 5.22		21.09	**9.68**
22	C-1 → C +2 3.55	C +2 → C +4 2.15	C +4 → C +6 6.26	C +6 → C +8 1.22	C +8 → **C +10** 12.07		25.25	**15.88**
19	C-1 → C +2 3.52	C +2 → C +4 4.53	C +4 → C +6 2.35	C +6 → C +8 5.63	C +8 → **C +8.5** 10.18		26.21	**11.32**
16	C-1 → C +2 0.98	C +2 → C +4 1.23	C +4 → C +6 4.20	C +6 → C +8 14.86	C +8 → **C +10** 11.81		36.76	**26.58**
17	C-1 → C +2 6.63	C +2 → C +4 6.32	C +4 → C +6 0.92	C +6 → C +8 9.89	C +8 → C +10 13.00	C +10 → **C +10.5** 3.19	39.95	**22.8**
13	C-1 → C +2 1.17	C +2 → C +4 1.75	C +4 → C +6 0.87	C +6 → C +8 5.87	C +8 → C +10 13.17	C +10 → **C +10.5** 7.66	30.49	**18.94**
27	C-1 → C +2 missing C +2 sample	C -1 → C +4 5.67	C +4 → C +6 2.20	C +6 → C +8 8.5	C +8 → **C +9** 10.65		27.02	**18.33**
26	C-1 → C +2 missing C -1 sample	C +2 → C +4 missing C +4 sample	C +2 → C +6 7.39	C +46→ C +8 8.64	C +8 → **C +9** 10.41		26.44	**18.05**
206	C-1 → C +2 3.39	C +2 → C +4 4.35	C +4 → C +6 5.05	C +6 → C +8 3.81	C +8 → **C +10** 14.24		30.84	**16.88**
106	C-1 → C +2 7.95	C +2 → C +4 4.05	C +4 → C +6 1.89	C +6 → C +8 2.49	C +8 → **C +8.5** 14.17		30.55	**17.44**
24	C-1 → C +2 5.01	C +2 → C +4 1.54	C +4 → C +6 3.43	C +6 → C +8 3.7	C +8 → **C +10** 8.53		22.21	**15.00**
BC.1	day 0 → day 2 1.88	day 2 → day 4 6.77	day 4 → day 6 3.19	day 6 → day 8 2.14	day 8 → day 10 4.70	day 10 → day 12 4.69	23.37	**7.94**
BC.2	day 0 → day 2 3.68	day 2 → day 4 1.45	day 4 → day 6 3.46	day 6 → day 8 4.31	day 8 → day 10 5.59	day 10 → day 12 3.01	21.5	**4.08**
BC.3	day 0 → day 2 missing day 0 sample	day 2 → day 4 3.12	day 4 → day 6 missing day 6 sample	day 4 → day 8 4.65	day 8 → day 10 4.92	day 10 → day 12 4.10	16.79	**5.05**
BC.4	day 0 → day 2 0.72	day 2 → day 4 0.51	day 4 → day 6 2.91	day 6 → day 8 13.51	day 8 → day 10 9.59	day 10 → day 12 missing day 12 sample	27.24	**7.96**

Appendix 5 | Within-volunteer "distance travelled" was calculated by assessing within-volunteer variation by Principle Component Analysis. By plotting each time point in the volunteer's time course on a 2D scale (as PC1 vs PC2), the “distance travelled” between each point could be calculated using “Pythagoras' Theorem” ($a^2 + b^2 = c^2$). “Total distance” was taken as the sum of each sequential distance travelled (a – b – c - d), and “final distance”, calculated by drawing a direct line between the first time-point and the last (a – d). Table shows a break-down of the measurements, for each of the 14 infected and 4 uninfected (baseline) controls through time. “Unknowns” = yellow, “non-classical” responders = blue, “classical” responders = red and “baseline controls” = black.

Appendix 6: Concentrations (pg/mL) of Cytokines and Chemokines in Volunteer Plasma

	Concentrations of **CXCL9** (pg/mL)						
volunteer i.d	C -1	C +2	C +4	C +6	C +8	C +10	DoD
12	76.53	25.045	58.5	41			58.99
13	70.75	104.9	47.86	54.2	44.07	158.4	157.88
16	96.98	60.82	91.84	42.51	405.04		3722.61
17	70.56	37.01	88.81	46.69	128	555.67	914.4
18	94.23	56.74	42.1	89.85	95.69		43.9
19	56.57	96.66	39.83	85.04	53.24		76.42
22	43.21	43.63	97.84	57.1	80.57		40.15
24	53.42	57.13	32.68	81.1	40		120.19
26	177.63	84.31	140.1	76.1	124.86		184.8
27	39.63	67.97	43.39	62.49	128.18		717.21
106	72.74	18.31	55.64	43.89	58.6		79.2
206	39.11	19.46	37.05	13.46	44.1		217.62
208	38.82	101.87	43.91	110.91	30.24		79

	Concentrations of **CXCL10** (pg/mL)						
volunteer i.d	C -1	C +2	C +4	C +6	C +8	C +10	DoD
12	261.47	207.11	203.29	222.16			196.04
13	251.43	290.53	254.08	199.83	263.82	645.02	991.39
16	289.47	444.66	322.35	270.9	1241.4		10,144.18
17	158.07	173.38	171.86	153.54	355.1	1711.75	2523.1
18	257.49	283.71	263.91	265.79	305.41		197.5
19	338.53	314.89	231.28	297.22	265.99		240.95
22	227.42	283.95	364.87	267.45	305.17		288.54
24	279.61	179.84	284.79	213.57	336.42		506.57
26	313.54	283.28	278.24	256.67	310.99		822.56
27	181.87	133.11	182.82	185.97	382.87		1918.48
106	184.93	179.46	214.21	230.64	205.61		644.28
206	267.18	303.51	286.92	286.57	285.29		1436.72
208	204.68	261.47	256.8	316.08	212.73		214.16

	Concentrations of **CCL2** (pg/mL)						
volunteer i.d	C -1	C +2	C +4	C +6	C +8	C +10	DoD
12	1431.14	810.635	1163.45	965.53			1407.01
13	919.85	1693.21	993.19	1143.65	854.92		1390.8
16	1325.46	1072.83	1307.22	1085.02	2567.33		7,752.66
17	1743.86	1160.05	1683.55	1523.47	1550.02		2710.17
18	1039.4	868.9	956.86	683.875	898.985		742.635
19	889.93	1419.1	896.705	1407.52	1009.52		1134.83
22	851.435	729.715	1171.92	794.175	985.005		1125.67
24	695.095	577.765	883.335	762.55	928.37		1099.15
26	1224.65	808.41	1140.05	889.87	943.505		1162.16
27	1177.79	1071.26	1725.68	1461.56	1021.62		3671.01
106	771.305	657.9	798.205	820.805	715.34		1051.02
206	927.23	985.99	1044.5	862.04	967.575		1829.07
208	1096.89	1161.85	1126.4	1231.74	901.105		1354.25

	Concentrations of **IL-18** (pg/mL)						
volunteer i.d	C -1	C +2	C +4	C +6	C +8	C +10	DoD
12	198.585	121.165	177.88	176.345			197.25
13	262.11	342.915	187.49	249.725	223.265	311.83	285.01
16	259.785	176.975	194.43	142.765	220.305		439.86
17	263.73	208.34	313.265	259.525	329.765	339.785	503.885
18	209.68	179.81	204.135	163.42	197.505		139.58
19	168.145	220.035	155.51	253.98	162.475		249.745
22	174.94	157.28	266.225	153.975	194.23		147.37
24	251.095	199.525	258.96	276.43	302.89		340.72
26	223.825	177.93	201.65	147.955	189.98		175.11
27	107.515	180.87	127.54	136.065	88.065		141.235
106	431.41	280.71	261.23	326.765	244.75		330.02
206	315.605	218.3	277.65	176.64	212.475		220.445
208	113.39	238.74	135.33	235.71	126.015		187.625

	Concentrations of **INFα** (pg/mL)						
volunteer i.d	C -1	C +2	C +4	C +6	C +8	C +10	DoD
12	481.585	219.83	403.905	132.715			342.32
13	29.24	68.43	67.685	37.615		34.17	15.43
16	35.625		22.595		42.315		
17							
18	117.835	25.8	66.25	28.095	84.14		
19	125.505	193.52	188.48	180.32	84.58		166.745
22	65.315	25.325	140.45	53.175	98.555		55.82
24	9.945	36.95	18.295	51.245	27.635		60.435
26	80.375	28.625	77.7	28.495	74.415		43.46
27	21.91	52.82		49.695			39.06
106	46.17		46.005		33.37		
206					16.95		
208		25.935	16.465	28.105			25.195

	Concentrations of **IL-17** (pg/mL)						
volunteer i.d	C -1	C +2	C +4	C +6	C +8	C +10	DoD
12	16.32		13.935				13.6
13	18.75	39.4		27.235		20.97	
16							
17							
18	37.11		19.525		20.65		
19		19.55		18.49			
22	19.565	37.905	86.115	54.905	67.41		60.88
24				18.805	19.035		49.785
26							
27							
106							
206							
208	115.76	242.565	102.065	162.41	65.9		77.965

	Concentrations of T**NFα** (pg/mL)						
volunteer i.d	C -1	C +2	C +4	C +6	C +8	C +10	DoD
12	19.66		16.2				17.33
13	23.005	27.85		24.36		22.07	
16	30.72		22.54		23.615		
17	13.745		16.23		15.365		17.345
18					16.79		
19		29.11		26.785	16.155		22.685
22	17.62		74.705	40.02	39.315		45.51
24				17.335			25.505
26	15.09				14.82		
27		20.56		18.78			19.365
106	3567.1	3165.28	3105.59	3631.08	2755.62		3265.72
206	14.015						
208		14.28		16.54			15.645

	Concentrations of **IFNγ** (pg/mL)						
volunteer i.d	C -1	C +2	C +4	C +6	C +8	C +10	DoD
12							
13							85.45
16							1,325.14
17						36.775	258.63
18							
19							
22							
24							
26							
27							
106							
206							
208							

	Concentrations of **IL-1β** (pg/mL)						
volunteer i.d	C -1	C +2	C +4	C +6	C +8	C +10	DoD
12	49.565		41.445				39.15
13		32.73		21.83		20.305	
16							
17							
18							
19		25.295		19.845			20.83
22			79.225	30.205	52.745		35.67
24							16.69
26							
27							
106							
206							
208		16.425		15.935			15.09

	Concentrations of **IL-8** (pg/mL)						
volunteer i.d	C -1	C +2	C +4	C +6	C +8	C +10	DoD
12	18.81						
13							
16							31.33
17							16.415
18	79.765				50.06		
19							
22							
24							
26							
27							
106							
206							
208							

	Concentrations of **IL-6** (pg/mL)						
volunteer i.d	C -1	C +2	C +4	C +6	C +8	C +10	DoD
12							
13		21.285		14.145		15.855	6.855
16							77.73
17							36.775
18	17.945						
19		21.75		15.06			16.265
22		21.17	77.535	34.645	49.01		45.49
24							17.915
26							
27							
106							
206				6.51			
208							

	Concentrations of **IL-10** (pg/mL)						
volunteer i.d	C -1	C +2	C +4	C +6	C +8	C +10	DoD
12	11.91		10.025				9.03
13	4.775	19.56	2.53	14.515	3.37	14.51	4.12
16	9.405				12.55		183.20
17							31.985
18	10.88		11.755		11.835		
19		13.885	2	13.275			9.87
22			11.43	2	10.5		
24			2	10.335			9.715
26	9.71		9.335				
27							21.2
106							
206							
208		9.03		9.635			

= Analyte undetectable

= Time-point subsequent to volunteer diagnosis (and treatment), therefore no available sample

Appendix 7: Volunteer Safety Data (temperature (ºC) and heart rate (BPM))

Temperature (°C)

volunteer i.d	C -1	C +2.0	C +2.5	C +3.0	C +3.5	C +4.0	C +4.5	C +5.0	C +5.5	C +6.0	C +6.5	C +7.0	C +7.5	C +8.0	C +8.5	C +9.0	C +9.5	C +10.0	C +10.5
18	36.9	36.9	36.7	36.8	37.2	36.2	37.4	36.4	36.1	36.9	36.7	36.8	36.7	36.6	37.4				
12	36.2	36.6	36.1	36.1	36.8	35.5	36.7	36	36.1	35.9	36.3	36.1	36.2						
208	36.2	36.5	37.1	36.6	36.6	36.2	36.4	36.4	36.6	36.3	36.8	37.1	36.1	37.1	36.9	36.9			
20	36.2	36.1	36	36	36	36.3	36	36.5	36.1	36.1	36	35.7	35.8	36.2	36.9				
Group Mean	36.4	36.5	36.5	36.4	36.7	36.1	36.4	36.3	36.2	36.3	36.4	36.4	36.0	36.6	37.1	36.9			
16	36.2	36.1	36.4	36.1	36.2	36.2	36.2	36.3	36.4	36	36	36.1	36.5	36.2	36.8	36.6	36.9	37.3	
17	36.2	36	36.1	36.8	36.3	36.2	36.1	36.1	35.9	36.8	36.1	36.6	35.9	36.7	35.7	36.8	37.6	36.2	38.2
13	36.7	36.1	36.6	36.4	36.5	36.7	36.5	36.1	36.3	36.6	37.5	36.3	36.2	36.5	36.1	36.3	37.1	36.2	37.0
27	36.7	35.8	35.8	37.1	36.3	36.1	36.7	36.4	36	36.3	36.8	36.5	36	36.2	36.4	36.8			
26	36.9	36.2	36.1	36.6	36.3	36.9	36.4	36.8	36.9	36.8	36.4	36.5	37	36.6	37.3	37.1			
206	36.4	36.4	36.3	36	36.4	36.2	35.6	36.1	36.7	36.1	36.6	35.9	36.9	36.3	36.7	36.8	37	36.8	
106	37.1	36.9	37.2	36.8	36.9	36.6	36.8	37.2	37.1	37.1	36.7	36.9	36.2	36.8	37.1				
24	36.4	36.2	36.2	36.7	36	36.3	36.2	36.2	36.2	35.9	36	36.1	36.2	36.1	36.6	35.8	37.1	36.0	
Group Mean	36.6	36.2	36.3	36.6	36.4	36.4	36.3	36.4	36.4	36.4	36.5	36.4	36.4	36.4	36.6	36.6	37.14	36.5	37.6
22	36.2	36.8	36.3	36.7	37.1	36.5	37.1	36.7	36.7	36.3	37.1	36.7	36.8	36.7	37.2	36.1	36.8	36.1	
19	36.8	36.1	36.2	36.2	35.8	36.4	36.2	36.1	36.1	36.3	36.2	36.2	36.7	36.1	36.7				
Group Mean	36.5	36.4	36.3	36.5	36.4	36.4	36.7	36.4	36.4	36.3	36.7	36.5	36.8	36.4	36.95	36.1	36.8	36.1	

day of diagnosis
fever (>37.6)

Heart Rate (BPM)

volunteer i.d	C -1	C +2.0	C +2.5	C +3.0	C +3.5	C +4.0	C +4.5	C +5.0	C +5.5	C +6.0	C +6.5	C +7.0	C +7.5	C +8.0	C +8.5	C +9.0	C +9.5	C +10.0	C +10.5
18	91	78	87	83	78	98	90	79	72	78	82	82	82	78	91				
12	68	65	74	103	68	63	75	64	83	68	84	86	64						
208	66	64	74	62	67	72	60	67	70	77	56	63	73	77	69	77			
20	58	64	55	90	57	70	47	76	53	78	55	67	N/A	55	87				
Group Mean	71	68	73	85	68	76	68	72	70	75	69	75	73	70	82	77			
16	72	49	60	102	89	57	64	57	78	65	59	54	53	65	67	76	73	93	
17	81	82	94	82	88	69	97	84	83	71	88	93	84	84	88	91	82	94	83
13	62	83	73	90	71	89	67	86	55	82	84	75	65	69	91	62	87	55	97
27	94	88	83	96	68	90	83	73	74	73	84	76	103	84	99	98			
26	79	65	90	86	71	75	67	73	79	84	67	77	66	77	88	73			
206	54	74	60	71	58	64	56	65	61	63	66	56	59	66	55	62	62	76	
106	88	93	79	86	103	89	80	65	95	93	80	94	80	96	79				
24	61	60	77	78	72	69	78	62	68	77	68	61	66	63	67	82	84	84	
Group Mean	74	74	77	86	78	75	74	71	74	76	75	73	72	76	79	78	78	80	90
22	74	68	70	66	71	67	68	72	68	74	67	59	58	69	77	63	68	63	
19	81	84	92	87	86	89	75	83	99	87	73	80	86	74	93				
Group Mean	78	76	81	77	79	78	72	78	84	81	70	70	72	72	85	63	68	63	

N/A heart rate not assesed

Appendix 7 Continued: Volunteer safety data (blood pressure (BP))

Blood Pressure (BP)

volunteer i.d	C -1	C +2.0	C +2.5	C +3.0	C +3.5	C +4.0	C +4.5	C +5.0	C +5.5	C +6.0	C +6.5	C +7.0	C +7.5	C +8.0	C +8.5	C +9.0	C +9.5	C +10.0	C +10.5
18	118	116	117	124	119	118	116	111	108	107	118	113	103	97	122				
	77	77	69	74	70	73	72	68	62	66	71	71	67	66	76				
12	68	65	74	103	68	63	75	64	83	68	84	86	64						
	117	112	132	139	120	125	124	124	125	114	125	129	122						
208	111	121	113	123	119	112	106	117	112	115	105	109	114	119	109	118			
	71	72	70	78	76	78	72	73	67	75	64	74	71	78	69	74			
20	118	126	129	146	133	119	141	119	114	116	123	137	N/A	116	113				
	74	70	77	76	82	74	72	70	70	71	73	76	N/A	65	72				
Group Mean	104	107	108	124	110	103	110	103	104	102	108	111	94	111	115	118			
	85	83	87	92	87	88	85	84	81	82	83	88	87	70	72	74			
16	123	118	119	145	126	116	116	119	142	110	122	117	110	123	123	123	124	123	
	74	68	73	82	71	72	61	67	77	65	68	78	66	76	68	70	67	68	
17	108	117	116	113	111	104	112	106	114	111	113	121	116	111	96	124	108	106	120
	73	80	74	73	73	78	74	73	76	70	73	77	83	76	64	77	69	71	77
13	98	135	135	153	142	136	139	141	129	133	142	119	150	125	135	122	140	123	134
	72	77	84	81	81	80	77	80	78	81	86	69	80	76	77	74	82	74	77
27	133	138	134	120	131	144	132	134	148	128	135	141	143	125	135	127			
	82	86	81	73	78	83	77	74	81	75	80	73	77	74	81	80			
26	104	105	106	103	103	102	109	106	105	102	111	112	102	106	108	102			
	72	71	67	69	70	72	67	61	64	60	66	66	65	62	61	63			
206	129	113	127	107	110	119	113	108	94	114	118	106	114	103	110	115	127	125	
	79	67	76	71	73	71	65	70	60	73	75	71	78	61	70	71	83	78	
106	114	105	120	106	126	102	106	114	114	114	112	107	104	118	112				
	70	71	73	66	80	65	66	75	73	70	70	69	64	74	76				
24	113	115	114	119	107	115	124	112	110	106	115	115	105	113	114	116	128	113	
	66	68	70	67	67	72	69	61	71	64	62	69	65	71	66	73	68	66	
Group Mean	115	118	121	121	120	117	119	118	120	115	121	117	118	116	117	118	125	118	127
	74	74	75	73	74	74	70	70	73	70	73	72	72	71	70	73	74	71	77
22	113	120	123	134	122	125	126	124	105	115	127	119	124	113	123	107	119	124	
	74	72	71	76	76	76	76	79	66	84	80	81	78	70	81	78	80	80	
19	120	117	129	119	129	124	130	114	128	118	117	136	130	113	122				
	72	72	74	73	73	73	76	71	81	77	76	80	79	71	75				
Group Mean	117	119	126	127	126	125	128	119	117	117	122	128	127	113	123	107	119	124	
	73	72	72.5	74.5	74.5	74.5	76	75	73.5	80.5	78	80.5	78.5	70.5	78	78	80	80	

	systolic BP
	diastolic BP
N/A	blood pressure not assessed

Appendix 8: List of (203) Differentially Expressed Genes Between Parasites Isolated From Volunteers at Day of Patent Infection and Parasites Recovered from Blood-stage Inoculum

UP in volunteer samples			
transcript id	log2FoldChange	adjusted p.value	description
PF3D7_0401600.1	7.589696519	0.000162813	rifin PIR protein
PF3D7_1222600	7.056450524	0.004128576	transcription factor with AP2 domain(s)
PF3D7_1004400	6.885845263	0.001193024	RNA-binding protein, putative
PF3D7_0621000	6.371605844	0.004967138	conserved Plasmodium protein, unknown function
PF3D7_0212300	6.316650195	0.001860276	peptide chain release factor subunit 1, putative
PF3D7_1307600	6.261076569	0.008576355	DNA-directed RNA polymerase alpha chain, putative
PF3D7_1021900	6.258342957	0.008554609	conserved Plasmodium protein (10b antigen), unknown function
PF3D7_1368200	6.210902227	0.005477977	RNAse L inhibitor protein, putative
PF3D7_1135900	5.869392045	0.005020867	3-oxo-5-alpha-steroid 4-dehydrogenase, putative
PF3D7_0310400	5.816774187	0.005900786	parasite-infected erythrocyte surface protein
PF3D7_1008900	5.777594785	0.008646082	adenylate kinase
PF3D7_0621700	5.595624295	0.007865631	conserved Plasmodium protein, unknown function
PF3D7_1215100	5.147264846	0.002093246	conserved Plasmodium protein, unknown function
PF3D7_0608800	4.852681574	0.000253703	ornithine aminotransferase
PF3D7_1035800	4.639032499	0.00661158	probable protein, unknown function
PF3D7_0313100	4.585079665	0.00098878	ubiquitin-protein ligase, putative
PF3D7_1017900	4.397342279	0.000483826	26S proteasome regulatory subunit p55, putative
PF3D7_1329100	4.325649942	0.002409188	myosin C
PF3D7_1402800	4.256969419	1.21145E-05	conserved Plasmodium protein, unknown function
PF3D7_0601900	4.169424174	0.000121686	conserved Plasmodium protein, unknown function
PF3D7_1030300	4.141242261	0.004128576	conserved Plasmodium protein, unknown function
PF3D7_1354200	4.131329319	0.002270942	inositol-polyphosphate 5-phosphatase, putative
PF3D7_1307800	4.058050673	0.000299532	fork head domain protein, putative
PF3D7_1323800	4.026533135	0.006341894	vacuolar protein sorting-associated protein 52, putative
PF3D7_1415600	3.978823292	0.007018203	conserved Plasmodium protein, unknown function
PF3D7_0913700	3.961248452	0.006681229	conserved Plasmodium protein, unknown function
PF3D7_1306400	3.909001017	0.000230448	26S protease regulatory subunit 10B, putative
PF3D7_1407300	3.896194195	0.000845152	pre-mRNA splicing factor, putative
PF3D7_1208900	3.874977254	0.002409188	conserved Plasmodium protein, unknown function
PF3D7_0717400	3.87078768	0.000177985	queuine tRNA-ribosyltransferase, putative
PF3D7_0802000	3.867459151	0.000202375	glutamate dehydrogenase, putative
PF3D7_1113600	3.842159963	0.004677872	Rpr2, RNAse P, putative
PF3D7_1366600	3.837084867	0.002203153	signal recognition particle receptor alpha subunit
PF3D7_1139300	3.816201815	2.21864E-06	transcription factor with AP2 domain(s)
PF3D7_1473200	3.806113656	0.000665293	DnaJ protein, putative
PF3D7_1021700	3.797870093	0.009692009	conserved Plasmodium membrane protein, unknown function
PF3D7_1004200	3.73798755	0.000371194	conserved Plasmodium membrane protein, unknown function
PF3D7_1306900	3.698760882	0.000310495	U1 small nuclear ribonucleoprotein a, putative
PF3D7_0415000	3.650658437	0.00857253	arsenical pump-driving ATPase, putative
PF3D7_1422800	3.642101843	0.004659408	actin-related protein, putative
PF3D7_0902200	3.634861136	0.0026505	serine/threonine protein kinase, FIKK family
PF3D7_1309000	3.613586507	2.97416E-06	conserved Plasmodium protein, unknown function
PF3D7_0801700	3.596528781	0.000843903	sentrin-specific protease 2, putative
PF3D7_1107800	3.57798007	0.000845152	transcription factor with AP2 domain(s)
PF3D7_0201500	3.559010391	0.009508445	Plasmodium exported protein (hyp9), unknown function
PF3D7_0410000	3.520026739	0.00471645	conserved Plasmodium protein, unknown function
PF3D7_0409400	3.510609487	0.000650811	heat shock protein 40
PF3D7_0506700	3.504809849	0.004508475	GTPase-activating protein, putative
PF3D7_0316700	3.465973839	0.007050907	HVA22/TB2/DP1 family protein, putative
PF3D7_1410000	3.462820348	0.004234528	tetratricopeptide repeat family protein, putative
PF3D7_0514900	3.441394338	0.001494755	conserved Plasmodium protein, unknown function
PF3D7_0811400	3.431857847	0.000483826	conserved protein, unknown function
PF3D7_0404600	3.41529078	5.10477E-05	conserved Plasmodium membrane protein, unknown function
PF3D7_0409100	3.41089642	0.000144259	U4/U6 small nuclear ribonucleoprotein PRP31, putative
PF3D7_0724200	3.406504374	0.004128576	type 2A phosphatase-associated protein 42, putative
PF3D7_0410900	3.399687981	0.000211196	conserved Plasmodium protein, unknown function
PF3D7_1472400	3.390692792	0.000665293	M1-family alanyl aminopeptidase, putative
PF3D7_0310500	3.38324818	0.001287094	DEAD box helicase, putative
PF3D7_0806500	3.381134406	0.001077071	DnaJ protein, putative
PF3D7_0821600	3.319163249	0.00077128	clp1-related protein, putative
PF3D7_1472300	3.295635351	0.006189479	conserved Plasmodium membrane protein, unknown function
PF3D7_0711500	3.291725131	0.002409188	regulator of chromosome condensation, putative
PF3D7_0625600	3.270147309	6.3738E-05	poly(A) polymerase PAP, putative
PF3D7_0215500	3.242430561	0.005562389	conserved Plasmodium protein, unknown function
PF3D7_1316600	3.221833194	0.003789631	choline-phosphate cytidylyltransferase
PF3D7_0323500	3.202768768	0.000477372	survival motor neuron-like protein

UP in volunteer samples			
transcript id	log2FoldChange	adjusted p.value	description
PF3D7_1446900	3.157589548	0.008674698	glutaminyl-peptide cyclotransferase, putative
PF3D7_1011600	3.152572994	0.006681229	conserved Plasmodium protein, unknown function
PF3D7_0217600	3.151321263	0.006415943	conserved Plasmodium protein, unknown function
PF3D7_1210400	3.134049237	0.002689235	general transcription factor 3C polypeptide 5, putative
PF3D7_0919100	3.133070031	0.003920393	DnaJ protein, putative
PF3D7_1122300	3.127968389	0.001562525	conserved Plasmodium protein, unknown function
PF3D7_1408400	3.120851274	0.001082668	DNA repair helicase, putative
PF3D7_0731600	3.117483393	0.006859746	acyl-CoA synthetase
PF3D7_1205400	3.090476908	0.002409188	conserved Plasmodium protein, unknown function
PF3D7_1450600	3.073778817	0.002779141	conserved Plasmodium protein, unknown function
PF3D7_1421400	3.067637897	0.000203053	DNA-directed RNA polymerase III subunit C, putative
PF3D7_0923900	3.03115755	0.000508993	RNA-binding protein, putative
PF3D7_1225500	3.009777073	0.007018203	small subunit rRNA processing factor, putative
PF3D7_0725300	3.006568515	0.005142894	conserved Plasmodium protein, unknown function
PF3D7_1038100	3.004726701	0.000508993	GDP dissociation inhibitor, putative
PF3D7_1323500	2.996151746	0.000578771	plasmepsin V PEXEL protease
PF3D7_0506800	2.977551073	0.002203153	transcription factor 25, putative
PF3D7_1134000	2.959348321	0.00183968	heat shock protein 70
PF3D7_0821700	2.953313306	0.000167765	60S ribosomal protein L22, putative
PF3D7_0630600	2.920112228	0.003739123	conserved Plasmodium protein, unknown function
PF3D7_1434300	2.919079953	3.74857E-06	Hsp70/Hsp90 organizing protein
PF3D7_0730900	2.899633149	0.003749965	EMP1-trafficking protein
PF3D7_1220100	2.890700194	0.008266248	pre-mRNA splicing factor, putative
PF3D7_0807900	2.878566748	0.002111257	tyrosine--tRNA ligase
PF3D7_1102500	2.87155595	0.006721578	Plasmodium exported protein (PHISTb), unknown function
PF3D7_1117800	2.867525797	0.005834226	DNA mismatch repair protein MLH
PF3D7_1307700	2.859846433	0.000208979	conserved Plasmodium protein, unknown function
PF3D7_0920900	2.851240596	0.003635992	U4/U6 snRNA-associated-splicing factor, putative
PF3D7_1317000	2.804908929	0.006197414	U4/U6.U5 tri-snRNP-associated protein 2, putative
PF3D7_1478600	2.770861538	0.003350396	EMP1-trafficking protein
PF3D7_1231600	2.761053926	0.000320171	pre-mRNA-splicing factor ATP-dependent RNA helicase PRP2, putative
PF3D7_1439100	2.739988871	0.000716273	DEAD/DEAH box helicase, putative
PF3D7_0211800	2.730267399	5.08668E-05	asparagine--tRNA ligase
PF3D7_1207600	2.726138975	0.007509846	tRNA delta(2)-isopentenylpyrophosphate transferase, putative
PF3D7_1005600	2.680673175	4.51981E-05	DnaJ protein, putative
PF3D7_1242800	2.667853101	0.004576557	rab specific GDP dissociation inhibitor
PF3D7_0610100	2.663432925	3.29865E-05	pre-mRNA-splicing factor SLU7, putative
PF3D7_1343700	2.654159529	0.006415943	kelch protein K13, putative
PF3D7_0925200	2.6314443	0.000664728	rRNA processing and telomere maintaining methyltransferase, putative
PF3D7_0912900	2.625869565	6.1697E-05	26S proteasome regulatory subunit RPN8, putative
PF3D7_1455500	2.620644125	0.009980309	AP-1 complex subunit gamma, putative
PF3D7_1237600	2.606180959	0.008576355	rRNA processing WD-repeat protein, putative
PF3D7_1135100	2.597667236	0.000821409	protein phosphatase 2C, putative
PF3D7_1249300	2.591251287	0.008674698	protein phosphatase, putative
PF3D7_1339300	2.483464709	1.36143E-05	conserved Plasmodium protein, unknown function
PF3D7_1224400	2.40845892	0.000295317	conserved Plasmodium protein, unknown function
PF3D7_0929200	2.397921949	1.95153E-05	RNA-binding protein, putative
PF3D7_0411000	2.391703614	2.64352E-05	conserved Plasmodium protein, unknown function
PF3D7_1353000	2.310334837	0.000162813	tryptophan-rich antigen, pseudogene
PF3D7_1466400	2.308592188	2.96614E-09	transcription factor with AP2 domain(s)
PF3D7_0813900	2.292206969	0.002270205	40S ribosomal protein S16, putative
PF3D7_0802300	2.28234867	0.002108594	rRNA processing WD-repeat protein, putative
PF3D7_1119300	2.26879073	0.000967908	U2 snRNP auxiliary factor, small subunit, putative
PF3D7_0501000	2.255275362	0.007235025	Plasmodium exported protein, unknown function
PF3D7_1340600	2.254006078	0.008576355	RNA lariat debranching enzyme, putative
PF3D7_0615600	2.091958312	0.000202375	conserved Plasmodium protein, unknown function
PF3D7_0904000	2.020687425	4.07114E-05	GTPase-activating protein, putative
PF3D7_0716800	1.969573584	0.003237866	eukaryotic translation initiation factor 3 37.28 kDa subunit, putative
PF3D7_1353400	1.8645978	0.008373671	Ran-binding protein, putative
PF3D7_1450100	1.842473303	1.95153E-05	signal recognition particle subunit SRP54
PF3D7_0720700	1.815932955	0.002409188	phosphoinositide-binding protein, putative
PF3D7_0206000	1.791970021	0.007923738	DNA repair endonuclease, putative
PF3D7_1309700	1.747188261	0.00093173	vacuolar protein sorting-associated protein 18, putative
PF3D7_1350500	1.596525609	0.009744215	conserved Plasmodium protein, unknown function
PF3D7_1227800	1.566859513	0.000162301	histone S-adenosyl methyltransferase, putative
PF3D7_1470600	3.160090769	0.002409188	RAP protein, putative

Appendix 8 continued: List of (203) Differentially Expressed Genes Between Parasites Isolated From Volunteers at Day of Patent Infection and Parasites Recovered from Blood-stage Inoculum

DOWN in volunteer samples			
transcript id	log2FoldChange	adjusted p.value	description
PF3D7_0719900	-0.978419593	0.005668415	conserved Plasmodium membrane protein, unknown function
PF3D7_1349200	-1.250190149	0.000211196	glutamate--tRNA ligase, putative
PF3D7_0819000	-1.276686744	0.007018203	conserved Plasmodium protein, unknown function
PF3D7_1341200	-1.305171203	0.00471645	60S ribosomal protein L18, putative
PF3D7_0106700	-1.327991758	0.002474345	small ribosomal subunit assembling AARP2 protein
PF3D7_0801800	-1.413621719	0.00553724	mannose-6-phosphate isomerase, putative
PF3D7_0617900	-1.460222023	0.005811386	histone H3 variant, putative
PF3D7_0321800	-1.466029802	3.66904E-07	conserved Plasmodium protein, unknown function
PF3D7_1408700	-1.471323798	0.002354089	conserved Plasmodium protein, unknown function
PF3D7_0820000	-1.533245901	4.98854E-06	Snf2-related CBP activator, putative
PF3D7_0518500	-1.542409885	0.008554609	ATP-dependent RNA helicase DDX23, putative
PF3D7_1349500	-1.581279415	0.008373671	conserved Plasmodium protein, unknown function
PF3D7_1248700	-1.827383977	0.007050907	conserved Plasmodium protein, unknown function
PF3D7_1407100	-1.936893935	0.003749965	fibrillarin, putative
PF3D7_0628200	-1.987880431	0.000330297	protein kinase PK4 eukaryotic translation initiation factor 2-alpha kinase
PF3D7_1003800	-2.047587809	0.000162813	U5 small nuclear ribonuclear protein, putative
PF3D7_1427100	-2.112371598	0.002270205	lipase, putative
PF3D7_0206500	-2.118661143	0.001195824	conserved Plasmodium protein, unknown function
PF3D7_1142400	-2.144827789	4.51131E-07	coproporphyrinogen-III oxidase
PF3D7_0922600	-2.186275798	0.006197414	glutamine synthetase, putative
PF3D7_1123100	-2.218855177	0.001000142	calcium-dependent protein kinase 7
PF3D7_0409800	-2.342523298	0.000125273	zinc finger protein, putative
PF3D7_0918700	-2.350466897	0.001644286	conserved Plasmodium protein, unknown function
PF3D7_0922500	-2.460567397	0.000243325	phosphoglycerate kinase
PF3D7_0309500	-2.504671843	0.008744462	asparagine synthetase, putative
PF3D7_1202600	-2.516073357	0.003724837	conserved protein, unknown function
PF3D7_0505700	-2.627650403	0.000719992	conserved Plasmodium membrane protein, unknown function
PF3D7_0621900	-2.676647384	0.004128576	signal recognition particle subunit SRP68, putative
PF3D7_1228900	-2.918995136	0.000377563	conserved Plasmodium protein, unknown function
PF3D7_1001800	-3.000665691	0.002530902	Plasmodium exported protein (PHISTc), unknown function
PF3D7_1459200	-3.01436934	0.002270205	conserved Plasmodium protein, unknown function
PF3D7_1209000	-3.038602704	0.000693761	conserved Plasmodium protein, unknown function
PF3D7_1034000	-3.054691395	0.000719992	Sec1 family protein, putative
PF3D7_0610800	-3.111696467	0.002029505	transketolase
PF3D7_0804300	-3.128554613	0.001136993	conserved Plasmodium protein, unknown function
PF3D7_1352400	-3.156730331	0.000766316	conserved Plasmodium protein, unknown function
PF3D7_0526500	-3.17122799	1.09742E-12	conserved Plasmodium protein, unknown function
PF3D7_0622100	-3.182788596	0.002530902	conserved Plasmodium protein, unknown function
PF3D7_0309800	-3.187445029	0.000283252	YTH domain-containing protein, putative
PF3D7_1113300	-3.338219552	0.00153738	UDP-galactose transporter, putative
PF3D7_1407600	-3.42414992	0.007150283	conserved Plasmodium protein, unknown function
PF3D7_0304300	-3.458913235	0.002401704	conserved Plasmodium protein, unknown function
PF3D7_0405300	-3.603500019	0.000115301	liver specific protein 2, putative 6-cysteine protein
PF3D7_1302500	-3.647871616	2.97416E-06	conserved Plasmodium protein, unknown function
PF3D7_0632800	-3.738616926	0.000729613	erythrocyte membrane protein 1, PfEMP1
PF3D7_1120300	-3.995245692	4.07114E-05	metal ion channel - Mg2+, Co2+ and Ni2+
PF3D7_0112000	-4.018303524	6.00944E-07	TatD-like deoxyribonuclease, putative
PF3D7_1251100	-4.121413205	6.1697E-05	conserved Plasmodium protein, unknown function
PF3D7_0217900	-4.210780603	0.006873667	conserved Plasmodium protein, unknown function
PF3D7_0912200	-4.216400356	4.93262E-06	conserved Plasmodium membrane protein, unknown function
PF3D7_0223500	-4.265234687	0.009355964	erythrocyte membrane protein 1, PfEMP1
PF3D7_0511600	-4.615520172	0.002401704	apical rhoptry neck protein
PF3D7_0604600	-4.667514797	0.003237866	DNA helicase, putative
PF3D7_0209600	-4.683750805	0.000162301	transporter, putative
PF3D7_1406300	-4.690373539	0.009592626	glycerophosphodiester phosphodiesterase
PF3D7_1300100	-4.840764226	0.000508993	erythrocyte membrane protein 1, PfEMP1
PF3D7_0315200	-4.914366545	0.004127674	circumsporozoite- and TRAP-related protein
PF3D7_0415500	-4.916812243	0.00072182	nuclear cap-binding protein, putative
PF3D7_0111900	-5.21421173	1.95153E-05	conserved Plasmodium protein, unknown function
PF3D7_1117500	-5.217339031	0.000211196	tyrosine--tRNA ligase
PF3D7_1011300	-5.651434127	0.00054578	conserved Plasmodium membrane protein, unknown function
PF3D7_1411400	-5.740537929	0.001692076	plastid replication-repair enzyme
PF3D7_1039100	-6.072440815	0.00553724	DnaJ protein, putative, pseudogene
PF3D7_1136000	-6.413824044	0.004226415	conserved Plasmodium protein, unknown function
PF3D7_0916000	-6.597749567	0.001562525	sugar transporter, putative
PF3D7_1217600	-6.716201129	0.007453375	anaphase promoting complex subunit 10, putative
PF3D7_0100100	-6.840804674	0.000115301	erythrocyte membrane protein 1, PfEMP1
PF3D7_0712000	-6.858380099	0.000663224	erythrocyte membrane protein 1, PfEMP1
PF3D7_1033400	-6.875761214	0.000240065	haloacid dehalogenase-like hydrolase, putative
PF3D7_0730800.2	-28.87174117	2.96614E-09	Plasmodium exported protein, unknown function
PF3D7_1235600	-29.02807788	2.96614E-09	serine hydroxymethyltransferase

Appendix 9: Optimising the PCR cycle number for use with Smart-seq2

	cDNA yield (ng)										
	13 cycles	14 cycles	15 cycles	16 cycles	17 cycles	18 cycles	19 cycles	20 cycles	21 cycles	22 cycles	25 cycles
10 pg starting RNA						8.2	10.4	6.04	32	65.3	908.0
						4.9	9.7	10.2	36.7	59.6	900.0
						4.9	8.4	18.8	39.5	34.8	2,690.0
mean of replicates						**6.0**	**9.05**	**11.7**	**36.1**	**53.2**	**1499.3**
(-RT control)						< 0.2	< 0.2	< 0.2	< 0.2	< 0.2	< 0.2
Experiment Repeat						4.3					
						3.9					
						7.8					
mean of replicates						**5.3**					
(-RT control)						< 0.2					
50 pg starting RNA					6.8	9.3	17.8				
					6.5	8.9	19.5				
					4.6	9.7	24.5				
mean of replicates					**6.0**	**9.3**	**20.6**				
(-RT control)					< 0.2	< 0.2	< 0.2				
Experiment Repeat					4.7	18.5					
					11.5	18.7					
					10.4	14.3					
mean of replicates					**8.9**	**17.2**					
(-RT control)					< 0.2	< 0.2					
100 pg starting RNA			4.2	10.6	15.6	56.9	148.0				
			3.6	11.2	17.9	34.8	127.1				
			3.6	14.7	17.5	65.7	144.0				
mean of replicates			**3.8**	**12.2**	**17.0**	**52.5**	**139.7**				
(-RT control)			< 0.2	< 0.2	< 0.2	< 0.2	< 0.2				
Experiment Repeat			2.3	9.6	28.6		182.7				
			2.2	7.9	19.4		123.1				
			3.4	5.2	18.6		82.3				
mean of replicates			**2.6**	**7.6**	**22.2**		**129.4**				
(-RT control)			< 0.2	< 0.2	< 0.2		< 0.2				
500 pg starting RNA			15.6	25.7	34.2						
			8.83	24.9	33.5						
			6.9	21.2	26.9						
mean of replicates			**10.4**	**23.9**	**31.5**						
(-RT control)			< 0.2	< 0.2	< 0.2						
Experiment Repeat			16.2	12.9	39.4						
			13.4	17.4	35.4						
			13.9	25.9	35.8						
mean of replicates			**14.5**	**18.7**	**36.9**						
(-RT control)			< 0.2	< 0.2	< 0.2						
1 ng starting RNA	2.8	11.5	59.6		72.1						
	3.4	11.9	38.2		75.5						
	3.4	7.9	48.4		71.1						
mean of replicates	**3.2**	**9.9**	**48.7**		**72.9**						
(-RT control)	< 0.2	< 0.2	< 0.2		< 0.2						
Experiment Repeat	11.8	22.6									
	11.2	15.8									
	12.6	12.2									
mean of replicates	**11.9**	**14**									
(-RT control)	< 0.2	< 0.2									

PCR cycle number not assessed
(-RT control) Minus Reverse Transcriptase control
< 0.2 Sample below the quantitation range for the Qbit fluorometer and dsDNA HS kit (0.2 ng)

Appendix 9 | Optimising the PCR cycle number for use with Smart-seq2. Smart-seq2. PCR cycle number was optimised using variable starting quantities of RNA, (10 pg, 50 pg, 100 pg, 500 pg and 1 ng), to cover the predicted range for parasite preparations following isolation from the human host during mosquito-bite CHMI. Each experiment included three replicate samples (means shown in red), and a Minus Reverse Transcriptase control (-RT control).

Appendix 10: List of detectable *var* and *rif* genes following mosquito-bite CHMI

volunteer 1074		
***P. f* (3D7) transcript I.D**	***var/ rif* group**	**read count**
C +9		
PF3D7_0426000	B (*var*)	66
PF3D7_1300100	B (*var*)	15
PF3D7_0223500	B (*var*)	6
C +10		
PF3D7_0401600	A (*rif*)	12
C +11		
PF3D7_0632800	B (*var*)	1,660
PF3D7_0426000	B (*var*)	946
PF3D7_1255200	B (*var*)	880
PF3D7_0400400	A (*var*)	795
PF3D7_0632500	B/A (*var*)	766
PF3D7_0400100	B (*var*)	739
PF3D7_0223500	B (*var*)	734
PF3D7_0425800	A (*var*)	683
PF3D7_1300100	B (*var*)	611
PF3D7_0733000	B (*var*)	509
PF3D7_1373500	B (*var*)	475
PF3D7_0937800	B (*var*)	456
PF3D7_1100200	A (*var*)	422
PF3D7_1041300	B (*var*)	418
PF3D7_0115700	B (*var*)	413
PF3D7_1100100	B (*var*)	406
PF3D7_1200400	B/A (*var*)	387
PF3D7_0401600	A (*rif*)	344
PF3D7_0100100	B (*var*)	315
PF3D7_1200600	var2csa (E)	252
PF3D7_0800100	B (*var*)	236
PF3D7_0200100	B (*var*)	191
PF3D7_0300100	B (*var*)	147
PF3D7_1200100	B (*var*)	145
PF3D7_0421100	B/C (*var*)	119
PF3D7_1240400	B/C (*var*)	105
PF3D7_0809100	B/C (*var*)	94
PF3D7_0400500	A (*rif*)	90
PF3D7_0800300	B/A (*var*)	87
PF3D7_1240600	C (*var*)	74
PF3D7_0712400	B/C (*var*)	64
PF3D7_0712000	C (*var*)	17
PF3D7_0420900	C (*var*)	9
PF3D7_0412700	C (*var*)	8
PF3D7_1300300	A (*var*)	6

volunteer 1068		
***P. f* (3D7) transcript I.D**	***var/ rif* group**	**read count**
C +9		
PF3D7_0800300	B/A (*var*)	16
C +10		
PF3D7_1255200	B (*var*)	46
PF3D7_0400100	B (*var*)	40
PF3D7_0401600	A (*rif*)	14
C +11		
PF3D7_0937800	B (*var*)	287
PF3D7_1255200	B (*var*)	277
PF3D7_0300100	B (*var*)	211
PF3D7_0400400	A (*var*)	176
PF3D7_0632500	B/A (*var*)	141
PF3D7_1100200	A (*var*)	136
PF3D7_1100100	B (*var*)	120
PF3D7_1041300	B (*var*)	117
PF3D7_0632800	B (*var*)	115
PF3D7_0800100	B (*var*)	111
PF3D7_1373500	B (*var*)	100
PF3D7_1200400	B/A (*var*)	96
PF3D7_1300300	A (*var*)	89
PF3D7_1240400	B/C (*var*)	88
PF3D7_0401600	A (*rif*)	86
PF3D7_0400100	B (*var*)	82
PF3D7_1200100	B (*var*)	82
PF3D7_0733000	B (*var*)	80
PF3D7_0100100	B (*var*)	79
PF3D7_1200600	var2csa (E)	75
PF3D7_0421100	B/C (*var*)	62
PF3D7_0600200	B/A (*var*)	54
PF3D7_0426000	B (*var*)	53
PF3D7_0324900	B (*var*)	43
PF3D7_0400500	A (*rif*)	34
PF3D7_0712400	B/C (*var*)	34
PF3D7_0712800	B/C (*var*)	23
PF3D7_0425800	A (*var*)	21
PF3D7_0420900	C (*var*)	19
PF3D7_0712300	B/C (*var*)	16
PF3D7_1300100	B (*var*)	12
PF3D7_1200500	A (*rif*)	6
PF3D7_0617400	C (*var*)	6
PF3D7_1240600	C (*var*)	5

volunteer 1037		
***P. f* (3D7) transcript I.D**	***var/ rif* group**	**read count**
C +9		
PF3D7_1200600	var2csa (E)	33
PF3D7_0733000	B (*var*)	15
C +10		
PF3D7_0712800	B/C (*var*)	55
PF3D7_0115700	B (*var*)	34
PF3D7_0425800	A (*var*)	29
PF3D7_0833500	B (*var*)	28
PF3D7_1200100	B (*var*)	22
PF3D7_1200600	var2csa (E)	20
PF3D7_0937800	B (*var*)	19
PF3D7_0632800	B (*var*)	13
C +11		
PF3D7_1255200	B (*var*)	137
PF3D7_0300100	B (*var*)	81
PF3D7_0632800	B (*var*)	81
PF3D7_0223500	B (*var*)	64
PF3D7_0401600	A (*rif*)	53
PF3D7_0800100	B (*var*)	50
PF3D7_0937800	B (*var*)	45
PF3D7_0400100	B (*var*)	44
PF3D7_0733000	B (*var*)	40
PF3D7_1373500	B (*var*)	39
PF3D7_1041300	B (*var*)	33
PF3D7_0632500	B/A (*var*)	32
PF3D7_0200100	B (*var*)	30
PF3D7_1200400	B/A (*var*)	30
PF3D7_0426000	B (*var*)	27
PF3D7_1240600	C (*var*)	24
PF3D7_1200600	var2csa (E)	22
PF3D7_0421100	B/C (*var*)	20
PF3D7_1100100	B (*var*)	19
PF3D7_0115700	B (*var*)	18
PF3D7_1200100	B (*var*)	17
PF3D7_1300100	B (*var*)	15
PF3D7_0100100	B (*var*)	14
PF3D7_0712300	B/C (*var*)	12
PF3D7_0425800	A (*var*)	11
PF3D7_0712400	B/C (*var*)	11
PF3D7_0412700	C (*var*)	8
PF3D7_0809100	B/C (*var*)	8
PF3D7_0324900	B (*var*)	7
PF3D7_0400400	A (*var*)	5

volunteer 1073		
***P. f* (3D7) transcript I.D**	***var/ rif* group**	**read count**
C +9		
PF3D7_0711700	C (*var*)	88
C +10		
PF3D7_0400100	B (*var*)	544
PF3D7_1255200	B (*var*)	390
PF3D7_0400400	A (*var*)	299
PF3D7_1300100	B (*var*)	190
PF3D7_0200100	B (*var*)	172
PF3D7_0426000	B (*var*)	172
PF3D7_0712800	B/C (*var*)	112
PF3D7_0833500	B (*var*)	103
PF3D7_0711700	C (*var*)	82
PF3D7_0617400	C (*var*)	75
PF3D7_1200600	var2csa (E)	70
PF3D7_1041300	B (*var*)	42
PF3D7_0632500	B/A (*var*)	29
PF3D7_0600200	B/A (*var*)	20
PF3D7_1100100	B (*var*)	20
PF3D7_0632800	B (*var*)	13
PF3D7_0733000	B (*var*)	12
C +11		
PF3D7_1041300	B (*var*)	854
PF3D7_0400100	B (*var*)	381

volunteer 1076		
***P. f* (3D7) transcript I.D**	***var/ rif* group**	**read count**
C +9		
PF3D7_0100100	B (*var*)	145
C +10		
PF3D7_1373500	B (*var*)	41
PF3D7_0600200	B/A (*var*)	33
PF3D7_0833500	B (*var*)	31
PF3D7_0425800	A (*var*)	26
PF3D7_0800300	B/A (*var*)	22
PF3D7_1100200	A (*var*)	21
PF3D7_0712300	B/C (*var*)	14
PF3D7_0400100	B (*var*)	12
PF3D7_0632800	B (*var*)	8
PF3D7_0115700	B (*var*)	5
PF3D7_1200500	A (*rif*)	5

Appendix 10 | List of detectable *var* and *rif* genes (with associated read counts) following mosquito-bite CHMI (n = 5 volunteers). Tables show the *P. falciparum* transcript i.d and associated reads counts for the *var* and *rif* genes detected at each of the 3 time points for which parasite samples were sequenced (C +9, C +10 and C +11), for each of the 5 volunteers (1074, 1068, 1037, 1073 and 1076). For each time point, genes have been ordered by read count (highest to lowest). *Var* genes have been colour coded according to group (A, B/A, B, B/C, C, and E), and *rif* genes are highlighted in yellow. Note that data are not normalised and hence read counts are not directly comparable between volunteers.